We shall write this relationship as follows

$$\Delta T = \tfrac{1}{3} C \tau L'^2 / L^2. \tag{7.23-1}$$

Here, C is a constant which was experimentally found to be equal to $7.4 \cdot 10^{-9}$ deg/(dynes $\cdot$ cm^{-2}).

The speed of sliding S_A of a glacier is equal to the volume of ice melted per unit time in front of an obstacle divided by the cross-sectional area of the obstacle. The melting process, however, will be caused by heat-flow across each obstacle at which the difference in temperature ΔT exists as calculated above. Thus

$$S_A = \frac{1}{L^2} \Delta T \frac{DL}{H\rho} = \frac{\tau C D}{3 H \rho L} \left(\frac{L'}{L}\right)^2 \tag{7.23-2}$$

where D is the coefficient of heat conductivity of the rock, H is the heat of fusion of the ice and ρ is its density.

If there is a whole spectrum of protuberances present in the glacier bed (L'/L being constant), then it becomes obvious that the larger the obstacle, the less likely it is that sliding by the above mechanism can take place.

Fortunately, it can be shown that the second effect (that of stress concentration) can precisely account for the sliding of glaciers over *large* obstacles. Stress concentrations will again be of the order of $\tau(L'/L)^2$. Using the power law of creep for ice (cf. Sec. 2.33), the creep rate K due to this stress concentration will be

$$K = \text{const}\, \tau^n \left(\frac{L'}{L}\right)^{2n}. \tag{7.23-3}$$

Furthermore, it stands to reason that this creep rate is effective over the distance L; hence the sliding velocity S_B due to the stress concentration is (writing the constant somewhat differently)

$$S_B = B(\tfrac{1}{2} \tau L'^2 / L^2)^n L. \tag{7.23-4}$$

This vanishes for very small obstacles. WEERTMAN now argues that the sliding will take place with just such a speed which is the same for the two types of sliding, because for each type, the speed is controlled by the most unfavorable obstacle size. Thus, setting $S_A = S_B$ and eliminating L (assuming the ratio L'/L as given), WEERTMAN obtained for the sliding velocity S

$$S = S_A = S_B = \left(\frac{2BCD}{3H\rho}\right)^{\frac{1}{2}} \left(\frac{\tau}{2}\right)^{\frac{1+n}{2}} \left(\frac{L'}{L}\right)^{1+n}. \tag{7.23-5}$$

The main result of the above analysis is that sliding of glaciers can and will indeed take place. WEERTMAN, using reasonable values (*viz.*

Adrian E. Scheidegger

Theoretical Geomorphology

Second, Revised Edition

With 207 Figures

Springer-Verlag Berlin · Heidelberg · New York 1970

Dr. ADRIAN E. SCHEIDEGGER
Professor of Petrophysics

University of Illinois
Dept. of Mining, Metallurgy, and
Petroleum Engineering
Urbana 61801/U.S.A.

Title-No. 0892

To my Parents

Preface

The surface features of the Earth are commonly split into two categories, the first of which comprises those features that are due to processes occurring inside the solid Earth (endogenetic features) and the second those that are due to processes occurring outside the solid Earth (exogenetic features). Specifically, the endogenetic features are treated in the science of geodynamics, the exogenetic features in the science of *geomorphology.*

I have treated the theoretical aspects of the endogenetic features in my "*Principles of Geodynamics*", and it is my aim to supplement my earlier book with a discussion of the theory of the exogenetic features. It is my hope that the two books will together present a reasonably coherent, if necessarily incomplete, account of theoretical geology.

Contrary to endogenetic phenomena, exogenetic processes can often be directly observed as they occur: the action of a river, the development of a slope and the evolution of a shore platform are all sufficiently rapid so that they can be seen as they take place. This has the result that in geomorphology one is generally on much less speculative ground regarding the mechanics of the processes at work than one is in geodynamics.

The book follows a pattern which is, *mutatis mutandis*, analogous to that of my "*Principles of Geodynamics*". First, a brief description is given of the physiographic facts of geomorphology, after which some of the basic physics is reviewed which is necessary for the understanding of the subsequent exposition. Then, the body of the book presents in sequence the pertinent subjects which are (i) the mechanics of slope formation, (ii) the theory of river action, (iii) drainage basin and large scale landscape development, (iv) the theory of subaquatic effects, (v) niveal effects and (vi) some special features.

The present edition is the second of this book. A comparison with the first edition will show that some sections have been extensively rewritten. Chapter V on basin development is completely new, inasmuch as the past eight years have brought an entirely new approach to the problem, based upon statistical mechanics.

Some of the sections in the present book are based upon articles of my own which appeared in the *Bulletin of the Geological Society of America*, in the *Journal of the Alberta Society of Petroleum Geologists*, in *Geofisica Pura e Applicata*, in *Geologie und Bauwesen*, in the *Bulletin*

of the International Society of Scientific Hydrology and in *Water Resources Research*. I am grateful to the Editors of these Journals for the permission to draw freely from my articles published therein. Professor BERNAL of the University of London kindly gave permission to quote from an unpublished letter of his, Dr. CRICKMAY of Calgary, Dr. STEKETEE of Delft, Mr. BRIGHAM of Urbana and Dr. WEERTMAN of Evanston have assisted me with much valuable advice and Dr. POKHSRARYAN of Erevan has patiently explained some of his theories to me. My thanks are also due to the Springer-Verlag who has again been most cooperative in effecting a speedy publication of the manuscript.

Urbana/Ill., 1969. A. E. SCHEIDEGGER

Contents

I. Physical Geomorphology

1.1. Introduction

Geomorphology, in its widest sense, is that branch of the geosciences which concerns itself with the development of the surface features of the Earth. In a more restrictive sense, geomorphology is the science of those surface features whose shape is determined by the action of *exogenetic* processes, i.e. of processes which originate *outside* the solid Earth. It is with this latter concept of geomorphology that we shall concern ourselves.

Any discussion of the mechanical and physical processes active in the shaping of the Earth's surface features has to start with a discussion of the physiography of these features. This is what we propose to do in this first chapter of our monograph.

The basic constituents of any landscape are *slopes*. The term "slope" may refer to a mountain side, to a river bed, or to a cliff on a coast line. If the development of individual slopes is understood, the development of a landscape can be synthesized.

Some of the most striking features in geomorphology are linear, i.e. they are formed by curved lines. One therefore must discuss the means by which such linear features can be described.

Such linear features may be caused by the work of *rivers*. A brief description of the physiography of river erosion, including river bed processes and meander formation, will therefore be provided.

Making the transition from one river to many rivers, one arrives at an analysis of whole *drainage basins*,—a description of which rounds out the discussion of features caused by the action of water on the land surface of the Earth.

Most of the Earth's surface (about 71 per cent) is covered by the sea. Processes connected with the motion of large bodies of water are therefore of great importance with regard to the evolution of geomorphological features. Accordingly, we shall give a brief review of coastal and submarine geomorphology.

Subsequently, we shall turn to features caused by some specific exogenetic agents: this includes niveal features caused by the action of ice and snow and aeolian features created by the direct action of wind.

Finally we shall discuss some phenomena which are due to a variety of processes:—this includes karsts and caves, badland erosion and geysers.

The description of physical geomorphology will be held brief here as it is to serve only as a preliminary for a discussion of the exogenetic geodynamic processes at work. Many more details may be found in pertinent textbooks on geomorphology[1–26]. Treatises bearing upon specific geomorphological questions will be listed when the particular problems are under discussion.

1.2. Development of Slopes

1.21. General Remarks. Slopes are the constituent elements of mountains, river banks, coasts;—in short of all the features that are characteristic of the geography of our globe. Some of these slopes may

1. AIGNER, A.: Geomorphologie. Die Formen der Erdoberfläche. Berlin, Leipzig 1936.
2. BLOOM, A. L.: The Surface of the Earth. New York, Prentice-Hall 1968.
3. COTTON, C. A.: Geomorphology. 5th Ed. New York 1949.
4. DE MARTONNE, E.. Traité de géographie physique, 2nd. vol.: Le relief du sol. 8th ed. Paris 1948.
5. DERRUAU, M.: Précis de géomorphologie. Paris: Masson & Cie. 1956.
6. DURY, G. H.: Essays in Geomorphology. Amsterdam: Elsevier Publ. Co. 1966.
7. DYLIC, J.: Dynamical geomorphology, its nature and methods. Bull. Soc. Sci. Amer. Let. Lodz (Classe III, VIII, 12, p. 1–42 [1957]).
8. FAIRBRIDGE, R. W. (ed.): The Encyclopedia of Geomorphology. New York: Reinhold 1968.
9. GRESSWELL, R. K.: Physical Geography. London: Longmans & Green 1967.
10. HINDS, N. E. A.: Geomorphology. New York: Prentice-Hall 1943.
11. KING, L. C.: The Morphology of the Earth, 2nd ed. London: Oliver & Boyd 1967.
12. KLIMASZEWSKI, M.: Geomorfologia ogolna, Warsaw 1963.
13. LOBECK, A. K.: Geomorphology. New York, London 1939.
14. LOUIS, H.: Allgemeine Geomorphologie. Berlin: W. de Gruyter 1960.
15. MACHATSCHEK, F.: Geomorphologie. 5th Ed. Leipzig: Teubner 1952.
16. MARKOV, K. K.: Основы проблемы геоморфологии. Moscow: OGIZ 1948.
17. MAULL, O.: Geomorphologie. Wien: Deuticke 1938.
18. PANZER, W.: Geomorphologie: die Formen der Erdoberfläche. Braunschweig: Westermann.
19. PENCK, A.: Morphologie der Erdoberfläche. 2 vols. Stuttgart 1894.
20. ROVERETO, G.: Forme della terra, trattato di geologie morphologica. 2 vols. Milano 1924/25.
21. SHCHUKIN, I. S.: Общая морфология. 2 vols. Moscow 1964.
22. SPARKS, B. W.: Geomorphology. London: Longmans 1960.
23. STRAHLER, A.: Physical Geography. New York: John Wiley & Sons, 1st ed.: 1951; 2nd ed.: 1960.
24. THORNBURY, W. D.: Principles of Geomorphology. New York: J. Wiley & Sons 1954.
25. TRICART, J.: Principes et méthodes de la géomorphologie. Paris: Masson & Cie. 1965.
26. VON ENGELN, O. D.: Geomorphology. New York: Macmillan 1942.

have been formed by endogenetic processes, such as by the thrusting up of a mountain range or by the opening up of a rift valley. However, the "primary" slopes, if one whishes to call them thus, will soon be acted upon by external ("exogenetic") agents such as wind, water ice, and residual stresses, so that their shape will change. If it can be understood how slopes change under the influence of exogenetic processes, then it is obviously possible to explain physical geography.

1.22. Quantitative Description of Slopes. As always when quantitative methods of analysis are contemplated, it is necessary to describe the field data in quantitative terms as well. Slopes are fundamentally inclined surfaces, and as such one might think that all one has to do is to give the equation describing the surface in question in, say, Cartesian co-ordinates. Needless to say, this would be a very difficult undertaking: The surfaces in question are extremely irregular; this becomes obvious if one thinks of the individual pebbles etc. that might comprise it. However, one is generally only interested in the *average* properties of a hill-side, not in all of its intricate details. Thus, the true hillside is approximated by a smooth surface passing through such points as have been measured. Of this approximate surface it is then possible to determine characteristic parameters.

Moreover, one is generally not concerned with the entire hillside, but only with its *profile.* In order to obtain a profile, a horizontal straight base line is chosen more or less parallel to the general declivity of the area in question (there is a certain amount of arbitrariness in choosing this line). Common parameters that are listed are then the elevation H of the slope profile above the base line, the distance L along the base line from an arbitrarily chosen initial point thereon, and the (local or average) gradient given by

$$G = \Delta H / \Delta L. \qquad (1.22\text{-}1)$$

1.23. Agents in Slope Formation. As noted, slopes change under the influence of exogenetic agents. The net effect is called denudation. Depending on climate and season, it may occur rather rapidly[1,2]. A compilation of the various agents that might cause the shapes of slopes to change, has been given, for instance, by PENCK[3]. Accordingly, the processes that are effective in slope formation can be classified as follows: (i) reduction of rocks, (ii) spontaneous mass movement, (iii) corrasion, (iv) erosion, (v) transport of mass and (vi) accumulation. The terminology used by PENCK is somewhat different from that in other writings on

1. SCHUMM, S. A.: Z. Geomorphol., Suppl. 5, 215 (1964)
2. GERBER, E.: Mitt. Aargauischen Naturforsch. Ges. 26, 86 (1961)
3. PENCK, W.: Geomorphologische Analyse. Stuttgart: J. Engelhorn's Nachf. 1924.

geomorphology, but the processes considered are usually of the same general nature as those listed above.

Looking at the various processes in somewhat greater detail, we note that the *reduction* (cf. also Sec. 3.2) of rocks represents their disintegration into small pieces. It takes place by weathering due to their exposure to wind and water. It may be mechanical or chemical. Mechanical reduction may be due to the action of freezing and melting of the water in the cracks and pores of the rocks, or to the thermal expansion of the rocks themselves under temperature variations. Mechanical reduction of rocks may also be due to the action of internal stresses[1]. Chemical reduction is due to the action of the water on the chemical composition of the rocks. The amount of reduction of a particular rock depends on its exposure to the elements of the weather. For given climatic conditions, the latter decreases if the weathered débris are not transported away by some other process.

The reduction of rocks alone does not produce any changes in the existing slopes. In order to produce such changes, it is necessary to have processes that can effect a transfer of mass. All such mass transfers are due to the action of gravity in some form. First of all, one has *spontaneous mass movement.* With no interference from any carrying medium, the débris produced by weathering may start to slide downhill. On steep rock walls, any loosened particles will immediately drop to the bottom and form a pile of débris. Generally, such piles of débris are steeper at the top than at the bottom, and at the same time the individual pebbles are larger at the bottom than at the top. It has been contended that the size-grading *causes* the change in steepness (cf. MACHATSCHEK[2], p. 39), but this statement would appear to require further analysis (see Sec. 3.36). The slopes vary from 25 – 40°. On lesser slopes, spontaneous mass movement may express itself as a landslide, sometimes of spectacular magnitude.

The material moving over a slope by the above-mentioned process helps further wearing down the slope. This wearing-down process has been termed *corrasion.* It occurs without the intermediary of any further medium. In contrast to corrasion one has *erosion.* This process is caused by the intermediary of some moving medium such as wind, water or ice. It also causes the wearing down of the slope. The combined effect of the above agents is termed "*denudation*".

In order to achieve further slope development, the material that has been loosened and that may have slid into the lower parts of the area under consideration, must somehow be removed. This occurs by the various processes of *transport of mass.* In such transport processes, the

1. GERBER, E., and A. E. SCHEIDEGGER: Ecl. Geol. Helv. 1969.
2. MACHATSCHEK, F.: Geomorphologie. 5th ed. Leipzig: Teubner 1952.

appearance of a carrying medium is of prime importance. A case in point is represented by rivers. The latter, however, have only an indirect effect on slope formation by making space for more débris to form. On the slopes themselves, running water or blowing wind may directly affect the shape and thus have a far more direct effect. The end stage of transport of mass is *accumulation.* The transporting agents (water, wind, ice) may dump material in some areas which by its very presence forms a slope. This occurs not only in alluvial plains and in sheet-floods, but also in any place where the material is transported by external agents. Thus,

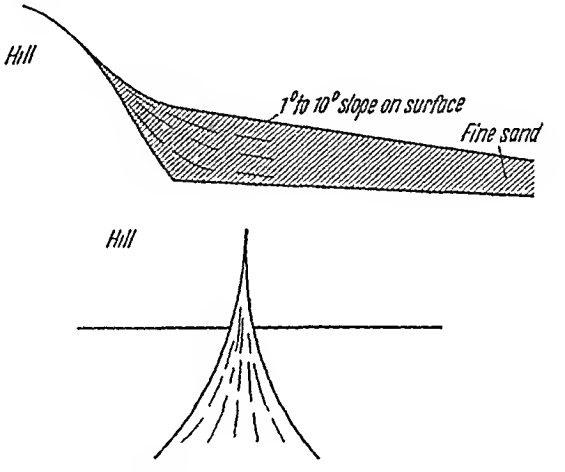

Fig. 1. Alluvial fan: top cross section; bottom: view in plan

near mountains, material might for instance be deposited in the form of alluvial fans which occur at the edge of hills and mountains. Their slopes are from 1 – 10 degrees, the finest deposits are always found at the periphery (Fig. 1). The opposite arrangement with regard to the grading of deposits is found in alluvial cones and talus accumulations. Here the slopes are from 10 to 50 degrees. Boulders are found at the base, sand and gravel at the top (Fig. 2). These features are caused by small intermittent streams.

1.24. Differential Development of Slopes. The discussion given earlier sets the agents which act upon the shape of slopes entirely apart from those processes that caused uplifted areas on the Earth's crust in the first place. It would therefore appear that one could treat the development of a landscape in terms of a *cycle* in which uplift and planation alternate. In fact, this is the old classic view amongst geomorphologists and will be treated in detail in Sec. 1.51. However, a somewhat different point of view has been taken by PENCK[1]. Accordingly, there is little reason to

1. PENCK, W.: Die geomorphologische Analyse. Stuttgart: J. Engelhorn's Nachf 1929. English translation by H. CZECH and K. C. BOSWELL. London: Macmillan 1953.

believe that uplift and planation are taking place alternately; rather, uplift and planation are concurrent phenomena and should be treated as such. Thus, according to PENCK, there is little justification in speaking of a "cycle". There is no true beginning nor any end to such a cycle; slope development is a differential process in which, at best, several typical quasistationary stages can be discerned. Such stages are the following: (i) waxing development[1] in which the uplift is faster than the denudation (leading to convex slope profiles); (ii) stationary development[2] in which uplift and denudation proceed at an equal rate (leading to straight slopes

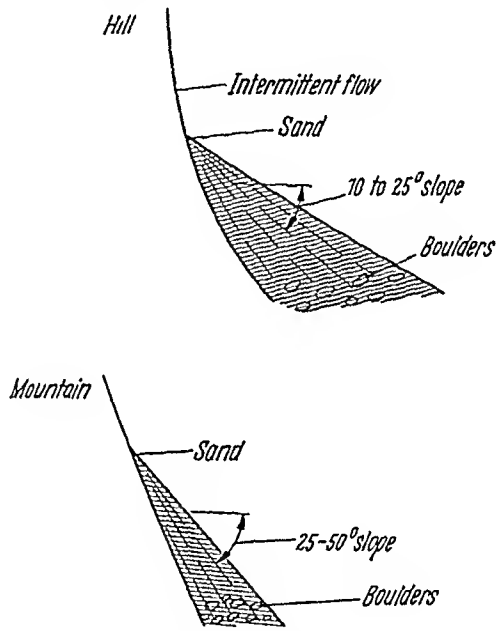

Fig. 2. Alluvial cone (top) and talus accumulation (bottom)

and parallel slope recession) and waning development[3] in which the denudation rate exceeds the rate of uplift (leading to concave slopes).

PENCK's ideas have met with considerable opposition. However, the criticisms are directed toward PENCK's interpretation of particular slopes rather than against his endeavor to consider slopes as the outcome of a differential process. It is therefore mainly the relative importance of the various processes envisaged by PENCK which is in doubt.

In a vein similar to that of PENCK, WHITE[4] has noted that equilibrium slope profiles have generally a tripatite classification: An upper convex element, a middle straight element, and a lower concave element. A series of slope profiles measured by WHITE in an area about 15 km East of Dayton, Ohio, is reproduced here in Fig. 3.

1. Aufsteigende Entwicklung.
2. Gleichformige Entwicklung.
3. Absteigende Entwicklung.
4. WHITE, J. F.: Ohio J. Sci. 66. 592 (1966).

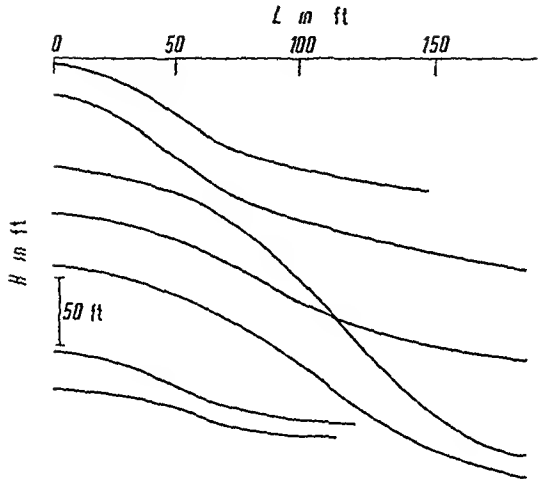

Fig. 3. Sample profiles of slope profile near Dayton, Ohio Note smoothness and similar form, but contrasting size, gradient, and shape. After WHITE

1.3. Curved Lines in Geomorphology

1.31. General Remarks. Many features in geomorphology are represented, on a map at least, by lines.

The most obvious of such "linear" features are rivers, although, in fact, a river has actually a finite width and is therefore, in nature, not the realization of a mathematical line.

A true linear feature is the course of each bank of a given river (for, say, mean water level). The course of the water's edge represents, in fact, a mathematical line. A similar true linear feature is a coastline. Here the natural feature is again a mathematical line: the course of the water's edge at mean sea level. This line represents, in effect, an isohypse; all other isohypses also represent geomorphic "lines". Another linear feature is the course of a mountain-crest, or of any other watershed. This is again a mathematical line.

All the above geomorphic lines have an obvious characteristic: They are "wiggly". While the general trend of these lines is very often quite straight, the details, if one cares to look closely, are extremely complex and difficult to ascertain. It is the purpose of this chapter to touch upon some problems, old and new, which are caused by the "wiggliness" of geomorphic lines and by the task of quantitatively describing such lines.

1.32. The Length of Wiggly Lines. The problem of measuring the length of a line is an old one. In general, not much thought is given to this problem by geomorphologists, inasmuch as it is simply assumed that the length be measured by some type of integrating device.

However, the fact that natural geomorphological lines are wiggly, introduces certain complications. It is clear that more and more "wiggles" tend to disappear, the smaller the scale of the map is. Thus, the "length" of a geomorphic line does not have a meaning *per se*, inasmuch as it depends very much on the scale of map used: The better the map, the greater the length of a given natural feature.

RICHARDSON[1] has studied this problem, based on the usual idea of Riemann integration: The curved line is approximated by polygons of smaller and smaller edge-length l (in practice, a divider is "walked" along the line on a map), the last edge being taken as a fraction of l; then the length is approximated by the sum $\sum l$ of the lengths of all the polygon-edges. The results of RICHARDSON's measurements for three natural coasts, viz. the West Coast of Great Britain, the Coast of South Africa, and the Coast of the Australian Mainland, are reproduced here in Table 1. From his numerical values, RICHARDSON deduced empirically a law

$$\sum l = l^{-\alpha} \tag{1.32-1}$$

with $\alpha = 0.25$ for the West Coast of Great Britain, $\alpha = 0.02$ for South Africa, and $\alpha = 0.13$ for Australia. Thus, according to "Richardson's law", the "length" of a geomorphic feature would be given by stating three

Table 1. *Lengths of wiggly lines as a function of polygon side. (After* RICHARDSON[1]*)*

West Coast of Britain						
Polygon side l km	971	490	200	100	30	10
$\sum l$ km	971	980	1,180	1,540	2,073	2,931
Coast of South Africa						
Polygon side l km	1,000	500	215.5	100		
$\sum l$ km	4,120	4,155	4,263	4,334		
Coast of Australian Mainland						
Polygon side l km	2,000	1,000	500	250	100	
$\sum l$ km	9,400	11,040	11,950	13,200	14,420	

parameters: the edge-length l of the polygon, the length $\sum l$ measured using this edge length, and the "Richardson parameter" α.

MANDELBROT[2] noted that Richardson's law could be the outcome of a general self-similarity property of the geomorphic curves in question. In this case, the curves would be treated as non-rectifiable, self-similar, and their mathematical fractional dimension D would then be

$$D = 1 + \alpha. \tag{1.32-2}$$

However, it should be noted that Richardson's law has not been verified over a range greater than that of a factor of 97 (in the case of Great

1. RICHARDSON, L. F.: General Systems Yearbook 6, 139 (1961).
2. MANDELBROT, B.: Science 156, 636 (1967).

Britain; in the other cases only over that of a factor of 10) with rather large (10 km in the case of Great Britain and 100 km in the other cases) minimum l. It seems physically absurd to postulate the validity of Richardson's law for *all* l. In the limit, one arrives at the size of the pebbles on the coasts in question and at the molecular interstices of those pebbles, etc. To postulate the validity of self-similarity for all these size-ranges of l seems absurd.

Thus, in practice, if the "length" of a geomorphic feature is to be determined, the length l of the polygon by which it was measured should be stated. In the case of a river, l should obviously not be smaller than the width of that river. If it is empirically found that Richardson's law holds, the Richardson parameter α may be given, and the *range* over which the validity of Richardson's law was verified. It is doubtful that, in general, α will be the same for small scale ($l<1$ km) and large scale ($l>10$ km) "wiggles". At least there is no obvious reason why there should be self-similarity over such ranges.

A different approach to the problem of length from that described above has been taken by STEINHAUS[1]. STEINHAUS bases his argument on ideas of measure theory and Lebesgue integration, and goes back to the possibility of defining the "length" of a point-set by a double integral[2] as the mean of the lengths of all projections of the set. CROFTON[3] described this idea by using an infinite sum which permitted a probabilistic interpretation. This leads to a practical way of measuring lengths of a geomorphic curve. Without going into the details and the proof of the method, which the reader may ascertain in STEINHAUS[1] article, we simply describe it here.

One takes a transparent sheet with a family of equidistant parallels L_i ($i=\ldots,-2,-1,0,1,2,\ldots$). Any arc A whose length is to be measured cuts L_i in a_i points. One denotes the number of all intersections by

$$S_0=\sum a_i. \tag{1.32-3}$$

Then one turns the transparent sheet through an angle $\pi k/m$ ($k=0,1,\ldots,m-1$); we get S_k intersections; the number of *all* intersections is then

$$N=\sum_{k=0}^{k=m-1} S_k. \tag{1.32-4}$$

If the distance between the parallel lines be d, the approximate length $|A|$ of A is given by

$$|A|\cong\frac{N d\pi}{2m}. \tag{1.32-5}$$

1. STEINHAUS, H.: Coll. Math. 3, No. 1, 1 (1954).
2. CAUCHY, L. A.: Oevres Compl. Sér. I, 2, 167 (1832).
3. CROFTON, M. W.: Phil. Trans. Roy. Soc. 158, 181 (1868).

This approximation gets better and better as $d \to 0$, $m \to \infty$. In most practical cases, STEINHAUS claims that $d = 2m$ and $m = 6$ give a sufficient accuracy, since this seems to correspond to the accuracy of given maps; i.e., taking more closely spaced lines at more angular positions of the transparent sheet does not seem to change the obtained length-values much from any given map.

In order to introduce a limitation as to the accuracy with which one would like to follow the details of the wiggles of a given geomorphic line, one sets an upper limit to the numbers of intersections of each of the parallel lines with the geomorphic feature which will be counted. If this upper limit be M, then it is said that one is measuring a "length of order M". Clearly, this procedure will eliminate wiggles. It enables one to compare lengths of lines on maps of different accuracy. The highest accuracy that can be obtained for a length is of that order indicated by the largest number of intersections which a straight line can have with the feature in question.

It is not immediately obvious to what order (M) a measurement to a given Riemann-approximation (polygon length l) corresponds. It does not seem to be possible to make an easy correspondence between M and l for corresponding accuracies, as one type of measurement is based on the Riemann, the other on the Lebesgue approximation to integration.

In practice, it seems easier to stick with the Riemann-type of approximation, stating the polygon-length $\sum l$ and the side l of the polygon used to approximate a wiggly geomorphic line.

The same problems as with the measurement of length would occur with the measurement of areas of geomorphic features, if the true surface area of the ground were desired. However, one defines as "area" generally the simple vertical projection onto a horizontal surface (geoid) whose area is always clearly defined.

1.33. Spectrum of a Wiggly Line. The length of a line is only one of its characteristic features. It is evidently desirable to use additional characteristics to describe it.

The most obvious one that comes to one's mind is the *power spectrum* of the line.

In general, in order to define a power spectrum, one starts with a function of one variable

$$x = f(t) \tag{1.33-1}$$

where x is a univalued function of t. In practice, if x is measured for a sequence of t_i, one will only have a discrete "sequential" set of measurements x_i, with $0 \leq i \leq N$, say.

The first task, thus, is to define the geomorphic curve in terms of a sequential set x_i, t_i. Any plane curve, of course, can be given as a rela-

tionship between two variables ξ, η, say (e.g., the Cartesian coordinates of the arbitrary point on the curve) such that

$$F(\xi, \eta)=0. \tag{1.33-2}$$

However, this representation will not generally be univalued for ξ as a function of η nor η as a function of ξ, so that it is unsuitable for calculating spectra.

One will therefore have to choose a parameter other than ξ or η for use as independent parameter t for the spectrum analysis. As such, the arc length along the curve, measured from a fixed point 0, comes to one's mind. However, here the difficulties enter which were encountered in defining "length" along geomorphic curves, discussed in the last section.

Thus, we choose a polygon length l, as described in the last section, and define measurement-points along the curve by giving the distance $t_n=n\,l$ along the polygon, assuming that only measurement points with $n=$integer are admissible. Then, n will be our independent variable.

At each point thus defined, we define as dependent variable the angle φ_n which a straight line drawn through the points $n\,l$ and $(n-1)\,l$ forms with a given datum-line. The measured pairs of variables are thus (n, φ_n), for $n=1, 2, \ldots, N$. On the sequence of values $\varphi_1 \ldots \varphi_n \ldots \varphi_N$ the customary types of spectral analyses can then be made[1].

Thus, we first define the correlation function $C_\varphi(r)$

$$C_\varphi(r)=\left\{\sum_{S=1}^{N-r} \varphi_n\,\varphi_{n+r}\right\} -(N-r)\,\bar{\varphi}^2. \tag{1.33-3}$$

The spectral function $X(k)$ is then

$$X(k)=\frac{1}{N}\left[C_\varphi(0)+\sum_{r=1}^{m-1} C_\varphi(r)\left(1+\cos\frac{\pi r}{m}\right)\cos\frac{\pi k r}{m}\right] \tag{1.33-4}$$

where m is the number of frequency-bands of interest. Naturally, the above quantities depend very much on the polygon-length l. If they are found not to depend on l, at least for a certain range of l, then the curve is self-similar (in a statistical sense) over that range.

1.4. River Erosion

1.41. General Remarks. Rivers are very powerful agents in shaping our globe's surface. They act in essentially two fashions: by removing material from its confines, and by transporting it.

1. Blackman, R. B., and J. W. Tukey: The Measurement of Power Spectra. New York: Dover 1958.

The removal of material by flowing water from the confining channel, in turn, can occur in two ways: either the channel is being scoured out and thereby deepened, or the removal occurs on the side. The latter case is referred to as sideways erosion, the former is normally considered jointly with transportation phenomena, and the two referred to as *river bed processes.*

We shall consider the phenomenology of these various cases in their turn below.

1.42. River Bed Processes. Turning first to river bed processes, we note that this includes every kind of interaction of a river with its bed, such as the entrainment of particles of which the river bed is composed, the formation of bottom ripples, the silting up and scouring out of a channel, the contrition of bed particles, the gradation of pebbles and so on. Erosional processes proper, however, are usually dealt with separately.

The requirements for measurements on rivers have been set forth on several occasions[1-4]. Accordingly, many field measurements have been made of various typical river bed processes. However, these were usually made in connection with special mechanical investigations and it is therefore difficult to give a meaningful summary in connection with a general discussion of physiography. These investigations will be referred to when the appropriate mechanical theories will be discussed.

1.43. Total Material Transport. As we have seen earlier, mass may be transported over the Earth's surface by a variety of means, However, it is only the *rivers* which are able to transport material over large distances. Thus, if one would like to know the total denudation rate in any one area, he has to look towards the rivers as the main removing agents.

It is to be expected that the fact of mountain ranges being worn down has an effect on the equilibrium of geodynamic forces; therefore the problem of determining the *total* amount of material that is being carried away from any given area per unit of time, is of major importance. The method of attacking this problem is by measuring the total mass flux in a river at successive points. The increase in mass flux between two points must be due to the denudation of the area drained between those two points. In making the appropriate measurements, it must be noted that a large part of the material is being transported in *solution.*

1. TRICART, J.: Inform. Geol. **24**, No. 5, 210 (1961).
2 SCHUMM, S. A.: U.S. Geological Survey Circ. No. 477 (1963).
3. LEOPOLD, L. B , and H. E. SKIBITZKE: Geografiska Ann. **49**A, 2 (1967).
4. MORISAWA, M.: Streams, Their Dynamics and Morphology. New York: McGraw-Hill Book Co. 1968.

Analyses of the pertinent mass transport data for various rivers have been reported on many occasions; a convenient summary of the earlier literature has been given by HOLEMAN[1]. CORBEL[2] investigated the dependence of denudation rates on climatic and relief conditions; his results are given in Table 2. In this table, the first column of numbers

Table 2. *Table of total denudation rates. (After* CORBEL[2]*)*

	mm/1,000 years	% in solution
A. Lowlands		
Climate with cold winter	29	93
Intermediate maritime climate (lower Rhine, Seine)	27	83
Hot dry climate (Mediterranean, New Mexico)	12	10
Hot-moist climate with dry season	32	34
Equatorial climate (dense rain forest)	22	70
B. Mountains		
Semi-humid periglacial climate	604	34
Extreme niveal climate (South-East Alaska)	800	24
Climate of Mediterranean, high mountain chains	449	18
Hot-dry climate (South-East U.S.A., Tunesia)	177	4
Hot-moist climate	92	33

represents the denudation in millimeters per thousand years, the second column the percentage that is being carried off in *solution*. From this table one may see that the denudation rates in mountainous areas are very substantial indeed. This, in turn, signifies that the sum total of the exogenetic processes in geodynamics is anything but negligible and that there might even be an interaction of the latter with endogenetic processes.

An estimate of the total material lost by erosion from the entirety of the non-submerged areas of the world has been made by FOURNIER[3] who arrived at a value of 400 mm per thousand years. SCHUMM[4] notes that this is about one-eighth of the present day rates of orogenesis.

1.44. Sideways Erosion. As noted earlier, rivers not only have a tendency to deepen their channels (under certain circumstances), but also to scour *sideways*.

It has been observed that the course of a river is almost never straight. Close to the source, there are V-shaped gorges with a sinuous course. Similarly curved courses occur in plains where rivers have a definite

1. HOLEMAN, J. N.: Water Resources Res. 4, 737 (1968).
2. CORBEL, J.: Z Geomorphol. 3, 1 (1959).
3. FOURNIER, F.: Débit solide des cours d'eau. Paper presented at the 12th General Assembly, Association of Scientific Hydrology, U.G.G.I., Helsinki, 1960.
4. SCHUMM, S. A.: U.S. Geol Survey Profess. Papers 454, H 1 (1963).

tendency to meander (i.e. to form loops; cf. Fig. 4a) or to form braids (cf. Fig. 4b). The meanders have a tendency to grow and to wander, presumably until they become so big that no further sideways erosion (scouring) can take place. On occasion, this causes meanders to touch and to short-circuit each other; the "dead" loops then form lakes which are called *oxbow lakes* (cf. Fig. 4a).

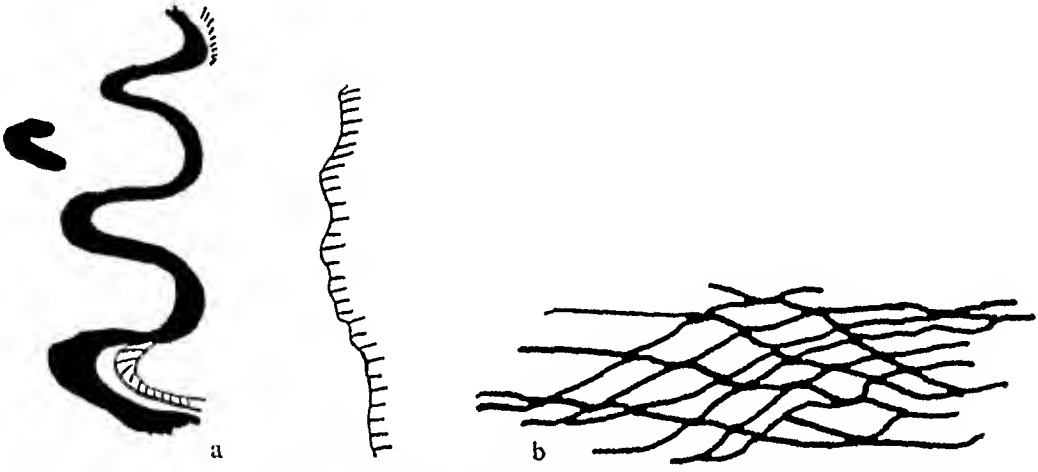

Fig. 4a and b. Meandering (a) and braided (b) river. Note the "oxbow lake" in the meandering river; this lake represents a meander that has been cut off

If one wishes to make quantitative studies of meanders, one is first of all faced with the problem of having to describe a geomorphic *line*. The pertinent questions in this connection have been discussed in Sec. 1.3 of this monograph. Accordingly, the river is approximated by a smooth curve, called "talweg" which is differentiable and rectifiable.

Once this is done, geometrical studies of meander loops can be made. This has been done, for instance by JEFFERSON[1], INGLIS[2,3], BATES[4], SCHUMM[5] and particularly by LEOPOLD and co-workers (LEOPOLD and MADDOCK[6], LEOPOLD and MILLER[7], LEOPOLD and WOLMAN[8,9], WOLMAN and LEOPOLD[10]) who investigated many rivers in the United States. In

1. JEFFERSON, M.: Nat. Geog. Mag **13**, 373 (1902).
2. INGLIS, C. C.: Ann. Rept. (Techn.), Central Board of Irrig. (India) 1938-to 1939, **49**, (1939).
3. INGLIS, C. C.. The Behaviour and Control of Rivers and Canals. Res Pub. Centr. Waterpower, Irrigation and Navigation Research Station, Poona 1949.
4. BATES, R. E.: Bull. Geol. Soc. Amer. **40**, 819 (1939).
5. SCHUMM, S. A.: Science **157**, 1549 (1967).
6. LEOPOLD, L. B., and T. MADDOCK: U.S. Geol. Survey Profess. Papers **252** (1953).
7. LEOPOLD, L. B., and J. P. MILLER: U.S. Geol. Survey Profess. Papers **282-A** (1953).
8. LEOPOLD, L. B., and M. G. WOLMAN: U.S. Geol. Survey Profess. Papers **282-B** (1957).
9. LEOPOLD, L. B., and M. G. WOLMAN: Bull. Geol. Soc. Amer. **71**, 769 (1960).
10. WOLMAN, M. G., and L. B. LEOPOLD: U.S. Geol. Survey Profess. Papers **282-C** (1957).

characterizing a meander, it is common to use its *length* L, its *amplitude* A, its *talweg* T, its *sinuosity* P ($P=T/L$) and its *radius of curvature* R. The meaning of some of these quantities is illustrated in Fig. 5. The aim is, then, to correlate these geometrical quantities with the channel width w, with

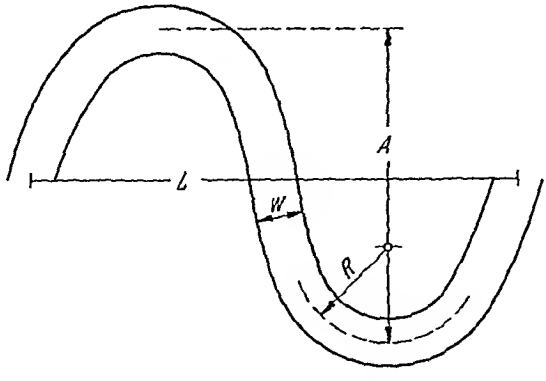

Fig. 5. Geometrical characteristics of a meander

the (average) depth d (or the width-to-depth ratio $F=w/d$) with the bankful discharge Q and with the bed slope S. In this instance, some of the formulas that have been proposed are the following

(i) by INGLIS[1] (English units; everything in feet)

$$L=6.6\,w^{0.99} \tag{1.44-1}$$

$$A=18.6\,w^{0.99}, \tag{1.44-2}$$

(ii) by LEOPOLD and WOLMAN[2] (English units; everything in feet)

$$L=10.9\,w^{1.01} \tag{1.44-3}$$

$$A=2.7\,w^{1.1} \tag{1.44-4}$$

$$L=4.7\,R^{0.98}, \tag{1.44-5}$$

(iii) by ZELLER[3] (metric units)

$$A=4.5\,w^{1.00}, \tag{1.44-6}$$

$$L=10.0\,w^{1.025}, \tag{1.44-7}$$

1 INGLIS, C. C: The Behaviour and Control of Rivers and Canals Res Pub. Centr. Waterpower, Irrigation and Navigation Research Station, Poona 1949.

2. LEOPOLD, L. B., and M. G. WOLMAN: *U.S. Geol. Survey. Profess. Papers 282-B (1957).*

3. ZELLER, J.: Int. Assoc. Sci. Hydrol., Symposium on River Morphology, Gen. Ass. Bern, Trans p. 174 (1967).

(iv) by SCHUMM[1] (English units)

$$P = 3.5\, F^{-0.27}, \tag{1.44-8}$$

(v) by MAKKAVEEV[2] (any units)

$$R = k\sqrt{Q}/S^n. \tag{1.44-9}$$

In the last formula, k and n are constants. It expresses the observed fact that a large discharge and low bed slope are conducive to an enlarging of the meanders.

The above formulas imply that the meander length generally ranges[3] from 7 to 10 times the width of the stream. However, the amplitude correlates only poorly with meander length. The ratio R/w tends to lie near 2 or 3.

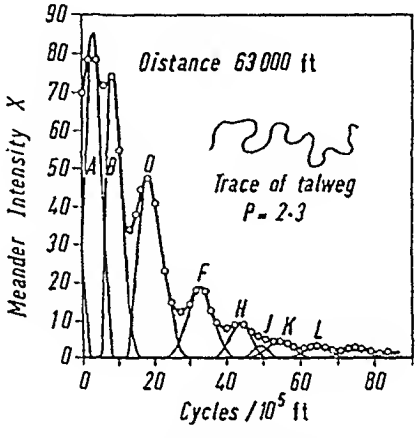

Fig. 6. Spectrum of the 1957 upper plains course of the Angabunga River in New Guinea. After SPEIGHT[4]

It should be noted that the meander wavelength L, its amplitude A etc. are not really well defined quantities in nature, inasmuch as it is difficult, in an irregular sequence of loops, to choose them unequivocally. Therefore, a more sophisticated approach to the problem of describing the geometry of a string of meanders is by means of a power-spectrum analysis, as this was described for general geomorphic lines in Sec. 1.3. Thus, a spectral meander intensity X can be obtained, using Eq. (1.33-4), in which the peaks describe the prevailing meander wave lengths. This method of describing meanders was apparently suggested for the first time by SPEIGHT[4] in connection with a study of the Angabunga River in New Guinea. An example of such a spectrum is shown in Fig. 6.

1. SCHUMM, S. A.: Bull. Geol. Soc. Amer. 74, 1089 (1963).

2. in SAMOILOV, I. V.: Устья рек. Moscow: Geografgiz 1954. German translation (title: Die Flußmündungen) by F. TUTENBERG. Gotha: Hermann Haack Verlag 1956; see particularly, p. 79, thereof.

3. LEOPOLD, L. B., and M. G. WOLMAN: Bull. Geol. Soc. Amer. 71, 769 (1960).

4. SPEIGHT, J. G.: J. Hydrology 3, No. 1, 1 (1965).

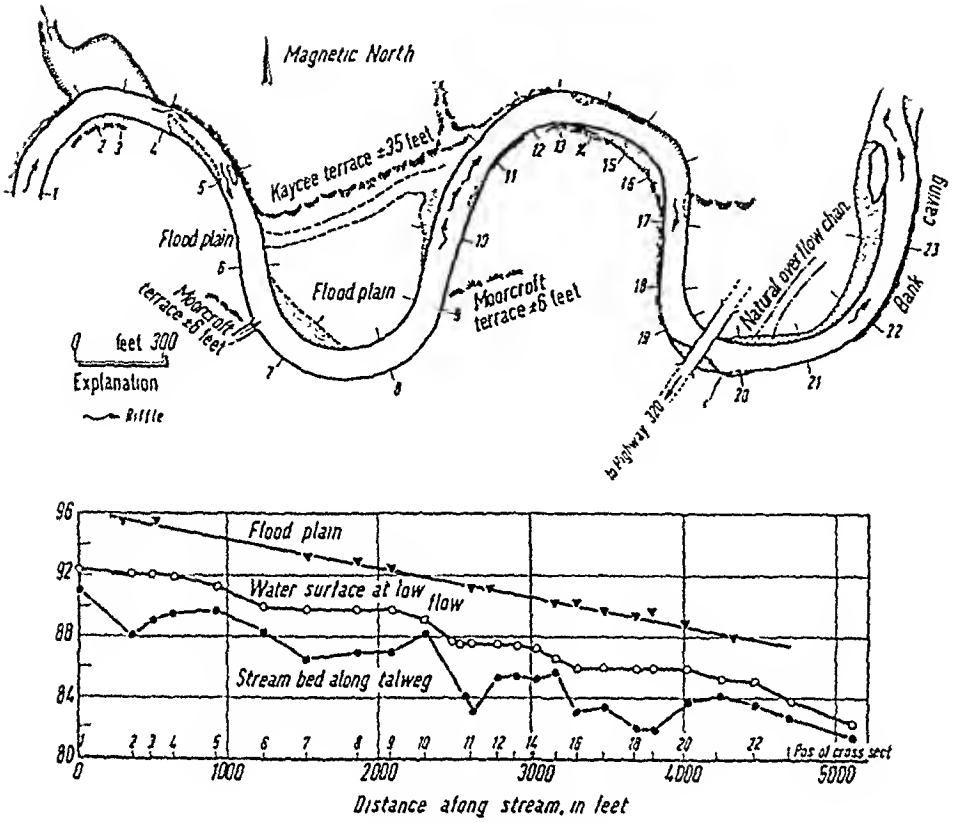

Fig. 7. Plan and profile of a meandering reach of the Popo Agie River near Hudson, Wyo. After LEOPOLD and WOLMAN[1]

Some of the above-mentioned empirical relations introduce the depth d of the meandering river. However, this depth is not very well defined either, inasmuch as there is a sequence of shallow "riffles" and deeper "pools" along a meandering river stretch. Much of the pertinent data in this regard has been summarized by LEOPOLD and WOLMAN[1]. The riffles occur generally in the more straight parts of a meander reach, but this relation is not entirely unequivocal, as is seen from an inspection of Fig. 7.

1.45. Morphometry of Particles. Since the river action is essentially concerned with the direct entrainment and deposition of particles, it may be well at this point to mention a few concepts which are of importance with the description of particles. This is useful not only in connection with the discussion of river action, but whenever individual particles are involved in geomorphic features (such as sandy deserts and beaches).

1. LEOPOLD, L. B., and M. G. WOLMAN: U.S. Geol. Survey Profess. Papers 282-B (1957).

2 Scheidegger, Theoretical Geomorphology, 2nd Ed.

One generally likes to speak of the "size" of a particle. However, particles have generally an irregular shape and hence "size" does not have an obvious meaning. Nevertheless, the "largest diameter" d has always a geometrically clearly defined meaning: It is the largest distance between points on the surface of the particle. When speaking of "diameter", we always mean this quantity. This diameter has the dimension of a length, and thus may be given in cm or mm. However, one finds commonly in the literature a different type of unit, called φ (phi) unit. The number of φ units is related to the diameter d in mm as follows:

$$d(\text{mm}) = (\tfrac{1}{2})^{\varphi}. \qquad (1.45\text{-}1)$$

Diameters of particles other than the largest are much more difficult to define. One could introduce a "small" diameter as the diameter of the largest totally inscribed sphere, and an "intermediate" diameter as the diameter of the smallest circumscribed circular cylinder. Similarly, attempts have been made to introduce such quantities as "roundness", "angularity" of the grains etc. However, these concepts are only incidental to the subject of the book, and the reader is therefore referred to the pertinent literature[1-3] for further details.

1.5. The Form of Drainage Basins

1.51. The Concept of a Geomorphological Cycle. We have already mentioned (in Sec. 1.24) that the development of a landscape can often be treated in terms of a *cycle*. As a most natural unit of a landscape one might consider a drainage basin which embodies all the area from which water proceeds to an arbitrarily chosen point on a river. Our attention will primarily be directed toward such drainage basins.

The concept of a cycle with regard to the general development of the Earth's surface features is very old and goes back to ancient Greek philosophy[4]. In connection with geomorphology, the cycle concept seems to have been applied primarily by DAVIS late in the nineteenth century[5]. According to DAVIS, the geomorphological cycle has its beginning soon after an endogenetic geodynamic process has completed creating an uplifted area, such as a mountain range. Weathering, erosion

1. KRUMBEIN, W. C., and F. PETTIJOHN: Manual of Sedimentary Petrography. London: Appleton-Century (1938).

2. HAWKSLEY, P. G.: Bull. Brit. Coal. Util. Res. Ass. **15**, 105 (1951).

3. KONZEWITSCH, N.: La Forma de los Clastos. Buenos Aires: Servic Hidrograf. Naval, Rep. Argentina (1961).

4. Cf. ENGELHARDT, W. v.: Nova Acta Leopoldina, N.F. **21**, No. 143, 85 (1959) for a good summary of the philosophical aspects of cycle theory.

5. DAVIS, W. N.: Die erklärende Beschreibung der Landformen. 2nd ed. Leipzig: Teubner 1924. (This summarizes DAVIS' work.)

and detrition begins to act on the uplifted area and gradually proceeds to reduce it to a base level. This completes the cycle. A new cycle starts when a new endogenetic diastrophism occurs.

DAVIS recognizes three distinct stages in the geomorphological cycle which may be termed *youth*, *maturity*, and *old age*. In a humid climate, these are as follows:

In *youth*, one has some trunk streams but not many large tributaries. The valleys are strongly V-shaped, their depth depends on their height above sea level. Lithologic variations cause waterfalls and rapids for which there has not been sufficient time to disappear.

In *maturity*, the drainage system becomes more integrated. Any waterfalls and rapids evident in youth have disappeared and most of the rivers are in a dynamic equilibrium condition. The extent of the relief represents the maximum that is possible. In a fully matured river, one discerns (see e.g. HOLMES[1]) a sequence of three tracts. At its head is the *mountain* (or: torrent) *tract* which is either a gorge or V-shaped with slope angles from 30 to 90 degrees. In the middle of its course is the *valley tract*: the gorge has opened up, the slopes are gentler and the valley is wider. This opens up into a *plain tract*, at the bottom of the valley there is now a "flood plain" which, as its name implies, gets flooded whenever there is a high discharge of water. A cross-section of a flood plain shows fine, essentially horizontally stratified deposits. Often the rivers in flood plains are braided, representing bifurcating flow with islands in between or they meander (form loops, cf. Sec. 1.44).

In *old age*, valleys become very broad, most of the relief has disappeared due to continental planation. The level of the drainage basin approaches the base level of erosion. The final stage of the cycle is reached when *all* relief has been reduced to the base level, leading to a gently undulating plain which DAVIS called a "peneplain".

The above interpretation of the development of a drainage basin in terms of a geomorphological cycle has been widely accepted. An illustration of the cycle, after HOLMES[1], is shown in Fig. 8. Objections against the cycle theory and different interpretations of the development of drainage basis will be presented in Sec. 1.54.

1.52. Climatic Effects. In the development of a drainage basin, climate obviously plays a major rôle. The most commonly encountered climate in inhabited land areas is a humid one which consequently has been called "normal". In its effect on a drainage basin, it leads to a *normal* geomorphological cycle. The latter corresponds to the conditions as they have been described in the last section (1.51). However, in addition to the normal cycle, DAVIS considered an *arid* and a *glacial* cycle. In these

1. HOLMES, A.: Principles of Physical Geology. London: T. Nelson & Sons 1944.

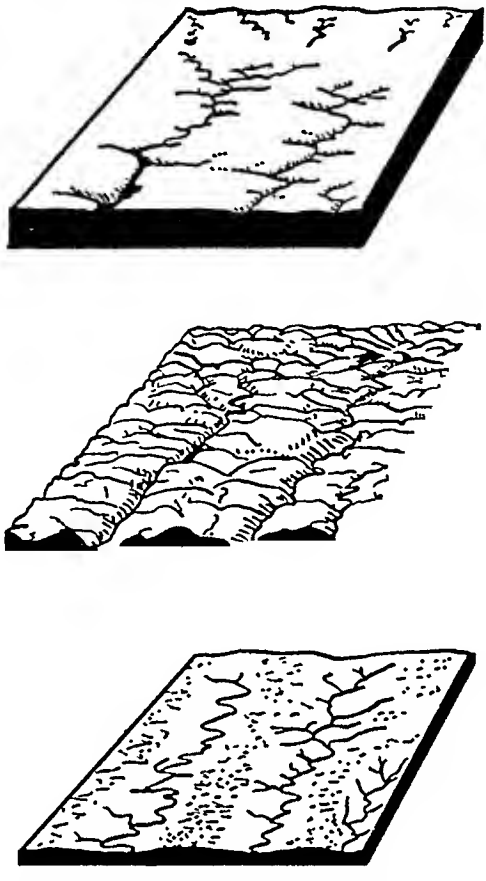

Fig. 8. Young (top), mature (center) and old (bottom) drainage basins. After HOLMES[1]

types of cycles, similar agents are active as in a normal cycle but their relative importance is different. In order to demonstrate this, let us investigate the arid and the glacial cycles in some detail.

A. Arid Cycle. First, we shall turn our attention to the *arid* cycle. The arid climate is characterized by very infrequent, but when they occur, terrific rainfalls. DAVIS assumed that the arid cycle starts with an uplifted mass of land that contains irregularities in the form of hollows. The rivers in arid areas are intermittent (wadis) as they carry water only very infrequently. Hence they will be oriented radially toward these hollows where they get lost in the ground. This is the *youthful stage* of the arid cycle. Deposition takes place in the hollows which are therefore being built up to a higher level. At the same time, the originally higher parts become severely cut with many gorges. This leads to the *mature stage* which is reached as soon as several original hollows become connected with the deepest depression, the latter forming a central focus. Finally,

1. HOLMES, A.: Principles of Physical Geology. London: T. Nelson & Sons 1944.

in *old age*, the central depression becomes shallower and wider to form a playa. The gorges and the débris become worn down; instead of rivers, sheet floods take over the agency of mass transport and, with the wearing down of the differences in elevation, wind erosion takes on significance by producing shifting dunes.

B. Glacial Cycle. Corresponding to the arid cycle, DAVIS also mentioned a *glacial* geomorphic cycle. A true glacial cycle would occur if in a certain locality the glacial climate would reach to the very surface of the sea, so that after an endogenetic uplift, all the landforms would be caused solely by glacial erosion. DAVIS notes that it may be possible through induction to infer what the typical forms of youth, maturity, and old age in such a glacial landscape would look like, but that it would hardly ever be possible to find actual examples thereof in nature.

The general procedure is therefore one of investigating glacial effects that have occurred at one stage or another during the course of an otherwise "normal" (i.e. humid) geomorphic cycle. This seems to correspond to actual natural conditions where it has been noted that at one time or another the climate may have changed for a relatively brief period from a normal humid one to a glacial one. This is particularly evident in the effects that have been left in many parts of the world by the Pleistocene ice ages. However, the details of the morphological forms that have thus been created will be discussed in a different section of this book.

1.53. Quantitative Description of Drainage Basins. In order to proceed with a rational explanation of the development of a drainage basin, it is necessary to describe its features in numerical terms. Thus, one can define a series of parameters which are characteristic of a drainage system:

(i) The *order* of a river segment. In order to define this fundamental term, one first has to introduce a series of concepts. The *stream net* is the interrelated drainage pattern formed by a set of streams in a certain area (omitting the possible downstream splitting of channels). A *junction* is the point where two channels meet. The *source* of a river is the beginning of the blue line on a map (in nature there may be some ambiguity in defining this term), a *link* is any unbroken stretch of river between two junctions (interior link) or between a source and the first junction (exterior link).

We then define the STRAHLER[1] order of a link as follows: We assign the order l to all the exterior links in the net. When two first order links meet, they form a second order link; when two second order links meet, they form a third order link etc. However, when a N-th order link meets a link of order $P<N$, the resulting link will have order N, i.e. the lower-order link gets "swallowed up". The formation of Strahler orders of

1. STRAHLER, A. N.: Trans. Amer. Geophys. Un 38, 913 (1957)

links can be written as an algebraic operation. Let us denote the meeting of links of orders N, P by an asterisk; then we have

$$N * P = N + 1 \quad \text{if} \quad N = P, \tag{1.53-1}$$

$$N * P = \sup(N, P) \quad \text{if} \quad N \neq P. \tag{1.53-2}$$

A stretch of river over which the Strahler order does not change is called a Strahler segment. The Strahler ordering of a hypothetical stream system is shown in Fig. 9B.

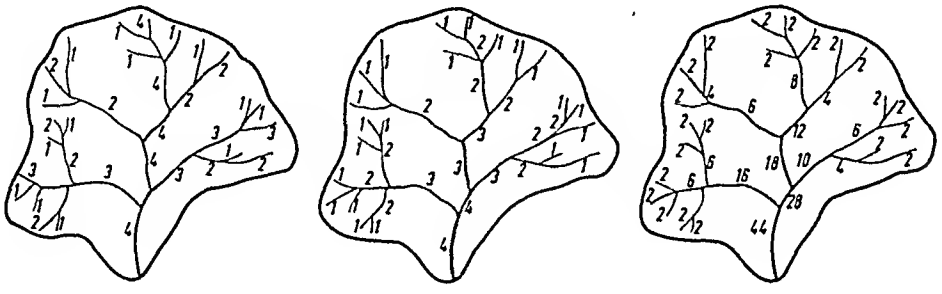

Fig. 9. Stream-ordering systems of HORTON (A), STRAHLER (B) and SCHEIDEGGER (C) as applied to a hypothetical stream net. In C the italic numbers are the associate integers. After SCHEIDEGGER

A slight modification of the above scheme was the (earlier!) notion of Horton[1] order. In this scheme it is considered that the "main stream" in a river net should be denoted by the same order number all the way from its moth to its headwaters. Thus, at every junction where the order changes, one of the lower order streams (usually either the longest or the most direct upstream continuation of the main stream) is renumbered to the higher order. The resulting stream ordering system is exemplified in Fig. 9A.

The stream ordering systems above have the disadvantage that the distributive law does not hold: If, say, two third-order segments combine to form a fourth-order segment before joining another fourth-order segment, the result of the last junction is a fifth-order link. On the other hand, if the two third-order segments are simply individual tributaries to a fourth-order segment, the result is a fourth-order link. However, it could be argued that the hydraulic properties of a link should only depend on the number of lower-order tributaries, not on the sequence in which they join. Thus, a *consistent* ordering system of stream nets has been postulated by SCHEIDEGGER[2] in which the distributive law holds. In order to deduce this, we proceed as follows.

1. HORTON, R. E.: Bull. Geol. Soc. Amer. **56**, 275 (1945).
2. SCHEIDEGGER, A. E.: U.S. Geol. Survey Profess. Papers **525-B**, B 187 (1965).

The basic property of stream-order numbers is that if two orders N be combined (operation denoted by an asterisk as above), the resulting stream is of order $N+1$. Hence

$$N*N=N+1. \tag{1.53-3}$$

In order that the distributive law be valid, it is postulated

$$[N*(N-1)]*(N-1)=N*[(N-1)*(N-1)] \tag{1.53-4}$$

and so that the commutative law be satisfied, it is required

$$N*P=P*N. \tag{1.53-5}$$

The above postulates completely define an algebra of consistent stream order numbers. Any integral N can be expressed in terms of smaller orders:

$$\begin{aligned} N&=(N-1)*(N-1)=(N-2)*(N-2)*(N-2)*(N-2)\\ &=P*P*P*\cdots*P \end{aligned} \tag{1.53-6}$$

where the number of "factors" P is equal to 2^{N-P}. Thus we may write

$$N=P^{*2^{N-P}} \tag{1.53-7}$$

where the asterisk in the "exponent" indicates that the "multiplications" refer to junctions. Continuing the algebraic analysis to the hypothetical zero-order streams (which do not exist in nature), we have

$$N=O^{*2^N} \tag{1.53-8}$$

and

$$N*P=O^{*2^N}*O^{*2^P}=O^{*(2^N+2^P)}. \tag{1.53-9}$$

Hence, setting

$$X=N*P \tag{1.53-10}$$

we have from a combination of the three previous relations

$$2^X=2^N+2^P=I \tag{1.53-11}$$

or

$$P*N=X=\frac{\log(2^N+2^P)}{\log 2}=\log_2(2^N+2^P)=\log_2 I. \tag{1.53-12}$$

The quantity I has been called "associated integer" of the link in question; it is evidently simply double the number M of sources which feed into that link. This number M has been called "magnitude"[1] of that link. The consistent stream ordering system is demonstrated in Fig. 9C.

1. Shreve, R. L.: J. Geol. 75, 178 (1967).

(ii) The *stream length.* The problem of defining the length of a stream (or a link, a segment etc.) has been touched upon on several occasions. As noted in Sec. 1.3, it is necessary to approximate the natural stream course by a smooth curve which is differentiable and rectifiable. Then no further problems in stating stream lengths are encountered.

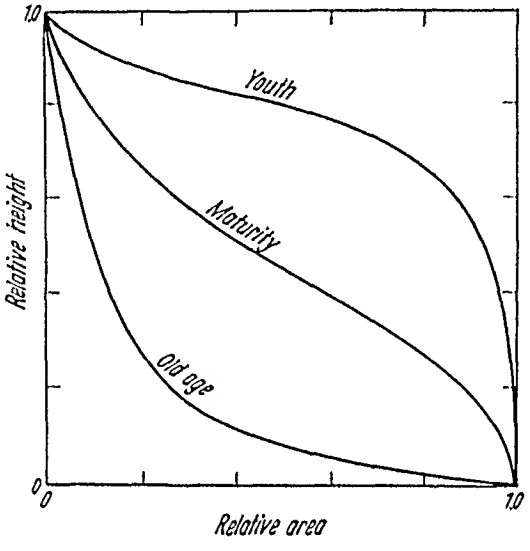

Fig. 10. Characteristic integrals of the hypsometric curve of drainage basins (after STRAHLER[1])

(iii) The *drainage density.* This is defined as the sum of the channel lengths divided by the drainage area. This yields an important measure of the drainage pattern. It ranges from as low as 2.3 miles per square mile ($\sim 1.5\ \mathrm{km}^{-1}$) in massive sandstone to values of 500 to 1,000 miles per square mile (~ 300 to $600\ \mathrm{km}^{-1}$) or more for badlands.

(iv) The *hypsometric curve.* The hypsometric curve is defined in exactly the same manner for drainage basins as this is done for the Earth as a whole[2]. However, it is usually customary to divide the heights and areas by the total height (measured from the lowest to highest point in the basin) and total area, respectively, so that one is dealing with "relative" quantities. The hypsometric curve is not Gaussian, so that there is a significant skewness and kurtosis which can be used to characterize an area. It is often convenient to plot the integral of the hypsometric curve. These integrals for young, mature, and old-age drainage patterns have characteristic shapes which are shown in Fig. 10.

(v) The *channel frequency.* If one counts all the stream segments up to a given order which are present in a drainage basin, and divides this

1. STRAHLER, A. N.: Trans. Amer. Geophys. Union 38, 913 (1957).
2. Cf. SCHEIDEGGER, A. E.: Principles of Geodynamics. 2nd ed. Berlin-Göttingen-Heidelberg: Springer 1963.

by the area drained by the streams up to that order, the quotient is called "channel frequency".

It turns out that the channel frequency F is not independent of the drainage density D. MELTON[1], for mature drainage basins, established the following dimensionally homogeneous relation (any consistent units):

$$F = 0.694\, D^2. \tag{1.53-13}$$

The principle of measuring the various quantities introduced above has been applied to a variety of drainage basins by MELTON[1–3], CHORLEY[4], COATES[5] and others[6–15]. In the course of these studies, various statistical relationships between the quantities introduced above, valid for certain conditions, have been deduced.

In addition to the various parameters introduced above for a quantitative characterization of river nets, this is the place to mention attempts that have been made at setting up systems of stream coding. A comparison of such systems has been made, e.g., by RANALLI and SCHEIDEGGER[16]. Accordingly, such coding systems have as their aim the assignment of code numbers (and/or letters) to stream segments and junctions in such a fashion that each segment in the net is given a unique label.

One such method of labeling stream segments is due to MILTON and OLLIER[17]: In a given net or subnet, the main river is labeled by assigning

1. MELTON, M. A.: J. Geol. 66, 35 (1958).

2. MELTON, M. A : List of sample parameters of quantitative properties of landforms: T. R. No. 16, Proj. ONR-NR-389-042, Columbia Univ. New York 1958.

3. MELTON, M. A.: Bull. Geol. Soc. Amer. 71, 133 (1960).

4. CHORLEY, R. J.: J. Geol 65, 628 (1957)

5 COATES, D. R.: Quantitative geomorphology of small drainage basins of southern Indiana. T. R. No. 10, Proj. ONR-NR-389-042, Columbia University, New York 1958.

6. PELTIER, L. C.: Paper No. I, 3, Sympos. Quant. Terr. Stud., Chicago (Amer. Assoc. Adv. Sci.), 1959.

7. SNELL, J. B : Paper No. II, 1, Sympos. Quant. Terr. Stud., Chicago (Amer. Assoc. Adv. Sci.) 1959.

8. TANNER, W. F.: Amer. J. Sci. 257, 458 (1959).

9. TANNER, W. F.: Bull. Geol. Soc. Amer. 70, 1813 (1959).

10. TANNER, W. F.: Paper No. I, 5, Sympos. Quant. Terr. Stud., Chicago (Amer. Assoc. Adv. Sci) 1959.

11. TANNER, W. F.: Science 131, No. 3412, 1525 (1960).

12. THOMPSON, W. F.: Paper No. I, 2, Sympos. Quant. Terr. Stud., Chicago (Amer. Assoc. Adv. Sci.) 1959.

13. WOOD, W. F.: Paper No. I, 1, Sympos. Quant. Terr. Stud., Chicago (Amer. Assoc. Adv. Sci) 1959.

14. YUNG, A.. Paper No. I, 7, Sympos. Quant. Terr. Stud., Chicago (Amer. Assoc. Adv. Sci) 1959.

15. STRAHLER, A. N.: Trans. Amer. Geophys. Union 38, 913 (1957).

16. RANALLI, G., and A E. SCHEIDEGGER: Bull. Intern. Assoc. Sci. Hydrol. 13, No. 2, 142 (1968).

17. MILTON, L. E., and C. D. OLLIER: J. Hydrol 3, 66 (1965)

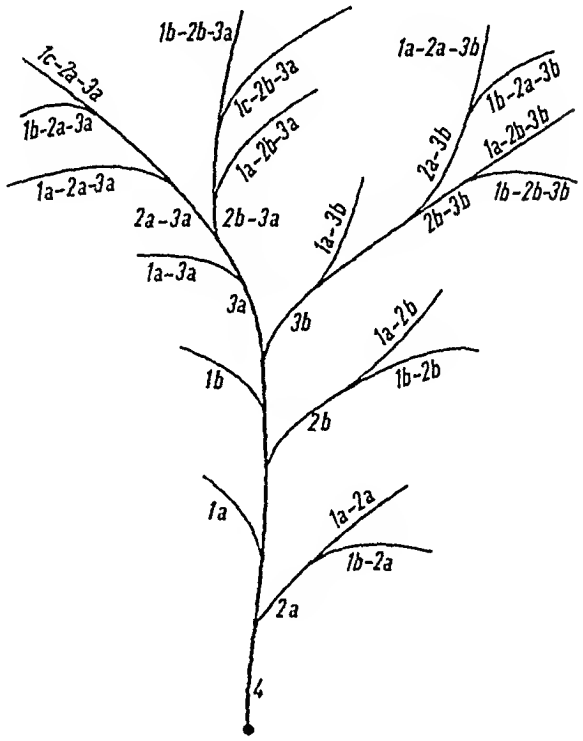

Fig. 11. Milton-Ollier Stream Coding System

to it its Strahler order; the in-flowing tributaries are given a label consisting of both order and a letter (*a*, *b*, *c* etc.) which takes into account the order of junctions (looking upstream). Then, the labeling is repeated in the same fashion in the lower order subnets. In this fashion, each stream segment in a given channel network has a unique code label. An example is shown in Fig. 11.

Another procedure for labeling basins, rivers, and junctions has been devised by the Division of Water Supply and Pollution Control of the U.S. Public Health Service (STORET system).[1] In the STORET system location code, streams are labeled using the concept of "stream level": This is an inverse, so to speak, of stream order. The main river (flowing into an ocean, sea or lake) is assigned the level 1, all tributaries thereto level 2, all tributaries to level 2 rivers are assigned level 3 etc. Once the levels have been assigned, tributaries of the same level along a given river (and thereby their junctions with this river) are assigned increasing stream index numbers going upstream (an even number or even ten for tributaries entering on the left, an odd number or odd ten for tributaries entering from the right looking upstream). Finally, for a particular location, the mileage to the nearest junction downstream is given.

1. GREEN, R. S., D. P. DUBOIS, and C. W. TUTWILER: J. San. Eng. Div. Amer. Soc. Civ. Eng. **92(SA)**, Proc. Pap. 4652, p. 55 (1966).

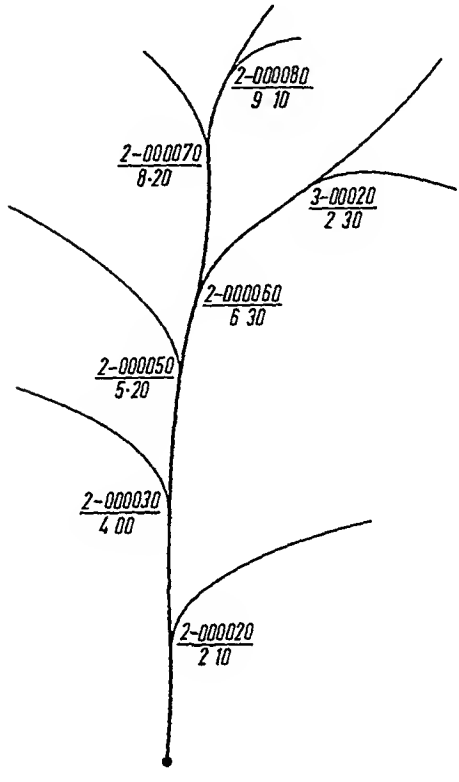

Fig. 12. STORET Location Code

Fig. 12 gives an example of STORET location coding: The code is given as a fraction whose numerator gives the stream level (first digit) and the stream index numbers as defined above (remaining digits), and whose denominator gives the mileage to the nearest junction downstream.

1.54. Possible Interpretations of Landscape Development. As already stated in Sec. 1.24, the interpretation of the development of landscapes in terms of a cycle is not the only one that is possible. Criticisms of the cycle theory have appeared immediately after its invention (see e.g. TARR[1] and SHALER[2]); however, they have become more numerous only recently. An outstanding critic of the cycle theory has been PENCK[3] who viewed the development of a whole drainage basin as the result of the development of each individual slope it contains (cf. Sec. 1.24). It is to the credit of PENCK to have emphasized that slope *recession* might be an ubiquitous phenomenon which could be basic to the understanding of

1. TARR, R. S.: Amer. Geologist **21**, 341 (1898).
2. SHALER, N. S.: Bull Geol. Soc. Amer. **10**, 263 (1899).
3. PENCK, W.: Die morphologische Analyse. Stuttgart: Verl. von Engelhorn's Nachf. 1924.

landscapes. The slopes, according to PENCK, recede individually owing to the various agents considered in Sec. 1.23.

Another form of criticism of the cycle theory has been advanced by the adherents of the "equilibrium theory"[1] who regard the present appearance of a landscape as the outcome of a dynamic equilibrium of the forces in action. Accordingly, a landscape preserves its character if the forces stay the same; some slopes will waste away whilst others are being created.

All the above interpretations of landscape development assume a more or less equal activity of the various slope forming agents with regard to the individual slopes. The whole principle of equal activity has recently been challenged by CRICKMAY[2, 3] who maintains that the activity of the exogenetic agents is unequal. According to CRICKMAY, a slope bank can recede only if there is a river (or surf) cutting away laterally at its bottom. The lateral action of rivers is connected with their tendency to meander. Slope wastage without lateral action of a river (or surf) simply produces a slow decline in slope angle without a recession at the foot. Thus, according to CRICKMAY, there is again no distinct meaning to a geomorphic cycle. Endogenetic movements may lift parts of the Earth's crust at a slow or rapid rate while denudation is also taking place. This is the *anagenetic* stage of the development. Once the endogenetic movements cease, denudation will continue and one has the *catagenetic* stage of landscape development. Since denudation (according to CRICKMAY) is mostly achieved by rivers cutting away at the bottom of slopes while they meander in the valleys, some parts of a landscape may never be touched by slope recession (*stagnation* of development) and their "youthful" (in the Davisian sense) forms may locally subsist to a very late stage. Therefore one can no longer speak of the stages of youth, maturity and old age. The ultimate result, however, is again a gently undulating plain caused by meandering rivers.

Summarizing, one may say that field geomorphologists have advanced four distinct theories regarding the development of landscapes. The first is DAVIS' *cycle* theory in which valleys develop through deepening (and wasting of the sides) from youth to old age, the second is PENCK's differential theory in which each slope *recedes* according to its own pattern, the third is the *equilibrium* theory, and the fourth is CRICKMAY'S *principle of unequal activity* according to which each valley develops in correspondence with the intensity of lateral river action.

1. Cf. e.g. HACK, J. T.: Amer. J. Sci. 258A, 80 (1960).

2. CRICKMAY, C. H.: A Preliminary Inquiry into the Formulation of the Geological Principle of Uniformity. Calgary: Evelyn de Mille Books 1959.

3. CRICKMAY, C. H.: J. Geol. 68, 377 (1960).

The cycle theory of DAVIS is to-date probably still the most widely accepted one, but we shall try to investigate the dynamics of all four possibilities.

1.6. Subaquatic Effects

1.61. General Remarks. Most of the surface of the Earth is covered by water. It stands to reason, therefore, that a knowledge of the processes that are active below the water line is extremely important for an understanding of the evolution of the morphology of our globe.

Knowledge of the morphology of water-covered areas has been accumulated only very recently. Whereas the physiography of the land areas has been the object of the study of geologists for hundreds of years, the investigation of the water-covered areas had to await the advent of refined measuring techniques, such as echo-sounding, deep sea coring, underwater photography and others.

During the course of modern investigations it turned out that the deep sea is not just a bottomless abyss as was originally thought, but that there is a rather varied topography. Many of the observed features are due to endogenetic processes and will not be discussed here, but others are properly dealt with in a study of geomorphology.

Apart from the development of truly submarine phenomena, the dynamics of the sea has also had a pronounced effect upon some land areas as seen in the evolution of coasts and river mouths.

We shall give below a review of some of the pertinent facts borne out by the study of the morphology of subaquatic features. This refers to coasts (Sec. 1.62), to river mouths (Sec. 1.63) and to truly submarine features (Sec. 1.64). Finally, we shall discuss some morphological aspects of turbidity currents which have been advocated as a powerful agent in shaping submarine features (Sec. 1.65).

The facts thus compiled will form the basis for our further theoretical studies.

1.62. Coastal Geomorphology. We first turn to a discussion of the physical geomorphology of *coasts*. In the present section (1.62) we shall confine ourselves to those parts of a coastline which are not obviously influenced by a river. The morphology of river mouths will be discussed separately in Sec. 1.63.

First, we have to clarify the term *coast* somewhat, since the line between the water and the land (owing to tides, storms etc.) is not entirely definite. Thus, the *coast proper* is that part near the water's edge which *never* gets wet. The part which is affected by the action of the water (generally this may be above or below the water line) is properly called

shore. A normal shore profile, after ALEXANDER[1], in which the various features involved are explained, is shown in Fig. 13. The dynamic interaction between the water and the land takes place on the shore.

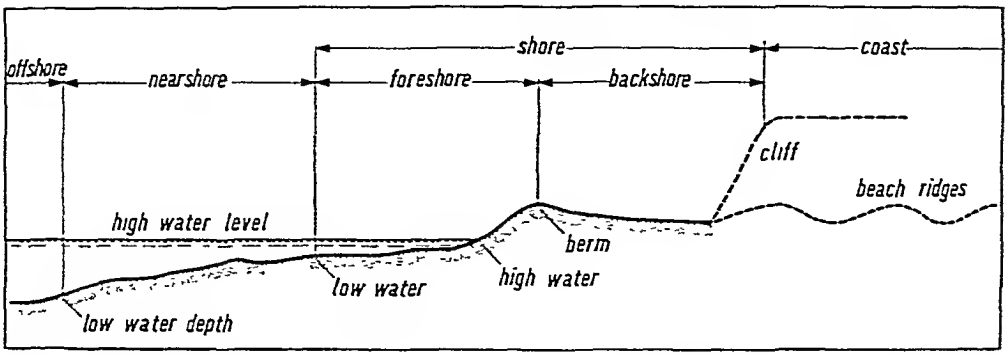

Fig. 13. Schematic diagram showing features usually associated with a normal shore profile. After ALEXANDER[1]

There are then several methods of classifying coasts:

a) Genetically, one distinguishes between coasts of emergence and coasts of submergence[2]. The meaning of these terms is self-evident. The phenomena of emergence and submergence of land are primarily due to endogenetic causes, but fluctuations of sea level may also be involved. More sophisticated schemes of genetic classification introduce also such terms as "advancing" and "retreating" coasts[3,4].

b) Tectonically, one distinguishes coasts of the *Atlantic* type, where the axes of the tectonic system near the coast intersect the latter at more or less right angles, from coasts of the *Pacific* type, where the tectonic axes are more or less parallel to the shore line[5].

c) Morphologically, a classification of shore lines can be made which is entirely independent of the genetic or tectonic interpretation of the surrounding area[6]. Thus, the shore profile may be either cliffed or non-cliffed, and in plan the coast may be regular or irregular.

Of primary interest for theoretical geomorphology is how the endogenetically determined features are modified by exogenetic agents. First of all, this concerns the detailed features of a coast: In many instances, a beach is formed which may consist of sand or shingle. It slopes gently towards the sea with somewhat of a step at the line where the waves

1. ALEXANDER, C. S.: Ann. Assoc. Amer. Geogr. 56, No. 1, 128 (1966).
2. JOHNSON, D. W.: Shore Processes and Shoreline Development. New York: Wiley 1919.
3. VALENTIN, H.: Peterm. Mitt. Erg.-H. 246 (118 p.) (1952).
4. BLOOM, A. L.: Z. Geomorph., N.F. 9, 422 (1865).
5. RICHTHOFEN, F. F. v.: Führer für Forschungsreisende. Hannover 1901.
6. ALEXANDER, C. S.: California Geogr. 3, 131 (1962).

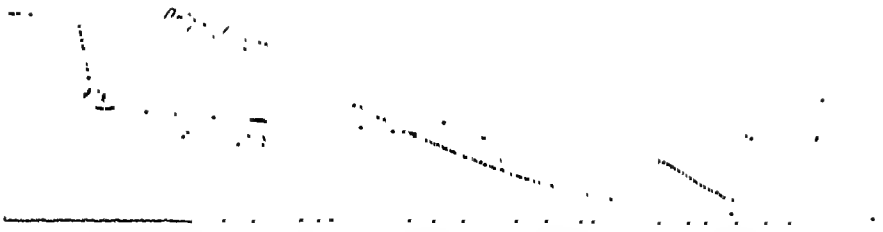

Fig 14. Cliff recession and formation of a shore platform. After HOLMES[1]

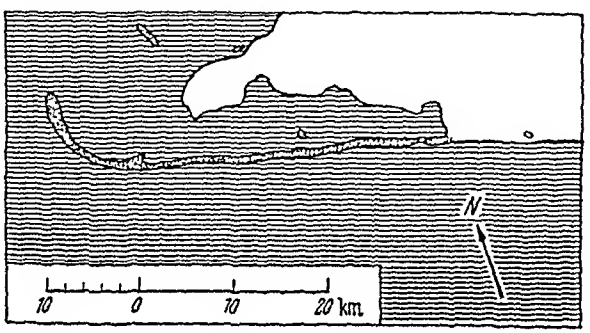

Fig. 15. Offshore hook (Kosa Tendra in the Black Sea). After ZENKOVICH[2]

commonly break. The sand in beaches appears to be graded, although no general empirical laws can be established regarding the grading. Beaches may change their shape due to a variety of factors, not all of which are understood as of yet. For the hydrodynamic conditions prevailing in any one area, there exists an *equilibrium state* for the beach which, if disturbed, will re-instate itself.

Beaches are commonly found on coasts where the land *gently dips* toward the sea. On steep coasts, beaches may or may not form. The principal action of the waves in this case is one of undercutting the coastal slope. If the material is hard rock, *cliffs* are formed which are gradually receding. Below the cliffs there may be a *beach* (as implied above) or a *shore platform* consisting of solid rock. The process of cliff development is schematically shown in Fig. 14. On coasts of emergence, a series of former shore platforms may often be observed high above the present water level.

On flat, sandy coasts, *spits* and *hooks* may be formed, presumably by the action of currents in the water. An example of a hook is shown in Fig. 15. Features related to spits and hooks are *barrier islands* (often called *offshore bars*). These are low islands which occur on many shallow

1. HOLMES, A.: Principles of Physical Geology. London: T. Nelson & Sons 1944
2. ZENKOVICH, V. P.: Trudy Inst. Okeanologii Akad. Nauk SSSR 21, 3 (1957).

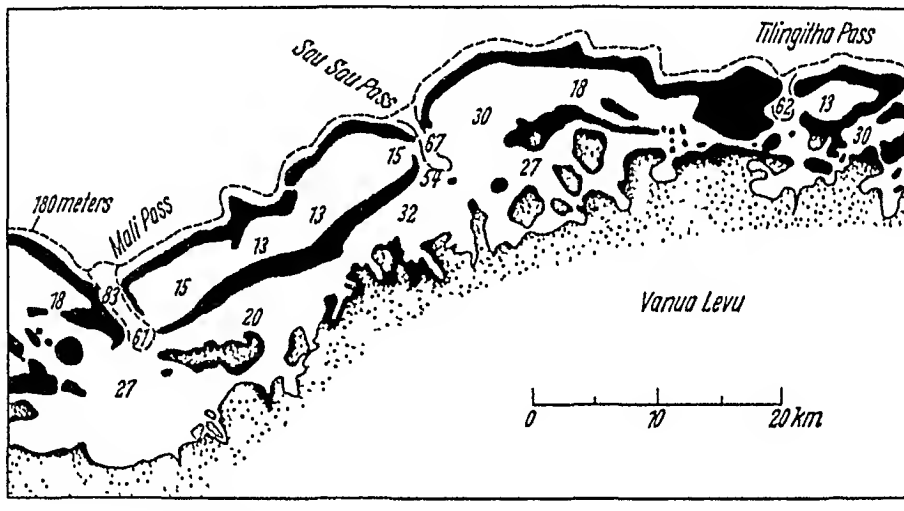

Fig. 16. Coral barrier reef off Fiji. After KUENEN [1]

coasts, such as on the Gulf of Mexico. An extensive bibliography of the physiography of barrier islands (offshore bars) has been published by SHEPARD[2]. Offshore bars are often linked with the emergence of a shore line.

Other actions of the sea are connected with the scooping out of bays[3] and indirectly, by providing the right environment for corals to grow, with the growth of barrier reefs near a coast line. A typical configuration of a coast with a reef is shown in Fig. 16.

More details about the above physiographic features of coasts may be found in general monographs on geomorphology (see Sec. 1.1) and also in treatises specifically concerned with coasts, particularly those authored by JOHNSON[4], by GUILCHER[5] by KING[6] and by ZENKOVICH[7].

1.63. Morphology of River Mouths. In the vicinity of the places where rivers empty into the sea, the coasts are disturbed in a peculiar fashion. In such places, the steady trend of the shoreline is generally disrupted by either an *estuary* or a *delta* which represent the two principal types of river mouths. In an estuary, the sea forms a funnel into the land, and on

1. KUENEN, P. H.: Marine Geology. New York: J. Wiley & Sons 1950.
2. SHEPARD, F. P.: in "Recent Sediments, Northwest Gulf of Mexico, 1951 to 1958", p. 197ff. Tulsa: Amer. Assoc. Petroleum Geolog. Spec. Pub. (1960).
3. Cf. e.g. IONIN, A. S.: Trudy Okeanogr. Kommiss. Akad. Nauk. SSSR **1**, 82 (1956).
4. JOHNSON, D. W.: Shore Processes and Shore Line Development. New York: J. Wiley 1919.
5. GUILCHER, A.: Coastal and Submarine Morphology (Transl. from French) London: Methuen & Co. 1958.
6. KING, C. A. M.: Beaches and Coasts. London: E. Arnold & Co. 1959.
7. ZENKOVICH, V. P.: Processes of Coastal Development. London: Oliver & Boyd 1967.

a delta the land protrudes into the sea. A physiographic study of river mouths has been made e.g. by SAMOILOV[1].

Geomorphologists discern various regions on a river mouth. For the two basic types of the latter (i.e. deltas and estuaries), the various regions are shown in Fig. 17. The general river mouth region comprises the area between the first widening or division of the river channel and the underwater step some distance away from the mouth, in the sea. Under certain circumstances, a river may give rise to a *land spit.*

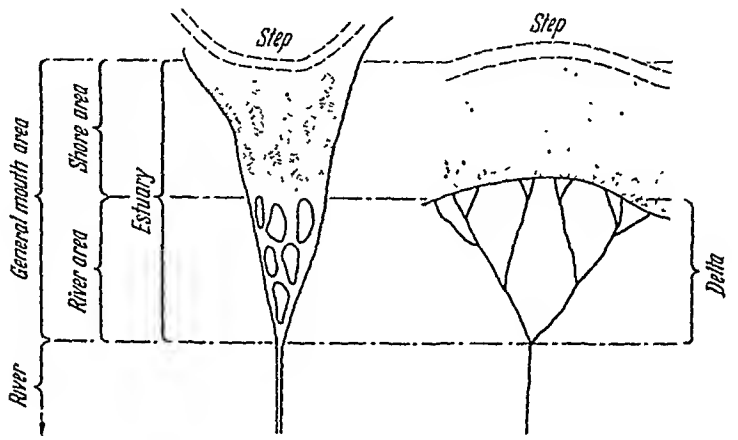

Fig. 17. Morphology of a river mouth. After SAMOILOV[1]

Whether a delta or an estuary is formed depends on the presence or absence of lateral currents in the sea: if the currents in the sea are weak, the river will dump its load near its mouth and thus form a delta. Otherwise, the sediments introduced may be removed from the area and an estuary is the result. It has been observed that two types of deltas are possible which have been called *arcuate deltas* (example: Nile Delta) and *birds foot deltas* (example: Mississippi Delta). The two types of deltas are illustrated in Fig. 18. The steeper the slopes of a delta are, or the smaller it is, the coarser are usually the materials of which it consists.

Attempts have been made to apply DAVIS' geomorphological cycle theory (cf. Sec. 1.51) to the development of deltas. The stages of youth, maturity, and old age for delta development (after BARRELL and CLARK[2]) are shown in Fig. 19. However, as with regard to the geomorphological cycle theory in general, corresponding objections have also been raised against the application of the cycle theory in the development of deltas.

1. SAMOILOV, I. V.: Устья рек. Moscow: Geografgiz 1954. German translation by F. TUTENBERG under the title: Die Flußmündungen. Gotha: Herm. Haack Verlag 1956.
2. BARRELL, J., and G. N. CLARK: Bull. Geol. Soc. Amer. 23, 377 (1912)

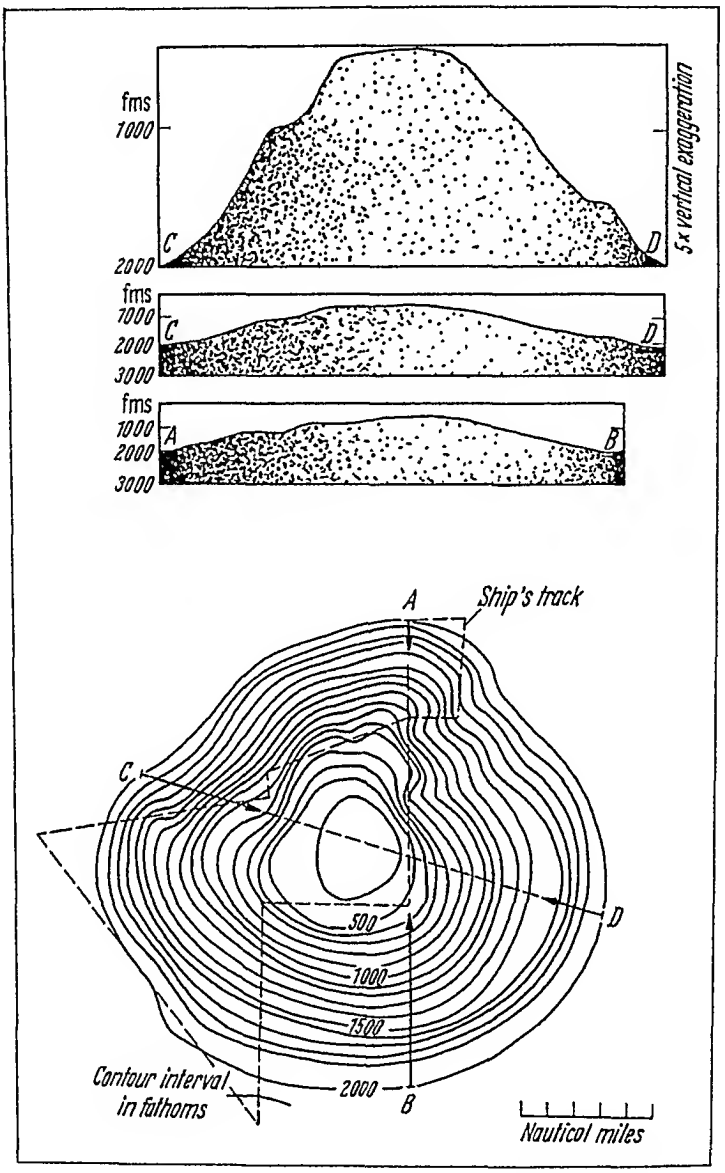

Fig. 20. Drawing of a typical guyot. After MENARD[1]

and that wave action levelled their tops. This points towards a relative subsidence of many features in the ocean. Coral atolls seem to point in the same direction, since on a subsiding sea mount, under favorable climatic conditions, coral growth can just keep up with the subsidence. In fact, from a hole drilled on Bikini where Miocene sediments were found at a depth of 300 m, KUENEN[2] (p. 467) estimated a rate of subsidence (before glacial times) of less than 0.5 cm/century. It would thus appear that sea mounts and atolls are of endogenetic origin. After their formation, they start sinking owing to the extra weight caused by their presence.

1. MENARD, H. W.: Bull. Geol. Soc. Amer. 66, 1149 (1955).
2. KUENEN, P. H.: Marine Geology. New York: J. Wiley & Sons 1950.

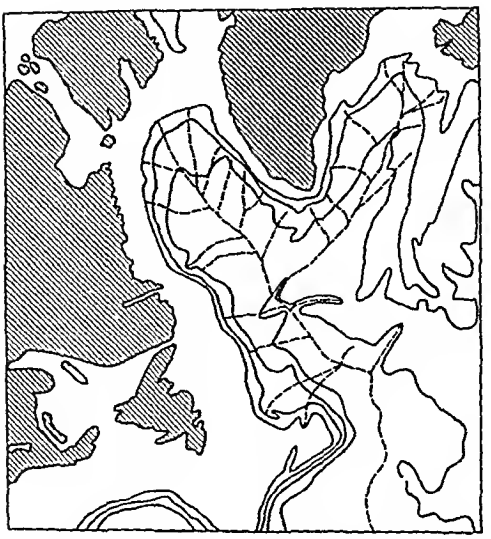

Fig. 21. Mid-Ocean Canyon. After ELMENDORF and HEEZEN[1]. Contour intervals in kilometers

A further prominent physiographic feature of the sea bottom is the existence of *submarine canyons*[2, 3]. These canyons are in appearance very similar to subaerial valleys[4] and may have deltas at their mouths[5]. Most of them are found on the continental shelf; many appear as continuations of rivers. The largest canyons stretch over an entire ocean such as the recently discovered Mid-Ocean Canyon in the Northwest Atlantic Ocean[1] (see Fig. 21).

In summary, it may be said that many features of submarine geomorphology have a great resemblance with subaerial features[6]. Since it is impossible to concede that the oceans at one time were empty of water for these features to develop by subaerial erosion, a different explanation has to be sought after.

1.65. Morphology of Turbidity Currents. We have noted above (Sec. 1.64) that in submarine topography there exist features that look just like erosional features on land. It has been postulated that such features have been carved out by a type of current which is called *turbidity current*. Such *turbidity currents* are assumed to be currents of dense fluid

1. ELMENDORF, C. H., and B. C. HEEZEN: Bell System Techn. J. **36**, 1047 (1957).

2. SHEPARD, F. P., and R. F. DILL: Submarine Canyons and Other Sea Valleys. Chicago: Rand McNally & Co. 1966.

3. LAUGHTON, A. S.: Deep Sea Res. **15**, 2 (1968).

4. See e g. DIETZ, R. S.: New Scientist **4**, 946 (1958).

5. BATES, C. C., and A. R. MOONEY: Trans. Internat. Oceanogr. Congr. Washington, p. 595 (1959).

6. HEEZEN, B. C.: Geophys. J. Roy. Astron. Soc. **2**, 142 (1959).

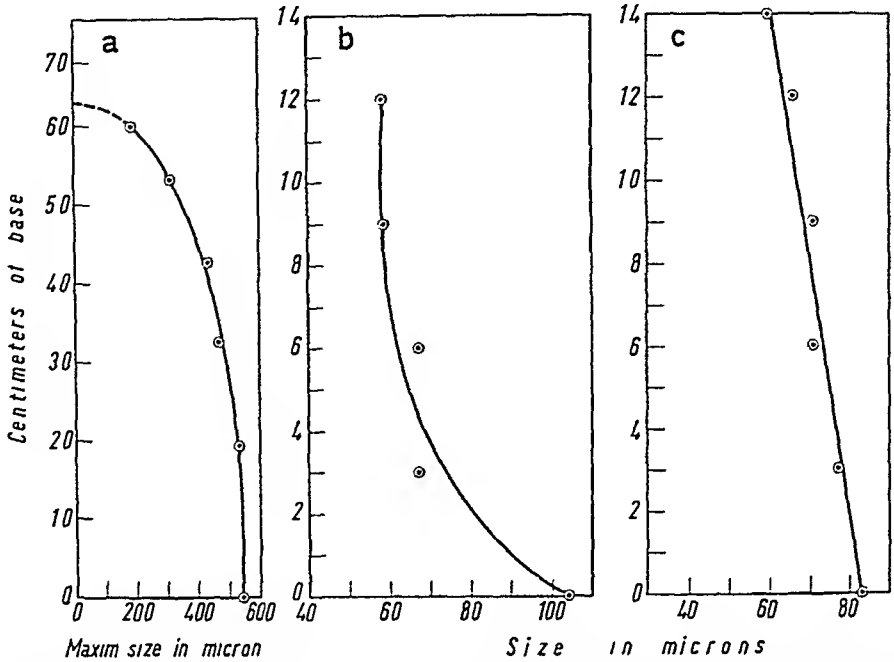

Fig. 22 a–c. Vertical grading curves in turbidites. *a* Martinsburg formation (Ordovician) at Hamburg, Berks Co., Pa., U.S.A.[1]. *b* Upper Broverian turbidite (DANGEARD[2] et al. sample R 2, Table 1). *c* same as *b*, but sample R 1

inside a less dense one. The density difference is commonly thought to be due to the content of suspended sediments.

There are, in fact, additional physiographic observations which point toward the existence of turbidity currents, quite apart from the reasons given above:

a) *Graded Deposits.* In general, the farther out one goes into a body of water, the smaller is the grain size of the deposits. There are many instances, however, where a graded sequence of particles is found seemingly out of its place: Large pebbles, graded with distance and height, are suddenly found where they do not seem to belong. An example of three vertical grading curves is shown in Fig. 22. It has been suggested that such deposits have been positioned by turbidity currents; the grading, then, would be the result of the slowing down of the current over the length of its course. An exhaustive bibliography of references to geological investigations of such deposits has been given by BALLY[3]. Much information is also contained in reviews edited by BOUMA and BROUWER[4], and by ANONYMOUS[5].

1. SCHEIDEGGER, A. E., and P. E. POTTER: Sedimentology 5, 289 (1965).
2. DANGEARD, L., et al.: Rev. Géograph. Phys. Géol. Dyn. Sér. 4, 251 (1961).
3. BALLY, A.: J. Alberta Soc. Petrol. Geol. 5, 89 (1957).
4. BOUMA, A. M., and A. BROUWER (ed.): Turbidites, Developments in Sedimentology, vol. 3. Amsterdam: Elsevier. 1964.
5. ANONYMOUS: Spec. Pub. Soc. Econom. Palaeont. Mineral. 12, 253 (1965).

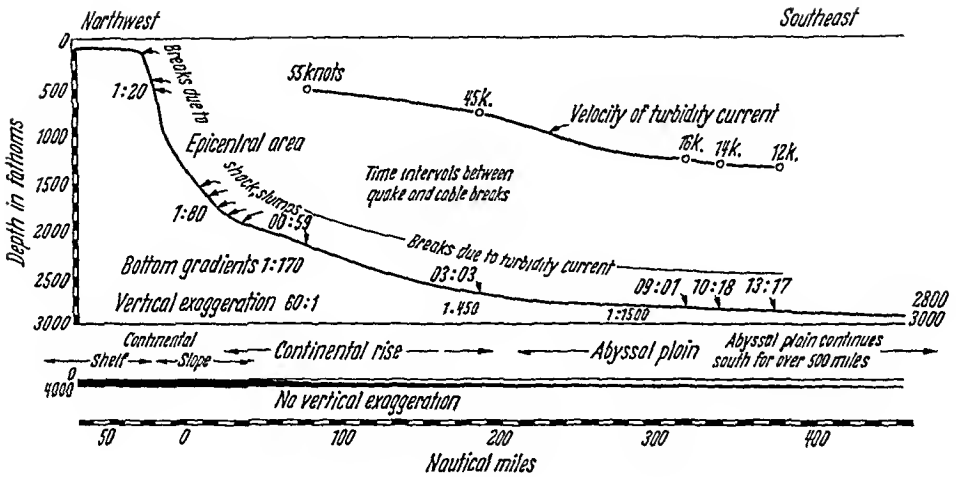

Fig. 23. Cable breaks and profile after the Grand Banks earthquake in 1929. After HEEZEN, ERICSON and EWING[1]

b) *Broken Telegraph Wires.* After the earthquake on November 18, 1929, on the continental shelf South of Newfoundland, many telegraph cables went dead. HEEZEN, ERICSON and EWING[1] made an analysis of the times at which these breakdowns occurred and correlated them with the position of the cables from the epicenter of the earthquake. The picture that was found is shown in Fig. 23. This picture is in good agreement with the hypothesis that the cables were broken by a turbidity current generated by the earthquake. The velocity of the current as it travelled down the continental slope and into the abyssal plain could be calculated. The result is also shown in Fig. 23.

c) *Direct Observation.* Turbidity currents have actually been observed in Lake Mead. Lake Mead is an artificial reservoir which has been created on the Colorado River (U.S.A.) by the erection of Hoover Dam. A convenient summary of the turbidity currents observed over the years has been given by GOULD[2]. Accordingly, whenever the density of the turbid river water entering the lake is greater than that of the lake water, the former follows a course along the bottom of the lake. Such turbid water has been observed to travel distances of up to 125 km. The average velocity of the largest underflows has been estimated as of the order of 25.2 cm/sec. The velocity of the underflows that do not reach so far is considerably less, of the order of 9 cm/sec. The underflows are generally only a few feet thick, a typical measured density distribution is shown in Fig. 24.

1. HEEZEN, B. C, D. B. ERICSON, and M. EWING· Deep Sea Res. 1, 193 (1954).
2. GOULD, H. R.: Soc. Econ. Paleon. Min. Spec Pub. 2, 34 (1951)

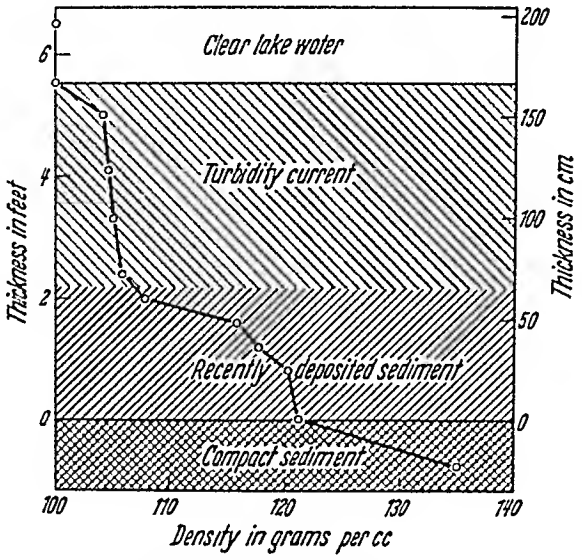

Fig. 24. Distribution of density (centigrams per cc) in a turbidity current in Lake Mead. After GOULD[1]

Apart from in Lake Mead, modern turbidity currents have also been observed directly in the ocean[2]. They occur, for instance, quite frequently off the mouths of great rivers, such as of the Congo and the Rio Magdalena. An extensive study of the Rio Magdalena turbidity currents has been reported by HEEZEN[3].

In view of the various observations just mentioned, there is little doubt that turbidity currents must be considered as possible geodynamic agents.

1.7. Niveal Features

1.71. General Remarks. Niveal features are due to the action of snow and ice. This action manifests itself in a variety of ways. Snow, if it accumulates, consolidates eventually into ice which may form giant streams proceeding downhill in a manner similar to that of rivers. The giant moving masses of ice are called *glaciers*. We shall describe (in Sec. 1.72) some features bearing out the morphology of glaciers as this is important for the understanding of the geomorphological action of ice.

The effect of glaciers upon the appearance of the Earth's surface occurs in two ways: by erosion and by deposition. The erosional activity of glaciers manifests itself in the scouring out of valleys and hollows in a special manner, the depositional activity in the dumping of moraines and similar features. Both types of glacier activity will be discussed in some detail (in Sec. 1.73 and 1.74, respectively).

1. GOULD, H. R.: Soc. Econ. Paleon. Min. Spec. Pub. **2**, 34 (1951).
2. HEEZEN, B. C.: Eclog. Geolog. Helv. **51**, 521 (1958).
3. HEEZEN, B. C.: Bol. Socied. Geograf. Columbia Nos. **51–52**, p. 135 (1956).

Table 3. *Summary of the earth's glacial epochs, their ages, and the affected areas.* (After EMILIANI and GEISS[1])

Glacial Epoch	Time (10^6 years)	Main glaciated areas
Pleistocene	0.6 to 0	North America; central and northern Europe; northern Siberia; Alps; Himalaya; Andes; Patagonia; New Zealand; Tasmania; Antarctica
Upper Paleozoic	250–200	South America; central and South Africa; Madagascar; India; southern Australia
Late Pre-Cambrian	550	Spitzbergen; Greenland, Scandinavia; southern Australia; Yang-tze, China (?)
Transvaal-Nama-Katanga	600	South-West Africa; Angola; Republic of the Congo; Rhodesia; Transvaal; Simla, India (?); Broken Hill, New South Wales (?)
Huronian	800	Cobalt, Ontario; Witwatersrand, Transvaal
Bothnian	1,000	Finland; Western Australia (?)
Damara	1,200 (?)	Chuos District, South-West Africa
(No name)	1,500 (?)	Medicine Bow Mountains, Wyoming

Finally, we shall discuss some peculiar features which also have been ascribed to the action of ice: niveal solifluction, the upheaval of pingos, and the formation of pressure ridges. These features are peculiar to specific areas of the world as they require the presence of permafrost in the ground. They will be described in Sec. 1.75. Finally we discuss the phenomenon of varves (Sec. 1.76).

Before starting with a description of the various geomorphological features caused by ice and snow, it may be well to note that the abundance of these substances upon the Earth's surface has been much greater during certain earlier periods during the Earth's evolution than it is at present. Such periods are called *ice ages*. Geologists have noted ice ages at various epochs; a suggested time table thereof (after EMILIANI and GEISS[1]) is shown in Table 3.

During an ice age, some of the water originally in oceans is locked up in continental ice sheets. Hence sea-level fluctuations may occur. COTTON[2] quotes sea-levels 139 m below the present sea level during the Pleistocene ice age.

Of the various ice ages, the most recent one, i.e. the Pleistocene ice age, has been studied best. It turns out that this last ice age consisted of a sequence of glacial and interglacial cycles of a duration of about

1. EMILIANI, C., and J. GEISS: Geol. Rdsch. 46, 576 (1957).
2. COTTON, C. A.: Trans. Roy. Soc. New Zealand, Geology 1, No. 16, 249 (1962).

40,000 years (EMILIANI[1]). Our present time may be considered as an interglacial stage of this most recent ice age; the end of the last glaciation has been estimated by EWING[2] as having occurred about 11,000 years ago.

The recognition of the occurrence of ice ages has a geomorphological significance inasmuch as effects of glacier action may be sought not only in presently glaciated regions, but also in areas that are now ice-free.

1.72. Morphology of Glaciers. Turning to the morphology of *glaciers*, we note that one generally (HOLMES[3]) discernes three classes of such features.

The *first* class contains *ice sheets* and *ice caps* covering large continental areas such as Greenland and Antarctica. The ice creeps slowly towards the margins of these features. Ice sheets may be up to 3 km thick. During the ice ages, such ice sheets existed in many now ice-free areas.

The *second* class contains *mountain or valley glaciers.* These have again been split into two groups[4] which represent glaciers of the first and of the second order, respectively. *Glaciers of the first order* represent the true valley glaciers which are veritable rivers of ice extending for many miles along a mountain valley. They move with speeds in the Alps of 30 – 150, in the Himalayas of 700 – 1,300 and in Greenland of 1,000 – 3,000 m per year[4]. On their surface, longitudinal, transverse and marginal crevasses may arise. The longitudinal crevasses are roughly parallel to the direction of flow, transverse crevasses cut across a valley glacier whenever a steepening of its course occurs, and marginal crevasses may point upstream from its rim. At the end of a valley glacier there is commonly a snout. *Glaciers of the second order* are those that hang from the side of a mountain, unable to reach the outflow of the drainage areas. These features include *cirque glaciers.*

Finally the *third* class of glaciers contains *piedmont* glaciers which are formed by coalescence when several valley glaciers reach into a plain at the foot of a mountain range.

The physiography of glaciers has been described in a number of books on general glaciology some of which are mentioned below[5–10].

1. EMILIANI, C.: J. Geol. **63**, 538 (1955).
2. cf. e.g. EWING, M.: J. Alberta Soc. Petrol. Geol. **8**, 191 (1960).
3. HOLMES, A.: Principles of Physical Geology. London: T. Nelson & Sons 1944.
4. NEUMAYR, M., and F. E. SÜESS: Erdgeschichte, 3d. ed. Stuttgart: Bibliogr. Inst. 1920.
5. FLAIG, W.: Das Gletscherbuch. Leipzig 1938.
6. HEIM, A.: Handbuch der Gletscherkunde. Stuttgart 1885.
7. HESS, H.: Die Gletscher. Braunschweig 1904.
8. KLEBELSBERG, R. v.: Handbuch der Gletscherkunde und Glazialgeologie. 2 Vols. Vienna (1948/49).
9. KOECHLIN, R.: Les glaciers et leur mécanisme. Lausanne 1944.
10. FRISTRUP, B.: The Greenland Ice Cap. Copenhagen: Rhodos Internat. Pub. 1966.

1.73. Effects of Glacier Scouring. Glaciers move and thereby scour out their bed. There are several large-scale effects due to this scouring that have been noted by geomorphologists.

The first such effect is the development of a *step-shaped longitudinal profile* of a glaciated valley. The situation is described in most textbooks of geomorphology (see e.g. MACHATSCHEK[1]) and has been analyzed in great detail by GERBER[2]. It is illustrated in Fig. 25. It appears that at

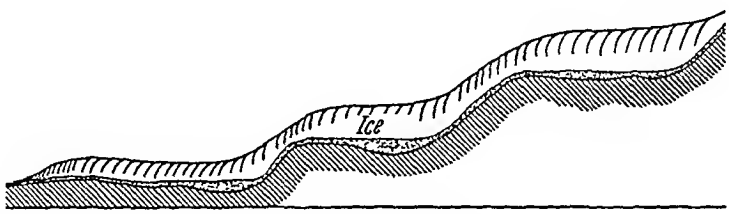

Fig. 25. Step-shaped longitudinal profile of a glaciated valley. After MACHATSCHEK[1]

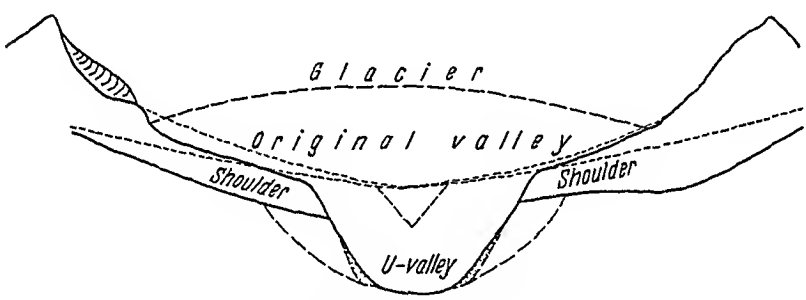

Fig. 26. Cross-section through a glaciated valley. After MACHATSCHEK[1]

least some of the steps were present before the existence of a glacier and that the glacier accentuated the structure. However, it should be noted that BAKKER[3] disclaims the action of glaciers in such cases, likening step-shaped valleys to pluvial preglacial conditions.

The second effect due to the scouring of a glacier is the characteristic *transverse profile* of a valley that was carved out by the glaciers of the ice ages. Such valleys are generally U-shaped with broad shoulders (see Fig. 26). Geomorphologists have been unable to reconstruct the glacial processes that led to the profile described above. The most satisfactory physiographic interpretation of the observed facts is probably that of DISTEL[4] according to whom the profile was created in two stages. The first stage, purely due to water erosion, was responsible for the broad valley (at this stage the "shoulders" are assumed as connected together);

1. MACHATSCHEK, F.: Geomorphologie 5th ed. Leipzig: Teubner 1952.
2. GERBER, E : Geograph Helvet. 11, 160 (1956).
3. BAKKER, J. P.: Z. Geomorphol. 9, 18 (1965).
4. DISTEL, L.: Mitt Geogr. Ges. München 7, 1 (1912).

for some reason, probably due to an orogenetic uplift, a somewhat deeper valley was incised into the broad valley, which was eventually transformed by a glacier into the characteristic U-form. An alternative attempt at a physiographic explanation of the valley profiles has been suggested by HESS[1, 2] who claimed that the latter are the result of the various repeated glaciations that have taken place in Europe. Thus, the problem of the origin of the profile of a once glaciated valley is still unsolved.

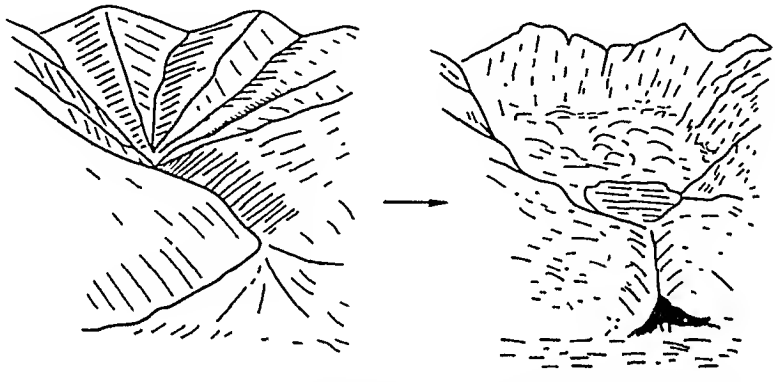

Fig. 27. Transformation of a drainage basin into a glacial cirque. After MACHATSCHEK[3]

A further effect due to the scouring of glaciers is the transformation of an erosional basin into a *glacial cirque* (see Fig. 27). This type of transformation occurred many times in the Alps during the ice ages and has been well documented. This transformation, however, may be partly stress-included[4].

Finally, features which also may be due to glacier action are those described as ice-thrust features by CHARLESWORTH[5], FLINT[6] and MACKAY[7]. These represent tilted, folded and contorted sediments with truncated beds, thrust faults, closely spaced shear planes, clastic dykes, arcuate to irregular ridges and linear streams. They indicate that a glacier is able to produce thrust forces when it is moving over an area.

1.74. Drumlins, Eskers, Moraines. After having discussed the scouring effects of glaciers, we turn our attention to some other features whose existence is commonly ascribed to glacial action. These include drumlins, eskers and moraines.

1. HESS, H.: Pet. Geogr. Mitt. 49, 73 (1903).
2. HESS, H.: Z. Gletscherkunde 2, 321 (1907/08).
3. MACHATSCHEK, F.: Geomorphologie. 5th ed. Leipzig: Teubner 1952.
4. GERBER, E. K., and A. E. SCHEIDEGGER: Ecl. Geol. Helv. 62, No. 2 (1969).
5. CHARLESWORTH, J. K.: The Quaternary Era, 2 vols. London: E. Arnold & Co. 1957.
6. FLINT, R. F.: Glacial and Pleistocene Geology. New York: J. Wiley & Sons 1957.
7. MACKAY, J. R.: Geograph. Bull. 13, 5 (1959).

Let us begin with *drumlins*. These are features which have been described by a variety of authors such as ALDEN[1], ARONOW[2], CHORLEY[3] and ZOLLINGER[4]. ALDEN[1] stated that one may regard as a typical drumlin a hill of glacial drift which approximates the form of an elongated ovoid. The highest point coincides with the center of the greatest breadth. Thus, a typical (lengthwise) cross section is that of a drumlin near Gossau in Switzerland shown in Fig. 28[4]. As noted above, drumlins are somehow connected with former glaciers: They occur in areas that have been glaciated; their long axes are parallel to the flow direction of the glacier and their steep sides face upstream.

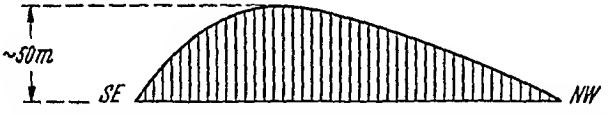

Fig 28. Longitudinal profile of a drumlin. After ZOLLINGER[4]

The next phenomena to be discussed are *eskers*. Eskers are gravel walls of more or less straight strike, parallel or orthogonal to the edge of a former glacier. Eskers are long features that may stretch over some 20 km. In cross-section, they appear irregularly layered.

Finally, we mention *moraines* which are heaps of débris that are left by glaciers after their retreat. Most conspicuous are terminal moraines consisting of material that a glacier had accumulated on its tongue and which was left in an arcuate position after its melting. Terminal moraines often cause the formation of a lake. Of interest are also longitudinal moraines which may have left along the walls of a formerly glaciated valley, creating several parallel valleys.

1.75. Pingos, Solifluction, Pressure Ridges. Finally, we shall discuss some types of geomorphological features which are presumably due to frost action and thus are properly considered together with other niveal features.

The first of these features are *pingos*. Pingos, sometimes also called *hydrolaccoliths*, are ground-ice mounts which occur in areas where permafrost is prevalent. They have been described, e.g. by SHARP[5], PIHLAINEN et al.[6], MAARLEVELD[7], MACKAY[8], and, in a very extensive study, by

1. ALDEN, W. C.: U.S. Geol. Surv. Bull. 273, 18 (1905).
2. ARONOW, S.: Amer. J. Sci. 257, 191 (1959)
3. CHORLEY, R.J.: J. Glaciol. 25, 339 (1959).
4. ZOLLINGER, J.: Leben u. Umwelt 15, 145 (1959)
5. SHARP, R. P.: Geograph. Rev. 32, 417 (1942).
6. PIHLAINEN, J. A., R. J. E. BROWN, and R. F. LEGGET: Bull. Geol. Soc. Amer. 67, 1119 (1956).
7. MAARLEVELD, G. C.: Meded. Geol. Stich., N.S No. 17 (1965).
8. MACKAY, J. R.: Proc Permafrost Int. Conf., Lafayette, 71 (1963).

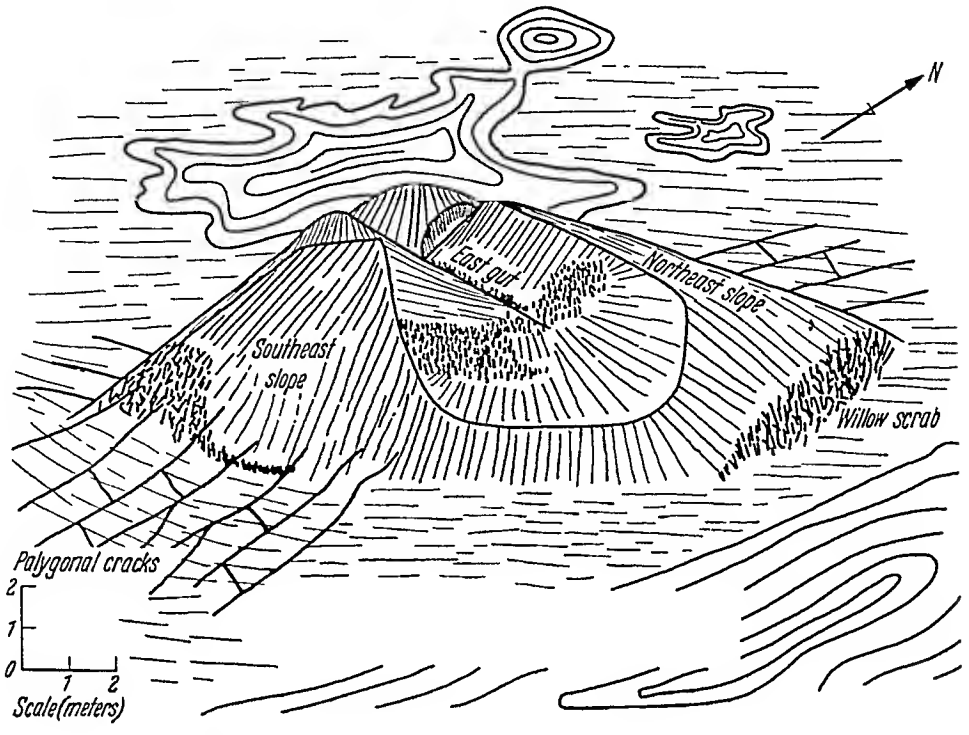

Fig. 29. Sketch of a pingo. After PIHLAINEN et al.[1]

MÜLLER[2]. Pingos have the appearance of more or less regular cones up to 100 m in height with a crater-like depression in the center. Their body contains an ice lens. Tensional cracks on the side of the cones indicate that pingos were formed by some kind of diapirism. A drawing of a pingo (after PIHLAINEN et al.[1]) is shown in Fig. 29. Evidence of fossil pingos (from the last ice age) has also been discovered[3,4].

The second feature to be discussed is that of *niveal solifluction*. Under arctic conditions, it is observed that soil may be slowly creeping downhill on a slope. This is called "solifluction". The presence of frost action is essential for this phenomenon to occur. It has been described in the literature on many occasions (cf. HOLMES' book[5]). Movements of the soil are particularly noticeable in spring. WILLIAMS[6], in an investigation

1. PIHLAINEN, J. A., R. J. E. BROWN, and R. F. LEGGET: Bull. Geol. Soc. Amer. 67, 1119 (1956).

2. MÜLLER, F.: Medd. Grønland 153, No. 3, 1 (1959).

3. WIEGAND, G.: Fossile Pingos in Mitteleuropa. Würzburg: Verl. Geogr. Inst. Univ. No. 16 (1965).

4. SLOTBOOM, R. T.: Comparative Geomorphological and Palynological Investigation of the Pingos (Viviers) in the Hautes Fagnes (Belgium) and the Mardellen in the Gutland (Luxemburg). Amsterdam: Univ.-Diss. 1963.

5. HOLMES, A.: Principles of Physical Geology. London: T. Nelson 1944.

6. WILLIAMS, P. J.: Amer. J. Sci. 255, 705 (1957).

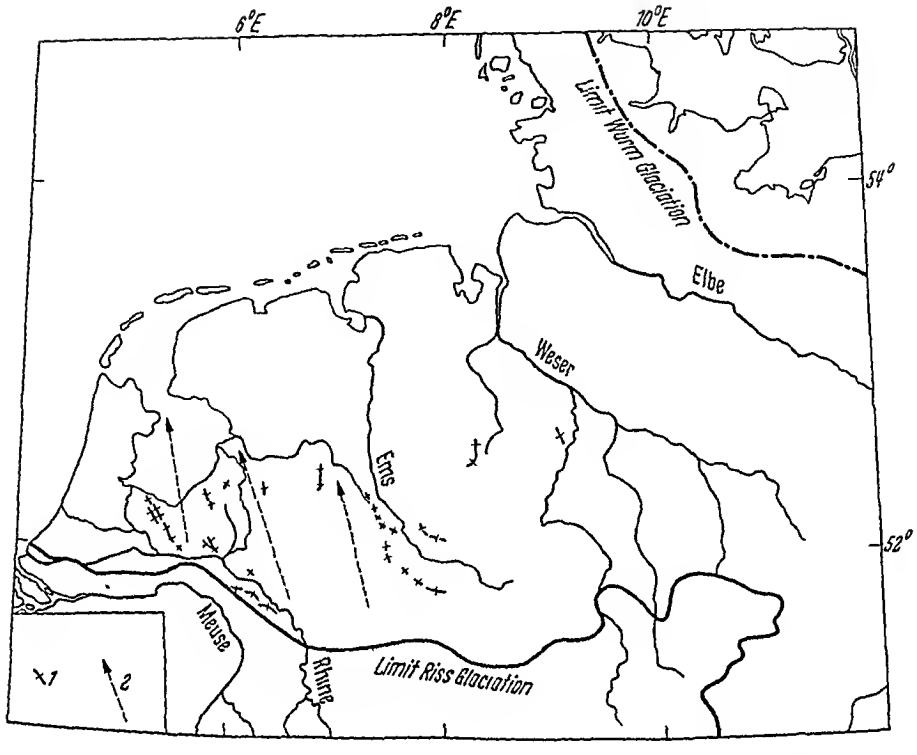

Fig. 30. Distribution of ice-pushed ridges in Europe 1 Ice pushed ridges; 2 Drainage direction during Riss glaciation. After RUTTEN[1]

of the solifluction phenomenon, measured displacements of 20 cm in one spring season on a slope of slope angle of 19°. The movements reached to a depth of 75 cm. Niveal solifluction should be distinguished from *aqueous solifluction* which also refers to soil creep, but without the presence of frost action in water-logged soils. The two phenomena, although superficially similar, are genetically different.

Another phenomenon to be discussed in the present section is that of *ice-pushed pressure ridges* which are conspicuous features in the plains of Europe and northwestern Canada[1] (cf. Fig. 30). They are structures of considerable dimensions. Their height may reach from 50–200 m above their surroundings and their linear extent may attain 100 km. They have often been confounded with moraines. It stands to reason that they are due to a combination of glacier pressure and freezing of the soil.

Features related to ice-pressure ridges may be polygons of patterned ground found in periglacial areas. Such polygons are cracks in the ground or may be manifest simply by a consistent sorting of the gravel. A description of such features from many parts of the world was given e.g.

1. RUTTEN, M. G.: Amer J. Sci. 258, 293 (1960).

by FURRER[1] and a summary of the recent literature on them by DYLIK and MAARLEVELD[2].

1.76. Varves. Varves are sedimentary laminae which are often observed in postglacial basins, such as the Baltic Sea. In a vertical section, dark and light colored bands alternate and the contention is that these bands correspond to yearly cycles of deposition[3], like the rings on a tree.

It has been observed[3] that, in varved clays, the yearly sedimentation rate decreases upwards. Sedimentation curves (annual rate *versus* height

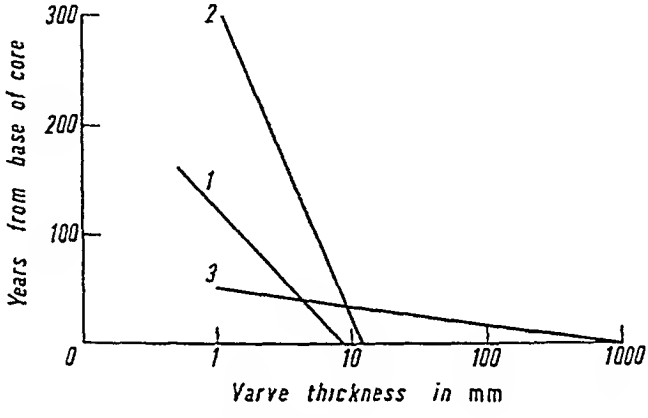

Fig. 31. Sedimentation curves of Baltic Sea Varves, on semilogarithmic paper (see text), drawn from data published by IGNATIUS[3]

in years above base) can be constructed; typical curves have for instance been published by IGNATIUS[3]. On semilogarithmic paper (abscissa: logarithm of varve thickness; ordinate: height or years above base of core) the latter are generally straight lines (see Fig. 31). Evidently, these observed features require a physical explanation.

1.8. Aeolian Features

1.81. Occurrence of Effects Due to Wind. The force of the wind can have great geomorphological significance. This occurs mostly in the dry areas of the world because wind forces have little room for attack on the soil if the surface of the Earth is covered by plants. Wind effects can also become significant if a plant cover has been prevented by some means other than lack of precipitation. This may have occured because of human activity, because of wave action on an oceanic coast, or because of the severity of the climate in high mountain regions.

1. FURRER, G. J.: Die Höhenlage von subnivalen Bodenformen. Habil.-Schr. Phil. Fak. II, Univ. Zürich (1965).
2. DYLIK, J., and G. C. MAARLEVELD: Meded. Geolog. Sticht. 18, 7 (1967).
3. IGNATIUS, H.: C.R. Soc. Geol. Finland 30, 135 (1958).

The action of the wind consists in the transportation of loose dust or sand particles. It is important to distinguish between "dust" and "sand"; the former is lifted by the turbulence of the air like suspended sediment in rivers, whereas the latter is dragged along like the bed load in a water stream. In the two cases, the morphological effects are entirely different.

Considering first the movement of sand, we note that the latter is particularly significant in *deserts*. Sand ripples, dunes and corrasive features are caused in this fashion. We shall discuss the morphology of such features in some greater detail in Sec. 1.82.

We shall then proceed to a discussion of dust movement. Soil erosion and the deposition of loess are probably the best known effects thereof. This will be described in Sec. 1.83.

Wind-borne features are also created after a volcanic eruption: Material is ejected from the volcano and then travels through the air. We shall discuss this in Sec. 1.84.

The best summary of aeolian features known to the author is a book by BAGNOLD[1]. Another, somewhat descriptive treatise of desert features has been written by CORNISH[2]. Most textbooks of geomorphology mentioned in Sec. 1.1 also contain chapters on wind action.

1.82. Desert Features. As noted above, the action of wind in a desert causes a variety of phenomena.

Thus, winds of varying strength and direction may cause *ripples* on a sand surface. These ripples are entirely ephemeral; they change their size and direction with the wind that happens to be blowing. They are distinguished from larger features not only by their impermanence, but also by the fact that the fine sand particles are always found in the troughs between the ripples, the coarse particles at the crests. This type of particle size grading is reverse to that observed in larger scale features. The ratio of height to wave length in ripples ranges from 1:10 to 1:70 (cf. BAGNOLD[1]) depending on the range of the grain size distribution of the sand; the ratio of height to wavelength of the ripples increases with the range of the grain size distribution of the sand. If ripples become large, they are called *sand ridges*. BAGNOLD[1] quotes cases where such ridges have been found in the Libyan Desert with wavelengths exceeding 20 m and with heights of over 60 cm. Ripples and ridges are genetically identical; there is no sharp distinction between the two types of features.

The above-mentioned features answer to the criteria of impermanence and sorting of the fine grains into the troughs, coarse grains onto the crests. With the so-called large-scale features, the reverse is true. These

1. BAGNOLD, R. A.: The Physics of Blown Sand and Desert Dunes. London: Methuen & Co 1941.

2. CORNISH, V.: Waves of Sand and Snow. London: T. Fisher Unwin 1914.

large-scale features are represented by *dunes*[1,2] and by modifications of dunes. There are essentially two types of dunes which have been called *barchan dunes* and *seif dunes*. Barchan dunes are crescentic mounds of sand which may occur singly or in groups, the horns of the crescents facing leeward (referring to the prevailing wind direction). The part of the dune between the horns on the leeward side is steep and represents a *slip face*. A schematic drawing of a barchan dune is shown in Fig. 32. The height of barchans may vary. Barchan dunes are observed to progress ("wander") downwind. Their speeds are variable and may be related to their heights. Some measurements have been reported by BEADNELL[3] whose results (for 5 dunes in the area of the Karga Oasis in Egypt) are shown in Table 4.

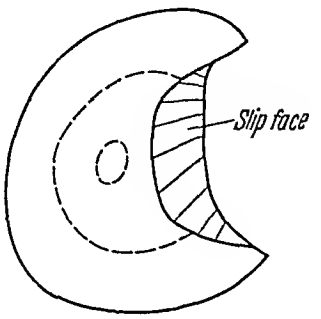

Fig. 32. Barchan dune: view in plan

Table 4. *Height (H), total advance (L) in one year and speed (C) of five barchan dunes in Egypt.* After BREADNELL[3]

H (cm)	L (cm)	C (cm/sec)
2,000	1,090	3.46×10^{-5}
1,700	1,080	3.42×10^{-5}
1,100	1,620	5.14×10^{-5}
1,050	1,880	5.96×10^{-5}
400	1,840	5.83×10^{-5}

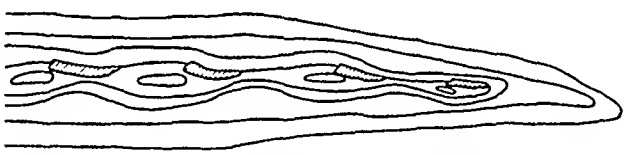

Fig. 33. A chain of seif dunes. Note the slip faces

As noted above, in addition to barchan dunes one may observe seif dunes (Fig. 33). These are longitudinal features which do not show the crescentic shape of the barchans. It may be that a barchan dune can develop into a seif dune if it becomes asymetrical (cf. Sec. 8.35). HOLMES[4] states that seif dunes commonly occur in parallel ranges of immense length (see Fig. 33).

Modifications of the two basic types of dunes have been termed as *whalebacks* and as *sand undulations*. The meaning of these terms is self-evident.

1 BAGNOLD, R. A.: The Physics of Blown Sand and Desert Dunes. London: Methuen & Co. 1941.

2. NORRIS, R. M., and K. S. NORRIS: Bull. Geolog. Soc. Amer. 72, 605 (1961).

3. BEADNELL, H. J. L.: Geogr. J. 35, 379 (1910).

4. HOLMES, A.: Principles of Physical Geology. London: T. Nelson & Sons 1944.

Finally, one may note that blowing sand can act as a corrasive agent on tectonic features in a desert. The result of this action is a sometimes weird *pillar-like structure* of the type known, for instance, from Monument Valley in Utah. The *island mounts* ("Inselberge") sometimes found in the tropics (particularly in Mozambique) are generally thought to be the remnants of the sandblasting action when the area was a desert.[1, 2]

1.83. Dust Movement. The desert features discussed in the last Section (1.82) are caused by the movement of *sand*. The finer particles, commonly called *dust*, also occur in deserts but they do not seem to be prominently involved in the formation of desert features.

However, the movement of dust has great significance in the plains areas of the world. It may become significant in two possible manifestations: the first representing removal of material and the second deposition.

The removal of dust from the surface of the earth is particularly evident where the phenomenon of *soil erosion* occurs. If the plant cover is destroyed by some means (such as human activity), the Earth is laid open to attack by the wind and great quantities of material may be removed. Dust removal, of course, also occurs in deserts but it is not so conspicuous there.

The *deposition* of dust may lead to a very characteristic phenomenon: the deposition of loess. It matters little whence the dust was taken, from a desert or from the rock flour of glacial deposits: the result of massive deposition in a plains area is in each case a *blanket of loess*. The dust is

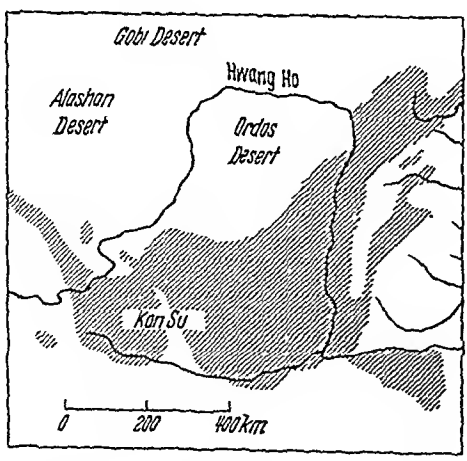

Fig. 34. The extent of loess coverage (shaded) in China (modified after HOLMES[3])

1. OLLIER, C. D., and W. G. TUTTENHAM: Z. Geomorphol. 5, No. 4, 257 (1962).
2. TWINDALE, C. R.: Trans. Inst. Brit. Geogr. 34, 91 (1964).
3. HOLMES, A.: Principles of Physical Geology. London: T. Nelson & Sons 1944.

trapped by the vegetation that is present; each year the blanket of loess grows a little higher as new dust is deposited. The loess blankets may stretch over immense areas. The extent of the loess deposits in China is shown in Fig. 34.

1.84. Volcanic Eruptions. During a volcanic eruption, large amounts of material may be ejected into the air. There are then two types of aeolian mechanisms by which this material may be transported and deposited.

The first is that of the *ash flow* represented by nuées ardentes. Such nuées represent downward-rolling hot clouds; a particularly notorious example of a nuée ardente occurred in 1902 after an eruption of Mt. Pelée on the island of Martinique and destroyed the city of St. Pierre. A classical description of nuées ardentes has been given by LACROIX[1] who visited Martinique after the eruption of Mt. Pelée. Nuées ardentes are also thought to give rise to welded tuffs[2]. Ash flows may travel a distance of up to 120 km from their source which represents a considerable distance. It thus appears that nuées ardentes are extremely mobile and can travel over large distances. Velocities of nuées ardentes have been estimated to reach up to 130 m/sec (during the Mt. Pelée eruption the distance of 8 km from the crater to the city was covered in somewhat less than a minute), their length 1 km and their height 4 km where, however, perhaps only a very small fraction of the total height contains coarse material.

The second type of mechanism is the *ash fall*. Ash falls are the products of aeolian differentiation wherein particles are segregated by their fall velocity as they are transported downwind. Ash fall deposits tend to have an exponential decay of thickness downwind and a corresponding decrease in grain size. A review of the available observations may be found in papers by FISHER[3] and by EATON[4].

1.9. Special Features

1.91. General Remarks. Finally, we shall briefly discuss the physiography of some special geomorphological features which cannot be grouped very well with the phenomena already described above.

These features include some very special erosional structures that are found in badlands: we mean particularly *hoodoos* (Sec. 1.92) which have the form of giant mushrooms with an overhanging hat. Next, we shall consider *geysers* (Sec. 1.93). Finally, we shall discuss the phenomenon of *karsts and caves* (Sec. 1.94).

1. LACROIX, A.: La montagne Pelée et ses éruptions. Paris: Masson & Cie. 1904.
2. SMITH, R. L.: Bull. Geol. Soc. Amer. **71**, 795 (1960).
3. FISHER, R. V.: J. Geophys. Res. **69**, 341 (1964).
4. EATON, G. P.: J. Geology **72**, 1 (1964).

1.92. Badland Erosion. In semi-arid, sandy or clayey areas where there is not enough moisture and time available between cloudbursts to allow vegetation to grow profusely, the water washes gulleys and valleys into otherwise undisturbed, flat strata. Due to the lack of vegetation, the sides of the gulleys remain bare of plant growth although the more level parts show some cover with such low-lying plants as prairie grass and cactus. The whole area thus takes on a bleak appearance; the type of landscape it represents is therefore referred to as "badlands".

Since erosion in badlands does not proceed at the same pace in all localities, characteristic and sometimes fantastic features result. At times, strata are encountered which present slightly more resistance to ablation and dissolution by water than others so that "islands" are formed around which erosion takes place at a faster pace. The water now collects even more in the deeper places and the more resistive top of the developing feature acts as a protection. Thus, a series of features will eventually stand out in an area which all around has been eroded to a lower level. In general, the features thus created are pyramidal structures and are referred to as *mesas* or *buttes*.

In addition to the pyramidal structures just mentioned, one occasionally finds clusters of more unusual structures which have a strange, mushroom-shaped form. Instead of being pyramidal, they have an overhanging "hat" so that they have the general appearance of giant mushrooms. Such structures are called *hoodoos*.

Table 5. *Measurements of three hoodoos*

No.	Height m	Waist m	Overhang m
1	3 0	0.6	0.4
		1.5	0.5
2	2.4	0.8	0.3
		1.4	0
3	1.6	0.8	0.2
		1.4	

The writer[1] took measurements on three hoodoos in the Alberta Badlands (near Drumheller); the result is shown in Table 5. On inspecting this table, it will be noted that in some instances, there are two numbers given. These indicate the maximum and minimum values for various cross-sections of the hoodoo in question. The most striking feature of hoodoos is the overhanging hat; the overhang may reach up to 50 cm.

1. SCHEIDEGGER, A. E : Geofis. Pura e Appl. 41, 101 (1958).

The occurrence of hoodoos in badlands requires an explanation. It is obvious that they are erosional features; — but so are mesas and buttes which have a pyramidal structure. The reasons for the different appearance of *hoodoos* are not at all *a priori* evident.

1.93. Geysers. A geyser is a special type of hot spring found in some volcanic areas, particularly in Iceland, in Yellowstone and in New Zealand. The discharge of geysers is intermittent, sometimes with great regularity, and often connected with a significant outburst of energy which causes the water to shoot to great heights into the air. The morphology of Icelandic geysers has been described in a notable monograph by BARTH[1], that of the Yellowstone geysers by ALLEN and DAY[2] and that of the New Zealand geysers by HERBERT[3]. Accordingly, the jets of hot water may reach a height of 457 m. The rest periods between eruptions may be anything from a few minutes to several days. The quantity of water ejected in one single eruption may reach 800 tons[4].

1.94. Karsts and Caves. Finally we shall discuss the *karst* phenomenon. In limestone areas water readily dissolves channels and caverns out of the rock and this produces characteristic features.

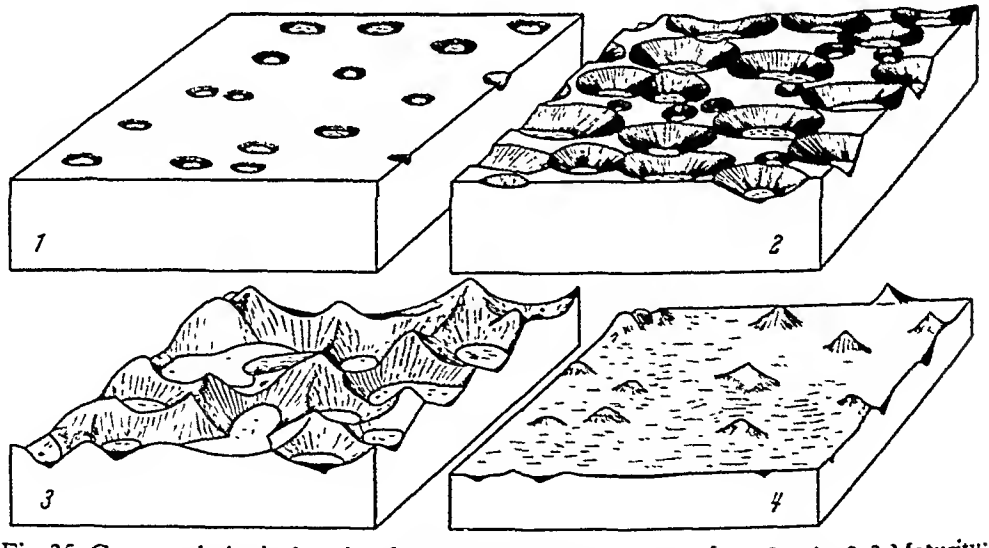

Fig. 35. Geomorphological cycle of a karst area. After GRUND[5]. *1* Youth; *2, 3* Maturity; *4* Old age

1. BARTH, T. F. W.: Publ. Carnegie Inst. Washington **587**, 1 (1950).
2. ALLAN, E. T., and A. L. DAY: Publ. Carnegie Inst. Washington **466**, 1 (1935).
3. HERBERT, A. S.: Hot Springs of New Zealand. London 1921.
4. The jet height of 457 m and water quantity of 800 tons refer to the Waimanga Geyser in the vicinity of Lake Tarawera in New Zealand. This geyser is now (since 1904) no longer active. The above information is from M. NEUMAYR and F. E. SÜESS: Erdgeschichte, 3d ed. Leipzig: Bibliogr. Inst. 1920, p. 227.
5. GRUND, A.: Z. Ges. Erdk. Berlin **1914**, 621 (1914).

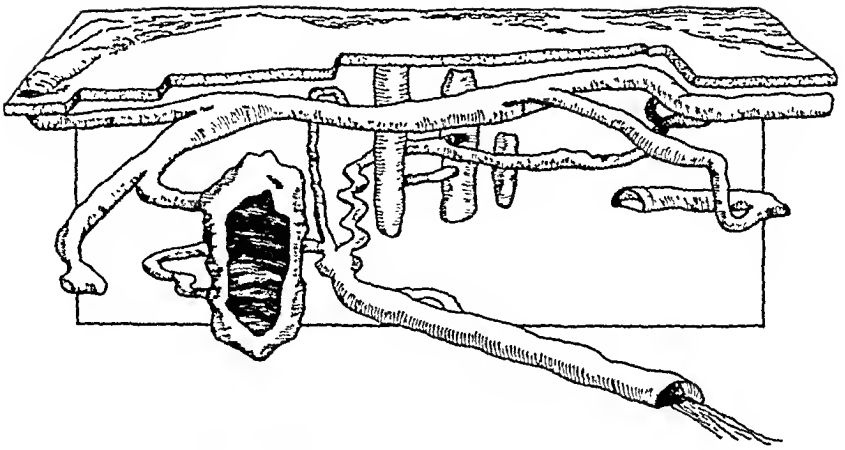

Fig. 36. Schematic drawing of a cave. After KUZNETSOV[1]

Originally small surface openings become gradually enlarged. As the leaching process continues, the openings begin to fuse together and a mountainous relief results. Finally, the peaks become worn down and the karst surface becomes level with the ground water niveau. Thus, the development of a karst region can be described in terms of a geomorphological cycle[1]. Its main features are shown in Fig. 35.

One of the most striking karst features are *caves*. Such caves are generally long, winding passages, but they may also be in the form of big rooms. One section in the Carlsbad Cavern in New Mexico is almost 1.2 km long with walls 180 m apart and a ceiling 90 m high. A schematic drawing of a cave is shown in Fig. 36.

1. KUZNETSOV, S.S.: Геология (динамическая). 2nd ed. Moscow: Uchpedgiz 1959.

II. Physical Background

2.1. Introduction

2.11. General Remarks. The materials that are of importance in causing exogenetic geodynamic effects are water, air and ice. Of these materials, water and air can be treated as viscous fluids to a high degree of approximation; ice, on the other hand, is a "solid" which must be treated by the general methods of rheology.

The present chapter will be devoted to a brief review of the basic dynamics of these substances, as far as this is of importance regarding geomorphological effects.

2.12. Hydrodynamics of Viscous Fluids. The general hydrodynamics of viscous fluids is wll known. Since many treatises exist on the subject[1-3], there is not much need of giving many details here. We shall simply briefly review a few of the basic concepts which will be of importance later.

Thus, we may note that for the complete description of the behavior of continuous matter (of which viscous fluids represent an example), one needs four types of relationships. The first is a kinematic condition, the second a continuity condition, the third an equation of motion and the fourth an equation of state. Since the above conditions lead to a system of differential equations, one will have to add suitable boundary and initial conditions to make a problem determined.

The set of above conditions can be combined to yield differential equations which are applicable under various conditions. A well-known equation of this type is the so-called Navier-Stokes equation which is

$$v \operatorname{grad} v + \frac{\partial v}{\partial t} = F - \frac{1}{\rho} \operatorname{grad} p - \frac{\eta}{\rho} \operatorname{curl} \operatorname{curl} v. \qquad (2.12\text{-}1)$$

Here, v is the local velocity vector of a point of the fluid, t is time, F is the volume force per unit mass, ρ is the density and η is the viscosity of the fluid. The Navier-Stokes equation applies to incompressible fluids.

1. Lamb, H.: Hydrodynamics. 6th ed. London: Cambridge Univ. Press 1932.
2. Pai, S. I.: Viscous Flow Theory (2 Vols.) New York: D. Van Nostrand 1957.
3. Goldstein, J.: Modern Developments in Fluid Dynamics (2 Vols.) Oxford: Oxford Univ. Press 1938.

It has been observed that the flow pattern of a fluid becomes transient at high flow velocities although the boundary conditions remain steady: eddies are formed which proceed into the fluid at intervals. The transient flow pattern is termed "*turbulent*". It appears that, for any one flow system, a transition velocity exists at which the flow becomes turbulent; at lower velocities the flow remains steady ("*laminar*"). The best-known criterion for this transition velocity is based on the *Reynolds number Re* which is defined as follows

$$\mathrm{Re} = \frac{\rho v d}{\eta} \tag{2.12-2}$$

where d denotes a characteristic diameter of the flow system. The criterion states that turbulence will occur if the Reynolds number reaches a critical value, commonly quoted as in the neighborhood of 2,200. However, this criterion is strictly applicable to straight tubes only; in other types of flow systems the critical Reynolds number may be different.

For further details regarding the hydrodynamics of viscous fluids, the reader is referred to standard textbooks.

2.13. Rheology. As noted in the Introduction to this chapter (Sec. 2.11), of the materials affecting the surface of the Earth exogenetically, ice must be treated as a general rheological substance. Ice is a solid, but it can flow; its flow is described by some non-viscous flow law.

The general theory of rheological substances has ably been described in a textbook by REINER[1]. In it is shown that the various possible rheological conditions (equations of state) which, in essence, comprise stress-strain relationships, can be arrived at in a systematic fashion. A brief review of REINER's procedures has also been given by the present writer[2]; the reader is reffered to the quoted references for details.

With regard to the physics of ice, we shall discuss in Sec. 2.33 some of the rheological conditions ("flow laws") that have been proposed in the literature. For geomorphological applications, this will suffice.

2.2. Dynamics of Flowing Water

2.21. Principles of the Statistical Theory of Turbulence. Fluids that cause hydraulic actions which have an effect upon geodynamics, are usually in a state of turbulence. The investigation of the dynamics of turbulent flow is therefore of utmost importance.

1. REINER, M.: Twelve Lectures on Theoretical Rheology. Amsterdam: North Holland Pub. Co. 1949.

2. SCHEIDEGGER, A. E.: Principles of Geodynamics. 2nd ed. Berlin-Gottingen-Heidelberg: Springer 1963. See p. 132ff. therein.

The fluids in question are generally ordinary, viscous (Newtonian) fluids. In principle, it should therefore be possible to solve any flow problems simply by solving the basic Navier-Stokes differential equations for the correct boundary conditions. Unfortunately, for the conditions prevailing in turbulent flow, this is impossible. Turbulent flow is characterized by irregular velocity fluctuations which are much too complicated for being followed in detail. It has therefore proven to be convenient to use the methods of statistical mechanics to deal with the problem.

Accordingly[1], the velocity-field $\boldsymbol{u}(x)$ (where *boldface* denotes vectors, x is the space coordinate) of a fluid in turbulent motion is considered as a field of a random variable. One can then define various types of averages. First of all, one has the average velocity $\bar{\boldsymbol{u}}(t)$, where the average has been taken with regard to the space coordinate x. The fluctuation of the velocity is then given by

$$\boldsymbol{u}' = \boldsymbol{u} - \bar{\boldsymbol{u}}, \tag{2.21-1}$$

or, in components

$$u_k' = u_k - \bar{u}_k, \tag{2.21-2}$$

where $k = 1, 2, 3$. It is then customary to define the *correlation tensor* R_{ik} by

$$R_{ik}(r) = \overline{u_i'(x)\, u_k'(x+r)}. \tag{2.21-3}$$

Eq. (2.21-3) represents a tensor field.

The correlation tensor, and most significantly, its Fourier transform (called *spectrum* tensor) can be taken as fundamental kinematic variables in (homogeneous) turbulence problems. The equations of motion for these variables can be deduced from the Navier-Stokes equations and one then arrives at a general theory of decay of turbulence. However, in the present context we shall be more interested in steady-state problems. It will be assumed that sufficient energy is available to maintain turbulence, and what is of significance are the *stresses* present in such systems.

2.22. Momentum Transfer and Eddy Viscosity. Let us assume that turbulence has been established in a system of two-dimensional flow, such as in a channel or in a pipe. Let the coordinate parallel to which the mean flow is taking place be denoted by x, the coordinate orthogonal to this by y. Let the mean velocity in the x-direction be $\bar{u}_x(y)$, the fluctuation u_x' and the fluctuation in the y-direction u_y'. The excess of momentum parallel to the mean flow is then $\rho\, u_x'$ per unit volume, and,

1. See e.g. BATCHELOR, G. K.: The Theory of Homogeneous Turbulence. Cambridge: University Press 1953.

consequently, the force per unit area (i.e. the shearing stress) is given by

$$\sigma = \rho \overline{u'_x u'_y}. \tag{2.22-1}$$

This is the general expression for the turbulent shearing stress.

In an ordinary, viscous fluid in laminar motion, the viscosity is defined in terms of the velocity gradient

$$\rho = \eta \frac{d\bar{u}_x}{dy}. \tag{2.22-2}$$

If, therefore, the turbulent shearing stress is expressed in terms of the average velocity gradient, then it can be said to be due to an "*eddy viscosity*". This "eddy viscosity" is a fictitious quantity; it can be used, however, to indicate the relationship between the turbulent stresses and the (average) velocity gradient.

The form (2.22-1) of the stress formula suggests that the drag R (a *force*) experienced by an object of linear dimension d immersed in turbulent flow is proportional to (for the x-component)

$$R_x \sim d^2 \rho \bar{u}_x^2. \tag{2.22-3}$$

The drag formula is commonly written as follows

$$R_x = \frac{\pi}{8} C_D d^2 \rho \bar{u}_x^2 \tag{2.22-4}$$

where C_D contains the correlation. The coefficient C_D is called "drag coefficient".

2.23. PRANDTL's Theory of Turbulence. PRANDTL[1,2] approached the problem of turbulent momentum exchange from a different angle. He introduced a *mixing length* l which he regarded as the mean distance which a small volume of fluid may travel normal to the main stream until it loses its identity by mixing. Assuming two-dimensional flow, with the mean velocity $\bar{u}$ being parallel to, say, the x-direction, but with a velocity gradient $d\bar{u}/dy$ being present in the y-direction, then the velocity of a mass of fluid arriving at a certain position will be proportional, in the first approximation, to $\bar{u} \pm l\, d\bar{u}/dy$, because l is precisely that (average) distance which it can travel without losing its identity. Hence the average velocity *fluctuation* u' will be proportional to $l\, d\bar{u}/dy$. In isotropic turbulence, the lateral velocity fluctuation v' will, *ab hypothesi*, be proportional to the same quantity. Hence one obtains for the stress according

1. PRANDTL, L.: Über die ausgebildete Turbulenz. Trans. 2nd Int. Congr. Appl. Mech., Zürich, p. 62 (1926)

2. See also DRYDEN, H. L., F. D. MURNAGHAN, and H. BATEMAN: Hydrodynamics. New York: Dover Publ. 1956; particularly, p. 396ff.

to general principles (cf. 2.22-1):

$$\sigma = \rho \overline{u' v'} = \text{const. } \rho \, l^2 \left(\frac{d\bar{u}}{dy} \right)^2 \tag{2.23-1}$$

where any correlation factor between u' and v' may be incorporated into the (unknown) quantity l. Taking into consideration the fact that the stress σ must change its sign if the velocity $\bar{u}$ does, one can write (incorporating the *const.* also into l):

$$\sigma = \rho \, l^2 \left| \frac{d\bar{u}}{dy} \right| \frac{d\bar{u}}{dy} = \rho \, \varepsilon \frac{d\bar{u}}{dy} = \varepsilon' \frac{d\bar{u}}{dy}. \tag{2.23-2}$$

Here, one can call ε' the "exchange coefficient" for the momentum. The last expression is that which was suggested by PRANDTL as describing the turbulent (shearing) stress. Comparison with Eq. (2.22-2), suggests that, in the present case, $\varepsilon' = \rho \, \varepsilon$ could also be called *eddy viscosity*, since it occupies the same position in the stress-velocity gradient relationship as does the viscosity in laminar flow.

2.24. Homogeneous Turbulence and Its Decay. In a stady state, the turbulence has to be maintained at a constant level. Because energy is dissipated into heat during the turbulent motion, turbulent energy has to be introduced at a rate which equals that of the dissipation. In this fashion, a steady state can develop.

The mechanism is therefore clear in principle: Turbulent energy is dissipated (into heat) at one end of the eddy-spectrum (at high wave numbers) and introduced at the other end (low wave numbers) from some external source; it thus "flows" from one end of the spectrum to the other. According to BATCHELOR[1], the energy relation in the linear case, for homogeneous, isotropic turbulence, originally due to BASS[2], is given by

$$E = A \, \varepsilon^{\frac{2}{3}} k^{-\frac{5}{3}} \tag{2.24-1}$$

where A is some constant, E is the total energy, k is the wave number (the Fourier transform of the space coordinate) and ε the rate of energy flux (dissipation).

When no more energy is introduced into a fluid volume in homogeneous, isotropic turbulent motion, the latter will start to decay. The decay laws for turbulence are fairly well understood[3]. In homogeneous turbulence, if the velocity fluctuations are denoted by u', the decay law

1. BATCHELOR, G. K.: The theory of homogeneous turbulence. London: Cambridge University Press 1953.

2. BASS, J.: C. R. Acad. Sci. Paris 228, 228 (1949).

3. HINZE, J. O.: Turbulence. New York: McGraw-Hill Book Co. 1959. See p. 164 therein.

may be written as follows

$$\overline{u'^2} = \text{const.}\, t^{-m} \tag{2.24-2}$$

where

$$m = 1 \text{ for the "initial range"}, \tag{2.24-3}$$

$$m = \tfrac{5}{2} \text{ for the "terminal" range}. \tag{2.24-4}$$

Numerical values for the instant when the "initial" time range ends and the "terminal" range begins, cannot easily be given. For turbulence created by obstacles of linear dimension M in a stream of mean velocity v, it was found that for the initial range

$$\frac{v\,t}{M} \leq 100 \tag{2.24-5}$$

and for the terminal range

$$\frac{v\,t}{M} \geq 500. \tag{2.24-6}$$

Writing $v\,t = x$, the above relations yield, together with some laws for the generation of turbulence, that the turbulent velocity fluctuations behind an obstacle are given by[1]

$$\left(\frac{v}{u'}\right)^2 = \alpha \frac{x}{\delta} - \beta \tag{2.24-7}$$

where α and β are constants; β is a small number.

2.25. Boundary Layer Theory. If there are boundaries in a (viscous) fluid which is in turbulent motion, then it has been noted long ago by PRANDTL that the amount of turbulence present in any one region of the fluid must be affected by the proximity of such a boundary.

In fact, the boundary condition usually applied in the case of a viscous fluid is that the latter must stick to the walls. Hence, the velocity of the fluid near the boundary must be reduced by viscous drag. One usually defines as "boundary layer" that region near the boundary in which the velocity differs by one per cent. from the mean fluid velocity.

The motion in the boundary layer may be either turbulent or laminar, depending on the velocity of the fluid. If it be turbulent, then it is clear that there must be a sublayer very close to the wall in which the velocity is so small that the Reynolds number is smaller than the critical Reynolds number necessary for the maintenance of turbulence. This region is then called the "laminar sublayer".

The existence of these various types of boundary layers has a certain significance in theoretical geomorphology.

1. HINZE, J. O.: Turbulence New York: McGraw-Hill Book Co. 1959. See pp. 216–217 therein.

2.26. The Stability of Superposed Streams of Different Densities. A further problem of fluid dynamics which has a bearing upon geomorphological effects is the question of stability of superposed streams of different density.

Let us suppose that one has two fluids of different densities, one beneath the other, moving parallel to, say, the x-direction. Let us assume that the interface is a horizontal plane and that it represents a discontinuity in the velocity by a finite amount. The stability of such a system has been analyzed long ago by HELMHOLTZ; his analysis has been reproduced, for instance, by LAMB[1].

The stability analysis can be accomplished by the method of small oscillations. Thus, small perturbations about the state of steady motion are introduced into the flow equations and it is investigated whether these will grow.

It turns out (see LAMB[1]) that the common boundary is *always* unstable for sufficiently small wave-lengths of the perturbations. If the relative velocity between the two fluids be V, and the densities ρ_1 and ρ_2, respectively, then those waves whose wave-lengths are shorter than

$$\lambda < 2\pi \rho_1 \rho_2 V^2/[g(\rho_1^2 - \rho_2^2)] \tag{2.26-1}$$

are unstable. Longer waves are propagated at a constant speed and constant amplitude. This result would indicate that, if there were no modifying influences, density currents would not be possible.

The above calculations have been extended by TAYLOR[2] to the case where there is more than one interface, i.e. to the case where there are several strata of fluids superimposed upon each other. The densities are taken as changing abruptly, but the velocity as changing continuously in the intermediate layers. A similar generalization has been made by GOLDSTEIN[3], who assumed three layers: a layer of constant velocity and density being on top, a layer of a different constant velocity and larger constant density being at the bottom, and a transition layer of varying velocity being in between.

The results of the calculations can be expressed in terms of two non-dimensional variables, viz. α, equal to

$$\alpha = 2\pi H/\lambda \tag{2.26-2}$$

where H is the thickness of the transition layer and λ is the wave-length of the disturbance; and n equal to

$$n = g \frac{\Delta\rho/\bar{\rho}\, H}{(\Delta n/H)^2} \tag{2.26-3}$$

1. LAMB, H.: Hydrodynamics. New York: Dover Publications 1945. See p. 373ff. therein.

2. TAYLOR, G. I.: Proc. Roy. Soc. A **132**, 499 (1931).

3. GOLDSTEIN, S.: Proc. Roy. Soc. A **132**, 524 (1931).

where $\Delta\rho$ is the difference in density, Δn the difference in velocity between the top and bottom layers, and $\bar{\rho}$ is the mean density in the transition layer.

If the density in the transition layer is assumed to be constant and equal to the mean of the densities above and below, and if the velocity is assumed to change linearly with height, and if, furthermore, the effect of the change in density upon inertia is neglected, then it can be shown that instability exists for

$$\frac{\alpha}{1+e^{-\alpha}}-1<n<\frac{\alpha}{1-e^{-\alpha}}-1. \tag{2.26-4}$$

The region of instability is that between the full line curves in Fig. 37. A correction to this result is obtained if the effect of the density change on inertia is not neglected. When the densities of the fluids are in ratio $1:\frac{3}{2}$, then the region of instability is that between the broken line curves in Fig. 37.

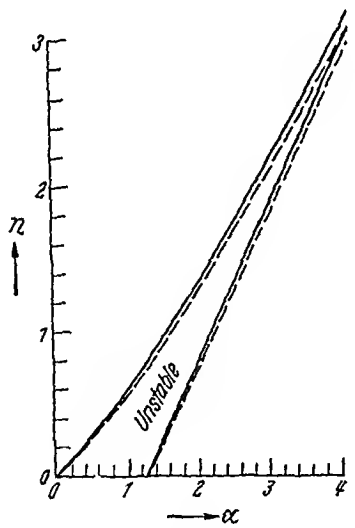

Fig. 37. Region of instability in stratified flows

The most significant feature of the above results is that there is *always* a region of instability.

The above investigations are valid for laminar flow. One might well ask himself what modifications are necessary if one of the fluids is in turbulent flow. This problem has been studied by KEULEGAN[1,2]. The latter author noted that if one fluid is at rest, then there must be a laminar sublayer in the turbulent fluid at the boundary between the two

1. KEULEGAN, G. H.: J. Res. U.S. Nat. Bur. Stand. 32, 303 (1944).
2. KEULEGAN, G. H.: J. Res. U.S. Nat. Bur. Stand 43, 487 (1949).

fluids. In consequence, one must study the phenomena that occur in the laminar boundary layer, using PRANDTL's theory (cf. Sec. 2.25).

The outcome of all these investigations is that the interface should become unstable at certain values for the velocity. Stratified flows, thus, should dissipate themselves in rather short order.

2.3. Dynamics of Flowing Ice

2.31. General Remarks. When water freezes, it becomes *ice*. Amongst solid substances, ice has the remarkable property that it is less dense than the corresponding molten phase (water). With most solids, the reverse is true.

Ice occurs in vast quantities in certain regions of the Earth. Its action is then that of an eroding and transporting agent which is similar to the action of water: for, as a polycrystalline aggregate, ice has certain rheological properties by which it is able to *flow*. In order to understand the transporting action of ice, it is necessary to give a brief review of its physical properties (Sec. 2.32) and of the various flow laws (Sec. 2.33) that have been suggested in the literature. These laws will form the basis for an understanding of the geomorphological significance of ice.

2.32. Some Physical Properties of Ice. Ice is a polycrystalline substance which exhibits a rather complicated mechanical behavior. The crystals belong to the hexagonal system which, in the aggregate, may be from less than one millimeter to over a meter long. The physical properties of ice have been extensively studied as witness for instance the reviews of BERNAL[1] and BUTKOVICH[2].

Upon being subjected to an external load, ice responds instantaneously by an elastic deformation; however, as time goes on, it keeps deforming at a varying *creep rate*. A typical loading-unloading curve of a polycrystalline aggregate, after JELLINEK and BRILL[3], is shown in Fig. 38. For a single ice crystal, the corresponding curve is different; – however, since the ice in nature (which is of geomorphological significance) is generally in a polycrystalline state, the behavior of a single ice crystal is of little concern here.

For the ultimate strength of polycrystalline ice, rather divergent values have been obtained. The compressive strength of lake ice was found[2] to range from 35 – 60 kg/cm^2 (in the temperature range from -5 to -15°C); for the tensile strength, values between 14 and 17.5 kg/cm^2 are generally accepted.

1. BERNAL, J. D.: Nature (Lond.) **181**, 380 (1958).
2. BUTKOVICH, T. R.: Quart. Colo. School Mines **54**, No. 3, 349 (1959).
3. JELLINEK, H. H. G., and R. BRILL: J. Appl. Physics. **27**, 1198 (1956).

An inspection of Fig. 38 shows that the flow behavior of ice cannot be characterized in any simple fashion. It is possible to define a pseudo-viscosity value (denoted by η in Fig. 38), but it may be preferable to describe the rheological behavior differently by empirical flow laws. Some of these will be discussed in the Section below.

It has been found that ice also develops *cracks* during flow. An extensive study of this phenomenon has been reported by GOLD[1]. It appears that part of the creep-time curve for ice (and hence also the form of the flow laws to be discussed below) is due to internal cracking.

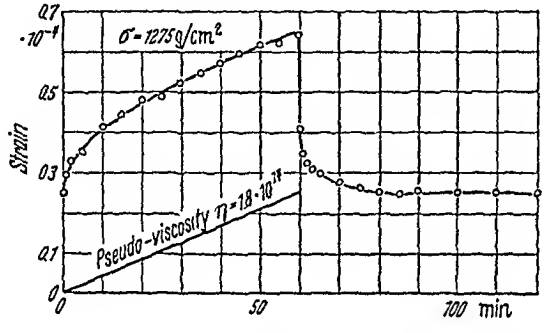

Fig. 38. Typical deformation-recovery curve for polycrystalline ice for a tension σ starting at zero and ending at 60 min. After JELLINEK and BRILL[2]

2.33. Various Flow Laws. We now turn to the rheological properties of ice upon which one might base the law of flow of bulk masses of that substance. A description of the historical development of ice flow laws has been given by FINSTERWALDER[3] and a review of various attempts has been published by GLEN[4].

The simplest attempt to describe the flow of ice is by means of the Navier-Stokes equations, i.e. by treating it as a viscous liquid. Upon this basis, the flow of glaciers has been studied, for instance, by SOMIGLIANA[5].

However, it soon became apparent that a viscous law does not really describe the flow properties of ice very well. Reference has therefore been made to the *theory of plasticity*[6]. In this theory, the stress conditions of MISES or TRESCA are assumed to hold for the flowing ice (for a description of the theory of plasticity, see loc. cit.[6]).

1. GOLD, L. W.: Canad. J. Phys. 38, 1137 (1960).
2. JELLINEK, H. H. G, and R. BRILL: J. Appl. Physics 27, 1198 (1956).
3. FINSTERWALDER, R.: Publ. Assoc. Int. Hydrol. Scient. 47, 5 (1958).
4. GLEN, J. W.: Phil. Mag. Suppl. 7, 254 (1958).
5. SOMIGLIANA, C.: Atti Acad. Nat. Lincei, Rend. Cl. Sci. fis., mat. e nat. 30, (5) 291, 323, 360 (1921).
6. HILL, R.: The Mathematical Theory of Plasticity. Oxford: Clarendon Press 1950.

However, recent experiments by GLEN[1] seem to indicate that plasticity theory represents still too simple a mathematical frame-work for the description of flow properties of ice, and that a power flow law suggested earlier by PERUTZ[2] would be more adequate. The latter is

$$\dot{\varepsilon} = B\,\tau^n \tag{2.33-1}$$

where $\dot{\varepsilon}$ represents the shear strain rate, τ the shear stress and B, n are constants. The quantity n is approximately equal to 4 ± 1[3]. More complicated flow laws have also been analysed by BUTKOVICH and LANDAUER[4]. The flow of ice seems to be due to the simultaneous operation of two processes: grain boundary creep at low stresses and intracrystalline gliding at high stresses[5].

In any application, power flow laws represent great mathematical difficulties. Fortunately, it turns out that the flow law of plasticity theory is in many problems quite adequate.

2.4. Dynamics of Blowing Wind

2.41. Statics of the Atmosphere. In addition to its rôle as a provider of rain and snow, the atmosphere may also have a geomorphological significance by its direct interaction with the Earth's surface. It is therefore of some importance to give a brief review of its physical behavior.

The study of the atmosphere is the subject of the science of *meteorology*. Many pertinent treatises exist[6–13] to which the reader is referred for details; in the present context we shall only give a short account of those meteorological results that are of importance with regard to geomor-

1. GLEN, J. W.: J. Glaciol. **2**, 111 (1952).
2. PERUTZ, M. F.: Observatory **70**, 64 (1950).
3. GLENN, J. W., and S. J. JONES: Proc. Internat. Conf. Low Temp. Sci., Sapporo, Japan **1**, Pt. 1, 267 (1966).
4. BUTKOVICH, T. R., and J. K. LANDAUER: The Flow Law for Ice. SIPRE report DA Proj. 8-66-02-400. Wilmette, Illinois 1959.
5. MEIER, M. F.: U.S. Geolog. Surv. Prof. Pap. **351** (1960).
6. BRUNT, D.: Physical and Dynamical Meteorology. London: Cambridge Univ. Press 1939.
7. HAURWITZ, B.: Dynamic Meteorology, New York: McGraw-Hill Book Co. 1941.
8. ELIASSEN, A., and E. KLEINSCHMIDT: Encycl. Phys. **48**, 1 (1957).
9. BERRY, T. A., E. BOLLAY and N. R. BEERS: Handbook of Meteorology, New York: McGraw-Hill Book Co. 1945.
10. ERTEL, H.: Methoden und Probleme der dynamischen Meteorologie. Berlin: Springer 1938.
11. EXNER, F. M.: Dynamische Meteorologie. Vienna: Springer 1923.
12. HOLMBOE, J., G. E. FORSYTHE, and W. GUSTIN: Dynamic Meteorology. New York: J. Wiley & Sons 1945.
13. KOSCHMIEDER, H.: Physik der Atmosphäre, Vol. 2. Leipzig: Akademische Verlagsges. 1951.

phology. Our main concern will be with climatic effects near the ground, i.e. with "micrometeorology", as this is of utmost geomorphological significance. Comprehensive treatises on this subject have been written by SUTTON[1] and by GEIGER[2].

Beginning with the statics of the atmosphere, we first of all note its *chemical composition* which is approximately that shown in Table 6.

Table 6. *Chemical composition of the atmosphere (volume per cent).* After PANETH[3]

Nitrogen (N_2)	78.08%	Argon	0.93%
Oxygen (O_2)	20.95%	Carbon dioxide	0.03%
Others (Ne, Kr, He, X, O_3)	0.01%		

For most practical purposes, the air forming the atmosphere can be regarded as an ideal gas. We have then the following well-known equation of state:

$$\frac{p}{\rho} = RT \tag{2.41-1}$$

where p is the pressure, ρ the density, T the absolute temperature (in degrees Kelvin) and R the universal gas constant divided by the molecular weight of the gas. For dry air we have $R \sim 2.87 \times 10^6\,\mathrm{cm^2\,sec^{-2}\,deg^{-1}}$. Since in a column of fluid in the gravity field (with acceleration g) the condition of static equilibrium yields

$$\frac{dp}{dz} = -\rho g \tag{2.41-2}$$

(z being a coordinate which is counted positive upward), one obtains the following expression for the pressure distribution

$$\frac{dp}{dz} = -g\frac{p}{RT} \tag{2.41-3}$$

and hence

$$\text{lognat}\, p = -\int_0^z \frac{g}{RT(z)}\,dz + \text{lognat}\, p_0 \tag{2.41-4}$$

$$p = p_0 \exp\left\{-\int_0^z \frac{g}{RT(z)}\,dz\right\}; \tag{2.41-5}$$

similarly, one obtains for the density distribution

$$\rho = \rho_0 \exp\left\{-\int_0^z \frac{g}{RT(z)}\,dz\right\}. \tag{2.41-6}$$

1. SUTTON, O. G.: Micrometeorology, New York: McGraw Hill Book Co. 1953.
2. GEIGER, R.: Das Klima der bodennahen Luftschicht, 3d. ed. Braunschweig 1950.
3. PANETH, F. A.: Sci. J. Roy. Coll. Sci. 6, 120 (1933).

This shows that it is possible to determine theoretically the pressure and the density if the variation of temperature with height is known.

This distribution of temperature with height, in the near to ground layer which alone is of geomorphological significance, can assume a wide variety of patterns. Stability is attained in the atmosphere if the temperature gradient is below a characteristic value. The latter can be calculated as follows: Assume that a volume of air is displaced upward through the distance dz. This causes a pressure decrease by the amount

$$dp = -g\,\rho\,dz = -g\,\frac{p}{RT}\,dz. \tag{2.41-7}$$

However, owing to the pressure change, the air will undergo an adiabatic temperature change given by [1]

$$dT = T\,\frac{dp}{p}\left(\frac{\gamma-1}{\gamma}\right), \tag{2.41-8}$$

with $\gamma \cong 1.41$ for dry air. If the air column is to be stable, this temperature change must produce a temperature which is not higher than that already present in the column. Thus, we have in the limiting case

$$\frac{dp}{p} = -g\,\frac{dz}{RT} = \frac{dT}{T}\left(\frac{\gamma}{\gamma-1}\right) \tag{2.41-9}$$

or

$$\frac{dT}{dz} = -\frac{g}{R}\,\frac{\gamma-1}{\gamma} \tag{2.41-10}$$

which, for air, represents a gradient of roughly $-1°$ C per 100 m. This is the critical pressure gradient ("dry adiabatic lapse gradient"); if the temperature change is less than (in absolute value) or equal to this gradient, the air column in question will be stable.

The above discussion refers to dry air only. For moist air, suitable modifications can be made which cause a change in the various constants occurring in the equations.

2.42. Quasistatic Flow in the Atmosphere. The atmosphere at rest obviously can have little effect upon the formation of the Earth's surface. We thus have to consider the *dynamics* of the atmosphere.

The air above the ground forms a complicated thermomechanical system. The basic equations of motion, which include the Navier-Stokes equations for a viscous fluid and the thermodynamic equations for a real gas, can be written down, but it turns out that solutions thereof can be

1. See e.g. PLANCK, M.: Treatise on Thermodynamics. 3d. ed., p. 63. New York: Dover Pub.-Co. 1945.

obtained only in the simplest of cases. One of the best known of these cases is the *quasistatic approximation*, in which the vertical acceleration is ignored in the motion and the horizontal component of the angular velocity-vector of the Earth is neglected.

A particular case of the quasistatic approximation is represented by *geostrophic* flow in which friction is also neglected. Then, the flow is subject essentially to two forces. One is the Coriolis force F_c (per unit mass) which is always normal to the (horizontal) wind velocity vector, to the right in the Northern hemisphere and to the left in the Southern. Its magnitude is

$$F_c = 2\omega v \sin\varphi \tag{2.42-1}$$

where ω is the angular velocity of the Earth, v the wind speed and φ the latitude. The other force is caused by horizontal pressure differences; denoting the pressure gradient normal to the isobaric lines by $\partial p/\partial n$, the force per unit mass (F_p) in question is

$$F_p = \frac{1}{\rho}\frac{\partial p}{\partial n} \tag{2.42-2}$$

where ρ is the density of the air.

In quasistatic equilibrium, the two forces must balance each other, which shows that the geostrophic wind will blow parallel to the isobaric lines with a velocity

$$v = \frac{1}{2\rho\omega\sin\varphi}\frac{\partial p}{\partial n}. \tag{2.42-3}$$

In particular cases of the quasistatic theory, it becomes possible to regard the air flow as potential flow. Consider two dimensions only and introduce a velocity potential ψ with

$$u = \frac{\partial\psi}{\partial x}, \qquad w = \frac{\partial\psi}{\partial z} \tag{2.42-4}$$

where u and w represent the horizontal and vertical velocity, respectively, and x, z the coordinates, z vertically upward. Then the continuity condition requires

$$\frac{\partial}{\partial x}(\rho u) + \frac{\partial}{\partial z}(\rho w) = 0. \tag{2.42-5}$$

If ρ varies with the vertical coordinate (z) only, we obtain

$$\operatorname{lap}\psi = -\frac{1}{\rho}\frac{\partial\rho}{\partial z}\frac{\partial\psi}{\partial z}. \tag{2.42-6}$$

This is the equation for the velocity potential. Choosing the following density variation

$$\rho = \rho_0 \exp(-q z), \tag{2.42-7}$$

Eq. (2.42-6) has been integrated by POCKELS[1] for frictionless flow over an undulating ground level. Using (2.42-7), the equation for ψ becomes

$$\operatorname{lap}\psi = q\frac{\partial\psi}{\partial z} \tag{2.42-8}$$

a solution of which is (v being a constant)

$$\psi = v\{x - b\cos m\,x\exp(-n\,z)\} \tag{2.42-9}$$

provided that

$$m^2 - n^2 = q\,n. \tag{2.42-10}$$

According to this solution, the wind has a constant velocity

$$u = v \tag{2.42-11}$$

at $z=\infty$. Any streamline of this solution can be taken as ground surface; it turns out that one possibility is a wavy surface of wavelength

$$\lambda = \frac{2\pi}{m}. \tag{2.42-12}$$

A discussion of the streamline pattern obtained in POCKELS' theory yields that the highest horizontal velocity occurs at the top of the undulation and that the maximum vertical velocity is attained at the middle of the windward side of the hills.

In general, the simplified theory exemplified by POCKELS' example yields acceptable results for the phenomena occurring at the windward side of the obstacles, but not at the leeward side, since it does not account for the existence of a wake. For the formation of the latter, friction is of fundamental importance. RAYLEIGH[2] discussed this problem and showed that the introduction of a small frictional force proportional to the perturbation velocity at an obstacle will prevent the motion process from being reversible which it otherwise is in the quasistatic theory. This idea has been applied by LYRA[3] to the calculation of the streamlines over a thin mountain ridge. LYRA's result is shown in Fig. 39. More accurate calculations have been made by SOKHOV and GUTMAN[4].

The assumption of a frictional force leads to the consideration of the effect of viscosity on quasistatic or stationary flow. As with all viscous fluids, viscosity has the effect that a laminar boundary layer must exist near a solid surface. It is possible to set up the equations of motion for

1. POCKELS, F. C.: Ann. Physik (4), 4, 459 (1901).
2. Lord RAYLEIGH: Sci. Papers 2, 258 (1883).
3. LYRA, G.: Z. angew. Math. Mech. 23, 1 (1943).
4. SOKHOV, T. Z., and L. N. GUTMAN: Izv. Akad. Nauk SSSR, Atm. Ocean. Phys. 4, 23 (1968).

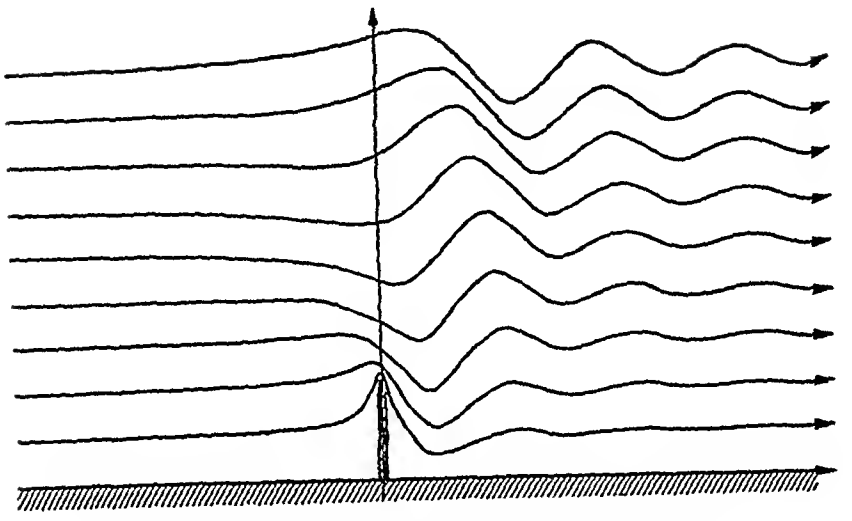

Fig. 39. Streamlines around a thin mountain. After LYRA[1]

this boundary layer. This has been done by PRANDTL in his investigations of turbulence (cf. Sec. 2.25). In the present context, we are interested only in the *laminar* boundary layer which corresponds to the laminar sublayer in the theory of turbulent flow. PRANDTL obtained his "boundary layer equations" by writing down the pertinent equations for a viscous fluid (cf. Sec. 2.12) in two dimensions (x, z) and consistently neglecting terms of an order higher than the first. He then obtained:

$$\left.\begin{aligned} \frac{\partial u}{\partial t}+u\frac{\partial u}{\partial x}+w\frac{\partial u}{\partial z}&=-\frac{1}{\rho}\frac{\partial p}{\partial x}+\nu\frac{\partial^2 u}{\partial z^2}\\ \frac{\partial p}{\partial z}&=0\\ \frac{\partial u}{\partial x}+\frac{\partial w}{\partial z}&=0. \end{aligned}\right\} \qquad (2.42\text{-}13)$$

As usual, in the above equations u, w signify the velocities in the x, z directions, respectively, t is time, p is the pressure, ρ is the density and ν is the kinematic viscosity. The boundary conditions require that

$$u=w=0 \qquad (2.42\text{-}14)$$

at the boundary surface and that

$$u=v; \quad w=0 \qquad (2.42\text{-}15)$$

1. LYRA, G.: Z. angew. Math. Mech. 23, 1 (1943).

at the "upper surface" of the boundary layer where v denotes as usual the velocity of the main stream of the wind. This cannot generally be achieved, but if the last condition is prescribed only to a certain accuracy consistent with the approximation under consideration, it can be done.

BLASIUS[1] has integrated PRANDTL'S boundary layer equations numerically for a particular case ($u=w=0$ for $z=0$ and $u=v$ for $x=0$ and $x=\infty$) and obtained an expression for the ground friction σ_0:

$$\sigma_0 = \frac{0.332\,\rho\,v^2}{\sqrt{\frac{v\,x}{\nu}}}. \tag{2.42-16}$$

2.43. Turbulent Flow in the Atmosphere. The theory of quasistatic flow in the atmosphere, as discussed in the last section, has relatively little importance with regard to geomorphological effects. It turns out that the air flow near the ground has to be *turbulent* if geomorphological changes are to be caused by it.

The theory of turbulent air flow near the surface of the ground is entirely analogous to the theory of turbulent flow of water near a surface. The general concepts of the statistical theory of turbulence, as outlined in Chap. 2.2, can therefore be directly applied to the flow of air. With regard to the velocity distribution near the ground, as will be discussed in more detail in Sec. 8.22, the theory is identical to that of turbulent water flow in open channels (Chap. 4.2). The details, therefore, will be discussed later in their proper context.

In all geomorphological applications, the origin of the motion of the wind or of the turbulence is of little importance, so long as its structure is known. Questions of general meteorology will therefore not be discussed here.

1. BLASIUS, H.: Z. Math. Physik 56, 4 (1908).

III. Mechanics of Slope Formation

3.1. Principles

Any cursory inspection of the shape of the surface of the Earth shows that *slopes* are the basic constituents of many features of interest. We therefore start the main part of our treatise on theoretical geomorphology with a description of what is known regarding the theory of slope evolution.

The exogenetic deformation of any slope starts with the *reduction* (i.e. decay) of the constituent material. This reduction may be chemical (corrosion), physical or even biological. The various possibilities will be discussed in Sec. 3.2.

After the material on a slope has been loosened up, further development takes place by the *removal* of the loose pieces from their original position. This removal may occur *spontaneously* (Sec. 3.3) or it may be due to the action of *various agents.* The agents that are able to remove material from a slope will be discussed in Sec. 3.4. The combined effect of all these agents upon a slope produces *slope denudation.* It is here that mathematical analysis has been most widely employed. The Section in question (3.5) will therefore be the most interesting one in the present Chapter (3) for the theorist.

Finally, endogenetic effects upon the development of slopes will be briefly discussed (Sec. 3.6). However, problems of mountain building, folding etc. will not be described here as they belong into a treatise on geodynamics rather than into one on geomorphology.

3.2. Reduction of Rocks

3.21. General Remarks. The effect of exogenetic agents upon the shaping of the Earth's surface is mostly a *destructive* one: Features built up by endogenetic processes are worn down and destroyed.

The destructive action of the exogenetic forces begins with the *reduction* of rocks. By "reduction" we mean the breaking up of the solid material of the Earth's surface into small particles which are subsequently susceptible to removal by a variety of transporting agents.

The processes that bring about the reduction of the rocks may be of diverse natures. Most effective are probably chemical processes which

alter the composition of the rocks so that actual *corrosion* is the result (Sec. 3.22). Next in line are physical processes. These, again, fall into a variety of categories. Thus, the *physical drag* (Sec. 3.23) of flowing water may be sufficient to separate loosely coherent substances into small particles. If the physical drag is exercised by "flowing" débris over a substratum, it has been termed *corrasion. Splattering action of raindrops* (Sec. 3.24) represents another type of physical rock reduction. The impact of rain may loosen up soil particles, and ready them for further transportation.

A peculiar form of reduction of rocks is due to *cavitation* in flowing water (Sec. 3.25). The term "cavitation" refers to the formation of bubbles which occur when the hydrodynamic forces in the fluid are so great that the local pressure becomes smaller than the vapor pressure. The destructive action of cavitation is probably due to the shock waves created when the bubbles collapse.

Another type of rock reduction owing to a physical process is due to *freezing* and *thawing* (Sec. 3.26) of water contained in the pores and cracks of the rock. This process can be very effective in destroying materials.

Other physical processes causing rock weathering will be discussed in Sec. 3.27.

Finally, rock reduction can also be brought about by plants and animals (Sec. 3.28).

We shall discuss the various modes of rock reduction in their turn below.

3.22. Chemical Effects. The decomposition of materials of the Earth's crust may occur by *chemical* weathering. This type of weathering always involves some reaction of water with the rock material. There are several reactions which are of particular importance with regard to geomorphology.

(i) *The Dissolution of Limestone.* It is well known that water can dissolve limestone (consisting mostly of $CaCO_3$)[1]. However, pure water has relatively little effect; the speed of the reaction is greatly enhanced if carbon dioxide is present in the water (the calcium carbonate is then slowly transformed into calcium bicarbonate and removed). If salts are present in the water, the dissolution of limestone becomes very complicated as complexing reactions may occur. This process is of some importance in connection with the development of coasts (cf. Sec. 6.33).

(ii) *The Breakdown of Feldspars into Clay Minerals*[2]. Clay formation occurs when slightly carbonated water comes into contact with plagioclase and similar minerals; the sodium (or, in other cases, calcium or po-

1. Ingle-Smith, D., and D. Mead: Proc. Univ. Bristol Speleolog. Soc. **9**, 188 (1962)
2. Heydemann, A.: Geochim. et Cosmochim. Acta **30**, 995 (1966).

tassium) is thereby removed from the feldspars and only the silicium and aluminium are left in the end product. The latter is clay.

(iii) *The Oxydation and Chemical Hydration* of many minerals. The phenomenon of serpentinization belongs into this category. Granites[1,2] and other igneous rocks[3] may decay in this fashion.

In addition to the above reactions there are many others that involve the reaction between water (containing impurities) and minerals. Many of these reactions have been studied e.g. by ROY and co-workers[4]. The details of these reactions are of little importance here as we are only concerned with the general effect of the chemical weathering phenomenon upon the morphology of the Earth's surface.

In this connection, one may note that the *geological effect* of chemical weathering is to loosen up the rock so that it can be further attacked by physical agents. In some instances, chemical weathering alone can directly produce large-scale geomorphological effects as witness the karst phenomena which are solely due to the dissolution of limestones. Chemical weathering may also have a pronounced effect upon shaping the flanks of mountain ranges as was shown by studies of HEMBREE and RAINWATER[5].

3.23. Physical Drag. Some materials of which the surface of the Earth is composed are so loose as to be almost without cohesion. In such cases, the physical drag of water flowing over these materials is by itself sufficient to separate the individual particles. This induces reduction of these materials.

The theory of the drag exercised by flowing water upon individual particles will be discussed in full in Sec. 4.43, in connection with an analysis of river bed processes, where it is of utmost importance.

If the physical drag is exercised by débris moving over a substratum it has been termed *corrasion*. This occurs mostly on mountain sides where rubble moves over rock strata below. The physical action of the rubble upon the rock is destructive as material is being abraded and the rock thus is being reduced.

3.24. Splattering of Drops. A notable denudational effect, particularly in soils, is caused by the *impact and splattering of raindrops*. This phenomenon has been studied by agricultural engineers and people connected

1. BAKKER, J. P.: Z. Geomorphol, Suppl. 1, 69 (1965).

2. BAKKER, J. P.: In: L'évolution des versants, ed. P. MACAR, vol. 1 of Symposium internat. de géomorphologie, Liège, 1967, p. 51.

3. NOSSIN, J. J., and T. W. M. LEVELT: Z. Geomorphol. 11, 14 (1967).

4. See e.g. NELSON, B. W., and R. ROY: Amer. Mineral. 43, 707 (1958); where further references may be found.

5. HEMBREE, C. H., and F. H. RAINWATER: Chemical Degradation on Opposite Flanks of the Wind River Range, Wyoming. Pap. Symp. Quantitative Terrain Studies, Chicago (Amer. Assoc. Adv. Sci) (1959).

with soil science, beginning with some pioneering work of ELLISON[1]. A good review of the current state of the work has been given by SMITH and WISCHMEIER[2].

The mechanics of loosening soil by raindrop impact involves two processes: first, particles are detached by direct impact and then they are dislodged a small distance by the splash.

Unfortunately, the mechanism of the impact of raindrops upon soil is very complicated and it appears as almost hopeless to try to construct a satisfactory theory thereof. Most of the investigations, therefore, have been directed toward establishing empirical correlations between the amount of soil loosened and several of the variables that one might assume as being important.

The first such variable which might come to one's mind is the *energy* of the raindrops. Most experimental studies attempt to establish universal curves purporting to show the raindrop energy *versus* the amount of soil loosened; such studies have been reported for instance by WOODBURN[3] and by EKERN and co-workers[4–6]. It was found as essential to specify the drop shape at the time of impact in order to come up with unequivocal relationships.

A different type of correlation has been sought after by ROSE[7]. ROSE plotted the amount of soil removed against the *momentum* (rather than the energy) of the rain. The correlation thus obtained is nonlinear. A typical result obtained by ROSE for a particular type of soil is shown in Fig. 40.

The above two hypotheses, viz. (i) that the erosive action (per unit time) of rain is proportional to the energy expended by the rain (per unit time) and (ii) that the erosive action of the rain (per unit time) is proportional to the momentum of the rain (per unit time) can be formulated mathematically as follows[8]

$$\text{(i)} \qquad Q = C q \rho v^2, \tag{3.24-1}$$

$$\text{(ii)} \qquad Q = C q \rho v \tag{3.24-2}$$

where Q is the rate of erosion (g/cm^2 sec), q the rate of rainfall (cm/sec), v the terminal velocity of the rainfall (cm/sec), ρ the mass density (g/cm^3) and C a constant.

1. ELLISON, W. D.: Agr. Eng. **28**, 145, 197, 245, 297, 349 (1947).
2. SMITH, D. D., and W. H. WISHMEIER: Adv. in Agronomy (Academic Press, N. Y.) **14**, 109 (1962).
3. WOODBURN, R.: Agr. Eng. **29**, 154 (1948).
4. EKERN, P. C., and R. J. MUCKENHIRN: Proc. Soil. Sci. Soc. Amer. **12**, 441 (1947).
5. EKERN, P. C.: Proc. Soil Sci. Soc. Amer. **15**, 7 (1951).
6. EKERN, P. C.: Agr. Eng. **34**, 23 (1953).
7. ROSE, C. W.: Soil Sci. **89**, 28 (1960).
8. SCHEIDEGGER, A. E.: Geofis. pura e appl. **56**, 58 (1963).

The above results are altered by the emergence of additional effects. The soil erosion can be slowed down by the formation of surface crusts [2, 3] which are harder than the material below. The formation of such crusts is due to the washing-in of fine particles into the pores of the soil and to surface-compaction of the latter. Similarly, if the rain is strong enough for a surface film of water to form upon the soil, the impact of the raindrops will no longer be directly affecting the soil below, but set up turbulent

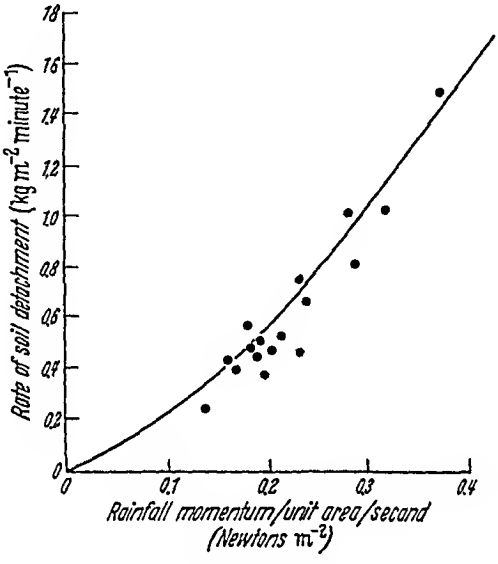

Fig. 40. Correlation between rainfall momentum and erosion for a particular soil. After ROSE [1]

motions in the water film already present. This will again cause soil erosion but of a different type than that considered above. A preliminary study of this process has been reported by KURON and STEINMETZ [4]. Unfortunately no quantitative estimates of this effect are as yet available.

As may be seen from an inspection of the above remarks, the phenomenon of soil erosion due to raindrop splattering is only qualitatively understood. For every type of soil, a different diagram of the type shown in Fig. 40 is required. The results quoted above were obtained on small scale experiments. In order to obtain a more trustworthy picture, ILLNER [5] laid out plots of land of various sizes, with and without vegetation, upon an inclined slope and measured the denudation during natural and arti-

1. ROSE, C. W.: Soil Sci. 89, 28 (1960).
2. MCINTYRE, D. S.: Soil Sci. 85, 185 (1958).
3. MCINTYRE, D. S.: Soil Sci. 85, 261 (1958).
4. KURON, H., and H. J. STEINMETZ: C. R. Assemb. Gen. Toronto, Assoc. Hydrol. Scient. 1, 115 (1957).
5. ILLNER, K.. Wiss. Z. Humboldt-Univ. Berlin 6, No. 4, 417 (1956).

ficial rainfalls. However, no attempts at any type of correlation were made; the results are simply reported as they were measured.

In summary, we may note that raindrop splattering has a pronounced erosional effect upon naked soil. For any particular soil, a useful correlation can be obtained between the amount of soil removed and the momentum of the rain. However, generalizations for *various* soil types cannot be made. A plant cover will effectively prevent raindrop erosion so that the phenomenon under discussion is of great importance only under circumstances where the natural state of the Earth's surface has been disturbed. An empirical "soil-loss" equation taking the type of plant cover into account, has been proposed by WISCHMEIER[1].

3.25. Cavitation. A peculiar form of denudation can occur owing to *cavitation* in rapidly moving water. Cavitation, i.e. the formation of bubbles, takes place if the hydrodynamic forces in the fluid are so great that the local pressure becomes smaller than the vapor pressure. Cavitation is known to be of great significance in hydraulic machinery where highly deleterious effects are known to be produced by it, particularly on turbine vanes and similar structures. The cavitation phenomenon has therefore been extensively studied by mechanical engineers. Bibliographies of these studies have been compiled for instance by EISENBERG[2] and by SHAL'NEV[3]. The destructive action of cavitation is probably due to the shock waves created when the bubbles collapse.

Since cavitation is of such great significance in eroding metal surfaces of engineering equipment, it stands to reason that it also is of importance with regard to geomorphological phenomena. The geological effects that may be ascribed to cavitation have been discussed by HJULSTRÖM[4] and by BARNES[5,6].

Accordingly, bubble formation and therewith geologic action of cavitation, will occur primarily during the rapid flow of water over a slope or within a river channel. One can give an estimate of the velocity required for water flow in order to produce cavitation based upon BERNOULLI'S equation

$$\frac{v_1^2}{2g}+\frac{p_1}{\rho g}+z_1=\frac{v_2^2}{2g}+\frac{p_2}{\rho g}+z_2. \qquad (3.25\text{-}1)$$

1. WISCHMEIER, W. H.: Proc. Soil Sci. Soc. Amer. **24**, No. 4, 322 (1960).
2. EISENBERG, P.: On the Mechanism and Prevention of Cavitation. D. W. Taylor Model Basin: Navy Dept., 1950.
3. SHAL'NEV, K. K.: Izv. Akad. Nauk SSSR, Otd. Tekh. Nauk 1956, No. 1, 3 (1956).
4. HJULSTRÖM, F.: Bull. Geol. Inst. Uppsala **25**, 221 (1935).
5. BARNES, H. L.: Bull. Geol. Soc. Amer. **64**, 1392 (1953).
6. BARNES, H. L.: Amer. J. Sci. **254**, 493 (1956).

This equation must be valid along any streamline if one neglects energy dissipation due to turbulence or bottom friction. In (3.25-1) v_1 is the flow velocity, p_1 the pressure, z_1 the height of the stream line above an (arbitrary) datum level and v_2, p_2 z_2, are the corresponding values at the cavitation point. In the latter, one has p_2 equal to the vapor pressure (p_D) of the water. Let us now consider (with HJULMSTRÖM) a case where the water at one point is at rest ($v_1 = 0$) and the corresponding pressure is the atmospheric pressure ($p_1 = p_{atm}$). These conditions will apply to the surface element of a puddle of water. If we neglect gravity, cavitation will occur if v_2 reaches the value

$$v_2 = \sqrt{\frac{2(p_{atm} - p_D)}{\rho}}. \tag{3.25-2}$$

From this, HJULSTRÖM calculated that v_2 must equal 14.3 m/sec for $p_{atm} = 760$ mmHg at 0° C. A similar calculation was made by BARNES who considered streamlines in which the maximum flow velocity v_2 is $2v_1$, v_1 denoting the initial flow velocity on the streamline. Again taking $p_1 = p_{atm}$ as initial pressure, he then calculated the initial flow velocity v_1 required to produce cavitation and obtained from (3.25-1), discounting gravity:

$$v_1 = 8.1 \text{ m/sec}. \tag{3.25-3}$$

The result of the above investigation is that the flow velocity of water has to be rather high in order to produce cavitation. Such flow velocities can be realized in waterfalls and in rapids. Potholes near glacier margins may have been caused by miniature waterfalls. Since the erosive action of cavitation is very great, such waterfalls need not exist for a very long time to start the holes.

Since most water flow in nature is turbulent and not laminar, the use of the Bernoulli equation (3.25-1) is, strictly speaking, not justified. However, as long as only orders of magnitude are involved in the velocity estimates, it stands to reason that the latter are acceptable in spite of the obvious energy dissipation.

3.26. Temperature Effects. If water invades surface cracks and pores of rocks and freezes therein, the latter become very quickly destroyed. This is due to the fact that ice occupies a greater volume than the same mass of water which results in tremendous pressures being built up within the invaded rock.

It turns out that in many instances, the actual displacements caused by water freezing in the surface material of the Earth are much greater than can be explained simply by assuming that the volume expansion is solely due to the volume increase undergone by the water contained in the material in question when it becomes ice. This phenomenon is particularly

well known from the frost-heaving experienced under many circumstances. Therefore, a destructive process in addition to the simple volume expansion of the water must be at work. Because of the importance of frost heaving in connection with many construction projects, the phenomenon has been studied by various people for some time[1–3]. The efforts of engineers have been mostly to get experimental criteria with regard to whether or not a certain type of soil will exhibit frost heaving[4, 5].

The characteristic feature of frost heaving lies in the fact that layers of ice (often called ice lenses) may form within a water-saturated porous medium, without the water freezing in the adjacent pores. An ice lens keeps growing by the addition of water which is being drawn from the porous medium. There are two theories of this process of which the writer is aware. The first is due to JACKSON and CHALMERS[6] based on nucleation theory, and the second is due to GOLD[7], based on capillary equilibrium. Some thermodynamic relationships for soils near the freezing point have also been published by LOW et al.[8]. A lengthy discussion of the theories available has also been published by MARTYNOV[9].

We shall discuss first the theory of JACKSON and CHALMERS. Accordingly, one must take the interfacial tensions between water, ice and the rock into account. One has generally

$$\sigma_{LB} = \sigma_{SB} + \sigma_{LS} \cos \alpha \tag{3.26-1}$$

where σ_{SB}, σ_{LB} and σ_{SL} are the interfacial tensions (interfacial energies) between the solid-rock, liquid-rock and solid-liquid interfaces, respectively; α is the contact angle.

According to nucleation theory, the initiation of solidification can occur in a capillary of radius r at a temperature T^* given by

$$T^* = T_E + \frac{\sigma_{LS} T_E \cos \alpha}{L r}, \tag{3.26-2}$$

where T_E is the usual equilibrium temperature and L the latent heat. It should be noted that, for $\cos \alpha$ negative, T^* will lie below T_E. This case occurs in the water-ice system where $\alpha = 180°$.

1. TABER, S.: J. Geol. 37, 428 (1924).
2. RUCKLI, R.: Der Frost im Baugrund. Vienna: Springer 1950.
3. JUMIKIS, A. R.: The Frost Penetration Problem in Highway Engineering. New Brunswick, N. J.: Rutgers Univ. Press 1955.
4. PENNER, E.: Bull. Highway Res. 135, 109 (1956).
5. BALDUZZI, F.: Experimentelle Untersuchungen über den Bodenfrost. Zürich: Mitt. Vers. Anst. Wass. Erdbau. No. 44 (1959).
6. JACKSON, K. A., and B. CHALMERS: J. Appl. Physics 29, 1178 (1958).
7. GOLD, L. W.: Bull. Highway Res. 168, 65 (1958).
8. LOW, P. F., P. HOEKSTRA, and D. M. ANDERSON: Water Resources Res. 4, 379, 541 (1968).
9. MARTYNOV, G. A.: In: Основы геокриологий. Acad. Sci. Moscow 1959. See Pt. 1, Chap. VI therein.

In a porous medium which may be regarded as an assemblage of capillaries, freezing will not be initiated until the temperature T^* is reached. Once this has happened, a nucleus will form which will rapidly grow to an ice lens, since T^* is below the equilibrium freezing temperature T_E – i.e. since the water in the system is supercooled. Water will be drawn from wherever it is available to let the ice lens grow. Thus, volume expansions much greater than those corresponding to the freezing of the water originally contained in the pores, may occur.

The reasoning of GOLD to explain the occurrence of frost heaving is similar to that of JACKSON and CHALMERS, but the rôle of the freezing-temperature depression due to the prevention of nucleation is replaced by a direct shifting of the freezing-temperature due to capillary forces. It

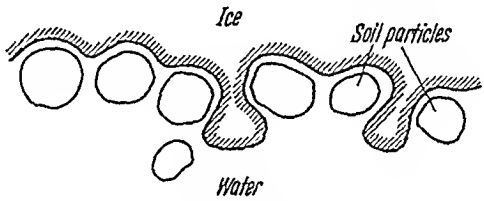

Fig. 41. Ice-water interface in a porous medium. After GOLD[1]

turns out that parts of the ice-water interface in the pores which are convex toward the water with a large radius of curvature will grow more rapidly than parts with a smaller radius of curvature. Thus, a picture as shown in Fig. 41 will result. This represents frost heaving.

Temperature changes may also cause a reduction of rocks without the help of the action of frost. The thermal expansion and contraction caused by extreme temperature variations may be sufficient to have a deleterious effect, although at a lower rate than if frost occurs. One may thus get actual thermal fragmentation of rocks[2] or be faced with dirt-cracking[3].

3.27. Other Physical Effects. In addition to the physical effects mentioned above, there are other such effects. An important one is aeolian abrasion[4, 5], in which rocks are blasted by windborne particles (usually sand) and thereby destroyed. This is the well-known sand-blasting action occurring mostly in deserts.

Another physical process is weathering by impact of extra-planetary objects[6]. As a landscape-forming process this is rather insignificant on

1. GOLD, L. W.: *Bull. Highway Res. 168, 65 (1958).*
2. MAROVELLI, R., T. S. CHEN, and K. F. VEITH: Trans. Soc. Mining Eng. 235, 1 (1966).
3. OLLIER, C. D.: Austral. J. Sci. 27, 236 (1965).
4. KUENEN, P. H., and W. G. PERDOK. Proc. Koninkl. Akad. Wetenschap. Amsterdam B 64, 343 (1961).
5. KUENEN, P. H , and W. G PERDOK: J. Geol. 70, 648 (1962).
6. ROBERTS, W. A.: Icarus 5, 459 (1966).

the Earth in contrast, for instance, to on the Moon; however, the occurrence of craters caused by meteor impact associated with much destruction in the surrounding landscape, is well known.

The final physical process to be considered here is "weathering" due to the action of tectonic stresses [1]: Every rock mass is subject to a tectonic stress field; upon exposure of such rock masses to the surface, stress concentrations may occur which have a very wide-spread destructive effect on these rocks. This is particularly noticeable in the decay pattern of steep rocky walls and mountain peaks.

3.28. Biological Effects. Finally, it should be noted that life also may cause the reduction of rocks. Burrowing animals, such as earth-worms and rodents may make the rock susceptible to destruction, and plants may push their roots into rock cracks so as to cause their widening. Various forms of life also affect the chemistry of the environment (e.g. fungi causing the addition of carbon dioxide to the water), which then will exhibit a different chemical action upon the rocks than it would otherwise. Mostly, however, life in the form of vegetation acts as a protecting agent inhibiting the speed of denudation that would take place without it.

3.3. Spontaneous Mass Movement

3.31. Rankine States. The materials that form the land-surface of the Earth, such as earth, soil and rock, are in the solid state of aggregation. Our aim is to understand the deformations that they may undergo. The general investigation of the deformation in "solid" materials is the subject of the science of *rheology*. The application of this to soils etc. is the subject *of soil mechanics* [2, 3].

A general review of the mechanics of deformation, as it is of interest to Earth scientists, has been given by the writer [4] on an earlier occasion. We shall concern ourselves here only with those aspects of the theory that have a direct bearing on geomorphological problems. This concerns the stability of masses of rock débris and soil which can be described satisfactorily by means of a form of plasticity theory. Accordingly, as long as a pile of material is stable, it obeys the conditions of elasticity theory. Motion occurs if the shearing limit is being reached. The shearing limit s is satisfactorily expressed by COULOMB's empirical equation which reads (see TERZAGHI [2])

$$s = \sigma \tan \Phi + c \qquad (3.31\text{-}1)$$

1. GERBER, E., and A. E. SCHEIDEGGER: Ecl Geol. Helv. **62**, No. 2 (1969)
2. TERZAGHI, K.: Theoretical Soil Mechanics. New York: J. Wiley & Sons 1943.
3. JUMIKIS, A. R.: Introduction to Soil Mechanics. New York: Nostrand 1967.
4. SCHEIDEGGER, A. E.: Principles of Geodynamics. Second Ed. Berlin-Göttingen-Heidelberg: Springer 1963. See p. 132ff.

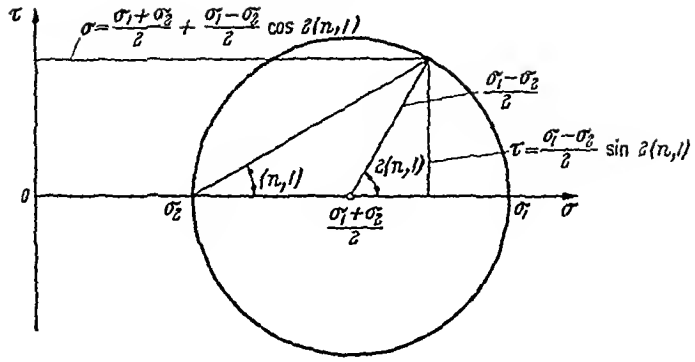

Fig. 42. Mohr circle for a two-dimensional stress state

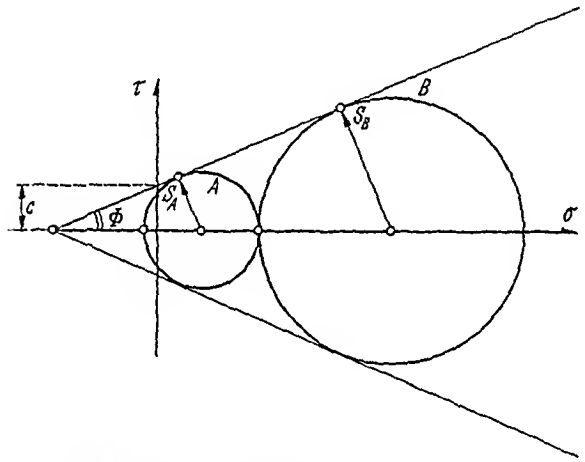

Fig. 43. Active and passive Rankine states

where c is indicative of the cohesion of the material, σ signifies the normal stress and Φ is commonly called the *angle of internal friction.*

The stress state at any one point in a material can easily be expressed by means of MOHR's circle[1]. For a two-dimensional stress state, MOHR's circle is shown in Fig. 42. In this Figure, it is assumed that the **1**-direction corresponds to a principal stress direction (shear stress τ zero, normal stress σ_1). If the normal stress in a direction normal to **1** be σ_2, then MOHR's circle is defined and can be drawn as shown in Fig. 42. The normal stress σ and shear stress τ acting on a surface element which forms the angle $(n, 1)$ with the direction **1**, are then read off from MOHR's circle as demonstrated in Fig. 42.

The limiting shear stress condition (3.31-1) of COULOMB is represented in MOHR's diagram by two lines (see Fig. 43). So long as the stress state is such that the corresponding Mohr circle does not touch these lines, the

1 MOHR, O.: Abhandlungen aus dem Gebiete der technischen Mechanik, 3. Aufl. Berlin: W. Ernst & Sohn 1928

material is in a stable condition. If the Mohr circle touches the limiting shear lines, the material is said to be in a *Rankine*[1] *state of plastic failure.* The stress state can never become such that the corresponding Mohr circle would *intersect* the limiting shear stress lines since motion will take place during which the mass will always be in a Rankine state.

If the normal stress acting on an element in the 1-direction is given, then there are two Rankine states of failure possible which are represented in Fig. 43 by the Mohr circles A and B. They are called *active* and *passive* Rankine states, respectively. The limiting shear (cf. 3.31-1) in these states is attained in elements represented by the arrows S_A and S_B; they are oriented in a direction that subtends an angle $\pm\left(45°+\frac{\Phi}{2}\right)$ and $\pm\left(45°-\frac{\Phi}{2}\right)$ towards the 1 direction, respectively. These directions are tangent to the *shear-lines of failure.*

There are two extreme cases of substances which may be considered here. The first occurs if $c=0$ so that Eq. (3.31-1) yields

$$s=\sigma \tan \Phi. \tag{3.31-2}$$

This corresponds to cohesionless materials, such as sands or piles of gravel. However, even sands may have a little cohesion, particularly if they are moist. If one forms a pile with *completely dry* sand, the material will slide and not come to rest until the angle of inclination of the slopes becomes equal to a certain angle which is called the *angle of repose.* This angle of repose is equal to the angle of internal friction if the sand is in its *loosest state.* For loose, dry sand the angle of repose is independent of the height of the slope. This can easily be demonstrated as follows. Assume a slope angle β and take a surface slice of material of length x (from the top of the slope) and height dh. (see Fig. 44). The force normal to the bed is then

$$F_n=x\,\rho\,g\,dh\,W\cos\beta \tag{3.31-3}$$

where W is the width of the slope and ρ, g are the density and gravity acceleration, respectively. If the slope is stable, but just on the verge of instability, then the forces parallel to the bed must exactly balance each other. These forces are the downslope component of the weight of the slice, and the frictional force. Thus (using 3.31-2)

$$x\,\rho\,g\,dh\,W\cos\beta\tan\Phi=x\,\rho\,g\,dh\,W\sin\beta \tag{3.31-4}$$

or

$$\cot\beta\tan\Phi=1 \tag{3.31-5}$$

and thus

$$\beta=\Phi \tag{3.31-6}$$

1. Rankine, W. J. M.: Phil. Trans. Roy. Soc. **147** (1857).

independently of the height of the slope, which is what was to be demonstrated.

For compacted sand or packed gravel the above relationship is no longer true because the formula for friction (3.31-2) does not hold for packed materials. The resistance to shearing motion in this case depends on the packing. It is then possible for two angles of repose to exist: One which corresponds to the slope angle at which sliding masses come to rest, and another, larger one, which corresponds to the slope at which stacked masses begin to slide.

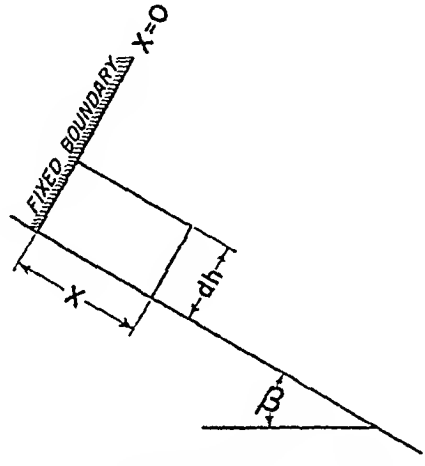

Fig. 44. Geometry of a slope

As noted, the above remarks refer to cohesionless substances. The other extreme case, mentioned earlier, is obtained if in Eq. (3.31-1) Φ is set equal to zero. This leads to the classical theory of plasticity[1]; the envelopes of the critical MOHR circles in the two-dimensional case are then straight lines parallel to the 1-axis. Wet clays show a behavior which fits this kind of description very well.

3.32. Stability of Slopes. The general principles of the stability of masses will now be applied to a discussion of the stability of slopes. Thus let us consider a slope bank of slope angle β and height h consisting of some material having certain values for the parameters c and Φ. The question is: What are the conditions for such a slope to become unstable[2]?

An excellent review of the possible methods to obtain answers to the above question has been given by CARILLO[3]. Accordingly, it has been

1. HILL, R.: The Mathematical Theory of Plasticity. Oxford: Clarendon Press 1950.

2. The practical implications of this problem have been discussed, for instance, by MÜLLER, L.: Geologie u. Bauw. 25, 203 (1960).

3. CARILLO, N.: Investigations on Stability of Slopes and Foundations. D. Sc. Thesis, Cambridge, Mass.: Harvard Univ. 1942

observed that an earth bank may become unstable in two ways; these have been termed *slope failure* and *base failure*. Base failure is caused by failure in the supporting base of the slope, whereas slope failure represents a collapse of the slope itself. We are concerned here only with slope failure since it bears out the possible events sufficiently accurately.

The crudest analysis of the stability of a slope is based on the assumption that the entire sliding portion is in an active Rankine state. The situation is illustrated in Fig. 45 for a vertical bank[1]. In this case, the po-

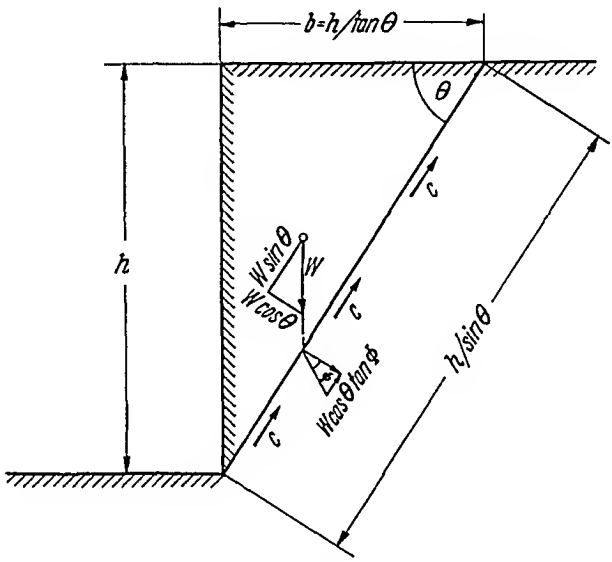

Fig. 45. Stability analysis of a vertical slope. Modified after TSCHEBOTARIOFF[1]

tential surface of sliding is inclined at an angle of $\Theta = 45° + \Phi/2$ towards the horizontal and the equilibrium condition along it can be formulated as follows. The weight W of the sliding slice per unit width is (where ρ, g denote density and gravity acceleration, respectively):

$$W = \frac{\rho g h^2}{2 \tan(45 + \Phi/2)}. \tag{3.32-1}$$

The component of W parallel to the sliding surface is

$$W_{\text{slide}} = W \sin(45 + \Phi/2) \tag{3.32-2}$$

and that normal to the sliding surface is

$$W_{\text{normal}} = W \cos(45 + \Phi/2). \tag{3.32-3}$$

1. TSCHEBOTARIOFF, G.: Soil Mechanics, Foundations and Earth Structures. New York: McGraw-Hill Book Co. 1952. See p. 169 ff.

The equilibrium condition for failure (COULOMB's equation, cf. 3.31-1) yields

$$W_{\text{slide}} = W \sin\left(45+\frac{\Phi}{2}\right) = \frac{c\,h}{\sin(45+\Phi/2)} + W\cos\left(45+\frac{\Phi}{2}\right)\tan\Phi. \quad (3.32\text{-}4)$$

Inserting the value for W and making an algebraic transformation yields for the *critical height* h_{cr} at which the bank becomes unstable

$$h_{cr} = \frac{4c}{\rho g}\tan(45°+\Phi/2). \quad (3.32\text{-}5)$$

As noted above, the theory leading to (3.32-5) is somewhat crude. It has, in fact, been observed that the surface of sliding is not plane but curved. As heuristic approximation, one might therefore assume it as cylindrical with a circular cross section[1]. This leads to the picture shown in Fig. 46. The potential circle of sliding is given by the chord angle α and the center angle 2Θ. The equations for stability are then determined by formulating the equilibrium conditions for the moments around the

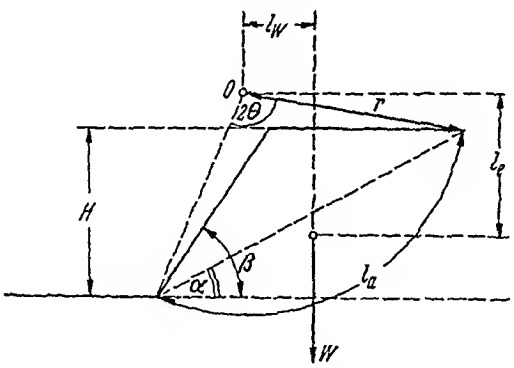

Fig. 46. Slope failure along a critical toe circle

point 0 (in Fig. 46). Assuming the angle of friction to be zero, the only force opposing sliding is that due to the cohesion c. The equilibrium condition is then[2]

$$W l_w - c\, l_a\, r = 0 \quad (3.32\text{-}6)$$

where l_a is the length of the arc. One can solve this for c which yields

$$c = W\frac{l_w}{r\, l_a}. \quad (3.32\text{-}7)$$

1. PETTERSON, K. E.: Tekn. Tidskr. 46, 289 (1916).
2. TERZAGHI, K.: Theoretical Soil Mechanics. New York: J. Wiley & Sons 1943. See p. 155.

The last equation can be regarded to be an expression for the cohesion c required to maintain stability. One can insert the various geometrical quantities in Fig. 46 into it and one then obtains an expression of the form

$$c = \rho g h \frac{1}{f(\alpha, \beta, 0)} \tag{3.32-8}$$

where h, β are the height and slope angle of the slope, respectively, and f denotes a certain function of α, β, Θ. Failure in a given slope would occur around such a circle that c is a minimum, i.e.

$$\frac{\partial c}{\partial \alpha} = \frac{\partial c}{\partial 0} = 0 \tag{3.32-9}$$

since β is fixed. This equation can be solved analytically and one thus obtains the "critical toe circle" for the failure of a slope. For each critical toe circle, one has a connection between c and h; hence one can determine the critical height h_c for any value of the cohesion c and slope angle β. The connection has the form

$$h_c = \frac{c}{\rho g} N_s \tag{3.32-10}$$

where N_s is a *stability factor*, depending on the slope angle β only. The calculations sketched above have been carried out by FELLENIUS[1]; his results are represented in the graph shown in Fig. 47. The constants α and Θ of the corresponding toe circles are shown in Fig. 48.

FELLENIUS also carried out calculations for a friction angle $\Phi \neq 0$. The stability factor $N_{\Phi S}$ tends to infinity for $\beta \to \Phi$; i.e., as long as the slope angle β is smaller than Φ, the slope can be made arbitrarily high. The results of the calculations of FELLENIUS are also shown in Fig. 47.

The above theory has been modified to allow for sliding surfaces which are different from circles. Thus, RENDULIC[2] has used logarithmic spirals and formulated a theory which is analogous to that of FELLENIUS. It can be shown[3], however, that the results differ only negligibly from those obtained by using circles.

Slope stability calculations based upon the above theories have also been made for complicated conditions, such as layered and anisotropic soils[4, 5]. In such cases, the use of computers has to be resorted to[6].

1. FELLENIUS, W.: Erdstatische Berechnungen. Berlin: W. Ernst & Sohn 1927.
3. RENDULIC, L.: Der Bauingenieur **16**, 230 (1935).
3. TAYLOR, D. W.: J. Boston Soc. Civ. Eng. **24**, 226 (1937).
4 HORN, J. A.: Proc. Amer. Soc. Civ. Eng. **86**, SM 3 (J. Soil. Mech. Found. Div.) 1 (1960).
5. LO, K. Y.: Proc. Amer. Soc. Civ. Eng. **91**, SM4 (J. Soil Mech. Found. Div.), pt. I, 85 (1965).
6. WHITMAN, V , and W. A. BAILEY: Proc. Amer. Soc. Civ. Eng. **93**, SM 4 (J. Soil Mech. Found. Div.) 475 (1967).

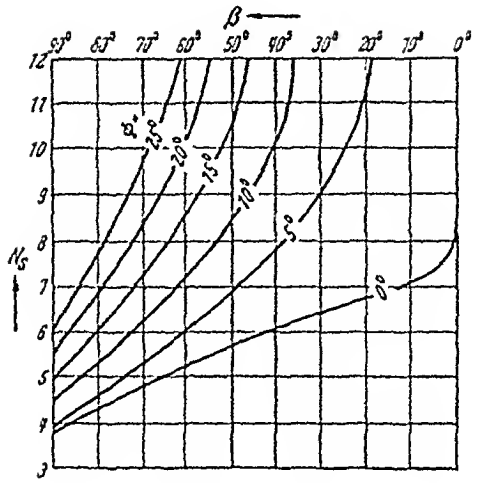

Fig. 47. Stability factors as a function of slope angle for various values of Φ

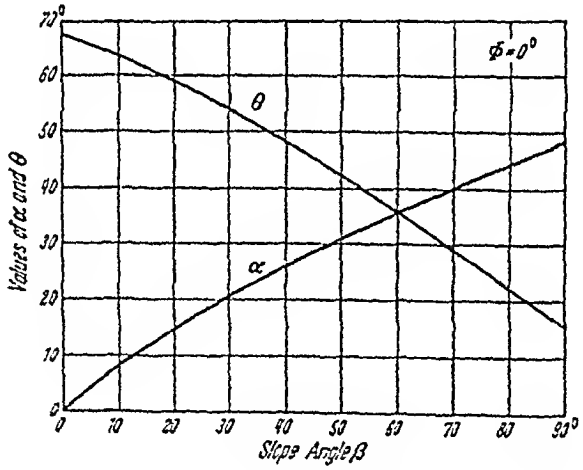

Fig. 48. The angles x and θ of the critical toe circle for $\Phi=0$. After FELLENIUS[1]

In conclusion of the present Section on slope stability, we may mention some work by TROLLOPE and co-workers[2,3] who approached the stability problem from a microscopic standpoint. They considered the *arching* effect in regular piles of spherical grains.

3.33. Landslides. The considerations about the stability of slopes which were presented in the last Section (3.32) lend themselves to an application to the phenomenon of landslides. Landslides are a type of

1. FELLENIUS, W.: Erdstatische Berechnungen. Berlin: W. Ernst & Sohn 1927.
2. TROLLOPE, D. H.: Proc. 4th Conf Soil Mech. & Found. Eng. 2, 387 (1957).
3. TROLLOPE, D. H., and J. R. MORGAN: Inst. Eng. Australia, Civ. Eng. Trans. CE 1, No. 1, 18 (1959).

rapid mass-movement which may suddenly occur on a slope. During the movement, the center of gravity of the moving mass moves downward and outward with a velocity increasing from zero to at least 1 m in 3 hours. A discussion of landslides in phenomenological terms has for instance been given by SHARPE[1] in a monograph which contains many references to descriptions of individual slides.

Any attempt at a theoretical explanation of landslides has to account for the fact that slides may occur on slopes that have been stable for a long time, sometimes for many thousands of years. Thus, if a slide occurs,

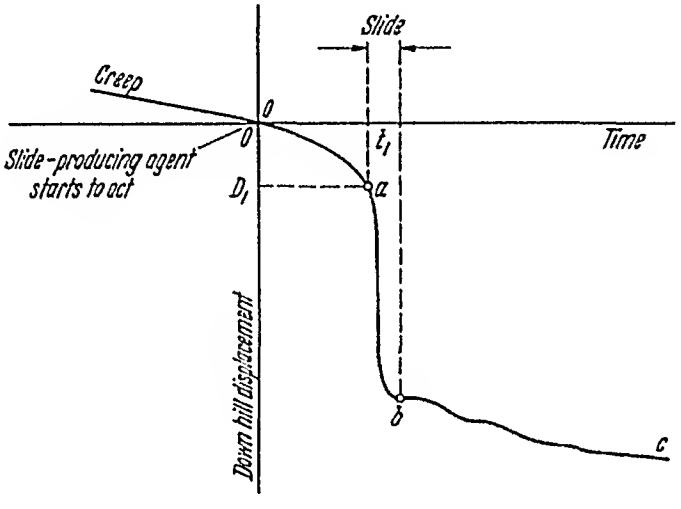

Fig. 49. Graph of the downhill motion just prior to, during and after a landslide. After TERZAGHI[2]

there must have been an agent which caused a decrease of the stability of the slope so as to make it collapse. In every landslide, there must therefore be a *direct mechanical cause.*

Once such an agent has caused a slope to become unstable, the latter will collapse. Little is known with regard to the actual dynamics of a landslide from a theoretical standpoint. TERZAGHI[2], has presented an empirical graph of the motions just prior to, during and after the actual slide (see Fig. 49). The slippage must be thought to take place along the critical toe circle, inasmuch as the latter is an acceptable approximation to the surface of sliding (cf. Sec. 3.32). The final result of a slide is as shown schematically in Fig. 50.

A good review of the possible mechanical causes (in the sense mentioned above) of landslides has been given by TERZAGHI[2]. Accordingly, one has to distinguish between *external and internal* causes of landslides.

1. SHARPE, C. F. S.: Landslides and Related Phenomena. New York: Columbia University Press 1938.

2 TERZAGHI, K.: Geol. Soc. Amer. Engineering Geology (Berkey) Volume, p. 83 (1950).

The external causes create an increase of the shearing stresses in the slope. They include e.g. the undercutting of the slope by a river, the effect of an earthquake shock and the deposition of material at the upper edge of the slope. Internal causes are those that create a decrease of the shearing resistance of the material. This may occur without a visible change of the conditions affecting the slope (hence their name) and may be due to an increase of the pore-water pressure or to a progressive decrease of the cohesion of the slope material.

TERZAGHI[1] discusses the various possibilities as follows.

A. Increase of Slope Steepness. A river undercutting a slope bank will generally cause the slope to collapse. This is simply due to an overall increase in slope angle which eventually may reach such a value so that the

Fig. 50. Schematic drawing of the final result of a landslide. After TERZAGHI[2]

stability criterion is no longer satisfied. A similar situation occurs if material is deposited at the upper edge of the slope, but this is rare under natural conditions although it is common enough in bad engineering practice. As soon as the stability condition is no longer satisfied, a slide will occur. According to earlier remarks the slide will consist in a slippage along the critical toe circle and the result will be as shown in Fig. 50.

B. Earthquakes. Another external cause of landslides may be represented by earthquakes[3,4]. The equilibrium condition for a slope has been given in Eq. (3.32-6). One can define a "safety factor" G for the slope by forming the quotient of resisting moment and driving moment (for an explanation of the symbols, cf. Fig. 46):

$$G = \frac{c\, l_a\, r}{W\, l_w}. \tag{3.33-1}$$

A slide will occur if $G < 1$ in conformity with the equilibrium condition (3.32-6).

1. TERZAGHI, K.: Geol. Soc. Amer. Engineering Geology Volume (Berkey Vol.) 83 (1950).

2. TERZAGHI, K.: Theoretical Soil Mechanics New York: J. Wiley & Sons 1943.

3. Examples are given e.g. in GLUKHOV, I. G.: Vestnik Moskovsk. Un-ta No. 4, 143 (1959).

4. SEED, H. B.: Proc. Amer. Civ. Eng. 93, SM 4 (J. Soil Mech. Found. Div.) 299 (1967).

An earthquake produces a horizontal acceleration g_e so that the equilibrium condition now reads: (cf. Fig. 46)

$$W l_w - c l_a r + \frac{W}{g} g_e l_e = 0. \tag{3.33-2}$$

Defining again a safety factor as the quotient between resisting moment and driving moment, we have during the earthquake

$$G' = \frac{c l_a r}{W(l_w + l_e g_e/g)}. \tag{3.33-3}$$

A side will occur if during the earthquake if $G' < 1$. For catastrophic earthquakes, g_e may reach $\frac{1}{2} g$. Thus the lowering of the safety factor evident in formula (3.33-3) explains how landslides may be caused by an earthquake.

C. Pore Water Pressure. Turning now to the *internal causes* of landslides, we note that the most common such cause is an increase in pore water pressure (piezometric landslides). In a water-saturated assemblage of grains, the relation for the shearing resistances (to failure) of a water-filled earth-material is (after TERZAGHI and PECK[1]):

$$s = c + (p_t - p_w) \tan \Phi \tag{3.33-4}$$

where c is the cohesion as before, p_t is the total earth pressure (due to the weight of the earth material and the water contained therein), p_w is the pore-water pressure ($= \rho g H$ with ρ density of the water, g the gravity acceleration and H the "hydraulic head") and Φ as usual, the angle of internal friction. Eq. (3.33-4) is based upon the notion that it is the "effective pressure" $p_t - p_w$ which determines the deformation of a porous medium. This assumption seems to be borne out as correct in many instances, but deviations from it have been observed on several occasions[2].

If one again calculates the "safety factor" G (following the procedure leading to 3.33-1), he has to replace c in (3.33-1) by s from (3.33-4) and obtains

$$G = [c + (p_c - p_w) \tan \Phi] \frac{l_a r}{W l_w}. \tag{3.33-5}$$

As usual, a slide will occur if, along the critical toe circle, the quantity G becomes smaller than 1. It is obvious that this is possible if the pore water pressure p is sufficiently increased. This may occur due to soaking

1. TERZAGHI, K., and R. B. PECK: Soil Mechanics in Engineering Practice. New York: J. Wiley & Sons 1948.

2. cf. SCHEIDEGGER, A. E.: The Physics of Flow through Porous Media. Second edition. Toronto: University of Toronto Press 1960.

of the ground in rainstorms[1]. However, since such rainstorms occur regularly, a slope that has been stable for thousands of years, cannot suddenly fail due to this cause alone. Other progressive changes may be present, and the slope then fails at a time when the pore water pressure assumes one of its periodic maxima. As such possible progressive changes TERZAGHI mentions a gradual tectonic increase of the slope angle, a gradual decrease of the cohesion c (due to chemical or mechanical weathering) and human activity.

A peculiar instance of the failure of slopes due to piezometric effects is encountered if an originally submerged slope is suddenly laid bare to the air. This causes a rapid drawdown of the hydraulic head which can be shown to lead to the possibility of a slide. However, the phenomenon is of importance mainly with regard to man-made structures and thus of little importance in geomorphological problems.

D. Other Internal Causes. A mounting pore pressure is the most common cause of an internal change of the shear resistance of the material forming a slope. However, we have already stated above that structural changes may gradually occur in the slope material. These structural changes affect the cohesion of the material and may be due to chemical and physical weathering. Into a similar category belongs the phenomenon of "spontaneous liquefaction"[2-4] which may occur due to the change of the arrangement of the grains in water-logged fine sand or coarse silt. In all these cases, the shearing resistance is lowered to such an extent that the safety factor (cf. 3.33-1)

$$G=\frac{s\,l_a\,r}{W\,l_w} \tag{3.33-6}$$

becomes smaller than 1, and hence a slide results. Sometimes, the slow progressive changes are confined to the base upon which the slope rests; this too will lead to a slide.

3.34. Decay of Rock Walls and Mountain Peaks. An additional pattern of spontaneous decay may be observed in exposed rock masses, such as on a steep rock wall or on a mountain peak. In such cases, the decay is very often caused by the presence of tectonic stresses (see Sec. 3.27).

A tectonic stress field is present everywhere[5]. It is a tensor field like any other stress field (see Sec. 3.31). Thus, at any point in a medium, there

1. SCHUMM, S. A., and CHORLEY, R. J.: Amer. J. Sci. 262, 1041 (1964).
2. MCCRONE, A. W.: J. Sed. Petrol. 36, 270 (1960).
3. BAZANT, Z.: Proc. 3d World Conf. Earthq. Eng. 1, I 6 (1966).
4. KENT, P. E.: J. Geol 74, 79 (1966).
5 See SCHEIDEGGER, A. E.: Principles of Geodynamics, 2nd ed. Berlin-Göttingen-Heidelberg: Springer 1963. See p. 75ff.

are three orthogonal principal stress directions. The stress trajectories, being lines tangent at every point to the principal stress directions, provide a convenient representation of the tectonic stress field.

In geomorphology, we are interested in the surface-effects of the ever-present tectonic stress field. First of all, we note that the Earth's surface represents a boundary condition: Because it cannot transmit shear, one of the principal stress directions must be normal to it in its vicinity, the other two must be horizontal. This yields three possible "standard" large-scale stress states near the Earth's surface, depending on whether the vertical stress is the largest, intermediate or smallest of the three principal stresses (pressure counted positive; ANDERSON's[1] theory).

Rock near the surface responds to an overload by fracturing. According to the Mohr-Coulomb[2] theory, fractures occur such that the potential fracture surfaces are parallel to the intermediate principal stress and inclined at 30 to 45° toward the maximum principal stress (pressure positive). Thus, two conjugate potential fracture surfaces are present in any triaxial stress state.

There are two cases of geomorphic action of the tectonic stress field which can be discussed easily: The steep rock wall and the lone mountain peak.

Turning first to the steep (ideally vertical) rock wall[3, 4] we note that one can make some definite remarks about the course of the stress trajectories near such a feature. The vertical principal stress, σ_V, corresponds to the weight of the overlying rock. The closer one approaches the top edge of the wall, the smaller σ_V becomes. The principal stress σ_W normal to the exposed surface of the wall is evidently very small. Hence

$$\sigma_V > \sigma_W \sim 0. \tag{3.34-1}$$

Thus, solely the third principal stress σ_H (parallel to the wall and horizontal) can take on any large values at all. In a tectonic area characterized by crustal shortening (as are most mountainous areas), this must be a pressure; hence

$$\sigma_H > \sigma_V > \sigma_W. \tag{3.34-2}$$

Thus, under these conditions, σ_V is the intermediate principal stress; according to the Mohr-Coulomb fracture theory, the fracture surfaces must be vertical and inclined at some 30—45° towards the maximum

1. ANDERSON, E. M.: The Dynamics of Faulting and Dyke Formation with Applications to Britain. Edinburgh: Oliver & Boyd Ltd. 1942.

2. See e.g. SCHEIDEGGER, A. E.: Principles of Geodynamics, 2nd ed. Berlin-Göttingen-Heidelberg: Springer 1963. See p. 112.

3. GERBER, E. K.: Geograph. Helv. 18, No. 4, 331 (1963).

4. GERBER, E. K., and A. E. SCHEIDEGGER: Felsmech. Ing. Geol., Suppl. 2, 80 (1965).

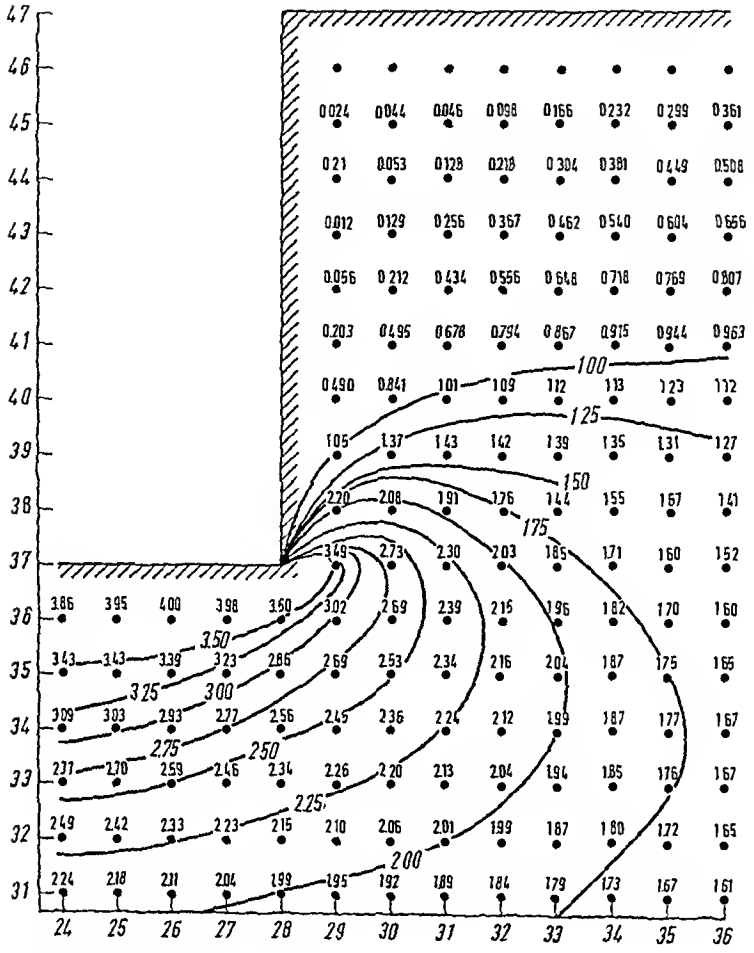

Fig. 51. Lines of equal maximum stress near a wall. At infinity, a unit stress normal to the wall is assumed After STURGUL and SCHEIDEGGER[2]

compression (parallel to the wall) which is exactly what is observed in nature: It is the well-known phenomenon of a "couloir".

Furthermore, it has been found that rock walls basically decay ("recede") at the bottom. This may be due to stress-concentrations which are always present at the foot of a wall[1]. Numerical calculations of the stresses near a wall, based on elasticity theory, have been made by STURGUL and SCHEIDEGGER[2]. Fig. 51 reproduces the maximum stress values obtained by STURGUL and SCHEIDEGGER[2] near a wall when the stress at infinity is a sole compression, acting normal to the wall. Naturally, the stresses only produce the tendency for cracks to form at the foot of the wall, but this enables other secondary agents, like freezing

1. GERBER, E. K., and A. E SCHEIDEGGER. Ecl. Geol. Helv. 62, No. 2 (1969)
2. STURGUL, J R., and A. E. SCHEIDEGGER. Rock Mech. Eng. Geol. 5, 137 (1967).

water etc., to act more effectively at the foot than elsewhere on the wall. Because of these secondary effects, the actual calculation of the stability of rocky slopes is todate still a very difficult problem[1-3].

Turning finally to mountain peaks, we note first of all that calculations by STURGUL and SCHEIDEGGER[4] have shown that one of the most characteristic features of protrusions is (provided they are high enough) that a stress reversal occurs at the top. Taking a section parallel to the maximum regional compression P across a mountain peak, one thus obtains a stress state[5] in which the horizontal stress normal to P is the intermediate stress, inasmuch as the stress parallel to the surface of the peak is a tension T, and the vertical stress is a compression W, due to the weight of the rock (see Fig. 52)[5]. In this fashion, the Mohr-Coulomb fracture surfaces M are normal to the cross-section, and inclined at an

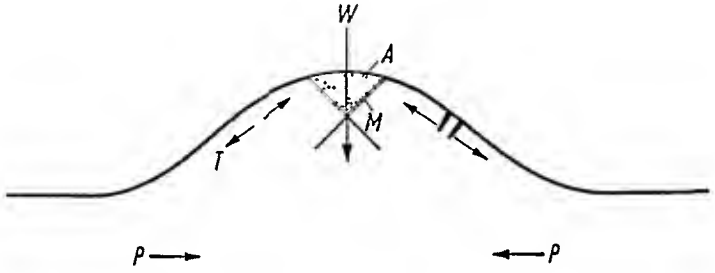

Fig. 52. Stress geometry on a mountain peak. After GERBER and SCHEIDEGGER[5]

angle of 30–45° to the vertical. This may cause breakouts to occur, indicated by A in Fig. 52. In fact, it is quite possible that the genesis of a glacial cirque is not primarily "erosional" at all (cf. Sec. 1.73), but stress-induced; naturally the action of ice thereafter intensifying the feature. Clearly, if this type of stress-induced action occurs, pyramidal forms like the Matterhorn in Switzerland will be the end product of the process.

3.35. Slow Spontaneous Mass Movement. The phenomena of mass movement that were discussed above are characterized by a rapid downhill movement of earth masses in the form of slides. However, mass movement may also occur in the form of *slow flowage*. Such slow flowage is almost imperceptible if it is not observed over a long period of time; it consists in a slow downslope movement of soil or rock, and affects only the surface layers of the Earth to a depth of a few feet[6, 7].

1. MÜLLER, L.: Int. J. Rock Mech. Mining Sci. **1**, 475 (1964).
2. WITTKE, W.: Felsmech. Ing. Geol., Suppl. **1**, 103 (1964).
3. PETZNY, H.: Felsmech. Ing. Geol., Suppl. **3**, 35 (1967).
4. STURGUL, J. R., and A. E. SCHEIDEGGER: Pure Appl. Geophys. **68**, 49 (1967).
5. GERBER, E. K., and A. E. SCHEIDEGGER: Ecl. Geol. Helv. **62**, No. 2 (1969).
6. See e g. HAEFELI, R.: Proc. 3d Conf. Soil Mech. Found. Eng. **3**, 238 (1953).
7. FISCHER, K.: Mitt. Geogr. Ges. München **52**, 231 (1967).

There are several types of slow flowage that may be discerned[1]. These depend to an extent on the climate that is prevalent. In temperate and tropical climates, one encounters rock-creep, talus-creep and soil-creep; in niveal climates, one has solifluction.

The most commonly encountered flowage phenomenon is *soil-creep* where the moving mass is top-soil, often including the vegetation thereon. It is believed that weathering, frost heaving and thermal expansion are all factors contributing to the creep.

If the moving masses consist of screes, one speaks of *talus-creep*. Talus-creep may be aided by freezing and thawing, but it occurs also in climates where the temperature never falls below the freezing-point of water. It stands to reason, therefore, that the daily temperature-changes are sufficient to induce rock movement. This is particularly evident in *arid* areas[2]. An indication that temperature changes might indeed be sufficient to cause creep, has been provided by MOSELEY[3] who experimented with a sheet of lead moving down an inclined board. Similar experiments have been performed by DAVISON[4] using brick and rock slabs.

If the moving masses are even larger than the screes considered above, one has *rock creep*.

In niveal climates, *solifluction* is an ubiquitous phenomenon. This is a slow flowing from higher to lower ground of masses of waste saturated with water. Frost action is playing a fundamental rôle in its occurrence.

In all the above cases, it can probably be said that the movement on the slope is due to the existence of a Rankine state (cf. Sec. 3.31) in the material in question. Thus, the slow spontaneous mass movement is essentially plastic flow[5]. The theory is entirely analogous to the flow of a glacier; it will be presented in detail in that context.

SOUCHEZ, in later papers[6, 7] also proposed the occurrence of viscous, rather than plastic flow on a slope. Viscous flow is characterized by the property that displacements take place as long as there is a shearing stress present in the material. The final equilibrium configuration, thus, is always a level distribution of material. Based upon the assumption of viscous flow, SOUCHEZ ended up with a diffusivity equation for the slope profile.

---

1. SHARPE, C. F. S.. Landslides and Related Phenomena. New York: Columbia University Press 1938.

2. Such as in the California Deserts. Cf. ANDERSON, H.W., G.B. COLEMAN, and P.J. ZINKE: Summer Slides and Winter Scour. Berkeley. U.S. Dept. Agric. Forest Service, Pacif. Southwest Exp. Stn. Tech Paper. No. 36. 1959.

3. MOSLEY, H.: Phil. Mag. (4) 38, 99 (1869).

4. DAVISON, C.: Quart. J. Geolog Soc London 44, 232 (1888).

5. SOUCHEZ, R.: Rev. Belge Géogr. 97, No. 1, 9 (1963).

6. SOUCHEZ, R.: Ciel et Terre 80, Nos. 11–12, 3 (1964).

7. SOUCHEZ, R.: Bull. Soc. Belge Géologie 74, 189 (1965).

It is difficult to judge whether the assumption of viscous flow is physically sound. Slurries, pastes etc. generall behave in a plastic fashion so that it would appear that viscous flow has no place on a slope. Nevertheless, we shall show later (Sec. 5.82) that the transport process on a slope is statistically such that the displacement rate is roughly proportional to the gradient of elevation (i.e. to the shear on a slope). Thus, phenomenologically it may be possible to describe mass transfer on a slope in such a fashion as if it *were* viscous. This transfer, however, is generally effected by external agents, not spontaneously. The assumption of viscous flow may thus lead to acceptable results although it is physically probably untenable.

3.36. Slopes of Screes. The Rankine theory of plastic creep can also be applied to the movements in slopes of screes. However, a quite different process evidently also takes place in scree slopes which can be explained most readily by the assumption of the occurrence of "miniature landslips"[1]. Thus, it has been observed in nature that a stair-shaped configuration may develop. The geometry of the slope is then as shown in Fig. 53: Small landslips occur in the layer (having a cohesion c and an angle of internal friction Φ) of scree of (minimum) thickness D and average slope angle α; h_c is the critical height (cf. Sec. 3.32) of the slope bank that is

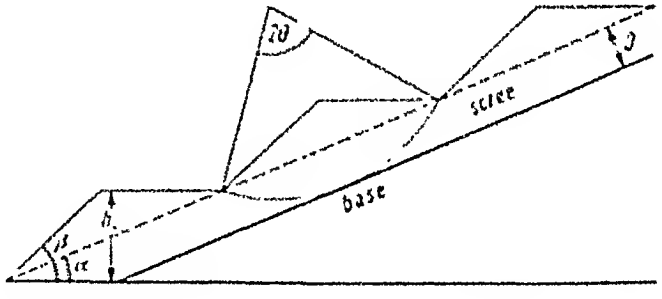

Fig. 53. Geometry of a scree slope. After Gerber and Schuppiger[1]

stable in the scree material with slope angle β, and 2θ is the central angle of the critical toe circle for the landslip (see Sec. 3.32) that is just possible. Inspecting the geometry of Fig. 53, one can calculate the critical thickness D_c

$$D_c = \frac{h_c(1-\cos\theta)}{2\sin\alpha\sin\theta}. \tag{3.36-1}$$

Using Eq. (3.32-10) and the curves of Fellenius (see Fig. 48) one has a connection between all the characteristic quantities. Thus, a scree thick-

1. Gerber, E. K., and A. E. Schuppiger: Geograph. Helv. 21, No. 1, 20 (1966).

ness $D > D_c$ is unstable, a thickness $D < D_c$ is stable. Material will therefore accumulate until $D = D_c$ and then will begin to slide by means of miniature landslides.

It has been noted that most scree slopes are concave upward. Since, in a cohesionless material the slope angle should be equal to the angle of repose which is independent of the height of the slope (cf. Sec. 3.31), one is faced with the problem of explaining this fact.

MACHATSCHEK (cf. Sec. 1.23) has ventured the opinion that the concavity of slopes of screes is due to the grading of material which is generally observed thereupon. However, it appears that the angle of repose, which would generally be believed to determine the slope angle, does not depend on the size of the screes, but rather on their angularity. A somewhat more convincing explanation has been advanced by SHARPE[1] who noted that there are, in fact, *two* angles of repose: one at which the material begins to slide, and another at which it is being deposited. The former angle is always greater than the latter. If the formation of the slope is due to talus creep, one would expect that at the top, the slope angle is close to the angle of repose for incipient sliding and at the bottom close to the angle of repose for deposition. This would at least partially explain the observed concavity, but no numerical comparisons are available. It would appear, however, that the two angles of repose do not differ sufficiently to account for all of the observed change in steepness.

A considerably greater difference in angle than that accounted for above may be caused by the fact that the packing of the screes becomes looser the further the material has moved from its source. We have noted in Sec. 3.31 that the customary angle of repose in a cohesionless material is reached for the loosest possible packing only. If the packing is denser than the loosest one possible, a slope of greatly increased slope angle is attained. This increase may be very substantial and can easily account for any increase of slope-angle with height that may be observed.

3.4. Discussion of Agents in Slope Formation

3.41. General Remarks. The weathering agents discussed thus far are concerned with the reduction and transportation of material. If the reduction and transportation takes place on a mountain side, the configuration of the latter will be affected.

Thus, slope development occurs only if weathering *and* removal takes place. There are several agents that may bring about slope development. One is *corrasion* (Sec. 3.42) which changes a slope by the abrasion initiated

1 SHARPE, C. F. S.. Landslides and Related Phenomena. New York. Columbia Univ. Press 1938 See p 30

by material moving over it. Another is *dry creep of rock* (Sec. 3.43) which effects a slope change due to the slow motion of the constituent material itself. A similar pattern of slope development is connected with *aqueous solifluction* (Sec. 3.44) which is caused by the water contained in the slope material. The most important agent in slope development is *erosion* (Sec. 3.45) caused by water flowing over a slope. Finally, we shall discuss the dynamics of alluvial fans (Sec. 3.46), and the dynamic similarily theory of slope agents (Sec. 3.47).

3.42. Corrasion. The term "corrasion" refers to the development of slopes as caused by the abrasion due to rock débris moving over them.

Corrasion may be attributed to the dry creep of screes over the rock beneath or to the contrition of the bed caused by the direct wearing of the rocks by silt-laden water. This phenomenon has been studied by HJULSTRÖM[1]. A marked striation of the bottom which is primarily subject to the current, may be caused by it.

3.43. Dry Creep of Rock[2]**.** We have seen previously in (Sec. 3.35) that there are indications that the daily and yearly temperature changes in a talus slope consisting of rock débris might be sufficient to cause "dry creep" of rock: as outlined earlier, by "dry creep" we understand the slow downhill motion of the screes without the help of any carrying agent. In order to provide a proper explanation of this phenomenon, we have to study it in somewhat more detail.

For this purpose we shall consider a variety of theoretical models. Starting with a relatively simple model, we shall introduce a series of refinements so as to arrive at the desired result.

In the first model, we consider a long straight slope of slope angle β. We shall assume that all the material is constrained from direct movement parallel to the slope. It is then possible to look at the effect of the daily temperature changes in the following manner: During the heating-up period each infinitesimal block of material $ABCD$ (cf. Fig. 54) will expand to the shape $A'B'CD$. This must be so if it be assumed that no sideways expansion can take place. During the cooling period, the particles will rearrange themselves and the shrinkage of any block $A'B'C''D''$ will then the result in the form $A''B''C''D''$ in Fig. 54. Thus, during one cycle, a net transport of surface material by the distance AA'' takes place. During this whole process no net sideways expansion (i.e. in the x-direction) occurs in correspondence with our assumption.

1. HJULSTRÖM, F.: Bull. Geol. Inst. Uppsala **25**, 219 (1935). See particularly p. 305 and ff. thereof.

2. This Section in after SCHEIDEGGER, A. E.: J. Alberta Soc. Petrol. Geol. **9**, No. 4, 131 (1961).

Let us now calculate the amount of displacement taking place during one temperature cycle. The original volume of $ABCD$ is

$$V = V_{ABCD} = W \Delta x \, \Delta h \tag{3.43-1}$$

where W represents the width of the slope and the explanation of the other symbols is evident from an inspection of Fig. 54.

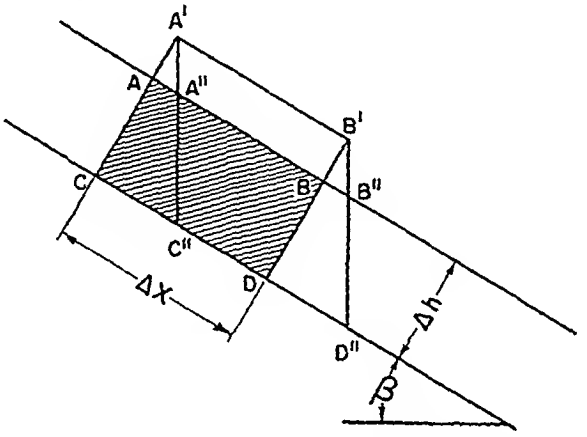

Fig. 54 Geometry of constrained thermal expansion

If the temperature cycle produces a maximum temperature increase by the amount δT, then the new volume will be

$$V' \equiv V_{A'B'CD} = V(1 + 3\kappa \, \delta T) \tag{3.43-2}$$

where κ is the coefficient of linear thermal expansion of the material. Thus

$$AA' = (V' - V)/(W \Delta x) = 3 \Delta h \, \kappa \, \delta T. \tag{3.43-3}$$

Hence we have

$$AA'' = AA' \tan \beta = 3 \Delta h \, \kappa \, \delta T \tan \beta. \tag{3.43-4}$$

This represents the average increase in surface displacement if one proceeds through a layer of thickness Δh. Taking the limit and integrating gives the surface displacement s_K per cycle in an infinitely deep slope:

$$s_T = -\int_0^\infty 3\kappa \, \delta T(h) \tan \beta \, dh \tag{3.43-5}$$

where $\delta T(h)$ is the maximum temperature difference that is reached at the depth h during the cycle. Assuming that the cycle has the period τ, the average surface velocity v turns out to be

$$v = \frac{s_T}{\tau} = -\frac{1}{\tau} \int_0^\infty 3\kappa \, \delta T(h) \tan \beta \, dh. \tag{3.43-6}$$

We now assume that the temperature fluctuation during any one cycle is harmonic at the surface with the maximum temperature difference being δT_0, then it is well known (see e.g. CARSLAW and JAEGER[1] p. 64) that in a heat-conducting medium the maximum temperature difference at depth h is

$$\delta T(h) = \delta T_0 \, e^{-mh} \tag{3.43-7}$$

with

$$m = \sqrt{\frac{\omega}{2A}} \tag{3.43-8}$$

with

$$\omega = 2\pi/\tau \tag{3.43-9}$$

$$A = k/(\rho \, c_p) \tag{3.43-10}$$

where k is the thermal conductivity, ρ the density and c_p the specific heat of the substance.

Inserting (3.43-7) into (3.43-6) and carrying out the integration yields

$$v = \frac{1}{\tau} 3\kappa \tan\beta \, \delta T_0 \int_{\infty}^{0} e^{-mh} \, dh = 3\sqrt{\frac{\kappa^2 k}{\pi \tau \rho \, c_p}} \tan\beta \, \delta T_0 \tag{3.43-11}$$

and hence

$$v = 3\kappa \tan\beta \, \delta T_0 \sqrt{k/(\tau \pi \rho \, c_p)}. \tag{3.43-12}$$

Taking as representative values (for granite) $c_p = 0.192$ cal/deg/gram, $\kappa = 8.3 \cdot 10^{-6}$ deg^{-1}, but $\rho = 2$ g/cm^3 and $k = 0.00033$ cal/(cm deg sec) (the last two values are not the values for solid granite, but some values thought to be representative for a loose pile of granite-rubble), $\beta = 45°$ $\delta T_0 = 30°$ C and $\tau = 1$ day ($= 8.64 \cdot 10^4$ sec) yields

$$v \sim 1.3 \text{ cm/year}. \tag{3.43-13}$$

This is obviously far too little to account for any appreciable rock creep. It therefore appears that the model based on the assumption that there is no lateral expansion in any one layer, is unrealistic. Let us therefore modify the above model and investigate another one based on the opposite extreme in which it is assumed that some of the expansion takes place laterally. Looking at Fig. 55 this means that it is assumed that an elemental block of material $ABCD$ expands during the heating cycle to $A'B'C'D$. During the cooling cycle, it contracts again, but only

1. CARSLAW, H. S., and J. C. JAEGER: Conduction of Heat in Solids. 2nd Ed. Oxford: University Press 1959.

in the direction of h. The net effect is thus an elongation of the layer in the x-direction. The latter is

$$s_T(h)=\delta T \int_0^x \kappa \, dx=\kappa x \, \delta T(h). \tag{3.43-14}$$

The surface velocity, thus, increases with increasing distance from the top of the slope. Using again the earlier value for κ ($8.3 \cdot 10^{-6}$ deg^{-1}), and a cycle of 1 day duration with a maximum temperature difference of 30° C, we obtain

$$\begin{aligned} v &= x \, 30 \cdot 8.3 \cdot 10^{-6} \cdot 360 \\ &= 8.96 \cdot 10^{-2} \, L \text{ per year} \end{aligned} \tag{3.43-15}$$

where L is the length of the slope. For $L=100$ meters we have

$$v=8.96 \text{ metres per year}, \tag{3.43-16}$$

at the bottom of the slope.

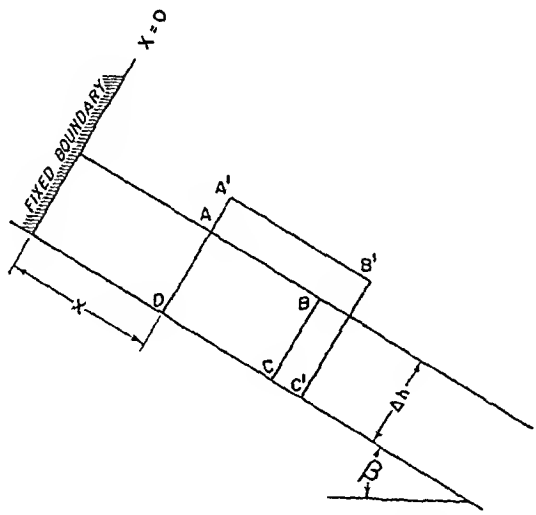

Fig 55. Geometry of unconstrained thermal expansion

According to the above model, the velocity of the surface layer depends on the length of the slope. Thus, if the slope be infinitely long, the velocity at the bottom becomes infinitely great. This, also, is obviously an unrealistic result.

It stands to reason that a reasonable model lies somewhere in between the two extremes: Only part of the slope can be effective in the downward push; if the strength limit of the screes is exceeded, the material will pile up vertically as envisaged in the first model considered.

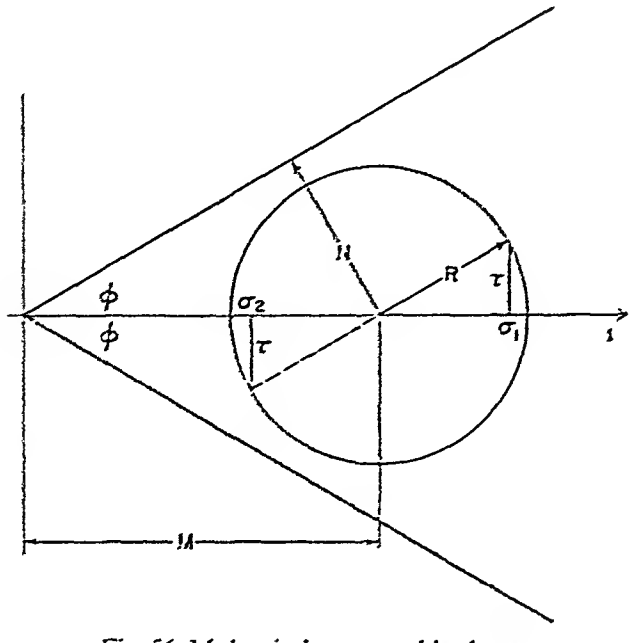

Fig. 56. Mohr circle on a stable slope

In order to investigate this stability limit of the screes we assume that COULOMB's strength law applies; viz. we have for stability (cf. 3.31-2)

$$\tau_{max} = \sigma \tan \Phi \tag{3.43-17}$$

where the cohesion of the material is assumed to be zero. In this case, the angle of repose is equal to the angle of internal friction Φ. In the MOHR diagram (cf. Sec. 3.31), the strength limit is given by two straight lines through the origin that have the slope $\pm \tan \Phi$. (See Fig. 56.)

If we consider an element of material of cross-section dx, dh (and unit width) at the depth h below the surface and at the distance x from the top of the slope (cf. Fig. 57), then the equilibrium conditions are

$$\frac{\partial \sigma_1}{\partial x} + \frac{\partial \tau_1}{\partial h} - \rho g \sin \beta = 0, \tag{3.43-18}$$

$$\frac{\partial \sigma_2}{\partial h} + \frac{\partial \tau_2}{\partial x} - \rho g \cos \beta = 0, \tag{3.43-19}$$

$$\frac{\partial \tau_1}{\partial h} = -\frac{\partial \tau_2}{\partial x} \tag{3.43-20}$$

and from the frictional formula we have

$$\frac{\partial \tau_1}{\partial h} = \rho g \cos \beta \tan \Phi. \tag{3.43-21}$$

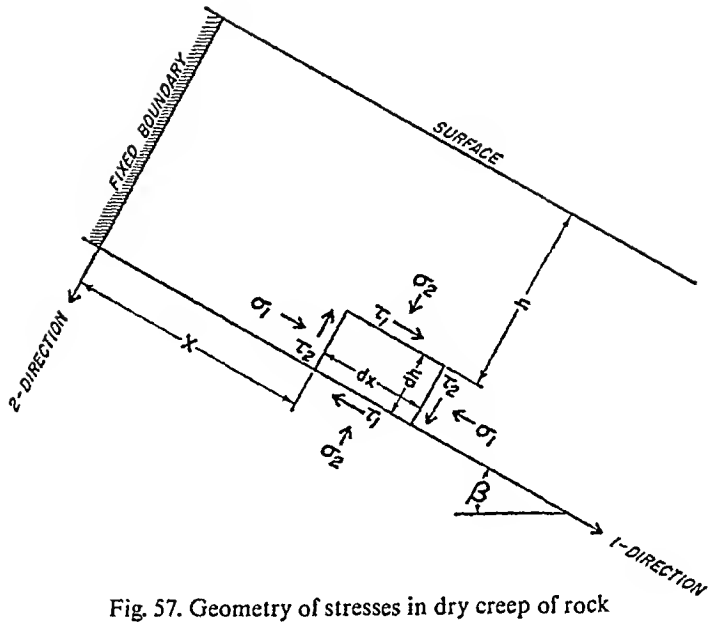

Fig. 57. Geometry of stresses in dry creep of rock

Integrating, this yields (with proper constants)

$$\sigma_1 = g\,\rho(L-x)\,\alpha \tag{3.43-22}$$

with

$$\alpha = \cos\beta\tan\Phi - \sin\beta. \tag{3.43-23}$$

The stress normal to the bed (σ_2) at the point x is

$$\sigma_2 = g\,\rho\,h[\cos\beta\tan\Phi + \cos\beta] = g\,\rho\,h\,\gamma \tag{3.43-24}$$

with

$$\gamma = \cos\beta\tan\Phi + \cos\beta \tag{3.43-25}$$

and the shearing stress, due to the friction, is

$$\tau_1 = \rho\,g\,h\cos\beta\tan\Phi. \tag{3.43-26}$$

The quantities σ_1, σ_2 and τ at the point (x, h) determine a stress state; the corresponding Mohr circle is drawn in Fig. 56. The material will slide downhill if the Mohr circle lies inside the two straight lines that go through the origin and subtend an angle $\pm\Phi$ with the 1-axis, i.e. as long as $R<N$ in Fig. 56. If $R=N$ the material will be in a Rankine state and move vertically. Thus, $R=N$ is the limiting condition for which the material will be able to slide downhill as envisaged.

We have

$$N = M\sin\Phi = \tfrac{1}{2}(\sigma_1+\sigma_2)\sin\Phi \tag{3.43-27}$$

$$R = \sqrt{\left(\frac{\sigma_1-\sigma_2}{2}\right)^2 + \tau^2}. \tag{3.43-28}$$

The condition for stability $N>R$ or $N^2>R^2$ is

$$\left(\frac{\sigma_1+\sigma_2}{2}\right)^2 \sin^2\Phi > \left(\frac{\sigma_1-\sigma_2}{2}\right)^2+\tau^2 \tag{3.43-29}$$

or

$$\left(\frac{(L-x)\alpha+h\gamma}{2}\right)^2 \sin^2\Phi > \left(\frac{(L-x)\alpha-h\gamma}{2}\right)^2+h^2\cos^2\beta\tan^2\Phi. \tag{3.43-30}$$

It should be noted that a true instability can occur only if $\sigma_1>\sigma_2$ (this corresponds to the "passive" Rankine state; in the "active" Rankine state, i.e. if $\sigma_1<\sigma_2$, one has no piling up of material). Thus the conditions for *in*stability are

$$\{\tfrac{1}{2}[(L-x)\alpha+h\gamma]\}^2\sin^2\Phi < \{[(L-x)\alpha-h\gamma]/2\}^2 + h^2\cos^2\beta\tan^2\Phi, \tag{3.43-31}$$

$$h\gamma<(L-x)\alpha. \tag{3.43-32}$$

If either of these conditions is *not* satisfied, the material will move downhill and not pile up on the slope.

Thus, if we set

$$\xi=(L-x)/h \tag{3.43-33}$$

the first limiting condition is

$$(\xi\alpha+\gamma)^2\sin^2\Phi=(\xi\alpha-\gamma)^2+4\cos^2\beta\tan^2\Phi \tag{3.43-34}$$

or

$$\xi=\frac{\gamma(1+\sin^2\Phi)\pm\sqrt{\gamma^2(1+\sin^2\Phi)^2-\gamma^2\cos^4\Phi-4\cos^2\beta\sin^2\Phi}}{\alpha\cos^2\Phi} \tag{3.43-35}$$

or, inserting the values for α, γ:

$$\xi=\frac{(\tan\Phi+1)(1+\sin^2\Phi)\pm\sqrt{(\tan\Phi+1)^2[(1+\sin^2\Phi)^2-\cos^4\Phi]-4\sin^2\Phi}}{\cos^2\Phi(\tan\Phi-\tan\beta)}. \tag{3.43-36}$$

One can prove that this represents the onset of a true instability if the upper sign is used. We set

$$\xi=f(\Phi)\frac{1}{\tan\Phi-\tan\beta} \tag{3.43-37}$$

with

$$f(\Phi)=\frac{(\tan\Phi+1)(1+\sin^2\Phi)+\sqrt{(\tan\Phi+1)^2[(1+\sin^2\Phi)^2-\cos^4\Phi]-4\sin^2\Phi}}{\cos^2\Phi}. \tag{3.43-38}$$

It can then be shown that the second instability condition is satisfied. We have

$$\frac{\gamma}{\alpha}=\frac{\cos\beta(\tan\Phi+1)}{\cos\beta\tan\Phi-\sin\beta}=\frac{\tan\Phi+1}{\tan\Phi-\tan\beta}=F(\Phi)\frac{1}{\tan\Phi-\tan\beta} \tag{3.43-39}$$

with

$$F(\Phi)=\tan\Phi+1. \tag{3.43-40}$$

It is obvious that

$$f(\Phi)>F(\Phi) \tag{3.43-41}$$

so that

$$\xi>\frac{\gamma}{\alpha}. \tag{3.43-42}$$

This is the second instability condition and we see that we have indeed a true instability if the larger root is chosen in (3.43-36).

Summarizing, we note that instability occurs if

$$\frac{L-x}{h}>f(\Phi)\frac{1}{\tan\Phi-\tan\beta}; \tag{3.43-43}$$

if $\Phi=\beta$, one can make the slope as long as he likes.

For $\beta<\Phi$, $f(\Phi)$ is some given quantity. The slope then can have the following maximum length

$$(L-x)_{\max}=f(\Phi)\frac{h}{\tan\Phi-\tan\beta}. \tag{3.43-44}$$

However, h is the depth to which the temperature change is felt. We have seen earlier that (cf. 3.43-7/8)

$$\delta T(h)=\delta T_0\, e^{-\sqrt{\omega/(2A)}h}=\delta T_0\, e^{-mh}. \tag{3.43-45}$$

Thus, the lengthwise displacement s_T per cycle is [for the definition of κ see (3.43-2)]

$$s_T=\kappa(L-x)_{\max}\delta T(h)=\kappa(L-x)_{\max}\delta T_0\, e^{-mh} \tag{3.43-46}$$

and therefore we have

$$s_T(h)=\kappa h f(\Phi)\frac{1}{\tan\Phi-\tan\beta}e^{-mh}\delta T_0. \tag{3.43-47}$$

During the above deduction, it has been assumed that each layer at any given depth h acts independently of all others, except that it is impli-

cit in the stress formulas that all layers above a given layer must be sliding *faster* than the layer under consideration. Since $s_T(h)$ as given by (3.43-47) has a maximum (cf. Fig. 58), all layers above this maximum will slide *en bloc*.

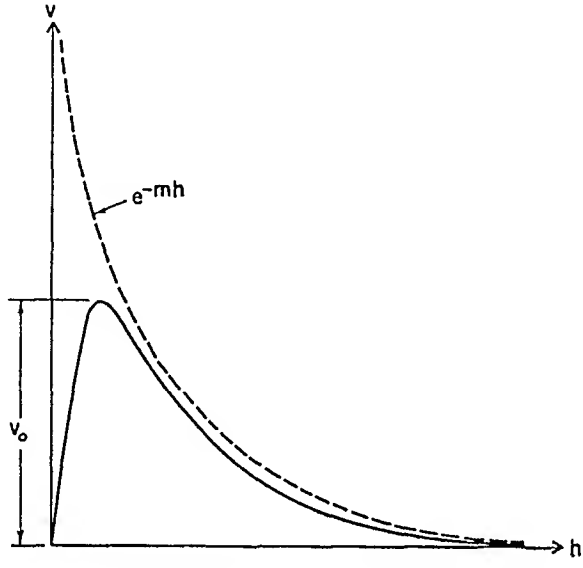

Fig. 58. Creep velocity as a function of depth

3.44. Aqueous Solifluction. The phenomenon of *aqueous solifluction* is one which is very similar to the dry creep of soil, except that now the soil is water-logged instead of dry.

It turns out that the flow of soil in aqueous solifluction is analogous to that of ice in glaciers, at least if the latter is treated by the method of plasticity theory. Ice flow is, in its own turn, very similar to the theory of the Rankine state of the slow downhill flowage of loose material discussed in Sec. 3.31. Thus, there is no fundamental difference between dry creep of rock and solifluction. It should be noted, however, that the driving force in solifluction is not provided by temperature changes, but by gravity alone: the material is so waterlogged that it becomes mobile. As has been shown in Sec. 3.31, the material can flow in either an *active* or a *passive* Rankine state. The formulas that apply are similar to those in glacier flow, and will be discussed in detail in Sec. 7.22 (since glacier flow is a more important geomorphological agent than solifluction). The mechanics of the two phenomena, as long as simple plasticity theory is used for glaciers, is analogous except for one interesting feature. In an active Rankine state in glacier flow, snow has to be added to keep the slope angle constant. In solifluction, of course, nothing can be added. This requires, in the light of condition (7.22-5), that deeper and deeper layers begin to flow. This, however, is reasonable.

Geomorphologists usually term as "solifluction" something that is different from the phenomenon discussed here; hence we have added the qualifying adjective "aqueous". Unqualified "solifluction" generally refers to an effect caused by freezing and thawing and will be discussed in connection with other niveal phenomena.

3.45. Slope Development by Water Erosion. The process of erosion can have a direct effect upon slope development. This is particularly evident if the slope consists of the very material which the eroding agent carries, i.e. in alluvial slopes if the carrying agent is water.

Let us briefly discuss the mechanism of the slope recession that is directly induced by erosion. Water, carrying material, is moving over a slope consisting of the same material. In general, there will be a relationship between the speed of flow and the carrying capacity of the water. If the water happens to carry less material than is its capacity, it will take on more material from the slope underneath and thus erode it. Conversely, if the flow gets slowed down, the carrying capacity will decrease and therefore material will be deposited. It is thus apparent that there exists a dynamic equilibrium between an alluvial slope and water flowing over it. If there is any deviation from such an equilibrium, the slope will be eroded or will be built up.

It becomes evident thus, that the process of water erosion cannot be treated separately from the process of accumulation of eroded material further downhill: on a steep part of the slope, one will generally find that mass-removal is taking place, whereas on a less steep part accumulation occurs. After an initial phase, a quasistationary process will develop in which material is being transferred from the steep to the flat parts of the slope at a quasi-steady rate (i.e. a rate which changes only very slowly with time under constant external conditions). Concurrently, the slope will slowly change its shape.

It will be necessary to put the above intuitive arguments onto a more analytical basis. Whereas it is intuitively quite clear that the slowing down of a carrying medium which is originally in dynamic equilibrium with regard to mass transport, will cause some of this mass to be deposited, one would like to know just how the slowing down will affect the slope.

Thus, let us assume that the mass-transporting medium be water. Further, let us assume[1] that the water hits a flat part of ground with a constant velocity v_1. The water carries with it a certain amount of material c per unit volume. Due to its being slowed down it will start building up a slope on the originally flat ground. It is clear that the mass-carrying

1 SCHEIDEGGER, A. E.: Geol. u. Bauw. 25, 3 (1959).

capacity of the water increases with the velocity v, and hence one may set as a first approximation

$$v \sim c \tag{3.45-1}$$

for a *particular body of water*. Furthermore, we also assume that the velocity of the water is proportional to the instantaneous slope S over which it travels

$$v \sim S. \tag{3.45-2}$$

The last assumption implies that we neglect the effects of momentum which, in turn, means that the layer of water carrying the mass is not very thick[1].

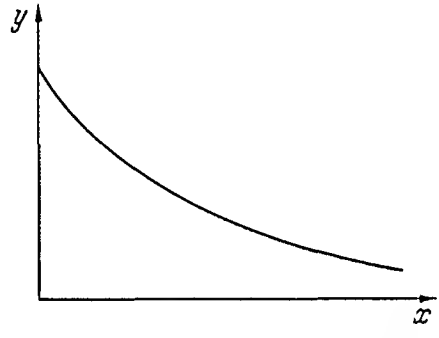

Fig. 59. General geometry of a slope

We now introduce coordinates x (horizontal), y (vertical, upward) and t (time), and assume that the mass-carrying water hits the originally flat surface at $x=0$, with a constant velocity v_1. The geometrical layout is shown in Fig. 59. In the slope that will develop, the increase in height is due to the loss of mass from the water; hence

$$\frac{\partial y}{\partial t} \sim -\frac{\partial (v\, c)}{\partial x}. \tag{3.45-3}$$

Eq. (3.45-2) yields, in terms of x and y

$$v \sim -\frac{\partial y}{\partial x}. \tag{3.45-4}$$

Thus

$$\frac{\partial y}{\partial t} \sim -\frac{\partial v^2}{\partial x} \sim -\frac{\partial}{\partial x}\left(\frac{\partial y}{\partial x}\right)^2. \tag{3.45-5}$$

1. Relation (3.45-2) has been confirmed, for instance, for sheet floots by HORTON, R. E., H. R. LEACH, and R. VAN VLIET: Trans. Amer Geophys. Union **15**, 393 (1934). For river flow, a different relation (see Sec. 4.22) is generally used.

Differentiating with regard to x

$$\frac{\partial^2 y}{\partial x\,\partial t} \sim -\frac{\partial^2}{\partial x^2}\left(\frac{\partial y}{\partial x}\right)^2 \tag{3.45-6}$$

and setting

$$\zeta = -\frac{\partial y}{\partial x} \tag{3.45-7}$$

yields

$$\frac{\partial \zeta}{\partial t} \sim \frac{\partial^2 \zeta^2}{\partial x^2} \tag{3.45-8}$$

or, written as an equality

$$\frac{\partial \zeta}{\partial t} = a\frac{\partial^2 \zeta^2}{\partial x^2} \tag{3.45-9}$$

where a is some constant. The above differential equation has to be solved for the following boundary condition implicit in our assumptions:

$$\zeta(t, 0) = \zeta_1 = \text{const} \tag{3.45-10}$$

and the initial condition

$$\zeta(0, x) = \zeta_0 = 0 \tag{3.45-11}$$

since ζ is proportional to the velocity.

The differential equation (3.45-9) is nonlinear and is thus difficult to solve. However, it is the same differential equation that occurs in the description of the flow of gas through porous media. It has received a great amount of attention since it describes the flow, say, of natural gas into a well. The equation cannot be integrated in closed form, but can be solved by an approximation method on a computer. Various undertakings along these lines have been collected by the writer[1]. Unfortunately, however, these solutions cannot be used for our problem because, in studies of flow through porous media, the initial value is different from zero. However, GREEN and WILTS[2] have suggested a way to linearize the equation so that it will read:

$$\frac{\partial \zeta^2}{\partial t} = a'\frac{\partial^2 \zeta^2}{\partial x^2} \tag{3.45-12}$$

where a' is a new constant depending on the old constant a and on an intermediate value ζ' between ζ_0 and ζ_1:

$$a' = a/\zeta'. \tag{3.45-13}$$

1. SCHEIDEGGER, A. E.: The Physics of Flow Through Porous Media Second edition. Toronto: University of Toronto Press. 1960 See p. 108.

2 GREEN, L., and C H. WILTS. Proc 1st U S Nat. Congr. Appl Mech., p 777 (1952).

Since we are interested only in general features of the solution, it will be sufficient to deal with the linearized equation. The latter can easily be solved; the required solution is:

$$\zeta^2 = \zeta_1^2 \left(1 - \operatorname{erf} \frac{x}{\sqrt{4a't}}\right) \equiv \zeta_1^2 \operatorname{erfc} \frac{x}{\sqrt{4a't}}. \tag{3.45-14}$$

Hence, we obtain for the slope

$$S \cong -\zeta_1 \sqrt{\operatorname{erfc} \frac{x}{\sqrt{4a't}}}, \tag{3.45-15}$$

for the velocity

$$v \sim v_1 \sqrt{\operatorname{erfc} \frac{x}{\sqrt{4a't}}}, \tag{3.45-16}$$

and for the height of the accumulation

$$y \cong -\int_{\infty}^{x} \sqrt{\operatorname{erfc} \frac{x}{\sqrt{4a't}}}\, dx. \tag{3.45-17}$$

Since the error function complement behaves for large x just like e^{-x^2}/x (see e.g. PRANGE[1]) and its square root just like $e^{-\frac{1}{2}x^2} x^{-\frac{1}{2}}$, one does not have to fear any difficulties with regard to the convergence of the integral. The shape of the $y = y(x)$ curve is thus exactly as was anticipated in Fig. 59.

The last equation obtained (3.45-17), thus, gives a description of what accumulative slopes should look like: They should be essentially concave. Gradually, with time, they should approach a horizontal level.

It may be noted that the above theory can also be extended to that part of a slope where material transport effects a removal of mass. In this instance, it leads to a case of *slope recession*. This can be demonstrated as follows.

The differential Eq. (3.45-12), being a diffusivity equation, has solutions of the form (cf. Fig. 60)

$$Y' \equiv \zeta^2 = \frac{\text{const}}{\sqrt{t}} \exp\left\{-\frac{x^2}{\sqrt{4at}}\right\}. \tag{3.45-18}$$

Thus, the slope itself has the form

$$-y' = S = \frac{\text{const}}{\sqrt[4]{t}} \exp\left\{-\frac{x^2}{4\sqrt{at}}\right\}, \tag{3.45-19}$$

1. PRANGE, G.: Vorlesungen über Differential- und Integralrechnung. Berlin: Springer 1943.

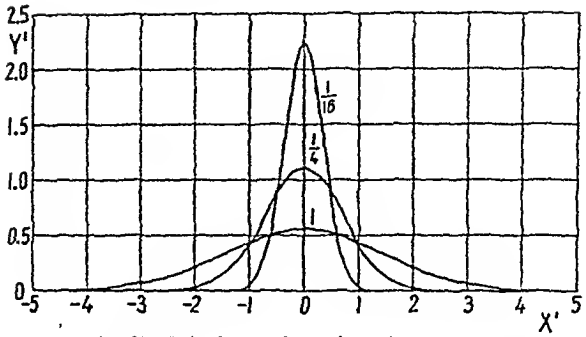

Fig. 60. Solutions of the diffusivity equation

which, qualitatively, leads to the picture shown in Fig. 61. The figure indicates that a lowering of the slope is taking place on one side of the axis of symmetry, a rising on the other side. The equation of the slope, being given by the negative integral of the expression (3.45-19), is always an error function complement. The transport of mass, thus, effects erosion on one side of the center of the slope and accretion on the other side.

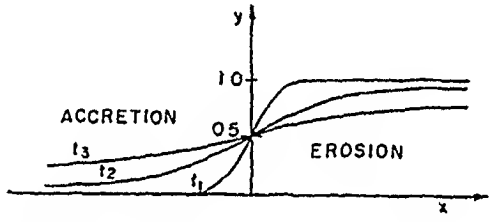

Fig. 61. Slope development by accumulation and erosion. After SCHEIDEGGER[1]

Some of the difficulties inherent in the above discussion are due to the nonlinear character of the basic Eq. (3.45-9). Although the latter can be linearized, as shown above, it may also be possible to justify physically the assumption of a *linear* differential equation in the first place, viz. of

$$\frac{\partial y}{\partial t} = a \frac{\partial^2 y}{\partial x^2}. \tag{3.45-20}$$

This, in fact, has been proposed by CULLING[2] by assuming (a) that the *mass flow* velocity (and not the velocity of the mass-carrying water as assumed above) is proportional to the slope $\partial y/\partial x$ and, (b) that the deposition is proportional to the mass flow velocity gradient. This immediately yields Eq. (3.45-20). The solutions of this equation are the well-known solutions of the heat conductivity equation as they have been discussed above in the analysis of the linearized Eq. (3.45-12).

It remains to compare the analytically predicted slope-shapes of accumulations with observations in nature. In this connection, we note

1. SCHEIDEGGER, A. E.: Bull. Geol. Soc. Amer. 72, No. 1, 37 (1961).
2. CULLING, W. E. H.: J. Geol. 68, 336 (1960).

that the slopes observed in natural accumulations fit very well indeed with those postulated in the analytical theory outlined above. Similarly, the concave nature of the slopes of most volcanoes also fits the above analytical theory. SCHUMM[1] has shown that pediment profiles also fit the above characteristics.

The universality of the concavity of accumulative slopes has led STRAHLER[2] to postulate a concave shape *a priori* from which it would then be possible to calculate the change of shape with time. STRAHLER took as fundamental equation (as an *a priori* assumption) for slopes caused by accumulation (especially river beds)

$$y = A\, e^{-kx}. \tag{3.45-21a}$$

He then introduced the assumption that the rate at which the slope is lowered at a given point is proportional to the slope at that point. This immediately leads to an exponential lowering of the slope with time; one ends up with

$$y = A\, e^{-k_1 x - k_2 t}. \tag{3.45-21b}$$

It should be noted, however, that the above procedure does not really predict what the shape of a slope should be (since this has been introduced as an *a priori* assumption). Furthermore, it is doubtful whether the rate of lowering of the slope can indeed be regarded as proportional to the slope. If the flow of the water is in dynamic equilibrium on the slope, this is certainly not true. The theory given earlier would therefore appear to be preferable.

One can now try to investigate the sequence of the pebble sizes found in natural slopes in terms of the analytical theory of the preceding paragraphs. Remarks with regard to the observed grading have been made in Chap. I.

In order to explain the observed grading of pebble sizes, one can proceed as follows. It is often assumed that the weight W of the pebbles that can just be moved by flowing water is proportional to the sixth power of the velocity v of the water:

$$W = \text{const}\, v^6. \tag{3.45-22}$$

Reasons for this assumption will be given later (in Sec. 4.43). Combining (3.45-22) with the velocity formula (3.45-16) yields

$$W = \text{const}\left[\operatorname{erfc}\frac{x}{\sqrt{4a't}}\right]^3. \tag{3.45-23}$$

This predicts that the pebble sizes become smaller the farther away one moves from the beginning of the slope. This is indeed confirmed in nature, as it immediately explains the sequence of pebble sizes found in flood

1. SCHUMM, S. A.: Bull. Geol. Soc. Amer. **73**, 719 (1962).
2. STRAHLER, A.: Bull. Geol. Soc. Amer. **63**, 923 (1952).

plains and alluvial fans. The reason for this sequence to be seemingly reversed in alluvial cones and talus accumulations lies in the observation that these features are being accumulated by *intermittent* streams. The largest flash floods reach furthest over the heap of débris until they get slowed down. However, these are the floods that carry the largest boulders. Hence the boulders are found at the base of the accumulation.

It may therefore be said that the analytical theory of slopes formed by mass accumulation explains the observed facts reasonably well. The application of the above ideas to the slope of river beds will be discussed further in Sec. 4.7.

In conclusion of the present section on water erosion, one may mention that such erosion can also be caused by a groundwater stream on a surface of seepage[1]. A surface of seepage is a surface which is intersected by the streamlines of the groundwater flow and from which, therefore, water is seeping out. During the process of seepage, the flowing water exerts a force upon the soil particles. Using the notion that it is the "effective pressure" which causes the deformation of the soil, as was already discussed in Sec. 3.33 in connection with piezometric landslides (*quo vide*), we note that the effective pressure may become such that the shearing limit of the soil (see Eq. 3.33-4) becomes zero. In this case, the emerging groundwater stream will carry away soil particles from the surface of seepage. This represents a special type of water erosion.

3.46. Alluvial Fan. Alluvial fans are quasi-conical structures, as described in Sec. 1.23. Because of this, they can no longer be described by simply giving their profile. The agents which cause fans to be deposited may be braided streams as well as periodic sheet-floods.

It is difficult to describe the genesis of an alluvial fan theoretically, and therefore semi-empirical studies have been made[2–4]. BULL[2] and DENNY[3] came up with the following relationship between the fan area A_f and the drainage-basin area A_d

$$A_f = c\, A_d^n \tag{3.46-1}$$

where c and n are constants; HOOKE[4] found for the mean value of n

$$n = 0.90. \tag{3.46-2}$$

A study by HOOKE[4] suggested that the relationship (3.46-1) may be due to the establishment of a steady state between deposition and erosion in a fan. However, actual calculations of the steady state conditions do not seem to have been made.

1. See BRINCH HANSEN, J., and H. LUNDGREN: Hauptprobleme der Bodenmechanik. Berlin-Göttingen-Heidelberg: Springer 1960. (Esp. p. 102ff. therein.)
2. BULL, W. B.: U.S. Geol. Surv. Prof. Pap. 437A, A 1 (1964).
3. DENNY, C. S.: U.S. Geol. Surv. Prof. Pap. 466 (1965).
4. HOOKE, R. L.: Amer. J. Sci. 266, 609 (1968).

3.47. Dynamic Similarity in Slope Development Agents[1]. Whenever it is difficult to describe a process analytically, recourse may be taken to scale model experiments. In order to set up such scale model experiments, the appropriate dynamic similarity conditions must be observed.

The scaling relations are developed simply by postulating that the fundamental equations be valid in the prototype as well as in the model. The fundamental equations are first written down in terms of dimensionless variables; requiring then that the equations be indentical in prototype and model yields the required scaling relations[2].

Of the slope development agents discussed above, we turn first to raindrop action. Of the possibilities discussed in Sec. 3.24, the hypothesis referring to the significance of the *momentum* rather than of the energy in rain action will be used here, as implied in Eq. (3.24-2). In that case, the constant C is a measure of the "ruggedness" r (cm/sec) of the soil, i.e. a measure of its resistance to erosion. The first fundamental equation of raindrop action becomes therefore:

$$Q=\frac{1}{r}\,q\,\rho\,v \tag{3.47-1}$$

where all the symbols have been defined in Sec. 3.24. Because of turbulent drag, the terminal velocity v of the raindrops is approximately proportional to $a^{\frac{1}{2}}$, where a is their diameter (see Eq. 4.42-10); thus:

$$Q=K\frac{1}{r}\,a^{\frac{1}{2}}. \tag{3.47-2}$$

Here ρ, the density of the water, has been incorporated into the constant K which has the dimension $g\ \mathrm{cm}^{-\frac{1}{2}}\ \mathrm{sec}^{-1}$.

Now, the last Eq. (3.47-2) must be written in terms of dimensionless variables, following the general scheme[2]. In order to do this, the gravity acceleration g has to be introduced as a reference parameter. We can then set (bars denoting dimensionless quantities)

$$\bar{Q}=Qg^{\frac{1}{2}}/(Kr), \tag{3.47-3}$$

$$\bar{q}=q/r, \tag{3.47-4}$$

$$\bar{a}=a\,g/r^2. \tag{3.47-5}$$

The fundamental equation is then indeed dimensionless:

$$\bar{Q}=\bar{q}\,\bar{a}^{\frac{1}{2}} \tag{3.47-6}$$

1. This Sec. after SCHEIDEGGER, A. E.: Geofis. Pura Appl. **56**, 58 (1963).

2. See e.g. FOCKEN, C. M.: Dimensional Methods and Their Application. London: E. Arnold & Co. 1953.

and the scaling relations (α_i denoting the *ratio* of the variable i in prototype and model) are

$$\alpha_Q = \alpha_K \alpha_r / \alpha_g^{\frac{1}{2}}, \tag{3.47-7}$$

$$\alpha_q = \alpha_r, \tag{3.47-8}$$

$$\alpha_q = \alpha_r^2 / \alpha_g. \tag{3.47-9}$$

Next, we turn to spontaneous mass transport. We have to go to the fundamental equation given as (3.32-10). The transformation to make this dimensionless is (see Sec. 3.32 for the definition of the symbols involved)

$$\bar{h}_c = h_c \rho g / c, \tag{3.47-10}$$

$$\bar{N}_s = N_s(\beta). \tag{3.47-11}$$

Then, indeed, (3.32-10) becomes

$$\bar{h}_c = \bar{N}_s \tag{3.47-12}$$

and we obtain the scaling conditions:

$$\alpha_{h_c} = \alpha_c / (\alpha_\rho \alpha_g) \tag{3.47-13}$$

$$\alpha_{N_s} = 1. \tag{3.47-14}$$

Finally, the slope development by water erosion was given by (3.45-5) which may be written as follows:

$$\frac{\partial y}{\partial t} = -c \frac{\partial}{\partial x} \left(\frac{\partial y}{\partial x} \right)^2 \tag{3.47-15}$$

where c is a constant and the other symbols have been defined in Sec. 3.45. This constant is connected with the erodibility of the material over which the water flows and with the quantity of water that is available. The latter is best measured as the water volume that flows per unit time across a slope profile of unit width. We shall denote this quantity by Q; the dimensions are obviously $L^2 T^{-1}$. The relation is then,

$$c = Q / r \tag{3.47-16}$$

where r *defines* the resistance to erosion of the material on the slope, the quantity r is dimensionless (note, however, that Q and r are not the same quantities as in the previous paragraph).

Substituting this value of c in the basic equation results in

$$\frac{\partial y}{\partial t} = -\frac{Q}{r} \frac{\partial}{\partial x} \left(\frac{\partial y}{\partial x} \right)^2. \tag{3.47-17}$$

It may be of some interest to compare slopes with different slope angles β. In this case, one has to differentiate the fundamental differential equation with regard to x

$$\frac{\partial^2 y}{\partial t\,\partial x} = -\frac{Q}{r}\frac{\partial^2}{\partial x^2}\left(\frac{\partial y}{\partial x}\right)^2; \tag{3.47-18}$$

then, it is possible to introduce as a new (dimensionless) variable (instead of y):

$$\zeta = \tan\beta = \frac{\partial y}{\partial x} \tag{3.47-19}$$

so that one obtains

$$\frac{\partial \zeta}{\partial t} = -\frac{Q}{r}\frac{\partial^2 \zeta^2}{\partial x^2}. \tag{3.47-20}$$

Assuming a slope bank of height H and slope angle β_0 (so that $\zeta_0 = \tan\beta_0$), the complete system of equations defining the process is then

$$\frac{\partial \zeta}{\partial t} = -\frac{Q}{r}\frac{\partial^2 \zeta^2}{\partial x^2}, \tag{3.47-21}$$

$$\begin{aligned} \zeta(t=0) &= \zeta_0 \quad \text{for } 0 \le x \le H/\zeta_0 \\ &= 0 \quad \text{otherwise.} \end{aligned} \tag{3.47-22}$$

This system of equations can be made dimensionless by the transformation

$$\bar{t} = t\,Q\,\zeta_0^3/(r\,H^2), \tag{3.47-23}$$

$$\bar{x} = \zeta_0\,x/H, \tag{3.47-24}$$

$$\bar{\zeta} = \zeta/\zeta_0. \tag{3.47-25}$$

Then,

$$\frac{\partial \bar{\zeta}}{\partial \bar{t}} = -\frac{\partial^2 \bar{\zeta}^2}{\partial \bar{x}^2}, \tag{3.47-26}$$

$$\begin{aligned} \bar{\zeta}(t=0) &= 1 \quad \textit{for } 0 \le \bar{x} \le 1 \\ &= 0 \quad \text{otherwise.} \end{aligned} \tag{3.47-27}$$

Thus, the dynamic similarity conditions are

$$\alpha_t = \alpha_r\,\alpha_H^2/(\alpha_Q\,\alpha_{\zeta_0}^3), \tag{3.47-28}$$

$$\alpha_x = \alpha_H/\alpha_{\zeta_0}, \tag{3.47-29}$$

$$\alpha_\zeta = \alpha_{\zeta_0}. \tag{3.47-30}$$

3.5. Combined Effect: Denudation

3.51. Models of Slope Recession. The various agents of mass transport have a combined effect upon the development of a slope which is commonly called "denudation". Microscopically, such denudation may occur, for instance, by the effect of rain. Little rivulets and gulleys may form which carry material away. The way in which this might happen

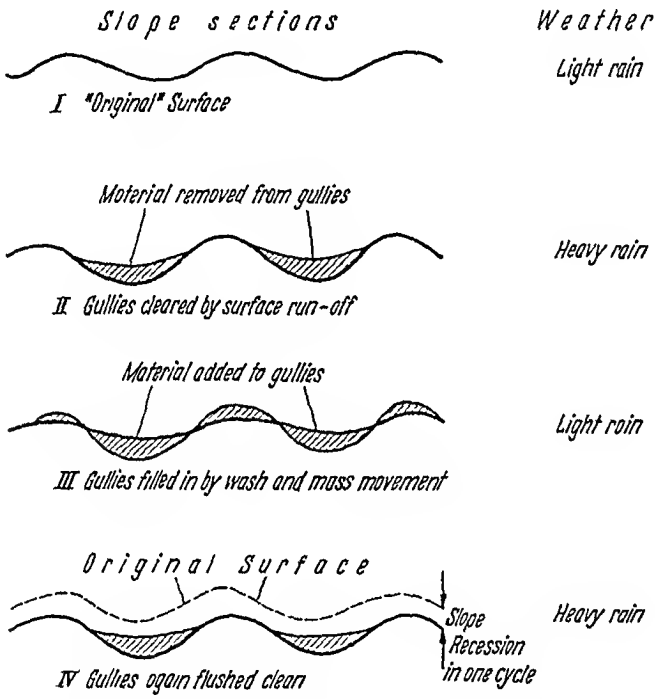

Fig. 62. Diagrammatic representation of slope retreat by gullying. After BEATY[1]

has for instance been discussed by BEATY[1] whose diagrammatic representation of slope retreat is shown in Fig. 62. However, in spite of the rather complicated aspects of such "microscopic" processes, the development of a slope bank can usually be treated in a macroscopic fashion by simply considering its over-all cross-section.

The development of this over-all cross-section has been phenomenologically studied and the observed patterns have been classified by many people. Thus, TAKESHITA[2] and SCHUMM[3] discussed various possibilities, distinguishing between mountain, hill, and valley slopes; and

1. BEATY, C. B.: Bull. Geol. Soc. Amer. 70, 1479 (1959)
2. TAKESHITA, K : Bull. Fukuoka-Ken Forest Exp. Stn. 17, 1 (1964).
3. SCHUMM, A.: J. Geolog. Educ. 14, 98 (1966).

MACAR[1] edited a volume containing many papers on the evolution of slopes mostly concerned with phenomenological development-patterns. However, in order to investigate the various possible modes of slope development, the most useful way appears to be the creation of a series of mathematical models. Such models are only concerned with the large-scale (macroscopic) aspects of the development of a slope as discussed above. They are based upon different physical pictures and thus represent the outcome of a variety of mechanical assumptions. If then the actually observed large-scale development of a natural slope be compared with the type of development obtained in the various models, the model that is applicable and therewith the underlying physical causes, can be determined.

A variety of mathematical models of slope development will be discussed below.

3.52. Parallel Rectilinear Slope Recession. The first model of slope recession which we shall consider is the following:

(i) the rock is homogeneous so that its reduction by weathering proceeds at an equal rate at all points of the slope that are exposed;

(ii) all material is instantly removed due to mass transport so that the exposure to the reducing elements is the same everywhere.

The above assumptions imply that the denudation proceeds at an equal rate everywhere on the slope. It is easy to see that this leads immediately to parallel slope recession. If the slope is rectilinear to begin with, then it will remain so and one has the case of parallel rectilinear slope recession.

The above condition represents a rather trivial case. However, things become more interesting if it is taken into account that the débris must go somewhere. One can assume that the débris will accumulate at the bottom of the slope and form a pile of screes which is leaning against the original slope. The slope angle α of the pile (screes angle) will be determined by the geometrical properties of the weathered material according to the conditions established in Sec. 3.31.

As the pile of débris grows, it will cover up more and more of the original slope and thereby protect it from further denudation. Underneath the pile, the originally straight slope will evolve into a curved one, an occurrence which had already been noted by FISHER[2] in the last century. The problem, now, is to determine more exactly the shape of the curve[3].

1. MACAR, P.: L'évolution des versants (vol. 1, Symp. Internat. Géomorphologie, Liège, 1966).

2. FISHER, O.: Geol. Mag. 3, 354 (1866).

3. A review of this problem has, for instance, been provided by BAKKER, J. P., and A. N. STRAHLER: Congr. Int. Geogr., 1er Rapp. Comm. étude des versants. Rio de Janeiro (1956).

An attempt in this direction has been made by LEHMANN[1] who envisaged the following model of a receding slope (cf. Fig. 63): A steep slope of angle β is bounded by two horizontal planes which are the (vertical) distance h apart. Each individual amount weathering off the slope will pile up at the bottom, the pile forming a screes angle α. Some of the material, however, may get lost during the transfer, or else its volume

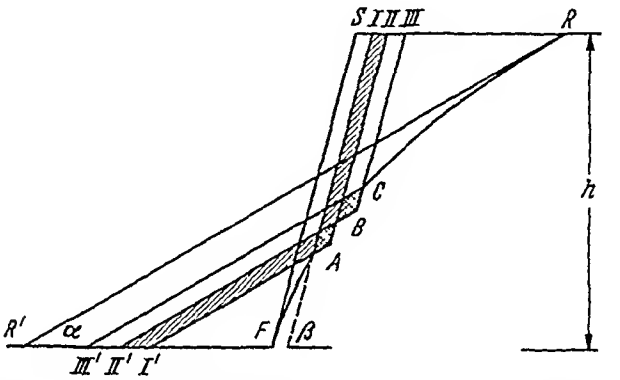

Fig. 63. Building up of a pile of débris at the bottom of a steep slope. After LEHMANN[1]

might increase since the density of the débris may be less than that of the slope-material. Hence one has to set

$$V_R/V_D = 1-c \tag{3.52-1}$$

where V_R is the volume of slope material removed and V_D the corresponding volume of débris piling up at the bottom of the slope. Expressing the condition (3.52-1) for each infinitesimal amount of slope recession, one obtains (from a inspection of Fig. 64)

$$(dx-dy\cot\beta)(h-y)=(1-c)\left(dy-\frac{dx}{\cot\alpha}\right)y\cot\alpha \tag{3.52-2}$$

or

$$\frac{dx}{dy}=\frac{h\cot\beta+(\cot\alpha-c\cot\alpha-\cot\beta)\,y}{h-cy}. \tag{3.52-3}$$

This is a differential equation which may easily be integrated. One obtains (choosing as a suitable boundary condition $y=0$ for $x=0$):

$$x=k(l+m)\,\text{lognat}\frac{m}{m-y}-ky \tag{3.52-4}$$

1 LEHMANN, O.: Viertelj.schr. Natf. Ges. Zurich 78, 83 (1933)

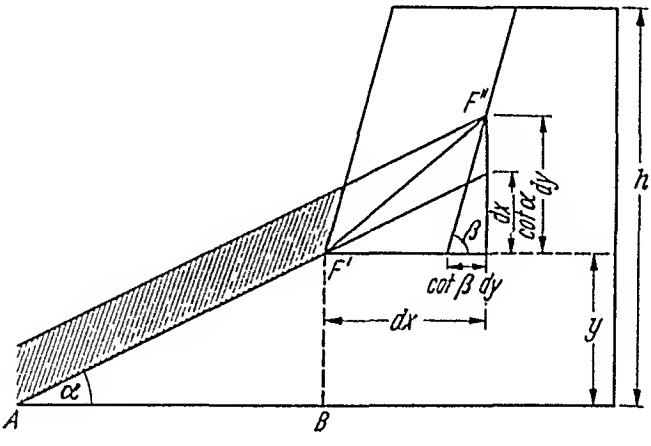

Fig. 64. Infinitesimal increase of the heap of débris at the bottom of a slope. After LEHMANN[1]

with

$$m = h/c, \tag{3.52-5}$$

$$k = \frac{(1-c)\cot\alpha}{c} - \frac{\cot\beta}{c}, \tag{3.52-6}$$

$$l = \frac{h\cot\beta}{\cot\alpha - \cot\beta - c\cot\alpha}. \tag{3.52-7}$$

In order to investigate the meaning of these equations, it is convenient to consider two limiting cases. If one sets $c=0$, $\beta=90°$, one has

$$y = \sqrt{2h\,x\tan\alpha} \tag{3.52-8}$$

which corresponds to the case where all the débris are piled up against the slope; the latter, then, underneath takes on the shape of a parabola.

A second limiting case is obtained by setting $c=-\infty$. One then obtains

$$y = x\tan\alpha. \tag{3.52-9}$$

This corresponds to the case where all the débris disappears somehow. It indicates that, under these circumstances, the slope will become rectilinear and that the slope angle will become equal to the screes angle. This result, in fact, has been enounced as a geomorphological law by BAKKER and LE HEUX[2]. The latter authors stated it as follows:

"*In every type of weathering-removal recession of steep walls, a denudation slope with a rectilinear cross-profile and a constant slope angle equalling the screes angle in nature will be formed, provided no or hardly any screes are deposited on the terrace at the foot of the initial wall*".

1. LEHMANN, O.: Viertelj.schr. Natf. Ges. Zürich **78**, 83 (1933).

2. BAKKER, J. P., and J. W. N. LE HEUX: Proc. Koninkl. Akad. Wetenschap. Amsterdam B **55**, 399 and 554 (1952).

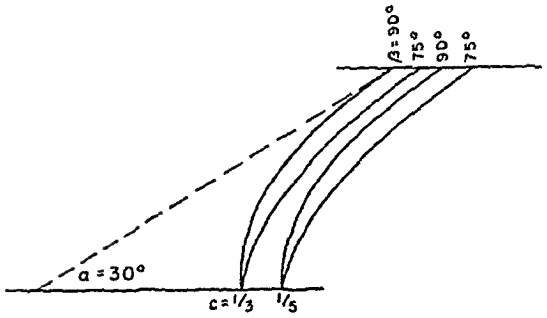

Fig. 65. The influence of the original slope angle on the shape of the slope underneath the debris for $c = {}^1/_3$ and ${}^1/_5$, $\varkappa = 30°$. After BAKKER and LE HEUX[1]

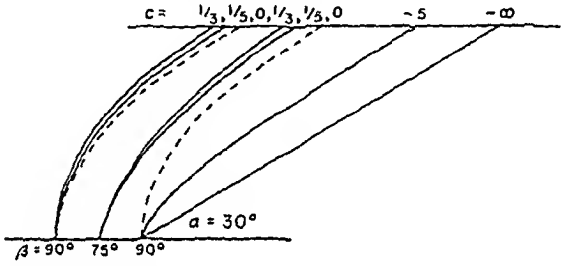

Fig. 66. The influence of the constant c on the shape of the slope underneath the debris. After BAKKER and LE HEUX[1]

BAKKER and LE HEUX[2] also provided physiographic examples to show that their law is indeed obeyed in nature. The end-result of the process envisaged by them had, in fact, been known for some time as "RICHTER's[3] slope of denudation".

It is rather difficult to visualize the curves that are represented by the Eqs. (3.52-4/7) for general values of the parameters. Points on the curves can be calculated, but there is equally the possibility of constructing them graphically. Such a method has also been described by BAKKER and LE HEUX[1]. The detailed technique to do this will not be described here, we only show some of the results that have been obtained. Thus, Fig. 65 demonstrates the influence of the original slope angle β on the curvature of the convex slope underneath the débris, and Fig. 66 demonstrates the influence of the constant c.

The above discussion deals only with the denudation of a slope bounded by two plateaux. One can extend the theory to the weathering of a

1 BAKKER, J. P., and J. W. N. LE HEUX. Proc Koninkl Akad. Wetenschap. Amsterdam 49, 533 (1946).

2. BAKKER, J. P., and J. W. N. LE HEUX: Proc. Koninkl. Akad. Wetenschap. Amsterdam B 55, 399, 554 (1952).

3 RICHTER, E.: Petermann's Geograph. Mitt., Ergänzungsbd. 24, 1 (1901).

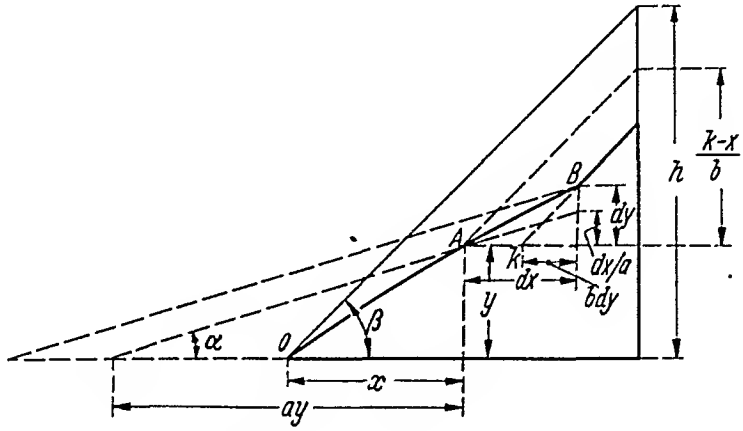

Fig. 67. Geometry of a weathering, symmetrical crest. After VAN DIJK and LE HEUX[1]

(symmetrical) crest. This has been done by VAN DIJK and LE HEUX[1]. The mass balance equation, corresponding to (3.52-3) looks for a weathering crest somewhat different from that for a weathering plateau. Using again (3.52-1), one obtains from an inspection of Fig. 67:

$$\frac{k-x}{b}(dx-b\,dy)=(1-c)\left(dy-\frac{dx}{a}\right)a\,y. \tag{3.52-10}$$

Here, second order quantities have been neglected and h is the height of the crest, $2k$ is its base, β is again the original slope angle and α is the screes angle. Furthermore

$$\cot\alpha=a, \tag{3.52-11}$$

$$\cot\beta=b. \tag{3.52-12}$$

An analysis of the slopes that will develop, rests with a discussion of the differential Eq. (3.52-10). First of all, it will be convenient to write the latter as follows:

$$\frac{dy}{dx'}=-\frac{(1/b)\,x'+(1-c)\,y}{x'+(1-c)\,a\,y} \tag{3.52-13}$$

where the substitution

$$x'=k-x \tag{3.52-14}$$

has been performed. This puts the zero point for x' below the center of the crest. One then can discuss easily some special cases:

(i) If $a=b$, one has

$$\frac{dy}{dx'}=-\frac{1}{a}. \tag{3.52-15}$$

1. VAN DIJK, W., and J. W. N. LE HEUX: Proc. Koninkl. Akad. Wetenschap. Amsterdam B **55**, 115, 123 (1952).

Hence

$$y=-\frac{1}{a}x'+C=-\frac{1}{a}(k-x)+C \tag{3.52-16}$$

where C is a constant of integration. If one requires $y=0$ for $x=0$, this yields

$$y=\frac{1}{a}x. \tag{3.52-17}$$

(ii) If $c=-\infty$, one has also

$$\frac{dy}{dx'}=-\frac{1}{a}. \tag{3.52-18}$$

Hence, with the usual boundary condition, again:

$$y=\frac{1}{a}x. \tag{3.52-19}$$

Thus, in the two special cases considered above, the crest develops into straight slopes of slope angle α.

In the general case, a more elaborate discussion is required. Setting

$$u=y/x' \tag{3.52-20}$$

$$dy=u\,dx'+x'\,du \tag{3.52-21}$$

yields from (3.52-13):

$$\frac{dx'}{x'}=-du\frac{1+(1-c)\,a\,u}{\frac{1}{b}+(2-c)\,u+(1-c)\,a\,u^2} \tag{3.52-22}$$

which is a differential equation with separated variables. It can therefore be integrated. Depending on the sign of the discriminant

(i) $$(1-c)\frac{a}{b}-\frac{(2-c)^2}{4}>0, \tag{3.52-23}$$

(ii) $$(1-c)\frac{a}{b}-\frac{(2-c)^2}{4}<0, \tag{3.52-24}$$

(iii) $$(1-c)\frac{a}{b}-\frac{(2-c)^2}{4}=0 \tag{3.52-25}$$

one has three possible solutions. Transforming back to the old coordinate system and using the usual boundary condition, these solutions are for the three cases (i), (ii), (iii) (according to VAN DIJK and LE HEUX[1]):

1. VAN DIJK, W., and J.W.N. LE HEUX: Proc. Koninkl. Akad. Wetenschap. Amsterdam B 55, 115, 123 (1952).

Case (i)

$$(1-c)\,a\,b\,y^2+(2-c)\,b(k-x)\,y+(k-x)^2$$
$$=k^2\exp\left\{\frac{2c}{\sqrt{4(1-c)\frac{a}{b}-(2-c)^2}}\arctan\frac{-a\,b\,y\sqrt{4(1-c)\frac{a}{b}-(2-c)^2}}{2a(k-x)+(2-c)\,a\,b\,y}\right\}. \tag{3.52-26}$$

Case (ii)

$$(1-c)\,a\,b\,y^2+(2-c)\,b(k-x)\,y+(k-x)^2$$
$$=k^2\exp\left\{\frac{c}{\sqrt{(2-c)^2-4(1-c)\,a/b}}\right. \tag{3.52-27}$$
$$\left.\cdot\,\mathrm{lognat}\frac{2a(k-x)+(2-c)\,a\,b\,y+a\,b\,y\sqrt{(2-c)^2-4(1-c)(a/b)}}{2a(k-x)+(2-c)\,a\,b\,y-a\,b\,y\sqrt{(2-c)^2-4(1-c)(a/b)}}\right\}.$$

Case (iii)

$$(1-c)\,a\,b\,y^2+(2-c)\,b(k-x)\,y+(k-x)^2$$
$$=k^2\exp\left\{\frac{-4c(1-c)\,a\,y}{2(1-c)(2-c)\,a\,y+(2-c)^2(k-x)}\right\}. \tag{3.52-28}$$

The geometrical properties of the curves represented by Equations (3.52-26/28) have been studied by LOOMAN[1]. This author noted first of all that all possible positions of the original slope can be obtained from the case $\beta=90°$ by an affine transformation. In these affine transformations, the constants a and b change independently into some other constants, whereas c remains an invariant. This follows simply from an inspection of Fig. 67. Making use of this property, LOOMAN was able to show:

(i) In case (i) the curves are affine transformations of logarithmic spirals (BERNOULLI's spirals), circles being included among them.

(ii) In case (ii) the curves are affine transformations of the line

$$y=x^n \tag{3.52-29}$$

(polytropic lines) with n satisfying the equation

$$n+\frac{1}{n}-2=\frac{c^2\,b}{(1-c)\frac{a-b}{b}}-4 \tag{3.52-30}$$

for the relevant values a, b, c.

1. LOOMAN, H.: Proc. Koninkl. Akad. Wetenschap. Amsterdam B 59, 259 (1956).

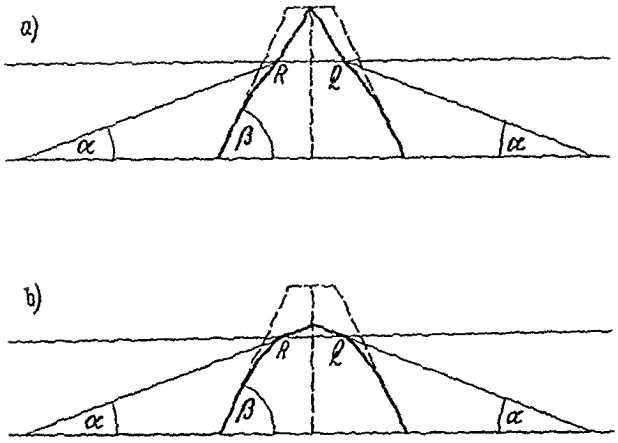

Fig 68. Two successive stages of the weathering of a symmetrical plateau of finite width. After VAN DIJK and LE HEUX[1]

(iii) In case (iii) the curves are affine transformations of

$$y = x \log |x|; \tag{3.52-31}$$

hence projective representations of the logarithmic line.

The proof of these statements is rather cumbersome and will therefore not be repeated here.

VAN DIJK and LE HEUX[1] also combined their theory of weathering of a plateau with that of a crest. Thus, suppose that one starts with a symmetrical plateau of finite width. Eventually, a stage will be reached where the two weathering edges meet at the top (Fig. 68a). The further progress will be by symmetrical crest recession, but without a plateau being present at the level RQ (Fig. 68). Thus, the development is supposed to be somewhat as it is shown in Fig. 68b.

3.53. Central Rectilinear Slope Recession. The theory of parallel rectilinear slope recession discussed above has certain unsatisfactory aspects. It stands to reason that the amount of denudation at the top is greater than the amount of denudation at the bottom and that one should take such variations into account. This has been done by BAKKER and LE HEUX[2] by their postulate of *central* rectilinear slope recession.

The postulates basic to central rectilinear slope recession can best be seen by inspecting Fig. 69 representing the case of a steep slope of

1. VAN DIJK, W., and J. W. N. LE HEUX: Proc. Koninkl. Wetenschap. Amsterdam B 55, 115, 123 (1952).

2. BAKKER, J. P., and J. W. N. LE HEUX: Proc. Koninkl. Akad Wetenschap. Amsterdam 50, 959, 1154 (1947)

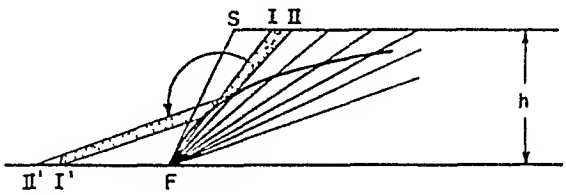

Fig. 69. Central rectilinear slope recession. After BAKKER and LE HEUX[1]

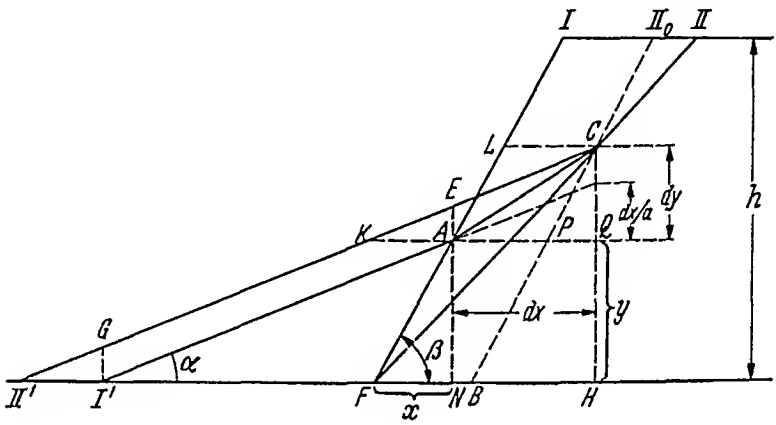

Fig. 70. Diagram for the deduction of the differential equation of central rectilinear recession of a plateau. After BAKKER and LE HEUX[1]

slope-angle β that is bounded by two plateaux which are the (vertical) distance h apart. During each infinitesimal time interval, the cross-sectional area weathering off the slope is bounded by two straight lines that always meet at the focal point F which is the original foot-point of the slope. As in Sec. 3.52, the débris then accumulates at the bottom of the slope forming a pile of screes with screes angle α and thereby protects part of the slope from further denudation. During the denudation-process, the slope angle β changes.

In order to deduce the relevant differential equation for the slope underneath the débris, we investigate the geometry of an infinitesimal change in some detail as shown in Fig. 70. From an inspection of this Figure, and again using (3.52-1) and (3.52-11/12), we obtain (after BAKKER and LE HEUX[1])

$$(1-c)\cdot II'I'AK = LCII_0I + II_0CII, \tag{3.53-1}$$

$$II'I'AK = GI'AE = a\,y(dy - dx/a), \tag{3.53-2}$$

$$(1-c)\,y(a\,dy - dy) = (dx - b\,dy)(h-y) + II_0CII. \tag{3.53-3}$$

1. BAKKER, J. P., and J. W. N. LE HEUX: Proc. Koninkl. Akad. Wetenschap. Amsterdam **50**, 959 (1947).

But

$$II_0\,CII:FCB=(h-y)^2:y^2, \tag{3.53-4}$$

$$II_0\,CII:\tfrac{1}{2}(dy-b\,dy)\,y=(h-y)^2:y^2, \tag{3.53-5}$$

$$II_0\,CII=\frac{(h-y)^2}{2y}(dx-b\,dy) \tag{3.53-6}$$

and hence

$$(1-c)\,y(a\,dy-dx)=(dx-b\,dy)(h-y)\left\{1+\frac{h-y}{2y}\right\}. \tag{3.53-7}$$

Using the fact that the variable slope angle β can be expressed as follows

$$\cot\beta=b=\frac{x}{y} \tag{3.53-8}$$

one has finally

$$\frac{dx}{dy}-\frac{h^2-y^2}{[h^2+(1-2c)\,y^2]\,y}x=\frac{2a(1-c)\,y^2}{h^2+(1-2c)\,y^2} \tag{3.53-9}$$

as the final differential equation for the slope. One may immediately solve it for the special case $c=-\infty$. One has then

$$dx/dy=a \tag{3.53-10}$$

or

$$y=x\tan\alpha \tag{3.53-11}$$

which means that in this limit one again approaches RICHTER's slope of denudation (cf. Sec. 3.52).

In the general case, the differential equation (3.53-9) is of the form

$$\frac{dx}{dy}+P(y)\,x=Q(y) \tag{3.53-12}$$

whose solution is well known:

$$x=e^{-\int P(y)\,dy}\{\int Q(y)\,e^{\int P(y)\,dy}\,dy+C\}. \tag{3.53-13}$$

Thus, the solution of (3.53-9) is

(i) for $c\neq\frac{1}{2}$

$$x=a\,y-(a-b_0)\,y\left[\frac{h^2+(1-2c)\,y^2}{h^2}\right]^{\frac{c-1}{1-2c}} \tag{3.53-14}$$

(ii) for $c=\frac{1}{2}$

$$x=a\,y-(a-b_0)\,y\exp\left\{-\frac{y^2}{2h^2}\right\}. \tag{3.53-15}$$

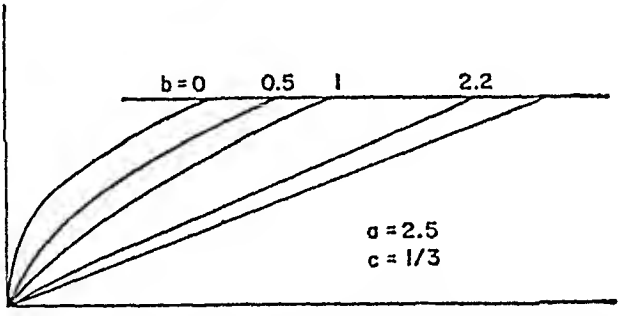

Fig. 71. Central rectilinear recession of a plateau. After BAKKER and LE HEUX[1]

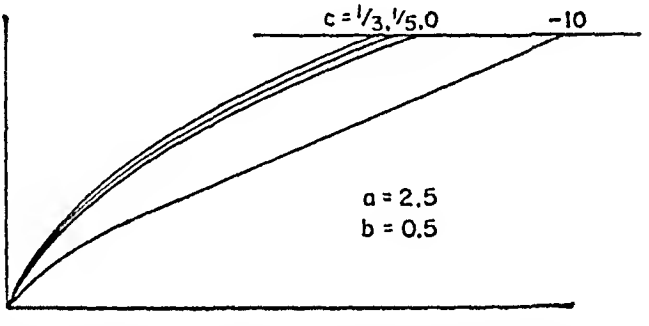

Fig. 72. Central rectilinear recession of a plateau. After BAKKER and LE HEUX[1]

Here, b_0 is the cotangent of the *initial* slope angle and the boundary conditions have been chosen so that $y=0$ for $x=0$. Several curves that can be drawn from the solution (3.53-14/15) are shown in Figs. 71 and 72. These curves represent slopes that may develop underneath a heap of débris according to the central rectilinear recession theory.

As in the case of parallel slope recession, the above theory has also been extended to receding (symmetrical) crests (BAKKER and LE HEUX[2]). Using the same geometrical layout as in Fig. 68 (showing a symmetrical crest), but expressing the condition of *central* slope recession, one immediately ends up with the differential equation

$$y(1-c)(a\,dy-dx)=\frac{k^2-x^2}{2x^2}(y\,dx-x\,dy) \qquad (3.53\text{-}16)$$

where the symbols have the meaning adopted in Sec. 3.52. Written in a more standard form, the last equation is

$$\frac{dx}{dy}=\frac{x(k^2-x^2)+2a x^2 y(1-c)}{y[2x^2(1-c)+k^2-x^2]}. \qquad (3.53\text{-}17)$$

1. BAKKER, J P, and J. W. N. LE HEUX: Proe Koninkl. Akad. Wetenschap. Amsterdam **50**, 959 (1947).

2. BAKKER, J. P., and J. W. N LE HEUX: Proc. Koninkl. Akad. Wetenschap. Amsterdam **53**, 1073, 1364 (1950).

The integration of this differential equation has been performed by LOOMAN[1] who noted that it can be done by the following substitution of variables:

$$v = a^2 y^2 / k^2, \tag{3.53-18}$$

$$t = x/(a y). \tag{3.53-19}$$

This leads to

$$\frac{dv}{dt} = \frac{1-2c}{1-c} \frac{v}{1-t} + \frac{1}{(1-c)\, t^2 (1-t)} \tag{3.53-20}$$

which is linear in v. Integration with the initial condition $y=0$ for $t=b_0/a$ yields the solution:

$$v = (1-t)^{-\frac{1-2c}{1-c}} \frac{1}{1-c} \int_{b_0/a}^{t} \frac{(1-\lambda)^{-c/(1-c)}}{\lambda^2} d\lambda, \tag{3.53-21}$$

or, in the old coordinates x, y:

$$(a y)^{\frac{1}{1-c}} (a y - x)^{\frac{1-2c}{1-c}} = \frac{k^2}{1-c} \int_{b_0/a}^{x/(a y)} \frac{(1-\lambda)^{-c/(1-c)}}{\lambda^2} d\lambda. \tag{3.53-22}$$

A particular curve of this type is shown in Fig. 73. This curve had been obtained by BAKKER and LE HEUX utilizing a graphical method before LOOMAN integrated the differential equation in closed form.

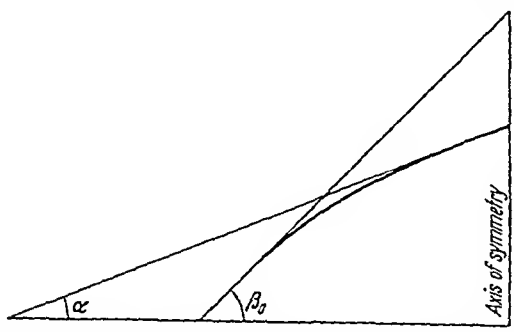

Fig. 73. Central rectilinear recession of a symmetrical crest for $\beta_0 = 45°$, $\alpha = 22°$, $a = 2.5$, $c = 0$
After BAKKER and LE HEUX[2]

An interesting observation regarding the integral curves in central rectilinear slope recession theory concerns the occurrence of *kinks*. Let us consider the case of plateau recession. Because of the symmetry of the solution (3.53-14 or 15) with regard to the origin ($x=0$, $y=0$), all the corresponding curves must have an inflexion point, and therefore zero

1. LOOMAN, H.: Proc. Koninkl. Akad. Wetenschap Amsterdam B 59, 259 (1956).
2. BAKKER, J. P., and J. W. N. LE HEUX: Proc. Koninkl. Akad. Wetenschap Amsterdam 53, 1073, 1364 (1950).

curvature, at that point. For large values of x, the curvature is again very small since the curves approach straight lines with the angle α (provided c is small enough; cf. 3.53-11). Hence, there must be a maximum of curvature somewhere and this represents a kink. Similar observations can be made in the case of *crest* recession. BAKKER and LE HEUX claim that this explains geomorphological observations in which such kinks were actually noted near the bottom of a slope. Naturally, for such phenomena to become visible, the screes that had originally been formed, must later have been removed. However, the possibility of this happening without the kink being destroyed would appear as somewhat doubtful.

3.54. Variations of Exposure: Linear Theory[1]. The models of denudation reviewed above are concerned with the shape of a rocky core beneath a pile of débris. However, BAKKER and his followers also applied this theory to the shapes of *visible* slopes. In order for these slopes to become uncovered, the débris above them must somehow be removed which must necessarily be achieved by the action of some eroding agent. It then appears as very doubtful indeed that the original shape of the slopes existing beneath the débris could possibly remain unaffected thereby, although LAWSON[2] maintains that slopes may develop in this fashion in arid climates.

In the theory of central rectilinear slope recession, an attempt was made to take variations of the rapidity of denudation into account. However, this was done by a postulate regarding the geometry of the slope without justifying it by a proper model of mass transport. One might therefore want to analyze systematically the effect of various assumptions regarding the rapidity of denudation upon the shape of the slope. At the same time, one might entertain the hope that the various shapes encountered in nature could be obtained directly from appropriate postulates regarding the process of denudation.

Assuming a homogeneous slope material, variations of the rapidity of denudation will be due to variations of exposure of the rock to the elements of the weather. One might think of the following possibilities:

Case 1. The denudation is independent of the slope and proceeds at an equal rate at any exposed portions of the slope.

Case 2. The denudation is proportional to the height of the point under consideration above a certain base level. This could be justified by the observation that in certain areas, precipitation increases with height.

Case 3. The denudation is proportional to the steepness of the slope. This could be justified by noting that the weathering is due to the expo-

1. This and the next section (3.55) are after SCHEIDEGGER, A. E.: Bull. Geol. Soc. Amer. 72, 37 (1961).

2. LAWSON, A. C.: Public. Univ. Calif., Dept. Geology 9, 3 (1915).

sure of the slope. The steeper the slope, the faster will the débris be removed. Thus, the steeper slopes will generally be more exposed than less steep ones.

Let us investigate how the denudation affects the shape of slopes in the above three cases. In order to do this, we assume that the lowering of the slope per unit time at any given point is proportional to a constant

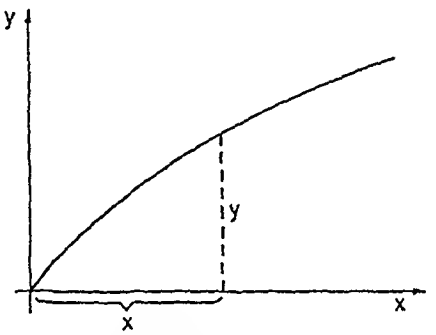

Fig. 74. General geometry of a slope

(case 1), to the height of the slope (case 2) or to the slope (case 3). Thus, denoting the height by y, the location by x, we have (cf. Fig. 74)

$$\frac{\partial y}{\partial t} = -\text{const}\ \Phi \tag{3.54-1}$$

with

$$\text{case 1:}\quad \Phi = 1 \tag{3.54-2}$$

$$\text{case 2:}\quad \Phi = y \tag{3.54-3}$$

$$\text{case 3:}\quad \Phi = \partial y/\partial x. \tag{3.54-4}$$

It is obviously always possible to change the time scale in such a fashion that the constant in (3.54-1) can be set equal to 1. Thus, one has a partial differential equation to solve; the shape of the original slope represents the arbitrary function that enters into the solution of every partial differential equation. In the three cases under consideration, the solution is very easily obtained.

Case 1. The differential equation is

$$\frac{\partial y}{\partial t} = -1 \tag{3.54-5}$$

with the initial condition $y = f_0(x)$. The solution is

$$y = f_0(x) - t. \tag{3.54-6}$$

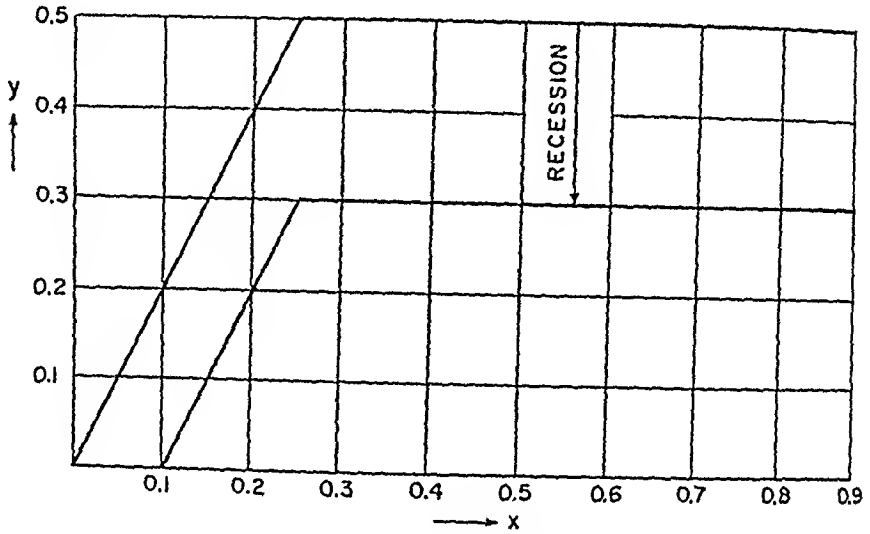

Fig. 75. Slope recession in case 1 of the linear theory

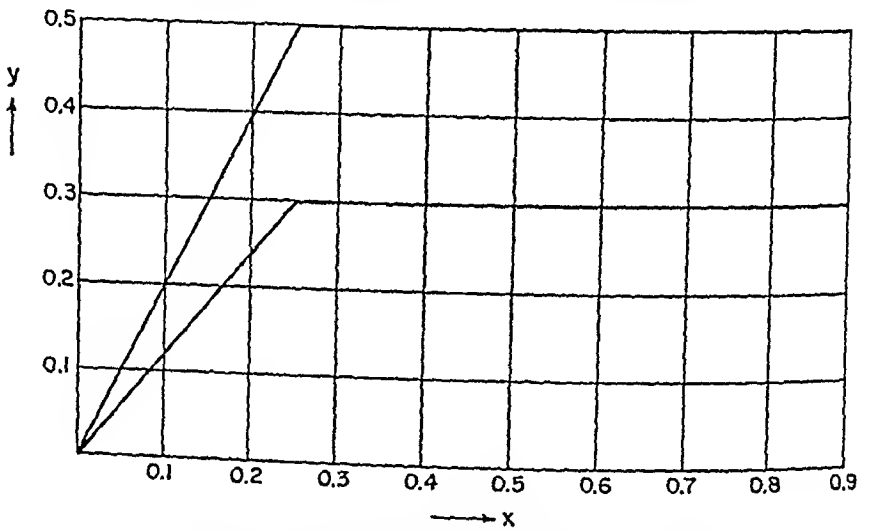

Fig. 76. Slope recession in case 2 of the linear theory

This represents the case of equal slope recession. The slope retains its shape and simply downward (see Fig. 75). If the slope is rectilinear to begin with, then one has *parallel slope recession* downward.

Case 2. The differential equation is

$$\frac{\partial y}{\partial t} = -y \tag{3.54-7}$$

with the same initial condition $y_0 = f_0(x)$. The solution is

$$y = f_0(x)\, e^{-t}. \tag{3.54-8}$$

At any time, all slope-heights, therefore, are reduced proportionately (see Fig. 76). If the slope is rectilinear to begin with, then this indeed represents

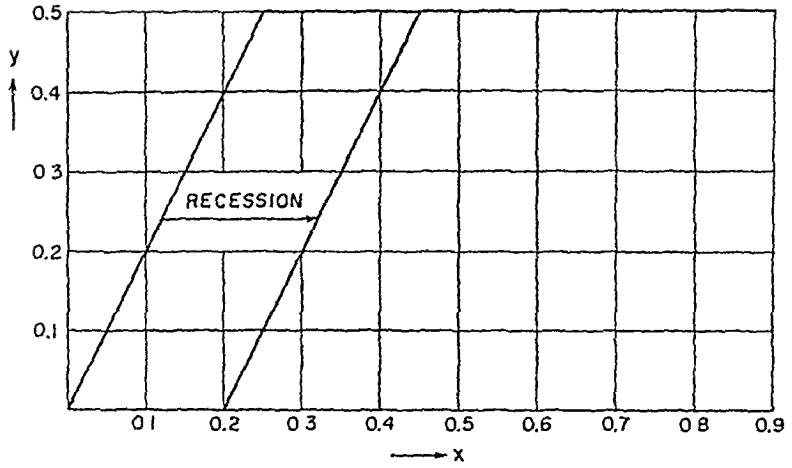

Fig. 77. Slope recession in case 3 of the linear theory

central slope recession. The latter has, thus, been given a clear physical justification.

Case 3. The differential equation is

$$\frac{\partial y}{\partial t} = -\frac{\partial y}{\partial x}. \tag{3.54-9}$$

Using the usual initial condition $y_0 = f_0(x)$, the solution is

$$y = f_0(x - t). \tag{3.54-10}$$

This solution signifies that any given slope profile will wander to the right with time (see Fig. 77). If the slope is rectilinear, this means *parallel slope recession* as in *case 1*. One has thus the interesting fact that parallel rectilinear slope recession can occur in case 1 as well as in case 3.

The various cases discussed above are in fact those that have been treated in the earlier work of BAKKER and followers. During its recession, a rectilinear slope remains rectilinear; the development is either parallel or central, depending on the model that is chosen. One may note that the physical conditions leading to central slope recession are, in fact, not very satisfactory, as it appears as very artificial indeed to assume that weathering is proportional to the height of the slope above a certain base level. It is much more natural to assume that the rapidity of weathering is proportional to the slope itself which, according to the above discussion, leads to parallel slope recession.

The basic shape of the slope remains unaltered in all three cases treated above. The hope that a variation of exposure would change the slope-shapes is therefore not fulfilled in the above mathematical models. In order to obtain such changes, one still has to take recourse to the idea of building up and afterwards destroying piles of screes.

3.55. Variation of Exposure: Nonlinear Theory. The mathematical models of slope development discussed so far appeal very much to one's imagination because of their basic simplicity. However, precisely because of the latter, some important conditions obtaining in nature have been neglected and the calculated slope profiles appear therefore as far too simple.

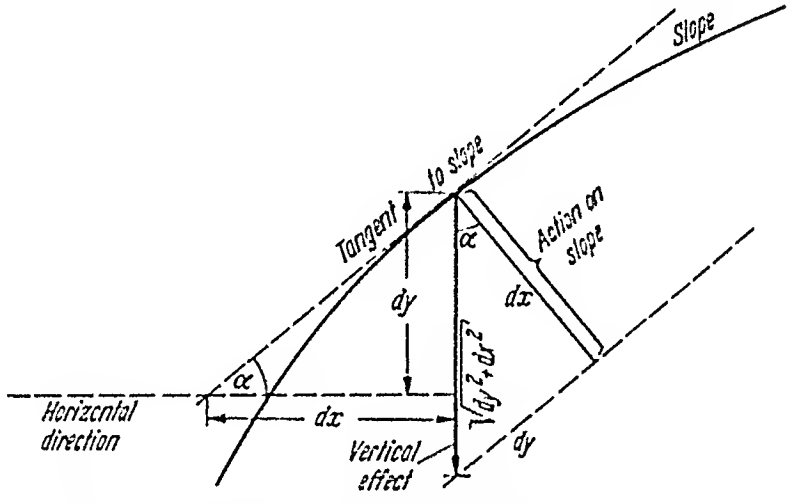

Fig. 78. Vertical effect of weathering action normal to the slope

A serious oversimplification has been made in the models when the *vertical* lowering of the slopes was set proportional to some expression which was either a constant, equal to y, or equal to $\partial y/\partial x$. One really should allow for the fact that weathering acts *normal* to the slope so that the vertical lowering is then represented by the vertical effect of the weathering-action (the latter being taken as proportional to a constant, y, or $\partial y/\partial x$ according to the case under consideration) which is directed *normally* against the slope. From an inspection of Fig. 78 which shows the geometrical layout of the weathering action, one can see that the slope development is then represented by the differential equation

$$\frac{\partial y}{\partial t} = -\sqrt{1+\left(\frac{\partial y}{\partial x}\right)^2}\,\Phi \qquad (3.55\text{-}1)$$

where Φ is again given by one of the expressions (3.54-2/3/4) corresponding to the three possible cases under consideration.

The improved "new" differential equation (3.55-1) of slope development differs from the old one in a very fundamental regard: it is nonlinear. Easy solutions of the new equation can therefore no longer be obtained. Although analytical solutions are possible[1,2] (using a Legendre

1. Mitin, A. V., and A. M. Trofimov: Uch. Zap. Kazansk. Gos. Un-ta **124**, No. 4, 112 (1964).

2. Trofimov, A. M.: Izv. Vsesoy. Geograf. Ob-va **98**, No. 2, 166 (1966).

transformation for case 2 and the theory of characteristics for cases 1 and 3) one ends up with a system of equations which can be written down in a reasonably simple form only for the case of an infinitely long straight slope as initial condition. The latter has not much relation to conditions in nature. If one wishes to have actual numerical results that have a visualizable meaning, it is best to solve the equations directly by means

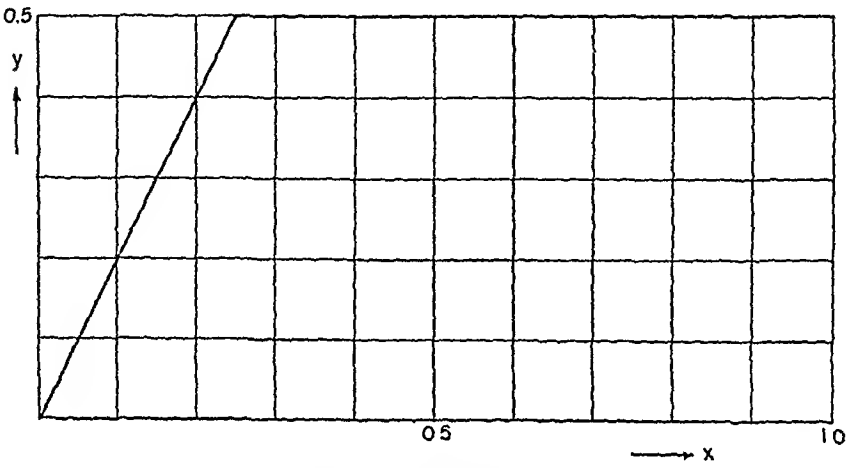

Fig. 79. Original slope step

of an electronic computer. As always with nonlinear hyperbolic partial differential equations, the choice of the steps in the approximation procedure is critical. The steps for Δx and Δt have to be consistent with the domain of influence defined by the net of characteristics (see e.g. COLLATZ[1]), but this is merely a necessary, not a sufficient condition for achieving stability for the solution.

In all cases considered, the development of a slope step was studied (in profile). The original height of the step was assumed as equal to 0.5 (arbitrary) scale units of y, the original slope at one end of the slope as equal to 2. The coördinate x varies from 0 to 1 in 100 steps. The original slope, thus, has the shape shown in Fig. 79. Then, the procedure adopted in the individual cases was as follows.

Case 1. The differential equation is

$$\frac{\partial y}{\partial t} = -\sqrt{1+\left(\frac{\partial y}{\partial x}\right)^2} \tag{3.55-2}$$

1. COLLATZ, L.: Numerische Behandlung von Differentialgleichungen. Berlin-Göttingen-Heidelberg: Springer 1951.

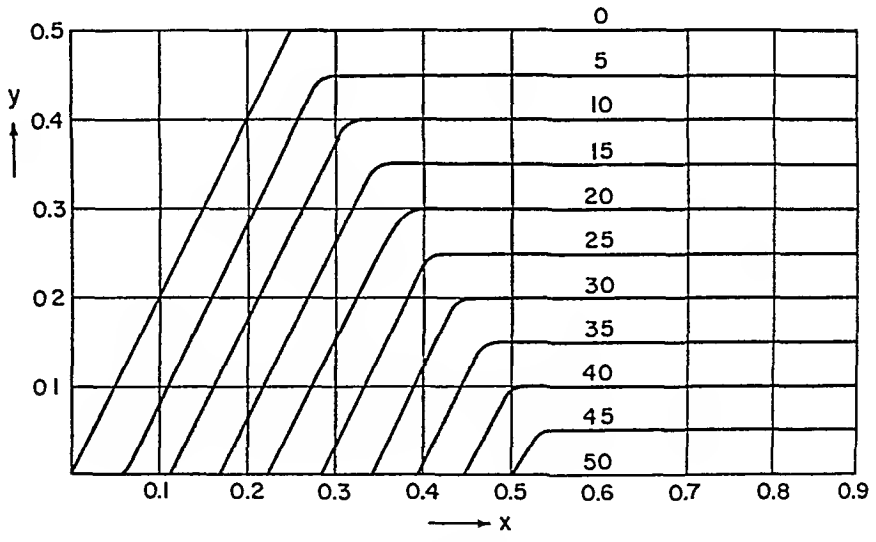

Fig. 80. Slope recession in case 1 of the nonlinear theory

which was approximated by the following difference equation

$$(y_{t_{m+1}} - y_{t_m})\Big|_n = -\sqrt{1+\left(\frac{y_n - y_{n-1}}{x_n - x_{n-1}}\right)^2}\Big|_m (t_{m+1} - t_m). \qquad (3.55\text{-}3)$$

The characteristics are (using e.g. the formula given by COLLATZ[1] p. 241)

$$dt/ds = 1 \qquad (3.55\text{-}4)$$

$$\frac{dx}{ds} = \frac{\partial y/\partial x}{\sqrt{1+(\partial y/\partial x)^2}} \qquad (3.55\text{-}5)$$

with s = arc length on the characteristics. This yields as a necessary condition for stability

$$\Delta t < \Delta x \sqrt{1+1/(\partial y/\partial x)^2} \qquad (3.55\text{-}6)$$

with

$$\Delta t = t_{n+1} - t_n; \qquad \Delta x = x_n - x_{n-1}.$$

Since the right-hand side of this inequality is always larger than 1, one can safely set

$$\Delta t = \Delta x. \qquad (3.55\text{-}7)$$

The result of carrying out the approximation procedure is shown in Fig. 80; some of the numerical values are tabulated in Table 7.

It is evident that there is a difference if the present case be compared with the analogous one of the linear theory. The recession is now no

1. COLLATZ, L.: Numerische Behandlung von Differentialgleichungen. Berlin-Göttingen-Heidelberg: Springer 1951.

Table 7. *Slope recession in case 1 of the nonlinear theory*

x	Time								
	5	10	15	20	25	30	35	40	45
0 00	0.00000	0.00000	0.00000	0.00000	0.00000	0.00000	0 00000	0.00000	0 00000
0.02	0.00000	0.00000	0.00000	0.00000	0.00000	0.00000	0.00000	0.00000	0.00000
0.04	0.00000	0.00000	0 00000	0.00000	0.00000	0.00000	0.00000	0.00000	0.00000
0.06	0.00000	0.00000	0.00000	0.00000	0.00000	0.00000	0.00000	0.00000	0.00000
0 08	0.04820	0.00000	0.00000	0.00000	0.00000	0.00000	0 00000	0.00000	0 00000
0.10	0 08820	0.00000	0 00000	0 00000	0.00000	0.00000	0.00000	0.00000	0.00000
0 12	0 12820	0 01639	0 00000	0.00000	0 00000	0.00000	0 00000	0.00000	0.00000
0 14	0 16820	0 05639	0 00000	0 00000	0.00000	0.00000	0.00000	0.00000	0 00000
0.16	0.20820	0.09639	0.00000	0.00000	0 00000	0.00000	0 00000	0.00000	0 00000
0 18	0 24820	0 13639	0.02458	0 00000	0.00000	0.00000	0 00000	0.00000	0.00000
0 20	0.28820	0.17639	0.06458	0 00000	0 00000	0.00000	0.00000	0.00000	0 00000
0.22	0.32820	0.21639	0.10458	0.00000	0.00000	0.00000	0.00000	0.00000	0.00000
0 24	0.36820	0.25639	0.14458	0.03278	0 00000	0.00000	0.00000	0.00000	0.00000
0.26	0 40820	0.29639	0 18458	0.07278	0 00000	0.00000	0.00000	0 00000	0.00000
0.28	0 42811	0 33639	0.22458	0 11278	0.00098	0.00000	0 00000	0.00000	0.00000
0.30	0.45000	0.37630	0 26458	0.15278	0 04098	0.00000	0.00000	0 00000	0.00000
0 32	0 45000	0.39999	0.30458	0 19278	0.08098	0.00000	0.00000	0.00000	0.00000
0.34	0.45000	0.40000	0.34302	0.23278	0.12098	0.00917	0.00000	0.00000	0 00000
0 36	0 45000	0.40000	0 35000	0 27273	0.16098	0.04917	0 00000	0 00000	0.00000
0.38	0 45000	0 40000	0.35000	0.29994	0.20097	0.08917	0 00000	0.00000	0.00000
0.40	0.45000	0.40000	0 35000	0.30000	0 24006	0.12917	0 01736	0.00000	0 00000
0.42	0 45000	0.40000	0.35000	0.30000	0.25000	0.16914	0.05736	0.00000	0 00000
0 44	0.45000	0.40000	0.35000	0 30000	0 25000	0.19969	0 09736	0.00000	0 00000
0.46	0.45000	0 40000	0 35000	0.30000	0.25000	0.20000	0.13684	0.02556	0.00000
0 48	0 45000	0.40000	0 35000	0 30000	0 25000	0.20000	0.15000	0.06554	0.00000
0.50	0 45000	0.40000	0.35000	0.30000	0.25000	0.20000	0.15000	0.09900	0.00000
0 52	0 45000	0 40000	0.35000	0.30000	0.25000	0.20000	0.15000	0.10000	0.00355
0 54	0 45000	0.40000	0.35000	0.30000	0.25000	0.20000	0.15000	0.10000	0.05000

longer straight downward, but partly sideways. At the same time, the sharp edge becomes rounded.

Case 2. The differential equation is

$$\frac{\partial y}{\partial t} = -y\sqrt{1+\left(\frac{\partial y}{\partial x}\right)^2}. \tag{3.55-8}$$

The difference equation approximating this is

$$y_{t_{m+1}} - y_{t_m}\Big|_n = -\sqrt{1+\left(\frac{y_n - y_{n-1}}{x_n - x_{n-1}}\right)^2}\, y_n\Big|_m (t_{m+1} - t_m). \tag{3.55-9}$$

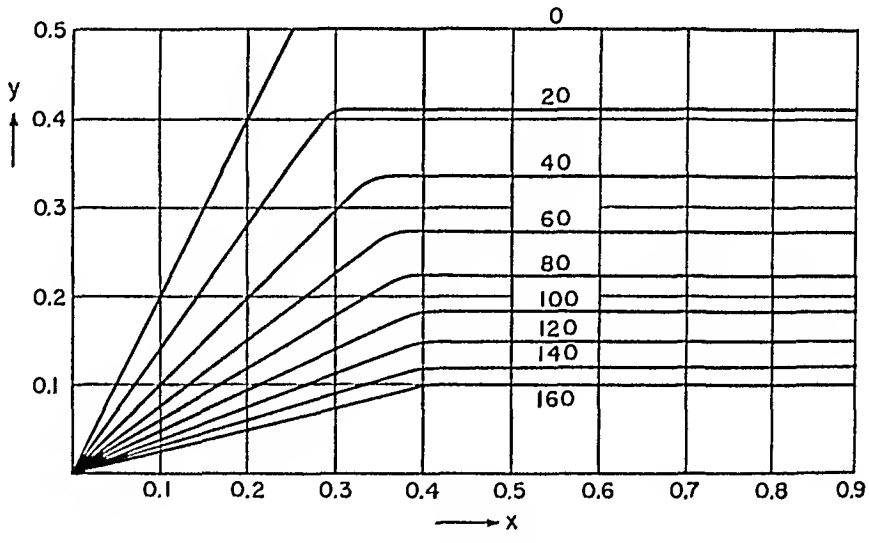

Fig. 81. Slope recession in case 2 of the nonlinear theory

The equations for the characteristics are

$$dt/ds = 1 \tag{3.55-10}$$

$$\frac{dx}{ds} = y\frac{\partial y/\partial x}{\sqrt{1+(\partial y/\partial x)^2}} \tag{3.55-11}$$

which leads to the condition

$$\Delta t \leq \Delta x \frac{1}{y}\sqrt{\frac{1}{(\partial y/\partial x)^2}+1}. \tag{3.55-12}$$

Since y is always smaller than 0.5, it is safe to set

$$\Delta t = 2\Delta x. \tag{3.55-13}$$

The results obtained by this approximation procedure are shown graphically in Fig. 81. Some of the values are tabulated in Table 8. In presenting these results, the time steps have been measured in units of Δx.

It is seen that the slope recession is now no longer "central" as was the case in the linear theory. One also has a rounding of the top edge.

Case 3. The differential equation is

$$\frac{\partial y}{\partial t} = -\frac{\partial y}{\partial x}\sqrt{1+\left(\frac{\partial y}{\partial x}\right)^2}. \tag{3.55-14}$$

This is approximated by the difference equation

$$y_{t_{m+1}} - y_{t_m}\Big|_n = -\frac{y_n - y_{n-1}}{x_n - x_{n-1}}\sqrt{1+\left(\frac{y_n - y_{n-1}}{x_n - x_{n-1}}\right)^2}\Bigg|_m (t_{m+1} - t_m). \tag{3.55-15}$$

Table 8. *Slope recession in case 2 of the nonlinear theory*

x	Time							
	20	40	60	80	100	120	140	160
0 00	0.00000	0.00000	0.00000	0 00000	0.00000	0.00000	0.00000	0.00000
0 02	0.02705	0 01983	0.01518	0.01188	0.00944	0.00758	0.00612	0 00496
0.04	0.05410	0.03968	0.03036	0.02366	0.01889	0.01516	0 01224	0.00992
0.06	0.08115	0 05952	0.04554	0.03565	0.02833	0 02274	0.01836	0 01488
0.08	0.10820	0.07936	0.06073	0.04753	0 03778	0.03032	0.02448	0.01985
0.10	0.13525	0.09920	0 07591	0.05941	0.04722	0.03790	0.03060	0.02481
0.12	0.16230	0.11904	0.09109	0 07130	0.05667	0.04547	0.03672	0 02977
0 14	0.18935	0.13888	0.10627	0 08318	0.06611	0.05305	0.04284	0.03473
0.16	0.21640	0.15718	0 12145	0.09506	0.07555	0 06063	0.04896	0 03969
0.18	0.24345	0.17856	0.13664	0 10695	0.08500	0.06821	0.05508	0.04465
0.20	0.27050	0 19840	0.15182	0 11883	0 09444	0.07579	0.06120	0 04961
0 22	0.29755	0 21824	0.16700	0.13071	0.10389	0.08337	0.06732	0.05458
0.24	0.32460	0.23808	0.18218	0 14259	0.11333	0 09095	0 07344	0 05954
0.26	0.35165	0.25792	0.19736	0 15447	0.12278	0.09853	0 07956	0.06450
0.28	0.37854	0.27778	0.21254	0.16636	0.13222	0.10611	0 08568	0.06946
0.30	0.40242	0.29757	0.22773	0.17824	0.14166	0.11368	0.09180	0.07442
0.32	0.40895	0.31706	0 24289	0.19012	0 15111	0 12126	0.09792	0.07938
0 34	0.40895	0.32434	0.25790	0.20199	0.16055	0.12884	0.10404	0 08434
0.36	0.40895	0.33449	0.27075	0.21367	0.16996	0.13641	0.11015	0.08930
0.38	0.40895	0 33449	0 27358	0.22265	0.17884	0.14382	0.11620	0.09423
0.40	0.40895	0.33449	0.27358	0.22353	0.18262	0.14893	0 12117	0.09857
0.42	0 40895	0.33449	0.27358	0.22353	0 18264	0.14923	0.12193	0.09963
0.44	0.40895	0.33449	0.27358	0.22353	0.18264	0.14923	0.12193	0.09963

The equations for the characteristics are

$$dt/ds = 1 \tag{3.55-16}$$

$$\frac{dx}{ds} = \sqrt{1+\left(\frac{\partial y}{\partial x}\right)^2} + \frac{(\partial y/\partial x)^2}{\sqrt{1+(\partial y/\partial x)^2}} \tag{3.55-17}$$

which yields the condition

$$\Delta t \leq \frac{\Delta x}{\sqrt{1+\left(\frac{\partial y}{\partial x}\right)^2} + \frac{(\partial y/\partial x)^2}{\sqrt{1+(\partial y/\partial x)^2}}}. \tag{3.55-18}$$

The machine was programmed to have the last condition always satisfied. Starting with $\Delta t = \Delta x$, the computer would keep halving the time steps until the inequality was satisfied and then it would proceed with the calculation. It was found, at the beginning, that it was necessary to use

$$\Delta t = \tfrac{1}{8}\Delta x. \tag{3.55-19}$$

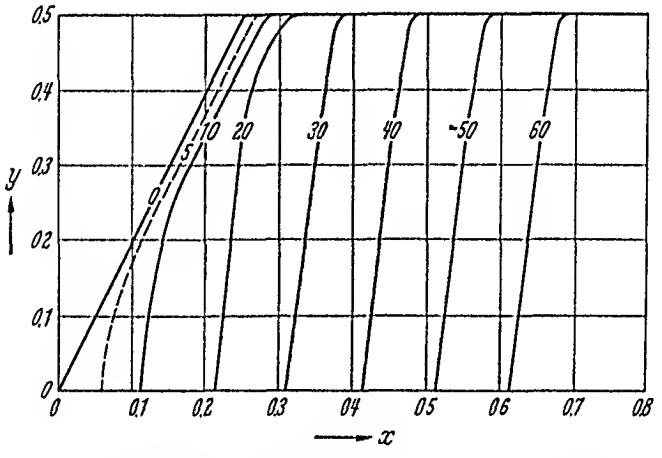

Fig. 83. Slope development with an undercutting river

Eq. (3.55-1) with $\Phi = \partial y/\partial x$. At the same time, we assume that a river is cutting away at the bottom of the slope. Its action is accounted for by the assumption that the river is able to carry away a certain amount of material (per unit length) m per unit time. This can be done very easily by introducing into the computer program for the solution of equation (3.55-1) a correction accounting for the action of the river after every time step. This is achieved simply by calculating the integral $\int y\,dx$ from zero to a point X so that

$$\int_0 y\,dx \leq m\,\Delta t \tag{3.56-1}$$

and setting y for all

$$x \leq X \tag{3.56-2}$$

equal to zero. The tests for the characteristics etc. can be used as before (cf. 3.55-18) and the program, with the modification, can be run for any number of iterations. The time steps will adjust themselves automatically to assure convergence as the calculation proceeds. The calculation, for an initial slope bank of the usual type as shown in Fig. 79, was carried out on an internally programmed computer for

$$m = 0.5 \tag{3.56-3}$$

and some 120 iterations. The result, in terms of time steps of duration

$$\Delta t = \tfrac{1}{8}\Delta x \tag{3.56-4}$$

is shown graphically in Fig. 83. In the presentation of the results, the time steps as given by (3.56-4) have been adhered to, although for the calculations, Δt adjusted itself as equal to $\Delta x/16$ in the later stages.

An inspection of the results presented above shows that the action of a river fundamentally changes the development-pattern of a slope. The

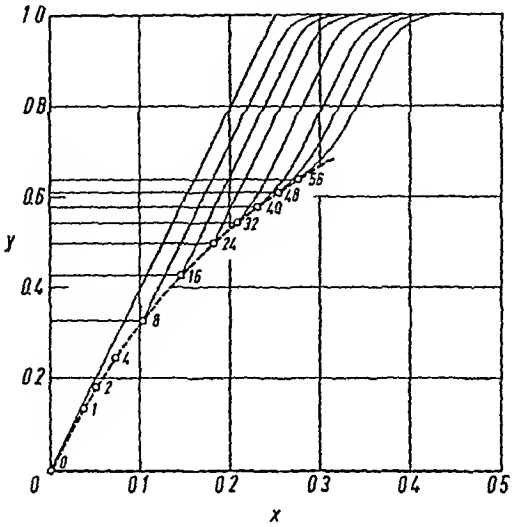

Fig. 84. Denudation of a valley side, the debris filling in the valley. (After SCHEIDEGGER[1])

slope now becomes steeper as time goes on and reaches asymptotically an inclination determined by the rapidity of the two types of erosion that are involved. The development in its latter stages is essentially a parallel slope recession.

It thus turns out that, if an undercutting river be involved in the development of a slope, *parallel slope recession* is the ultimate outcome. Some slopes will exhibit more resistance to surface denudation than others, in which cases the absence of an undercutting river may well bring about *stagnation* of development. In other slopes this may not be the case.

B. Deposition of Debris as Aprons[1]. The above slope-development models assume that all debris is completely carried away from the slope during its development; — which is evidently an oversimplification of what occurs in nature. Thus, we shall now investigate the case where all the debris from the lowering of the slope is deposited in a horizontal apron in front of the slope bank. This case may occur if a V-shaped valley is being filled up by the debris.

The above case can be investigated on the basis of Eq. (3.55-14) where now, however, the conditions are arranged in the numerical solution that the total volume of material which is taken off the slope during each time step is calculated and then spread horizontally between the zero abscissa and the slope. The results of this calculation, starting with a straight original slope bank (see Fig. 79), are shown in Fig. 84. As the valley fills up, part of the slope becomes covered by debris and is therefore protected from further attack by the weathering agents. This may give

1. SCHEIDEGGER, A. E.: Geophys. J. Roy. Astron. Soc. 7, 40 (1962).

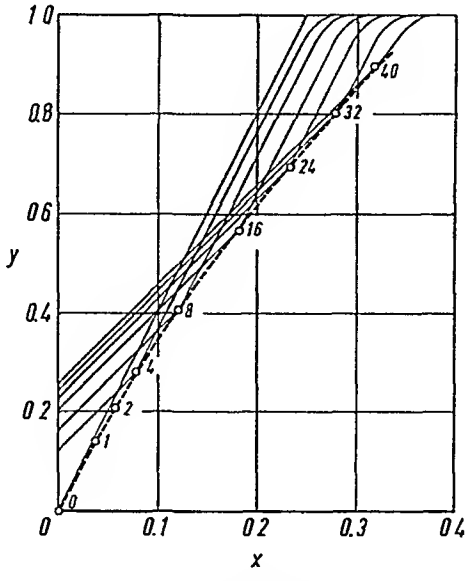

Fig. 85. Denudation of a slope bank, the debris forming an inclined apron. (After SCHEIDEGGER[1])

rise to a "rocky core" of the final slope, similarly as this was envisaged in Sec. 3.52. The rocky core forms an enveloppe to the various stages of the receding slope; it is shown as a dotted curve in Fig. 84.

The above model can be further modified by assuming that the debris piles up at the foot of the slope, forming an inclined apron corresponding to the angle of repose of the material. Starting again with a straight slope bank (Fig. 79) as before, it was assumed that the tangent of the angle of repose was $\frac{1}{2}$ of the tangent of the slope angle of the original slope bank. Then, it is assumed that the total volume of material taken off the slope during each time step is spread over an inclined strip at the foot of the slope. The results of the calculations are shown in Fig. 85. It is noted that the debris will again protect a rocky core beneath the slope from further weathering; it is shown as a dotted line in Fig. 85. The calculations cannot be carried on indefinitely, inasmuch as the apron eventually becomes tangent to the slope. corresponding to Richter's slope of denudation (cf. Sec. 3.52).

C. Influence of Lithologic Variations[2]. Another important feature which can easily be taken into account in the solution of Eq. (3.55-14) is the influence of lithologic variations in the slope. For doing this, one can simply introduce a function $a(y)$ into Eq. (3.55-14) so that it reads

$$\frac{\partial y}{\partial t} = -a(y)\frac{\partial y}{\partial x}\sqrt{1+\left(\frac{\partial y}{\partial x}\right)^2}. \tag{3.56-5}$$

1. SCHEIDEGGER, A. E.: Geophys. J. Roy. Astron. Soc. 7, 40 (1962).
2. SCHEIDEGGER, A. E.: U.S. Geological Survey Circ. No. 485 (1964).

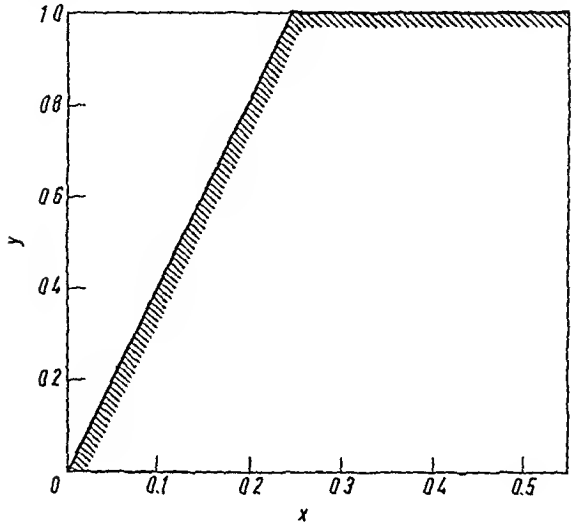

Fig. 86. Original slope bank for the calculation of the influence of lithologic variations

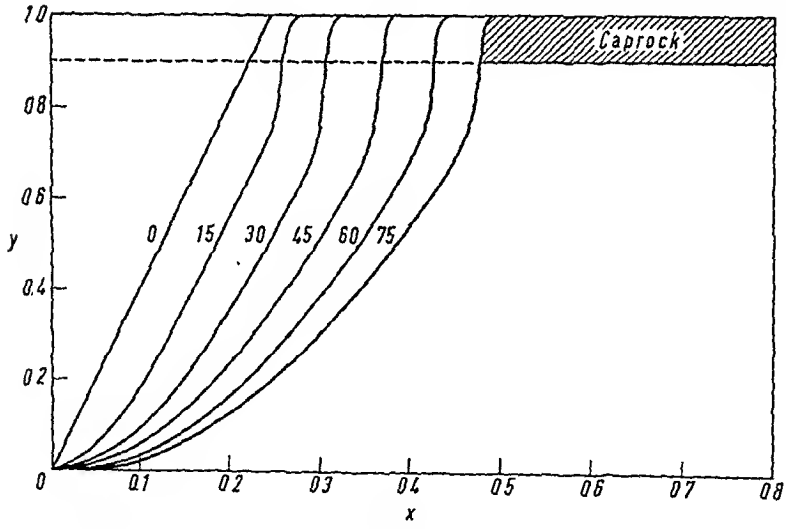

Fig. 87. Graph showing slope with caprock. (After SCHEIDEGGER[1])

Then, choosing suitable values for $a(y)$ models the influence of lithologic conditions.

Thus, starting with a slope bank of the form shown in Fig. 86, one can choose

$$\begin{aligned} a &= 1.0 \quad \text{for} \quad 0 \leq y \leq 0.9 \\ a &= 0.1 \quad \text{for} \quad 0.9 \leq y \leq 1.0. \end{aligned} \tag{3.56-6}$$

This represents a slope with a cap-rock which is ten times more resistant to erosion than the parts below. The solution is shown in Fig. 87. The

1. SCHEIDEGGER, A. E.: U.S. Geolog. Survey Circ. No. 485 (1964)

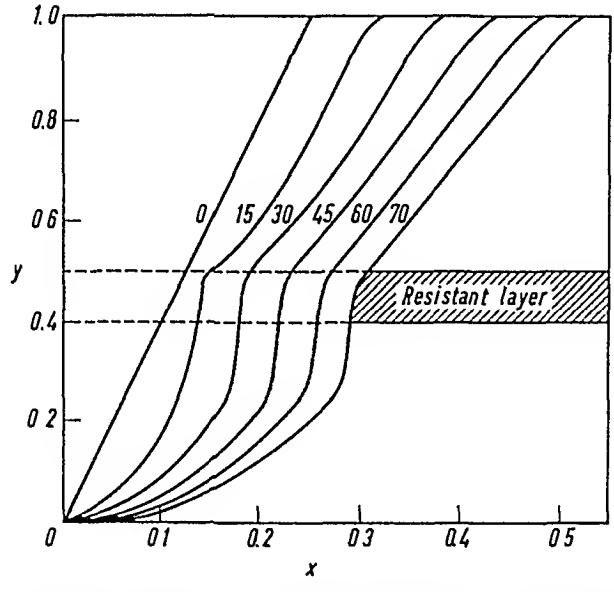

Fig. 88. Graph showing slope with resistant layer. (After SCHEIDEGGER[1])

calculated profiles are very good representations of mesa-type structures found in nature.

The influence of a horizontal resistant layer can be calculated by setting (cf. Fig. 86):

$$\begin{aligned} a &= 0.1 \quad \text{for } 0.4 \leq y \leq 0.5 \\ a &= 1.0 \quad \text{for all other values of } y. \end{aligned} \tag{3.56-7}$$

The solution obtained under these conditions is shown in Fig. 88.

The reverse condition to that considered above is that of a slope with a horizontal soft layer. It is assumed that

$$\begin{aligned} a &= 1.0 \quad \text{for } 0.4 \leq y \leq 0.5 \\ a &= 0.1 \quad \text{otherwise} \end{aligned} \tag{3.56-8}$$

and the solution of Eq. (3.56-1) is recalculated for these values of $a(y)$. The results are shown in Fig. 89.

The condition of a slope with a soft bottom is obtained if it is assumed that

$$\begin{aligned} a &= 0.1 \quad \text{for } 0.1 \leq y \\ a &= 1.0 \quad \text{for } 0 \leq y \leq 0.1. \end{aligned} \tag{3.56-9}$$

The results of the calculations are shown in Fig. 90.

An inspection of the various figures presented here shows that the calculated models correspond to observed conditions very well.

1. SCHEIDEGGER, A. E.: U.S. Geolog. Survey Circ. No. 485 (1964).

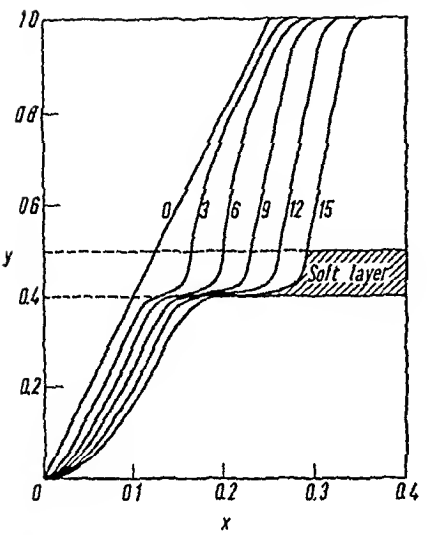

Fig. 89. Graph showing slope with soft layer. (After SCHEIDEGGER[1])

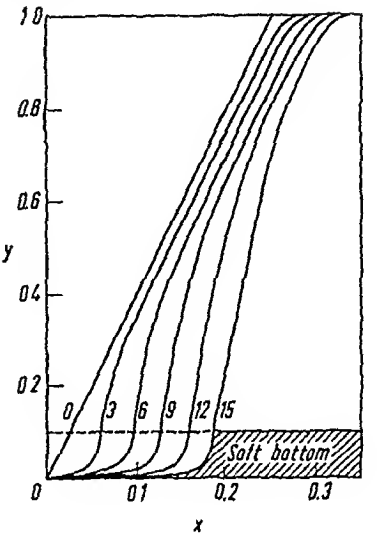

Fig. 90. Graph showing slope with soft bottom. (After SCHEIDEGGER[1])

3.57. Modifications of Nonlinear Slope Development Theory. The nonlinear theory discussed above can evidently be modified by choosing functions Φ in Eq. (3.55-1) which are different from those given in the preceding sections.

Thus, ESIN[2] discussed various possibilities. In particular, he considered the expression

$$\Phi=\frac{0.26}{y+7} \tag{3.57-1}$$

which he applied to underwater slopes.

Another possibility was considered by TAKESHITA[3] and by YOUNG[4] who both assumed the proportionality (s is the arc length)

$$\Phi\sim\frac{d(\partial y/\partial x)}{ds} \tag{3.57-2}$$

which implies that the "weathering" action normal to the slope is proportional to the curvature of the slope. Solutions of the basic nonlinear slope equations (3.55-1), using the expression (3.57-2) for Φ have been calculated; we present an example of the results of TAKESHITA[3] in Fig. 91.

1. SCHEIDEGGER, A. E.: U.S. Geolog Survey Circ. No. 485 (1964).
2. ESIN, N V.: Izv. Akad. Nauk SSSR, Ser. Geogr. No. 3, 126 (1968).
3. TAKESHITA, K.: Bull. Fukuoka-ken Forest Exp. Stn. **16**, 115 (1963).
4. YOUNG, A.: Nachr. Akad. Wiss. Gottingen, II. Math -Phys. Kl. No. 5, 45 (1963)

The physical justification for the choice of Φ given by (3.57-2) is that it follows from the hypothesis that the normal lowering or raising of the slope is proportional to the change dM/ds in down-hill mass flux M; the mass flux M, in turn, is assumed to be proportional to the steepness of the slope. Contrary to the hypothesis in the preceding sections, where all material "eroded" from the slope was assumed to be taken off the slope, Eq. (3.57-2) is the result of the postulate of complete mass-balance of the material moving along the slope. These conditions may be thought to be applicable under conditions of soil-creep, solifluction etc.

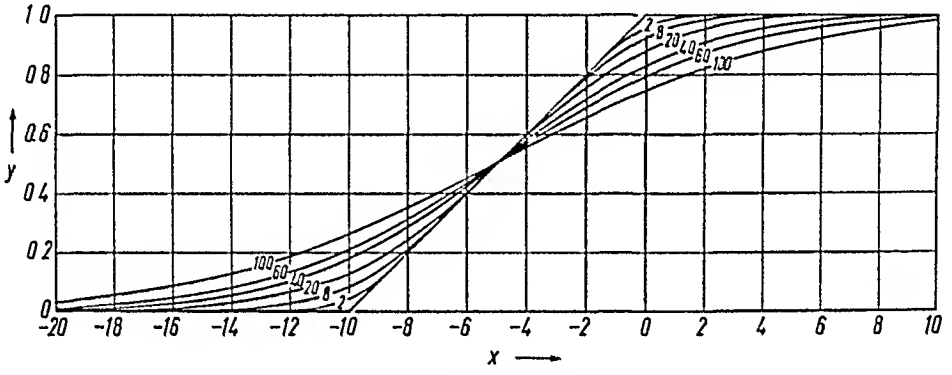

Fig. 91. Time-evolution of a slope bank where Φ is given by Eq. (3.57-2) (arbitrary units). (After TAKESHITA[1])

3.58. Evaluation of Slope Recession Theories[2]. In the theories of slope recession presented above, little has been said regarding their domain of application.

Under slopes, one may understand mountain sides, river banks, or even actual valley slopes. In all these instances, different slope recession theories must be assumed to apply.

The models of slope recession discussed in the present section (3.5) on "denudation" may be assumed to refer to any mountain side or river bank. In highly cohesive material, such as rock, it may be assumed that the direct action of external agents on the whole surface of the slope is small, so that the observed development will be either that envisaged by BAKKER et al. (see Secs. 3.52, 3.53) which occurs under a scree, or else that envisaged by CRICKMAY (see Sec. 3.56) which is due to rivers cutting away at the bottom. The direct slope recession caused by action of eroding agents upon the whole surface of the slope will probably most commonly be observed in materials of little cohesion such as clay, shale and incompletely consolidated sandstone. Actual valley slopes may be expected to have developed in conformity with the erosion and deposition caused

1. TAKESHITA, K.: Bull. Fukuoka-ken Forest Exp. Stn. 16, 115 (1963).
2. Cf. SCHEIDEGGER, A. E.: J. Alberta Soc. Petrol. Geol. 9, 15 (1961).

by flowing water (Sec. 3.45). The latter also may act on mountain sides and shape the slopes involved if sheet flooding is common in the area.

It appears that the theoretically postulated slope types have actually been observed in nature. In natural slopes, the various agents must be assumed to occur all at the same time[1]. Thus, undercutting by rivers may cause landslides whose faces then may be directly affected by surface action of slope-changing agents. Therefore, landscapes characteristic of the various processes discussed above have been found, depending on which agent has been the most powerful one.

3.6. Endogenetic Effects in Slope Development

3.61. General Remarks. The various mathematical models of slope development that have been discussed in Sec. 3.5 do not take any endogenetic movements into account. They thus fit into the Davisian concept of a geomorphic cycle: It is assumed that an original slope bank is somehow created by a diastrophic process and that for ever thereafter the denudation proceeds at a steady pace. If one wishes to introduce Penckian ideas which postulate that endogenetic and exogenetic geodynamic processes occur *simultaneously*, then endogenetic movements have to be superimposed upon the exogenetic development patterns.

In other words, we shall now study the modifications that are required in the various models of slope recession discussed earlier, if endogenetic effects are assumed to occur simultaneously with exogenetic phenomena.

3.62. Surface Action and Endogenetic Effects[2]. The models of slope development due to surface action that have been discussed in Sec. 3.55 lend themselves easily to a modification so as to describe external effects, simply by introducing an additional function F into the basic differential Eq. (3.55-1). The latter then becomes

$$\frac{\partial y}{\partial t} = -\sqrt{1+\left(\frac{\partial y}{\partial x}\right)^2}\,\Phi + F. \tag{3.62-1}$$

It is at once apparent that there exist many possibilities for the choice of F. We assume that F is a function of x and y and thus set

$$F = F(x, y). \tag{3.62-2}$$

In the present context, two cases can easily be investigated. In the first case one may assume an endogenetic *decrease* of the slope and therefore one may set

$$F = -\text{const}\, y. \tag{3.62-3}$$

1. See e.g. TANNER, W. F.: Trans Amer. Geophys. Union 37, 605 (1956)
2. This section is after SCHEIDEGGER, A. E.: Bull. Geol. Soc. Amer. 72, 37 (1961).

Only the possibility

$$\Phi=\frac{\partial y}{\partial x} \tag{3.62-4}$$

deserves analysis because the corresponding model of weathering appears to be the most reasonable one. Using (3.62-3) would presumably give a good picture of a body of mass (such as a rapidly thrown-up volcanic island) sinking due to its tendency of achieving isostasy. The speed of sinking is then proportional to the height of the mass above a certain base level; this is expressed by Eq. (3.62-3).

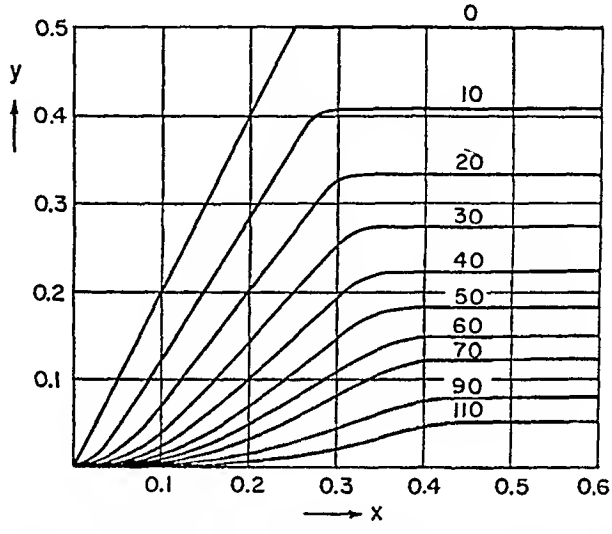

Fig. 92. Development of an endogenetically decreasing slope

The above case was solved on an electronic computer, using a procedure analogous to that employed in Sec. 3.55. The time steps, at the beginning at least, had to be chosen as follows:

$$\Delta t=\Delta x/8 \tag{3.62-5}$$

which corresponds to Eq. (3.55-19), since the characteristics were the same as those given in (3.55-16/17). The constant in (3.62-3) was chosen equal to 16; thus

$$F=-16y. \tag{3.62-6}$$

The results obtained in this manner are shown graphically in Fig. 92.

The second case investigated corresponds to that discussed above, but with a reversed sign. Thus:

$$F=16y. \tag{3.62-7}$$

This yields a slope whose height is endogenetically increasing; the rate of increase is proportional to the height already reached. This may

perhaps correspond to conditions obtaining in recent orogenetic belts that are still active. At the beginning of the calculation, one could choose the same time steps as in (3.62-5), but as the computation went along, these had to be shortened so as to fulfill the conditions for stability imposed by the characteristics. Of course, only the possibility for Φ represented by Eq. (3.62-4) was considered. The results obtained are shown graphically

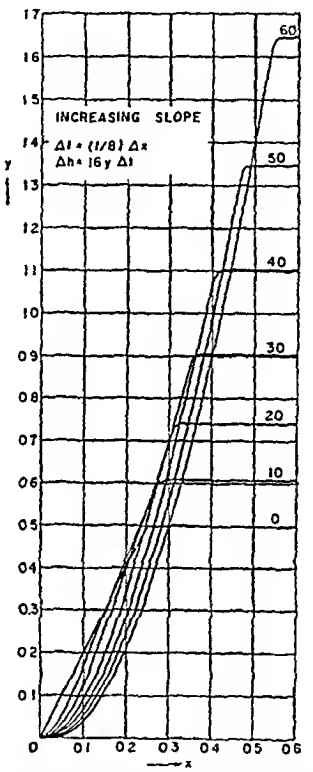

Fig. 93. Development of an endogenetically increasing slope

in Fig. 93. In these presentations, time is measured in units Δt as given in (3.62-5) although the steps, as mentioned above, were shortened in the latter stages of the computation.

It appears from the results obtained above that the superposition of an endogenetic displacement does not materially affect the character of the slope that will develop. An originally straight slope bank will become concave at the toe, convex at the head, with the toe being much broader than the head.

Similar calculations as those reported above have also been made by DEVDARIANI[1], but using a much simpler model for the "erosion", viz. one of the type considered in Sec. 3.45. Thus, DEVDARIANI had to solve a

1. DEVDARIANI, A. S : Izv. Akad. Nauk SSSR, Ser. Geograf. No. 3, 7 (1966).

non-homogeneous diffusivity equation rather than an equation of the type of (3.62-1). The result is a diffusive-type of "damping" of the tectonic motion, as might be expected. HIRANO[1] also based calculations on similar assumptions.

3.63. Sideways Erosion and Endogenetic Movements. It remains to analyse the effect of endogenetic movements if, as postulated by CRICKMAY (see Sec. 1.54) slope recession is assumed to be due to the sideways erosion of rivers at the bottom of such slopes.

It would appear that in this case, the endogenetic movements would not affect the slope recession in its pattern. On a slope consisting of gravel or débris, an essentially parallel slope recession will always be maintained no matter whether there is or is not an endogenetic movement occurring at the time. The same is true if the slope recession occurs by successive landslides.

The general patterns of receding slopes should therefore be independent of endogenetic movements, if these patterns are due to the sideways erosion of rivers.

3.64. Evaluation of Endogenetic Effects in Slope Development. Finally, we shall discuss the bearing of the various theories of endogenetic effects upon the slope development theories advanced by field geomorphologists.

An inspection of Figs. 92 and 93 shows at once that there is no support for PENCK's ideas regarding a characteristic form of *waxing* and *waning* slopes: All slopes, notwithstanding the endogenetic movements, are essentially concave upward. There is no indication from theory that slopes ever become convex, at least as long as there is no lateral river action.

On the other hand, we have noted that the action of a laterally eroding river will produce essentially parallel slope recession, regardless of endogenetic movements. Before a dynamic equilibrium is attained, the slope may be convex. This appears to support the principle of unequal activity outlined in Sec. 1.54, just as the latter was supported by the mathematical slope development theories which did make no allowance for endogenetic movements.

1. HIRANO, M.: Chikyu Kagaku **21**, No. 5, 27 (1967).

IV. Theory of River Action

4.1. General Remarks

On the land areas of the world, rivers are undoubtedly some of the most important geomorphological agents. Rivers act geomorphologically in fundamentally two fashions: first by interaction with their bed, i.e. downwards (this type of action is usually referred to as "river bed process") and second, by interaction with their banks (sideways erosion). It is the purpose of this Chapter (IV) to present the theories of these processes.

4.2. Flow in Open Channels

4.21. General Principles. In order to understand the mechanics of river action properly, it is first of all necessary to acquaint oneself with the fundamentals of open channel flow.

Flow in rivers is basically turbulent, but reasonable approximations can often be obtained by considering laminar flow, treating the ever-present turbulence as a "perturbation". Thus, turning first to (frictionless) laminar flow, we note that it is characterized by the existence of stream lines. The flow along each streamline is determined by the well-known Bernoulli equation:

$$H = z + \frac{p}{\rho g} + \frac{v^2}{2g} = \text{const}, \tag{4.21-1}$$

where z is the vertical co-ordinate, p the pressure, ρ the fluid density, v the flow velocity and g the gravity acceleration. The Bernoulli equation is an expression of the principle of conservation of energy. H represents the energy content at the point under consideration expressed as a height (hydraulic head).

It is often convenient to write the Bernoulli equation for the bottom-streamline in a stream of depth h; then, assuming static pressure distribution, (4.21-1) becomes (with $z=0$):

$$H = h + \frac{v^2}{2g}. \tag{4.21-2}$$

Disregarding the change of velocity with depth, and introducing into the above equation for v the value of the average velocity

$$v=\frac{Q}{A} \tag{4.21-3}$$

(Q denoting the volume flow rate and A the cross-sectional area), we obtain

$$H=h+\frac{Q^2}{2g\,A^2}. \tag{4.21-4}$$

Again, the quantity H represents the energy content expressed as a height above the river bottom. If we denote the distance along the river by s, then $H(s)$ defines a line which has been called *energy line.*

Let us assume that the channel is rectangular of width b. Then (4.21-4) becomes

$$H=h+\frac{Q^2}{2g\,b^2\,h^2} \tag{4.21-5}$$

or:

$$Q=\sqrt{(H-h)\,2g\,b^2\,h^2}. \tag{4.21-6}$$

From this equation (see Fig. 94) it is at once abvious that if H (the energy) and Q (the volume flow) be given, there are two possible water

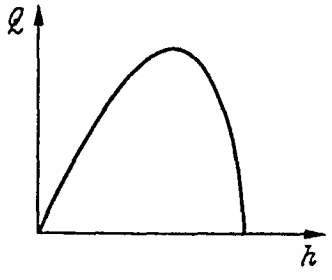

Fig. 94. Curve of Q as a function of h for a constant value of H

depths h (and corresponding velocities v) with which the flow may occur, provided, of course, that H be large enough. The faster one of these flows is termed *shooting* (or "*supercritical*") flow, the other *streaming* (or "*subcritical*") flow. One can show that, in streaming flow, the flow velocity v is always less than the shallow water wave velocity u

$$v<u\equiv\sqrt{g\,h} \tag{4.21-7}$$

(for u, cf. Eq. 6.22-28); in shooting flow, the reverse is true:

$$v>u\equiv\sqrt{g\,h}. \tag{4.21-8}$$

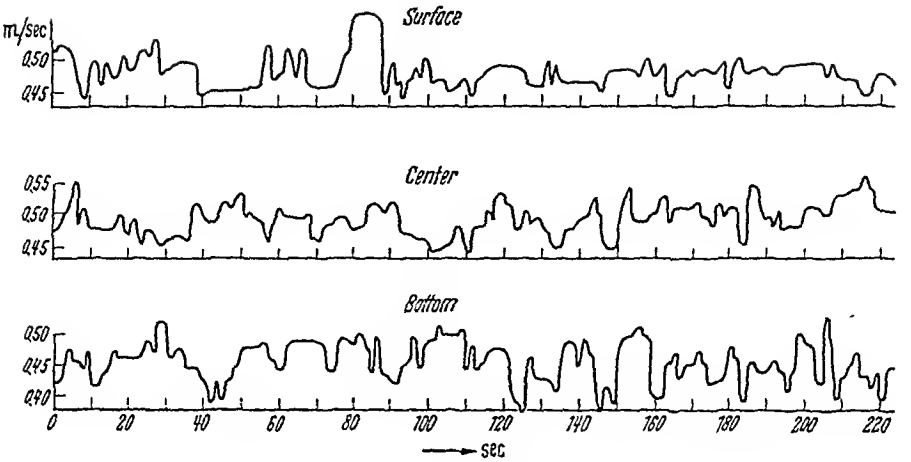

Fig. 95. Velocity fluctuations in an open channel. After VELIKANOV[1]

If

$$v = u, \tag{4.21-9}$$

the flow is termed "*critical*".

It is possible to build the whole structure of flow theory upon the Bernoulli equation. However, as noted above, it turns out that most river flow is turbulent. Measured turbulent velocity fluctuations in a channel are shown in Fig. 95. The study of turbulent flow in open channels is of particular interest with regard to a solution of the problem as to how sediment is being transported in rivers. There are several monographs bearing upon this subject[2-12].

In the present context, we shall study only (quasi-) stationary flow in open channels. If "stationary" flows are under investigation, one has to average out all the velocity fluctuations that characterize the turbu-

1. VELIKANOV, M. A.: Динамика русловых потоков, Том. I: Структура потока. Moscow: Gos. Izd. Tekh. Teoret Lit. 1954

2. CHOW, V. T.: Open-Channel Hydraulics New York. McGraw-Hill Book Co 1959.

3. HOMMA, M.: Hydraulics. Tokyo: Maruzen Book Co. 1952.

4. IWAGAKI, Y.: Theory of Flow in Open Channels. Congress of Modern Hydraulics, Chap. 1, Jap Soc. Civ. Eng. (1953).

5. LEVI, I. I.: Динамика русловых потоков. Moscow: Gosenergoizdat 1958.

6. MINSKII, E. M.: Турбулентность руслового потока. Moscow: Gidrometeorizdat 1953.

7. MOSTKOV, A.W.: Handbuch der Hydraulik (transl. from Russian). Berlin: Verlag Technik 1960.

8. ROUSE, H.: Engineering Hydraulics. New York: J. Wiley & Sons 1950.

9. SCHMIDT, M.: Gerinnehydraulik. Wiesbaden: Bauverlag 1957.

10. SCHOKLITSCH, A.: Handbuch des Wasserbaues. 2 Vols. Vienna: Springer 1950.

11. VELIKANOV, M. A.: Динамика русловых потоков. 2 Vols. Moscow: Gos. Izdat. Tekh.-Teoret. Lit. 1954.

12. WECHMANN. A.. Hydraulik. Wiesbaden· Bauverlag 1960.

lence. Moreover, only the variation of average flow with *height* above the river bed is usually considered which represents somewhat of an oversimplification. In Fig. 96 we show the average flow velocities as they have been measured in a regular channel. Whereas in this case there is a fairly regular velocity distribution over the cross section, this is no longer the case in a natural channel (see Fig. 97). Nevertheless, without the assumption of a certain regularity of the velocity distribution, it is almost impossible to arrive at any theory at all. The above remarks will serve to bear out some of the limitations of the investigations that will follow.

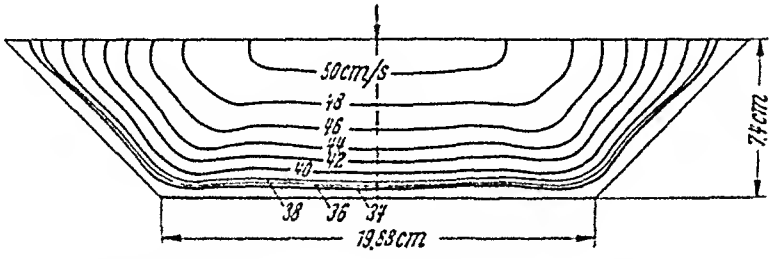

Fig. 96. Velocity distribution in a prismatic channel. After SCHMIDT[1]

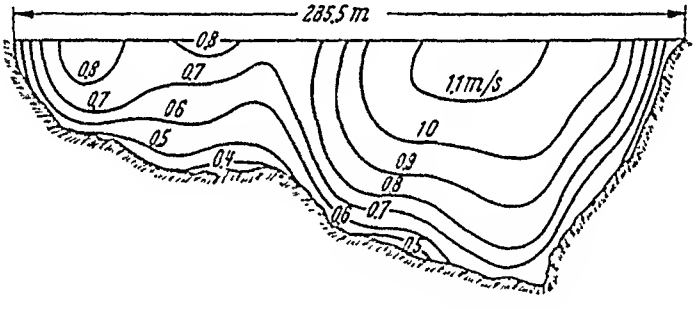

Fig. 97. Velocity distribution in a river. After SCHMIDT[1]

In developing the formulas which are of interest in connection with geomorphological questions, we shall first mention some empirical investigations. Then we shall proceed to the theory of turbulent flow in clean channels and in channels with a movable ("dirty") bottom, and finally discuss the theory of non-uniform flow.

After stating the possibility of existence of two types of flow, viz. of laminar and of turbulent flow, one now might ask the question as to under which conditions each type occurs in nature. As was noted above, river flow is usually turbulent. In spite of this, it may be possible to apply the Bernoulli equation as an approximation for large scale motions. The turbulence which is responsible for the transportation of sediment, can then be regarded as a perturbation causing energy dissipation. The quantity H in the Bernoulli equation (cf. 4.21-4) is then no longer

1. SCHMIDT, M.: Gerinnehydraulik. Wiesbaden: Bauverlag 1957.

constant, and the *energy line* $H(s)$ (where H is measured *from the river bottom*) will be a curved line running roughly parallel to the surface of the river. Our main emphasis will be on turbulent flow in open channels, but on occasions we shall mention investigations based upon the Bernoulli equation.

4.22. Empirical Formulas. In our discussion of flow in open channels, we shall first turn towards empirical flow formulas. Such formulas are commonly quoted in the form

$$v = \text{const}\, h_m^a S^b \tag{4.22-1}$$

where v is the average flow velocity in the channel, h_m its mean depth and S the bed slope. The quantities a and b, as well as the "const", are empirical constants. Instead of h_m, it is often convenient to introduce a hydraulic radius R, defined as follows:

$$R = \frac{A}{P} \tag{4.22-2}$$

where A denotes the cross-sectional area and P the wetted perimeter of the section under consideration. For large rivers, R evidently becomes equal to h_m. With a slight change of constants, it is usually possible to write the empirical formulas to be discussed here, in terms of either h_m or R.

Various values have been suggested in the literature for the constants a and b occurring in (4.22-1). A well-known relationship is of the form

$$v = R^{\frac{2}{3}} S^{\frac{1}{2}}/n \tag{4.22-3}$$

which is called *Manning*[1] *formula.*

In the Manning formula (4.22-3), the quantity n is a constant (the "roughness" of the channel), whose value varies from river stretch to river stretch. A catalog of representative values of n, with many colored pictures illustrating the river reaches in question, has been published by BARNES[2]. Accordingly, the values of n found vary between 0.029 and 0.075 (metric units).

A more elaborate form of Eq. (4.22-1) has been suggested by BESSREBRENNIKOV[3]. It is

$$v^n = \text{const}\, h^m S \tag{4.22-4}$$

where n and m are supposedly connected in such a fashion that

$$m + n = 3. \tag{4.22-5}$$

1. MANNING, R.: Trans. Inst. Civ. Eng. Ireland, **20**, 161 (1890). See also SCHMIDT, M.: Gerinnehydraulik, p 53. Wiesbaden: Bauverlag 1957.

2. BARNES, H. H.: Roughness Characteristics of Natural Channels. U.S Geolog Surv. Water Supply Paper No. 1849. Washington: U.S. Government Printing Office 1967.

3. BESSREBRENNIKOV, N.K.: Dokl. Akad. Nauk Belorussk. SSR **2**, No. 1, 30 (1958).

BESSREBRENNIKOV[1] quotes investigations bearing out that, in weedy channels, n equals 1, in nonweedy channels, n equals 2.

Another well-known formula for the average flow velocity v in a channel has been proposed by CHÉZY[2]. CHÉZY's formula is also essentially empirical, but one can give a somewhat rational deduction of it. Thus, let us write down the force balance equation for a slug of water flowing downstream. In order to do this, we consider a section of a stream of length L, cross-section A, wetted perimeter P, hydraulic radius R [defined by (4.22-2)] and slope S. The forces parallel to the current then are: (*a*) from the weight of the water

$$F_w = A L \rho g S \tag{4.22-6}$$

where ρ is the density of the water and g the gravity acceleration; (*b*) the frictional force

$$F_R = \sigma_m L P \tag{4.22-7}$$

where σ_m is the tractive force per unit surface (commonly referred to as *drag*). A reasonable assumption for the drag is (which can be justified because each obstacle offers quadratic resistance to the flow; see Eq. 2.22-3):

$$\sigma_m = C^2 v^2 \tag{4.22-8}$$

where C is called CHÉZY's *coefficient*. In flow that is essentially uniform, the sum of the forces acting upon a slug of water must be zero. Hence

$$A L \rho g S = \sigma_m L P = C^2 v^2 L P \tag{4.22-9}$$

whence we obtain CHÉZY's equation

$$v = \frac{1}{C}\sqrt{S \rho g \frac{A}{P}} = \frac{1}{C}\sqrt{S \rho g R}. \tag{4.22-10}$$

Furthermore, we have

$$\sigma_m = \rho g \frac{A}{P} S, \tag{4.22-11}$$

or, if P is large (h = depth)

$$\sigma_m = \rho g h S. \tag{4.22-12}$$

This is the basic formula of the *drag theory*.

Experimental evidence seems to show that C is, in fact, not independent of the hydraulic radius. Remembering MANNING's formula (4.22-3), we can write:

$$c \equiv \frac{1}{C} = k R^{\frac{1}{6}} \approx k h^{\frac{1}{6}} \tag{4.22-13}$$

---

1. BESSREBRENNIKOV, N. K.: Dokl. Akad. Nauk Belorussk. SSR **2**, No. 1, 30 (1958).
2. CHÉZY, A. DE, and M. PERRONET: Unpublished report on the Yvette Canal. (1775) See HERSCHEL, C.: J. Assoc. Engin. Soc. **18**, 363 (1896).

where the last approximation holds for wide rivers. The Manning formula, and hence also Eq. (4.23-13), are based upon observational data. Tables giving values for the constant k for various cases are available[1] and can also be calculated from values of the MANNING n mentioned above.

A different presentation of CHÉZY's formula is the so-called Darcy-Weisbach equation[2] which reads

$$v = K\sqrt{hS} \tag{4.22-14}$$

where the factor K contains everything which was written ont explicitely in (4.22-10). This factor is commonly written as follows

$$K = \sqrt{\frac{8g}{f}} \tag{4.22-15}$$

where g is the gravity acceleration and f the Darcy-Weisbach friction factor. If the appropriate dependence of f on h is inserted, one ends up with the CHÉZY or MANNING equation.

It has been pointed out by FRANCIS[3] that formulas of the type of (4.22-1) can be shown to be approximations to the theoretical formulas (logarithmic laws) which we shall deduce in the next section (4.23).

4.23. Turbulent Flow in Clean Channels. Turning now to the *theory* of open channel flow, we may remark that the latter has been developed by KEULEGAN[4] in analogy with investigations of the theory of flow in *pipes*. Such investigations had been undertaken by KARMAN[5], NIKURADSE[6] and others around 1930. Accordingly[4], the expression of PRANDTL[7] (cf. Sec. 2.23) for the turbulent shear stress σ at any point in a fluid moving past a solid wall is (cf. Eq. 2.23-2)

$$\sqrt{\sigma/\rho} = l\, d\bar{u}/dy \tag{4.23-1}$$

where ρ is the density of the fluid, $\bar{u}$ the (time-averaged) velocity in question, y the distance from the wall, and l is the turbulent mixing length. The last equation can also be written

$$u_* \equiv \sqrt{\frac{\sigma_m}{\rho}} = l\frac{d\bar{u}}{dy}\sqrt{\frac{\sigma_m}{\sigma}} \tag{4.23-2}$$

1 Cf. SCHMIDT, M.: Gerinnehydraulik. Wiesbaden: Bauverlag 1957.

2. See CHOW, V. T.: Open Channel Hydraulics New York: McGraw-Hill 1959. See p. 8 therein.

3 FRANCIS, J. R. O.: Engineer **203**, No. 5280, 519 (1957).

4. KEULEGAN, G. H.: J. Res. Natl. Bur. Standards **21**, 707 (1938).

5. KARMAN, T.. Nachr. Ges. Wiss. Göttingen, Math.-phys. Kl. **1930**, 58 (1930).

6 NIKURADSE, J.: Forsch.h Ver. Deut. Ing. No **356** (1932).

7. PRANDTL, L.: Trans. 2nd Int. Congr. Appl. Mech. Zurich, p. 62 (1926).

where σ_m is the maximum shear stress which occurs at the wall (i.e. for $y=0$). The abbreviation u_* is frequently used; the quantity it denotes is often called *shear velocity*.

Dimensional analysis then yields

$$l = -k \frac{d\bar{u}/dy}{d^2\bar{u}/dy^2} \tag{4.23-3}$$

where k is KARMAN's universal dimensionless constant of turbulence (equal to roughly 0.4). Substituting the expression for l into that for u_* yields

$$u_* = -k \frac{(d\bar{u}/dy)^2}{d^2\bar{u}/dy^2} \sqrt{\frac{\sigma_m}{\sigma}}. \tag{4.23-4}$$

For small values of y, the square root approaches 1 and one ends up with

$$u_* = -k \frac{(\bar{u}')^2}{\bar{u}''}. \tag{4.23-5}$$

This can be integrated to yield

$$\frac{\bar{u}}{u_*} = \frac{1}{k} \operatorname{lognat} \frac{y}{y_0}, \tag{4.23-6}$$

where y_0 is a constant of integration. This is KARMAN's *law of velocity distribution* in the neighborhood of a solid wall.

If the surface of the wall is smooth, y_0 will depend solely on u_* and ν, the latter denoting the kinematic viscosity. Dimensional analysis then yields

$$\frac{y_0 u_*}{\nu} = m \tag{4.23-7}$$

where m is a constant (generalized Reynolds number). Hence

$$\frac{\bar{u}}{u_*} = a_s + \frac{1}{k} \operatorname{lognat} \frac{y u_*}{\nu}. \tag{4.23-8}$$

Experimental evidence yields[1]

$$a_s = 5.5. \tag{4.23-9}$$

If the surface is rough, then the "constant" m must depend on the heigh k_s of the surface roughnesses. Dimensional analysis yields

$$\frac{y_0 u_*}{\nu} = f\left(\frac{k_s u_*}{\nu}\right). \tag{4.23-10}$$

1. See KEULEGAN, G. H.: J. Res. Natl. Bur. Standards **21**, 707 (1938)

Again using experimental data, one obtains for water[1]:

$$\frac{\bar{u}}{u_*}=8.5+\frac{1}{k}\,\text{lognat}\left(\frac{y}{k_s}\right). \tag{4.23-11}$$

In order to obtain expressions for the average flow velocity in the channel, the above expressions must be integrated from δ to R where R is again a hydraulic radius

$$R=\frac{A}{P} \tag{4.23-12}$$

(with A=cross-sectional area and P the wetted perimeter) and δ the thickness of the laminar sublayer. This thickness δ, from dimensional reasoning, must be proportional to ν/u_*; KEULEGAN[1] quotes the following relationship as determined from experiments:

$$\delta=11.5\frac{\nu}{u_*}. \tag{4.23-13}$$

One then obtains for the average channel velocity v (after KEULEGAN[1])

(a) for smooth channels

$$\frac{v}{u_*}=3.5+5.75\log_{10}\left(\frac{R\,u_*}{\nu}\right) \tag{4.23-14}$$

(b) for rough channels

$$\frac{v}{u_*}=6.25+5.75\log_{10}\left(\frac{R}{k_s}\right). \tag{4.23-15}$$

The expressions for smooth and rough channels can be taken together if one writes

$$\frac{v}{u_*}=5.75\log_{10}\left(12.27\frac{R\,x}{k_s}\right)\equiv 5.75\log_{10}\left(12.27\frac{R}{\Delta}\right) \tag{4.23-16}$$

where x is a correction factor shown in Fig. 98 and Δ is simply

$$\Delta=\frac{k_s}{x}. \tag{4.23-17}$$

As noted in Sec. 4.22, it can be shown that the Chézy formula (4.22-10) is an approximation to (4.23-16).

The above formulas are valid for open channels with a smooth or rough bottom, as the case may be. However, in many natural rivers there

1. See KEULEGAN, G. H.: J. Res. Natl. Bur. Standards **21**, 707 (1938).

are sand bars at the bottom which create an additional resistance. This can be taken into account by introducing a ficticious hydraulic radius. In view of the various limitations of the theory, it is not too surprising that TAYLOR[1] did not find too good an agreement between measured and theoretical values for the velocity distribution in a river.

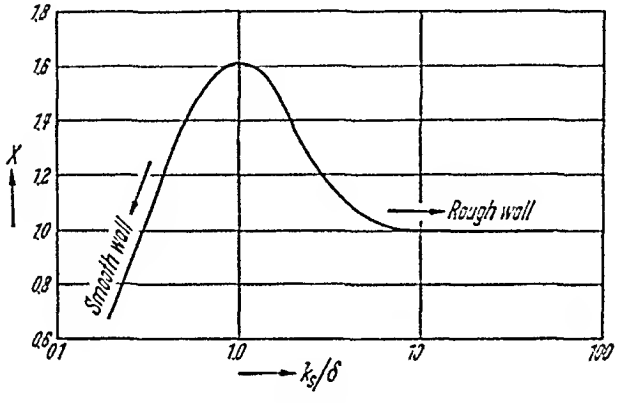

Fig. 98. Correction factor in open channel flow

4.24. Turbulent Flow in Channels with Movable Bottom. The formulas of open channel flow discussed thus far refer to channels with an immovable bottom. However, the river bed consists of movable sediment (is "dirty") and it stands to reason that an interaction will take place between the bed and the flow. The action of the river on its bottom cannot in fact be separated from the reaction of the bottom on the flow, but for purposes of classification we shall discuss the two problems separately. At the present time we are concerned with the flow of the water in the river and with the reaction which the movability of the bed might have on this flow.

Early studies of this problem were undertaken by GILBERT[2] who argued that the energy loss in a flowing river was incurred in two ways, first, in overcoming the hydraulic friction of the flow and, second, in transporting the sediment. On the one hand, this leads directly to the Chézy formula of flow (4.22-10) of which a more sophisticated deduction has been given in Sec. 4.22, and on the other hand, it was concluded that a clear stream must flow faster than a comparable one laden with sediment.

Special studies to investigate the validity of the clean channel flow formulas for dirty channels have been undertaken by LIU and HWANG[3]

1. TAYLOR, E. H.: Trans. Amer. Geophys. Union **20**, 631 (1939).
2. GILBERT, G. K.: Amer. J. Sci. **12**, 16 (1876).
3. LIU, H. K., and S. Y. HWANG: Proc. Amer. Soc. Civ. Eng. **85**, Hy 11. (J. Hydr. Div.) 65 (1959).

and by VANONI and coworkers[1-3]. In all these studies it turned out that the formulas for clean channel flow are indeed no longer valid. LIU and HWANG[4] started with the assumption of a formula of the type of (4.22-1) and gave empirical correlation curves for the constants occurring therein. VANONI and BROOKS made special studies[1,2] to determine the influence of the sediment load upon the discharge. Their data are best represented by the introduction of a friction factor f defined as follows:

$$f=8(u_*/v)^2 \tag{4.24-1}$$

where u_* is the shear velocity (cf. 4.23-2) and v the average velocity in the river. This friction factor does not vary in accordance with the ideas of GILBERT, in that it does not increase with sediment load. In fact, it turned out that there is no single-valued relationship between the velocity and any combination of depth and slope of the river. The results of VANONI and coworkers in this regard, however, are purely empirical and no theoretical explanation could be given. It also turned out that KARMAN'S "universal constant" (cf. 4.23-3) is not, in fact, a constant but varies with sediment load.

4.25. Non-Uniform Flow. The formulas deduced thus far refer to *uniform* flow in channels in which the cross-section of the flow is assumed as constant along the whole length of the channel. It is of interest to investigate the changes in these formulas that are necessary if the flow is assumed to be non-uniform.

The problem has been treated by many authors, for instance by OVSEPYAN[5] and in a book by ROUSE[6]. A physically most satisfactory deduction of the relevant formulas has been given by LIU[7], based upon the Bernoulli equation with turbulent energy dissipation treated as a perturbation. Accordingly, we envisage the geometry of the flow as shown in Fig. 99. The theory can best be represented if we introduce the hydraulic head H at every section (located by giving x); the former is given by

$$H=\frac{v^2}{2g}+h+z \tag{4.25-1}$$

1. VANONI, V. A., and N. H. BROOKS: Laboratory Studies of the Roughness and Suspended Load of Alluvial Streams. Report, Sedimentation Laboratory, California Institute of Technology, Pasadena, 1957 (121 pp.)

2. BROOKS, N. H.: Trans Amer Soc. Civ. Eng. **123**, 526 (1958)

3. VANONI, V. A., and G. N. NOMICOS: Trans. Amer. Soc Civ. Eng. **125**, pt. 1, 1140 (1960)

4. LIU, H. K., and S. Y. HWANG: Proc. Amer. Soc. Civ. Eng. **85**, Hy 11, (J. Hydr. Div.) 65 (1959).

5. OVSEPYAN, V. M.. Sb. Nauchn. Trud Erevansk. Politekhn. In-ta No. 9, 81 (1955).

6. ROUSE, H.: Engineering Hydraulics. New York: J. Wiley & Sons (1950).

7. LIU, H. K.: Trans. Amer. Geophys. Union 39, 939 (1958).

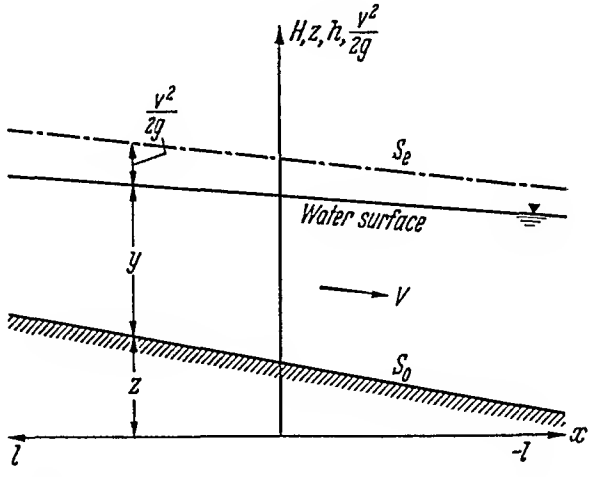

Fig. 99. Geometry of non-uniform flow. After Liu[1]

where v is the average velocity corresponding to the section under consideration, and h is the depth of the river for that section.

Differentiating (4.25-1) with regard to $l\,(=-x)$ yields

$$\frac{dH}{dl}=\frac{d}{dl}\left(\frac{v^2}{2g}\right)+\frac{dh}{dl}+\frac{dz}{dl}. \tag{4.25-2}$$

The slope of the energy line is denoted by S_e, the slope of the bottom by S_0. Thus

$$S_e=\frac{d}{dl}\left(\frac{v^2}{2g}\right)+\frac{dh}{dl}+S_0. \tag{4.25-3}$$

Introducing x instead of l, we have

$$-S_e=\frac{d}{dx}\frac{v^2}{2g}+\frac{dh}{dx}-S_0 \tag{4.25-4}$$

According to the Chézy relation (4.22-10), the velocity for a wide channel ($R\sim h$) and *constant slope* is a function of the depth:

$$v^2=\text{const}\,h. \tag{4.25-5}$$

Differentiating this with regard to x and substituting it into (4.25-4) yields

$$\frac{dh}{dx}=\frac{S_0-S_e}{1+K}, \tag{4.25-6}$$

where K is some constant. This is a differential equation for the variation of the river depth.

1. Liu, H. K.: Trans. Amer. Geophys. Union 39, 939 (1958).

4.3. Motion in River Bends

4.31. The Problem. Up to now, we have regarded a river as straight. However, in the development of drainage basins, the *lateral action* of rivers is of extreme importance. The latter is mostly connected with flow in river bends which, therefore, will form our present topic of study.

Much information on water movement in curved channels may be found in the general textbooks on open channel hydraulics already mentioned in Sec. 4.21. In addition, WITTMANN and BÖSS[1] wrote a monograph on water and bed load movement in curved river reaches and ROZOVSKII[2] as well as ANANYAN[3] published books on water movement in a curved channel. References to specific investigations will be given in their proper context.

As a very crude approximation, the flow in curved channels can be described as a two-dimensional process. This leads to the discussion of "primary" currents in river bends (Sec. 4.32). This is generally done by treating the two-dimensional flow as potential flow, the (turbulent) energy dissipation being considered as a perturbation. Whereas the potential-flow-type of an approximation might lead to acceptable results in *straight* river reaches, this is not the case in *curved* reaches. In the latter case, helicoidal cross-currents ("secondary" currents) are of great importance. Some aspects and a few of the standard theories for the explanation of such secondary currents will be discussed in Sec. 4.33. However, it will also be shown that these "standard" explanations are really inadequate. Therefore, in Sec. 4.34, we shall present some attempts to explain the existence of the helicoidal cross-currents in terms of more basic principles.

Finally, we shall discuss (Sec. 4.35) some shock phenomena that may occur in very rapid flow around corners in curved channels.

4.32. Primary Currents in River Bends. As mentioned above, the flow in a river, in a first approximation, may be treated as two-dimensional, and, furthermore, the energy dissipation may be neglected. We have noted in the section on general principles of flow in open channels (4.21) that frictionless laminar flow is characterized by the existence of streamlines. If the flow is also irrotational, then it can be represented by the introduction of a velocity potential Φ. It is well known that, if one restricts himself of two dimensions, the streamlines can be represented as the equipotential curves of a stream function Ψ which is connected with the velocity potential Φ by the Cauchy-Riemann differential equations.

1. WITTMANN, H., and P. BÖSS: Wasser- und Geschiebebewegung in gekrummten Flußstrecken. Berlin: Springer 1938.

2. ROZOVSKII, I. L.: Движение воды на повороте открытого русла. Kiev: Izd Akad. Nauk. Ukr. SSR 1957.

3. ANANYAN, A. K.: Движение жидкости на повроте водовода. Erevan: Izdat. Akad. Nauk Armyan SSR 1957.

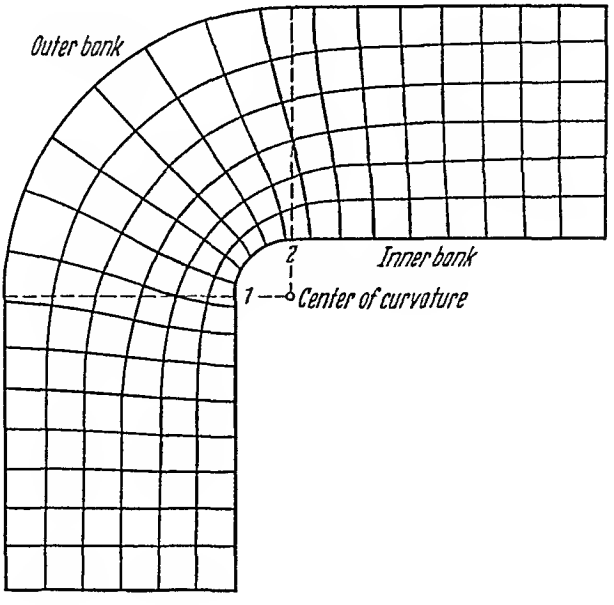

Fig. 100. Flow lines and potential lines in a circular river bend of 90°. After WITTMANN and BÖSS[1]

Both, Φ as well as Ψ are subject to the Laplace equation:

$$\text{lap } \Psi = \text{lap } \Phi = 0. \tag{4.32-1}$$

Because of the Cauchy-Riemann differential equations, the absolute value of the velocity vector is equal to the absolute value of the gradient of Ψ as well as of Φ.

The velocity field derived from a potential is often called the field of "primary currents" in a river. These primary currents may be considered as a first approximation of river flow.

Let us calculate the velocity in a circular river. In this case, the stream lines must be circular, hence the stream function may be assumed to be a function of the distance r from the center of the circle only. The Laplace equation for Ψ yields in polar co-ordinates:

$$\frac{\partial^2 \Psi}{\partial r^2} + \frac{1}{r} \frac{\partial \Psi}{\partial r} = 0. \tag{4.32-2}$$

However, $\partial \Psi / \partial r = v$, where v denotes the absolute value of the velocity. Hence

$$\frac{dv}{dr} + \frac{1}{r} v = 0 \tag{4.32-3}$$

or

$$v = \frac{\text{const}}{r}. \tag{4.32-4}$$

1. WITTMANN, H. P., and P. BÖSS: Wasser- und Geschiebebewegung in gekrümmten Flußstrecken. Berlin: Springer 1938.

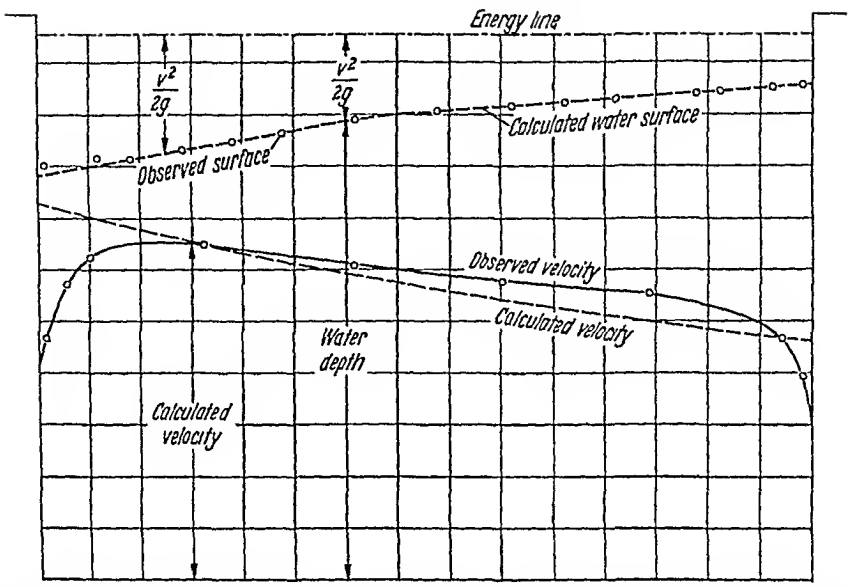

Fig. 101. Superelevation and velocity in a river bend (comparison between calculated and observed values). After WITTMANN and BÖSS[1]

Thus, the primary-current velocity is greatest on the *inside* of the curved river stretch, smallest on the outside. The stream lines are concentric circles, the lines of equal velocity potentials are radial lines.

The above simple pattern of stream lines is somewhat distorted if the river does not form a complete circle. In Fig. 100, we show the stream-lines in a 90° bend as calculated by WITTMANN and BÖSS[1].

The decrease of velocity from the inner to the outer bank has the effect that a superelevation of water occurs at the outer bank. If one assumes that the energy is constant and equal to H along any one radius in a curve, then the water depth can be calculated by means of the Bernoulli equation (4.21-2). Thus

$$h = H - \frac{v^2}{2g} \tag{4.32-5}$$

which yields with (4.32-4):

$$h = H - \text{const}\,\frac{1}{2g\,r^2}. \tag{4.32-6}$$

The last formula gives the water height (above a datum) as a function of r. One can also set up similar formulas for velocity distributions that are more complicated. In Fig. 101, we present the water depth (and the

1. WITTMANN, H. P., and P. BOSS: Wasser- und Geschiebebewegung in gekrümmten Flußstrecken. Berlin: Springer 1938.

velocity) as calculated for the velocity distribution shown in Fig. 100 (in the vertex position). We also show some measured values in comparison with the calculated curves (after WITTMANN and BÖSS[1]). As is seen, the agreement between theory and observations is not bad.

4.33. Elementary Theory of Secondary Currents in River Bends. It has been known for a long time[2] that potential flow does not describe the flow around river bends correctly. In addition to the primary currents, there are closed cross-currents, which have been called "secondary flows". A recent summary of the observations of such cross-currents has been given, for instance, by BRADEN[3]. An inexpensive model to study such currents has been described by TANNER[4].

There have been many attempts to give a rational theory of the secondary currents in river bends. Some general discussions of the phenomenon have been published by PRUS-CHACINSKI[5] and by SHAPIRO[6]. Our present concern will be only with helicoidal currents in *streaming* flow (cf. Sec. 4.21); in *shooting* flow additional complications occur since *cross-waves* will arise which are analogous to shock waves. This will be discussed later (Sec. 4.35).

We shall now give a review of the commonly quoted elementary theories of secondary currents in curved open channels.

One of the earliest theories of secondary currents has been proposed by BOUSSINESQ[7] who started from an analogy of flow in rivers with flow in pipes. Using some semi-empirical formulas for pipe flow, he postulated corresponding formulas for river flow. Thus, according to BOUSSINESQ, the loss of head in a straight river (per unit length) is given by (v is the velocity, h the depth of the river)

$$\Delta H_1 = \beta \frac{v^2}{h} \tag{4.33-1}$$

where β represents some coefficient. In a curved channel, BOUSSINESQ postulates an additional loss (α is another coefficient, R the radius of the curve and b is the width of the river):

$$\Delta H_2 = \frac{\alpha}{h} \sqrt{\frac{b}{R}}\, v^2 \tag{4.33-2}$$

---

1. WITTMANN, H. P., and P. BÖSS: Wasser- und Gesehiebebewegung in gekrümmten Flußstreeken. Berlin: Springer 1938.
2. THOMSON, J.: Proe. Roy. Soe. **25**, 5 (1876).
3. BRADEN, G. E.: Proe. Oklahoma Acad. Sei. **39**, 115 (1959).
4. TANNER, W. F.: J. Geolog. Edue. **10**, No. 4, 116 (1962).
5. PRUS-CHACINSKI, T. M.: Dock and Harbour Authority **36**, No. 417, 81 (1955).
6. SHAPIRO, KH. SH.: Trudy Vsesoyuz. In-ta Gidromekh. i Melior. **28**, 171 (1958).
7. BOUSSINESQ, J. M.: Mém. Aead. Sei. Paris **23**, Ser. 2, No. 1, Supplement **24**, 1 (1877).

and hence

$$\frac{\Delta H_2}{\Delta H_1}=\frac{\alpha}{\beta}\sqrt{\frac{b}{R}}. \tag{4.33-3}$$

The *total* loss in a curved river is then

$$\Delta H=\Delta H_1+\Delta H_2=\beta\frac{v^2}{h}+\frac{\alpha}{h}\sqrt{\frac{b}{R}}v^2=\frac{v^2}{h}\left(\beta+a\sqrt{\frac{b}{R}}\right). \tag{4.33-4}$$

BOUSSINESQ then reasons that in a river composed of straight and curved stretches, the head-loss per unit distance must be the same. Hence

$$\frac{\beta}{h_{\text{straight}}}v^2=\frac{v^2}{h_{\text{curved}}}\left(\beta+\alpha\sqrt{\frac{b}{R}}\right) \tag{4.33-5}$$

or

$$h_{\text{curved}}=h_{\text{straight}}\left(1+\frac{\alpha}{\beta}\sqrt{\frac{b}{R}}\right). \tag{4.33-6}$$

This gives a correlation between the depth of water in straight and in curved stretches of the river. It is obvious from the structure of the formula that the depth increases if the radius of curvature decreases. BOUSSINESQ concludes that, the deeper the channel, the more effective must be the cross-currents.

The Boussinesq formulas are semi-empirical because they are based upon a rather tenuous analogy with empirical formulas found for curved pipes. It would be desirable to devise a more analytical theory describing secondary currents in a curved channel.

Such an analytical theory may be based on the hypothesis that the flow in a river may be described by a velocity potential (cf. Sec. 4.32). According to the potential flow theory, the flow is fastest at the inner (convex) side of the river (see Sec. 4.32). However, such a distribution of flow cannot exist if the drag force at the bottom of the river is considered. The latter will cause the velocity to decrease from the surface to the bottom in a vertical column of water. The individual fluid particles moving with their individual velocities v (cf. Eq. 4.32-4) are forced around their circular paths with a radius of curvature r by a radial pressure drop of dp/dr (centrifugal force) across the channel which is given by the following equation:

$$dp/dr=\rho\, v^2/r \tag{4.33-7}$$

where ρ is the density of the water. In a slow-moving river, the radial pressure gradient dp/dr will not change along a vertical line, and hence its value is too great to keep the slow-moving bottom fluid (which is retarded by the drag) on the same curvature as the fast moving fluid particles at the surface. Hence, the fluid at the bottom of the river is

forced inward onto paths with stronger curvature. This gives rise to secondary currents which, if superimposed upon the mean flow, will create a helicoidal flow pattern as shown in Fig. 102.

The above explanation of secondary flow in curved channels is the standard one found in the textbooks[1]. It seems to be due to EINSTEIN (senior)[2]. However, the basic assumption, viz. that river flow is fundamentally irrotational so that it can be described by potential flow theory, is certainly not tenable. It is for this reason that the above explanation of the onset of secondary currents in river bends is scarcely acceptable.

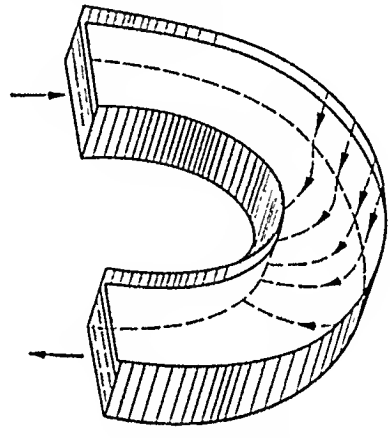

Fig. 102. Effect of secondary currents to produce helicoidal flow in a river bend

4.34. Basic Theory of Helicoidal Flows. The discussion presented thus far leaves one with the task of finding an acceptable explanation for the existence of the cross currents in river bends. It would be desirable to find such an explanation in terms of basic principles, viz. in terms of the Navier-Stokes equation and in terms of the statistical theory of turbulence. A clue to how to do this might be presented by the fact that secondary currents have been observed not only in curved channels, but also in straight ones[3]. Therefore, a basic instability in turbulent flow might be involved. An attempt to uncover such an instability by theoretical reasoning has been reported by EINSTEIN and LI[4].

Accordingly, the existence of secondary currents in straight channels can be explained if one starts from the formulation of the Navier-Stokes equations in terms of the vorticity (ξ, η, ζ)

$$\xi = \frac{\partial w}{\partial y} - \frac{\partial v}{\partial z} \text{ etc.} \qquad (4.34\text{-}1)$$

1. See e.g. SCHMIDT, M.: Gerinnehydraulik. Wiesbaden: Bauverlag 1957.

2. EINSTEIN, A.: Naturwissenschaften **14**, 223 (1926). I am grateful to Dr. STEKETEE for having drawn my attention to this paper.

3. See e.g. MUROTA, A.: Technol. Rep. Osaka Univ. **10**, 85 (1960).

4. EINSTEIN, H. A., and H. LI: Trans. Amer. Geophys. Union **39**, 1085 (1958).

with

$$\frac{\partial \xi}{\partial x}+\frac{\partial \eta}{\partial y}+\frac{\partial \zeta}{\partial z}=0. \tag{4.34-2}$$

Here $x\,y\,z$ are Cartesian co-ordinates, $u\,v\,w$ are the velocity components. The Navier-Stokes equations then read as follows (cf. LAMB[1], p. 578)

$$\frac{D\xi}{Dt}=\xi\frac{\partial u}{\partial x}+\eta\frac{\partial u}{\partial y}+\nu\,\mathrm{lap}\,\xi\ \text{etc.}, \tag{4.34-3}$$

where D/Dt is the total time derivative moving with the fluid and ν is the kinematic viscosity. One now introduces the concept of mean and fluctuating velocity components

$$u=\bar{u}+u', \tag{4.34-4}$$

where

$$\overline{u'}=\overline{\frac{\partial u'}{\partial t}}=0. \tag{4.34-5}$$

This is introduced into the Navier-Stokes equations, the average is taken, and one then ends up with

$$\overline{\frac{\partial \xi}{\partial t}}=\frac{\partial^2}{\partial y\,\partial z}(\overline{v'^2}-\overline{w'^2})+\frac{\partial^2}{\partial z^2}(\overline{v'\,w'})-\frac{\partial^2}{\partial y^2}(\overline{v'\,w'}). \tag{4.34-6}$$

The last Eq. (4.34-6) shows that in turbulent flow, the x-component of the vorticity need not necessarily vanish and therewith that secondary currents are possible. True, the terms on the right-hand-side of (4.34-6) add up to zero in *isotropic* turbulence, but in a river, particularly near its bed, the turbulence is not isotropic. Hence, EINSTEIN, and LI conclude that secondary currents must be expected even in straight channels.

The above theory does not have a bearing upon the *initiation* of secondary currents in straight channels. However, it has been shown by DELLEUR and MCMANUS[2] that the boundary-shear in a straight open channel can initiate the secondary flow.

A very interesting analysis of the origin of cross-currents based upon the basic equations of turbulent flow, has also been made by ANANYAN[3] who actually carried out calculations of the turbulent instability for flow in curved open channels. ANANYAN started with a set of fundamental flow equations which are based upon REYNOLDS'[4] equations for the

1. LAMB, H.: Hydrodynamics. New York: Dover Publications 1945.

2. DELLEUR, J. W., and D. S. MCMANUS: Proc. 6th Midwest Conf. Fluid Mechanics, Austin, Texas, p. 81 (1959).

3. ANANYAN, A. K.: Движение жидкости на повороте водовода. Erevan: Izvo Akad. Nauk Armyan. SSR 1957.

4. REYNOLDS, O.: Phil. Trans. Roy. Soc. Lond. A 186. 123 (1894).

turbulent stresses

$$\rho\left(\frac{\partial \bar{u}_i}{\partial t}+\bar{u}_j\frac{\partial \bar{u}_i}{\partial x_j}\right)=\rho F_i+\frac{\partial}{\partial x_j}(\tau_{ij}-\rho\,\overline{u_i' u_j'}). \tag{4.34-7}$$

Here, the x_i are the co-ordinates, the $\bar{u}_i$ are the average velocities, the u_i' are the velocity fluctuations, the τ_{ij} are the average hydrodynamic stresses,

$$\sigma_{ij}=\rho\,\overline{u_i' u_j'} \tag{4.34-8}$$

are the turbulent stresses, F_j is the external volume force and ρ is the fluid density. The viscosity term has been neglected because it is insignificant in relation to the turbulent stresses.

ANANYAN then introduced a heuristic assumption for the turbulent stresses, viz.

$$\sigma_{ij}=\varepsilon'(x_i)\left(\frac{\partial \bar{u}_i}{\partial x_j}+\frac{\partial \bar{u}_j}{\partial x_i}\right) \tag{4.34-9}$$

where $\varepsilon'(x_i)$ is the eddy viscosity (cf. Sec. 2.23). Following PRANDTL, the latter may be expressed as follows (see Eq. 2.23-2)

$$\varepsilon'(z)=\rho\,l^2\left|\frac{d\bar{u}_x}{dz}\right| \tag{4.34-10}$$

where x is the horizontal, z the vertical co-ordinate and l is PRANDTL'S mixing length (cf. 4.23-3):

$$l=-k\frac{d\bar{u}_x/dz}{d^2\bar{u}_x/dz^2}. \tag{4.34-11}$$

If all the above equations are taken together, if the continuity equation

$$\operatorname{div}\bar{u}=0 \tag{4.34-12}$$

is added, and if the boundary conditions are specified, then one has a problem which is, in principle, determined. ANANYAN wrote the equations in cylindrical co-ordinates, he specified the boundary conditions pertaining to a circular river bend, and showed that there are solutions which represent cross-circulations.

ANANYAN'S treatment of the cross-circulation problem in river bends is the most satisfactory one available to-date. Difficulties still exist in the introduction of PRANDTL'S heuristic theory into the fundamental equations of REYNOLDS. Furthermore, in obtaining his final solutions, ANANYAN had to make a series of approximations. It is not certain whether the solutions of ANANYAN are unique and, furthermore, what the fundamental influence of the channel curvature is.

Because of the difficulty in describing secondary flows analytically, methods of dimensional analysis and experimental correlations have also been tried. A lengthy review of such investigations has been published by KOLÁŘ[1]. As usual with such investigations, these do not explain the physical facts but only make them more accessible to observation.

4.35. Shooting Flow Around Corners. Peculiar phenomena occur in shooting (supercritical) flow around river bends. In shooting flow, the wave propagation velocity u with which disturbances travel, is smaller than the flow velocity v. The behavior of such a flow in a curved channel has, for instance, been analyzed by KNAPP[2].

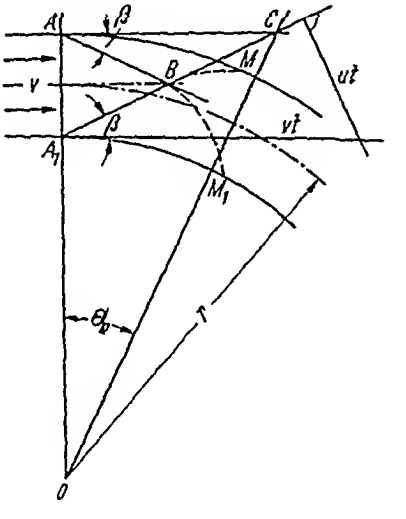

Fig. 103. Geometry of shooting flow at the beginning of a river bend

Thus, let us consider the beginning of a channel bend containing shooting flow. (See Fig. 103). If the flow is smooth in the straight section above the bend, the first disturbance due to the bend will start at the points A and A_1. At A, a pilling up of water will be created, at A_1, a lowering of the level. The disturbance travels with the wave velocity u, and hence it cannot make itself felt above the point B (see Fig. 103) where

$$\sin\beta=\frac{ut}{vt}=\frac{u}{v}=\frac{\sqrt{gh}}{v}. \tag{4.35-1}$$

Here, the shallow water formula (6.22-28) has been used for the wave velocity; t denotes some arbitrary time and h the river depth. The disturbances will reach the opposite bank at the points M and M_1 which lie approximately on the radius 0 C. For the angle Θ_0 determining the

1. KOLÁŘ, V.: Rozpravy Československ. Akad. Věd, Řada Technic. Věd 66, 105 (1956).
2. KNAPP, R. T.: Trans. Amer. Soc. Civ. Eng. 116, 296 (1951).

position of this radius. one has (see Fig. 103)

$$\Theta_0 = \arctan \frac{b}{\left(r + \frac{b}{2}\right) \tan \beta} \tag{4.35-2}$$

where b denotes the width of the river. The disturbances which arrive at the banks at the radius with angle Θ_0 will again start further disturbances of the same nature, and hence a pattern of *cross waves* will be the result which have a wavelength λ of

$$\lambda = 2r\,\Theta_0. \tag{4.35-3}$$

The disturbances being reflected from the banks of the channel have a scouring effect.

It is obvious that the propagation phenomena of disturbances in shooting flow are analogous to the corresponding phenomena in gas dynamics. Particular problems arise when $v = u$ ("critical" flow) where shock fronts, analogous to the "sonic boom" in gases, can arise. The geomorphological effects of shooting flow, thus, consist in a high stressing of the banks.

4.4. Forces of Fluids on Particles

4.41. General Remarks. In many instances, the surface of the Earth consists of loose particles. This is particularly the case in alluvial areas, on beaches and in river beds. The morphology of such surfaces is conditioned by the interaction of water with the individual particles.

Therefore, our next task is to study the forces that act on individual particles immersed in a fluid. First, we shall study the gravity force with its attendant effect on the settling velocity of particles in water. Then we shall turn to the scouring effect of flowing water on river bed particles and finally we shall study the modes by which flowing water can actually lift particles from a river bed to bring them into suspension.

4.42. Gravity Force: Settling Velocity. If we consider a particle suspended in a liquid, we note that amongst all the forces acting upon it, the best known is the gravity force. It is due to the gravity acceleration and is equal to the underwater weight W of the particle given by (making use of ARCHIMEDES' principle):

$$W = Vg(\delta - \rho). \tag{4.42-1a}$$

Here, V is the volume of the particle, δ is the density of the particle, ρ the density of the fluid and g is the gravity acceleration.

Owing to the gravity force, a submerged particle has the tendency to settle towards the bottom, regardless of whether the liquid be at rest or whether it be flowing. During the settling process, the resistance that the particle has to overcome may either be caused by viscous drag or by turbulence, depending on the relative velocity of fluid and particle. We shall investigate these two possibilities in turn.

A. Viscous Drag. In case the resistance is due to viscous forces, the settling velocity can easily be calculated from STOKES' law. As is well known, the resistance F_R of a sphere of radius a to flowing liquid is given by

$$F_R = 6\pi a \eta v$$

where η is the viscosity of the fluid and v the relative velocity between fluid and sphere. Setting this equal to the underwater weight W of the sphere (cf. 4.42-1a)

$$W = \tfrac{4}{3}\pi a^3 g(\delta - \rho) \qquad (4.42\text{-}1b)$$

yields the following settling velocity of the particle

$$v = \frac{2}{9}\frac{a^2(\delta-\rho)g}{\eta}. \qquad (4.42\text{-}2)$$

If the particles are not spherical, one has to introduce a shape factor κ, and one then has

$$F_R = 6\pi\kappa\eta v. \qquad (4.42\text{-}3)$$

The length κ can be calculated theoretically for various simple shapes. In the case of a circular disk of radius c moving broadside on, one has[1]

$$\kappa = 0.85\, c \qquad (4.42\text{-}4)$$

and in the case of a disk moving edgewise[1]

$$\kappa = 0.556\, c. \qquad (4.42\text{-}5)$$

The viscous drag formulas are good for particles settling in water on the Earth of a radius up to about 0.114 mm. For larger particles, the formulas given under (B) and (C) of this Section have to be used.

The gravity and inertial forces acting upon a spherical particle in a moving fluid can be combined and an equation of motion can be deduced. This has been done by TCHEN[2] who started with a discussion of the problem of slow motion of a spherical particle under the influence of gravity in a fluid at rest. The latter problem had been studied previously

1. Cf. LAMB, H.: Hydrodynamics, 6th ed., p. 605. New York: Dover Pub. Co. 1945.

2. TCHEN, C. M.: Mean Value and Correlation Problems Connected with the Motion of Small Particles Suspended in a Turbulent Fluid. Diss., Tech. Hoogesch. Delft. The Hague. M. Nijhoff 1947. See p. 73 ff.

by BASSET[1], BOUSSINESQ[2] and OSEEN[3]. OSEEN arrived at the following equation of motion in the direction of the axis $O\,y$ ($+y$ being directed vertically upward):

$$\frac{4\pi a^3}{3}\delta\dot{v}=-\frac{2\pi a^3}{3}\rho\,\dot{v}^2-6\pi\eta\,a\left\{v+\frac{a}{\sqrt{\pi\nu}}\int_{t_0}^{t}dt_1\,\frac{\dot{v}(t_1)}{\sqrt{t-t_1}}\right\}-\frac{4\pi a^3}{3}(\delta-\rho)\,g. \tag{4.42-6}$$

In this equation, $v(t)$ is the velocity of the particle, ρ, δ are density of fluid and particle, respectively, a is the radius of the (spherical) particle, g is the gravity acceleration and η, ν are viscosity and kinematic viscosity, respectively. In deriving OSEEN's equation, it had been assumed that the particle as well as the fluid had been at rest until $t=t_0$. It will usually be expedient to assume $t_0=-\infty$.

TCHEN now rewrote the Oseen equation in terms of a particle whose velocity is $(v-u)$ and endowed the entire system (particle plus fluid) with a uniform rectilinear velocity $u(t)$. The result of performing this operation is

$$\frac{4\pi a^3}{3}\delta\dot{v}=\frac{4\pi a^3}{3}\delta\dot{u}-\frac{2\pi a^3}{3}\rho(\dot{v}-\dot{u})-6\pi\eta\,a(v-u)-6\pi\eta\frac{a^2}{\sqrt{\pi\nu}}\int_{-\infty}^{t}\frac{\dot{v}(t_1)-\dot{u}(t_1)}{\sqrt{t-t_1}}dt_1-\frac{4\pi a^3}{3}g(\delta-\rho). \tag{4.42-7}$$

This is TCHEN's equation.

B. Turbulent Drag. We now direct our attention to the settling velocities of particles where the resistance is due to turbulent energy dissipation. Turbulence occurs if the relative velocity between fluid and particle exceeds a critical value given by

$$Re=\frac{2\rho v a}{\eta}\geqq Re_{\text{crit}} \tag{4.42-8}$$

where Re is commonly called Reynolds number. As usual, ρ denotes the density of the fluid, v the relative velocity, a the radius of the particle and η the viscosity of the fluid.

Turbulent settling has mostly been studied by meterologists since it is the mode by which rain drops fall from the sky.

1. BASSET, A. B.: A Treatise on Hydrodynamics. Cambridge 1888. See Vol. 2, Ch. 4.
2. BOUSSINESQ, J.: Théorie analytique de la chaleur. Paris 1903. See Vol. 2, 224.
3. OSEEN, C. W.: Hydrodynamik. Leipzig: Akademische Verl ges. 1927. See p. 132.

The settling velocity in purely turbulent flow can be calculated in the same fashion as that for laminar flow by setting the underwater weight of the particle (cf. 4.42-1a) equal to the well-known expression for turbulent drag: (cf. 2.22-4)

$$F_R = C_D \pi a^2 \frac{\rho v^2}{2} \tag{4.42-9}$$

(cf. also Eq. 4.43-1 in the next section), where C_D is some drag coefficient equal[1] to about 0.79 for spherical particles. We then obtain

$$C_D \pi a^2 \frac{\rho v^2}{2} = \frac{4}{3} \pi a^3 g(\delta - \rho),$$

or for the settling velocity:

$$v = \sqrt{\frac{8}{3} \frac{g a(\delta - \rho)}{\rho C_D}}. \tag{4.42-10}$$

C. Intermediate Flow Régime. Recently, SHIFRIN[2] gave a general formula for the settling rate of a sphere in a fluid, which encompasses both, the turbulent and the viscous settling formulas into one expression.

SHIFRIN assumes that, for low Reynolds numbers, the factor C_D is a function of the Reynolds number

$$C_D = f(Re). \tag{4.42-11}$$

Then, setting the drag equal to the underwater weight, one obtains[3] the following relation under steady state conditions

$$\alpha a^3 = \frac{1}{24} Re^2 f(Re) \tag{4.42-12}$$

with

$$\alpha = \frac{4}{9} \frac{\rho(\delta - \rho) g}{\eta^2} \tag{4.42-13}$$

where $(\delta - \rho)$ is the difference between the density of the sphere and that of the fluid. We then set

$$F(Re) \equiv \frac{1}{24} Re^2 f(Re). \tag{4.42-14}$$

The determination of the settling velocity (or of the corresponding Reynolds number) is then accomplished by a solution of the equation

$$F(Re) - \alpha a^3 = 0. \tag{4.42-15}$$

1. See LELIAVSKY, S.: An Introduction to Fluvial Hydraulics, p. 36. London: Constable & Son 1955.

2. SHIFRIN, K. S : Izv Akad. Nauk SSSR, Ser. Geofiz. 1958, 280 (1958).

3. SHIFRIN, K. S.: The Kinetics of Precipitation. Trudy Obshch. Geofiz Obs. No. 31 (1951).

Denoting the inverse function of F by Φ

$$\Phi \equiv F^{-1}$$

we can write the solution of (4.42-15) as follows

$$Re = \Phi(\alpha a^3). \tag{4.42-16}$$

Thus, we have for the settling velocity

$$v = \frac{\eta}{2\rho a} \Phi(\alpha a^3). \tag{4.42-17}$$

This is SHIFRIN's general formula for the settling velocity which is valid for the turbulent and laminar flow régimes alike. This can be verified as follows. The function $f(Re)$ in Eq. (4.42-11) has been discussed by GOLDSTEIN[1] who gave a series development for small values of Re. Using GOLDSTEIN's series leads to the following expression of Φ for small Re:

$$\Phi(F) = F\left\{1 - \frac{3}{16}F + \frac{109}{1280}F^2 - \frac{1031}{20480}F^3 + \cdots\right\} \tag{4.42-18}$$

and hence one obtains

$$v = \frac{\eta}{2\rho a} \alpha a^3 = \frac{2}{9} \frac{(\delta - \rho) g}{\eta} a^2 \tag{4.42-19}$$

which is indeed STOKES' formula (4.42-2). For large Re, C_D is constant; thus

$$F(Re) = \frac{C_D}{24} Re^2 \tag{4.42-20}$$

$$\Phi = \sqrt{24 F / C_D}. \tag{4.42-21}$$

Hence

$$\begin{aligned} v &= \frac{\eta}{2\rho a} \sqrt{\frac{24 \alpha a^3}{C_D}} \\ &= \sqrt{\frac{8(\delta - \rho) g a}{3\rho C_D}}, \end{aligned} \tag{4.42-22}$$

which is indeed the formula found earlier (4.42-10). Thus, SHIFRIN's general formula for the settling velocity of a spherical particle indeed yields the correct limiting values for high and low Reynolds numbers and hence it stands to reason that it correctly describes the intermediate flow régime, too.

1. GOLDSTEIN, S.: Modern Developments in Fluid Dynamics, Vol. 2. Oxford: Clarendon Press 1938.

The above investigations refer to the settling velocity of a single particle. If there are many particles present, it may be expected that an interaction effect occurs. The interaction between several particles following each other whilst they are settling, has received some attention in the literature; convenient reviews of the theory have recently been given by HAPPEL and coworkers[1,2]. In general, it is found that two particles will fall faster than one. Experiments seem to bear out this prediction.

4.43. Scouring Force. Another type of force of flowing fluids whose existence is intuitively well known is the *scouring force*. It acts upon particles sitting at the bottom of a stream bed.

A simple theory for the scouring force can be obtained by regarding a particle as sitting alone on the bottom of an otherwise smooth container with the fluid streaming by it. It is well known that such a particle offers a resistance to the fluid that varies with the square of the velocity (provided the Reynolds number is high enough), as this is implicit in the momentum transfer theory (cf. Sec. 2.22). By the principle of action and reaction this is also the force experienced by the particle. Thus, the scouring force F_s acting upon the particle can be expressed as follows

$$F_s = C_D \frac{\pi}{4} d^2 \frac{1}{2} \rho_F v^2. \tag{4.43-1}$$

In this equation, d is the diameter of the particle, ρ_F is the density of the fluid, v is the fluid velocity at the particle level and C_D is a drag coefficient, depending on the size of the particle and on the Reynolds number. Expression (4.43-1) is the well-known expression for turbulent drag (cf. 4.42-9). As noted in Sec. 4.42, in the case of the particle being spherical, the drag coefficient is given by $C_D = 0.79$ at high Reynolds numbers.

The scouring force will be able to *move* a (spherical) particle if it is large enough to overcome the frictional resistance F_f

$$F_f = \varepsilon(\rho_s - \rho_F)\, g \tfrac{1}{6} \pi d^3$$

where ε is the coefficient of friction, ρ_s the density of the particle, g the gravity acceleration and the other symbols have the previously defined meaning.

Equating the two forces and solving for v yields an expression for the critical velocity v_{cr} of the stream which will just be able to move bottom

1. HAPPEL, J., and R. PFEIFFER: J. Amer. Inst. Chem. Eng. 6, 129 (1960).
2. HAPPEL, J., and H. BRENNER: Low Reynolds Number Hydrodynamics. Englewood Cliffs: Prentice-Hall (1965).

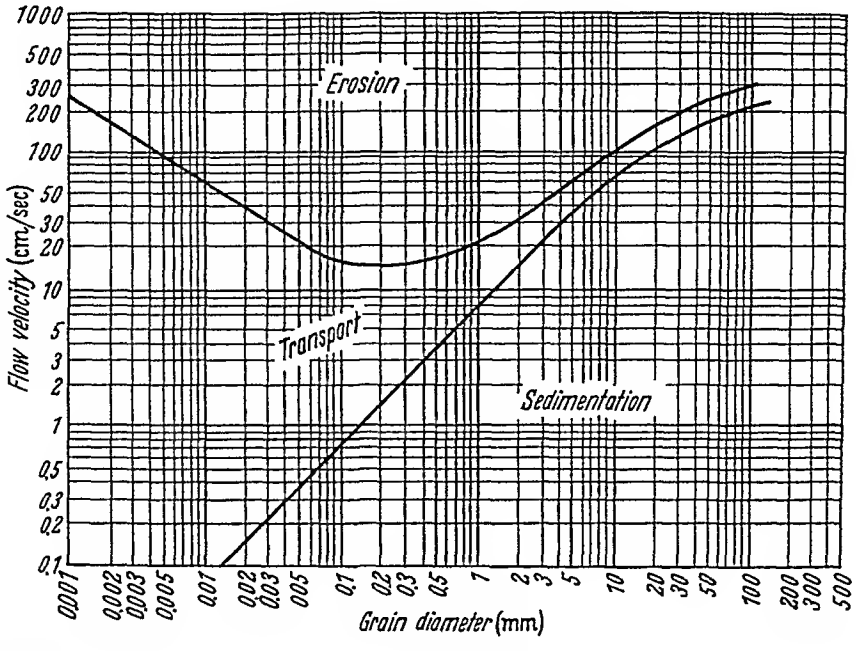

Fig. 104. HJULSTRÖM's[1] critical drag curves, separating the flow regions where entrainment, deposition, and steady carriage occurs

particles. It is:

$$v_{cr}^2 = \frac{4g}{3} \frac{\varepsilon(\rho_s - \rho_F)}{C_D \rho_F} d. \tag{4.43-2}$$

The square of the critical velocity, thus, turns out be proportional to a linear dimension of the particle. However, the latter is roughly proportional to the cube root of its weight W, and hence we can write

$$v_{cr} \sim W^{\frac{1}{3}}, \tag{4.43-3}$$

This is a correlation (BRAHMS' *equation*) which had been found from empirical data over two hundred years ago. More modern experiments have yielded a somewhat more complicated picture. Thus, HJULSTRÖM[1] established empirically critical drag curves separating the flow regions where entrainment, deposition and steady transportation occurs (see Fig. 104).

The above theory is obviously somewhat oversimplified. More generally, in newer investigations, it is therefore assumed that it is a critical value for the bottom tractive force σ_m (also called drag force) introduced in Sec. 4.22 which starts the bottom-particles moving. This critical drag may be related to the mechanics in the turbulent and laminar boundary layer in rough channels. Microscopically, the phenomena taking place are not entirely clear; it may be that grain entrainment results from the

1. HJULSTRÖM, F.: Bull. Geol. Inst. Uppsala 25, 221 (1935).

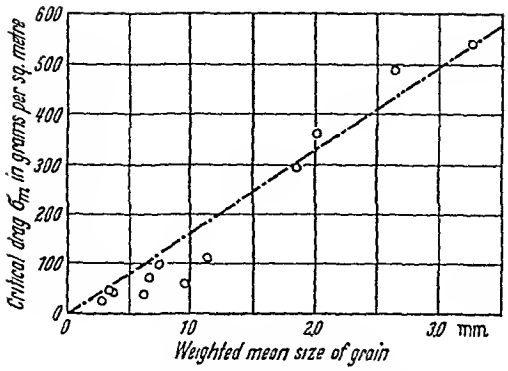

Fig 105. Chart showing critical drag (ordinate) in g/m² as function of grain diameter (abscissa) in mm compared with experimental results (circles) from various laboratories. After LELIAVSKY[1]

interaction between fluid elements within an eddy and the sediment grains[2]. Phenomenologically, SHIELDS[3] postulated a general relation for the critical drag force $\sigma_m = \sigma_{crit}$

$$\frac{\sigma_{crit}}{\rho_s - \rho_w} = f\left(\frac{u_* d}{\nu}\right) \tag{4.43-4}$$

where ρ_s is the sediment density, ρ_w the water density, u_* the shear velocity (cf. Eq. 4.23-2), d the grain diameter, ν the kinematic viscosity of the water and f denotes a universal function.

Measurements have been made of σ_{crit} for various types of sedimentary particles. These measurements, originating from various laboratories, have been collected by LELIAVSKY[1] and the result is shown in Fig. 105. This figure bears out a definite correlation (the circles are the values measured by various laboratories). From LELIAVSKY's graph, one takes the following formula for the critical drag force

$$\sigma_{crit} = \text{const} \cdot d \tag{4.43-5}$$

where d is the particle diameter. A variety of formulas of this type has been suggested in the literature, most of which, if dimensionally correct, can be reduced to the form[4] (being a simplified version of 4.43-4)

$$\frac{\sigma_{crit}}{g(\rho_s - \rho_F)d} = A \tag{4.43-6}$$

1. LELIAVSKY, S.: An Introduction to Fluvial Hydraulics. London: Constable & Sons 1955.

2. SUTHERLAND, A. J.: J. Geophys. Res. **72**, 6183 (1967).

3. SHIELDS, A.: Mitt. Preuss. Vers. Anst. Wasserbau & Schiffbau, No. 26 (1936).

4. CARTER, A. C.: Critical Tractive Forces Which Start Movement of Sediment in a Channel. U.S. Bureau of Reclamation, Hyd. Lab. Rept. HYD-296 (1950).

where again ρ_s and ρ_F are the densities of sediment and fluid, respectively, g is the gravity acceleration, d the particle diameter and A is a dimensionless parameter. The latter may be taken as a function of d/D where D is the thickness of the laminar sublayer. Most of the experiments have been made on beds consisting of uniform grains. Attempts to obtain empirical correlations for mixtures of grains of different sizes have been reported by GESSLER[1].

The above theory has been generalized somewhat by SUNDBORG[2] who introduced modifications to allow for *cohesion* between sand grains to exist and also to allow for a *slope* (angle α) that may not be small. The formula corresponding to (4.43-5) then becomes

$$\sigma_{crit} = \text{const}_1 [g\, d(\rho_s - \rho_F)(\varepsilon \cos\alpha - \sin\alpha) + \text{const}_2 \cdot C] \quad (4.43\text{-}7)$$

where C represents the cohesion and ε is a coefficient of friction.

4.44. Lifting Force. The forces acting on particles contained in a flowing fluid discussed so far, are not able to explain the lifting and transportation of sediment. The scouring force might at best provide for an explanation of the inception of motion of bottom sediment, but for an explanation of the well-known transportation of sedimentary particles in suspension, a *lifting* force is required.

It has long been recognized that *turbulence* must play a fundamental rôle for this lifting force. In this instance, turbulence, in sediment transportation, plays a similar rôle as in the dynamics of flight. A semi-theoretical discussion of this fact has been given for instance by LEIGHLY[3]. A modern analytical theory in terms of the statistical theory of turbulence has been provided by FRIEDLANDER[4].

Accordingly, each particle is assumed to be contained in an *eddy* of fluid, large compared with the former, but still small compared with the dimensions of the container of the fluid. Let the velocity of the eddy be u_F and its acceleration a_F. Correspondingly, the velocity and acceleration of the particle are u_P and a_P.

The force balance equation, neglecting gravity, for the particle can now be written down. If the Reynolds number

$$Re = d_P \sqrt{\overline{u_R^2}}\, \rho_F / \eta \quad (4.44\text{-}1)$$

is less than 1 (where d_P is the particle diameter, furthermore

$$u_R = u_F - u_P, \quad (4.44\text{-}2)$$

1. GESSLER, J.: Mitt. Vers. Anst. Wasserbau & Erdbau, Eidg. Techn. Hochsch. Zürich, No. 69 (1965).
2. SUNDBORG, A.: Geografiska Ann. 38, 174 (1956).
3. LEIGHLY, J.: Geograph. Rev. 24, 453 (1934).
4. FRIEDLANDER, S. K.: J. Amer. Inst. Chem. Eng. 3, 381 (1957).

ρ_F is the fluid density and η the fluid viscosity), then the resistance F_f is given by STOKES' law which may be written as follows, to allow for the various shapes of the particles (cf. 4.42-3):

$$F_f = -f(u_P - u_F). \tag{4.44-3}$$

In addition to this resistance, the particle will be subject to a force F_b because of the pressure gradient in its vicinity. If the Reynolds number is high, then the Stokesian force can be neglected and one has (by NEWTON'S law of motion; p is pressure):

$$\frac{\partial p}{\partial x} = \rho_F a_F. \tag{4.44-4}$$

The force F_b is then given by (m_F being the mass of the displaced fluid)

$$F_b = m_F a_F \tag{4.44-5}$$

so that the force balance equation yields (m_P being the mass of the particle)

$$m_P a_P = m_F a_F - f(u_P - u_F) \tag{4.44-6}$$

or

$$\frac{du_P}{dt} + \beta u_P = \beta u_F + \gamma \frac{du_F}{dt} \tag{4.44-7}$$

where β is some coefficient (depending on f and the particle inertia) and

$$\gamma = \rho_F / \rho_P. \tag{4.44-8}$$

FRIEDLANDER now obtains the rate of eddy diffusion of the suspended particles by expressing their mean square displacement $\overline{x_P^2}$ as a function of time. The distance travelled by a particle which at $t=0$ is at the position $x=0$, is obtained by integrating equation (4.44-7):

$$x_P + \frac{u_P - u_{PO}}{\beta} = \int_0^t u_F(T)\, dT + \frac{\gamma(u_F - u_{FO})}{\beta}. \tag{4.44-9}$$

Squaring and averaging this yields

$$\begin{aligned} \overline{x_P^2} + \frac{2}{\beta} \int_0^t \overline{u_P(T)[u_P(t) - u_{PO}]}\, dT + \frac{\overline{(u_P - u_{PO})^2}}{\beta^2} \\ = \int_0^t \int_0^t \overline{u_F(T_1)\, u_F(T_2)}\, dT_1\, dT_2 \\ + \frac{2\gamma}{\beta} \int_0^t \overline{u_F(T)[u_F(t) - u_{FO}]}\, dT \\ + \frac{\gamma^2 \overline{(u_F - u_{FO})^2}}{\beta^2}. \end{aligned} \tag{4.44-10}$$

We now introduce a correlation function

$$R(\Theta)=\frac{\overline{u(t)\,u(t+\Theta)}}{\overline{u^2}}.$$

Then, one can make the following transformations

$$\int_0^t\int_0^t \overline{u(T_1)\,u(T_2)}\,dT_1\,dT_2=\overline{u^2}\int_0^t\int_0^t R(T_2-T_1)\,dT_1\,dT_2$$

$$=\overline{u^2}\int_0^t dT_1\int_{-T_1}^{t-T_1} R(\Theta)\,d\Theta$$

$$=\overline{u^2}\left[\int_0^t dT_1\int_0^{T_1} R(\Theta)\,d\Theta+\int_0^t dT_1\int_0^{t-T_1} R(\Theta)\,d\Theta\right]$$

(integrating by parts)

$$=2\overline{u^2}\int_0^t (t-\Theta)\,R(\Theta)\,d\Theta$$

and

$$\int_0^t \overline{u(T)[u(t)-u_0]}\,dT=\int_0^t \overline{u(T)\,u(t)}\,dT-\int_0^t \overline{u(T)\,u_0}\,dT$$

$$=\overline{u^2}\int_0^t R(t-T)\,dT-\overline{u^2}\int_0^t R(T)\,dT$$

$$=-\overline{u^2}\int_t^0 R(\Theta)\,d\Theta-\overline{u^2}\int_0^t R(\Theta)\,d\Theta=0.$$

For large t, the terms containing β^2 in the denominator remain finite. Hence, they may be disregarded in setting up an asymptotic expression for large t. The same is true for the integral $\int_0^{t\to\infty}\Theta R(\Theta)\,d\Theta$. Thus one obtains asymptotically

$$\overline{x_P^2}=2\overline{u_F^2}\,t\int_0^{t\to\infty} R(\Theta)\,d\Theta. \qquad (4.44\text{-}11)$$

This is an expression characteristic of *diffusion.*

There is some question as to what the correlation function should be. TCHEN[1] took it as equal to the correlation function of the fluid and interpreted the last equation as meaning that fluid and particles diffuse at the same rate. However, FRIEDLANDER points out that the correlation functions which should be used range between two extremes: the Lagrangian

1. TCHEN, C. M.: Mean Value and Correlation Problems Connected With the Motion of Small Particles Suspended in a Turbulent Fluid (125 pp.). Diss. Tech. Hoogeschool, Delft. The Hague: M. Nijhoff 1947.

function for small particles able to follow the fluid, and the Eulerian function for particles which remain almost fixed.

At any rate, the existence of diffusion in turbulent flow provides a means for keeping particles in suspension against gravity.

4.5. Sediment Transportation

4.51. General Remarks. Sediments in a river are mixtures of particles of various kinds, sizes and shapes. Mechanically, the "kind" of particle expresses itself in the grain density ρ_s, the size by its largest diameter d and the shape by some measure of ellipticity. Measurements of these properties consist in sieve analyses leading to weight-fractions etc.[1]

The particles making up the sediment-mixture in a river are often subject to ROSIN'S[2] law, expressible by the equation

$$R = 100\, e^{-bx^n} \tag{4.51-1}$$

which can be directly obtained from probability considerations[3]. In Eq. (4.51-1) R is the weight percent retained on a sieve of mesh x, and b and n are constants for any given material. For the study of sedimentary *structures*, the orientation of grains relative to each other and in space is of importance, but in the present context, this is not of much significance.

There are two fundamentally different modes by which sediment can be transported in a river. These modes are called *suspended* sediment transportation and *bottom* sediment transportation. In the former, the particles in transit are in suspension within the river, whereas in the latter they are dragged along at the bottom. The transitional stage between these two modes of sediment transportation has been called *saltation;* in it particles perform jumping motions.

The characteristics of sediment transportation have been described in various places in the literature. Much information is contained in general textbooks on river bed processes[4–10]. In addition, the problem

1. Cf. e.g. GRIFFITH, J. C.: J. Geol. 69, 487 (1961).
2. ROSIN, P. O., and E. RAMMLER: Kolloid-Z. 67, 16 (1934).
3. KRUMBEIN, W. C., and F. W. TISDEL: Amer. J. Sci. 238, 296 (1940).
4. HJULSTRÖM, F.: Bull. Geol. Inst. Uppsala 25, 221 (1935)
5. MEINZER, O. E. (ed.): Hydrology. New York: McGraw-Hill Book Co. 1942.
6. LELIAVSKY, S.: An Introduction to Fluvial Hydraulics. London: Constable & Son 1955
7. BLIZNYAK, E. V., and A. YUFIN. Гидравлика сооружений и динамика речных русел. Moscow: Iz-vo Akad. Nauk SSSR (1959).
8. KONDRAT'EV, N. E., A. N. LYAPIN, and I. V. POPOV: Русловой процесс. Leningrad: Gidrometeoizdat (1959).
9. VELIKANOV, M. A.: Динамика русловых потоков. 2 Vols. Moscow: Gos. Iz-vo Tekh. Teoret. Lit. 1954–55.
10. VELIKANOV, M. A.: Русловой процесс. Moscow: Gos. Iz-vo Fiz.-Mat. Lit. 1958.

has been reviewed by BENEDICT[1], JAROCKI[2], MITCHELL[3], YALIN[4] and EGIAZAROV[5]. References to the original investigations which are basic to the various theories that will be presented below, will be given in their proper context.

In order to characterize sediment transport, it is customary to introduce a Reynolds number Re

$$Re = \frac{u_* d}{\nu} \tag{4.51-2}$$

where u_* is the shear velocity (cf. 4.23-2) in the river, d the particle diameter and ν the kinematic viscosity of the water. It then is thought that definite values of Re separate the various modes of sediment transportation from each other.

It turns out that the Reynolds number is only a rather inaccurate criterion for determining what type of sediment transportation can be expected in a river whose velocity and bed composition are known. A more elaborate attempt to arrive at a criterion, based on similarity considerations, has been undertaken by ABDURAUPOV[6]. However, it would appear that criteria regarding the type of sediment transportation based on similarity considerations could never be very satisfactory. A direct solution of this problem should be sought by actually studying the various modes of sediment transportation; the fraction and type of material that will be subject to each mode will then automatically follow.

Unfortunately, a complete analysis of the general problem of sediment transportation has not yet been achieved. We shall, in the next two Sections, describe the theories that have been proposed for an explanation of suspended and bottom sediment transportation, respectively, and then return to the general questions regarding total sediment load transportation.

4.52. Suspended Sediment Transportation. We shall first look at the mechanism of suspended sediment transportation. As outlined earlier, it must be held that it is *turbulence* which keeps the particles in suspension. However, there are two theories with regard to the manner in which this turbulence might act. The first theory assumes that there is an effect acting on the particles which is analogous to diffusion (eddy diffusion),

1. BENEDICT, P.: Trans. Amer. Geophys. Union **38**, 897 (1957).
2. JAROCKI, W.: Ruch rumowieska w riekach. Gdynia: Wydawictwo Morskie 1957.
3 MITCHELL, R.: Cahiers Géol. **44**, 440 (1957).
4. YALIN, S.: Houille Blanche **13**, No. 6, 607 (1958).
5. EGIAZAROV, I. V.: in: Проблемы использования водных рессурсов, pp. 49–86. Moscow: Iz-vo Akad. Nauk. SSSR, 1960.
6. ABDURAUPOV, R. R.: Izv. Akad. Nauk Uzbek. SSR, Ser. Tekh. Nauk 1958, No. 5, 67 (1958).

and that the vertical concentration of the particles is therefore subject to a diffusivity equation. This leads to the *diffusivity theory* of suspended sediment transportation. The second theory is based directly upon the dynamics of the supporting stream. This leads to the *gravitational theory* of suspended sediment transportation. We shall discuss these two theories in their turn.

Let us discuss first the diffusivity theory. As noted above, the mass exchange in turbulent flow may be regarded as analogous to diffusion (cf. Sec. 4.44). We therefore start with a suitable diffusivity equation for the vertical particle density which might be written as follows:

$$\frac{\partial n}{\partial t}=\frac{\partial}{\partial z}\left(\varphi\frac{\partial n}{\partial z}\right). \tag{4.52-1}$$

Here, n is the particle number per unit volume, φ is a suitable diffusivity factor, t is time and z is the vertical co-ordinate. Every particle, if left alone, will tend to settle downward with the settling velocity w; hence the above diffusivity equation should apply only in a system which is moving downward with the velocity w (assuming that all particles have the same settling velocity). Hence, in a rest system (co-ordinates y, t), the diffusivity equation becomes

$$\frac{\partial n}{\partial t}=\frac{\partial}{\partial y}\left(\varphi\frac{\partial n}{\partial y}\right)+w\frac{\partial n}{\partial y} \tag{4.52-2}$$

where

$$y=z-wt. \tag{4.52-3}$$

Eq. (4.52-2) is the well-known diffusivity equation with a mass transport term.

Seeking a steady state solution, one obtains

$$\varphi\frac{\partial n}{\partial y}+nw=0. \tag{4.52-4}$$

An inspection of the last equation shows that it can be interpreted as a continuity equation: in a steady state, the rate of particle settling (nw) must be exactly balanced by some quantity which must be equal to the rate of particles being transferred upward by the turbulence. Hence, φ must be the turbulent transfer coefficient for the particles.

One could have arrived at the above relationship also directly by writing down the balance equation for the particles[1]

$$-\varphi\frac{\partial n}{\partial y}=nw \tag{4.52-5}$$

1. Vanoni, V. A.: Trans. Amer. Geophys. Union 22, 608 (1941).

where φ is *defined* as the transfer coefficient for the particles. The recourse to the diffusivity equation (4.52-2) is then not necessary.

Integrating equation (4.52-4/5) yields (n_0 = particle number at $y = y_0$)

$$\frac{n}{n_0} = e^{-w \int_{y_0}^{y} dy/\varphi}. \tag{4.52-6}$$

Now, the problem is to find an expression for φ. This problem is solved by making the basic assumption that the transfer coefficient for the particles and the transfer coefficient for the momentum are identical. Thus, using (2.23-2) one can write

$$\sigma = \varphi \rho \frac{d\bar{u}}{dy} \tag{4.52-7}$$

where $\bar{u}(y)$ is the time-averaged velocity at the height y, σ is the turbulent shear stress and ρ is the density of the fluid. It may then be assumed that the stress σ is a linear function of the depth concerned

$$\sigma = \sigma_m \left(1 - \frac{y}{h}\right) \tag{4.52-8}$$

where σ_m signifies the maximum stress which is reached at the bottom ($y = 0$) and h the total depth of the river. Hence, one obtains

$$\varphi = \frac{\sigma_m}{\rho} \frac{1 - y/h}{d\bar{u}/dy}. \tag{4.52-9}$$

The further discussion of the problem depends on the assumption of the vertical velocity distribution in the stream. Using KARMAN's logarithmic law (cf. Eq. 4.23-6), i.e.

$$\frac{u_{max} - \bar{u}}{\sqrt{\sigma_m/\rho}} = \frac{1}{k} \operatorname{lognat} \frac{h}{y} \tag{4.52-10}$$

yields

$$\varphi = \sqrt{\frac{\sigma_m}{\rho}} \left(1 - \frac{y}{h}\right) k y$$

$$\frac{n}{n_0} = \left[\frac{h - y}{y} \frac{y_0}{h - y_0}\right]^K \tag{4.52-11}$$

with

$$K = \frac{w}{k} \sqrt{\frac{\rho}{\sigma_m}}. \tag{4.52-12}$$

Here, k is as usual KARMAN's "universal" constant of turbulence (cf. Eq. 4.23-3) which is approximately equal to 0.4, and h is the total depth

of the stream[1]. The above equation applies to a suspended load where the particles are characterized by the settling velocity w. In a mixture of particles, one has to sort out the individual fractions.

A similar relation was obtained by CONOVER and MATALAS employing a statistical model of sediment transport[2].

In an attempt at checking Eq. (4.52-11) experimentally, VANONI found that, in absolute terms, the agreement is not very good. However, the general *shape* of the curves found experimentally agrees reasonably well with that postulated by the theory.

From a practical standpoint, it is extremely important to proceed from the above formulas (which explain the distribution of sediment with height in a stream) to a quantitative expression of the carrying capacity of streams with regard to given sediment sizes. An attempt in this direction has been made by EINSTEIN[3], simply by integrating the last equation over the vertical, assuming that in the *horizontal* direction, the speed of the particles is identical to that of the surrounding fluid, corresponding to Eq. (4.52-10). He obtained:

$$q_s = \int_y^h n_y \bar{u}\, dy$$
$$= \int_y^h n_0 \left[\frac{h-y}{y}\,\frac{y_0}{h-y_0}\right]^K \left[\sqrt{\frac{\sigma_m}{\rho}}\,\frac{1}{k}\,\text{lognat}\,\frac{y}{h} + u_m\right] dy \qquad (4.52\text{-}13)$$

where q_s is the sought-after sediment flux. This integral cannot be expressed in closed form, it can only be evaluated numerically. For this purpose, tables supplied by EINSTEIN[3] must be applied. Furthermore, the integral cannot be valid down to the bottom of the bed but must be broken off at the "laminar sublayer" since it becomes infinite.

Thus, an inspection of the above formula immediately shows up the difficulties that are inherent in the method. First of all, the integral is extremely sensitive to the lower limit of integration. Second, the concentration of sediment at the level y_0 enters as a parameter into the formulas. It is therefore impossible to calculate, say, the total amount of sediment suspended in a particular stream: one must always have at least one value that is measured.

The "diffusivity" theory of suspended sediment transportation is based essentially on the hypothesis that an exchange coefficient exists

1. The equation (4.52-11/12) appears to have been given for the first time by: ROUSE, H.: Trans. Amer. Soc. Civ. Eng. 102, 534 (1937).

2. CONOVER, W. J., and N. C. MATALAS: U.S. Geolog. Survey Profess. Papers 575-B, B60 (1967).

3. EINSTEIN, H. A.: The Bed-Load Function for Sediment Transportation in Open Channel Flows. U.S. Dept. Agric. Soil Cons. Serv. Tech. Bull. No. 1026, 71 pp. (1950).

for the solid particles which is proportional to the exchange coefficient of water in the river. This is a somewhat indirect approach to the sediment transportation problem. It might be considered as preferable if it were possible to write down the equations of motion of the particles and take directly into account the forces exerted by the turbulent river. This type of an approach has been called *gravitational theory*; it seems to have been initiated by VELIKANOV[1,2] whose original approach gave rise to much controversy[3]. A similar theory applicable to small sediment particles and small accelerations in the river has later been proposed by BARENBLATT[4]. It is also controversial[5,6].

The difficulties in these theories arise from the fact that somehow the equations of motion for the river must be averaged since the local fluctuating velocity is of very little use in applications. VELIKANOV uses a doubtful energy relationship to achieve this, BARENBLATT follows some relationships of KOLMOGOROV[7] which are somewhat more reliable, but still open to objections. VELIKANOV's theory[8] leads to an exchange equation although its deduction is quite novel. BARENBLATT ends up with a formula relating the turbulent energy in the river with the suspended sediment content.

The theories of VELIKANOV and BARENBLATT turn out to be mathematically quite involved. In view of this and in view of the fact that the various controversies have not yet been finally settled, the reader is referred to the original papers for further details.

There is no doubt that a "gravitational" type of a theory of suspended sediment transportation will ultimately provide the most satisfactory description of the suspended sediment transport phenomenon. However, the structure of the turbulence in the river must be known accurately to carry this approach to a satisfactory stage. This has not yet been achieved. Thus, the "diffusivity theory" of suspended sediment transportation is still the most useful one to date.

4.53. The Transportation of Bottom Sediment. We investigate now the mechanisms that might be responsible for transporting *bottom sediments*. A good summary of the present state of knowledge about this subject

1. VELIKANOV, M. A.: Izv. Akad. Nauk, SSSR, Otd. Tekh. Nauk **1944**, No. 3 (1944)

2. VELIKANOV, M. A.: Движение наносов. Moscow: Rechizdat (1948).

3 See e.g. the issues No. 5 (1946) and Nos. 2, 6, 8, 9, 11, 12 (1952) of Izv. Akad Nauk, SSSR, Otd. Tekh. Nauk.

4. BARENBLATT, G. I.: Prikl. Mat. Mekh. **17**, 261 (1953).

5. See VELIKANOV, M. A.: Vest. Mosk. Un-ta No. 12, 1954. — BARENBLATT, G. I : Vest. Mosk. Un-ta No. 8, 53, 1955.

6 ROMANENKO, B. E.: Trudy Akad. Morsk. Flota No. 4, 158 (1956).

7. KOLMOGOROV, A. N.: Izv. Akad. Nauk. SSSR, Ser. Fiz. 6, No. 1–2 (1942)

8. VELIKANOV, M. A.: Izv. Akad. Nauk, SSSR (Otd. Tekh. Nauk) **1951**, 1731 (1951); see particularly p. 1742.

has for instance been given by CHIEN[1]. There are essentially three theories of bottom sediment transportation which may be called the *drag theory*, the *bedload function theory* and the *Meyer-Peter theory*. We shall discuss these theories in their turn below.

A. Drag Theory. It is expectable that the scouring force discussed in Sec. 4.43 would cause movement of bottom sediment. Theories of bottom sediment transportation based upon this scouring force are called *drag theories.*

Accordingly, the forces acting upon a bottom particle are

(i) The *gravity force* as given in (4.42-1), acting vertically downward

$$W=(M_s-M_f)\,g \tag{4.53-1}$$

where M_s denotes the mass of the particle under consideration and M_f the mass of the displaced fluid.

(ii) The *scouring force* F_s from (4.43-1):

$$F_s=C_D\frac{\pi}{4}d^2\frac{1}{2}\rho(v_f-v_s)^2, \tag{4.53-2}$$

where v_f denotes the fluid velocity and v_s the velocity of the sediment particle. The scouring force acts parallel to the stream bed.

(iii) The *bottom friction force* due to the friction of the particle at the bottom, acting parallel to the stream bed. This can be represented most easily in terms of a frictional coefficient ε (cf. Sec. 4.43)

$$F_f=-\varepsilon W\cos\alpha \tag{4.53-3}$$

where α denotes the angle of the stream bed with the horizontal.

According to the drag theory, these are *all* the forces that act upon the sedimentary particles, provided forces due to the acceleration of the flowing water are neglected.

The equation of motion for the particle can be obtained in the usual fashion by equating all the forces acting in the direction of the stream bed to the product of mass and acceleration of the particle:

$$\begin{aligned}M_s\frac{dv_s}{dt}=C_D\frac{\pi}{8}d^2\rho(v_f-v_s)^2-(M_s-M_f)\,g\sin\alpha\\-(M_s-M_f)\,\varepsilon\,g\cos\alpha.\end{aligned} \tag{4.53-4}$$

For the steady-state case one postulates $dv/dt=0$, and hence one has

$$v_s-v_f=\sqrt{\frac{8\,g}{C_D\pi\,d^2\,\rho}(M_s-M_f)(\sin\alpha-\varepsilon\cos\alpha)}. \tag{4.53-5}$$

1. CHIEN, N.: Proc Amer. Soc. Civ Eng. 80, No. 565 (1954)

This is the expression for the velocity of a bottom sediment particle, provided, of course, the drag is large enough to overcome the frictional force. The above equation has been deduced by EAGLESON, DEAN and PERALTA[1] for use in an investigation of bottom sediment on a beach due to shoaling waves where it has yielded reasonable results.

The principles of the drag theory have been known for a long time. Early advocates of it were DU BOYS[2], CHANG[3], and O'BRIEN and RINDLAUB[4]. The best known of these early formulations is that of DU BOYS[2] based upon a model of sliding layers of bed material being kept in motion by the drag exerted by the fluid so that the shearing force parallel to the bed decreases with distance downward. Thus:

$$q_B = c_B \sigma(\sigma - \sigma_{cr}) \tag{4.53-6}$$

where q_B is the transport rate (in weight per unit width and time), σ is the drag force, σ_{cr} the critical drag force (cf. Sec. 4.43) and c_B is some parameter. The Du Boys formula has been generalized by O'BRIEN and RINDLAUB[4] to

$$q_B = c'_B(\sigma - \sigma_{cr})^m \tag{4.53-7}$$

where c'_B and m are two new constants. This has been done by assuming that in a state of dynamic equilibrium, the shearing force must be constant on planes parallel to the bottom.

It may be noted[5] that, in cohesive soils, one ought to introduce an additional term into the drag theory which expresses the cohesion (cf. also Sec. 4.43).

The various versions of the drag theory have not proven to be too satisfactory with regard to bottom sediment transportation in rivers. Different approaches have therefore been sought after.

B. Bed Load Function Theory. Such an approach, based upon statistical considerations, has been developed by EINSTEIN and POLYA[6]; it was later summarized and expanded by EINSTEIN[7]. Accordingly, every particle in a river bed has a finite probability to be lifted off the bed (due to turbulent velocity fluctuations) and to be carried a certain distance.

1. EAGLESON, P. S., R. G. DEAN and L. A. PERALTA: The Mechanics of the Motion of Discrete Spherical Bottom Sediment Particles Due to Shoaling Waves. – M.I.T. Hydrodyn. Lab. Tech. Rep. No. 26 (1957).

2. DU BOYS, P.: Ann. Ponts et Chauss. (5) **18**, 141 (1879).

3. CHANG, Y. L.: Trans. Amer. Soc. Civ. Eng. **104**, 1246 (1939).

4 O'BRIEN, M. P., and B. D. RINDLAUB: Trans. Amer. Geophys. Union **15**, 593 (1934).

5. SUNDBORG, A.: Geografiska Ann. **38**, 125 (1956).

6. EINSTEIN, H. A., and G. POLYA: Mitt. Versuchsanst. Wasserbau E.T.H. Zurich: Verlag Rascher 1937.

7. EINSTEIN, H A.: The Bed-Load Function for Sediment Transportation in Open Channel Flows. U.S. Dept. Agric. Soil Cons. Serv. Tech. Bull. No. 1026, 71 pp. (1950)

The rate at which particles of a given size are eroded from the stream bed is proportional to the number of such particles present and to the probability of each particle being eroded. If i_b denote the fraction of (resting) bed sediment of the size range considered (characterized by the "diameter" d), then the number of particles per unit area is $i_b/(A_1 d^2)$ where A_1 is a corrective coefficient so that $A_1 d^2$ is the exposed cross-section. If we denote by p the probability of erosion of a particle, and by t_1 the time necessary to replace a bed particle by a similar one (*exchange time*), then the number of particles eroded per unit time and area is

$$N_E = i_b\, p/(A_1 d^2 t_1). \tag{4.53-8}$$

The exchange time may be assumed to be proportional to the time necessary for a particle to fall in the fluid through a distance equal to its own diameter; thus (with w=settling velocity; cf. 4.42-10)

$$t_1 = A_3' \frac{d}{w} = A_3 \sqrt{\frac{d\rho_f}{g(\rho_s - \rho_f)}} \tag{4.53-9}$$

(where ρ_f is the density of the fluid and ρ_s that of the particle) so that the number N_E referred to above becomes

$$N_E = \frac{i_b\, p}{A_1 d^2 A_3} \sqrt{\frac{g(\rho_s - \rho_f)}{d\rho_f}}. \tag{4.53-10}$$

If there be dynamic equilibrium in the stream, then the number of particles eroded per unit time (N_E) must be equal to the number deposited (N_d). The latter number can be calculated as follows.

The rate at which particles of the given size move through the unit width of the stream is $i_B q_B$ where q_B equals the rate at which the bed moves per unit width and i_B is the fraction of particles of the given size in the *moving* bed. All the particles of the given size (diameter d) perform "jumps" of length $A_L d$. When these particles pass through a particular cross-section of the stream, it is not known where in its "jump" each of the particles is. It must be assumed, therefore, that a particular particle may be deposited anywhere in an area of length $A_L d$ and unit width downstream from the cross-section under consideration. If q_B is measured in dry weight per unit time and width, and if $A_2 d^3$ is the volume of each particle, then

$$N_d = \frac{q_B\, i_B}{A_L d A_2 d^3 \rho_s g}. \tag{4.53-11}$$

Equating N_E to N_d yields the *bed load equation:*

$$\frac{i_B q_B}{\rho_s A_2 A_L g d^4} = \frac{i_b\, p}{A_3 A_1 d^2} \sqrt{\frac{g(\rho_s - \rho_f)}{d\rho_f}}. \tag{4.53-12}$$

There must obviously be a connection between the distances travelled by the particles ($A_L\, d$) and the probability of erosion p. As long as p is small, A_L is a general constant λ, roughly equal to 100. If p is large, however, then deposition cannot occur on that part of the bed (p) where the lifting force exceeds the particle weight. Thus, only $(1-p)$ particles (of the unit available) are deposited after travelling a distance λd, p particles are not deposited. Of these $(1-p)$ are deposited after travelling $2\lambda d$ so that p^2 are not yet deposited, etc. Hence

$$A_L\, d = \sum_{n=0}^{\infty} (1-p)\, p^n (n+1)\, \lambda\, d = \frac{\lambda\, d}{1-p}. \tag{4.53-13}$$

Thus, the bed load equation may be written as follows:

$$\frac{p}{1-p} = A_*\, \Phi_* \tag{4.53-14}$$

with

$$A_* = A_1\, A_3/(\lambda\, A_2) \tag{4.53-15}$$

and

$$\Phi_* = \frac{i_B}{i_b}\left\{\frac{q_B}{\rho_s\, g}\sqrt{\frac{\rho_f}{\rho_s-\rho_f}}\sqrt{\frac{1}{g\, d^3}}\right\} \equiv \frac{i_B}{i_b}\,\Phi. \tag{4.53-16}$$

Thus, the bed load equation relates the bed velocity (this is essentially what Φ or Φ^* is) to the probability of erosion p.

It remains to express the probability of erosion p in terms of the river flow velocity in order to obtain a direct relationship between flow and bed load transportation. This can be done by taking the dynamic lift L of the water into consideration which acts upon each particle. The probability p, then, is equal to the probability that this lift is greater than the underwater weight W' of the particle. This underwater weight is, as usual:

$$W' = g(\rho_s-\rho_f)\, A_2\, d^3 \tag{4.53-17}$$

whilst for the lift L we can write, in conformity with the general principles of turbulent action

$$L = c_L\, \rho_f\, \tfrac{1}{2}\, u^2\, A_1\, d^2. \tag{4.53-18}$$

The factor c_L has been found from experiments to be equal to 0.178, and the velocity u occurring in (4.53-18) must be taken as that velocity which obtains at a level 0.35 X from the "theoretical" bed surface, where

$$\begin{aligned} X &= 0.77\,\Delta \quad \text{if } \Delta/\delta > 1.80 \\ X &= 1.39\,\delta \quad \text{if } \Delta/\delta < 1.80. \end{aligned} \tag{4.53-19}$$

For the meaning of the Greek symbols in the above equations, the reader is referred to Sec. 4.23.

Eq. (4.53-18) represents the average lift. The instantaneous lift is subject to random fluctuations which can be expressed as follows:

$$L_{\text{inst.}} = L_{\text{aver.}}(1+\eta) \tag{4.53-20}$$

where η is some random function. The last equation can be further evaluated by introducing the value for u from the various theories presented earlier, in terms of the (energy) slope S and the hydraulic radius R.

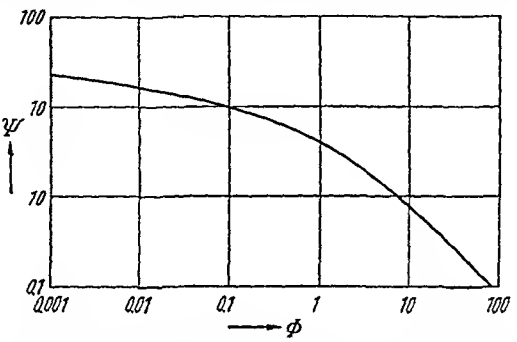

Fig. 106. EINSTEIN's[1] relationship between Ψ and Φ (note Ψ is essentially $1/v^2$ with v mean river velocity; Φ is bed load velocity)

EINSTEIN assumes that η follows a Gaussian distribution where the standard deviation η_0 is a universal constant. Then the probability p is equal to the probability of W'/L to be smaller than unity. What one ends up with, thus, is a relationship between

$$\Psi = \frac{\rho_s - \rho_f}{\rho_f} \frac{d}{RS} \tag{4.53-21}$$

(note that Ψ is essentially $1/v^2$ with v equal to the mean river velocity) and Φ_* (or Φ) in which some constants enter. It is

$$1 - \frac{1}{\sqrt{\pi}} \int_{-B_*\Psi - 1/\eta_0}^{B_*\Psi - 1/\eta_0} e^{-t^2}\, dt = \frac{A_* \Phi}{1 + A_* \Phi}. \tag{4.53-22}$$

This relationship, in essence, represents a relationship between bedload movement and flow intensity. EINSTEIN's plot of it is shown in Fig. 106. The constants are[2]

$$\begin{aligned} A_* &= 43.5 \\ B_* &= 1/7 \\ \eta_0 &= 1/2. \end{aligned} \tag{4.53-23}$$

1. EINSTEIN, H. A.: The Bed-Load Function for Sediment Transportation in Open Channel Flows. U.S. Dept. Agric. Soil Cons. Serv. Tech. Bull. No. 1026, 71 pp. (1950).

2. The equation (4.53-22) and the values for the constants are given here as corrected by CHIEN, N.: Proc. Amer. Assoc. Civil. Eng. 80, No. 565 (1954).

When using EINSTEIN's plot, it should be noted that there are various parameters in it. First of all there is R, the hydraulic radius of the river. Second, EINSTEIN gives various correction factors to account for the effect of the sandbars, the effect of small particles hiding behind large ones, etc., which may be incorporated in Φ, Ψ. Third, the universal constants A_1, A_2, η_0 are not very well defined. Thus, although it is in principle possible to calculate the bed load transport of a river from its characteristics, it is in practice very difficult to arrive at the correct numerical values.

C. Meyer-Peter Formula. The third theory of bed load transportation which has attained a considerable amount of popularity is that developed by MEYER-PETER and coworkers[1, 2]. It is a semiempirical theory which is based upon transport experiments. Using FROUDE's law of similarity as a guide, it may be expected that the quantity Q

$$Q = q_s^{\frac{2}{3}} S/d \tag{4.53-24}$$

should be independent of the scale used. Here, S is the slope, d is the diameter of the particles and q_s is the specific discharge quantity (mass of water flowing per unit width of bed and per unit time). MEYER-PETER and coworkers plotted the quantity Q against G

$$G = g_s^{\frac{2}{3}}/d \tag{4.53-25}$$

where g_s is the dry mass of the bedload transported per unit width of bed and per second. The resulting points from various sources fell all near a straight line given by

$$S\, q_s^{\frac{2}{3}}/d = a + b\, g_s^{\frac{2}{3}}/d. \tag{4.53-26}$$

The situation is demonstrated in Fig. 107 (after MEYER-PETER and MÜLLER[2]). In the m-k-s system, the values of the constants are

$$\begin{aligned} a &= 17\ \mathrm{kg^{\frac{2}{3}}\, m^{-\frac{5}{3}}\, sec^{-\frac{2}{3}}} \\ b &= 0.4. \end{aligned} \tag{4.53-27}$$

MEYER-PETER and coworkers[2] have generalized the above equation from further empirical tests to include the effect of sediment density and also to account for channel roughness. The formula then reads

$$\rho_f R \left(\frac{k_s}{k_r}\right)^{\frac{3}{2}} S = A(\rho_s - \rho_f)\, d + B \left(\frac{\rho_f}{g}\right)^{\frac{1}{3}} \left(\frac{\rho_s - \rho_f}{\rho_s} g_s\right)^{\frac{2}{3}}. \tag{4.53-28}$$

1. MEYER-PETER, E., H. FAVRE and H. EINSTEIN: Schweiz. Bauztg. **103**, No. 13, 147 (1934).

2. MEYER-PETER, E., and R. MÜLLER: Trans. 2nd Meeting, Int. Assoc. Hydraul. Struct. Res., Stockholm, Appendix **2**, 1 (1948).

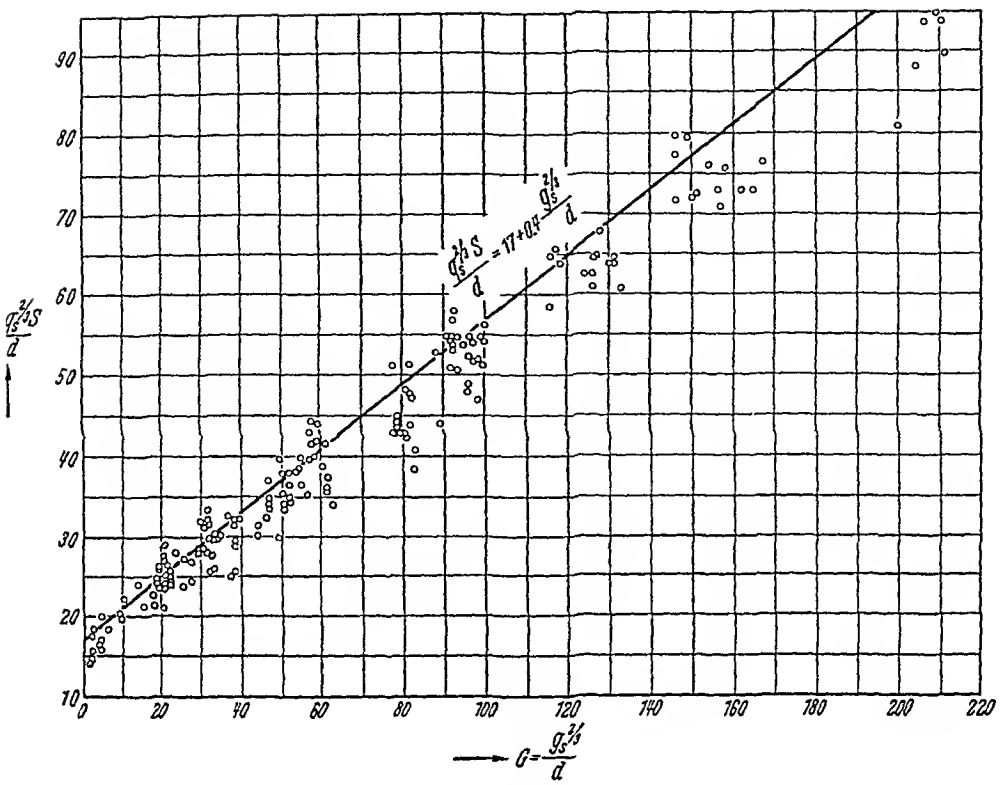

Fig. 107. The Meyer-Peter line in comparison with a series of experimental results. After MEYER-PETER and MÜLLER[1]

Here, all the symbols have the previously defined meaning; in addition R is the hydraulic radius of the channel, ρ_s, ρ_f are the densities of sediments and fluid, respectively, and g is the gravity acceleration. A and B are constants, and the ratio k_s/k_r is indicative of the roughness of the channel (the ratio decreases with increasing roughness). The modified Meyer-Peter formula (4.53-28) is dimensionally homogeneous so that A and B are dimensionless constants. Their values are[1]

$$A = 0.047$$
$$B = 0.25. \tag{4.53-29}$$

It has been shown by CHIEN[2] that the empirical (modified) Meyer-Peter formula, in fact, gives results which are in excellent agreement with the Einstein bed load theory. A comparison of the results is shown in

1. MEYER-PETER, E, and R. MÜLLER: Trans. 2nd Meet., Int. Assoc. Hydraul. Struct. Res. Stockholm, Appendix 2, 1 (1948).

2. CHIEN, N.: Proc. Amer. Soc. Civ. Eng. 80, No. 565 (1954).

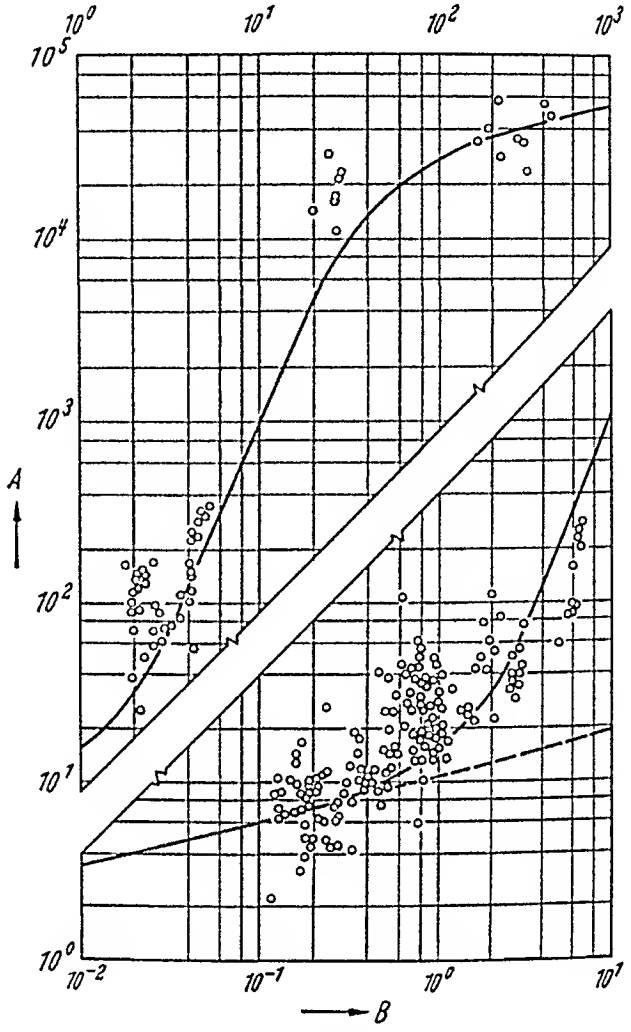

Fig. 109. Correlation between sediment transportation (dotted line: bottom load; solid line: total load) and river characteristics. (The measured points are indicated by dots.) After LAURSEN[1]

where q_s is the volume rate of sediment transport, and q is the volume rate of flow. Furthermore, d is the particle diameter, h is the depth of the river, σ_c is the critical drag (cf. Eq. 4.43-5), σ_m is the boundary shear (cf. Eq. 4.22-8), ρ is the density of the water, w is the settling velocity of the particles (cf. Sec. 4.42), and

$$\sigma'_o = \frac{v^2 d^{\frac{1}{3}}}{30 h^{\frac{1}{3}}} \tag{4.54-4}$$

where v is the mean flow velocity of the river. In terms of A and B, LAURSEN obtained a universal curve which is shown in Fig. 109. In this Figure, the dashed line represents the bed load, the solid line the total load. The relationship, according to LAURSEN, is valid for each size fraction of

1. LAURSEN, E. M.: J. Hydr. Div. Amer. Soc. Civ. Eng. **84**, Pap. 1530 (1958).

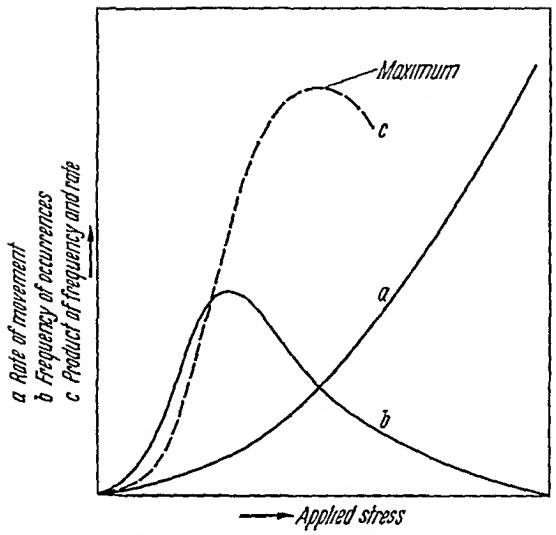

Fig 110. Relation between transport rate, frequency of occurrence, and effectiveness of an erosional process. After WOLMAN and MILLER[1]

the bed; in order to obtain the total sediment load composition, an appropriate summation over each fraction has to be performed.

Based upon the above empirical relationship, LAURSEN was able to predict, at least within an order of magnitude, the composition and the amount of sediment load in various creeks in the United States.

Another semi-empirical attempt at finding the total load in a river is by establishing a relationship between total load and the apparent bed load; the latter being more easily measurable. Flume experiments to achieve this have been reported by STEIN[2].

At this juncture, it might be attempted to deduce theoretically the cumulative erosion taking place in a drainage basin over a long period of time. The discussion by LAURSEN gives only the total load as a function of discharge; however, the discharge changes with time. It is thus necessary to obtain a frequency curve for discharge values that may be observed in a drainage basin, as it is apparent that the frequency of occurrence of an erosive process is just as important as its magnitude. This has been pointed out, for instance, by WOLMAN and MILLER[1]. The situation is illustrated in Fig. 110. The total of the erosive processes in an area can be determined if one combines the frequency distribution of each discharge rate with the corresponding carrying capacity. No tests, however, seem ever to have been made to investigate whether the total denudation rates listed in Sec. 1.43 are reasonable in terms of the observed discharge rates of the streams in the corresponding areas.

1 WOLMAN, M. G., and J. P. MILLER: J Geol. 68, 54 (1960)
2. STEIN, R. A.: J. Geophys. Res. 70, 1831 (1965)

The above considerations completely neglect the material which is transported in *solution* in a river. Since this may amount to more than half of the total (cf. Sec. 1.43), any attempts to correlate the rates quoted in this Section (4.54) with the actually observed denudation rates of an area, are necessarily somewhat shaky.

4.6. Mutual Interaction of Bed, Flow, and Sediment Transport

4.61. General Remarks. Thus far in the present Chapter, we have discussed how the shape of the river bed affects the flow velocity, and how the flow velocity affects the sediment discharge. However, in reality all these effects react mutually with each other and it is not really permissible to treat them in the sequence indicated above.

Therefore, we shall discuss in the present Section (4.6) how the turbulent river acts upon the bed (where it causes bottom ripples) and then how the bed acts upon the sediment transportation pattern. It will turn out, in essence, that every one of these phenomena depends on all others and that there are various possibilities for the establishment of stationary states. The difficulties encountered in defining these states forces one to introduce the semi-empirical concept of a "graded river", which designates a river which is in dynamic equilibrium, i.e. which does neither silt up nor scour. The conditions for a river to be graded will be given.

Subsequently, we shall present the theories that have been advanced for an explanation of the observed river profiles, both longitudinal and transverse. Finally, we shall give a review of the scaling laws that have been proposed for making model experiments of river bed processes.

4.62. Bottom Ripples. The first question which we shall analyze in connection with the interaction between the river bed and the flowing water, is the origin of the ripples and bars which are commonly found at the bottom of a river bed.

The formation of these ripples has been considered by LIU[1] to be the expression of instability between superimposed stratified flows. LIU's argument is mainly qualitative and is based upon the fact that, even in turbulent flow, there is a laminar boundary layer or sublayer very close to the boundary. He then treats the river bed as an extreme case of a *density current:* the movable layer containing the bed load of the river is treated as one dense fluid of (almost) infinite viscosity, the laminar sublayer of clear water attached thereto as another. One has thus, in essence, two fluids – the layer containing the bed load and the laminar boundary layer – which are both in laminar motion but with a different velocity. According to investigations reported in Sec. 2.26, this causes an instability at the interface which could create the ripples.

1. LIU, H. K.: Proc. Amer. Soc. Civ. Eng. 83, Pap. No. 1197 (1957).

LIU was not able to substantiate his claims by an actual calculation of the size of the ripples as a function of the size of the bed-particles and the flow velocity. His explanation of the bottom ripples in rivers must therefore be regarded as a conjecture.

A similar approach, treating the formation of sediment ripples as an instability phenomenon, has been reported by KENNEDY[1]. This analysis led KENNEDY to the hypothesis that ripples result from a perturbation of the bed load movement, whereas the larger dunes result from a perturbation in the movement of the suspended sediment load.

Another theory of ripple formation has been proposed by ANDERSON[2] who assumed a resonance effect between the river bed with waves on the surface of the water. The surface waves were assumed as corresponding to those found by the *laminar* flow theory. ANDERSON's theory is therefore similar to the theory of particle movement on beaches to be discussed in Sec. 6.43. A similar attempt was made by KONDRAT'EV[3]. However, the application of laminar flow theory to sediment ripple formation in a river is questionable, since it stands to reason that the ripples are intimately connected with the turbulence of the water.

Another approach to the problem of sediment ripple formation has been taken by VELIKANOV[4]. The latter author assumes that there is a connection between the bottom ripples and the large-scale turbulence in a river. Commonly, the statistical theory of homogeneous turbulence is applied to the turbulence which is present in a river only in the high-frequency end of the spectrum. The low-frequency part is not homogenous and it stands to reason that the velocity fluctuations will come into resonance with the walls. Unfortunately, the statistical theory of turbulence has not been develped to such an extent where the question as to the *form* of turbulence could be posed. However, it has been shown by VELIKANOV and MIKHAILOV[5] by direct measurements that the periods of the fluctuation of the turbidities are very close to the periods of the large-scale velocity fluctuations and these in turn to the periods of the sand ripples just when the latter begin to be formed.

A completely different approach to the problem of ripple formation has been taken by LANGBEIN and LEOPOLD[6] who noted that during the downstream movement of sediment, individual particles will tend to

1. KENNEDY, J. F : J Geophys Res. **69**, 1517 (1964).

2. ANDERSON, A. G.: Proc. Third Midwest. Conf. Fluid Mechanics, Univ. Minnesota, p. 379 (1953).

3. KONDRAT'EV, N. E : Trudy Gos. Gidrol. In-ta No. 116, 3 (1964)

4. See e.g. VELIKANOV, M. A.· Izv. Akad. Nauk, SSSR, Ser Geofiz **1957**, No. 1, 71 (1957).

5. VELIKANOV, M. A., and N. A. MIKHAILOV: Izv. Akad. Nauk, SSSR, Ser. Geogr Geofiz. **1950**, No. 5 (1950).

6. LANGBEIN, W. B., and L. B. LEOPOLD: U.S. Geolog Survey Profess Papers **422 L**, L 1 (1968).

impede each other's progress. Thus, once several particles have accidentally come together, they impede the progress of others and thus create a phenomenon analogous to a "traffic jam". These are the dunes and bars. In a similar vein, NORDIN and ALGERT[1] have shown that the process of ripple formation can be represented by a Markov second-order linear model[1].

Finally, as always when it is difficult to arrive at unequivocal theoretical relationships for a phenomenon, people have turned to its empirical investigation. Thus, a number of empirical correlations for the onset and characteristics of ripple and dune formation have been proposed. Most of these correlations refer to flume experiments[2-7], but some are deduced from actual measurement in rivers[8].

4.63. Cross-Bedding. The ripples and dunes mentioned in the last section give rise to the phenomenon of cross-bedding in sandstones: the total height H of a layer of cross-bedded sediments corresponds to the height of the sandwaves in a stream. In cross-bedded sediments, relationships between mean grain size diameter d and the height H of cross-bedded sediments is of the following type[9] (β is a constant):

$$d = \text{const } H^{\beta}. \tag{4.63-1}$$

This relationship appears to be quite universal[9]. It can be explained theoretically by assuming the following model[9]: Due to the presence of the ripples, the turbulence in the stream is affected; the latter, in turn, is directly related to the carrying capacity (with regard to the grain sizes involved) of the stream. This chain of interactions leads to a relation between H and d.

Thus, from Eq. (4.23-15) we have, taking the height of the surface roughnesses k_s equal to the sand-wave height H:

$$v = K_1 \log\left(\frac{R}{H}\right) + K_2 \tag{4.63-2}$$

1. NORDIN, C. F., and J. H. ALGERT: J. Hydr. Div., Proc. Amer. Soc. Civ. Eng. HY 5, 95 (1966).
2. BAREKYAN, A. S.: Met. i. Gidrol. No. 8, 33 (1962).
3. ZNAMENSKAYA, N. S.: Trudy Gos. Gidrol. In-ta No. 108, 89 (1963).
4. HILL, H. M.: J. Hydr. Div. Proc. Amer. Soc. Civ. Eng. 92, HY 2, 127 (1966).
5. VANONI, V. A., and L.-S. HWANG: J. Hydr. Div. Amer. Soc. Civ. Eng. 93, HY 3, 121 (1967).
6. HARMS, J. C.: Bull. Geolog. Soc. Amer. 80, 363 (1969).
7. SIMONS, D. B., and E. V. RICHARDSON: Proc. Federal Interagency Sedimentation Conf., U.S. Agric. Res. Serv. p. 193 (1963).
8. SNISHCHENKO, B. F.: Trudy Gos. Gidrol. In-ta No. 136, 82 (1966).
9. SCHEIDEGGER, A. E., and P. E. POTTER: Sedimentology 8, 39 (1967).

where v is the mean flow velocity, R the hydraulic radius of the river and K_1, K_2 are constants. Henceforth R will be assumed as equal to 1 (i.e. the river "depth" is approximately taken as unit length), so that H represents the "relative" roughness; it is a number $H \ll 1$.

An obstacle of height H creates turbulent velocity fluctuations u' of magnitude (cf. Eq. 2.24-7; neglecting β)

$$\text{const}\, u'^2/v^2 = H. \tag{4.63-3}$$

Furthermore, the carrying capacity of a river must be constant over the whole rippled bed; an inspection of (4.52-6) shows that for this to be the case, the ratio of the settling velocity w to the turbulent diffusion φ must be constant. However, from Eq. (4.42-2) we have

$$w \sim d^2 \tag{4.63-4}$$

where d is the grain diameter, and from Eq. (4.44-1) we have

$$\varphi \sim u'^2. \tag{4.63-5}$$

Therefore, we have a constant carrying capacity if

$$d \sim u'^2. \tag{4.63-6}$$

Thus, taking (4.63-2), (4.63-3) and (4.63-6) together, we obtain

$$d \sim H(\log H)^2 + \text{small terms} \sim H^\beta \tag{4.63-7}$$

where the last proportionality results if the upper bound is taken instead of the logarithm of H. Thus, the empirical relation (4.63-1) has been explained.

4.64. Concept of Graded River. From the above discussion of the mutual interaction between a river bed, the total flow and the sediment transported therein, it becomes obvious that the problem of finding the correct relationship between these phenomena is a very difficult one. People have therefore tried to at least establish the conditions for channel-equilibrium empirically.

Thus, the notion has been introduced of a river being "at grade". By this term one understands a condition of dynamic equilibrium in river flow in which just as much material is being deposited in the river bed as is being eroded (in the average over several seasons). In engineering use, this condition is often referred to by saying that the river is "in régime" rather than "at grade". The concept itself goes back to GILBERT[1] and DAVIS who worked before the turn of the century[2].

1 GILBERT, G. K.: Report on the Geology of the Henry Mountains, Washington (1877).

2. See for instance: MACKIN, J. H.: Bull Geol Soc. Amer. 59, 463 (1948).

Whether a river is at grade or not, depends on a variety of variables. Its depth h, its width b, the discharge Q and the material of which the channel is composed, are of prime importance. Many experiments have been performed, notably by hydraulic engineers, to determine when a channel is at grade (in régime). Also, innumerable data have been collected from actual canals in order to determine what the values of the external variables are that determine whether a channel is at grade. A summary of the "régime theory" of channel flow as used by engineers has been given in monographs by BLENCH[1,2]. Assuming that the kind of material that is being transported and the total discharge are given by nature, then there remain three self-adjusting variables which are the depth h, the gradient S and the width b of the channel. In order to determine the values of these variables in a particular case, one needs obviously three independent relationships between them.

These empirical relationships form the body of what engineers call "régime theory" of channel formation. It was probably first developed by LACEY[3] and as noted, has been summarized by BLENCH[1,2]. Accordingly, from innumerable factual data, the first equation of régime theory turns out to be

$$v^2/h = B \tag{4.64-1}$$

where v is the mean velocity of the flow, h is the depth of the water and B is a bed factor related to the type of bed load carried by the river.

The second equation of régime theory is

$$v^3/b = s \tag{4.64-2}$$

where b is that width which multiplied by h yields the cross-sectional area of the flow. The quantity s is a side-factor depending on the interaction of the river with the material of which the sides consist.

The third equation of régime theory is

$$\frac{v^2}{ghS} = c\left(\frac{vb}{\nu}\right)^{\frac{1}{4}} \tag{4.64-3}$$

where S is, as usual, the slope, ν is the kinematic viscosity and c is a dimensionless constant.

The above three equations are the conditions required by the régime theory for a channel to be at grade. One can manipulate these equations algebraically to obtain "design equations", giving the width, depth and slope that are required to produce a channel which is to be at grade, in

1. BLENCH, T.: Regime Behaviour of Canals and Rivers. London: Butterworth's Scientific Publications 1957.

2. BLENCH, T.: Mobile-Bed Fluviology. 2nd Ed. Edmonton: Alberta Univ. Press 1969.

3. LACEY, G.: Minutes of Proceedings, Inst. Civ. Eng. London 237, 421 (1933/34).

terms of the total discharge Q and the constants c, s, B. The values of these constants pose some problem. From the wealth of data pertaining to canals in the alluvial plains of India, BLENCH concluded that, in British engineering units, the value of $cg/\nu^{\frac{1}{4}}$ averages 2080 when ν equals 10^{-5} (water in British engineering units). The lowest value of B found in Indian canals is about 0.6, the highest 1.25 with $B=1.00$ representing a good average. Finally, the value for s turns out to be equal to 0.3 for glacial till, 0.2 for silty clay-loam material, and 0.1 for material with little cohesion.

It may be remarked that the first equation of régime theory (i.e. Eq. 4.64-1) is equivalent to the statement that stable flow is only possible if the Froude number

$$F_r=\frac{v}{\sqrt{gR}} \tag{4.64-4}$$

(where R is the hydraulic radius of the river, equal to h for wide rivers) is less than a certain critical value. This is a condition of the régime theory which has often been used by geologists. It is then generally said that for Froude numbers below a certain critical value (in the neighborhood of *l*), one has turbulent flow in which stable conditions are possible; for Froude numbers above the critical value, one has turbulent flow in which stable conditions are no longer possible. Bottom slopes that produce flow at a subcritical Froude number are then termed *mild*, otherwise they are termed *steep*.

The régime theory, as is evident from the discussion above, only establishes conditions for the existence of equilibrium. It does not, however, specify how this equilibrium is being attained if one starts with non-equilibrium conditions.

4.65. Longitudinal Profile of a River. One may now ask himself what the general form of the river bed slope would be from source to mouth or, at least, from the beginning to the end of a given limited reach. Since the river bed is very much like an erosional "slope", it may be permissible to postulate a similar law for the slope angle as was done in Sec. 3.45. Thus, using the general principles employed in Sec. 3.45, one again ends up with a slope equation of diffusivity-type identical to that given as formula (3.45-12). Unfortunately, this equation cannot be easily handled since its solution contains an error function complement. However, we have already mentioned in Sec. 3.45 that its main significance is that it predicts that the (accumulative part of the) slope decreases with increasing distance. In analogy with the procedure of Sec. 3.45, one might therefore again postulate an exponential law which may be written as follows:

$$S=S_0\exp(-aL). \tag{4.65-1}$$

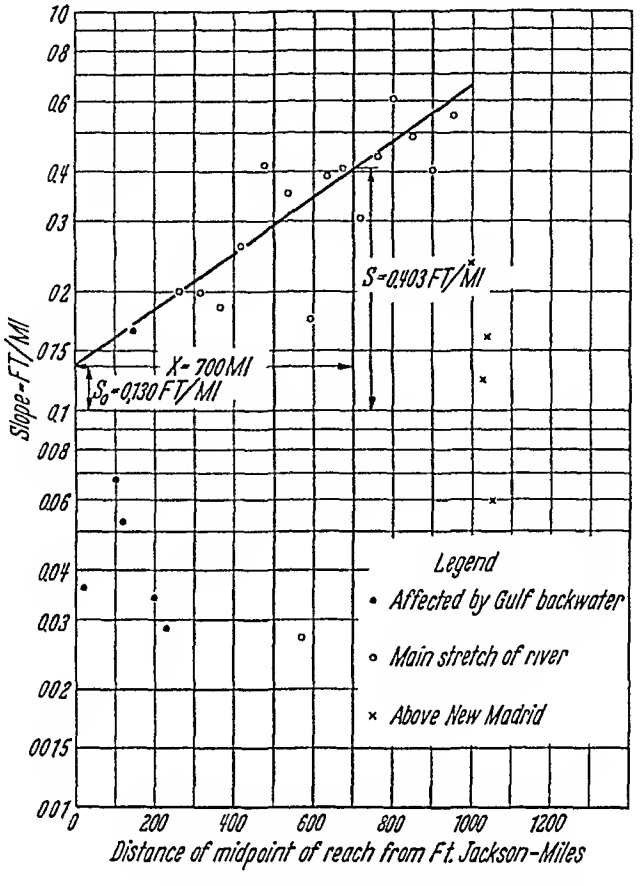

Fig. 111. Variation of slope along Mississippi River. After SHULITS[1]

Here, S is the slope, L the distance from the source (or from the beginning of the river reach under consideration) and a is a constant. A test of the above equation was made by SHULITS[1] using data from the Mississippi River between Cairo, Illinois and Fort Jackson, Louisiana and reasonable agreement was obtained, at least in the main stretch of the river below New Madrid and above the reach affected by Gulf backwater (see Fig. 111).

The principles indicated above can be further refined. Thus, DEVDARIANI[2] used some additional boundary conditions and ended up with a series of possible river profiles. Similarly, SAITO[3] started basically with a diffusivity equation and calculated river bed profiles upon its basis.

The fact that a diffusivity equation seems to be the correct basis for calculating river bed profiles can also be explained by referring to general systems theory: The adjustment of systems affected by random influ-

1. SHULITS, S.: Trans. Amer. Geophys. Union **22**, 622 (1941).
2. DEVDARIANI, A. S.: Voprosy Geografii No. 63, 33 (1963).
3. SAITO, Y.: J. Geosciences, Osaka City Univ. **7**, 145 (1963).

ences and subject to external constraints generally leads to equations of this type. The theory in question is of utmost importance with regard to the evolution of drainage basins and will therefore be developed in the latter context. The reader is referred to Sec. 5.83 of this book for further details of the application of the general theory to river profiles.

Peculiar phenomena occur if there are abrupt changes ("knick-points") in the bed-slope of a river. In this case, the flow is nonuniform (cf. Sec. 4.25). The conditions obtaining in such cases can be discussed in terms of the régime theory. Above a knick-point, the river slopes are "mild" (in the sense of Sec. 4.64), below it, "steep". Hence, no equilibrium

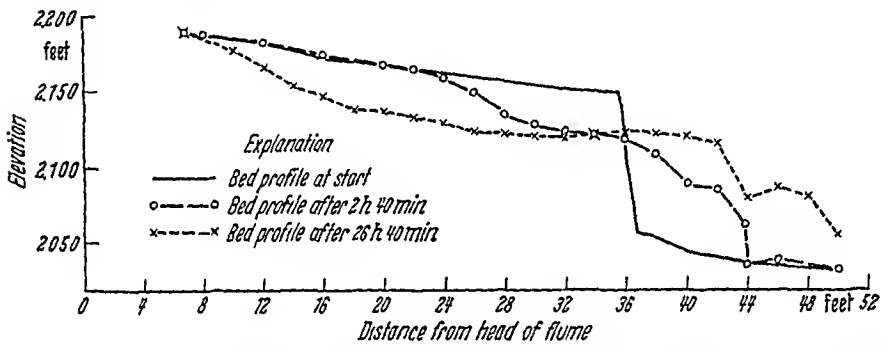

Fig. 112. Recession and disappearance of a knick-point in an experiment representing a river bed After BRUSH and WOLMAN[1]

is possible below the knick-point and the latter must wander upstream. Experiments to demonstrate this have been reported by BRUSH and WOLMAN[1]. A typical result obtained by these authors is shown in Fig. 112. In every experiment, the knick-point wandered upstream and eventually disappeared.

4.66. Transverse Profile of a River. We now come to a discussion of the development of the transverse profile in a stable river. This question is tied up with the cross-circulation across the river bed.

The problem of the development of the transverse profile in a stable river has been analyzed some 40 years ago by KOECHLIN[2], and somewhat more recently in investigations by IBAD-ZADE[3], POKHSRARYAN[4] and BRETTING[5]. In these investigations, a force-balance equation was

1. BRUSH, L. M., and M. G. WOLMAN: Bull. Geol. Soc. Amer. **71**, 59 (1960)
2. KOECHLIN, R.: Mécanisme de l'eau et principes généraux pour l'établissement d'usines hydroélectriques. Paris 1924.
3. IBAD-ZADE, YU. A.: Gidrotekh. Stroitel. **1952**, No. 12 (1952).
4. POKHSRARYAN, M. S.: Izv. Akad. Nauk Armyan SSR, Ser Tekh Nauk **10**, No. 6, 85 (1957); **11**, No. 6, 31 (1958).
5. BRETTING, A E.. Acta Polyt. Scand. Ci 1 (245/1958) (1958).

written down for a bottom particle being at rest. This yields a relationship between the bottom slope (in profile) and the local bottom velocity. In order to arrive at a differential equation of the profile, it is evident that a further relationship is needed. This additional relationship is provided by some more or less justified assumptions regarding the distribution of either the shearing stress or the bottom velocity with height.

We shall present here the exposition of POKHSRARYAN in some detail.

POKHSRARYAN bases his connection between slope angle and velocity upon the drag theory (cf. Sec. 4.22), but in doing this he allows for the

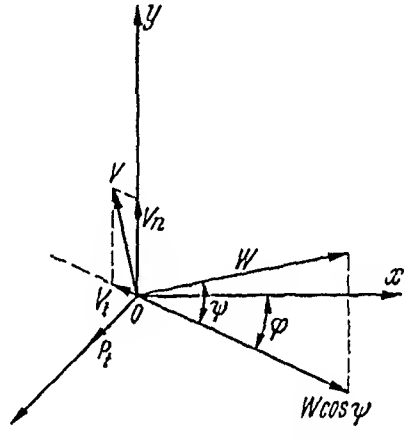

Fig. 113. Geometry of forces at the bottom of a river. After POKHSRARYAN[1]

possibility that the bottom velocity, although parallel to the bottom, may have a component in the transverse cross section because of the possibility of existence of an overall circulation. Furthermore, POKHSRARYAN assumes that the drag force vector is not necessarily parallel to the velocity vector, although the general quadratic form of the relationship (cf. Eq. 4.22-8) is retained.

Thus, taking the general geometry indicated in Fig. 113 where the flow velocity is parallel to the vector W, we have the following forces:

(a) the "frontal drag force" which we shall denote here by W

$$W = c_f \rho \frac{\pi d^2}{4} v_{bot}^2, \tag{4.66-1}$$

where c_f is the "frontal drag coefficient", ρ the fluid density, and d the particle diameter;

1. POKHSRARYAN, M. S.: Izv. Akad. Nauk Armyan. SSR, Ser. Tekh. Nauk **10**, No. 6, 85 (1957); **11**, No. 6, 31 (1958).

(b) the "transverse drag force" V (cf. Fig. 113) which is perpendicular to the flow velocity and perpendicular to the profile-cross-section

$$V = c_t \rho \frac{\pi d^2}{4} v_{bot}^2 \tag{4.66-2}$$

where c_t is a "transverse drag coefficient";

(c) the underwater weight P of a particle

$$P = g(\delta - \rho)\frac{\pi d^3}{6} \tag{4.66-3}$$

where δ is the density of the particle and g the gravity acceleration;

(d) and finally the frictional force (cf. Eq. 4.43-2)

$$F = \varepsilon(P_n - V\cos\psi) \tag{4.66-4}$$

where P_n is the component of P normal to the bed

$$P_n = P\cos\alpha \tag{4.66-5}$$

(α being the bed slope angle, cf. Fig. 114) and ψ is an angle as shown in Fig. 113. Furthermore, ε is a coefficient of friction.

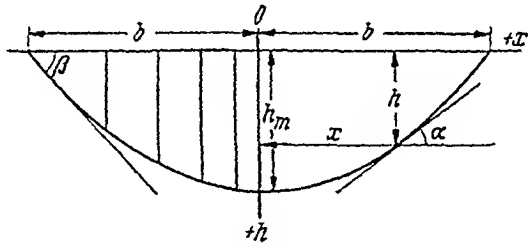

Fig. 114. Geometry of the bottom-profile of a river. After POKHSRARYAN[1]

One can now express the condition of force balance for a particle on the surface of the bed which must obviously be satisfied in a stable channel. This yields

$$[(W\cos\psi - V\sin\psi)\cos\varphi]^2 + [(W\cos\psi - V\sin\psi)\sin\varphi + P_t]^2 = F^2 \tag{4.66-6}$$

where P_t is the tangential component of the underwater weight:

$$P_t = P\sin\alpha. \tag{4.66-7}$$

1 POKHSRARYAN, M. S.: Izv. Akad. Nauk Armyan. SSR, Ser. Tekh. Nauk. 10, No. 6, 85 (1957); 11, No. 6, 31 (1958).

Introducing the individual expressions for the various forces and solving for v_{bot} yields

$$v_{bot}=\sqrt{\frac{2g}{3c_f}\left(\frac{\delta}{\rho}-1\right)\{-A\pm\sqrt{A^2-B}\}} \tag{4.66-8}$$

with

$$A=\frac{\left[\cos\psi-\frac{c_t}{c_f}\sin\psi\right]\sin\varphi\sin\alpha+\frac{c_t}{c_f}\varepsilon^2\cos\psi\cos\alpha}{\left(\cos\psi-\frac{c_t}{c_f}\sin\psi\right)^2-\varepsilon^2\left(\frac{c_t}{c_f}\right)^2\cos^2\psi} \tag{4.66-9}$$

$$B=\frac{\left[\left(\cos\psi-\frac{c_t}{c_f}\sin\psi\right)^2-\varepsilon^2\left(\frac{c_t}{c_f}\right)^2\cos^2\psi\right][\sin^2\alpha-\varepsilon^2\cos^2\alpha]}{\left(\cos\psi-\frac{c_t}{c_f}\sin\psi\right)^2-\varepsilon^2\left(\frac{c_t}{c_f}\right)^2\cos^2\psi}. \tag{4.66-10}$$

In the special case when there is no circulation, the above formula can be simplified. Setting

$$m_0\equiv\cot\beta=\frac{1}{\varepsilon} \tag{4.66-11}$$

where β is the angle of repose (cf. Fig. 114) in still water, formula (4.66-8) reads:

$$v_{bot}=\sqrt{\frac{2g}{3c_f}d\left(\frac{\delta}{\rho}-1\right)}\cdot\sqrt{\frac{-\frac{c_t}{c_f m_0^2}\cos\alpha\pm\sqrt{\left(\frac{c_t}{c_f m_0^2}\cos\alpha\right)^2-\left(1-\frac{c_t^2}{c_f^2 m_0^2}\right)\left(\sin^2\alpha-\frac{1}{m_0^2}\cos^2\alpha\right)}}{1-\frac{c_t^2}{c_f^2 m_0^2}}}. \tag{4.66-12}$$

If we take the average non-scouring velocity $\bar{v}$ at position x in the river instead of the bottom velocity v_{bot}, a correction factor must be inserted; using Eq. (4.63-1), (4.23-2) and (4.22-12), POKHSRARYAN writes this factor as follows

$$\bar{v}=v_{bot}\left(\frac{h}{d}\right)^{\frac{1}{6}}. \tag{4.66-13}$$

We now write formula (4.66-12) using (4.66-13) for the center line of the flow, where $\alpha=0$, and obtain ($\bar{v}_m$ at center line)

$$\bar{v}_m=\sqrt{\frac{2g}{c_f}d\left(\frac{\delta}{\rho}-1\right)}\left(\frac{h_m}{d}\right)^{\frac{1}{6}}\left[\left(1+\frac{c_t}{c_f m_0}\right)m_0\right]^{-\frac{1}{2}}. \tag{4.66-14}$$

Hence:

$$\bar{v}=\bar{v}_m\left(\frac{h}{h_m}\right)^{\frac{1}{6}}\frac{1}{\sqrt{1-\frac{c_t}{c_f m_0}}}$$

$$\cdot\sqrt{-\frac{c_t}{c_f m_0}\cos\alpha\pm\sqrt{\left(\frac{c_t}{c_f m_0}\cos\alpha\right)^2-\left(1-\frac{c_t^2}{c_f^2 m_0^2}\right)(m_0^2\sin^2\alpha-\cos^2\alpha)}}\,. \tag{4.66-15}$$

Using now an analogy with CHÉZY's relationship (cf. 4.22-10) embodying

$$\bar{v}=c\sqrt{hS}, \tag{4.66-16}$$

$$\bar{v}_m=c_m\sqrt{h_m S} \tag{4.66-17}$$

and employing formula (4.22-13) for c, POKHSRARYAN sets

$$\bar{v}=\bar{v}_m\left(\frac{h}{h_m}\right)^{\frac{1}{4}}. \tag{4.66-18}$$

Inserting this into (4.66-15) yields an equation for α and hence the bottom profile can be found theoretically by an integration. Neglecting the factor $c_t/(c_f m_0)$ (no transverse drag force), POKHSRARYAN obtained the following approximate expression

$$\frac{b}{h_m}x'=m_0\int_{h'}^{1}\frac{\sqrt{1+\frac{h'^2}{m_0^2}}}{\sqrt{1-h'^2}}dh'. \tag{4.66-19}$$

In this equation, h' and x' are relative coordinates, both varying from 0 to 1 (b being the width of the river).

An approximation integral of this is

$$x=m_0 h_m\left[\arccos h'+\frac{1}{4m_0^2}(\arccos h'+h'\sqrt{1-h'^2})\right.$$
$$\left.-\frac{1}{64m_0^4}(3\arccos h'+3h'^2\sqrt{1-h'^2}+2h'^3\sqrt{1-h'^2})\right]. \tag{4.66-20}$$

A comparison of the calculated values with experimental observations is shown in Fig. 115.

The above analysis is valid only for a straight stretch of river where no transverse circulation is present. The analysis, however, can be extended to river bends where such a circulation is present – in which

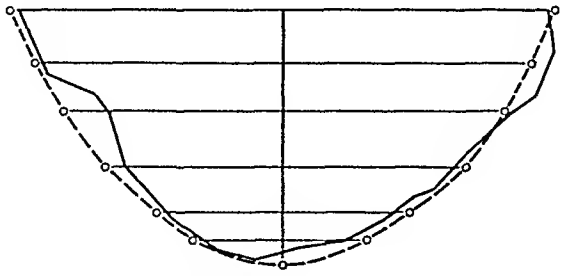

Fig. 115. Comparison of measured values for the cross-section of a river compared with those calculated from POKHSRARYAN's theory. After POKHSRARYAN[1]

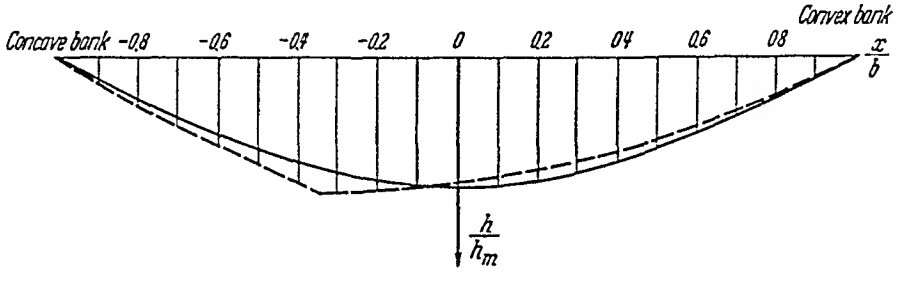

Fig. 116. Comparison of the transverse profile in a river in a straight stretch (solid line) with that in a curved (dotted line) stretch. After POKHSRARYAN[1]

case it is no longer true that $\varphi = \psi = 0$ in (4.66-6). Starting with a prismatic channel at the angle of repose, POKHSRARYAN obtained a result which is shown in Fig. 116.

Finally, it may be worth while to make a few remarks regarding BRETTING'S[2] treatment of the problem of the cross section of a stable river. BRETTING, essentially, writes down a basic force balance equation which is very similar to that of POKHSRARYAN (4.66-6), but he considers from the beginning only the forces parallel to the mean flow; he then introduces a hydrodynamic lifting force L

$$L = c\,\sigma_{\text{bottom}} \tag{4.66-21}$$

which corresponds to POKHSRARYAN's V (see Eq. 4.66-2).

The force balance equation, again, yields essentially a relation between v_{bot} and α. In order to calculate the profile, a further relation is needed. BRETTING chooses

$$\frac{\sigma_{\text{bottom}}}{\sigma_{\max}} = \frac{h}{h_{\max}\cos\alpha} \tag{4.66-22}$$

which replaces (4.66-18) in POKHSRARYAN's theory. One duly ends up with a differential equation for the profile. BRETTING, in his study,

1. POKHSRARYAN, M. S.: Izv. Akad. Nauk Armyan. SSR, Ser. Tekh Nauk **10**, No. 6, 85 (1957); **11**, No. 6, 31 (1958)

2. BRETTING, A. E.: Acta Polytech. Scand. Ci 1 (245/1958) (1958).

supplies a series of tables giving the numerical results which he obtained. He claims good agreement with tests; a representative result obtained by him is shown in Fig. 117.

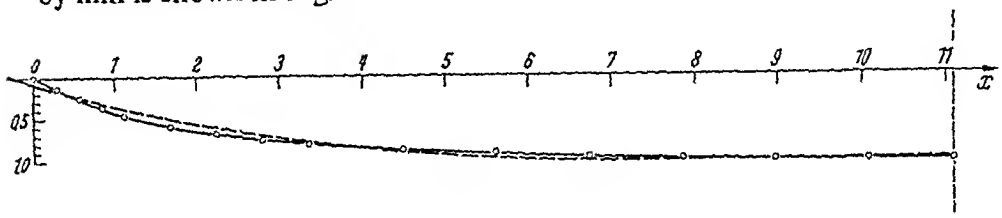

Fig. 117. Comparison of measured values of a river profile with those calculated according to BRETTING's theory. After BRETTING[1]

4.67. Scaling of River Bed Processes. An inspection of the discussion of river bed processes presented up to this point makes one recognize that it is possible only in a very few cases to give an actual physical theory of the phenomena that have been observed. Even if such a theory can be given, it is usually found that it involves many constants which have to be determined empirically. As usual in circumstances where the available theories are inadequate, it is useful to take recourse to model experiments. The problem therefore arises how best to scale river-bed processes.

In order to develop suitable scaling laws, one may assume as a first approximation that *gravity forces* and *turbulent forces* are the only forces that are acting in river bed processes. This leads immediately to the condition that the Froude numbers F_r

$$F_r = \frac{v}{\sqrt{g\,l}} \tag{4.67-1}$$

(where v is a characteristic velocity, l a characteristic length and g the gravity acceleration) must be equal in the prototype and in the model. One can prove this easily as follows. In order to scale *any* force f, NEWTON's law of motion (m denotes mass, v velocity, t time)

$$f = m\frac{dv}{dt} \tag{4.67-2}$$

has to be satisfied equally in the model as in the prototype. This implies the following conditions for the scaling ratios of force (α_f), mass (α_m), length (α_l), time (α_t) and velocity (α_v):

$$\alpha_m\,\alpha_v\,\alpha_t^{-1} = \alpha_m\,\alpha_l\,\alpha_t^{-2} = \alpha_f. \tag{4.67-3}$$

1. BRETTING, A. E.: Acta Polytech. Scand. Ci 1 (245/1958) (1958).

However, the gravity force is

$$f = mg. \tag{4.67-4}$$

Hence

$$\alpha_f = \alpha_m \tag{4.67-5}$$

which yields

$$\alpha_l = \alpha_t^2. \tag{4.67-6}$$

For the velocity ratio α_v this yields

$$\alpha_v = \alpha_l/\alpha_t = \alpha_l^{\frac{1}{2}}. \tag{4.67-7}$$

Writing

$$\alpha_v = V/v \tag{4.67-8}$$

$$\alpha_l = L/l \tag{4.67-9}$$

(where capitals denote variables in the prototype, lower case letters variables in the model) this can be written

$$\frac{v}{\sqrt{g\,l}} = \frac{V}{\sqrt{g\,L}} = F_r, \tag{4.67-10}$$

so that one has the result that gravity forces are correctly scaled if the Froude numbers are equal.

In order to scale turbulent forces, one starts with PRANDTL's equation (2.23-1)

$$\sigma = \text{const. } \rho\, l^2 (dv/dy)^2 \tag{4.67-11}$$

(see Sec. 2.23 for a definition of symbols). This yields the following expression for the various ratios:

$$\alpha_f\, \alpha_l^{-2} = \alpha_m\, \alpha_l^{-3}\, \alpha_l^2\, \alpha_v^2\, \alpha_l^{-2}. \tag{4.67-12}$$

Inserting this into (4.67-3) leads to

$$\alpha_l^2\, \alpha_t^{-2} = \alpha_v^2 \tag{4.67-13}$$

which does not yield a new condition. Hence, equality of the Froude numbers is the only scaling condition that is required to model gravity and turbulence effects correctly. This "Froude condition" can be written as follows:

$$\alpha_v^2\, \alpha_l^{-1} = 1. \tag{4.67-14}$$

It turns out that scaling experiments based upon FROUDE's similarity criterion alone are not always satisfactory. The reason for this is, of course, that gravity and turbulent forces are not the only ones that are

present. Thus, in addition to FROUDE's criterion, other conditions, corresponding to the various sediment transportation formulas, have to be used. Investigations into various possibilities have been made by numerous people. NAZARYAN[1] and coworkers based their scaling law on a generalized Manning (cf. 4.22-3) relationship

$$v=\beta\left(\frac{h}{d}\right)^n\sqrt{g\,h\,S} \tag{4.67-15}$$

where, as usual, v is the average velocity, h the river depth, d the particle diameter and S the slope. The quantities n and β are empirical constants. This leads immediately to the following scaling law:

$$\alpha_v=\alpha_h^{n+\frac{1}{2}}\,\alpha_d^{-n}\,\alpha_S^{\frac{1}{2}} \tag{4.67-16}$$

where the α's again denote the scaling ratios of the quantities indicated in their indices. In addition, NAZARYAN et al.[1] based further scaling laws upon some morphometric formulas of VELIKANOV[2].

Similarly, EINSTEIN and CHIEN[3,4] also used the above generalized Manning formula, but, in addition, based further scaling laws upon the bed load function theory outlined in Sec. 4.53 (e.g. the condition that the dimensionless functions Φ and Ψ introduced in Sec. 4.53 remain the same in model and prototype, immediately yields two scaling laws). All in all, EINSTEIN and CHIEN ended up with 9 conditions for 10 independent scaling ratios, which were later modified somewhat by BOGARDI[5].

Other attempts at setting up scaling relations for special conditions have been reported by various authors[6–12].

As with all model experiments, the latter never *explain* any physical facts but only make their characteristics accessible to laboratory investigations.

---

1. NAZARYAN, A. G., M. S. POKHSRARYAN, and M.I. TER-ASTABATSATRYAN: Izv. Akad. Nauk Armyan. SSR. Ser. Tekh. Nauk **12**, No. 5, 60 (1959).

2. VELIKANOV, M. A.: Динамика русловых потоков. Gos. Izd. Tekh. Teoret Lit. (1955).

3. EINSTEIN, H. A., and N. CHIEN: Trans. Amer. Soc. Civ. Eng **121**, Pap. 2805, 440 (1956).

4. CHIEN, N.: Academia Sinica, Bulletin No. 1 (1957).

5. BOGARDI, J.: Acta Tech. Acad. Sci. Hung. **24**, No. 3–4, 417 (1959).

6. RAZUMIKIN, N. V.: Vestn. Leningr. Un-ta No. 24, 93 (1960).

7. YALIN, S.: Dtsch. Wasserwirtsch. 50, 244 (1960).

8. CHAUVIN, J. L.: Bull Centre Rech. Essais Chaton. No. 1, 64 (1962).

9. AMOROCHO, J., and W. E. HART: J. Hydrol. 3, 106 (1965).

10. ZELLER, J.: Schweiz. Bauztg. 83, No. 42 (1965).

11. ZNAMENSKAYA, N. S.: Trudy Gos. Gidrol. In-ta, No. 136, 45 (1966).

12. BRUUN, P.· Bull. Geolog Soc. Amer. 77, 959 (1966).

4.7. Pebble Gradation and Bottom Slopes in Rivers

4.71. Possible Causes of Gradation. It is common knowledge that the sediment particles in an alluvial reach show a gradation of size. The finest particles are found furthest away from the source of the carrying water. There are several possible explanations of this phenomenon.

First, it has been proposed that the particles undergo contrition during their down-stream journey so that the finest particles would be those that have travelled farthest. This leads to a formula first proposed by STERNBERG[1]. Second, it has been postulated that the gradation is in fact due to a sorting effect. There are two possible explanations for the occurrence of such a sorting effect. First, the sorting may be due to the fact that only a certain size of particles can remain fixed on any one slope angle of the bed, the finest particles requiring the smallest slope angle. Since the slope angle generally diminishes in rivers if the distance from the source increases, this could account for the observed pebble gradation. Second, the sorting may not be the result of a fixation of particles on a certain slope, but of differential transportation.

The various theories that have been proposed as an explanation of pebble gradation will be discussed below and a section containing an evaluation of these possible explanations will be added.

4.72. Contrition of Pebbles. The best known explanation of the gradation of sediment particles in an alluvial reach, such as the course of a river, is that given by STERNBERG[1] in the last century.

STERNBERG based his explanation on the assumption that particles become smaller during their journey because of frictional forces which cause contrition of the material.

Thus, it stands to reason that the change in weight dW of a given particle is proportional to its weight W and the distance dL through which it travels; hence (with α a proportionality constant)

$$dW = -\alpha W dL \tag{4.72-1}$$

or

$$W = \text{const}\, e^{-\alpha L}. \tag{4.72-2}$$

The last equation is known as STERNBERG's *formula.*

The assumption that pebbles become contriturated during their downstream journey is beyond doubt. Experiments to study the contrition have been reported, e.g. by RAYLEIGH[2,3]. LORD RAYLEIGH was

1. STERNBERG, H. U.: Z. Bauw. **1875**, 483 (1975).
2. RAYLEIGH, LORD: Proc. Roy. Soc. (London) A **181**, 107 (1942).
3. RAYLEIGH, LORD: Proc. Roy. Soc. (London) A **182**, 321 (1944).

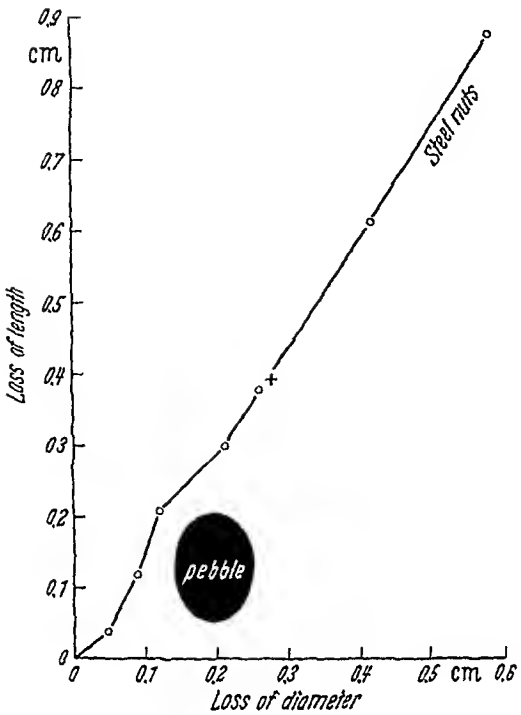

Fig 118

Fig 119

Fig 118. Loss of length correlated with loss of diameter of a spheroidal pebble during contrition. After LORD RAYLEIGH[1]

Fig. 119. Ultimate shape of a block of marble (shown on top) being contriturated by steel fragments (center) and by an artificial pot-hole mill (bottom) One-half of natural size After LORD RAYLEIGH[2]

mostly interested in the shape that pebbles adopt during their contrition. For this purpose, he made artificial pebbles of chalk and contriturated them by placing them into a metal box together with various kinds of abrasive particles (such as hexagon nuts). The box was kept in slow rotation. The result was that, if a spheroidal shape of pebbles was used to begin with, the shape did not change very much during the experiment. A curve of one of RAYLEIGH'S runs is shown in Fig. 118. The cross in that figure indicates the direction of a straight line which would correspond to the pebble retaining its original length-to-diameter ratio. Not all experimental runs of RAYLEIGH'S gave such a result; in most cases it was found that the pebbles became *more* spherical.

In his second paper, LORD RAYLEIGH repeated the experiments with a block of marble being contriturated by steel fragments. A typical

1. RAYLEIGH, LORD: Proc. Roy. Soc A 181, 107 (1942)
2. RAYLEIGH, LORD: Proc. Roy. Soc. A 182, 321 (1944).

result is shown in Fig. 119 (center) which shows how the edges become rounded. Somewhat different results are obtained if the contrition is achieved in an artificial pothole by rotating water in a vessel containing pebbles, forcing the latter to rub against the walls; the result of this type of an experiment is also shown in Fig. 119 (bottom). In some instances, almost perfectly spherical pebbles can be obtained in this fashion. Occasionally, a slightly *concave* shape is encountered. LORD RAYLEIGH suggested a qualitative explanation for this; the concavity is the result of the pebbles being nicked by other similar pebbles. The nicking process is more pronounced in the center than at the edges of a pebble (where nicking merely acts to round the corners) which gives rise to the concave shape.

RAYLEIGH'S work is only concerned with the *shape* of pebbles. Other experiments have been made to investigate the distance which a pebble has to travel to become contriturated. This will be more fully discussed in Sec. 4.75. It may be stated here, however, that it appears as uncertain whether the *amount* of contrition is sufficient to produce the actually observed gradation of bottom sediment in a river.

4.73. Bed Slope and Pebble Size. The explanation of pebble gradation given in the last Section may not be the correct one, although it undoubtedly yields a qualitatively acceptable result. It is beyond question that particles become contriturated during their downstream journey, but, as noted above, it is not certain whether this phenomenon is large enough to produce the gradations observed.

An alternative explanation of size gradation may be postulated on a similar basis as the explanation of particle size gradation on alluvial slopes (cf. Sec. 3.45). It is a known fact that, in general, the slope of a river bed declines from its source to its end (cf. Sec. 4.65). In a river which is in dynamic equilibrium (so that in every one of its reaches just such particles are present that cannot be dragged along by the scouring force), the size gradation of pebbles ought to be given by the same equation (3.45-23) as the size gradation on alluvial slopes. Applied to rivers, taking all constants into the two factors α and β, this equation reads

$$W = \alpha(\operatorname{erfc} \beta L)^3 \qquad (4.73\text{-}1)$$

where W is the weight of the pebble and L the distance from the source.

In examining this equation, it should be noted that considerable simplifications had been made during the deduction of formula (3.45-23) which cannot be expected to be valid for the case of river flow: particularly Eq. (3.45-1) and (3.45-2) are in doubt for this case.

A somewhat more heuristic approach to the idea that it is essentially the slope of the river bed which determines the particle size to be found

there, has been provided by LOKHTIN[1]. In this approach, it has been assumed that for any single river, there exists a constant *coefficient of fixation* C_F defined as follows:

$$C_F = d/S \tag{4.73-2}$$

where d is the diameter of the pebbles and S the corresponding slope. The reason that this coefficient is assumed to be constant is that, by its definition, it represents the ratio of two forces: (i) of the resistance of a pebble to being moved which is proportional to its weight and hence to d^3 (cf. 4.43-2) and (ii) of the scouring force which tends to propel the pebble which is proportional to $d^2 v^2$ (cf. 4.43-1) and, in view of the Chézy relation (4.22-10) to $d^2 S$. If a river is in any sort of dynamic equilibrium, LOKHTIN reasons that the ratio of these two forces, and hence the coefficient of fixation C_F, must be constant.

Equation (4.73-2), if the left hand side be assumed as constant, yields a law for the size distribution of pebbles in rivers. Taking again the weight W instead of the diameter d as the criterion of pebble size, LOKHTIN'S relationship yields:

$$W = \text{const}\, S^3. \tag{4.73-3}$$

This becomes a relation for the pebble gradation with distance L from the source of the river, if S is inserted as a function of L. LOKHTIN assumed that this would be done empirically. However, we have noted in Sec. 4.65 that SHULITS postulated a general law for the decrease of slope angle in a graded river which he writes as follows (cf. 4.65-1):

$$S = S_0\, e^{-aL}. \tag{4.73-4}$$

Using SHULITS' equation, LOKHTIN'S formula becomes

$$W = \text{const}\, e^{-\alpha L} \tag{4.73-5}$$

where α is a new constant (equal to $3a$). It should be noted that this has the same form as the Sternberg formula, but the physical explanation of this equation is totally different.

4.74. Gradation by Differential Transportation. The theory of pebble gradation given above is essentially a heuristic one. It would appear as desirable to set the same basic idea upon a sounder mechanical basis.

This has been attempted by SUNDBORG[2] who showed how a sedimentation formula can be deduced in the following fashion. Let $\varphi(w)$ denote the ratio of the number of particles in a certain interval of grain

1. LOKHTIN(E), V.: Sur le mécanisme du lit fluvial. St. Petersburg 1897.
2. SUNDBORG, A.: C. R. Ass. Toronto, Assoc. Hydrol. Sci, U.G.G.I., 1, 249 (1957).

size (characterized by their settling velocity between w, $w+dw$) that are picked up to the number which are deposited. Furthermore, let s_w denote the average vertical concentration of the corresponding material in the stream. The concentration of that material immediately above the bed may similarly be denoted by $\Phi(w)\, s_w$. Then, conservation of mass yields

$$h\frac{ds_w}{dt} = -w\, s_w\, \Phi(w)\,[1-\varphi(w)] \tag{4.74-1}$$

where h is the mean depth of the river. The above equation is valid for any size fraction of particles characterized by the settling velocity w (i.e. the latter assumed as being between w and $w+dw$). Assuming $\varphi=0$, the above equation can be integrated to yield

$$s_w(t) = s_w(0)\, e^{-w\,\Phi(w)\,t/h}. \tag{4.74-2}$$

This is SUNDBORG'S formula. If we assume that the mean flow velocity of the river is constant (equal to $\bar{u}$), then we can write

$$s_w(L) = s_w(0)\, e^{-w\,\Phi(w)\,L/(\bar{u}\,h)} \tag{4.74-3}$$

where L denotes the distance from the source. The quantity s_w represents the concentration still in suspension. The amount of material deposited (per unit time and length) at the distance L from the source is thus

$$K(w,L) = -\frac{ds_w(L)}{dL}\,\bar{u} = \frac{w\,\Phi(w)}{h}\, s_w(0)\, e^{-w\,\Phi(w)\,L/(\bar{u}\,h)}. \tag{4.74-4}$$

As indicated by the notation, $K(w,L)$ represents the size distribution of particles at the distance L from the source. This equation embodies a decrease of grain size with distance L. This can be shown e.g., if $s_w(0)$ and $\Phi(w)$ are taken as independent of w. The grain size (characterized by w) which has the maximum frequency of occurrence is calculated by setting

$$\partial K/\partial w = 0. \tag{4.74-5}$$

This yields under the above assumptions

$$w = \frac{\bar{u}\,h}{\Phi\,L}. \tag{4.74-6}$$

Since w is proportional (for low settling velocities) to the $\frac{2}{3}$ power of the particle weight W, (cf. 4.42-2) we have

$$W \sim (1/L)^{\frac{3}{2}}. \tag{4.74-7}$$

This does not have the same form as the Sternberg formula although, qualitatively, it also embodies a decrease of particle size with distance from the source. However, it should be noted that the assumption of

independence of $s_w(0)$ and $\Phi(w)$ of w constitutes a great oversimplification. SUNDBORG[1] has given graphical curves for the determination of these quantities which are based upon observational data.

4.75. Evaluation of Theories of Pebble Gradation. It remains to give an evaluation of the various theories of pebble gradation presented above.

Starting with STERNBERG's formula, we note that the latter describes the facts accurately enough. A comparison of observational data with STERNBERG's formula has been given, for instance, by LELIAVSKY[2] for

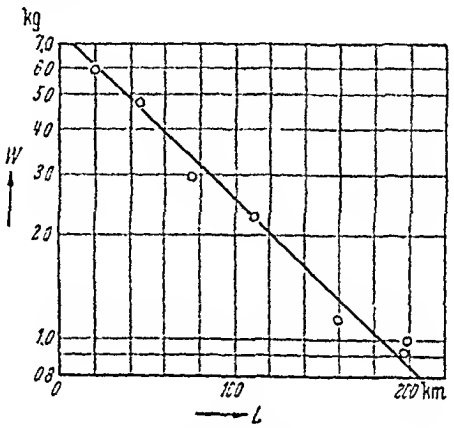

Fig 120. Relation of pebble weight W with distance L from source for the river Rhine, as plotted by LELIAVSKY[2]

the river Rhine. The measured points (pebble weight W as a function of distance L from source) fall fairly well onto a straight line on semi-logarithmic paper (see Fig. 120) which indicates the phenomenological validity of STERNBERG's formula. In the particular case of the Rhine, one obtains from Fig. 120:

$$\alpha \cong 0.01\,\mathrm{km}^{-1}. \tag{4.75-1}$$

However, it is not at all certain whether the physical postulates used in the deduction of STERNBERG's formula, are acceptable, particularly in view of the fact that LOKHTIN's theory, which is based upon an entirely different physical model, leads to an identical theoretical result. Whether STERNBERG's physical model is acceptable depends on whether the assumption that the contrition of a pebble is proportional to its size, is true.

1. SUNDBORG, A.: Geografiska Ann. 38, 127 (1956).
2. LELIAVSKY, S.: An Introduction of Fluvial Hydraulics. London: Constable & Co. 1955.

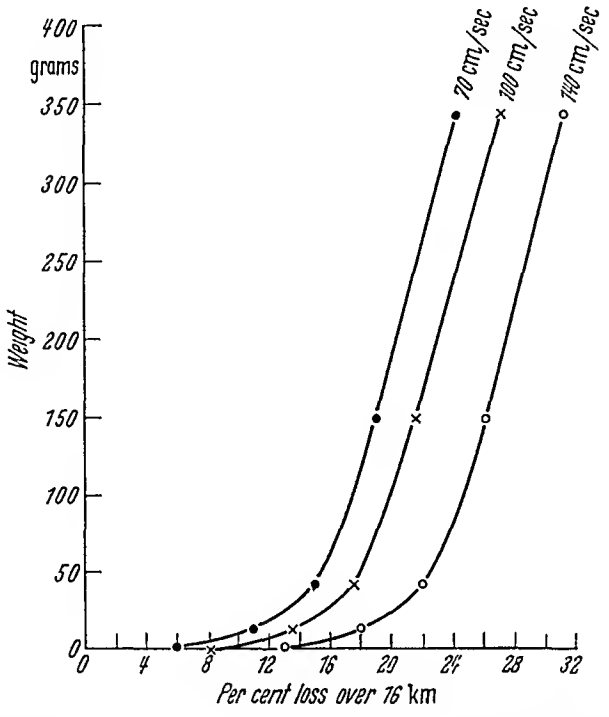

Fig. 121. Relation between per cent weight loss and weight for limestone cubes over the equivalent of 16 km travel distance on pebbly concrete floor, as deduced from KUENEN's experiments (after KUENEN[1])

Experiments to decide this question have been started in the last century by DAUBRÉE[2], who was followed by many investigators thereafter[3]. However, the experiments performed by these people seem to be inconclusive because the conditions under which they were performed, were rather far removed from those prevailing in a natural river. It was not until some investigations by KUENEN[4] that experimental results on pebble detrition could really be trusted.

KUENEN used a revolving current which drove pebbles over a concrete floor. The abrasion, expressed in distance travelled, was measured. Typical results obtained by KUENEN are shown graphically in Fig. 121.

It is immediately obvious from Fig. 121 that the per cent. loss of weight is not proportional to the weight of the pebble or boulder. Very small particles (such as quartz sand grains less than 0.5 mm in diameter) do not experience any appreciable loss of weight at all.

1. KUENEN, P. H.: J. Geol. **64**, 336 (1956).

2. Cf. DAUBRÉE, A.: Études synthétiques de géologie expérimentale, 2 vols Paris: Dunod 1879.

3. See e.g. KRUMBEIN, W. C.: J. Geol. **49**, 482 (1941) for a review.

4. KUENEN, P. H.: Leids. Geol. Med. **20**, 131 (1955). — J. Geol. **64**, 336 (1956) — Proc. Koninkl. Ned. Akad. Wetenschap. B **61**, 47 (1958). — Amer. J. Sci. **257**, 172 (1959). — Rept. Int. Geolog. Congr. 21st Sess., Pt. **10**, 50, Copenhagen (1960).

The percentage weight loss over 16 km corresponding to the Rhine river data (using Eq. 4.75-1) works out to 16 %. This value falls within the range acceptable according to KUENEN's experiments (see Fig. 121) so that the main objection to STERNBERG's model is the experimentally observed variation of the relative abrasion with pebble size. However, this objection is serious. Thus, in view of the fact that LOKHTIN's model (see Sec. 4.73) yields the same phenomenological result as STERNBERG's, and that there is therefore an alternative explanation of the observed data, STERNBERG's model ought to be rejected. No doubt, pebble abrasion plays *some* rôle in establishing the observed gradation patterns, but it cannot be the sole reason thereof.

Turning now to the second model, viz. to the hypothesis that the observed pebble gradation is the result of a differential sorting process rather than that of an abrasion of the pebbles, we note that the theory of LOKHTIN yields an acceptable result. A possible objection here lies in the definition of the coefficient of fixation which may vary widely from river to river. Nevertheless, the theory is most appealing in its simplicity, and has now also been experimentally verified[1]. The final model discussed (SUNDBORG's) represents basically the same idea as that adopted by LOKHTIN, but the treatment is much more sophisticated and also physically more satisfactory. Unfortunately, using some simple boundary and initial conditions, it does not yield the correct exponential law of gradation, but in view of the indeterminancy of the coefficients used, this is not too serious.

Therefore the most likely mechanism of pebble gradation in rivers consists of pebbles becoming contriturated due to the action of frictional forces, but being assigned their position along the stream bed by a sorting process due to differential transportation.

4.8. Meanders in Alluvial Channels

4.81. General Remarks. We have remarked earlier that, in general, rivers do not flow in a straight course. Intuitively, it would appear that the most natural course for a river to take on an incline would be along a straight line in the direction of steepest descent. If this were the case, nobody, presumably, would ask for any further explanations.

However, the course of rivers is not straight, but sinuous. It forms meanders and sometimes, braids, and this fact needs an explanation. In general terms, the problem of finding such an explanation has been discussed, e.g. by PRUS-CHACINSKI[2] and by LEOPOLD and WOLMAN[3].

1. JOPLING, A V.. J. Geophys. Res 69, 3403 (1964).
2. PRUS-CHACINSKI, T. M . New Scientist 4, No. 79, 16 (1958).
3. LEOPOLD, L. B., and M G. WOLMAN: Bull. Geol. Soc. Amer 71, 769 (1960)

A particularly noteworthy attempt has also been made by LEOPOLD and LANGBEIN[1].

The oldest explanation of meanders (presented in Sec. 4.82) is based on the concept of a graded river. However, it can be shown that it is not acceptable. The second explanation (presented in Sec. 4.83) is based on the circulatory (helicoidal) cross currents in rivers which must have a scouring effect upon the banks and hence produce meanders. It is probably correct, but the mathematical difficulties encountered in describing the effects of these currents analytically are almost unsurmountable. Thus, a statistical approach has been taken to the problem, in which meander formation is considered as the outcome of a constrained random walk (Sec. 4.84). Finally investigations turned to empirical approaches of the meander problem (Sec. 4.85). This, of course, will never produce an explanation of meandering in terms of basic physical principles but it might at least serve to delineate the variables that are involved.

Finally, we shall discuss a specific geomorphological effect of the meandering of rivers; this is the creation of terraces (Sec. 4.86).

4.82. Meanders in a Graded River. The first explanation of meandering that has been put forward is one based upon the concept of a graded river (cf. Sec. 4.64).

In any sedimentary plain, the size of the pebbles and the total water discharge of the river presumably would effect that the river is *not* at grade if it were to run in a straight course. Thus, the river would seek itself a crooked course until its bed has been lengthened to such an extent that the river would be at grade.

The above explanation of meanders, appealing though it might appear at first glance, nevertheless cannot be upheld in the light of criticism. For, even though a river be not at grade, there appears to exist no reason whatsoever why it should scour *sideways* in order to rectify the situation. The river might well simply deepen its channel and form a gorge. A different explanation of meanders is therefore required.

Nevertheless, one can make some general remarks upon meander mechanics based on such purely phenomenological terms as a graded river. Thus, SUNDBORG[2] has stated that a meander loop must of necessity widen until the radius of curvature has become so large that a further increase would slow down the flow velocity to such an extent that lateral erosion would cease. That such a state will be reached eventually

1. LEOPOLD, L. B., and W. B. LANGBEIN: Scient. Amer. **214**, No. 6, 60 (1966).
2. SUNDBORG, A.: Geografiska Ann. 38, 125 (1956)

may be ascertained from the principles of the drag theory of fluvial erosion. The shape of the meander loop, thus, depends on both the flow conditions and on the material constituting the river bed.

The fact, mentioned in Sec. 1.44, that the ratio of the radius of curvature R over the channel width w tends to lie around 2 or 3, has been explained by BAGNOLD [1] by noting that the resistance to flow in a channel falls sharply in the above range of the value of R/w.

Unfortunately, our present knowledge is not sufficient to exploit the above remarks any further.

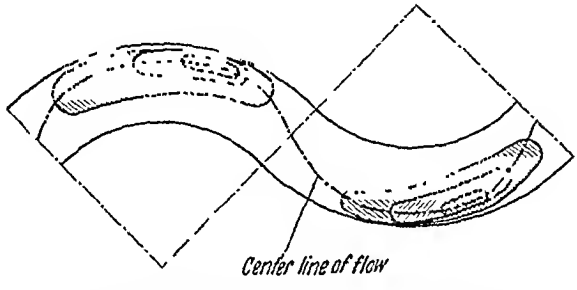

Fig. 122 Erosion at the outer and deposition at the inner bank in a meander coil. (Darker shades: deeper) After LELIAVSKY [2]

4.83. Helicoidal Flow. An explanation of the origin of meanders which is different from that attempted in the previous Section, may be based upon the existence of secondary flows in river bends.

According to the theories outlined in Sec. 4.33/4, helicoidal currents exist in river bends which have the form shown in Fig. 102. It stands to reason that such currents will cause erosion at the outer bank of a river bend and deposition at the inner bank (see Fig. 122), simply because there is a tendency to push high-velocity water towards the outer bank. Hence, the process of meandering, once it is initiated, is seen to intensify itself[3].

Unfortunately, no exact mathematical theory based upon a proper analysis of the effect of the helicoidal currents can be given which would correlate the size of meanders with other dynamical variables characterizing the river. However, a theory for the initiation of meanders has been given by WERNER [4] who based his considerations upon the assumption that the start of the cross currents might be connected with the propagation of a disturbance across the width b of the river. Referring

1 BAGNOLD, R. A : U S Geolog. Surv. Profess Paper 282-E, 135 (1960).

2. LELIAVSKY, S : An Introduction to Fluvial Hydraulics London: Constable & Co 1955.

3 See also TANNER, W F.: J. Geophys. Res. 65, 993 (1960).

4. WERNER, P. W.. Trans Amer Geophys. Union 32, 898 (1951)

to Fig. 123, WERNER argues that any disturbance originating at the point A will propagate itself to the point B, be reflected there and hit the original bank at the point C. The length AC, then, would correspond to the wave length λ of an incipient meander.

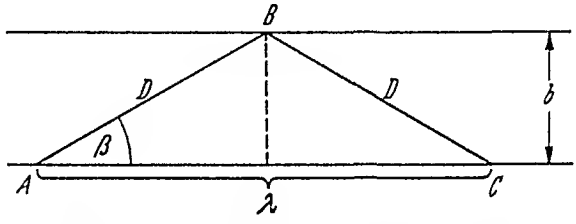

Fig. 123. Geometry of an incipient meander

If we denote the propagation velocity of a disturbance along the diagonal D (see Fig. 123) by v_c, we have (see Fig. 123).

$$\cos\beta = \frac{v}{v_c} \tag{4.83-1}$$

and hence

$$\lambda = 2b\cot\beta = 2b\frac{v/v_c}{\sqrt{1-v^2/v_c^2}}. \tag{4.83-2}$$

The velocity v_c is a "critical serpentine velocity"; WERNER represents it as follows:

$$v_c = \gamma\sqrt{g\,h} \tag{4.83-3}$$

where γ is an empirical constant ($\leqq 1$) depending on the silt content and h is the depth of the river (g is as usual the gravity acceleration). Then, we have

$$\lambda = 2b\frac{v}{\sqrt{\gamma^2 g\,h - v^2}}. \tag{4.83-4}$$

One can discuss the above meander formula further by introducing some drag formula such as MANNING's (cf. Eq. 4.22-3) into it. It is immediately obvious, however, that the meander length can be real only if

$$v < \gamma\sqrt{g\,h}. \tag{4.83-5}$$

The expression $\sqrt{g\,h}$ is the wave-velocity in the water (see Eq. 6.22-19), we have noted that $\gamma \leqq 1$; hence it is seen that meanders can form only if the flow velocity is smaller than the wave velocity. The latter condition characterizes streaming flow; in shooting flow, no true meanders are possible.

WERNER's theory is not based on a three-dimensional analysis of the effect of cross-currents. As noted above, such an analysis does not

seem to have been achieved as of yet. Thus, WERNER's theory, crude as it is, seems to be the best one available to-date to correlate meander length λ with other quantities characterizing the river flow.

4.84. Stochastic Theory of Meander Formation. A completely different approach to explaining meanders has been taken by LEOPOLD and LANGBEIN[1, 2] who assumed that a river follows the general proclivity of the area in question, but then, that random "wiggles" are superposed on the geologically conditioned course. Although these "wiggles", if considered in detail, are presumably caused by local physical conditions, they are so numerous and irregular that they cannot be followed in detail. The best way to deal with the "wiggles" is, therefore, to consider them as stochastic deviations from the geologically set trend.

LEOPOLD and LANGBEIN then proposed that the actual course of a river is the most frequent random walk of the set of random walks under the given geological constraints. It should be noted, however, that this line of reasoning is *not* in conformity with the commonly accepted principles of statistical mechanics (cf. Sec. 5.1): usually, the expectation value of an observable (the latter may be the "wiggly line" under consideration) is taken as its average over all the configurations of the ensemble in question. In LEOPOLD's and LANGBEIN's meander theory, however, the "characteristic" pattern is taken as that pattern of the observable which occurs in the most probable configuration of the ensemble. This is generally not satisfactory. Nevertheless, some interesting indications can be obtained from a consideration of such most frequent random walks in the meander case.

Thus, let us assume that, in a Cartesian coordinate system (x, y), a particle starts a random walk at the origin $(0, 0)$. Each step has the (constant) length l; there are a total of j steps after which the particle arrives at the point $J(x_j, y_j)$. The total length given of the walk is $L = jl$. Each step (number i) is a straight-line segment, whose angle with the $+x$ axis is φ_i.

One can then ask various types of questions: (a) Assume that the frequency distribution of angles φ_i be $f(\varphi_i)$, what is the most probable path (under the assumed constraints) from 0 to J? (b) Assume that the frequency distribution of the first differences $\Delta\varphi = \varphi_i - \varphi_{i-1}$ is $f(\Delta\varphi)$, what is the most probable path (under the assumed constraints) from 0 to J?

We turn first to the case where the probability distribution $f(\varphi_i)$ of the angles φ_i is given.

1. LEOPOLD, L. B., and W. B. LANGBEIN: Scient. Amer. **214**, No. 6, 60 (1966).
2. LANGBEIN, W. B., and L. B. LEOPOLD: U.S. Geolog. Survey Profess. Papers **422-H**, H 1 (1966).

Since the random walk, after j steps, must go through the point $x_j y_j$, we have the following constraints in the problem:

$$F \equiv \sum_{i=1}^{j} \frac{L}{j} \cos \varphi_i - x_j = 0, \tag{4.84-1}$$

$$G \equiv \sum_{i=1}^{j} \frac{L}{j} \sin \varphi_i - y_j = 0. \tag{4.84-2}$$

If the probability of finding a particular angle φ_i is $f(\varphi_i)$ (this is assumed to be the same for all steps), the total probability P of a random walk with angles $\varphi_1, \varphi_2, \ldots, \varphi_j$ is

$$P = f(\varphi_1) f(\varphi_2) \ldots f(\varphi_j). \tag{4.84-3}$$

Let us assume that the probability of f can be represented as follows

$$f = C e^{-g(\varphi)} \tag{4.84-4}$$

where C is a normalization constant. Then

$$P = C^j \exp\left(-\sum_{i=1}^{j} g(\varphi_i)\right). \tag{4.84-5}$$

We wish to find the most probable random walk, i.e. $P = \max$ or

$$Q \equiv \log P = \max \tag{4.84-6}$$

under the auxiliary conditions $F = 0$ and $G = 0$. In well-known fashion, this is achieved by maximizing

$$H = Q + \lambda F + \mu G \tag{4.84-7}$$

where λ and μ are Lagrange multipliers. Thus, we require $\partial H / \partial \varphi_i = 0$ for all i, which yields

$$0 = \frac{\partial H}{\partial \varphi_i} = -g'(\varphi_i) - \lambda \frac{L}{j} \sin \varphi_i + \mu \frac{L}{j} \cos \varphi_i. \tag{4.84-8}$$

This equation has, generally, a series of solutions for φ_i, so that the most probable random walk is a series of legs with certain angles whose sequence cannot further be ascertained. The minimization of H, thus, does not lead to a definite result: This is an indication that the positioning of the problem (most probable instead of expected state) is not fortunate.

We turn our attention now the case where $f(\Delta \varphi_i)$ is prescribed; i.e. a certain probability of the change of direction after each step in the

random walk is given. This case has been solved by VON SCHELLING[1,2]. The auxiliary conditions are now

$$F=\cos\Delta\varphi_i+\cos(\Delta\varphi_1+\Delta\varphi_2)+\cdots+\cos(\Delta\varphi_1+\cdots\Delta\varphi_j)-x_j=0$$
$$G=\sin\Delta\varphi_i+\sin(\Delta\varphi_1+\Delta\varphi_2)+\cdots+\sin(\Delta\varphi_1+\cdots\Delta\varphi_j)-y_j=0. \quad (4.84\text{-}9)$$

We again write the frequency distribution as an exponential

$$f(\Delta\varphi)=C\,e^{-g(\Delta\varphi)}. \quad (4.84\text{-}10)$$

The probability of a particular random walk is

$$P=f(\Delta\varphi_1)\,f(\Delta\varphi_2)\ldots f(\Delta\varphi_j) \quad (4.84\text{-}11)$$

which is a maximum if

$$Q=\log P=j\log C-\sum g(\Delta\varphi_i) \quad (4.84\text{-}12)$$

is a maximum. However, one has the auxiliary conditions (4.84-9) which can be taken into account by using Lagrange multipliers, λ, μ, and thus by maximizing the expression

$$H=Q+\lambda F+\mu G. \quad (4.84\text{-}13)$$

This yields

$$\frac{\partial H}{\partial\Delta\varphi_s}=-g'(\Delta\varphi_s)-\lambda\sum_{u=s}^{j}\sin\left(\sum_{i=1}^{u}\Delta\varphi_i\right)+\mu\sum_{u=s}^{j}\cos\left(\sum_{i=1}^{u}\Delta\varphi_i\right)=0. \quad (4.84\text{-}14)$$

We have

$$\varphi(s)=\Delta\varphi_1+\Delta\varphi_2+\cdots\Delta\varphi_s. \quad (4.84\text{-}15)$$

Going to the limit of $l/L=ds\to\infty$, $jl\to L$, s=arc length yields

$$-g'\left(\frac{d\varphi}{ds}\right)-\lambda\int_{u=s}^{L}\sin\varphi(u)\,du+\mu\int_{u=s}^{L}\cos\varphi(u)\,du=0 \quad (4.84\text{-}16)$$

and after some transformation (differentiation with regard to s, multiplying by $d\varphi/ds$, and integration)

$$\frac{d\varphi}{ds}\,g'\left(\frac{d\varphi}{ds}\right)-g\left(\frac{d\varphi}{ds}\right)+[\lambda\cos\varphi(s)+\mu\sin\varphi(s)]+\cos 2\omega=0 \quad (4.84\text{-}17)$$

where ω is a constant of integration. The term in square brackets can be written as $\nu\cos(\varphi-\alpha)$, where ν and α are two new constants; it is clear that setting $\alpha=0$, $\nu=1$ is no restriction of generality. Thus, one

1. SCHELLING, H v.: Trans Amer Geophys. Un. **32**, 222 (1951)
2 SCHELLING, H. v.. General Electric Report, No. 64GL92, Schenectady, N. Y. (1964)

has the differential equation

$$\frac{d\varphi}{ds}\, g'\left(\frac{d\varphi}{ds}\right) - g\left(\frac{d\varphi}{ds}\right) + \cos\varphi + \cos 2\omega = 0. \tag{4.84-18}$$

If the distribution f is specified as Gaussian, viz.

$$g = \frac{1}{2}\,\frac{1}{\sigma^2}\left(\frac{d\varphi}{ds}\right)^2 \tag{4.84-19}$$

the above differential equation can be solved. One has in parametric form

$$\begin{aligned} s &= \frac{1}{\sigma}\int \frac{d\varphi}{\sqrt{2(-\cos 2\omega - \cos\varphi)}} \\ x &= \frac{1}{\sigma}\int \frac{\cos\varphi\, d\varphi}{\sqrt{2(-\cos 2\omega - \cos\varphi)}}. \end{aligned} \tag{4.84-20}$$

Examples of these curves, for various values of ω, are shown in Fig. 124.

The curves, as is evident from their inspection, are fairly regular and, while reminiscent of stretches of river meanders, are too regular to describe a whole system of such features. The reason must be sought in the fact that the most frequent are not the expected random walks.

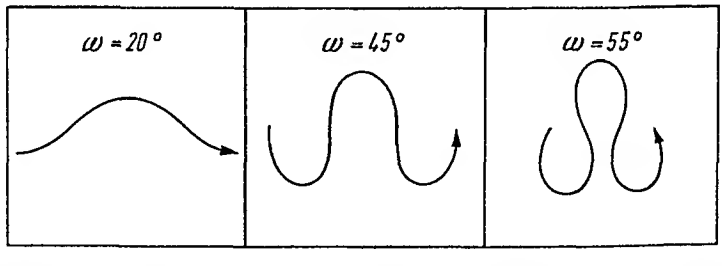

Fig. 124. Gaussian most frequent random walks (adapted from VON SCHELLING[1])

Some of the assumptions of the von Schelling theory can be tested. Thus, THAKUR and SCHEIDEGGER[2] made a test of the basic assumption (4.84-19) and found that it was indeed satisfied on three meandering rivers. However, what is needed at this juncture is an actual production of an expected (not most probable) meander spectrum (cf. Sec. 1.33) based on a statistical theory; this has not yet been achieved. Nevertheless, the meander theory of LANGBEIN and LEOPOLD is certainly a step in the right direction.

1. SCHELLING, H. v.: General Electric Report, No. 64GL92, Schenectady, N.Y. (1964).
2. THAKUR, T. R., and A. E. SCHEIDEGGER: Water Resources Res. 4, 317 (1968).

4.85. Experimental Investigations. The difficulty of giving a satisfactory theoretical description of meander formation has prompted investigators to try empirical methods. This, it may be expected, will at least produce an indication of the factors involved in meander formation if not a true explanation of the origin of the former in terms of basic physical principles. Such experimental studies have been performed, for instance, by TIFFANY and NELSON[1], FEDOROV[2], LEOPOLD and WOLMAN[3], JOGLEKAR[4], FRIEDKIN[5] and SHEN and KOMURA[6]. Of these investigations, that by TIFFANY and NELSON[1] is particularly noteworthy. Accordingly, it is possible to reproduce in flume experiments the meander develop-

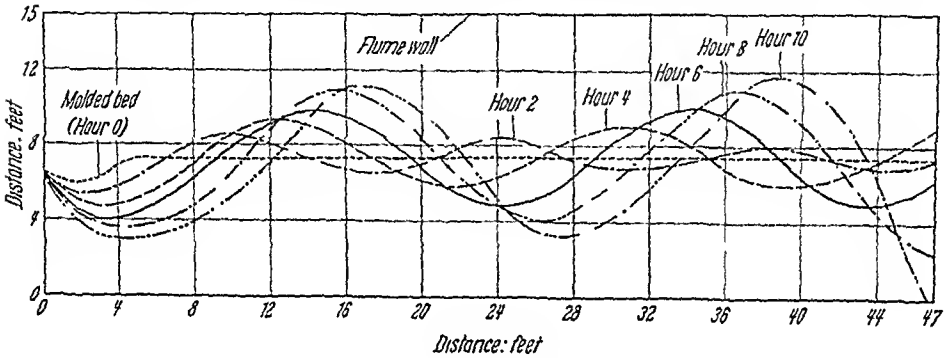

Fig. 125. Progressive changes of a channel in an experiment After TIFFANY and NELSON[1]

ment of alluvial rivers. The progressive changes in location of the channels as obtained by TIFFANY and NELSON is shown in Fig. 125. It was also noted that the rate of introduction of suspended material in to the flowing water materially affected the development-pattern of the meanders.

Furthermore, experimental investigations and field studies have shown that the formation of meanders is not the only possibility by which rivers may adjust to external conditions. It is also possible that braided channels are formed. An analysis of natural channels led LEOPOLD and WOLMAN to postulate that there is a dividing line between conditions producing braided and meandering channels. The results of these authors are reproduced in Fig. 126. Analytically, the dividing line between braids and meanders can be described by the equation

$$S = 0.06\, Q^{-0.44} \tag{4.85-1}$$

1 TIFFANY, J. B, and G. A. NELSON: Trans. Amer. Geophys. Union 20, 644 (1939)

2. FEDOROV, N. N . Trudy Gos. Gidrolog In-ta 44, 14 (1954).

3. LEOPOLD, L. B., and M. G. WOLMAN: U.S Geol Surv. Prof Pap. No. 282-B (1957).

4. JOGLEKAR, D. V.: J. Instn Eng India 39, No 7, Part I, 709 (1959)

5 FRIEDKIN, J. F : A Laboratory Study of the Meandering of Alluvial Rivers. Vicksburg, Miss.: U.S. Wways Exp Sta. 1945.

6 SHEN, H , and S. KOMURA: Proc. Am. Soc Civ Eng 94, J. Hydr Div. HY 4, 997 (1968).

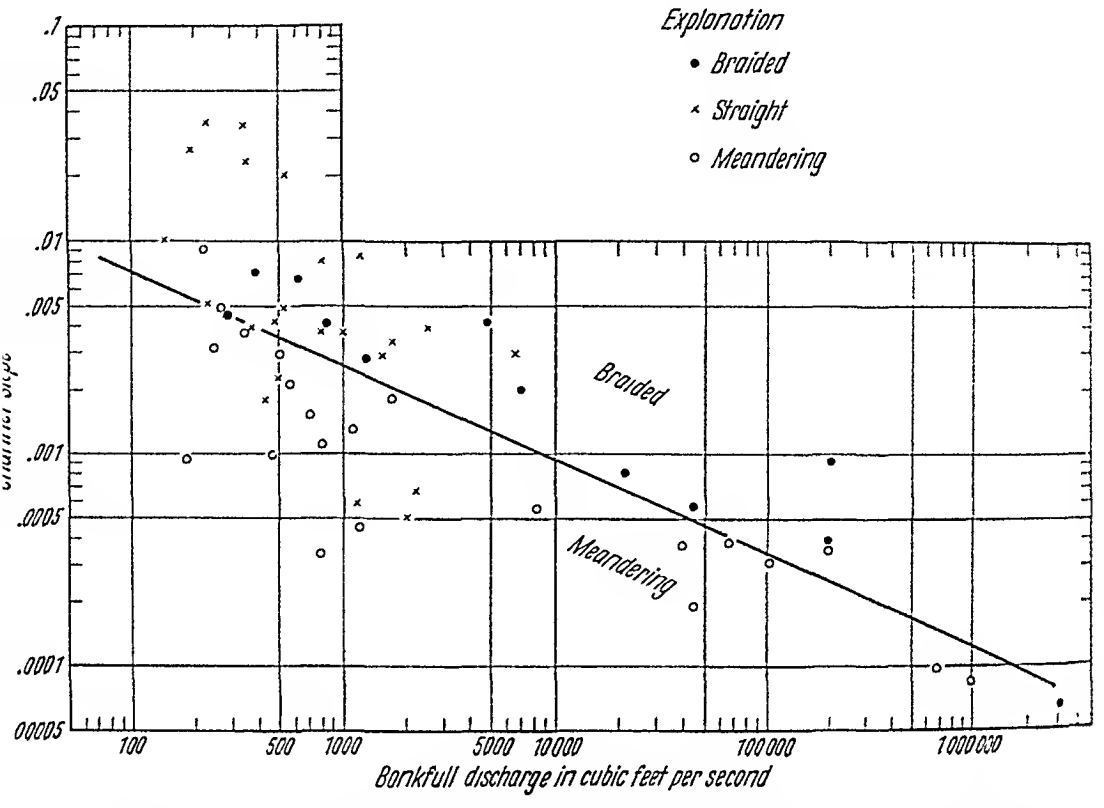

Fig. 126. Values of slope and bankfull discharge for various natural channels. After LEOPOLD and WOLMAN[1]

where S is the slope of the river and Q the bankfull discharge in cubic feet per second. The factors influencing the erosion of river banks have been studied by WOLMAN[2] in the field.

As noted earlier, empirical relationships do not really provide an explanation of why rivers meander or form braids; they do, at best, delineate some of the variables that are important.

4.86. Terraces in Alluvial Plains. As was noted in Sec. 1.44, some field geomorphologists contend that the lateral action of rivers is a most effective agent in the development of drainage basins. In the case of alluvial plains, this lateral action manifests itself primarily in meander formation: meanders swing back and forth across the plain. If a net removal of material (i.e. a net erosion) from the alluvial plain is connected with the meander action, then it stands to reason that *terraces* will be the result.

The above reasoning has been made the basis of a theory of the development of stepped erosion surfaces[3]. In this theory it is reasoned

1. LEOPOLD, L. B., and M. G. WOLMAN: U.S. Geol. Surv. Prof. Pap. No. 282-B (1957).
2. WOLMAN, M. G.: Amer. J. Sci. 257, 204 (1959).
3. GEYL, W. F.: J. Geol. 68, 154 (1960).

that ordinarily, no net removal takes place of material from an alluvial plain: The river dumps débris here and there and also erodes from here and there. In order to have net erosion, *endogenetic* effects must be involved: If a gradual uplift of the area occurs, then a river can maintain its general course only if it removes material from the region. Stepped erosion surfaces are the result.

4.9. Valley Formation

4.91. Requirements of a Physical Theory. Our next task is to investigate the formation of valleys. By "valleys" we mean river valleys which are primarily caused by flowing water. Some of the problems that are involved in this connection have been discussed in general terms e.g. by HOL[1].

The course of rivers at the bottom of a valley is generally very sinuous. This appears to be a characteristic feature of rivers which is evident not only in the meanders (as discussed in Sec. 4.8) that may be observed in an alluvial plain, but is a completely ubiquitous phenomenon. Thus, it is almost impossible to find a natural flow channel which is straight for any appreciable distance. It is this observation which, above all, calls for an explanation.

We have given earlier (Sec. 4.8) reasons for the sinuous course of graded river reaches, but it is doubtful whether the same explanation obtains under non-equilibrium conditions such as may occur in mountain streams. It is possible that the causes for the sinuosity are different in this case. This problem will be discussed first, in Sec. 4.92.

The reasons advanced for the explanation of meanders, however, may be applicable to those effects upon the course of rivers which have been ascribed to the rotation of the Earth. It appears that the Coriolis force is able to induce helicoidal currents in a river and thus affect the meanders. This question will be dealt with in Sec. 4.93.

4.92. Mountain Valleys. The most difficult problem in the development of valleys is to account for the shapes of mountain valleys. The latter are in a transient state which cannot be regarded as even remotely equilibriated. The flow of mountain streams is swift and generally of the shooting (supercritical) variety (cf. Sec. 4.21).

As with streams meandering in flood plains, it is again the sinuosity of the river courses in mountain areas which is a most striking feature. Interestingly enough, there seem to be no mathematical attempts in the literature to explain this feature. It is not possible to account for the bends in mountain streams in terms of cross currents of the type that have been advocated as the cause of alluvial meanders. We have shown in

1. HOL, J. B. L : Rev. Quest. Sci. 128, 195 (1957).

Sec. 4.83 that there are theoretical reasons which indicate that helicoidal currents cannot exist in shooting flow. Under such conditions, the arguments presented in Sec. 4.35 on shooting flow around corners must be advocated: cross waves will become established which have a high erosive power. Thus, one might argue that the sinuosity of mountain streams is initiated by tributary gulleys eroding the sides. Once kinks have been started in this fashion, the cross waves originating in the

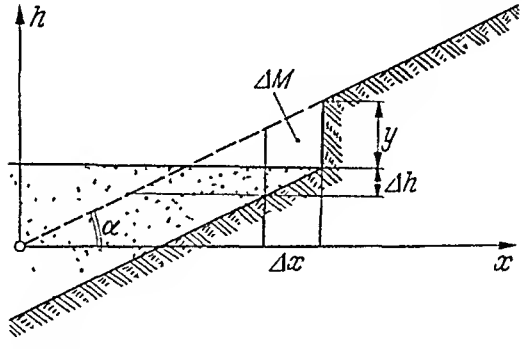

Fig 127. Geometry of the development of a mountain valley. Modified after GERBER[1]

corners will tend to intensify the latter owing to their erosive action. There are no reasons why this action should be regular in any way; this explains the absence of any regularity in the sequence of the bends in mountain streams.

A further complication occurs in mountain valleys because, in addition to eroding the valley sides, a mountain river generally also deposits a lot of débris on the valley floor. Thus, the latter is rising while the river eats its way into the mountain side. An analytical theory of this process has been proposed by GERBER[1]. Accordingly, if the slope of the mountain side is constant, the mountain river action may be envisaged as shown in Fig. 127. During a particular time interval Δt, the valley floor is raised by the amount Δh and the cross-sectional area ΔM is eroded from the mountain side. The ratio

$$\lambda = \frac{\Delta M}{\Delta h} \tag{4.92-1}$$

is indicative of the *erosive power* of the stream. If the mountain side has a constant slope of angle α, then the result of the process is a lowering of the slope; beneath the débris, the slope will be parallel to the original slope. This can be demonstrated as follows:

The (cross-sectional) area eroded is

$$\Delta M = y\,\Delta x = \lambda\,\Delta h. \tag{4.92-2}$$

1. GERBER, E.: Geograph Helv. **14**, 117 (1959).

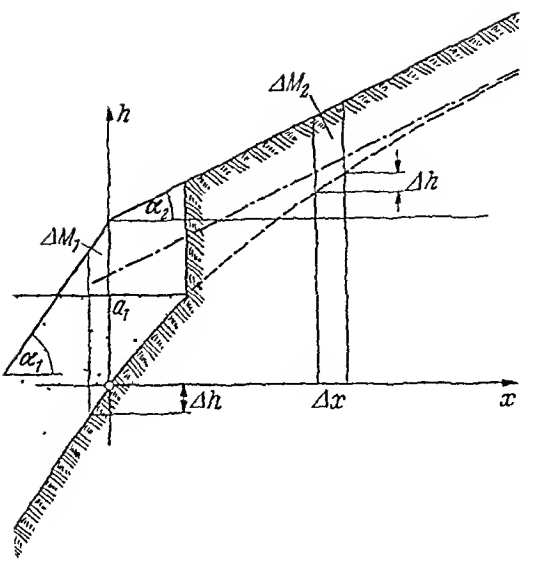

Fig. 128. Effect of a kink in the valley slope upon the development of a mountain valley. Modified after GERBER[1]

But

$$y = x \tan \alpha - h = \lambda \frac{\Delta h}{\Delta x}. \tag{4.92-3}$$

Hence, in the limit

$$\lambda \frac{dh}{dx} - x \tan \alpha + h = 0. \tag{4.92-4}$$

This is a differential equation whose solution is

$$h = x \tan \alpha - \lambda \tan \alpha \tag{4.92-5}$$

which is what was to be demonstrated.

GERBER also investigated the influence of a kink in the original mountain side upon the slope developing beneath the débris (cf. Fig. 128). Introducing the origin of the co-ordinate system (h, x) at that point on the lower slope (i.e. on the slope developing beneath the débris) which is exactly below the kink, we have from an inspection of Fig. 128:

$$\Delta M_2 = \lambda \Delta h \tag{4.92-6}$$

and

$$\Delta M_2 = \Delta x (a_1 + x \tan \alpha_2 - h). \tag{4.92-7}$$

Hence one obtains the differential equation

$$\lambda \frac{dh}{dx} - a_1 - x \tan \alpha_2 + h = 0. \tag{4.92-8}$$

1. GERBER, E.: Geograph. Helv 14, 117 (1959)

The solution of this equation for the boundary condition $h(x=0)=0$ is (note that $\tan\alpha_1=a_1/\lambda$; cf. Eq. 4.92-5):

$$h(x)=a_1\left(1-\frac{\tan\alpha_2}{\tan\alpha_1}\right)\left(1-\exp\left[-\frac{\tan\alpha_1}{a_1}x\right]\right)+x\tan\alpha_2. \quad (4.92\text{-}9)$$

This shows that the valley slope developing beneath the débris is an exponential curve: the kink disappears and is replaced by a rounded corner.

The physical model leading to Eq. (4.92-1) is probably somewhat of an oversimplification. Perhaps, the model could be improved upon by allowing for the fact that the valley becomes *wider* as it fills up. Then, instead of the ratio between ΔM and Δh, the ratio between ΔM and $x\,\Delta h$ should remain constant. Thus let us set

$$\lambda=\frac{\Delta M}{x\,\Delta h}. \quad (4.92\text{-}10)$$

This changes the differential Eq. (4.92-4) to

$$\lambda x\frac{dh}{dx}-x\tan\alpha+h=0 \quad (4.92\text{-}11)$$

whose solution is

$$h=\frac{\tan\alpha}{\lambda+1}x. \quad (4.92\text{-}12)$$

This shows that the slope beneath the débris is now no longer parallel to the original mountain side, but has a declivity which is smaller.

The above theories do not exactly explain the evolution of mountain valleys, but at least they provide some indications regarding the phenomena that might be expected. GERBER[1] gives some examples of geomorphological features of Alpine valleys which can be explained in terms of these theories.

4.93. Influence of the Earth's Rotation. It may be expected that the Earth's rotation has an effect upon the course of rivers. Accordingly, it has been proposed ("BAER's law")[2] that on the Northern hemisphere, the Coriolis force would cause rivers to have the tendency to erode preferentially their right bank and on the Southern hemisphere their left bank.

EINSTEIN[3] has given an explanation of "BAER's law" which is based on the same considerations as his explanation of the tendency of rivers to

1. GERBER, E : Geograph. Helv. **14**, 117 (1959).
2. BAER, K. E. v.: Bull. Acad. Imp. Sci. (St. Petersburg) **2**, 2, 218, 353 (1860)
3. EINSTEIN, A.: Naturwissenschaften **14**, 223 (1926).

meander. Accordingly, the Coriolis acceleration a_c in a river is given by

$$a_c = 2v\omega \sin\varphi \tag{4.93-1}$$

where v is the flow velocity, ω the angular velocity of rotation of the Earth, and φ the geographic latitude. If now the Coriolis force is balanced by a pressure drop across the width of a (straight) river, this can only be achieved for a given velocity v. From the surface to the bottom of the flowing water, however, the flow velocity of the river decreases, and thus the magnitude of a_c will decrease towards the bottom. In a slow-moving river, the local pressure is only conditioned by the height of the water above the point under consideration, and hence any lateral pressure *differentials* must be independent of the depth below the stream surface. Thus, the surface particles are forced towards one side more than the bottom ones. This should give rise to helicoidal cross-currents just as in the case of flow in a river bend discussed earlier. The theory of EINSTEIN, thus, appears to account for phenomena corresponding to BAER's law.

It should be remarked, however, that the very existence of BAER's law, i.e. the validity of the observation that the right hand bank of rivers is eroded more than the left hand bank on the Northern hemisphere, has been questioned by SCHMIDT[1] who based his criticism not upon actual observations in nature, but upon a series of experiments in which a stream of water was established upon a rotating sand bed. Subsequently, the propriety of SCHMIDT's experiments was questioned by EXNER[2] because the bed slope in SCHMIDT's experiments was much greater than what would correspond to nature. Thus, EXNER undertook to repeat SCHMIDT's experiments with some modifications. He took a basin filled with a mixture of sand and clay of 100 cm diameter which he rotated anti-clockwise once in 7 sec. In it was carved the channel of a river with a bed slope of 0.01. The flow velocity was chosen as $v = 50$ cm/sec. This yields a Coriolis acceleration in EXNER's experiments equal to about 90 cm/sec^2, which is about 36 times larger than the Coriolis acceleration of, say, the Danube near Vienna. If anything, it would thus appear that the effect of the Coriolis force is larger in EXNER's experiments than in nature. A typical result of EXNER's experiments is shown in Fig. 129.

It thus turns out that EXNER's experiments show a behavior of rivers which would correspond to BAER's law. EXNER proceeded to calculate the difference of erosive power at the two banks of the river, but these estimates do not seem to be based upon the helicoidal cross-currents postulated by EINSTEIN. For an establishment of the latter it would appear that the ratio of depth to width in the river must be of sufficient

1 SCHMIDT, W.: Festschr. Zentr Anst. Met. Geodyn. Vienna 1926.
2 EXNER, F. M: Geografiska Ann. 9, 173 (1926)

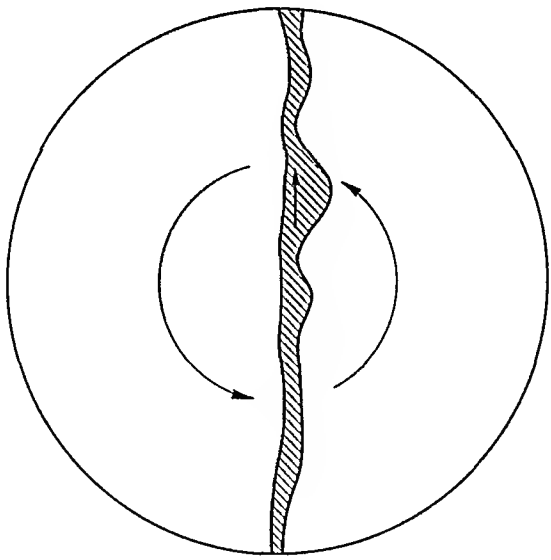

Fig. 129. Sideways erosion of a model river in a rotating basin. Drawn from a photograph by EXNER[1]

magnitude; however no attention was paid by the experiments to this ratio. It is thus not incomprehensible that different results were obtained by different experimenters. Nevertheless, the fact that *some* results corresponding to BAER's law were obtained, appears to speak for the validity of the latter.

1. EXNER, F. M.: Geografiska Ann. 9, 173 (1926).

V. Drainage Basins and Large Scale Landscape Development

5.1. General Remarks

The phenomena discussed thus far refer only to *single features* present on the Earth's surface. It is now time to consider the combined effect of the development of slopes and rivers, i.e. the development of whole landscapes. This leads us to the theory of the development of drainage basins and to the theory of large scale landscape development.

When investigating such large-scale features, it is no longer possible to follow in detail the development of each constituent (slope, river, etc.) in the systems under consideration, inasmuch as the various phenomena are so complex and complicated that a detailed follow-up of the individual microscopic events is simply beyond the capability of the human brain. As is often the case under such circumstances, progress can be made only by considering average properties of the systems under consideration using probabilistic concepts, i.e. by using the apparatus of statistical mechanics. The first to apply this idea, in entirely general terms, to landscape development appear to have been LEOPOLD and LANGBEIN[1] using a very simple analogy with thermodynamics. However, the procedure can be justified on a much deeper physical basis (cf. Sec. 5.8).

The basic philosophy of the statistical theory of the evolution of landscapes is that one assumes that there are innumerable influences which affect the form of the latter. Although each of these influences may be entirely deterministic (eddies around a stone in a river, scattered geological controls etc.), their combined effect is as if they had been acting "at random". This can be expressed mathematically by considering, instead of a particular system, a whole "ensemble" of systems which, within the limits of one's ignorance, one must regard as identical. The expected behavior of a particular system with regard to a given "observable" is then given by the expectation value (calculated as average) of that observable over the ensemble.

1. LEOPOLD, L. B, and W B. LANGBEIN· U.S. Geol. Survey Profess Papers 500-A, A 1 (1962)

This general scheme will be applied again and again in the present chapter, which will, thus, be found to be essentially an outline of the probabilistic theory of landscape evolution.

It may be useful at this juncture to also mention a procedure of setting up a stochastic theory of geomorphic features which is quite different from that sketched above. Thus, a fluctuating geomorphic system may be considered in which a property, x, exists at many points i so that the values x_i of the property at these points can be regarded as independent. Let us further assume that the fluctuations of the property x_i are given by the same Gaussian probability function p

$$p(x_i)=\text{const}\exp(-x_i^2/\alpha^2) \tag{5.1-1}$$

which, for the sake of simplicity, has been chosen such that the average

$$\bar{x}_i=0. \tag{5.1-2}$$

Then, the joint probability distribution $P(x_1, x_2 \dots x_n)$ is given by

$$P=\text{const}\exp\left\{\frac{-1}{\alpha^2}[x_1^2+x_2^2+\cdots x_i^2+\cdots x_n^2]\right\}. \tag{5.1-3}$$

This probability has evidently a maximum if the sum σ^2 of the "variances" x_i^2

$$\sigma^2=x_1^2+x_2^2+\cdots x_n^2 \tag{5.1-4}$$

has a minimum. This has been called the "principle of minimum variance"[1]. The result of the minimization is trivial, viz.

$$x_i^2=0 \tag{5.1-5}$$

unless constraints exist between the x_i. In the latter case, the minimization can be effected by using Lagrange multipliers. An example of this procedure has been presented in Sec. 4.84 of this book on meander theory where also the drawbacks of this type of approach have been mentioned: Calculating the most probable configuration of the system (implicit in the minimization of σ^2) and taking the value of an observable for it is not in conformity with the general principles of statistical mechanics; the accepted procedure is to calculate expectation values of an observable by averaging all its values over the ensemble rather than by taking its value for the most probable state in the ensemble. Nevertheless, the two procedures may not differ too much under particular conditions, viz. when the ensembles are such that the value for the most probable state of the ensemble and the mean value over the ensemble of an observable in question nearly coincide. Thus, useful results may be obtained sometimes from using the principle of minimum variance although it cannot be expected to hold under all conditions.

1. LANGBEIN, W. B.: J. Hydr. Div. Proc. Amer. Soc. Civ. Engr. HY 2, 1964, 301 (1964).

5.2. Empirical Relationships

5.21. The Law of Stream Numbers. Before proceeding with the theory of landscape development, we have to state some empirical relationships about drainage networks in regions where there is only little geological control, which turned out to have a fundamental significance in landscape theory.

The first of these relationships is HORTON's law of stream numbers[1]. Accordingly, if we denote by n_i the number of (STRAHLER) segments of order i in a given network, then the numbers $n_1, n_2, \ldots$ form (on the average) a geometric sequence:

$$n_{i+1} = \alpha\, n_i. \tag{5.21-1}$$

The inverse of the coefficient α, i.e. $1/\alpha$, is called the "bifurcation ratio"; it is often denoted by R_b. For the rivers in the United States of America, one finds approximately[2]

$$1/\alpha = R_b = 3.5. \tag{5.21-2}$$

HORTON's law was stated above in terms of Strahler segments. However, one can show[3] that, in a system in which the law of stream numbers is satisfied in the Strahler sense, it is also satisfied in the Horton sense and vice versa. We have (the superscript H stands for "Horton", the superscript S for "Strahler"):

$$n_i^H = n_i^S - n_{i+1}^S \tag{5.21-3}$$

since exactly n_{i+1}^S of the n_i^S Strahler segments have been relabelled to get Horton rivers. Thus

$$\frac{n_i^H}{n_{i+1}^H} = \frac{n_i^S - n_{i+1}^S}{n_{i+1}^S - n_{i+2}^S}, \tag{5.21-4}$$

but

$$n_{i+1}^S = \alpha\, n_i^S \tag{5.21-5}$$

because one is *assuming* the validity of HORTON's law. Thus

$$\frac{n_i^H}{n_{i+1}^H} = \frac{n_i^S - \alpha n_i^S}{\alpha n_i^S - \alpha^2 n_i^S} = \frac{n_i^S(1-\alpha)}{\alpha n_i^S - \alpha^2 n_i^s} = \frac{n_i^S(1-\alpha)}{\alpha n_i^S(1-\alpha)} = \frac{1}{\alpha} = \frac{n_i^S}{n_{i+1}^S} \tag{5.21-6}$$

which leads to the same bifurcation ratio for Horton and Strahler streams. Thus it is seen that it does not matter whether one uses Horton rivers or Strahler segments to state HORTON's law of stream numbers.

1. HORTON, R. E.: Bull. Geolog. Soc. Amer. 56, 275 (1945).

2. LEOPOLD, L. B., M. G. WOLMAN, and J. P. MILLER: Fluvial Processes in Geomorphology. San Francisco: Freeman & Co, 1964. See p. 138.

3. SCHEIDEGGER, A. E.: Water Resources Res. 4, 167 (1968)

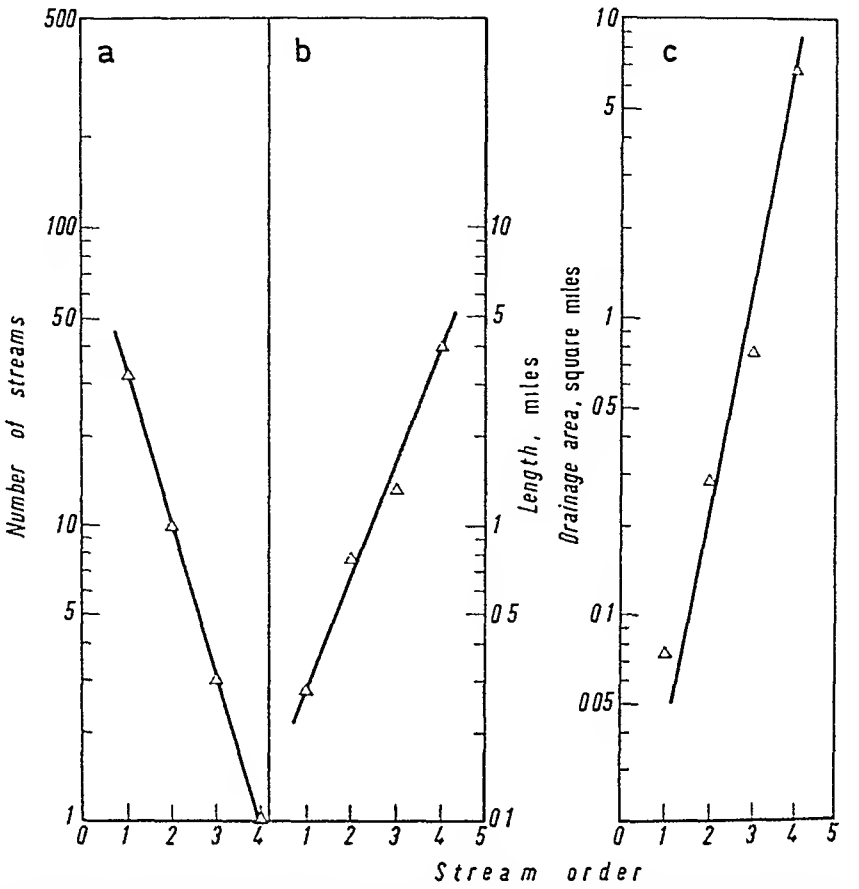

Fig. 130. Horton analysis of a drainage network (Watts Branch, near Rockville, Md., U.S.A.) A Stream numbers, B Stream lengths, C Drainage areas. After LEOPOLD et al.[1]

Based on HORTON's law of stream numbers, one can introduce the notion of a Horton net: this is simply a stream net in which HORTON's law of stream numbers is numerically satisfied.

In order to test whether a given river net is a Horton net, one performs a "Horton analysis"[1]: One plots the logarithm of the observed number of Strahler segments in each order in a drainage basin *versus* the Strahler order; if a straight line is obtained, the net is a Horton net (Fig. 130). It turns out that most river nets are indeed Horton nets.

5.22. The Law of Stream Lengths. A second empirical law due to HORTON[2] refers to some metric properties of river nets: viz. to the lengths of Strahler segments in various orders of a drainage basin. Here, the problem of measuring lengths enters; it is assumed, however, that reference is made to a given map on which the length of the river is simply the length of the corresponding blue line (see Sec. 1.32). Then the law of stream lengths can be stated as follows:

1. LEOPOLD, L. B., M. C. WOLMAN, and J. P. MILLER: Fluvial Processes in Geomorphology. San Francisco: Freeman & Co. 1964.

2. HORTON, R. E.: Bull. Geolog. Soc. Amer. 56, 275 (1945).

The lengths L_i of (STRAHLER) segments of order i in a given drainage basin form, on the average, a geometric sequence, so that

$$L_{i+1}=\beta L_i. \tag{5.22-1}$$

The factor β is called the "length ratio"; it turns out[1] that in nature, the length ratio is on the order of 2.1 to 2.9. Again, it does not really matter whether Horton lengths L^H or Strahler lengths L^S are used; if the length law is satisfied in terms of Strahler segments, then it is also satisfied in terms of Horton rivers[2]. One has evidently in approximation (this is only an approximation, because Horton renumbers the longest, not the average streams):

$$L_i^H \cong \sum_{j=1}^{j=i} L_j^S. \tag{5.22-2}$$

Then, assuming the length law to be valid for Strahler segments, one obtains:

$$\begin{aligned}\frac{L_i^H}{L_{i+1}^H}&=\frac{L_1^S+L_2^S+\cdots+L_i^S}{L_1^S+L_2^S+\cdots+L_{i+1}^S}=\frac{L_1^S(1+\beta+\cdots+\beta^{i-1})}{L_1^S(1+\beta+\cdots+\beta^i)}\\&=\frac{(\beta^i-1)/(\beta-1)}{(\beta^{i+1}-1)/(\beta-1)}=\frac{\beta^i-1}{\beta^{i+1}-1}\sim\frac{1}{\beta}\qquad \text{for } i>1.\end{aligned} \tag{5.22-3}$$

The validity of the length-law can again be tested by making a corresponding "Horton-analysis": one plots the logarithm of the (average) length of (STRAHLER) segments in a river net versus the order; the result is generally more or less a straight line, implying the validity of HORTON's law of stream lengths (Fig. 130).

5.23. The Law of Drainage Areas. A logical extension of the relationships discussed heretofore is obtained if one considers drainage areas. This extension leads to the following law[3]: The areas A_i drained by streams of Strahler order i in a given drainage basin form, on the average, a geometric sequence, so that

$$A_{i+1}=\gamma A_i. \tag{5.23-1}$$

The factor γ is called the area-ratio. For its value, LEOPOLD et al.[4] found, in the United States, approximately 4.8.

1 STRAHLER, A. N.: Quantitative geomorphology. In: Handbook of Applied Hydrology (ed. V T CHOW), see p 4–46 (1964).

2. SCHEIDEGGER, A. E : Water Resources Res. 4, 1015 (1968).

3 SCHUMM, S A.· Bull. Geolog. Soc. Amer. 67, 597 (1956)

4. LEOPOLD, L. B , M. C. WOLMAN, and J. P. MILLER: Fluvial Processes in Geomorphology. San Francisco: Freeman & Co See p. 142 (1964).

With regard to the law of areas, it is clear that it is immaterial whether it is stated with regard to Strahler or Horton orders, because, for whole drainage subbasins, these to concepts are identical.

Again, the law can be tested by making a corresponding "Horton-analysis": The logarithm of the drained area is plotted against the order. The result is generally a straight line, confirming the law of drainage areas (see Fig. 130).

5.24. Dimensional Analysis. Semiempirical relationships between parameters characterizing drainage basins can also be deduced by employing dimensional analysis. One of these attempts[1] has been directed towards the drainage density D.

The variables which must be assumed to affect the drainage density are: (i) The runoff intensity Q, measured as the volume rate of flow per unit area. This quantity Q is the difference between the precipitation per unit of area and time and the infiltration per unit of area and time. It thus has the dimension of a velocity. (ii) The erosion proportionality factor k_e as defined by HORTON[2]. It is the quotient of the mass rate of erosion per unit area and the eroding force per unit area. It thus has the dimension of an inverse velocity. The definition of the "erosional force" is somewhat vague, but it must be understood that, for various landscapes, it ought to be described in an analogous fashion so that the factor k_e will be indicative of the resistance to erosion that is offered by that landscape. (iii) The relief H. It is measured as the total difference of height between the summit in the area and the mouth of a river of a given, pre-selected order (see Sec. 1.53). The relief has the dimension of a length. (iv) The drainage density obviously must also be affected by the density of the fluid ρ (dimension ML^{-3}), the viscosity η of the fluid (dimension $ML^{-1}T^{-1}$) and the gravity acceleration g (dimension LT^{-2}).

Because these are *all* the variables that might interact with each other, there must exist a relationship of the form

$$f(D, Q, k_e, H, \rho, \eta, g)=0. \tag{5.24-1}$$

The usual way to attack this is by assuming that the relation (5.24-1) can be written as follows

$$D^{\alpha_1} Q^{\alpha_2} k_e^{\alpha_3} H^{\alpha_4} \rho^{\alpha_5} \eta^{\alpha_6} g^{\alpha_7}=\text{const}, \tag{5.24-2}$$

with the right-hand side dimensionless. Since there are three dimensions (L, M, T), one obtains three linear equations for the seven alphas; – which means that there are 4 linearly independent solutions. Each linearly independent solution represents a dimensionless number; the latter can

1. STRAHLER, A. N.: Bull. Geolog. Soc. Amer. **69**, 270 (1958).
2 HORTON, R. E.. Bull. Geol. Soc. Amer. **56**, 275 (1945).

be multiplied together with arbitrary exponents to yield a relationship of the required form.

It is thus evident that there must exist 4 independent dimensionless numbers in the present case. The latter may be chosen as follows

(i) $$R_u = HD \tag{5.24-3}$$

which is called the ruggedness number;

(ii) $$H_0 = Q k_e \tag{5.24-4}$$

which is called the Horton number;

(iii) $$R_e = \frac{HQ\rho}{\eta} \tag{5.24-5}$$

which is the well-known Reynolds number; and

(iv) $$F_r = \frac{Q^2}{Hg} \tag{5.24-6}$$

which is the Froude number.

The drainage-density equation must therefore be of the following form:

$$D = \frac{1}{H} f(H_0, R_e, F_r). \tag{5.24-7}$$

The four dimensionless products introduced above establish the criteria for scaling erosional patterns. As usual, scaling does not "explain" what is happening, but it does at least yield a means of determining the course of natural events by providing the means for making model experiments.

An interesting remark which may be made in connection with what was said above, is that HORTON noted that the ruggedness number R_u cannot assume entirely arbitrary values. If ϑ denote the average slope (tangent of slope angle) in the drainage basin under consideration, it turns out that for natural conditions

$$G_e = \frac{R_u}{\vartheta} = \frac{HD}{\vartheta} \sim \frac{1}{2}. \tag{5.24-8}$$

Here G_e is a dimensionless number which has often been called "*geometry number*". The factor 1/2 denotes an order of magnitude only; the actual values of G_e vary from about 0.38 to 1.00.

The relative constancy of the geometry number in natural basins is significant. It indicates, for instance, that if in a given drainage basin the drainage density be increased through removal of the plant cover, the slopes must also become steeper; this will produce the appearance of badlands.

5.3. Theoretical Explanations of the Law of Stream Numbers

5.31. Fundamental Remarks. The empirical laws mentioned above regarding the characteristics of drainage networks have evidently a very fundamental significance. If it is possible to give a rational explanation for the existence of these laws, the crucial phenomena governing the evolution of networks have evidently been explained. Hence much effort has been directed towards obtaining a rational explanation of these laws.

The laws mentioned above are statistical in nature: They make statements about the "average" behavior of a network. Because of this, and because drainage networks are evidently extremely complicated systems, it stands to reason that the methods of statistical mechanics touched upon in Sec. 5.1 will have to be used. Accordingly, one deals with a "system"; in our case with a river net. In this "system", there are "observables": stream numbers, bifurcation ratios etc. The system is so complex that it cannot be described in detail; hence, instead of one system, one considers all possible systems (an "ensemble") which, whithin the limits of one's ignorance, one must consider as equivalent. The expectation value of any observable is simply its average over the ensemble.

Based upon the above general remarks, a variety of probablisitic models for the explanation of the characteristics of river nets has been set up, which we shall discuss below.

5.32. Cyclic Models. HORTON[1] himself, in fact, has already proposed a physical explanation for his law of stream numbers: He assumed that a river net is the result of a regular, cyclic, growth process; internally, elements of the same structure are being built up, i.e. new parts of the drainage net are created with ever the same bifurcation ratio. The result is evidently a "structurally" Hortonian net (Fig. 131a) in which any N-th order stream receives only tributaries of order $N-1$. Each of these successive generations of rivers form a cycle; a cycle is complete when the Strahler order increases by 1.

This picture has been formalized by SCHEIDEGGER[2], based on the idea of branching processes, and by WOLDENBERG[3] based on the idea of allometric growth. Assuming that each cycle is geometrically similar to the previous ones, immediately yields HORTON's law of stream numbers. "Allometric" means that the growth rate of the system is proportional to the size of the system. The outcome of this hypothesis is that stream

1. HORTON, R. E.: Bull. Geolog. Soc. Amer. **56**, 275 (1945).
2. SCHEIDEGGER, A. E.: Water Resources Res. **2**, 199 (1966).
3. WOLDENBERG, M. J.: Bull. Geolog. Soc Amer. **77**, 431 (1966)

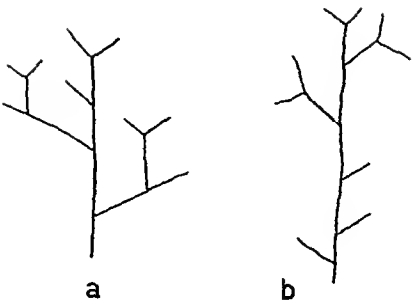

Fig 131 Two river nets with 9 first-order streams, 3 second-order streams, and 1 third-order stream, so that the bifurcation ratio is constant and equal to 3. However, (a) is structurally Hortonian, (b) is not. After SCHEIDEGGER[1]

nets should all be completely regular, i.e. structurally hortonian with constant bifurcation ratio R_b. The network then consists of entirely self-similar cycles. In such regular networks, there is a unique connection between the various characterizations of stream orders, at least for stream links that complete the cycles. Accordingly, WOLDENBERG[2] introduced an "absolute" stream order x

$$x = R_b^{N-1} \tag{5.32-1}$$

where N is the Strahler order and R_b the bifurcation ratio. Obviously

$$x = M = I/2 = R_b^{N-1} \tag{5.32-2}$$

where M is the magnitude and I the associated integer to the consistent order (see Sec. 153). It should be emphasized again, however, that the absolute stream order of WOLDENBERG can *only* be defined for structurally Hortonian networks.

Any deviations from complete structural regularity in a river net are, in the present model, explained away as spurious ("adventitious" streams); – a procedure which is evidently not satisfactory, inasmuch as RANALLI and SCHEIDEGGER[3] have shown, by a careful analysis of the Wabash River basin, that "adventitious streams" form a characteristic part of drainage basins.

5.33. Random Graph Models. As outlined above, it is not at all *a priori* clear that networks grow as has been hypothesized in the cyclic models discussed in Sec. 5.32. "Adventitious" streams seem to be an integral part of river networks and no cyclic models can account for

1 SCHEIDEGGER, A. E.: Water Resources Res 4, 655 (1968)

2. WOLDENBERG, M. J.: Bull. Geolog. Soc Amer 77, 431 (1966).

3. RANALLI, G., and A. E SCHEIDEGGER: Bull. Internat Assoc. Scient. Hydrol 13, No 2, 142 (1968)

them. Thus, different types of stochastic models have been proposed. Such models are based on the assumption that the topology of a network is completely random, i.e. that, for a given number of first order streams, all possible configurations are equally likely in the ensemble.

The idea of using topologically random networks appears to have been introduced for the first time by SHREVE[1]. Unfortunately, however, SHREVE did not then proceed to calculate expectation values of observables, but instead only looked at the most probable configurations and calculated the values of observables therefor. This is not generally a

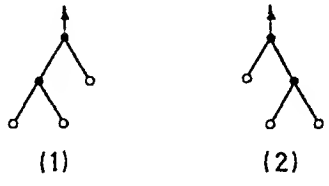

Fig. 132. Graphs of arborescences with 3 free vertices

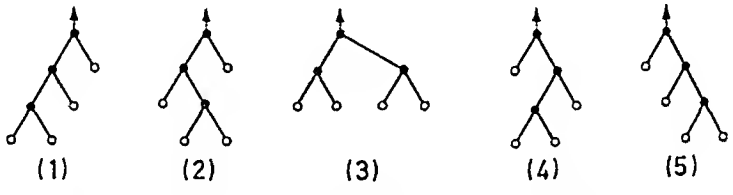

Fig. 133. Graphs of arborescences with 4 free vertices

satisfactory procedure (See discussion in Sec. 5.1). It was then SCHEIDEGGER[2] who first utilized random networks to calculate actual expectation values of such observables as stream numbers, bifurcation ratios etc.

In order to do this, a river network is represented by a special type of topological graph, called a bifurcating arborescence with a root and a given number of free ends[3]. The number N of topologically distinct such graphs with n free ends (first order streams) was first given by CAYLEY[4]. It is

$$N=\frac{1}{2n-1}\binom{2n-1}{n-1}=\frac{1}{2n-1}\binom{2n-1}{n}. \qquad (5.33\text{-}1)$$

As examples, the 2 graphs with 3 first order streams, the 5 graphs with 4 first order streams, the 14 graphs with 5 first order streams and the 42 graphs with 6 first order streams ("free vertices") are shown in Figs. 132–135.

1. SHREVE, R. L.: J. Geol. **74**, 17 (1966).
2. SCHEIDEGGER, A. E.: Proc. Internat. Assoc. Sci. Hydrol. Berne Meeting, vol. "Hydrological Aspects of the Utilization of Water", p. 415 (1967).
3. See e.g. BERGE, C.: Théorie des graphes et ses applications. Paris: Dunod, 1958.
4. CAYLEY, A.: Phil. Mag. **18**, 374 (1859).

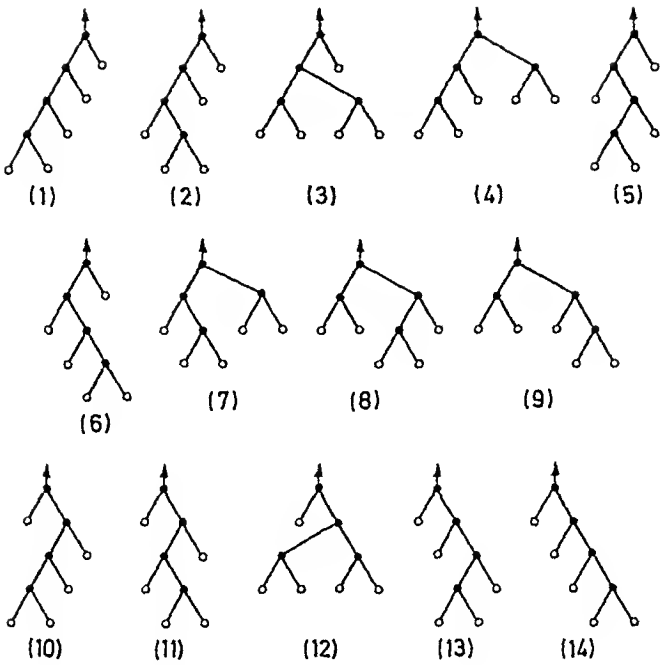

Fig 134. Graphs of arborescences with 5 free vertices

It is evident that the number N gets rapidly very large as the number n of first order streams increases. It is therefore not easily possible to enumerate the ensembles in question for the calculation of expectation values of observables. However, it is possible to random-generate (Monte Carlo technique) a representative sample of the ensembles required on a computer and to calculate the necessary expectation values thereform[1]. In order to do this, a representation of the graphs in question that is suitable for a computer is required. For this purpose, one best uses the Lukasiewicz representation of arborescences[2], in which a bifurcating arborescence, with its root at the top, is "read" from the top to the bottom and left to right, setting 1 for each junction and 0 for each first order stream (Fig. 136). Thus, a graph of n free ends is uniquely represented by a "word" consisting of n zeros and $n-1$ ones. Conversely, any word of n zeros and $n-1$ ones represents a rooted, bifurcating arborescence; in order to get the direct correspondence with the Lukasiewicz representation, a cyclic permutation in the word may be required. Thus, by random-generating words of the above type, river nets can be computer-generated.

1. Liao, K. H., and A. E. Scheidegger: Bull. Internat. Assoc. Sci. Hydrol. 13, No 1, 5 (1968).

2. Berge, C.: Théorie des graphes et ses applications. Paris: Dunod 1958.

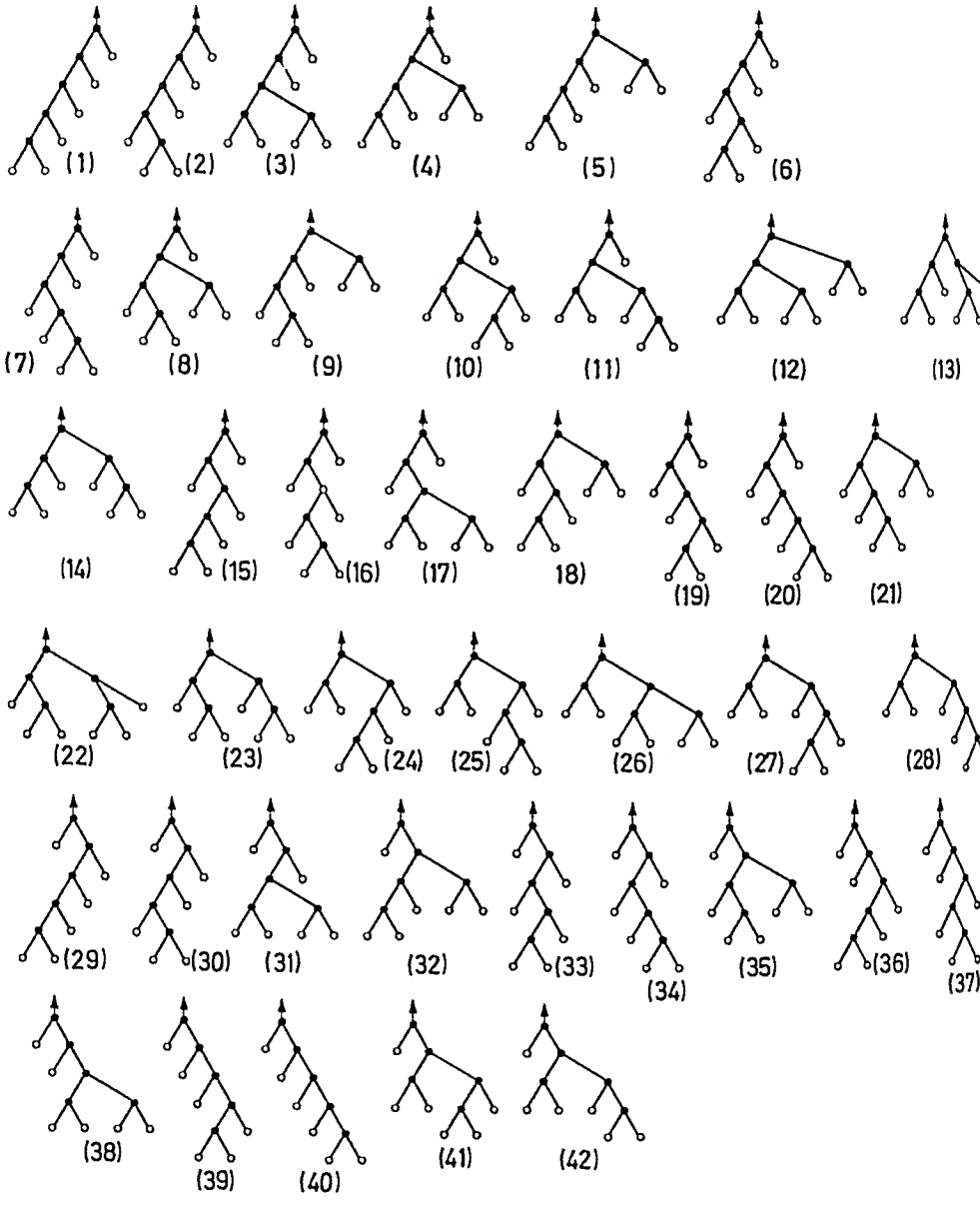

Fig. 135. Graphs of arborescences with 6 free vertices

The above technique has been used by LIAO and SCHEIDEGGER[1] to at least sample-generate the ensembles in question up to 500 ends and to calculate expectation values for stream numbers in various Strahler orders. The results are displayed in Table 10. It is seen that HORTON's law of stream numbers is fairly well satisfied, at least if a river net of a given order is fully developed. It is not surprising that discrepancies occur when a new order just starts to appear, inasmuch as the sampling

1. LIAO, K. H., and A. E. SCHEIDEGGER: Bull. Internat. Assoc. Sci. Hydrol. 13, No. 1, 5 (1968).

Table 10. *Results for random graph model of river net* (after LIAO and SCHEIDEGGER[1])

Number of first order streams	Number of segments, in Strahler order							Bifurcation Ratio R_b					
	1	2	3	4	5	6	7	$i=1$	2	3	4	5	6
3	3.00	1.00						3 00					
4	4.00	1.40	0.40					2 86	3 50				
5	5.00	1.50	0 50					3 33	3 00				
6	6.00	1.62	0 60					3 70	2 72				
7	7.00	1.86	0.70					3.77	2.66				
8	8.00	2.24	0 88	0.002				3.57	2 53	378.00			
9	9.00	2 43	0 94	0.014				3.70	2.57	67.43			
10	10 00	2.61	0.96	0 02				3 83	2.72	48.00			
12	12.00	3.18	1.07	0.08				3.78	2 98	12 88			
14	14.00	3.64	1.16	0.16				3.85	3.13	7.09			
16	16.00	4.13	1 25	0 25				3.88	3.29	5.03			
18	18.00	4.68	1.35	0.34				3 85	3.45	3.97			
20	20 00	5.11	1.46	0.43				3 91	3 50	3.39			
30	30.00	7.62	2 06	0.79	0.004			3.94	3 70	2.61	202.36		
80	80.00	20.20	5.10	1.50	0.46			3.96	3.96	3.40	3.26		
200	200.00	50.06	12.75	3.31	1.09	0.10		3.99	3 93	3.85	3.04	10.67	
500	500.00	129.78	31.39	8.00	2.06	0 80	0.01	4.01	3 98	3.92	3.88	2 58	120 00

1. LIAO, K. H , and A. E. SCHEIDEGGER· Bull. Internat. Assoc. Sci. Hydrol. **13**, No. 1, 5 (1968)

procedure is then felt. Although HORTON's law is fairly well satisfied, there are systematic deviations inasmuch as R_b decreases somewhat with stream order. This is also observed in nature.

The Monte Carlo results given above were somewhat improved upon by SMART[1] by using an implicit exact formula to make the required calculations. However, the computing effort in this connection is large and SMART had to stop at 80 free ends.

The random graph theory also allows one to obtain a model for the *evolution* of a river net[2]. One simply assumes that a network grows by a given rate of capture of first-order streams. Thus, the following questions may be asked:

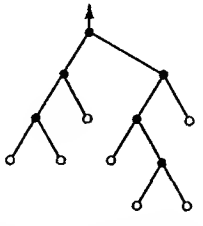

Fig. 136. Graph corresponding in Lukasiewicz representation to the word (1 1 1 0 0 0 1 1 0 1 0 0 0)

First, given the rate of capture $\dot{n}_1(t)$ of first order streams, what is the evolution of the structure of the network, i.e. what are the expectation values $n_i(t)$ in terms of $n_1(t)$, $\dot{n}_1(t)$?

Second, if a particular model for $\dot{n}_1(t)$ is adopted, e.g.

$$\dot{n}_1 = k n_1 \tag{5.33-2}$$

what is *then* the (expected) evolution of the structure of the network?

Table 10 immediately answers, in tabular form, the first of our questions. The first column corresponds to the "size" of the network, given by $\int \dot{n}_1(t)\, dt$. One can, therefore, immediately read off the increase in the expectation values n_i for a given increase in n_1. The maximum Strahler order is also determined from that table.

Turning to the second question, the assumption of (5.33-2) leads, upon integration, to

$$n_1(t) = e^{kt}. \tag{5.33-3}$$

The most visualizable way to describe the result is simply by plotting the values of Table 10 on semilogarithmic paper (logarithmic with regard to n_1). Since the growth in time of n_1 is given by an exponential function, equal distances on the (logarithmic) axis will simply present growths of $n_2 \ldots n_i$ in equal time intervals. This has been done in Fig. 137.

1. SMART, J. S.: Bull. Internat. Assoc. Scient. Hydrol. **13**, No. 4, 61 (1968).
2. SCHEIDEGGER, A. E.: Bull. Internat. Assoc. Scient. Hydrol. **15**, No. 1 (1970).

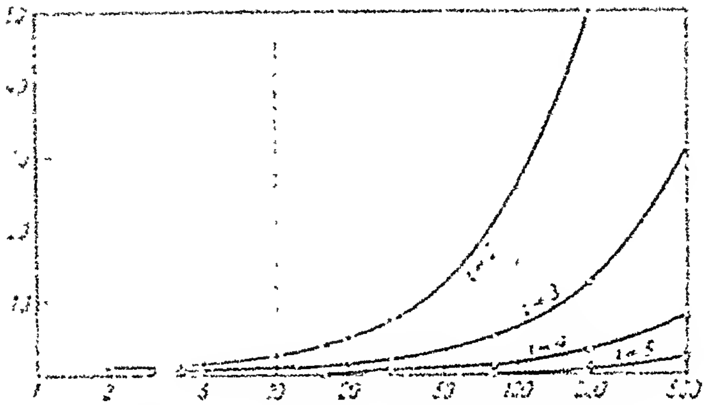

Fig. 137. n_1 as a function of n_1 (After Schmidt[illegible])

5.34. Other Models. Reviewing the stochastic models proposed for the explanation of the law of stream numbers, one might well ask himself whether models other than the two discussed are also possible. This question can be answered as follows.

Essentially, what one has for river nets is a "growth" process that leads to the final configuration which, then, is observed in nature. The "influences" that affect the final configuration are manyfold. What are now the possibilities for the structure of the final configuration? Clearly, either there are substructures ("cells" or "cycles") or there are none. In principle, the probability distribution in each cell could be anything. However, if one assumes many fluctuating influences that are (at least asymptotically) independent and additive, then the central limit theorem of probability theory ascertains that the system will have a Gaussian distribution; a special case thereof is a constant distribution. Modifications are possible only by introducing autocorrelation.

An inspection of the river net models given above shows that the two basic possibilities of constructing models have indeed been used up. Possible modifications are only obtained if one assumes that the probability distribution is Gaussian rather than constant in each (or the only) cycle, or the possibility of a change of the mean (autocorrelation) from cycle to cycle.

Thus it is clear that the two types of models discussed above for the explanation of Horton's law of stream numbers are essentially the only ones that are possible, except for minor modifications.

5.35. Test of Models with Nature. The theories given above purporting to explain Horton's law of stream numbers give correct results, i.e. the correct bifurcation ratio. However, before accepting any of these

[illegible] Bull. Internat. Assoc. Sci. Hydrol. 15, No. 4 (1970)

[illegible]

theories, one must test the validity of the basic hypotheses in nature. This alone will permit one to decide as to which is the truly correct explanation of HORTON's law of stream numbers.

In order to test the basic assumptions of the various theories given above, RANALLI and SCHEIDEGGER[1] made an investigation of the Wabash River system, choosing a root point near Terre Haute, Indiana. In order to test the law of stream numbers, a Horton analysis, plotting the stream numbers n_N against order N, was made, as reproduced here in Fig. 138. The highest order river obtained was of order 6. The Horton analysis

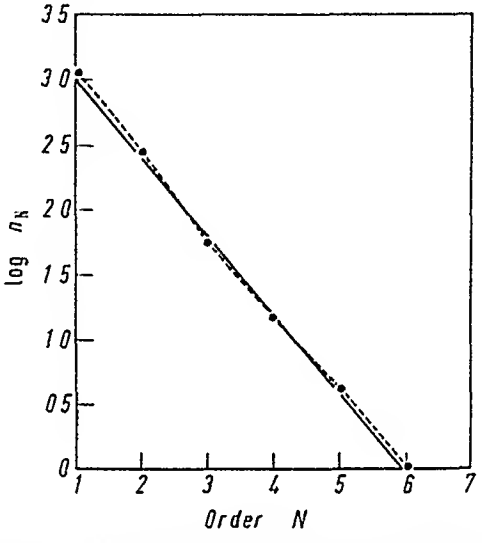

Fig. 138. Wabash river system, Horton diagram. (After RANALLI and SCHEIDEGGER[1])

yielded a bifurcation ratio $R_b = 4.088$, a little higher than common of U.S. river basins. An inspection of Fig. 138 yields that HORTON's law of stream numbers is well satisfied.

The next problem was to investigate the structure of the net. For a structurally regular (cyclic) Horton net, Eq. (5.32-2) has to be satisfied, which may also be written

$$m = 1 + (N-1)\log_2 R_b \tag{5.35-1}$$

where m is the consistent and N the Strahler order. This can be further transformed to

$$\Delta S = [(R_b - 1)/\log_2 R_b]\,\Delta m \tag{5.35-2}$$

where ΔS is the number of junctions required to increase the consistent order by Δm. In a regular net, $\Delta S/\Delta m$ is constant. The result of plotting this relation is shown in Fig. 139, which clearly indicates that $\Delta S/\Delta m$ is not constant so that the Wabash system clearly turns out to be not cyclic.

1. RANALLI, G., and A. E. SCHEIDEGGER: Bull. Internat. Assoc. Sci. Hydrol. 13, No. 2, 142 (1968).

Finally, a test for the randomness of interconnections in subbasins with 4 ends was made. The five possibilities denoted by (1) to (5) in Fig. 133 occur with the following relative frequencies: (1) 18.92%, (2) 21.62%, (3) 21.62%, (4) 18.92%, (5) 18.92%. This clearly indicates topological randomness, as assumed in the random graph theory.

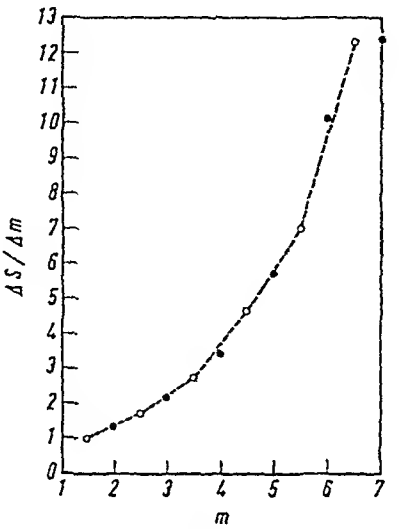

Fig. 139. Wabash river system, number of junctions per constant change in consistent order vs. consistent order. After RANALLI and SCHEIDEGGER[1]

Thus, the investigation of the Wabash River net by RANALLI and SCHEIDEGGER shows that the random-topology explanation of HORTON's law of stream numbers is correct in at least that case. On the other hand, the cyclic model does not seem to be applicable, inasmuch as river nets, in nature, do not seem to be structurally Hortonian: Adventitious stream appear to be part and parcel of natural networks and cannot be ignored.

5.4. Theoretical Explanations of the Law of Stream Lengths

5.41. General Remarks. We turn now to the possibilities of giving a rational explanation to HORTON's law of stream lengths. One attempts, of course, to use analogous models as before, but now one has to introduce at some stage or other a *metric* assumption; previously, one was dealing *with topology alone.*

Thus, the explanation will be based on the previous possibilities: cycle theory and random graph theory, *plus* some metric assumption.

1. RANALLI, G., and A. E. SCHEIDEGGER: Bull. Internat. Assoc. Sci Hydrol. 13, No. 2, 142 (1968).

5.42. Cycle Theory. The cycle theory, with the allometric growth assumption implying geometrical self-similarity between cycles, leads immediately to HORTON's law of stream lengths[1]. This can be formalized as follows[2]. Denoting the stream length of order i by L_i, self-similarity implies

$$\frac{L_{i+j+k}}{L_{i+k}} = \frac{L_{i+j}}{L_i} \qquad \text{for all } i, k. \tag{5.42-1}$$

Setting $j=k=1$ yields

$$\frac{L_{i+2}}{L_{i+1}} = \frac{L_{i+1}}{L_i} = \text{const} = \beta \tag{5.42-2}$$

and hence

$$\frac{L_{i+k+1}}{L_{i+k}} = \frac{L_{i+1}}{L_i} = \beta \tag{5.42-3}$$

for all i, which implies a geometric sequence (HORTON's law) for L_i. Thus, if the allometric growth idea is correct, HORTON's law of stream lengths is the automatic outcome. Furthermore, it turns out that the following relationship should hold[3] between the length ratio β and the bifurcation ratio R_b

$$\beta = R_b. \tag{5.42-4}$$

However, this relationship is not borne out in nature. Furthermore, cyclic models for the explanation of the law of stream lengths can be invoked only if river nets in nature are truly cyclic. Since this does not seem to be the case, a different explanation for the law of stream lengths must be sought.

5.43. Random Graph Theory. The random graph theory employed in connection with the law of stream numbers can be applied to the law of stream lengths provided a metric assumption is introduced. Evidently, the simplest such assumption is to assume that each link length in the graphs is constant; for simplicity's sake this link length may be taken as equal to 1.

With this assumption, it is then possible to calculate the expectation values for lengths of Strahler segments in the various orders in network ensembles with a given number of first order streams. This is not an easy task, and is best approached again by a Monte-Carlo technique of sampling the ensembles in question and calculating the expectation

1. WOLDENBERG, M. J.: Bull. Geolog. Soc. Amer. 77, 431 (1966).
2. SCHEIDEGGER, A. E.: Water Resources Res. 4, 1015 (1968).
3. SCHEIDEGGER, A. E.: Water Resources Res. 2, 199 (1966).

values on such samples. The problem was solved by LIAO and SCHEIDEGGER[1]; the result, up to networks with 1000 first order streams, is shown in Table 11.

It is clear that HORTON's law of stream lengths is approximately satisfied, but only in the headwater region. In the lowest orders, the stream length ratio starts from an asymptotie value of two whieh had already been found by SHREVE[2] for "infinite" networks, inereases somewhat, and then deereases to values well below one.

5.44. Comparison with Nature. We have already shown with regard to the law of stream numbers that the eyele theory does not eonform to the facts of nature. Hence it eannot be expected to be adequate with regard to stream lengths either, and one must eoneentrate on the random graph theory. This was done by GHOSH and SCHEIDEGGER[3], who found that the metrie assumptions made above are evidently too simple. There are two ways by which one ean change the metrie assumption: first, by assuming that the mean link lengths in all orders are the same, but that

Table 11. *Theoretical stream lengths and drainage areas in Horton nets of various orders (after* LIAO *and* SCHEIDEGGER*)*

Order	Av. length	Ratio	Av. drainage area	Ratio
Number of free vertices 20				
1	1.00		1.00	
		2.04		5.09
2	2.04		5.09	
		2.38		4.80
3	4.85		24.45	
		0.60		1.60
4	2.92		39.00	
Number of free vertices 30				
1	1.00		1.00	
		2.03		5.06
2	2.03		5.06	
		2.34		4.74
3	4.74		23.99	
		1.00		2.44
4	4.74		58.52	
		0.44		1.01
5	2.08		59.00	

1. LIAO, K. H., and A. E. SCHEIDEGGER: Water Resources Res. 5, 744 (1969).
2. SHREVE, R. L.: J. Geol. 75, 178 (1967).
3. GHOSH, A. K., and A. E. SCHEIDEGGER: Water Resources Res. 6, No. 1 (1970).

Table 11 (continued)

Order	Av. length	Ratio	Av. drainage area	Ratio
Number of free vertices 50				
1	1.00		1.00	
		2.02		5 05
2	2.02		5.05	
		2.12		4 41
3	4.29		22.27	
		1.89		3.97
4	8.09		88.50	
		0.40		1.12
5	3.21		99.00	
Number of free vertices 75				
1	1.00		1.00	
		2.01		5 02
2	2.01		5.02	
		2.05		4.31
3	4.13		21.65	
		2.35		4 61
4	9.70		99.79	
		0.56		1.49
5	5.41		149.00	
Number of free vertices 100				
1	1.00		1.00	
		2.00		5.00
2	2.00		5.00	
		2.06		4.30
3	4.12		21.52	
		2.34		4.62
4	9.65		99.35	
		0.79		2 00
5	7.59		198.36	
		0.36		1.00
6	2.75		199.00	
Number of free vertices 200				
1	1.00		1.00	
		1.99		4.97
2	1.99		4.97	
		2 06		4.28
3	4 10		21.27	
		2.03		4 26
4	8.34		90.52	
		2.08		3.97
5	17.35		359.77	
		0.36		1.11
6	6.25		399.00	

Table 11 (continued)

Order	Av length	Ratio	Av. drainage area	Ratio
Number of free vertices 500				
1	1.00		1.00	
		1.99		4.99
2	1.99		4.99	
		2.00		4.19
3	4.00		20 97	
		2.03		4.19
4	8.14		87.97	
		2 24		4 21
5	18 29		370 03	
		0 96		2 67
6	17.58		987.63	
		0 06		1 01
7	1.00		999 00	
Number of free vertices 1000				
1	1.00		1 00	
		1 99		4.98
2	1.99		4.98	
		2 00		4.20
3	4.00		21 00	
		2.03		4.12
4	8 13		86 60	
		2.04		4 00
5	16.57		346 35	
		2.08		4 29
6	34.98		1486.47	
		0.54		1.34
7	19 11		1999.00	

they are drawn from a somewhat lopsided population. Thus SHREVE[1] assumed that the link-lengths are subject to a log-normal distribution, but he also took different distributions for "exterior" and "interior" links. A more consistent application of this idea leads to the second possibility, which is to presuppose that the link lengths depend on Strahler order. This was consistently carried through by GHOSH and SCHEIDEGGER[2] who analyzed a series of networks on this basis and found that there is a definite increase of link length with Strahler order. This seems to be a natural law. The analysis was carried out by comparing the observed lengths of Strahler segments in natural networks with the theoretical values given in Table 11. Then, a matching of the observed and theoretical results can only be obtained by increasing the link lengths with order,

1 SHREVE, R. L.: J. Geol. 75, 178 (1967)

2. GHOSH, A K , and A. E. SCHEIDEGGER· Water Resources Res 6, No. 1 (1970).

Table 12. *Relation between link length E and stream order i (after* GHOSH *and* SCHEIDEGGER[1]*)*

Name of the basin	E_1	E_2	E_3	E_4	E_5	E_6	Link length ratio
Perth Amboy, N.J.	1	2 01	5.81	19.49	20.29		2.29
Chileno Canyon, Calif.	1	2.67	5.82	12.81	29.73		2.34
Mill Dam Run Basin, Md.	1	2.43	4.87	13.99	20.62		2.19
Tar Hollow, Ohio	1	1.21	3.65	3.82			1.74
Home Creek, Ohio	1	1.33	1.64	1.40	5.05		1 39
Mill Creek, Ohio	1	1.36	2.27	1.78			1 26
Green Lick, Pa.	1	1.52	4.56	3.02			1.55
Beech Creek, Ohio	1	1.12	1.56	1.83	2.59		1.26
Piney Creek, Md.	1	1.29	1.78	2.14	2.81		1.29
Casselman River, Md.	1	0.95	1.04	1.30	2.11	2.15	1.20
Emory River, Tenn.		1.00	1.40	2.00	2.65	2.80	1.30
Youghiogheny River, Md.		1.00	1.39	1.87	2.02	0.84	1.10
Daddy's Creek, Tenn.		1.00	1.18	1.30	1 26	1.42	1.10
Little Mahoning Creek, Pa.	1	1.64	2.21	2.60	2 65	6.74	1.38
Alleghony River, Pa.			1.00	1.55	2.19	3.05	1.45
Skin Creek, Pa.	1	0.78	0.73				
Black Water River, Pa.	1	1.53	1.58				1.26
Middle Fork, Pa.	1	1.80	3.09				1.78
Clear Creek, Ia.		1.00	1.05	1.79	0.92		1.04
Old Man Creek, Ia.			1.00	1.57	1.51	3.24	1.42

rather than assuming the latter to be constant and equal to 1. The results, showing the link lengths L_i required in Strahler orders i for a series of rivers, obtained by GHOSH and SCHEIDEGGER, are shown in Table 12. Accordingly, it is found that the link length always has a tendency to increase geometrically with the Strahler order. This leads to the conclusion that there really exists a *law of link lengths* similar to the laws of streams numbers etc. The link length ratios, according to GHOSH and SCHEIDEGGER[1], vary between 1.04 and 2.34.

5.5. Theoretical Explanations of the Law of Drainage Areas

5.51. Types of Explanations. The methodology for finding rational explanations of the law of drainage areas is exactly the same as with the law of stream lengths[2]: one has the cycle theory and the random graph theory, into which a metric assumption has to be introduced.

5.52. Cycle Theory. Again, the self-similarity between cycles yields immediately the required law. However, one must note that, in complete

1. GHOSH, A. K., and A. E. SCHEIDEGGER: Water Resources Res. **6**, No. 1 (1970).
2. SCHEIDEGGER, A. E.: Water Resources Res. **4**, 1015 (1968).

geometrical similarity, one has to have

$$\gamma^{\frac{1}{2}}=\beta \tag{5.52-1}$$

where, as before, γ is the area-ratio and β the length ratio. The above relation is not borne in nature. SMART and SURKAN[1] found

$$\gamma^{n}=\beta \qquad \text{with } n>\tfrac{1}{2}. \tag{5.52-2}$$

This is again an indication of the inadequacy of the cycle theory.

5.53. Random Graph Theory. In order to extend the random graph theory to the law of drainage areas, one needs again a metric assumption. The simplest such assumption is again that each link (of length L) drains an area proportional to L^2. One does not now have the simple relationship (5.52-1) above, but must figure out the actual relationship from the ensemble of graphs in question. The problem was again solved by LIAO and SCHEIDEGGER[2] by using a Monte Carlo technique; the results are shown in Table 11. As is seen, the law of drainage areas comes approximately out of the theory.

However, as with the length law, it is seen that the area law as well is only satisfied in the headwater region of a large, finite, network. The drainage area starts around 5 and then decreases towards 1.

Table 13. *Relation between areas drained F_i by a Link and Stream order 1 (After* GHOSH *and* SCHEIDEGGER[3]*)*

Name of the basin	F_1	F_2	F_3	F_4	F_5	F_6	F_7
Perth Amboy	1	0 81	1.36	1.95	1 04		
Chileno Canyon	1	1.04	1 09	1.19	1.39		
Mill Dam Run	1	0.65	0.71	1.05	0.66		
Tar Hollow	1	0.76	1.12	1.36			
Home Creek	1	0.58	0 62	0 39	0.78		
Mill Creek	1	0 97	1.08	1.07			
Green Lick	1	0.59	1.16	1.11			
Beech Creek	1	0.63	0.57	0.52	0 76		
Piney Creek	1	0.97	1.02	0.76	1 87		
Casselman River	1	0.89	0 94	0.70	1.40	1.37	
Emory River		1.00	0.99	0.90	1 57	0 87	0 80
Youghiogheny River		1.00	0.94	0.52	2.09	1.62	
Daddy's Creek		1.00	0.67	0.95	1.60	1.67	
Little Mahoning	1	0.99	0 95	1.07	1 27	2.09	
Alleghony River			1 00	1.41	1.86	3.15	1.72
Clear Creek		1.00	0 89	1.26	0.90		
Old Man Creek			1.00	1.18	0 91	1 16	

1 SMART, J. S., and A. J. SURKAN: Water Resources Res. 3, 963 (1967)
2. LIAO, K. H., and A. E. SCHEIDEGGER: Water Resources Res. 5, 744 (1969)
3. GHOSH, A. K., and A. E. SCHEIDEGGER: Water Resources Res. 6, No. 1 (1970).

5.54. Comparison with Nature. Finally, the theory must again be compared with nature. GHOSH and SCHEIDEGGER[1] analyzed the drainage areas of a series of river networks and compared the observed values with the theoretical ones given in Table 11. The results are shown in Table 13. It was found that the areas drained by each link are indeed constant, independently of the Strahler order of the link in question. This is somewhat startling, inasmuch as the length of the links does increase with Strahler order, contrary to the drained areas. This can only be explained by assuming that the sinuosity of the rivers increases with Strahler order.

Thus, all in all, the random graph theory appears to give a correct and adequate explanation of HORTON's laws: Networks simply evolve topologically random. Thus, of all the possibilities by which N first order streams can be connected, all theoretical possibilities are equally likely, at least in areas where relatively little geological control is present.

5.6. General Remarks on Stochastic Models

5.61. Growth Models. The stochastic models of river nets (Sec. 5.34) that have been discussed above are, in fact, absolutely general, and can be applied to all kinds of "systems".

Thus, we have shown that two types of models are possible: (i) a cyclic model (the system has "cells") and (ii) a random configuration model (the system consists of a single cell). As was shown above, there are no other models possible, except under very queer circumstances: If the evolution of the system is caused by many independent additive influences, the central limit theorem of probability theory asserts that the probability distribution is Gaussian around some mean. This was shown in Sec. 5.34 to apply to the topology of river nets, but it is obvious that the argument is independent of the interpretation of the "system" as a "river net".

5.62. The Steady State. Of particular importance is the investigation of a system in a steady state[2]. We assume that we are interested in an observable X, which is measured at a series of times $t_1, t_2, \ldots, t_i, \ldots$. The values obtained

$$X_i = X(t_i) \tag{5.62-1}$$

are called a "time series". An important question is that of extrapolation from a (finite) set of measurements to the future.

The configurations of the system at the times $t_1, t_2, \ldots, t_i, \ldots$ form an "ensemble". The expectation value of any observable is, as usual, simply

1 GHOSH, A. K., and A. E. SCHEIDEGGER: Water Resources Res. 6, No. 1 (1970).

2. SCHEIDEGGER, A. E.: Water Resources Res 6, in press (1970).

the average over this ensemble. In this connection, the ergodic hypothesis implies that, in a steady state, the ensemble of all possible configurations of the system at a given time is identical to the ensemble obtained by watching the system evolve through all times $t_1, t_2, \ldots, t_i, \ldots$. The ergodic hypothesis is justifiable under very broad conditions.

5.63. Brownian Conditions. We assume now that the influences that cause the fluctuations of the system are many, independent and additive. These assumptions are said to produce "Brownian" conditions, from the analogous case occurring in Brownian motion. The random variable (the observable) is denoted by $X(t)$ as above. One can then introduce the cumulative random variable:

$$x(t) = \int_{\text{const}}^{t} X(t)\, dt. \tag{5.63-1}$$

Then, under Brownian conditions, the distribution of X is Gaussian around some mean, and for the cumulative variable x the following relation holds:

$$\overline{(x-\bar{x})^2} = D\,t \tag{5.63-2}$$

where D is some constant.

5.64. Correlation. The above scheme can be modified by assuming that the influences are not independent, but are correlated. Then one can introduce the correlation function $C(s)$ for the random variable X:

$$C(s) = \frac{1}{\overline{X^2}} \int_0^{\infty} X(t)\, X(t+s)\, dt. \tag{5.64-1}$$

The correlation time is then defined as follows:

$$L_t = \int_0^{\infty} C(s)\, ds \tag{5.64-2}$$

assuming that the integral converges. Then, one has the following results:

(i) The original random variable X is still Gaussian (ultimate independence of the "influences", if one waits long enough).

(ii) For the cumulative variable x one has the following relations:

$$\overline{x^2(t)} \quad \text{proportional to } t \text{ for} \quad t \gg L_t \tag{5.64-3}$$

$$\overline{x^2(t)} \quad \text{proportional to } t^2 \text{ for} \quad t \ll L_t. \tag{5.64-4}$$

Thus, the behavior of the "cumulative" dispersion is bracketed between proportionality to t^2 (short times) and proportionality to t (long times).

5.65. Infinite Correlation Time. If the integral defining L_t (5.64-2) diverges, it is not possible to carry out the scheme outlined in the last section. In this case, the formalism can be salvaged, as outlined by MANDELBROT[1], by assuming that the time-series is entirely self-similar, for large and small time intervals. Then, one has for the cumulative variable x

$$\overline{x^2} \text{ proportional to } t^{2H}, \text{ with } \tfrac{1}{2} \leqq H \leqq 1 \qquad (5.65\text{-}1)$$

for large and small (i.e. *all*) times t. The quantity H has been called "Hurst-parameter", after HURST[2] who observed empirically such behavior in floods. However, if this argument is carried to short time intervals, the time-oscillations of $X(t)$ become so rapid that one has no longer a differentiable sequence (ultraviolet catastrophe). Also, physically there appears to be no reason for similarity between micro-fluctuations and secular fluctuations. The self-similar models of statistical time-series proposed by MANDELBROT, therefore, require, to say the least, a lot more substantiation.

5.66. Evaluation[3]. Of the models discussed above for the representation of time series, the simplest is evidently that corresponding to Brownian motion with an appropriately chosen correlation time L_t (the so-called Gauss-Markov model). This yields for the cumulative variable a dispersion proportional to t^{2H} with H between $\frac{1}{2}$ and 1. This is just, in fact, what is observed in nature.

To extrapolate beyond the time range over which measurements have been made, or to intrapolate into the intervals between the individual measurements, one has to proceed from a reasonable *physical* assumption. To simply postulate self-similarity for the series and extrapolate to infinitely long and to intrapolate to infinitely short time intervals seems physically absurd, as evidenced by the "ultraviolet catastrophe" mentioned above.

The model of hydrological phenomena that is physically most reasonable is therefore one of additive random events causing fluctuations in some observable. These events may be correlated by a series of effects with appropriate correlation time ranges L_t. The value of H for some time range T under investigation is empirically found, and the educated guess is then made that H does not change appreciably for an additional time interval of the size of maybe $T/2$. With this value of H, therefore, a cautious extrapolation can be made.

1. MANDELBROT, B : C.R. Acad. Paris **260**, 3274 (1965).
2. HURST, H. E.: Proc. Inst. Civil Engrs. Part I, 519 (1956).
3. SCHEIDEGGER, A. E.: Water Resources Res. **6**, in press (1970).

5.7. The Stochastic Simulation of Landscapes

5.71. The Idea. We have seen above that stochastic models have been very useful in explaining landscape evolution. The schemes presented let one actually predict the expectation values for certain observables.

The schemes can be further exploited by actually simulating numerically the evolution of the various systems in question instead of only predicting average values[1]. Some examples will illustrate this.

5.72. Random Model of a Stream Network. Beginning with a series of points 1 inch apart on a sheet of paper, LEOPOLD and LANGBEIN[2] constructed random walks by restricting the motion to steps to the right, left and forward (with equal probability). The several random walks were continued until junctions, representing confluences of rivers, were obtained. The random walk of the joined rivers was then continued;

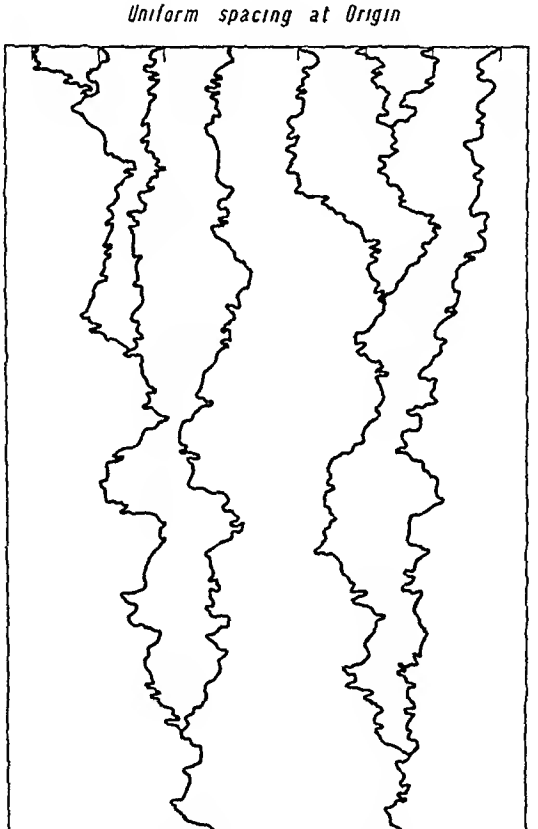

Fig. 140. Random-walk model of stream network. After LEOPOLD and LANGBEIN[2]

1. SEGINER, I.: Water Resources Res *5*, 591 (1969).
2. LEOPOLD, L. B., and W. B. LANGBEIN: U.S. Geolog. Survey Profess Papers *500A*, A 1 (1962).

the pattern obtained by LEOPOLD and LANGBEIN is reproduced here in Fig. 140. Evidently, the pattern is very reminiscent of a natural stream network. One can draw Horton diagrams for the observed patterns; the latter bear out the validity of HORTON's laws and therefore of the modeling procedure.

Similar drainage patterns were also produced on a computer by SMART and coworkers[1], by SEGINER[2] and by SCHENCK[3].

5.73. Intramontane Trench. When an essentially straight, primary valley runs roughly parallel to a continental divide, the total drainage area can be subdivided into first, second ... order "areas", ending with "valley sectors" (Fig. 141). [GERBER's[4] classification.]

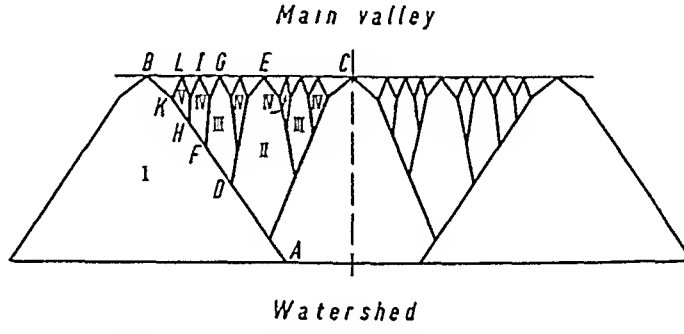

Fig. 141. GERBER's[4] scheme for the ordering of drainage areas. The smallest triangles touching the main valley are the "valley sectors"

On the north side of the Rhone Valley in the Canton of Wallis, Switzerland, there are 9 first-order, 6 second-order, 2 third-order, 2 fourth-order drainage basins and 18 valley sectors. With these numbers, it is possible to make an analysis in terms of a probabilistic model[5].

As an abstract model of the physical processes that are involved we assume that the formation of landforms is solely due to fluvial erosion. We further suppose that the drainage occurs in the manner of a random walk. We thus that the drainage in a unit step (time interval) is always "forward" (toward the main valley), but that it may randomly go one-half unit to the left or to the right. Thus, it is possible to model the drained strip by a grid of points; the points are arranged in rows where each subsequent row is displaced sideways by one-half of the lattice distance with regard to the former row. For the drainage of each

1. SMART, J. S., A. J. SURKAN, and J. P. CONSIDINE: General Assembly, Internat. Assoc. Scient. Hydrol., Bern, Vol. "on river morphology", p. 88 (1967).
2. SEGINER, I.: Water Resources Res. 5, 591 (1969).
3. SCHENCK, H.: J. Geophys. Res. 68, 5739 (1963).
4. GERBER, E.: Morphologische Untersuchungen im Rhonetal zwischen Oberwald und Martigny. E. T. H. Zürich, Arb. Geogr. Inst. No. 1 (1944).
5. SCHEIDEGGER, A. E.: Bull. Internat. Assoc. Sci. Hydrol. 12, No. 1, 15 (1967).

grid point there are two possibilities: to the nearest downward point to the left or to the right. The choice as to which of the two possibilities actually takes place is completely random. The grid, the "down" direction, and the possible choices (these may take place at each point) are illustrated in Fig. 142.

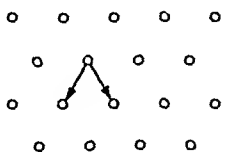

Fig. 142. The model grid showing the possibilities for each drainage point. After SCHEIDEGGER[1]

The simplest way for a deduction of the drainage patterns induced by the stochastic process described above is by simulating the latter directly on a computer (Monte Carlo method). Accordingly, random numbers were generated on a computer. The computer was instructed to print "1" when the number was larger that the mean, "0" when it was smaller. Twenty rows of 50 numbers each were printed, subsequent rows were staggered by one character so as to make the correspondence with the grid of Fig. 142 evident. The result is shown in Table 14.

Table 14. *Random numbers for model of trench. (After* SCHEIDEGGER[1]*)*

00101100100001010101111001101010110000011010110111110
10011010101101110010111101111100000111011010010000011001010110011111010000000001
01011110000000110110011000010101010111111100110101111110101111011000010
11001000011011111011101100110100001011111111110101001000101001011010110011000011000
11110010001101111010000111111001101010111101110110110011011001010011101
10001000010001010001111111001111110000101001000110001000111000010100
10010100111110000010110100110110010011100111111110111111111000101111
00010101010101010110110000001100010111010100001000011001010001100101101111000001
01000011001010011011111000000010100110111101010100011011000100000101111
01101100000000111011001110010110110011111001100110001101000000001010000101101110101101100110001
00101011010110011000110101010111100100100101010011001

1. SCHEIDEGGER, A. E.: Bull. Internat. Assoc. Scient. Hydrol. 12, No. 1, 15 (1967).

and other thermodynamic quantities. Furthermore, the quantity of heat introduced in a given substance is given by[1]

$$dQ = \gamma\, dT \tag{5.81-4}$$

with γ being a heat capacity coefficient. The analog of this in a landscape is

$$dM = \gamma\, dh \tag{5.81-5}$$

where γ is now an analog of the heat-capacity coefficient.

Our task is now to extend the above correspondences to energy terms. For a regular thermodynamic system, the first principle of thermodynamics states

$$U_2 - U_1 = Q + W \tag{5.81-6}$$

or, in differentials

$$dU = dQ + dW \tag{5.81-7}$$

where U is the internal energy, Q is the quantity of heat introduced from outside and W the work performed externally on the system. In landscape evolution, one would like to have, therefore, a similar relation, viz.

$$U_2 - U_1 = M + W \tag{5.81-8}$$

or, in differentials

$$dU = dM + dW \tag{5.81-9}$$

where U now signifies some potential, M the mass that was introduced and W some "fictitious work" whose physical meaning has yet to be defined.

For an ideal gas, W is

$$W = -\int_v p\, dV. \tag{5.81-10}$$

Here, V is the geometric domain in which the variables vary, and p the pressure. Because of the ideal gas law, the latter can be expressed as follows

$$p = \frac{RT}{V} = \text{const}\,\frac{T}{V}. \tag{5.81-11}$$

The last relation yields a means of setting up an analogy to "pressure" in landscapes. In the latter, V corresponds to the area A under consideration, T is the height h (see above) so that one has

$$p_{\text{landscape}} = \text{const}\,\frac{h}{A}, \tag{5.81-12}$$

at least in the equilibrium case.

1. Scheidegger, A. E.: Bull. Internat. Assoc. Sci. Hydrol. **12**, No. 4, 57 (1967).

If we are essentially interested in an "average" geographic cross section across a landscape, we have only one space-coordinate (x); denoting the total length of the section by L, we have (denoting the constant by α)

$$p_{\text{landscape}} = \text{const}\,\frac{h}{L} = \frac{h}{L}\alpha. \tag{5.81-13}$$

The analog of work is then

$$W = -\int p\,dV = -\int \alpha(h/L)\,dL. \tag{5.81-14}$$

5.82. The Diffusivity Equation of Landscape Decay. Because of the thermodynamic analogy, one must have similar equations for the analogous quantities in landscape theory as for the corresponding quantities in thermodynamics. As is well known, in heat conduction the temperature T in a thermodynamic system is subject to a diffusivity equation (D is some constant):

$$\frac{\partial T}{\partial t} = D\left[\frac{\partial^2 T}{\partial x^2} + \frac{\partial^2 T}{\partial y^2}\right]. \tag{5.82-1}$$

Correspondingly, the same equation must hold for the height h in a landscape:

$$\frac{\partial h}{\partial t} = D\left[\frac{\partial^2 h}{\partial x^2} + \frac{\partial^2 h}{\partial y^2}\right]. \tag{5.82-2}$$

For the diffusivity equation, one has the following well known solutions (in 1 dimension)

$$h = \frac{1}{(4\pi D t)^{\frac{1}{2}}} \exp\left(-\frac{x^2}{4Dt}\right), \tag{5.82-3}$$

$$h = \frac{1}{2} + \frac{1}{2}\,\text{erf}\left(\frac{x}{(4Dt)^{\frac{1}{2}}}\right). \tag{5.82-4}$$

These formulas represent a decay of initial structures; the first of an idealized mountain range (Fig. 145), the second of an idealized slope bank (Fig. 146). It is seen, thus, that based upon entirely general principles,

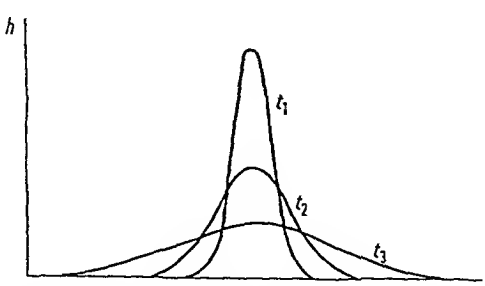

Fig. 145. Decay of an idealized mountain range (Eq. 5.82-3)

one must expect a decay of initial irregularities in a landscape. Obviously, we have an "end" to the decay process when $h=$const everywhere. This corresponds to the equipartition theorem in thermodynamics.

The diffusivity equation is the automatic outcome if many independent random influences act upon a system. Thus, a diffusivity equation is obtained whenever a stochastic model exhibiting these features is set up, regardless of what the mechanics of the influences happens to be. In this fashion, e.g., CULLING[1,2] obtained a diffusivity equation by setting up a stochastic model for soil creep.

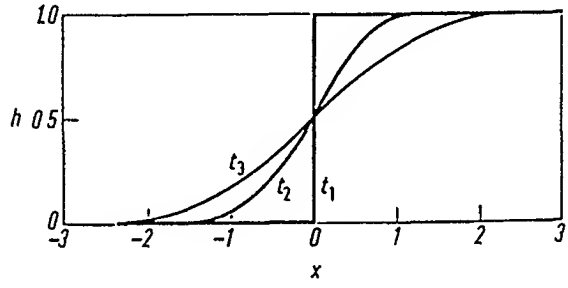

Fig. 146. Decay of an idealized slope bank (Eq. 5.82-4)

5.83. Steady State Conditions. In thermodynamics, we have as condition for the establishment of a steady state that the entropy production rate σ must be a minimum:

$$\sigma=-\sum\frac{\operatorname{grad}T}{T^2}J=\text{minimum}. \tag{5.83-1}$$

Here, J is the heat flux per unit time. Because of the analogy with landscape evolution, this immediately gives a condition for the establishment of a steady state in a landscape also. For a one-dimensional system one has:

$$\sigma=-\int\frac{T'}{T^2}J\,dx=-\int\frac{h'}{h^2}J\,dx=\text{minimum}, \tag{5.83-2}$$

where J is the mass flux per unit time.

The last formula may be applied to a river profile; the latter, indeed, can be regarded as a geomorphological profile[3]. For a steady state, one must have

$$\delta\sigma=-\delta\int\frac{h'}{h^2}J\,dx=0 \tag{5.83-3}$$

1. CULLING, W. E. H.: J. Geol. **71**, 127 (1963).
2. CULLING, W. E. H.: J. Geol. **73**, 230 (1965).
3. SCHEIDEGGER, A. E., and W. B. LANGBEIN: Bull. Internat. Assoc. Sci. Hydrol. **11**, No. 3, 43 (1966).

where J, being proportional to mass flow, represents sediment transport. Choosing intuitively $J=J(h')$ leads to the following Euler-Lagrange equation for the minimization:

$$h''\left[2\frac{J'(h')}{h^2}+h'\frac{J''(h')}{h^2}\right]-2\frac{J'(h')}{h^3}h'^2=0. \tag{5.83-4}$$

Choosing specifically

$$J=c\,h' \tag{5.83-5}$$

one obtains

$$\frac{h''}{h'}-\frac{h'}{h}=0 \tag{5.83-6}$$

which yields when solved

$$h=c_1\,e^{-c_2 x} \tag{5.83-7}$$

with c_1 and c_2 as constants of integration.

This formula is analogous to that obtained by a deterministic model.

The above theory may be modified by choosing

$$J=(-q\,h')^a \tag{5.83-8}$$

where q is the discharge volume per unit river width and a a constant. One may further assume that q is proportional to x (distance from source in the river basin), for the drainage area is roughly proportional to x^2, the river width proportional to x, hence q to x. This yields

$$J\sim(x\,h')^a. \tag{5.83-9}$$

Then, the solution of the corresponding Euler-Lagrange equation for the minimization of the entropy production rate (see Eq. 5.83-3) yields

$$h=\left[c\frac{a-1}{a+1}\ln k\,x\right]^{\frac{a-1}{a+1}} \tag{5.83-10}$$

where c and k are again constants of integration. Thus

$$h'=c\,h^{\frac{2}{1+a}}/x. \tag{5.83-11}$$

A regression analysis on 153–221 streams yields

$$a=1.5. \tag{5.83-12}$$

This is an excellent confirmation of the theory.

VI. Theory of Aquatic Effects

6.1. General Remarks

The theory of aquatic effects must of necessity start with a description of the theory of the movements in large bodies of water. In this connection, the mechanisms of waves, currents, tides and of turbidity currents are of prime importance and will be described in some detail (Sec. 6.2). This will constitute a necessary preamble to any theory of aquatic effects. Another preliminary discussion (Sec. 6.3) will have to deal with a description of the various agents that may be active in subaquatic geomorphology.

It will then be possible to proceed to a detailed description of the theory of the various aquatic features that may be of interest. First we shall discuss the theory of evolution of coasts (Sec. 6.4), then we shall proceed to a description of the dynamics of river estuaries (Sec. 6.5) and finally conclude the present chapter with a theoretical analysis of submarine geomorphology (Sec. 6.6).

6.2. Movements in Large Bodies of Water

6.21. Principles. As noted above, the first task in understanding marine geomorphology is to develop an understanding of the movements of large bodies of water.

In this connection, the prime phenomenon which comes to one's mind is that of *surface waves*. The theory of water waves is a very complex subject and much information exists in the literature. Those features of water waves which are of most importance in context with the subject matter of the present book will be discussed in Sec. 6.22.

We shall next proceed to a discussion of the phenomenon of *turbidity currents* which is of great importance with regard to the shaping of the submarine bottom relief of the Earth. Turbidity currents will be discussed at length in Sec. 6.23.

Finally, we shall give a brief description of the phenomena of *tides* (in Sec. 6.24) and of *ocean currents* (in Sec. 6.25) as far as they are of importance in connection with theoretical geomorphology.

6.22. Waves. For our study of coasts, we shall be concerned with waves. In this connection, it will not be necessary to investigate the

generation of waves on a body of water as we simply assume that waves exist and that they travel into a shoreline at a given angle. The main problem is to account for the changes in wave action due to the presence of a bottom relief. Comprehensive treatises on waves have been written by STOKER[1], SCHULEIKIN[2] and by TRICKER[3] who discussed all aspects of the problem. Other, brief expositions of the wave problem have been given e.g. by ROLL[4] and by PIERSON[5].

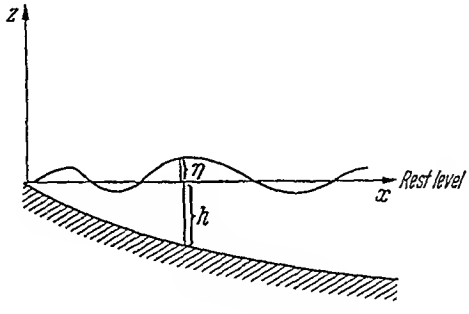

Fig 147. Geometry of water waves

Accordingly, one can describe the fluid motion in two dimensions (in x,z-space; z upward; u,w are the velocity components; cf. Fig. 147) by a velocity potential φ so that

$$u=-\frac{\partial\varphi}{\partial x} \tag{6.22-1}$$

$$w=-\frac{\partial\varphi}{\partial z}. \tag{6.22-2}$$

The velocity potential satisfies a Laplace equation (continuity equation)

$$\frac{\partial^2\varphi}{\partial x^2}+\frac{\partial^2\varphi}{\partial z^2}=0 \tag{6.22-3}$$

if the motion is assumed to be irrotational. The equations of motion reduce to BERNOULLI's equation if the external forces (gravity) have a potential:

$$\frac{p}{\rho}=\frac{\partial\varphi}{\partial t}-g\,z-\frac{1}{2}\left[\left(\frac{\partial\varphi}{\partial x}\right)^2+\left(\frac{\partial\varphi}{\partial z}\right)^2\right]. \tag{6.22-4}$$

1. STOKER, J. J.: Water Waves Interscience Publ Inc. New York 1957.
2. SCHULEIKIN, W.. Theorie der Meereswellen. (Transl from Russian by E. BRUNS.) Berlin: Akademie-Verlag 1959
3. TRICKER, R. A. R.. Bores, Breakers, Waves and Wakes (263 pp) Amsterdam: Elsevier (1965).
4. ROLL, H. U : Encycl. Phys. 48, 671 (1957).
5. PIERSON, J. D.: Appl Mech Revs. 14, 1 (1961)

Here p is the fluid pressure, ρ the density and g the gravity acceleration. The equations of motion enter only into the boundary conditions; the latter are

(i) $$\frac{d\varphi}{\partial n}=0 \qquad \text{for } z=-h(x) \tag{6.22-5}$$

if $z=-h(x)$ represents the equation of the bottom of the body of water (cf. Fig. 147) and n denotes the normal to the bottom surface;

(ii) $$\eta=\frac{1}{g}\frac{\partial\varphi}{\partial t}-\frac{1}{2g}\left[\left(\frac{\partial\varphi}{\partial x}\right)^2+\left(\frac{\partial\varphi}{\partial z}\right)^2\right] \qquad \text{for } z=\eta \tag{6.22-6}$$

where $z=\eta(x,t)$ represents the equation of the surface of the water, and we assume that $p=0$ thereon; finally, expressing the condition that

$$\frac{d}{dt}(z=\eta)=0$$

yields:

(iii) $$-\frac{\partial\varphi}{\partial x}\frac{\partial\eta}{\partial x}+\frac{\partial\varphi}{\partial z}=-\frac{\partial\eta}{\partial t} \qquad \text{for } z=\eta. \tag{6.22-7}$$

To this, one will add initial conditions of the form $\eta=\eta_0$ for $t=0$.

The above system of equations is nonlinear and has never been fully solved. There are two types of approximate solutions that have been obtained. The first is due to STOKES[1] who assumed that the amplitudes are small. The second assumes that the water is shallow; in this it is a nonlinear theory.

We shall first discuss the theory assuming that the amplitude and therewith the velocity-potential φ are so small that squares of φ and of its derivatives can be neglected. Then, the system of equations becomes linear; it may be written as follows

$$\frac{\partial^2\varphi}{\partial x^2}+\frac{\partial^2\varphi}{\partial z^2}=0, \tag{6.22-8}$$

$$\frac{p}{\rho}=\frac{\partial\varphi}{\partial t}-g\,z, \tag{6.22-9}$$

$$\frac{\partial\varphi}{\partial n}=0 \qquad \text{for } z=-h, \tag{6.22-10}$$

$$\eta=\frac{1}{g}\frac{\partial\varphi}{\partial t} \qquad \text{for } z=0, \tag{6.22-11}$$

$$\frac{\partial\eta}{\partial t}=-\frac{\partial\varphi}{\partial z} \qquad \text{for } z=0. \tag{6.22-12}$$

1. STOKES, G. G.: Trans. Camb. Phil. Soc. 8, 441 (1847).

Eliminating η from (6.22-11/12) yields

$$\frac{1}{g}\frac{\partial^2\varphi}{\partial t^2}+\frac{\partial\varphi}{\partial z}=0 \qquad \text{for } z=0. \tag{6.22-13}$$

One may now seek solutions of the above system which represent progressive waves. The best-known of these solutions is (its correctness may be verified directly by substituting it into the above system):

$$\varphi=-a\cosh m(z+h)\cos(m x\pm\sigma t+\delta) \tag{6.22-14}$$

with m and σ satisfying

$$\sigma^2=g m\tanh m h. \tag{6.22-15}$$

The frequency ν and the wave length λ of the waves are

$$\nu=\sigma/(2\pi), \tag{6.22-16a}$$

$$\lambda=2\pi/m. \tag{6.22-16b}$$

Furthermore, a and δ are arbitrary constants. The phase velocity c of the waves is (Stokes formula):

$$c=\lambda\nu=\frac{\sigma}{m}=\frac{\sigma\lambda}{2\pi}=\sqrt{\frac{g\lambda}{2\pi}\tanh\frac{2\pi h}{\lambda}}. \tag{6.22-17}$$

If $\lambda\ll 2h$, one has $\tanh\frac{2\pi h}{\lambda}\approx 1$, and hence one obtains the following formula for waves in deep water:

$$c=\sqrt{\frac{g\lambda}{2\pi}}. \tag{6.22-18}$$

Conversely, if $\lambda\gg h$, one has $\tanh\frac{2\pi h}{\lambda}\approx\frac{2\pi h}{\lambda}$, and hence one has for waves in shallow water:

$$c=\sqrt{g h}. \tag{6.22-19}$$

The displacements Δx, Δy corresponding to the above solution can also be calculated (simply by integrating the velocities over time). One obtains

$$\Delta x=\frac{a m}{\sigma}\cosh m(z+h)\cos(m x+\sigma t+\delta), \tag{6.22-20a}$$

$$\Delta z=\frac{a m}{\sigma}\sinh m(z+h)\sin(m x+\sigma t+\delta) \tag{6.22-20b}$$

which shows that the wave motion is elliptical. Of particular interest is that the tangential motion parallel to the bottom does not vanish for

$z=-h$. One also sees that the amplitude A (half the height from crest to through) is connected with the constant a as follows:

$$A=\frac{a\,m}{\sigma}\sinh m\,h.$$

There are instances where the above theory of "infinitesimal" waves is not entirely satisfactory. In this case, a second approximation of the theory may be considered. A particularly important result of the second approximation is that there is a net mass-transport in travelling waves. The velocity U of net mass transport at depth h in a wave of height H (crest to trough) is

$$U=\frac{1}{2}\left(\pi\frac{H}{\lambda}\right)^2 c\;\frac{\cosh\dfrac{4\pi(h-z)}{\lambda}}{\left(\sinh\dfrac{2\pi h}{\lambda}\right)^2} \tag{6.22-21}$$

where the wave velocity c is as given by (6.22-17).

Next, we shall discuss some of the results of the *nonlinear shallow water theory*. The procedures of the shallow water theory[1,2] are based upon the assumption that the vertical accelerations can be neglected with regard to the horizontal ones. Consequently, the pressure at any point in the body of water equals the static pressure.

$$p=g\,\rho(\eta-z) \tag{6.22-22}$$

where the pressure at the surface of the water is taken as zero and the other symbols have the same meaning as before (cf. Fig. 147). The (Eulerian) equation of motion $\left(du/dt=-\frac{1}{\rho}\,\partial p/\partial x\right)$ therefore yields

$$\frac{\partial u}{\partial t}+u\frac{\partial u}{\partial x}=-g\frac{\partial\eta}{\partial x}. \tag{6.22-23}$$

The continuity equation yields

$$-\frac{\partial\eta}{\partial t}=\frac{\partial}{\partial x}[u(\eta+h)] \tag{6.22-24}$$

since, in Fig. 147, $(\eta+h)$ can be regarded as a "linear density" σ; the continuity equation then is simply

$$-\partial\sigma/\partial t=\mathrm{div}(\sigma\,u).$$

1. Lamb, H.: Hydrodynamics, 6th Ed., p. 254. New York: Dover 1954.
2. Defant, A.: Encycl. Phys. 48, 846 (1957).

The two first-order differential Eqs. (6.22-23) and (6.22-24) are the differential equations of the shallow water theory; they are sufficient to determine the two functions η and u.

If we now linearize the shallow water theory by assuming that u and η are so small that square terms can be neglected, we end up with

$$\frac{\partial u}{\partial t} = -g\frac{\partial \eta}{\partial x}, \tag{6.22-25}$$

$$\frac{\partial}{\partial x}(u h) = -\frac{\partial \eta}{\partial t}. \tag{6.22-26}$$

Assuming that the depth h is constant, we find the wave equation

$$\frac{\partial^2 \eta}{\partial x^2} - \frac{1}{g h}\frac{\partial^2 \eta}{\partial t^2} = 0 \tag{6.22-27}$$

which has solutions representing waves progressing with the speed c given by

$$c = \sqrt{g h}. \tag{6.22-28}$$

This is the same result as was obtained from the "small amplitude theory" if it was applied to shallow water.

The nonlinearized shallow water theory has solutions corresponding to shock fronts as this is usually the case with nonlinear hyperbolic partial differential equations[1]. A corresponding situation occurs in gas dynamics; in water wave theory the shock fronts correspond to breakers. The analogy of the nonlinear water-wave theory with the equations of gas dynamics is complete. Introducing a ficticious density $\bar{\rho}$

$$\bar{\rho} = \rho(\eta + h) \tag{6.22-29}$$

and a ficticious pressure $\bar{p}$

$$\bar{p} = \int_{-h}^{\eta} p\, dy \tag{6.22-30}$$

the hydrostatic pressure law yields

$$\bar{p} = \frac{g}{2\rho}\bar{\rho}^2 \tag{6.22-31}$$

and the equations of motion become

$$\bar{\rho}\left(\frac{\partial u}{\partial t} + u\frac{\partial u}{\partial x}\right) = -\frac{\partial \bar{p}}{\partial x} + g\,\bar{\rho}\frac{\partial h}{\partial x}, \tag{6.22-32}$$

$$\frac{\partial}{\partial x}(\bar{\rho}\, u) = -\frac{\partial \bar{\rho}}{\partial t}. \tag{6.22-33}$$

1. See e.g. STOKER, J. J.: Water Waves. New York: Interscience Pub Co. 1957.

These are the exact analogues to the equations of gas dynamics. The "velocity of sound" is given by

$$c=\sqrt{\frac{\partial \bar{p}}{\partial \rho}}=\sqrt{\frac{g\,\bar{\rho}}{\rho}}=\sqrt{g(\eta+h)}. \tag{6.22-34}$$

The basic equations (6.22-23/4) can be reformulated in terms of this speed

$$\left.\begin{aligned}\frac{\partial u}{\partial t}+u\frac{\partial u}{\partial x}+2c\frac{\partial c}{\partial x}-\frac{\partial H}{\partial x}=0\\ 2\frac{\partial c}{\partial t}+2u\frac{\partial c}{\partial x}+c\frac{\partial u}{\partial x}=0\end{aligned}\right\} \tag{6.22-35}$$

with

$$H=g\,h. \tag{6.22-36}$$

It can be shown that c is indeed the propagation velocity of a disturbance. For infinitesimal disturbances, this can be verified directly. For constant bed slope ($\partial H/\partial x=m$) the system of equations can be treated by the method of characteristics. Along the lines

$$\begin{aligned}C_1\colon\ \frac{dx}{dt}&=u+c\\ C_2\colon\ \frac{dx}{dt}&=u-c\end{aligned} \tag{6.22-37}$$

the change of the following quantities

$$\begin{aligned}u+2c-m\,t&=k_1 \quad \text{on} \quad C_1\\ u-2c-m\,t&=k_2 \quad \text{on} \quad C_2\end{aligned} \tag{6.22-38}$$

is nil. Of course, on different characteristic lines, the respective constants (k_1 and k_2) are different.

Breaking of waves occurs when the characteristics of one family intersect each other.

Let us consider a case where the bottom is horizontal ($h=\text{const}$). We attempt to find a solution for the characteristic equations where, at $x=0$:

$$\eta(0,t)=A\sin\omega\,t \tag{6.22-39}$$

and where we assume that the C_1-family of characteristics are straight lines. Then, assuming that these lines issue from the t-axis at $t=\tau$, we have

$$\frac{dx}{dt}=u(\tau)+c(\tau). \tag{6.22-40}$$

On any characteristic of the family C_2 we have then (note that $m=0$):

$$u(\tau)-2c(\tau)=u_0-2c_0. \tag{6.22-41}$$

Hence, the slope of any straight characteristic of the family C_1 is given by

$$\frac{dx}{dt}=\frac{1}{2}[3u(\tau)-u_0]+c_0, \tag{6.22-42}$$

or

$$\frac{dx}{dt}=3c(\tau)-2c_0+u_0. \tag{6.22-43}$$

The values with the index 0 refer to the area where there is no disturbance, i.e.

$$c_0=\sqrt{gh}. \tag{6.22-44}$$

We have then for the C_1 family:

$$x=(t-\tau)[3c(\tau)-2c_0+u_0]. \tag{6.22-45}$$

As noted above, breaking occurs when the characteristics of one, say the C_1 family, intersect each other. This occurs on the points forming an envelope to the family. The latter is obtained by differentiation of the C_1-equation (6.22-45) with regard to the parameter (τ). The result is

$$\begin{aligned} x_{env}&=\frac{[3c(\tau)-2c_0+u_0]^2}{3c'(\tau)}\\ t_{env}&=\tau+\frac{3c(\tau)-2c_0+u_0}{3c'(\tau)}. \end{aligned} \tag{6.22-46}$$

Corresponding to our assumption for η, we have

$$c=\sqrt{g(h+A\sin\omega\tau)}. \tag{6.22-47}$$

Taking the first characteristic ($\tau=0$), we obtain the first breaking point

$$\begin{aligned} x_b&=\frac{2c_0(c_0+u_0)^2}{3gA\omega}\\ t_b&=\frac{2c_0(c_0+u_0)}{3gA\omega}. \end{aligned} \tag{6.22-48}$$

This shows that for higher frequencies, the breaking point occurs earlier.

The breaking point relation can be improved upon by using solitary wave theory. This has been done by MUNK[1] and by SVERDRUP and

1. MUNK, W. H.: Proc. N. Y. Acad. Sci. 51, 376 (1949).

MUNK[1]. These authors quote the following relationship between the wave height η, the depth of breaking h, and the cross-sectional area Q of the breaking wave;

$$Q=4h^2\sqrt{\frac{\eta}{3h}}. \tag{6.22-49}$$

The above formulas explain the occurrence of breakers.

The theories presented above are all based on approximations. Their validity is therefore fairly restricted. Other attempts at a solution of the nonlinear wave equations have e.g. been made by YIH[2] who investigated gravity waves in a stratified fluid, PHILLIPS[3] who studied the dynamics of nonsteady gravity waves of finite amplitude, CHAPPELEAR[4] who analyzed shallow water waves, KOH and LE MÉHAUTE[5] who investigated the phenomenon of wave shoaling and finally HASSELMANN[6] who gave a theory of wave-interaction based on statistical mechanics.

The *generation* of waves is commonly ascribed to the action of wind. This involves resonance and instability phenomena. A theory of this has been proposed and a review of earlier work has been given by BARNETT[7] according to which the wave spectrum caused by a wind fields can be predicted.

6.23. Turbidity Currents. As noted in Sec. 1.65, turbidity currents have been advocated as the explanation of some features of submarine geomorphology. It is therefore necessary to investigate the dynamics of such turbidity currents.

First of all, turbidity currents have been regarded as a case of stratified flow of fluids of different density and viscosity[8,9]. If such flow is laminar, however, one runs into difficulty with the investigations mentioned in Sec. 2.26 according to which the interface of two fluids of different densities superimposed upon each other and moving at different velocities, cannot possibly be stable under any circumstances. Hydrodynamics, therefore, requires that no stratified flows are possible for any length of time.

1. SVERDRUP, H. U., and W. H. MUNK: Trans. Amer. Geophys. Union **27**, 828 (1946).
2. YIH, C. S.: J. Fluid Mech. **8**, No. 4, 481 (1960).
3. PHILLIPS, O. M.: J. Fluid Mech. **9**, No. 2, 193 (1960).
4. CHAPPELEAR, J. E.: J. Geophys. Res. **67**, 4693 (1962).
5. KOH, R. C. Y., and B. LE MÉHAUTE: J. Geophys. Res. **71**, 2005 (1966).
6. HASSELMANN, K.: Rev. Geophys. **4**, No. 1, 1 (1966).
7. BARNETT, T. P.: J. Geophys. Res. **73**, 513 (1968).
8. HARLEMAN, D. R. F.: In STREETER, V. L. (ed.), Handbook of Fluid Dynamics, p. 26-2. New York: McGraw-Hill 1961.
9. BENJAMIN, T. B.: J. Fluid Mech. **31**, 209 (1968).

Upon further investigation it becomes obvious that turbidity currents cannot possibly represent laminar flow. Such currents consist of a suspension of various kinds of particles in water and it has been remarked earlier (in Sec. 4.44) that the lifting force keeping such particles in suspension, must of necessity be due to prevailing turbulence. Measurements of the Reynolds number in turbidity currents of Lake Mead have subsequently yielded the result that this number is of the order of 100,000, which is much higher than the critical Reynolds number at which turbulence is commonly thought to set in. Thus turbidity currents may safely be assumed to be highly turbulent, and it turns out that, physically, turbidity currents are "slugs" of fairly confined turbulent water mixed with debris which move downslope for a long distance until they come to rest.

If it is assumed that each turbidity flow is triggered by some external cause (earthquake, collapse of a pile of loose material etc.) which is of no interest for the intrinsic mechanics of a turbidity current, there remain three basic problems to be investigated: (A) Why does the turbulence remain confined in a steady-state slug; (B) how does the turbulent slug move; and (C) how does the turbulence decay after the slug has come to rest?

A complete solution of the above problems should be based on a solution of the Navier-Stokes differential equations for a viscous liquid with the appropriate boundary conditions. Needless to say, it is impossible to achieve such an exact solution. Nevertheless, it is possible to get at least partial solutions to the three fundamental problems mentioned above. We shall discuss these below.

Turning to the *first problem*, we note that a solution has been proposed by EINSTEIN[1] who ventured the opinion that the macroscopic rheological state of a sediment-laden stream is similar to that in a plastic substance. There are some indications that this might be so, particularly if the sediment is flocculated. The turbulence, thus, might be somehow confined inside the current, and the latter would move like a plastic body through the surrounding water. Naturally, EINSTEIN's plasticity assumption is purely heuristic. It does not explain why the turbulence does not get dissipated into the surrounding fluid, but simply assumes this as a fact and tries to give a semi-theoretical description of what happens in consequence of this assumption.

Thus, following EINSTEIN, let us consider a prismatic turbidity current of height h_0, viscosity η and density ρ. The corresponding values for the still water are η_0 and ρ_0 (see Fig. 148). If the material of which the turbidity current consists is uniform and "plastic", then the internal shear stress

1. EINSTEIN, H. A.: *Trans. Amer. Geophys. Union* **22**, 597 (1941).

must be a linear function of distance. The extreme values of this shear stress, τ_b at the bottom and τ_i at the top, must balance the gravity force F:

$$F = h_0(\rho - \rho_0)\, g \sin\alpha \tag{6.23-1}$$

to achieve dynamic equilibrium. The shearing stress will be zero at some distance y_0 from the bottom. On either side of this point, there will be points (denoted by A and B in Fig. 148) at which the value of the shear stress is equal to the "yield stress" of the turbidity current (since the latter is treated as a plastic substance). Between A and B, therefore, the current moves *en bloc* as a "frozen layer". Below the point B, the flow

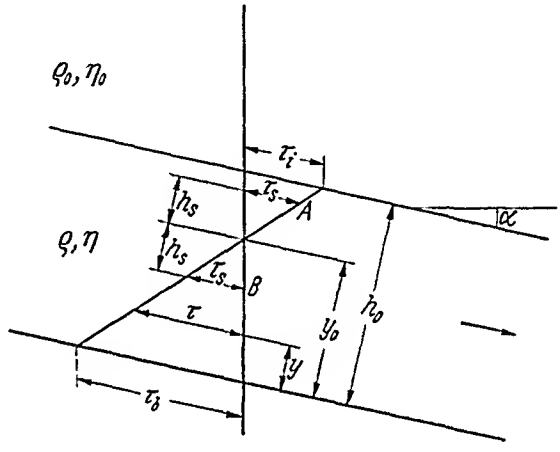

Fig. 148. Shearing stress in a turbidity current. After EINSTEIN[1]

is highly turbulent. From a comparison with measured values, EINSTEIN found that the thickness of the layer that moves *en bloc* in Lake Mead (cf. Sec. 1.65) may be of the order of 8.9 m.

As noted above, EINSTEIN's theory does not really provide a reason for the confinement of the turbulence of a slug. It stands to reason that somehow a steady state must develop in which the energy dissipated is constantly resplenished. This can be dealt with by means of statistical mechanics[2]: The conditions for the development of a steady state are that the production rate of entropy be a minimum; applying this to the energy "flux" between the various size eddies in the turbulent fluid yields at least an explanation in principle as to why the phenomenon of turbidity currents is mechanically possible.

Turning now to the *second problem*, viz. the question as to how the turbulent slug moves downhill, we note that most investigators in some fashion use a formula analogous to the Chézy relation (4.22-10) in rivers.

1. EINSTEIN, H. A.: Trans. Amer. Geophys. Union **22**, 597 (1941).
2. TOMKORIA, B. N., and A. E. SCHEIDEGGER: Canad. J. Phys. **45**, 3569 (1967).

Thus[1], one would expect for a turbidity current, assuming that it acts like a river

$$v = \text{const}\sqrt{RS\rho_e} \tag{6.23-2}$$

where v is the velocity of the slug, R is a "hydraulic radius" (the thickness of the current), s the (sine of the) slope, and ρ_e the effective density (i.e. the difference between the density of the current and that of the surrounding water). A somewhat more elaborate relationship is due to BLANCHET and VILLATTE[2] who take into account that there is friction not only at the bottom of the turbidity current (against the bed) but also at the top (against the still water; in a river no friction against the atmosphere is assumed). Further refinements can be made[3] by directly applying boundary layer theory to the turbulent slug.

Experiments aimed at checking out Eq. (6.23-2) are not entirely conclusive. KEULEGAN[4] and MIDDLETON[5], from tank type experiments, came up with the result that a relation of the following type should be used:

$$v = C\sqrt{\frac{\rho_e}{\rho} g R}. \tag{6.23-3}$$

Here, v is the velocity of the head of the density current, ρ_e is the density difference between current and surrounding water, R the thickness and ρ the density of the current, and g is the gravity acceleration. If the Chézy relation were valid, the value of C in (6.23-3) should be proportional to the square root of the slope S; however, KEULEGAN[4] found that C is largely independent of the slope, numerically equal to 0.7; MIDDLETON[5] found similarly that only a very slight increase of C with increasing slope takes place; his experimental value for C is 0.75 for $0.005 < S < 0.04$.

However, the above research of KEULEGAN[4] and MIDDLETON[5] concerns the velocity of the *head* of a turbidity current over short distances. Over longer distances (as e.g. in the Grand Banks event) MIDDLETON[6] still assumes that "uniform flow" is established for which he expects a Chézy-type relation to be valid. MIDDLETON's[6] general conclusion is, therefore, that large turbidity flows travelling a long distance over the sea floor experience very little resistance and are in a

1. KUENEN, P. H.: Soc. Econ. Pal. Min. Spec. Pub. 2, 14 (1951).

2. BLANCHET, C., and H. VILLATTE: Courants de densité. Confer. technique régionale, Tokyo 1954.

3. BATA, G. L.: Internat. Assoc. Hydraul. Res., 8th Congr., Montreal, Proc. 2, 12C 1 (1959).

4. KEULEGAN, G. H.: Repts. U.S. National Bureau of Standards Nos. 5168 (1957) and 5831 (1958).

5. MIDDLETON, G. V.: Canad. J. Earth Sci. 3, 523 (1966).

6. MIDDLETON, G. V.: Canad. J. Earth Sci. 3, 627 (1966).

state of "uniform flow" for which an equation of the type of (6.23-2) of CHÉZY's can be used.

Finally, the *third problem* concerns the mechanics of decay of the turbulence in a turbidity current. It stands to reason that this decay occurs at the end of the flow-process, when owing to the lack of further resplenishment, the turbulence decays according to the well known laws presented in Sec. 2.24 of this book.

6.24. Tides. Another phenomenon that may have a great effect upon coastal and submarine geomorphology, is that of the *tides.*

Tides are due to the attraction of the Sun and the Moon upon the water masses in the oceans and manifest themselves in a periodic rise and fall of the sea level with a period of about 12 hours in any part of the world. With regard to geomorphological questions, it is of little importance to present here a theory of the origin of tides; for such questions the reader is referred to suitable reviews such as those by BARTELS[1] and DEFANT[2]. For our purposes it is sufficient to realize that periodic fluctuations of the sea level *do* take place which, naturally, will cause *tidal currents* to arise. In the open ocean, the amplitude of the tidal fluctuations of the sea level reach only about a meter or so. A chart of the tides in the North Sea is shown in Fig. 149 (after SCHOTT[3]). However, in enclosed areas such as bays and estuaries, the tidal range may be very great (up to 15 meters in the Bay of Fundy on the Canadian East Coast).

The problem of tidal currents will be discussed in Sec. 6.5 with regard to river estuaries. However, tidal currents may also become established in necks between different bodies of water, such as at the inlet of a bay. In every case, they will exert a drag at the bottom and thus have a geomorphological significance. The surface speed of a tidal current over extensive areas may reach as much as 2 m/sec, and in isolated cases under special conditions (spring tides) up to 4.5 m/sec (e.g. in the Bristol channel[4]).

The structure of a tidal current has been measured and analysed by BOWDEN et al.[5]. These authors measured the flow velocity at various heights in Red Wharf Bay in North Wales where the water was 16 meters deep. The result is shown in Fig. 150. BOWDEN et al. then assumed that the profile of the velocity v near the bottom is given by the usual loga-

1 BARTELS, J.. Encycl. Phys. 48, 734 (1957).

2 DEFANT, A.: Encycl. Phys. 48, 846 (1957).

3. SCHOTT, G : Geographie des Atlantischen Ozeans. Hamburg: Boysen 1942.

4. See e.g. KUENEN, P. H.. Submarine Geology, p. 63. New York: J. Wiley 1950.

5 BOWDEN, K. F , L. A. FAIRBAIRN, and P. HUGHES: Geophys J Roy. Astron. Soc. 2, 988 (1959).

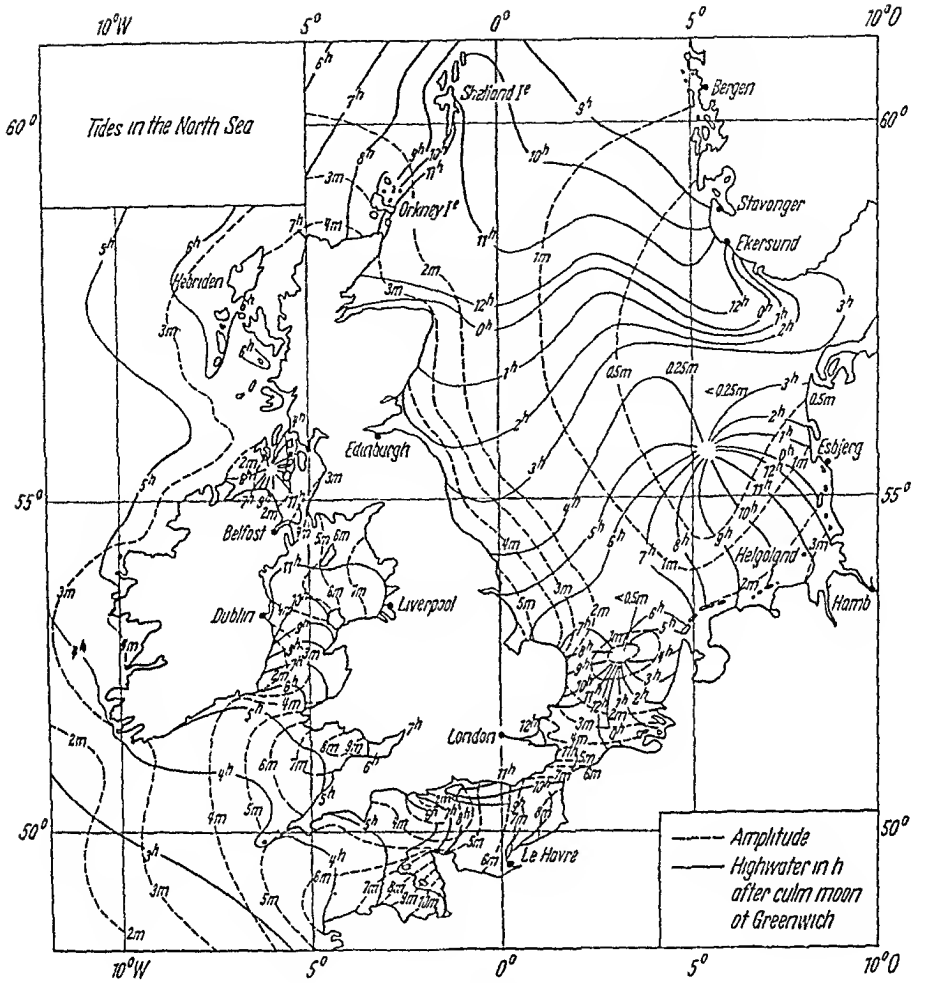

Fig. 149. Tides in the North Sea. After SCHOTT[1]

rithmic law of KARMAN (cf. Eq. 4.23-6), *viz:*

$$v = \frac{1}{k}\sqrt{\frac{\sigma_m}{\rho}}\,\text{lognat}\,\frac{z}{z_0} \tag{6.24-1}$$

where z denotes the height, k the Karman constant ($=0.4$), and z_0 the bottom roughness. Furthermore ρ is as usual the density, and σ_m the bottom shearing stress[2]. By a least squares solution using near-bottom data, σ_m and z_0 can be determined for a tidal cycle. The variation of bottom stress which corresponds to the velocity measurements given in Fig. 150, is shown in Fig. 151.

1 SCHOTT, G.: Geographie des Atlantischen Ozeans. Hamburg: Boysen 1942.

2. Regarding tidal bottom friction cf. also CHARNOCK, H.: Geophys. J. Roy. Astron. Soc. 2, 215 (1959)

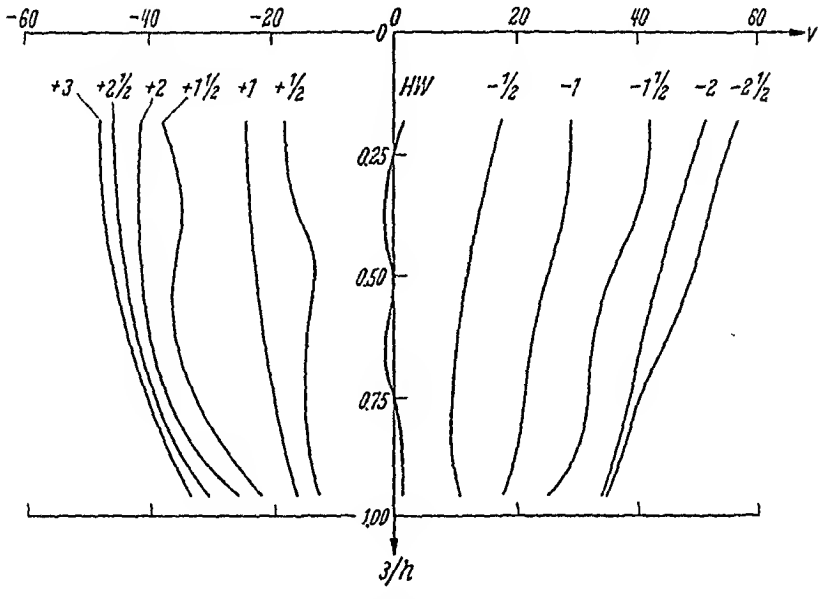

Fig. 150. Velocity as a function of relative depth in a tidal current, from $2^1/_2$ hours before to 3 hours after high water. After BOWDEN et al.[1]

It may be interesting to calculate the size of bottom particles which, according to the drag theory (see Sec. 4.43) will just be dislodged by the tidal bottom stress as estimated by BOWDEN et al. Referring to Eq. (4.43-5), we note that the bottom stress σ is related to the diameter d of the particles which are just being dislodged by

$$\sigma = A\,d \tag{6.24-2}$$

where A is a constant. From Fig. 105, we take the value of this constant A as equal to:

$$A = 166 \tag{6.24-3}$$

if d is given in millimeters and σ in units of g/m^2 (0.1 dynes/cm^2). Taking BOWDEN'S value for σ as approximately 5 dynes/cm^2 (50 g/m^2) yields

$$d = 0.3 \text{ mm}. \tag{6.24-4}$$

Thus, it may be seen that a tidal stress of some 5 dynes/cm^2 is able to start particles moving of about $\frac{1}{4}$ mm in diameter. In stronger tidal currents, the bottom effect will be correspondingly larger.

It cannot be assumed that the tidal current follows the logarithmic law of velocity distribution at all heights; in fact the velocity profiles shown in Fig. 150 speak against this. This is due to the circumstance that, in general, one has to deal with an unsteady state.

1. BOWDEN, K. F., L. A. FAIRBAIRN, and P. HUGHES: Geophys. J. Roy. Astron. Soc. 2, 988 (1959).

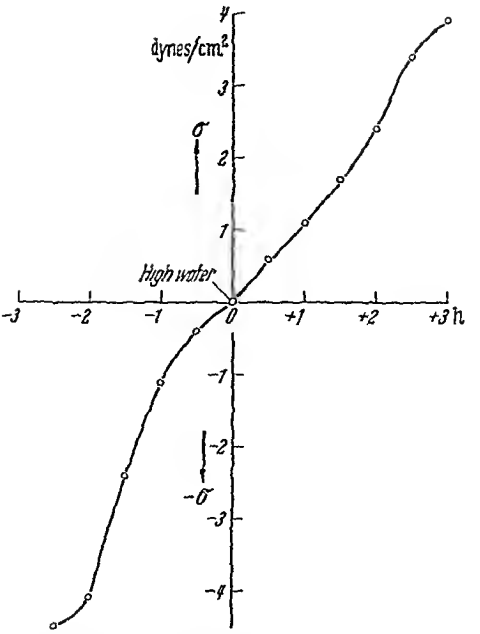

Fig. 151 Variation of bottom stress in a tidal current between $2^1/_2$ hours before and 3 hours after high water: drawn from data supplied by BOWDEN et al.[1]

6.25. Ocean Currents. The existence of currents in the ocean is well known from observations of mariners; the Gulf Stream, the Labrador current, and the Antarctic circulation are perhaps the most famous examples. The dynamical theory of such currents is fairly well established; it has been reviewed, for instance, by SVERDRUP et al.[2] and by DIETRICH and KALLE[3]. However, what is commonly referred to as "ocean currents", are currents at the surface of the sea, and it may be expected that such surface currents can have but little geomorphological significance. What is required is a knowledge of the bottom circulation in the sea, and here, unfortunately, our knowledge is rather scanty.

A short discussion of what is known about the bottom water circulation, has been given by SVERDRUP et al.[2] and by SVERDRUP[4]. Accordingly, conclusions regarding deep currents are based upon the temperature distribution, taking differences of oxygen content and other variable constituents into account. It is needless to say that, in

1. BOWDEN, K. F., L. A. FAIRBAIRN, and P. HUGHES: Geophys. J. Roy. Astron. Soc. 2, 988 (1959).

2 SVERDRUP, H. U., M. W. JOHNSON, and R. H. FLEMING: The Oceans. Englewood Cliffs, N. J.: Prentice-Hall, revised ed. 1946.

3. DIETRICH, G., and K. KALLE: Allgemeine Meereskunde. Berlin: Bornträger 1947

4. SVERDRUP, H. U.: Encycl Phys. 48, 608 (1957).

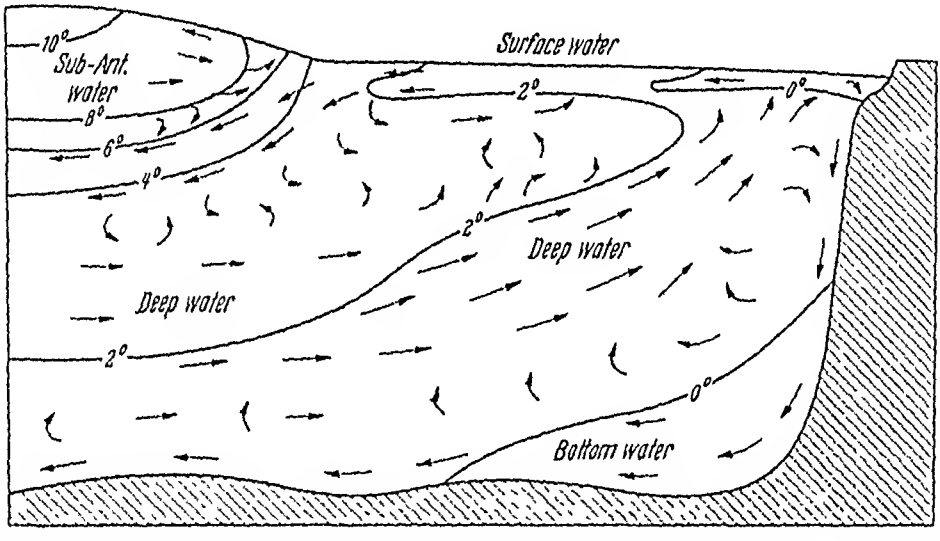

Fig. 152. Schematic diagram of deep-water circulation in a representative cross section of the Antarctic circulation. Modified from a drawing by SVERDRUP et al.[1]

this fashion, not much more than perhaps a qualitative idea about some features of the general deep water circulation can be obtained (cf. Fig. 152). It is almost hopeless to try to establish a quantitative picture of the prevailing velocities and frictional drag stresses at the ocean bottom. It is uncertain, therefore, whether these stresses are large enough to cause much transport of material. Until rather recently, it had been tought that the currents are not large enough, but photographs of scour marks[2] at depths of 6 km seem to indicate that deep water currents may cause at least some effects upon the bottom surface of the oceans (cf. also Sec. 6.65). Calculations by WÜST[3] indicate that values of bottom current velocities of up to 25 cm/sec do not seem to be unreasonable. Direct measurements[4, 5] have also indicated velocities of the same order of magnitude. DOEBLER[6] even found peak velocities of 40 cm/sec in a deep ocean current south of Plantagenet Bank near Bermuda. Such velocities can have a geomorphological significance: HEEZEN[7] investigated the sediment transport caused by the Antarctic bottom current on the Bermuda Rise.

1. SVERDRUP, H. U., M. W. JOHNSON, and R. H. FLEMING: The Oceans. Englewood Cliffs, N.J.: Prentice-Hall. Revised Edition (1946).
2. HEEZEN, B. C., M. THARP, and M. EWING: The Floors of the Oceans, I: The North Atlantic. Geol. Soc. Amer. Spec. Pap. 65. New York 1959. See especially Fig. 6 on Plate 11 thereof.
3. WÜST, G.: Wiss. Erg. dtsch. Atlant. Exped. METEOR 6, Pt. 2, 261 (1957).
4. SWALLOW, J. C., and V. WORTHINGTON: Nature (Lond.) 179, 1183 (1957).
5. LAIRD, N. P., and T. V. RYAN: J. Geophys. Res. 74, 5433 (1969).
6. DOEBLER, H. J.: J. Geophys. Res. 72, 511 (1967).
7. HEEZEN, B. C., et al.: Nature 211, 611 (1966).

6.3. Factors Acting in Subaquatic Geomorphology

6.31. General Review. The subaquatic features of the Earth's surface are affected by a variety of agents. These agents may be of a physical, chemical or biological nature. In addition, one perhaps ought to consider separately changes of the sea level (*eustatic changes*) which, although they are of a physical origin, are of a different nature than what is commonly included with the other physical agents in connection with geomorphology.

Summaries of the various aspects of the factors effective in shaping submarine features may be found in the general treatises on submarine geology which were already mentioned in Sec. 1.64. References to specific investigations will be given in their proper context.

We shall discuss below the various agents affecting submarine geomorphology in somewhat greater detail.

6.32. Physical Factors. The most important *physical* factors acting on coasts and on the ocean bottom are those connected with the movements of large bodies of water as discussed in Sec. 6.2. Thus, shoaling waves will displace material near the shore and large storm surges can directly erode pieces of the shore-rock through hydraulic action. It should be noted, however, that the presence of a large beach can often effectively protect the coast from attack by the sea.

Shoaling waves can only move material normal to the shore and are thus relatively ineffective in affecting the topography. However, longshore currents, even comparatively weak ones, always have a pronounced effect upon the topography, as they are capable of moving material out of the area. They often prevent the establishment of a beach and thus strip the coast of its protection against incoming waves. This, naturally enhances coastal erosion.

The tides also have a great effect upon coasts, particularly upon estuaries. The tidal action corresponds to that of a wave with a very great wave-length. Currents induced by the tides may be longshore currents or manifest themselves in the form of tidal "bores", bearing inshore and upstream in the estuary of a river.

Some of the most effective agents in the formation of submarine topography are *turbidity currents*. The latter seem to be the chief factors causing erosion and deposition in underwater areas.

Finally, of the movements in large bodies of water, it is vertical currents which can also cause changes in the sea-bottom topography.

The movements in large bodies of water, through their hydraulic action, are not the only physical agents that can affect the morphology of the Earth's surface. One of these other physical effects is *corrasion*

which implies the action of sand-laden waves upon the shore; another is *attrition* which implies the breaking down of loose pieces of rock; the latter then become tools of corrasion or parts of a beach. The mechanics of the attrition of pebbles on a shingle beach to their ultimate shape (which is that of sand grains) is the same as the attrition of pebbles on a river bed (cf. Sec. 4.72).

6.33. Chemical Factors. The next morphogenic agents which we shall consider are chemical ones. Of the chemical reactions that are important, we note particularly the dissolution of calcium carbonate from exposed

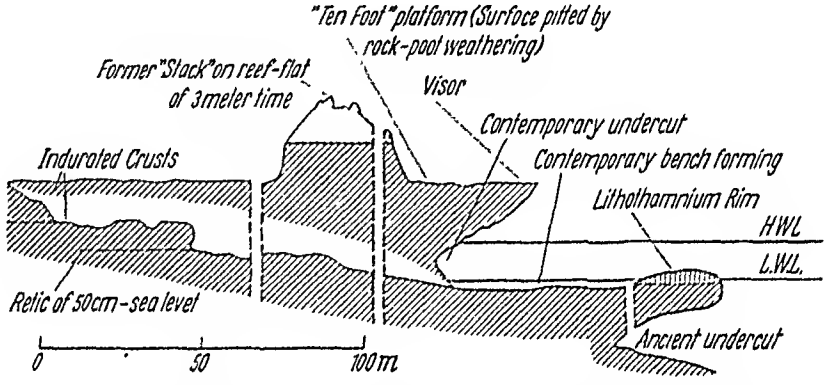

Fig. 153. Typical result (idealized section) of marine corrosion on the coastal limestone cliffs of Western Australia, corresponding to various levels of sea level. Modified from part of a drawing published by FAIRBRIDGE[1]. (Vertical scale twice horizontal scale)

rock. The result is commonly termed "corrosion" of the rock in question which can take place in sandstone where the bonding material between the quartz grains may be affected, and in limestone (such as reef rock) which may be attacked directly.

Morphological field studies have yielded the result that corrosion of beach and reef rock is most pronounced in the inter-tidal zone, i.e. in the zone between high and low tide. The surface of the rock becomes very irregular with many small depressions which are separated by narrow ridges. The depressions, or basins, remain filled by sea water at low tide and the corrosion taking place therein is very pronounced[1–4]. A typical result of marine corrosion is shown in Fig. 153.

It is, of course, well-known that water is able to dissolve calcium carbonate so that it would appear at first glance that there is little

1. FAIRBRIDGE, R. W.: Proc. 7th Pac. Sci. Cong. 3, 347 (1952).
2. MACFADYEN, G. A.: Geog. J. 75, 24 (1930).
3. GUILCHER, A.: Coastal and Submarine Geomorphology; transl. from French. London: Methuen & Co. 1958.
4. SMITH, C. L.: J. Marine Biol. Assoc. 25, 235 (1941).

difficulty in explaining the observed corrosion. However, it has been noted that in most instances, the basin water in which the dissolution of the calcium carbonate is supposed to take place, is in fact, supersaturated with that substance[1,2]. Therefore, the corrosion of limestone by sea water in the manner supposed above, poses somewhat of a puzzle.

The problem was analysed by REVELLE and EMERY[3] who discussed various attempts at an explanation which were based upon phenomena which are not chemical. However, they came to the conclusion that none of these explanations is satisfactory and that the cause of the rock-corrosion is in fact chemical. It appears that the mechanism of dissolution of calcium carbonate under the presence of other salts (sodium chloride etc.) and possibly organic matter, is not very well understood. Therefore, the possibility exists of complexing reactions[4] and hydration taking place which might explain the high rate of corrosion observed in intertidal limestone rocks[5,6].

6.34. Biological Factors. We have already mentioned earlier that biological agents have been advocated as geomorphologically effective. We shall investigate some of these agents somewhat further.

The best-known biological agents active in the formation of the Earth's surface are undoubtedly corals and calcareous algae. The limits for the environmental conditions under which corals can exist are rather narrow. The temperature of the water must never fall below 18° C or rise above 36° C with 25 to 30° C being most favorable. Light is also essential which restricts the depth at which reef building corals can grow to about 30 meters. Salinity must be between 27 and 40 parts per thousand. Much wind and sand are unfavorable[7].

Other biological factors in the formation of coastal morphology include animals burrowing into the rocks[8–10], algae growing below the rock surface[11] and snails[12] ingesting sand. In addition, it also appears that some fish eat coral, crabs and some gastropods may enter fissures in coastal rock and thereby help disintegrate it, and, acting in a fashion

1. WILLIAMS, J. E Geogr. Rev. 39, 129 (1949).
2. KUENEN, P. H : Marine Geology, New York: J. Wiley & Sons 1950.
3. REVELLE, R., and K. O. EMERY: U S Geol. Surv. Prof. Pap. 260-T, 699 (1957).
4. GARRELS, A. M , et al : Amer. J. Sci 259, 24 (1961)
5. HODGKIN, E. P · Z. Geomorph. 8, 385 (1964).
6. COLEMAN, J. M., et al.: Bull. Geolog. Soc. Amer. 77, 205 (1966).
7. See e.g. GUILCHER, A.: Coastal and Submarine Geomorphology. Transl. from French London: Methuen and Co. 1958.
8. DUERDEN, J E.: Bull. Amer. Mus. Nat. Hist. 16, 326 (1902)
9. GARDINER, J. S : Proc. Linnean Soc. London 1930/1, 65.
10 GINSBURG, R. N : Bull. Marine Sci. Gulf and Caribbean 3, 59 (1953)
11. NADSON, G.: C. R. Acad. Sci. (Paris) 184, 896, 1015 (1927)
12. NORTH, W. J.: Biol. Bull. 106, 185 (1954).

producing the opposite effect compared to the erosion considered above, seaweed may cause the sea floor to rise at a considerable rate. Most of the biological factors, thus, cause the disintegration of coastal material with only seaweed and corals acting contrariwise. Often, the disintegration is caused not directly, but the animals etc. create holes which lay the rock open to accelerated attack by other agents.

6.35. Eustatic Movements. Finally, coastal and submarine geomorphology has also been affected by eustatic movements. These eustatic movements may have been the result of endogenetic processes or they may have been due to climatic changes. Whatever their origin, their effect is approximately the same: At each level of the sea relative to the land, a typical coast line develops with beaches, wave terraces, etc. Thus, after several changes of sea level, a succession of coastal features remains, some drowned, some much above the most recent shore line.

The most thoroughly investigated features of the above type are related to the succession of Pleistocene ice ages. The varying amounts of sea water immobilized in the ice sheets and the isostatic movement of land caused the relative level of the sea to fluctuate to a considerable degree. The resulting sequences of coastal features have been found in many localities, as described for instance by GUILCHER[1] and by FAIRBRIDGE[2].

Studies of sea-level changes have been made up to the very present time. Thus, studying peats in Louisiana, COLEMAN and SMITH[3] found (allowing for the subsidence of the Gulf Coast) a linear rise in sea level of about 8.5 m from about 8,000 years before present (BP) time to about 3,500 years BP, with only a negligible change since then. Studying data from the present century, DONN et al.[4] found an average rise in sea level of between 12 and 21 cm per fifty years.

6.4. Coasts

6.41. General Remarks. Coasts are the most striking aquatic features on the Earth's surface that meet the eye of a casual observer. Whereas it is clear that the large-scale trend of coast lines is determined by endogenetic movements of the Earth, the finer features, such as the configuration of beaches etc., are due to exogenetic influences and are thus properly dealt with in a treatise of geomorphology.

---

1. GUILCHER, A: Coastal and Submarine Geomorphology; transl. from French. London Methuen & Co. 1958.

2. FAIRBRIDGE, R. W.: Sci. Amer. **202**, No. 5, 70 (1960).

3. COLEMAN, J. M., and W. G. SMITH: Bull. Geolog. Soc. Amer. **75**, 833 (1964)

4. DONN, W. L., J. G. PATULLO, and D. M. SHAW: In: Research in Geophysics, ed H. ODISHAW, vol. 2, p. 243. Cambridge, Mass.: M.I.T. Press 1967.

Monographs on the dynamics of coasts have recently been published by KING[1], ZENKOVICH[2,3] and IPPEN[4]. An older book, almost a classic, has been authored by JOHNSON[5]. Much pertinent information may also be found in the general treatises on geomorphology and physical geology which have been mentioned in Sec. 1.1.

The background for a study of the dynamics of coasts is supplied by an investigation of the *nearshore circulation system* (Sec. 6.42). It will then be possible to discuss the dynamics of *beaches* (Sec. 6.43) and of other characteristics of *gently dipping* shore lines (Sec. 6.44). Then, we shall analyze the dynamics of *steep coasts* such as of cliffs and shore terraces (Sec. 6.45). Finally, we shall discuss the possible explanations of large-scale features of shore lines (Sec. 6.46).

An inspection of the theories which will be presented below, shows that many individual traits of coast lines have been satisfactorily explained. However, most of these explanations are rather qualitative. In several instances, conditions for the equilibrium of a shore line have been devised; the process of the *evolution* of the various coastal features, assuming that there is no equilibrium, is frequently only very poorly understood.

6.42. The Nearshore Circulation System. We turn now our attention toward the *general dynamic processes* which occur on and near *coasts*.

The incoming swell is modified (refracted) by the bottom topography; at the same time, since there is a net mass transport in a wave in the direction of its propagation, currents are set up. These effects give rise to the establishment of a near-shore circulation system.

From STOKES' analysis of water waves, summarized in Sec. 6.22, it is seen that the velocity of water waves depends on the depth of the water. The Stokesian formula for the wave velocity c can be written as follows (cf. 6.22-17)

$$c^2 = \frac{g\lambda}{2\pi} \tanh \frac{2\pi h}{\lambda} \tag{6.42-1}$$

where h is the water depth, λ the wave length of the waves and g the gravity acceleration. If ocean swell is striking a coast, it stands to reason

1. KING, C A M.: Beaches and Coasts. London. E. Arnold & Co. 1959.
2. ZENKOVICH, V. P.: *Динамика и морфология морских берегов*. Moscow. Izd. Morsk. Transp. (1946)
3. ZENKOVICH, V. P.: Processes of Coastal Development, 738 pp Translated from Russian by D. G. FRY. London: Oliver & Boyd 1967.
4. IPPEN, A. T. (ed): Estuarine and Coastline Hydrodynamics. 744 pp. New York: McGraw-Hill 1966.
5. JOHNSON, D. W : Shore Processes and Shoreline Development. New York: J. Wiley & Sons 1919.

that its period T stays invariant. However, the period, the wave velocity c and the wave length are related by the following formula

$$c=\frac{\lambda}{T} \tag{6.42-2}$$

which is a general relationship valid for waves. It is therefore possible to eliminate the wave length λ from the two Eqs. (6.42-1) and (6.42-2) which yields a relationship expressing c as a function of h for any given period T.

If the bottom contours of an underwater region be known, it is possible to construct a corresponding chart, for each chosen period T, showing the wave velocity at each point. The areal variation of the wave velocity will cause incoming ocean waves of the corresponding period to be refracted in a pattern which is predictable. Starting with parallel wave crests in the area where the depth is great enough so as not to affect the wave velocity, one can construct the subsequent positions of the crests by successive approximations. O'BRIEN and MASON[1] coined the name "refraction diagram" for the resulting chart. An example of such a refraction diagram, constructed by MUNK and TRAYLOR[2] for swell of a period of $T=8$ sec hitting the California coast near La Jolla from a direction of WNW, is shown in Fig. 154. Naturally, the wave refraction diagrams are different for various periods in the same area.

From the refraction patterns it becomes quite obvious that the *wave crests tend to assume the shape of the depth contours.* This has been enunciated as a *law* by MUNK and TRAYLOR[2].

Wave refraction becomes significant only if the wave velocity is materially different from that for "deep" water, i.e. if the hyperbolic tangent in (6.42-1) is materially different from 1. This will be the case if, e.g.:

$$\frac{h}{\lambda}\leqq\frac{1}{2}. \tag{6.42-3}$$

The wave length λ for a given period T can be calculated approximately (using the deep-water formula) as follows:

$$c^2=\frac{\lambda^2}{T^2}=\frac{g\lambda}{2\pi}; \tag{6.42-4}$$

thence

$$\lambda=\frac{gT^2}{2\pi}\approx 160\,T^2 \tag{6.42-5}$$

1. O'BRIEN, M. P., and R. MASON: A Summary of the Theory of Oscillatory Waves. Tech. Rep. 2, Beach Erosion Board, 1940.

2. MUNK, W. H., and M. A. TRAYLOR: J. Geol. 55, 1 (1947).

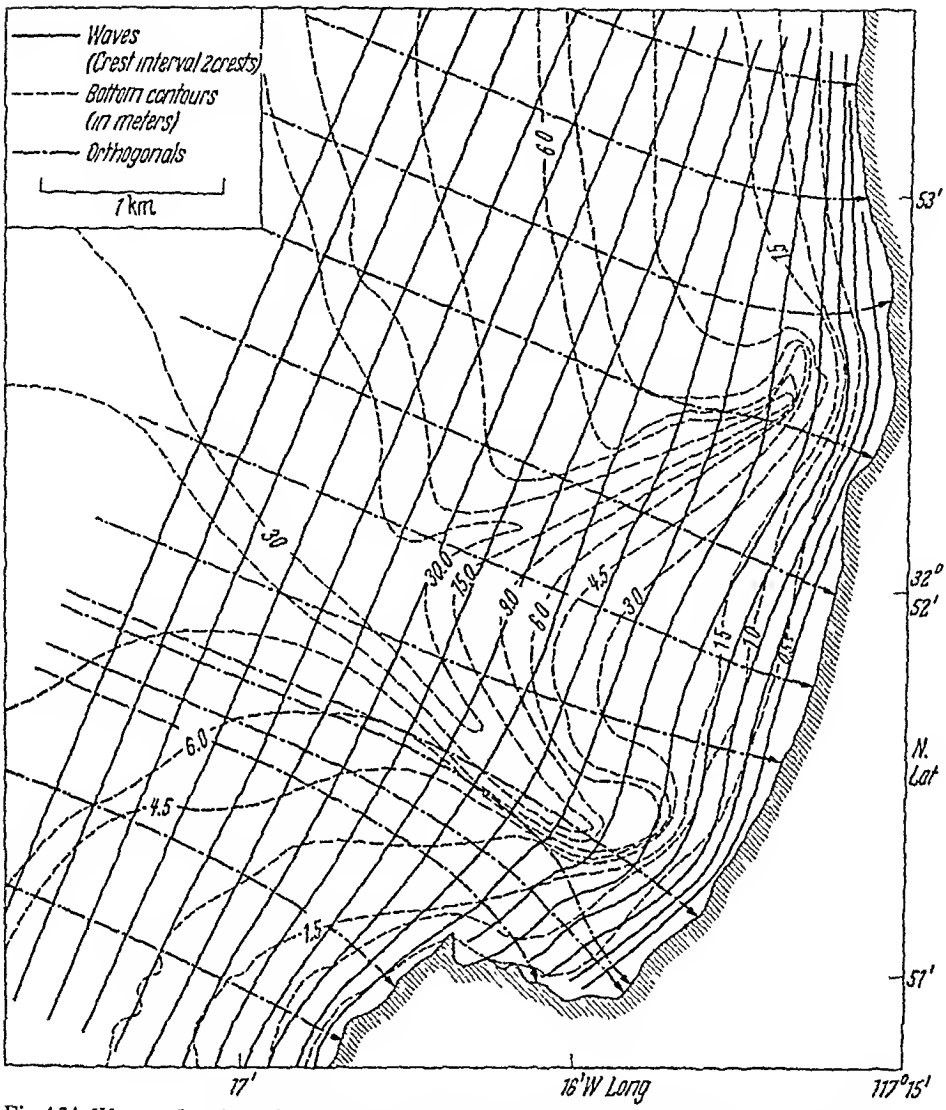

Fig. 154 Wave refraction diagram for 8-second swell striking Southern California from a direction of WNW. After MUNK and TRAYLOR[1]

where the last value is for the c.g.s.-system. Thus, the critical depth at which wave refraction becomes important, is from (6.42-3):

$$h = \frac{1}{4}\frac{gT^2}{\pi} \approx 80\,T^2 \text{ cm}. \qquad (6.42\text{-}6)$$

Ocean swell has seldom a period of more than 14 sec, hence the depth at which it becomes refracted is approximately

$$h = 160 \text{ meters}. \qquad (6.42\text{-}7)$$

1. MUNK, W. H., and M. A. TRAYLOR: J. Geol. 55, 1 (1947).

For a short period wind wave ($T=7$ sec), the corresponding value is

$$h=40 \text{ meters}. \tag{6.42-8}$$

The breaking waves, as they roll into the shore, give rise to currents near the shore. Our next problem is to discuss the dynamics of these currents.

If the waves break into the shore not absolutely orthogonally, but at an angle $\frac{1}{2}\pi-\alpha$, then it can be shown that a longshore current will be set up. A simple theory of how this may occur has been proposed by PUTNAM, MUNK and TRAYLOR[1].

Thus, let us consider waves striking the shore in a pattern as sketched in Fig. 155. We denote by Q the cross-sectional area of a breaking wave crest, by λ its wave length and by c its velocity. Then the average momentum M per unit surface area is (ρ is the density of water)

$$M=\frac{\rho Q c}{\lambda} \tag{6.42-9}$$

and hence the mean flux of momentum dF_M into the volume $ABCDE$ (cf. Fig. 155) is (u denoting some velocity-constant)

$$dF_M=u\frac{c\rho Q}{\lambda}\cos\alpha\, dx. \tag{6.42-10}$$

Consequently, the mean flux parallel to the shore line is

$$dF_{M\parallel}=u\frac{c\rho Q}{\lambda}\sin\alpha\cos\alpha\, dx. \tag{6.42-11}$$

After the water has been slowed down to form the longshore current with velocity v, the flux of momentum *after* the slowdown $dF'_{M\parallel}$ is

$$dF'_{M\parallel}=u\frac{v\rho Q}{\lambda}\cos\alpha\, dx. \tag{6.42-12}$$

The difference of $dF'_{M\parallel}$ and $dF_{M\parallel}$ represents the net flux of momentum, or the equivalent force, applied by the breakers upon the water mass in the surf zone. The latter is balanced by the frictional force acting on the volume $ABCDE$ in the longshore current which we assume, in conformity with the drag theory, as equal to (with k equal to some constant and l denoting the distance from the shore to the breaker line):

$$dF_{\text{friction}}=k\,u\,\rho\,v^2\,l\,dx. \tag{6.42-13}$$

1. PUTNAM, J. A., W. H. MUNK, and M. A. TRAYLOR: Trans. Amer Geophys. Union 30, 337 (1949).

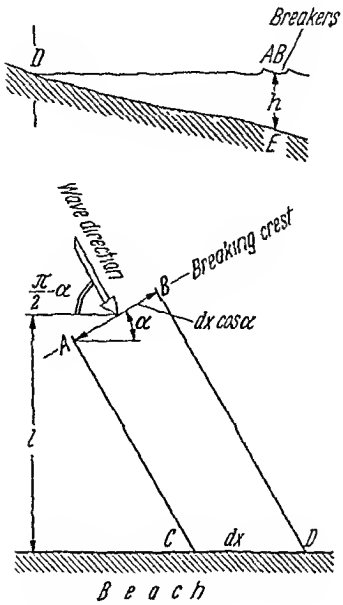

Fig 155. Geometry of waves breaking at an angle: top, view in section; bottom, view in plan After PUTNAM et al.[1]

Writing down the force balance equation yields an equation for v

$$\frac{c\rho Q}{\lambda}\sin\alpha\cos\alpha\,dx-\frac{v\rho Q}{\lambda}\cos\alpha\,dx-k\rho v^2 l\,dx=0. \quad (6.42\text{-}14)$$

Solving for v yields

$$v=\frac{a}{2}\left\{-1+\sqrt{1+4\frac{c\sin\alpha}{a}}\right\} \quad (6.42\text{-}15)$$

with

$$a=\frac{Q\cos\alpha}{k l\lambda}. \quad (6.42\text{-}16)$$

In the above equations, one can replace the value of Q by a relationship obtained from wave theory (cf. Eq. 6.22-49). Then, the formula (6.42-15) contains only one constant (k) which must be adjusted *a posteriori*.

The theory of PUTNAM et al. given above has been modified, still based on the assumption of momentum conservation, by various people (for a summary see the review of GALVIN[2]). Thus a modification of Eq. (6.42-15) introduced by GALVIN[2] is commonly used for engineering purposes. However, GALVIN[2] noted that the momentum theory implicitly requires that the longshore component of the speed of the breaking

1. PUTNAM, J. A., W. H MUNK, and M. A. TRAYLOR: Trans. Amer. Geophys. Union 30, 337 (1949).

2 GALVIN, C. J.· Revs. Geophys. 5, 287 (1967).

wave crests is larger than the velocity of the longshore current; this is, in fact, not borne out in nature so that there is a serious objection to this type of theory. Thus, it appears that empirical correlations exhibit, at the present time, the best hope for success. One of these correlations, obtained by a multi-regression analysis, is due to HARRISON[1]:

$$v = -0.170455 + 0.037376\alpha + 0.031801\,T + 0.241176\,H_{bs} + 0.030923\,\beta \tag{6.42-17}$$

where the symbols have the same meaning as above; in addition H_{bs} is the significant breaker height, T the period of the swell and β the beach slope. As units, meters, seconds and degrees (for the angles) are used.

In addition to longshore currents, another type of currents may be caused by the incoming waves. These are *rip currents* which have been described, for instance, by SHEPARD[2,3], INMAN[3,4] and BOWEN[4,5]. Such rip currents are seaward moving water masses which are restricted to relatively narrow lanes. They carry some of the backflow which has to compensate for the onshore water movement caused by the swell. A typical nearshore circulation pattern, after SHEPARD[2], which includes a rip current, is shown in Fig. 156.

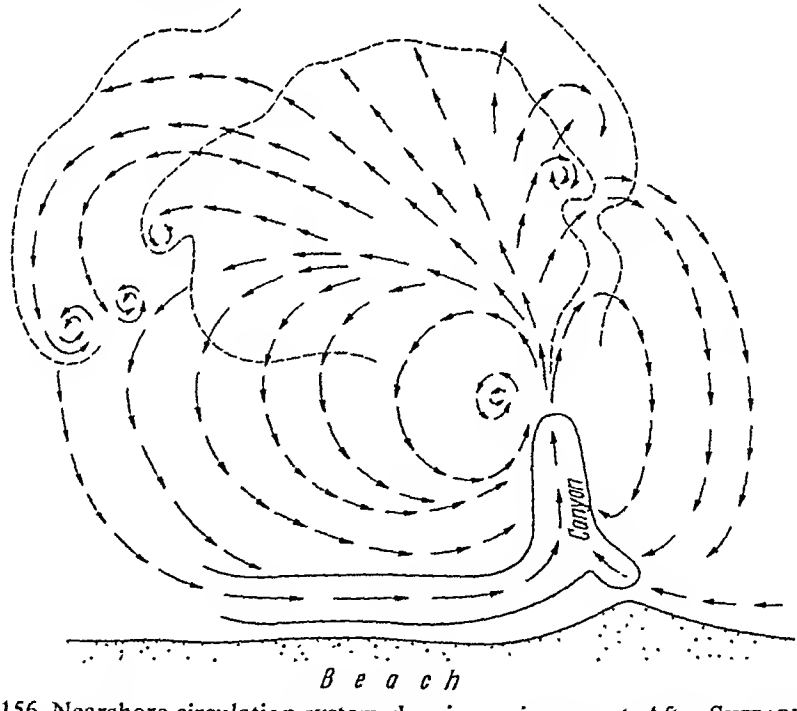

Fig. 156. Nearshore circulation system showing a rip current. After SHEPARD[2]

1. HARRISON, W.: J. Geophys. Res. 73, 6929 (1968).
2. SHEPARD, F. P.: Submarine Geology. New York: Harper 1948.
3. SHEPARD, F. P., and D. L. INMAN: Trans. Amer. Geophys. Union 31, 196 (1950).
4. BOWEN, A. J., and D. L. INMAN: J. Geophys. Res. 74, 5479 (1969).
5. BOWEN, A. J.: J. Geophys. Res. 74, 5467 (1969).

In effect, it may be argued that rip currents are not independent facets of the nearshore circulation system, but are intimately tied up with wave refraction and longshore currents. Thus, BRUUN[1] assumes that, as a wave breaks at an angle towards the shore, it contributes water to the surf zone which, because of mass conservation, creates alternate longshore and rip currents behind and across a system of bars (Fig. 157). Introducing a Chézy-type of friction for the longshore current,

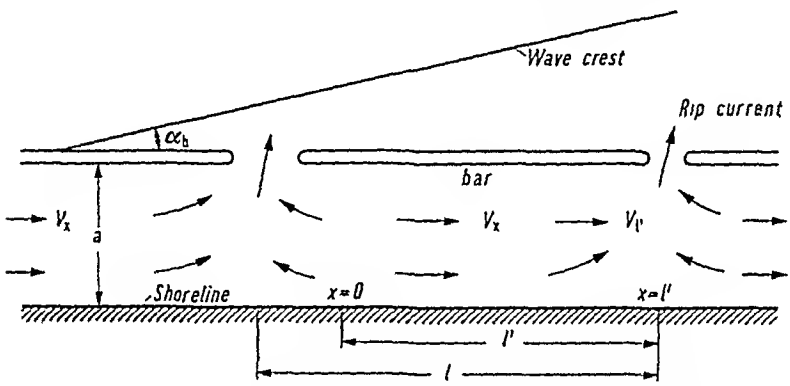

Fig. 157. System of rip and longshore currents. (After BRUUN[1])

GALVIN[2] deduced from BRUUN'S[1] theory the following formula for the average velocity of the induced longshore current:

$$v = C_f [H_{bs}^{\frac{5}{2}} \beta (\sin 2\alpha)/T]^{\frac{1}{2}} \qquad (6.42\text{-}18)$$

where C_f is a Chézy-type of friction factor and the other symbols have the same meaning as in the equation before. Thus, introducing mass conservation and a rip current system, a new theory of the origination of longshore currents is in fact arrived at.

The nearshore circulation system gives rise to littoral drift of sedimentary material. Attempts to calculate theoretically the amount of littoral drift from the wave pattern have been reported by SHVARTSMAN and MAKAROVA[3], but many assumptions regarding carrying capacity of certain types of currents etc. have to be made. INMAN and FRAUTSCHY[4] state that the sediment transport rate along most oceanic beaches is from about 45,900 to 764,500 m^3 of sand per year, the average being near 153,000 m^3 of sand per year.

1. BRUUN, P.: J. Geophys. Res. 68, 1065 (1963).
2. GALVIN, C. J.: Revs. Geophys. 5, 287 (1967).
3. SHVARTSMAN, A. YA., and A. I. MAKAROVA: Trudy Gos. Gidrol. In-ta 132, 57 (1966).
4. INMAN, D. L., and J. D. FRAUTSCHY: Proc. Santa Barbara Coastal Eng. Conf., Coastal Eng. 511 (1966).

6.43. Theory of Beaches. We now turn our attention to one of the most common coastal features: these are the beaches.

Our first interest concerns *the flow regime on a beach.* The theory of water waves presented in Sec. 6.22 can be applied to a discussion of the behavior of waves ascending a sloping beach. Most of the results that we are to use are based upon one of the two possible approximations (cf. Sec. 6.22), the complete problem of wave action being intractable.

Specific further calculations, based on the non-linear shallow water theory, have also been reported by CARRIER and GREENSPAN[1], by GREENSPAN[2] and by KELLER et al.[3]. The first two of these investigators show that it is, in fact, not always necessary that waves break on a shore; the last investigators achieve their solution of the wave problem by means of a digital computer.

For our further purposes, the theory as given in Sec. 6.22 will generally be adequate; for further refinements, the reader is referred to the papers cited above or to the pertinent monographs mentioned in Sec. 6.22.

An interesting modification of the wave theory has been made by allowing for the fact that the beach surface may be *permeable* to water. Essentially, this produces a dissipation of energy whilst the wave is ascending the beach. The problem has been studied by PUTNAM[4], by REID and KAJIURA[5] (actually only for deep water) and by HUNT[6] from a theoretical standpoint, and by GRANTHAM[7], SAVILLE[8] and by SAVAGE[9] from a experimental standpoint. From these investigations it appears that our picture of the wave dissipation process which occurs on a beach, is still quite incomplete. Nevertheless, SAVAGE presented graphs relating the run-up to wave steepness, slope roughness and slope permeability which he claims to be applicable to prototype conditions.

The particles making up a beach show some degree of sorting. Thus, we turn now to the *problem of finding the corresponding sorting-mechanism.*

First, we note that there are two types of beaches: shingle beaches (i.e. beaches where the particles are 1 cm or more in diameter) and sandy beaches (i.e. beaches where the particles are 1 mm or less in diameter). At the beginning of the present discussion, we shall concern ourselves with sandy beaches; a discussion of shingle beaches will be given later.

---

1. CARRIER, G. F., and H. P. GREENSPAN: J. Fluid Mech. 4, 97 (1958).
2. GREENSPAN, H. P.: J. Fluid Mech. 4, 330 (1958).
3. KELLER, H. B., D. A. LEVINE, and G. B. WHITHAM: J. Fluid Mech. 7, 302 (1960)
4. PUTNAM, J. A.: Trans. Amer. Geophys. Union 30, 349 (1949).
5. REID, R. O., and K. KAJIURA: Trans. Amer. Geophys. Union 38, 662 (1957).
6. HUNT, J. N.: J. Geophys. Res. 64, 437 (1959).
7. GRANTHAM, K. N.: Trans. Amer. Geophys. Union 34, 720 (1953).
8. SAVILLE, T.: J. Wwys. Div., Amer. Soc. Civ. Eng. 82, WW 2 (1956).
9. SAVAGE, R. P.: J. Wwys. Div., Amer. Soc. Civ. Eng. 84, WW 3 (1958).

With regard to sandy beaches, it has been noted that the action of the surface waves causes a certain amount of sorting of the grains. Detailed field observations of this phenomenon have been carried out, for instance, by TRASK and JOHNSON[1], by TRASK[2] and by GRIESSEIER and VOLLBRECHT[3]. The grain size distribution pattern on beaches was found to vary with the seasons because the prevailing wave patterns vary with the seasons.

On a beach there are several dynamic zones which are illustrated in Fig. 158. Most of the studies of sorting of grains are concerned with the zone of shoaling waves. We shall first discuss the sorting of the grains due to shoaling waves and later examine the other dynamic zones.

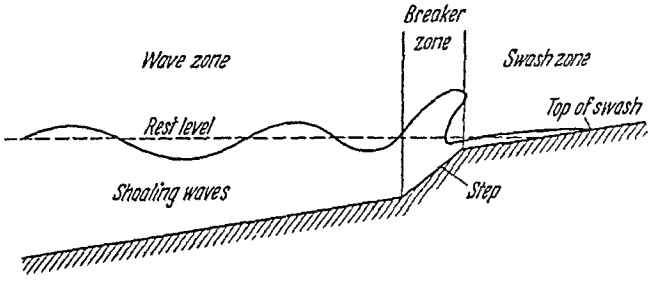

Fig 158. Schematic representation of the dynamic zones on a beach

The mechanism that is presumably responsible for the sorting of grains by wave action on a beach in the zone of shoaling waves has been discussed by KOLP[4] in qualitative terms. Accordingly, the sorting is due to the differential motion of individual grains, depending on their size, as they are being dragged along at the bottom by the orbital motion of the water caused by the waves.

A discussion of the phenomenon under consideration which can be regarded somewhat more justifiably as a "theory" has been given long ago by CORNAGLIA[5]. Accordingly, the crest velocity in a wave is greater than the trough velocity in shallow water. Hence the force moving a sand grain will tend to move the grain in the direction in which the crests are moving, a distance proportional to the difference between crest and through velocities. The difference between crest and trough velocities becomes less as the water depth increases, and at the same time the

1. TRASK, P. D., and C. A JOHNSON. Sand Variations at Point Rayes, California. Beach Erosion Board Tech. Mem 65 (1955).

2. TRASK, P. D. Change in Configuration at Point Rayes Beach, California. Beach Erosion Board Tech. Mem. 91 (1956)

3. GRIESSEIER, H., and K. VOLLBRECHT: Acta Hydrophys. **2**, No. 3, 87 (1955).

4 KOLP, O.: Petermann's Geogr. Mitt. **102**, No. 3, 173 (1958)

5 CORNAGLIA, P.: Sul regime delle spaggie e sulla regolazione dei porti Torino (1891)

influence of gravity becomes predominant tending to pull the particle seaward. Somewhere on the beach (null point), all the forces that act on one particular grain size are equal; seaward to this point the particles are drawn seaward, landward to it, they are dragged landward. The null point is the only place where a particle can remain in an equilibrium condition.

CORNAGLIA's "theory" was further tested by IPPEN and EAGLESON[1], who from a series of very careful experiments, arrived at the following dimensionless relation for the null-points

$$\left(\frac{H}{h}\right)^2 \left(\frac{\lambda}{H}\right) \left(\frac{c}{w}\right) = 11.6 \tag{6.43-1}$$

where H is the wave height, λ the wave length, c the wave velocity, h the still water depth and w the settling velocity of the grains in question. The use of Eq. (6.43-1) allows one to construct theoretical null line maps for a given type of swell on a beach.

EAGLESON and coworkers[2,3] have expanded their empirical approach by going back to the equation of motion for bottom sediments (4.53-4) in a river. However, they now replace the friction term (for the notation see Sec. 4.53

$$(M_s - M_f)\, \varepsilon\, g \cos\alpha$$

by

$$C_{Rx} \frac{\pi d^2}{8} (v_f - v_s)^2 \tag{6.43-2}$$

where C_{Rx} is a new coefficient. This, in fact, implies that the bottom resistance is not that which one would expect from the law of sliding friction, but allegedly that corresponding to rolling friction. In fact, the coefficient C_{Rx} is difficult to measure, and it is therefore usually incorporated into C_D (now denoted by C'_D) the two terms having the same form. Thus

$$M_s \frac{dv}{dt} = C'_D \frac{\pi}{8} d^2 \rho (v_f - v_s)^2 - (M_s - M_f)\, g \sin\alpha. \tag{6.43-3}$$

One can now average the above equation over one wave cycle. The acceleration term then drops out, and one is left with

$$C'_D \frac{\pi}{8} d^2 \rho \overline{(v_f - v_s)^2} = (M_s - M_f)\, g \sin\alpha. \tag{6.43-4}$$

---

1. IPPEN, A. T., and P. EAGLESON: A Study of Sediment Sorting by Waves Shoaling on a Plane Beach. M.I.T. Hydrodynamics Lab. Technol. Rept. No. 18 (1955).

2. EAGLESON, P. S., R. G. DEAN, and L. A. PERALTA: The Mechanics of the Motion of Discrete Spherical Bottom Sediment Particles Due to Shoaling Waves. – M.I.T. Hydrodyn. Lab. Tech. Rep. No. 26 (1957).

3. See also EAGLESON, P. S., and R. G. DEAN: J. Hydraul. Div., Proc. Amer. Soc. Civ. Eng. 85, No. 10, Part 1, 53 (1959).

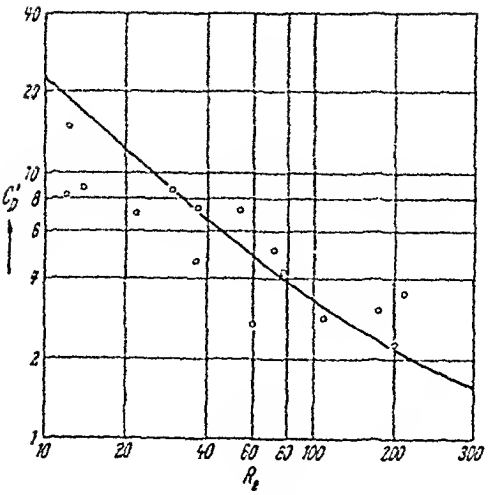

Fig. 159 Plot of resistance coefficient versus REYNOLDS number. After EAGLESON et al.[1]

EAGLESON et al. made experiments to check this equation. Since C'_D is only an empirical factor, the particular assumption made for the bottom friction force is really immaterial. It could equally well have been neglected entirely.

Using a special assumption for the shoaling wave form, EAGLESON et al. then showed that the average in Eq. (6.43-4) can also be written

$$C'_D \frac{\pi}{8} d^2 \rho (\bar{v}_f - \bar{v}_s)^2 = (M_s - M_f) g \sin \alpha. \tag{6.43-5}$$

The reason that this can be done lies in the fact that, if the wave motion is quasi-oscillatory, the sediment motion is also quasi-oscillatory, without any phase shift. This immediately allows one to form the averages as indicated above.

The last Eq. (6.43-5) was also investigated experimentally by EAGLESON et al. This was done by plotting the "coefficient" C'_D, as found experimentally by measuring all remaining quantities in Eq. (6.43-5), against a Reynolds number

$$R_e = (\bar{v}_f - \bar{v}_s)\, d/\nu \tag{6.43-6}$$

where ν is as usual the kinematic viscosity. The result obtained is that shown in Fig. 159. In that figure, the result is then compared with an empirical curve obtained by CARTY[2] (solid line in Fig. 159) giving the

1. EAGLESON, P. S., R. G. DEAN, and L. A. PERALTA: The Mechanics of the Motion of Discrete Spherical Bottom Sediment Particles Due to Shoaling Waves. Cambridge: M.I.T. Hydrodyn. Lab. Tech. Rept. No. 26 (1957).

2. CARTY, J. J.: Resistance Coefficients for Spheres on a Plane Boundary. B. Sc. Thesis, Massachusetts Inst. Techn., 1957.

resistance coefficient (corresponding to C'_D above) for a sphere rolling down an inclined slope in a liquid. According to EAGLESON et al., the agreement is excellent which, in turn, would establish the fact that sand particles on a beach are actually being rolled by the wave action. The curve around which the measured points scatter, is roughly of the form

$$C'_D = \text{const}/R_e. \tag{6.43-7}$$

Now, it has been found empirically in shoaling waves that the following relationship holds approximately

$$\bar{v}_f/\bar{v}_t = \text{const}(d/T^{1.43})^{\frac{1}{2}} \tag{6.43-8}$$

where T is the period of the waves and v_t is the fictitious bottom-velocity calculated from wave motion theory according to a formula by STOKES (cf. 6.22-21)

$$\bar{v}_t = \frac{1}{2}\pi^2 \frac{H^2}{\lambda^2} \frac{\text{const}}{\left(\sinh \frac{2\pi h}{L}\right)^2}. \tag{6.43-9}$$

Here, H is the height of the wave, h its depth, and λ its wavelength. Taking all the equations together yields

$$d^{\frac{1}{2}} \sin\alpha = \text{const}\, \bar{v}_t\, T^{-0.36}. \tag{6.43-10}$$

This shows that a particular size d of particles will collect at that point of the beach where the corresponding wave-period prevails. This gives an explanation for the empirically observed sorting of particles on a beach.

The above theory has been refined by RUSNAK[1] to include an analysis of the orientation of sand grains under conditions of unidirectional flow. He found that the most stable position which an elliptical particle acquires in depositional transport is one with its long axis lying parallel to the direction of the fluid motion.

Measurements of the size distribution and the motion of beach sand have been reported, e.g. by BLAU[2], by INMAN and CHAMBERLAIN[3] by INGLE[4] and by MILLER and ZEIGLER[5]. The last paper cited is of particular importance in that it contains a direct evaluation CORNAGLIA's and EAGLESON's theories. Null-lines are constructed and compared with the actual sand distribution on a natural beach. The agreement with the natural cases, although restricted by the information available, was found to be sufficiently good to warrant publication of the study.

---

1. RUSNAK, G. A.: J. Geol. 65, 384 (1957).
2. BLAU, E.: Wasserwirtsch.-Wassertechn. 6, 257 (1956).
3. INMAN, D. L., and T. K. CHAMBERLAIN: J. Geophys. Res. 64, 41 (1959).
4. INGLE, J. C.: The Movement of Beach Sand. 221 pp. Amsterdam: Elsevier 1966.
5. MILLER, R. L., and J. M. ZEIGLER: J. Geol. 66, 417 (1958).

As was noted earlier, the above discussion referred to the sorting of grains in the wave zone only: most investigations reported in the literature are concerned with the wave zone only. The paper by MILLER and ZEIGLER cited above, forms a notable exception in this regard as it contains at least a qualitative discussion of the phenomena occurring in the breaker zone and in the swash zone.

Turning first to the *breaker zone*, we note that the inshore velocity of the sediment is zero because in this zone the wave is met by the backwash. This is the reason for a step to form. Furthermore, it is in this zone where the coarsest sediments on a beach are found. Unfortunately, not much more can be said theoretically regarding the behavior of grains in the breaker zone.

A somewhat more elaborate study has been made of the *swash zone*, for which MILLER and ZEIGLER suggested a rather elaborate theoretical model. Their model consists of the following elements:

(i) an assumption regarding the size distribution left just at the end of any individual upswash. This size distribution is taken as graded with the finest particles being found near the top of the swash;

(ii) an assumption regarding the minimum velocity required to drag a given particle downslope by the backwash and

(iii) an assumption regarding the velocity distribution during the backwash.

MILLER and ZEIGLER use empirical relationships for (ii) and (iii) whose reliability is perhaps somewhat questionable. It is then possible to find the "theoretical" size gradation that should be left by a given backwash. MILLER and ZEIGLER claim reasonable agreement with observations, but in view of the many empirical relationships and indetermined constants employed by them, the problem of devising a completely satisfactory theory of the observed size distributions in the breaker and swash zones on a beach cannot be regarded as entirely solved as of yet.

So far, we have dealt with the sorting of grains on *sandy* beaches. However, not all beaches consist of sand, some consist of *shingle*. By the term "shingle" we mean as noted earlier, pebbles of about a centimeter or more in diameter.

It is an interesting observation that there are no beaches intermediate between shingle beaches and sandy beaches; in other words, the size distribution function of beach detritus is bimodal. This is a fact which requires an explanation in terms of physical principles.

The contrition of the original material to pebbles presumably takes place by the Rayleigh process which also applies to river pebbles; in the latter connection it was discussed in Sec. 4.72. The action of the waves upon the shingle is very similar to the action of the rotating can in

RAYLEIGH's experiments; the contrition, thus, corresponds to the first set of RAYLEIGH's experiments in which steel nuts were used as an abrasive material (cf. Sec. 4.72). Thus the standard shape of shingle particles may be assumed to be rather oblong as shown in Fig. 119 (see Sec. 4.72). Very large pebbles may be spherical[1].

As long as the shingle particles remain fairly large, the Rayleigh process is the only process causing size diminution. However, it has been suggested by BERNAL[2] that, once the shingle particles become smaller than a certain critical size, they also begin to break in two in the middle while being thrown around by the surf. This would greatly accelerate the contrition and the particles, once they are below the critical size, will

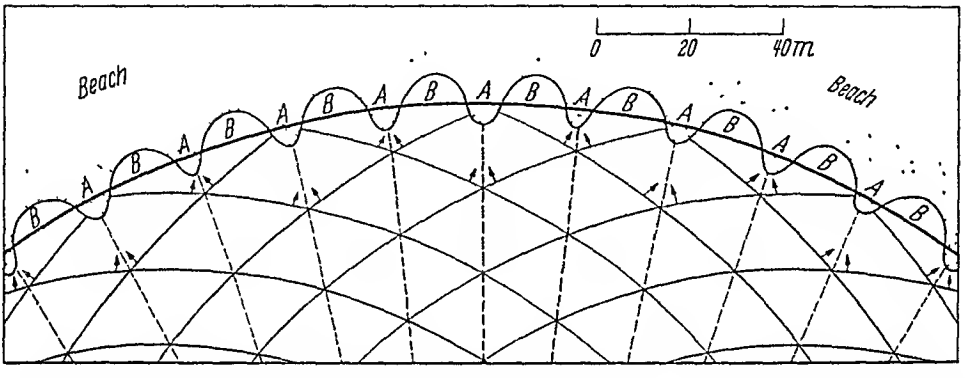

Fig 160. Diagram illustrating BRANNER'S[3] theory of beach cusp formation; after JOHNSON[4]

rapidly be reduced to sand. Hence shingle particles found on beaches will always be above a certain critical size, depending on the action of the surf; any particles below that size will be ground to sand almost immediately. This explains the bimodal size distribution of beach material.

After having discussed the sorting of particles on a beach, we now turn to *effects of a somewhat larger scale*, such as beach cusps and ripples.

With regard to *beach cusps*, we note that they have been regarded by BRANNER[3] as the result of a interference phenomenon between two sets of waves. A diagram, after JOHNSON[4], illustrating BRANNER's theory is shown in Fig. 160. Contrary to this, however, RUSSELL and MCINTYRE[5]

1. See KUZNETSOV, A. M., and V. A. KUZNETSOV: Izv Akad. Nauk, SSSR, Ser. Geofiz. **1959**, No. 8, 1247 (1959).

2. In a private communication to the writer, from which to quote Professor J. D. BERNAL has kindly given permission.

3. BRANNER, J. C.: J. Geol **8**, 481 (1900).

4. JOHNSON, D. W.: Shore Processes and Shore Line Development. New York: J. Wiley & Sons 1919.

5. RUSSELL, R. J., and W. G. MCINTYRE: Bull. Geolog. Soc. Amer. **76**, 307 (1965).

ascribe cusp formation to cellular flow patterns connected with the nearshore circulation system.

Turning now to *ripple marks*, we note that we have met such features already in the case of river beds. One can, therefore, regard the origin of beach ripples as due to essentially the same causes as river-bed ripples.

However, there is one difference: On a beach, the motion of the water is oscillatory, whereas on a river bed it is uniderectional. Nevertheless, this difference may not be essential; the "traffic-jam" idea (cf. Sec. 4.62) could evidently still be applied, inasmuch as kinematic interference between particles must be expected in oscillatory as well as in unidirectional flow.

A more specific approach has been taken by KENNEDY and FALCÓN-ASCANIO[1] who based their theory on a theoretical model involving a sediment-transport relation and a continuity condition for sediment transport. In this fashion, changes in the local bed deviation can be related to the local fluid velocity. This leads to a kinematic "feed-back" effect which leads to ripple-type of instabilities. It is seen that this is, in effect, nothing but a specific mechanical model for the traffic-jam idea.

Finally, we are now turning toward the *large scale changes that may be expected in the course of the life of beach.* A convenient general summary of the problem has been given by BASCOM[2].

Let us first investigate the conditions under which a beach will remain relatively *stable*. One may reckon that it will then be easy afterward to determine the changes that occur, simply by considering cases where conditions are such that a beach cannot be stable.

Of the theoretical attempts to calculate the equilibrium shore-profile, an investigation by WELLS[3] is noteworthy, who tried to get direct stability conditions from second-order gravity-wave theory. More macroscopic approaches have been made by NAGATA[4] who investigated the water-mass and sediment balance equations required for equilibrium, and by PRAVOTOROV[5] who looked at the composite energy flux.

There is a great number of surveys of beaches that have been made to ascertain the standard form. However, it is very difficult to bring all these surveys to a common denominator. In this connection, it has been noted by TANNER[6] that the concepts of régime theory of rivers (cf. Sec. 4.64) can also be applied to beaches. Accordingly, there are certain

1 KENNEDY, J. F., and M. FALCÓN-ASCANIO: Mass Inst. Technol, Hydrodynamics Lab. Staff Publ. No. 99 (1964).

2. BASCOM, W.: Sci. Amer. 203, No. 2, 80 (1960).

3 WELLS, D. R.: J. Geophys. Res. 72, 497 (1967).

4. NAGATA, Y.: Rec. Oceanogr. Wks. Japan 6, No. 1, 53 (1961).

5. PRAVOTOROV, I. A.: Okeanologiya 5, No. 3, 473 (1965).

6 TANNER, W. F.: Trans. Amer. Geophys. Union 39, 889 (1958)

combinations of beach parameters which effect that a beach is "at grade", and any deviations in these parameters from equilibrium combination will cause the beach to try to adjust itself in such a manner so as to reach equilibrium. Unfortunately, TANNER does not proceed to set up equations which would be analogous to the equations of régime theory of rivers (cf. Sec. 4.64), as this does not seem to be possible at the present stage of development of the beach erosion theory. However, LUDWIG[1] has at least been able to fix the values of some parameters (based on a statistical measure of the grain size distribution of the beach) necessary to achieve equilibrium which he deduced from field observations in the Baltic Sea. Nevertheless, a proper set of equations as in river theory, was not deduced either. The problem of establishing the pertinent equations of the equilibrium theory of beaches has obviously not yet been solved. The original thought of describing beach erosion processes as deviations from an equilibrium state can therefore not be followed up.

It is therefore necessary to turn our attention to a discussion of the various processes listed in Sec. 6.3 as active on coast lines and to investigate their significance with regard to beaches. We first consider the effect of swell. A recent monograph on this subject has been written by DJOUNKOVSKI and BOJITCH[2]; many original articles have also been published in the literature.

It stands to reason that the effect of swell on beach erosion is linked with the phenomenon of wave refraction. The problem has been examined from this angle in a study by MUNK and TRAYLOR[3]. The effect of the swell manifests itself in two ways: first sediment is transported by *direct action* associated with the swell and second *convection* occurs which is associated with the secondary currents created (such as longshore currents) by the swell.

The direct action manifests itself, for instance, in *diffusion*. This diffusion results from the variation of the wave heights along the beach. According to wave refraction theory, wave heights are small above the mouth of submarine canyons and large above their sides. Since large waves cause larger breakers than small ones, and larger breakers cause more turbulence than small ones, more sediment will settle out at the bottom of a canyon than on its sides. Thus, diffusion, for instance, tends to fill in submarine canyons. Similarly, it tends to obliterate submarine ridges.

1. LUDWIG, G.: Geol. Rdsch. **47**, 66 (1958).

2. DJOUNKOVSKI (DZHUNKOVSKII), N. N., and P. K. BOJITCH (BOZHICH): La houle et son action sur les côtes et les ouvrages côtieres (translated from Russian). Paris: Gauthier-Villars 1959.

3. MUNK, W. H., and M. A. TRAYLOR: J. Geol. **55**, 1 (1947).

The effect of diffusion is generally considered as small although no quantitative evaluations regarding its significance seem ever to have been undertaken. However, there is another way in which some direct action can be exercised by the swell upon the beach: this is *direct erosion* by the bottom drag of the waves. According to DAVIES[1], steep waves produce erosion and flat waves produce deposition. Elaborate experimental studies to ascertain the direct effect of the swell upon various types of sand have been reported by VINCENT and RUELLAN[2] and by LARRAS[3]. The last author arrived at numerical formulas for

(i) the smallest instantaneous (alternating) bottom velocity v_b at which erosion leads to the initiation of slight furrows after a (practically) infinite length of time; he obtained in the c.g.s.-system

$$v_b = w + 9.5 \frac{(\rho - 1)^{\frac{1}{2}}}{T^{\frac{1}{2}}} \tag{6.43-11}$$

where w is the settling velocity of the grains, ρ the density of the grains and T the period of oscillation;

(ii) the depth of erosion pits in the vicinity of obstacles; he found that the ultimate depth d of the erosion pits was sensibly unaffected by the shape of the obstacle and given by

$$d = \text{const} \log \frac{\left(\frac{H}{10}\right)^{3.5}}{\rho - 1} \tag{6.43-12}$$

where H is the height of the waves, ρ again the sediment density and the constant depends on the other parameters;

(iii) the time in which the erosion gradually reaches its maximum. The erosion proceeds according to an experimental law for whose halflife Θ LARRAS found (c.g.s.-system) independently of the sand:

$$\Theta = 360(\rho - 1)^2. \tag{6.43-13}$$

As is seen from the various remarks above, the direct action of the swell is rather small and insignificant. The secondary currents set up by the swell seem to be of much greater importance inasmuch as they may cause large scale *convection*. These secondary currents which have already been discussed above, are *longshore currents* and *rip currents* which are directed from shore to sea; the latter are most pronounced if the waves come straight toward the shore. It turns out that it is impossible

1. DAVIES, J. L : Austral. J. Sci. 20, 105 (1957)
2. VINCENT, G , and F RUELLAN: Houille Blanche 12, No. B, 693 (1957).
3. LARRAS, J.· Ann. Ponts et Chaussées 127, No 5, 599 (1957).

to find the effect of the currents on the shore by calculation. Thus, attention has been directed toward model experiments[1]. In an attempt at making models, SCHMITZ encountered insurmountable difficulties because of the impossibility to achieve sedimentological and hydrodynamic similarity at the same time. The latter fact has been demonstrated e.g. by GRIESSEIER and VOLLBRECHT[2] and by POPOV[3]. The problem of an explanation of the action of the near-shore circulation system upon the geomorphology of the area has therefore not yet been solved.

Difficulties are also encountered with regard to an explanation of the action of other types of currents upon the bottom topography, viz. of *tidal* currents. The action of such currents has been described in qualitative terms by INMAN and FILLOUX[4] by measurements on the California coast, but no quantitative laws have ever been deduced.

Finally, severe geomorphological changes on a beach may also be caused by catastrophic phenomena, such as great storms. Again, descriptions of observed changes may be found in numerous places in the literature[5], but any theory of the phenomena taking place is still completely lacking.

6.44. Theory of Special Features on Shallow Coasts. In Sec. 1.62 we have mentioned some features which occur specifically on shallow coasts. We shall now discuss the possible mechanical theories for their explanation.

First, turning to *spits* and *bars*, we note that their formation[6, 7] has generally been linked to the wave refraction phenomenon.

The spits may be curved to form *hooks*. The manner in which a hook may be formed has been illustrated by HOLMES[6] and is shown in Fig. 161. As the waves are refracted around the tip of a spit, the attendant longshore currents become weaker and hence material is deposited. This phenomenon was also studied experimentally by CASTANHO[8].

Second, we turn to a discussion of the origin of *offshore bars*. The cause of the formation of bars has generally been sought in the emergence of the coast line. A phenomenological theory based upon this hypothesis has been developed by JOHNSON[9]. Accordingly, bars are supposed to

1. See e.g. SAVILLE, T.: Trans. Amer. Geophys. Union **31**, 555 (1950).
2. GRIESSEIER, H., and K. VOLLBRECHT: Wasserwirtsch.-Wassertechn. **6**, 247 (1956).
3. POPOV, B. A.. Trudy Okeanogr. Kommiss. Akad. Nauk SSSR **1**, 120 (1956)
4. INMAN, D. L., and J. FILLOUX: J. Geol. **68**, 225 (1960).
5. E.g ZEIGLER, J. M., C. R. HAYES, and S. D. TUTTLE: J. Geol. **67**, 318 (1959)
6. HOLMES, A.: Principles of Physical Geology. London: T. Nelson & Sons 1944.
7. TANNER, W. F.: Science **132**, No. 3433, 1012 (1960).
8. CASTANHO, J. P.: Mém. Lab. Nac. Engenharia Civil, Lisboa **139**, 1 (1958).
9. JOHNSON, D. W.: Shore Processes and Shoreline Development. New York: J Wiley & Sons 1919.

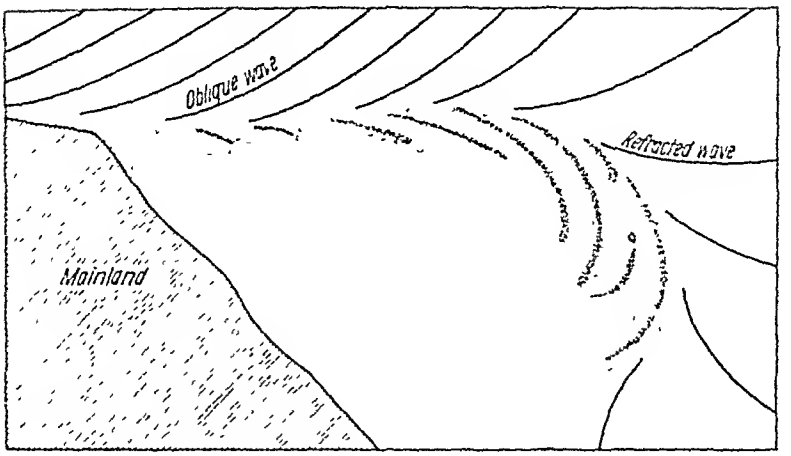

Fig. 161. Formation of a curved hook. After HOLMES[1]

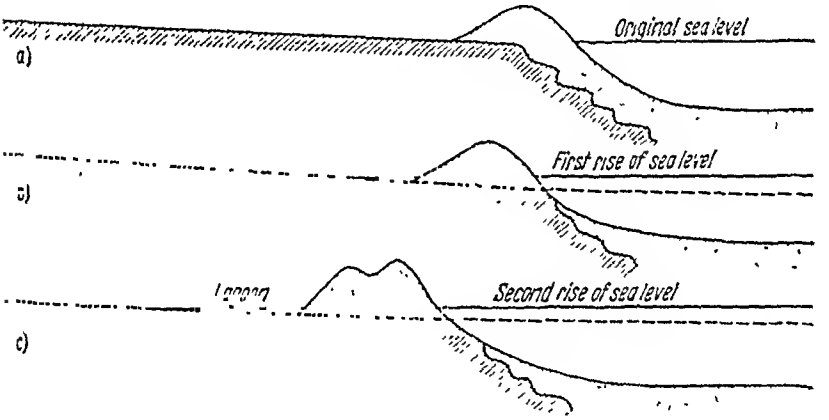

Fig. 162. Creation of an offshore bar on a submerging coast line. After ZENKOVICH[2]

develop at the youthful stage of the emergence of the coast line, owing to a process of transfer of bottom material from the shallow water towards the sea. First, a submerged bar is formed which later grows owing to the lowering of the sea level.

Although JOHNSON's theory has met with general acceptance, it has been pointed out by ZENKOVICH[2] that bars are found on *submerging* coasts as well as on emerging ones. A mechanism different from that suggested by JOHNSON must be advocated in coasts of submergence. ZENKOVICH suggested such a mechanism; it is illustrated in Fig. 162. In order for this mechanism to be operative, two elements are required: the existence of a rise above the water on the shore and the existence of an

1. HOLMES, A.: Principles of Physical Geology. London: T. Nelson & Sons 1944.
2. ZENKOVICH, V. P.: Trudy Inst. Okeanologii Akad. Nauk, SSSR 21, 3 (1957).

underwater slope which is steeper than the general slope of the land behind the ridge. As original rise, HOYT[1] assumed the existence of a beach ridge, whereas FISHER[2] proposed that it might be a subaerial dune. When the destruction of the whole complex begins, i.e. when the sea level rises, the rise wanders landward as the waves pass over its crest, at the same time heightening it through the deposition of material. This process keeps on being operative as long as there is a slow rise of sea level.

Further explanations of the origin of barrier islands (offshore bars) have been based upon the existence of longshore currents connected with the wave refraction phenomenon; thus GILBERT[3] supposed that these currents would deposit material where the islands are. Another explanation is due to DE BEAUMONT[4] who believed that the waves excavated the sea floor far out and piled the material up further inward so as to build up the barriers. SHEPARD[5] holds that probably all these processes were effective simultaneously.

Third, we shall investigate the depth distribution in *shallow bays.* In such bays, a special type of circulation may become established. Thus, one might reason that an onshore wind will, in addition to causing waves, also create an appreciable onshore flow of surface water which must be compensated by a seaward counter-current at the bottom. This type of circulation might be expected to be particularly pronounced in relatively small bodies of water such as a bay; it is called "vertical" circulation. Measurements of vertical currents have been made by RYZHKOV[6] on natural coasts.

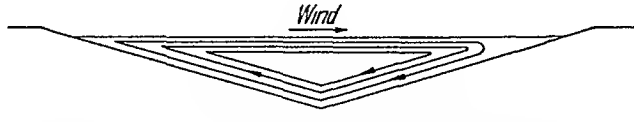

Fig. 163. Sketch of NAKANO's experiment showing the establishment of vertical currents. After NAKANO[7]

The above ideas have been tested in model experiments by KING[8] and by NAKANO[7]. A schematical view of NAKANO's experiment is shown in Fig. 163. The length and the width of the basin were 48 and 15 cm, respectively, and its greatest depth was 2.5 cm. It was filled with water

1 HOYT, J. C.: Bull. Geolog. Soc. Amer. **78**, 1125 (1967).
2 FISHER, J. J.: Bull. Geolog. Soc. Amer. **79**, 1421 (1968).
3. GILBERT, G. K.: U.S. Geol. Surv 5th Ann Rep. p. 87 (1885)
4 DE BEAUMONT, E : Leçons de géologie pratique. Paris (1845).
5. SHEPARD, F. P.: In "Recent Sediments, Northwest Gulf of Mexico, 1951 to 1958", Tulsa: Amer. Assoc. Petrol Geol. Spec. Pub. (1960).
6. RYZHKOV, YU. G.: Izv. Akad. Nauk, SSSR, Ser. Geofiz. No. 9, 1432 (1959).
7. NAKANO, M.: Rec. Oceanogr Wks. Japan **2**, No. 2, 68 (1955).
8. KING, C. A. M.: Beaches and Coasts. London: Ed Arnold & Co. 1959.

to a depth of 1.5 cm at the center and mounted into a corresponding opening of a wind tunnel. NAKANO investigated the circulation by inserting into the water about 12 grams of coal grains ($\rho = 1.42$ gram/cm^{-3}) of a diameter of 1 – 2 mm. The wind velocity in the tunnel was arranged to be about 7 m/sec. The result of the experiment showed that a circulation as indicated in Fig. 163 became indeed established by which the coal grains were transported little by little towards the side from which the wind blew until a certain equilibrium condition was reached.

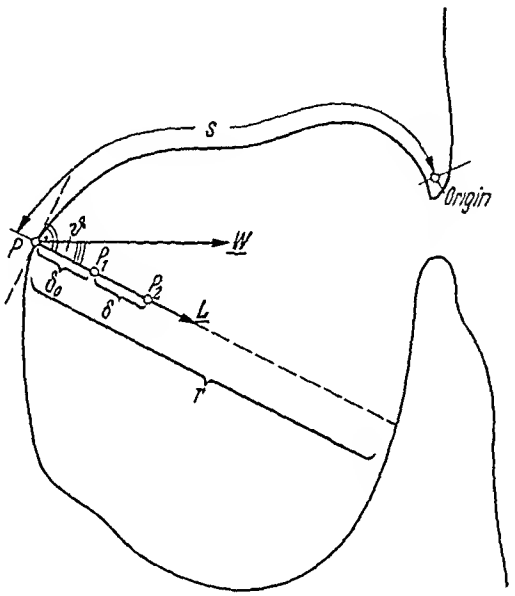

Fig. 164. Schematic view of a bay

In general, wave action will tend to accumulate material at a beach so that it would appear that beaches should grow indefinitely. However, the "vertical" circulation set up by prevailing onshore winds counteracts this so that the existence of stable beaches becomes possible.

The above model experiments demonstrating vertical circulation do not make allowance for the Coriolis force. The latter will cause a deflection in the circulation so that the bottom circulation will not be exactly antiparallel to the direction of wind flow. However, it stands to reason that in shallow bodies of water, the Coriolis force is relatively unimportant.

The above vertical circulation theory has been applied by NAKANO[1] to the bay-problem.

Thus, let us consider a bay (cf. Fig. 164) which is sufficiently shallow so that the Coriolis force can be neglected. We take an arbitrary point P

1. NAKANO, M.: Rec. Oceanogr. Works of Japan 2, No. 2, 68 (1955)

6.45. Theory of Steep Coasts. The action of waves upon steep coasts is somewhat different from the action on beaches. The sorting of sand and shingle is no longer a prominent phenomenon; it is rather the direct effect of the surf upon a cliff and the recession of the latter which will require an explanation.

The phenomenon of surf beating against a (vertical) cliff represents a process of extreme complexity. An inspection of the mere geometry of wave trains beating against a cliff, however, shows that a considerable amount of energy may be available for work on the cliff. The energy flux F carried by waves of wave length $\lambda=2\pi/m$ across a strip of unit width in water of depth h can be calculated (according to the theory of waves of small amplitude); it is[1]

$$F=U\frac{A^2\rho\sigma^2}{2g}\cosh^2 m h \tag{6.45-1}$$

with

$$U=\frac{1}{2}c\left(1+\frac{2mh}{\sinh 2mh}\right) \tag{6.45-2}$$

where c is the wave velocity (cf. 6.22-17):

$$c=\frac{\sigma}{m}=\sqrt{\frac{g\lambda}{2\pi}\tanh\frac{2\pi h}{\lambda}} \tag{6.45-3}$$

and σ is given by

$$\sigma=\sqrt{g\,m\tanh m h}. \tag{6.45-4}$$

It is clear that this energy flux is available for the destruction of the cliff if the waves are stopped by it, i.e. if no reflection is taking place.

It is in fact, possible to give a solution (in the small amplitude theory) for harmonic waves travelling from infinity in infinitely deep water toward a vertical cliff, their energy becoming absorbed there. In order to have the energy absorbed, a mechanism must be introduced to achieve this for which one can make the following suitable theoretical model: Let an external pressure fluctuation be operative between the cliff and the distance a from it:

$$p(x,t)=\left.\begin{cases}P\sin\sigma t & \text{for } |x|\leqq a\\ 0 & \text{for } |x|>a\end{cases}\right\} y=0 \tag{6.45-5}$$

where x denotes a co-ordinate parallel to the sea and normal to the cliff (the latter is at $x=0$) (see Fig. 166). Then it can be shown that the solution for the velocity potential φ in the small amplitude theory which represents waves travelling towards the cliff and being absorbed there,

1. See e.g. Stoker, J. J.: Water Waves, p. 50. New York: Interscience 1957.

is given by [1] (z represents the vertical co-ordinate):

$$\varphi(x,z,t)=-\frac{2P\sigma}{\rho g m}\sin m a\, e^{my}[\sin(m x+\sigma t)]+0(1/r) \quad (6.45\text{-}6)$$

where $0(1/r)$ is a function which behaves like $1/x$ at infinity. The surface $z=\eta$ is then given by (6.22-9).

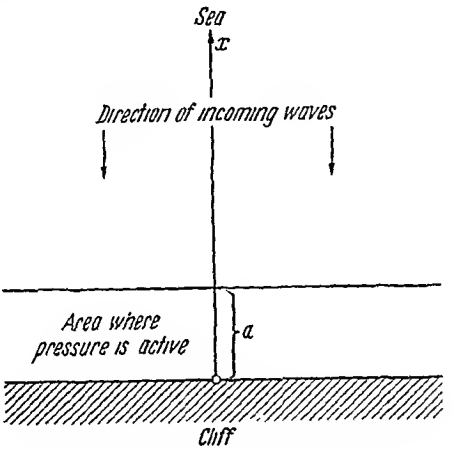

Fig 166. Waves travelling against a cliff

The amplitude A of the surface elevation η at infinity is given, from (6.22-11) and (6.45-6), by

$$A=\frac{2P}{\rho g}\sin m a. \quad (6.45\text{-}7)$$

It is obvious that P becomes infinite if $\sin m a$ is zero. This shows that, in the present model at least, conditions occur where the pressure fluctuations needed to absorb the wave energy must be infinitely great. The absorption mechanism introduced here is only a simple model, but the treatment does show that waves beating against a cliff may exert very great pressures upon the latter.

The amount of energy expended toward the destruction of a surf-beaten cliff depends on how much of the wave energy is reflected. It has been argued by RUSSELL and MACMILLAN [2] that the reflection is least (and thus the destruction greatest) if the waves break against a cliff in such a fashion that a pocket of air is trapped between the water and the cliff at impact time (cf. Fig. 167). No mathematical theory of the reflection coefficient can as yet be given. For a wave 3 m (10 feet) high and 46 m (150 feet) long, pressures of $7.25\cdot 10^7$ dynes/cm^2 (1210 lbs/sq. in)

1 See STOKER, loc. cit.; particularly on p. 67 thereof

2 RUSSELL, R. C. H., and D. H MACMILLAN: Water Waves and Tides. New York. Hutchinson 1952.

have been recorded. The maximum pressures ever recorded are about 10 times greater[1].

Pressures of the above magnitude make it understandable why a cliff can be eroded at its foot, since cavitation (cf. Sec. 3.25) must occur. Wave tank experiments to investigate the erosive action of waves beating against a rocky coast have been reported by SANDERS[2]. If it be assumed that the water is laden with rock débris, the erosive action is even more plausible. The action of the sea against a steep coast, thus, may be likened to that of a meandering river undercutting a slope. The development of a steep sea coast should therefore be explainable in terms of the same theory as that given in Sec. 3.56 for undercutting rivers; at

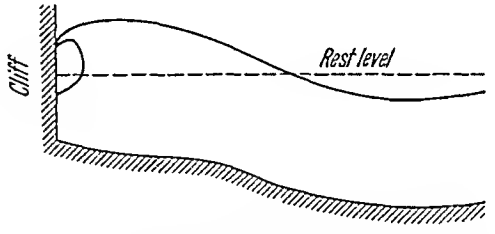

Fig. 167. Wave trapping a pocket of air when breaking against a cliff and thus likely to produce cliff recession

least for a certain time. Since the wave action is only effective near the still water line, erosion will proceed only above a certain level. Below it, a *shore platform* remains. After the latter has attained a certain breadth, it will retard the incoming waves and hence hinder further cliff recession, unless eustatic changes occur. With regard to such shore platforms, we note that there is a certain amount of controversy concerning their origin. They are due to erosion; some authors ascribe the erosion to chemical effects of the sea water, some to the action of the waves, and others to subaerial erosion near the coast. General reviews of the problem have been given, for instance, by WENTWORTH[3], by FAIRBRIDGE[4] and by GILL[5].

In general, the existence of shore platforms, sometimes much above the present shore line, is taken as evidence of the former position of the sea level at that locality. Thus, the shore platforms are regarded as evidence of an uneven change of the relative position of the sea level with regard to the land. However, POPOV[6] has maintained that this does not necessarily have to be so. POPOV considered a case where the speed of

1. Cf. KING, C. A. M.: Beaches and Coasts, p. 289. London: E. Arnold & Co. 1959.
2. SANDERS, N. K.: Pap. & Proc. Roy. Soc. Tasman. **102**, 11 (1968).
3. WENTWORTH, C. K.: J. Geomorph. **1**, 5 (1938).
4. FAIRBRIDGE, R. W.: Proc. 7th Pac. Sci. Congr. **3** (1952).
5. GILL, E. D.: Proc. Roy. Soc. Victoria **80**, No. 2, 183 (1967).
6. POPOV, B. A.: Trudy Okeanogr. Kommiss. Akad. Nauk SSSR **2**, 111 (1957).

lowering of sea level is constant and claimed that a series of terraces may be created. Again, it is seen, thus, that there is some controversy as to whether or not a series of shore platforms can result from a steady eustatic change. What is needed is evidently a theory of the creation of shore platforms and of their evolution.

Such a theory can be obtained[1] by considering the erosion on a shore profile as a form of slope recession. Thus, referring to Fig. 168,

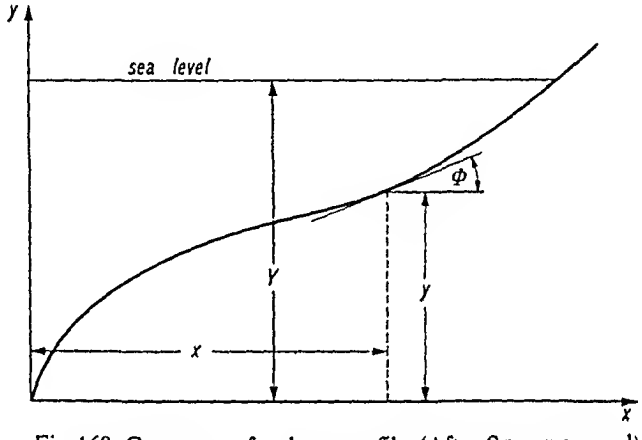

Fig. 168. Geometry of a shore profile. (After SCHEIDEGGER[1])

as exhibiting the general geometry of a cross-section of a coast, we can start with the fundamental equation of slope development (3.55-1)

$$\frac{\partial y}{\partial t} = -\Phi \sqrt{1+(\partial y/\partial x)^2} \tag{6.45-8}$$

adding suitable boundary conditions: In order to describe the erosive action on a shore, we assume that it becomes less and less the deeper we go below the surface of the water. We denote the height of the water surface above some base line by $Y(t)$; this may be a function of time. We then take our erosional function Φ proportional to an exponential and the sine of φ:

$$\Phi = a \sin\varphi \exp[-\alpha(Y-y)^2] \tag{6.45-9}$$

where α and a are some constants. This function has indeed the property that the erosion decreases with distance downward from the water level, and it also increases with increasing declivity of the slope. Expressing $\sin\varphi$ in terms of $\partial y/\partial x$ and inserting (6.45-9) into (6.45-8) yields the fundamental equation of shore development:

$$\frac{\partial y}{\partial t} = -a \exp[-\alpha(Y-y)^2] \cdot \frac{\partial y}{\partial x}. \tag{6.45-10}$$

1. SCHEIDEGGER, A. E.: Geofis. Pura Appl. 52, 69 (1962).

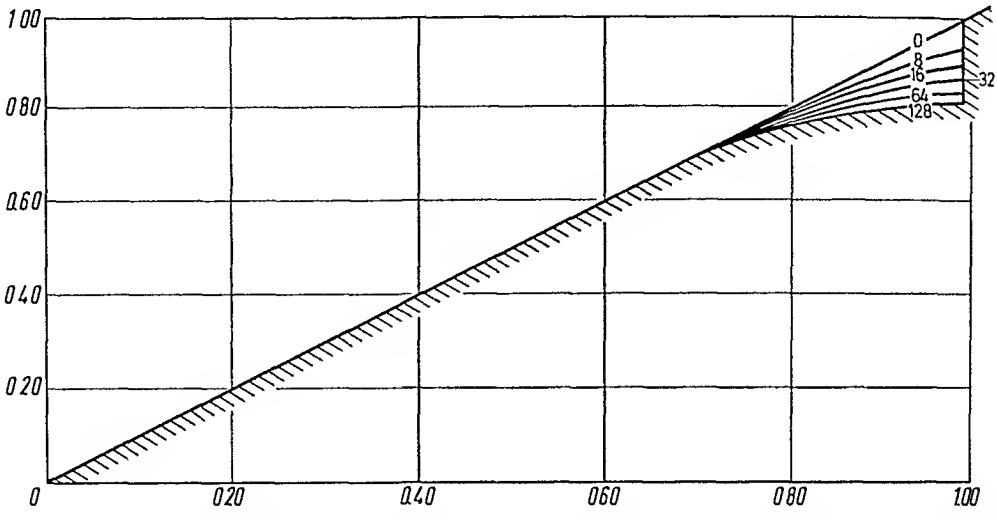

Fig. 169. Development of a marine terrace with constant sea level ($a=1$, $\alpha=64.0$). (After SCHEIDEGGER[1])

Naturally, this equation is only valid for $y \leqq Y$. Above the water line, no erosion occurs.

The basic shore development Eq. (6.45-10) is nonlinear and cannot be integrated in closed form. Thus, numerical methods may be used as in connection with the slope development theory presented in Sec. 3.55. The results of the calculations, starting with an initially straight profile, are shown for a constant sea level in Fig. 169. Similar calculations can be made for a sinking or rising sea level, assuming

$$Y(t) = Y_0 \pm t_{\text{const}}\, t. \tag{6.45-11}$$

The results are shown in Figs. 170 and 171.

The method of characteristics allows one to get an asymptotic solution of Eq. (6.45-10) for a rising or falling sea surface. The result is that the horizontal recession $R(y)$ at the level y is asymptotically independent of y (i.e. constant) and given by

$$R = \frac{a}{\sqrt{\alpha\, t_{\text{const}}}} \frac{\sqrt{\pi}}{2}. \tag{6.45-12}$$

Hence, we see that a eustatic change proceeding at a constant rate does not bear out POPOV's contention that a sequence of shore platforms should result: it simply leads to a recession by a constant amount of the slope profile. "Platforms" result only if there is a change in the rate of the eustatic changes. This result was also confirmed by more

1. SCHEIDEGGER, A. E.: Geofis. Pura Appl. 52, 69 (1962).

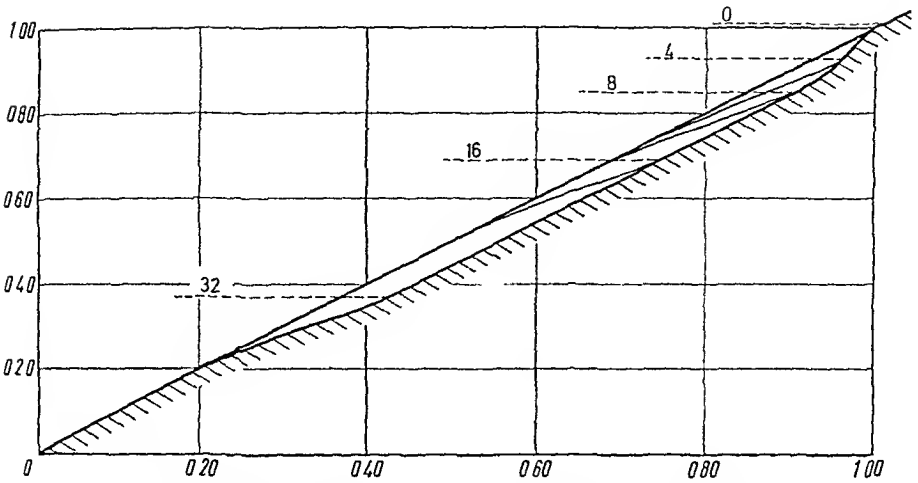

Fig. 170. Effect of a sinking sea level ($a=1.0$, $\alpha=64\,0$, $t_{const}=2.0$, $Y_0=1.01$). (After SCHEIDEGGER[1])

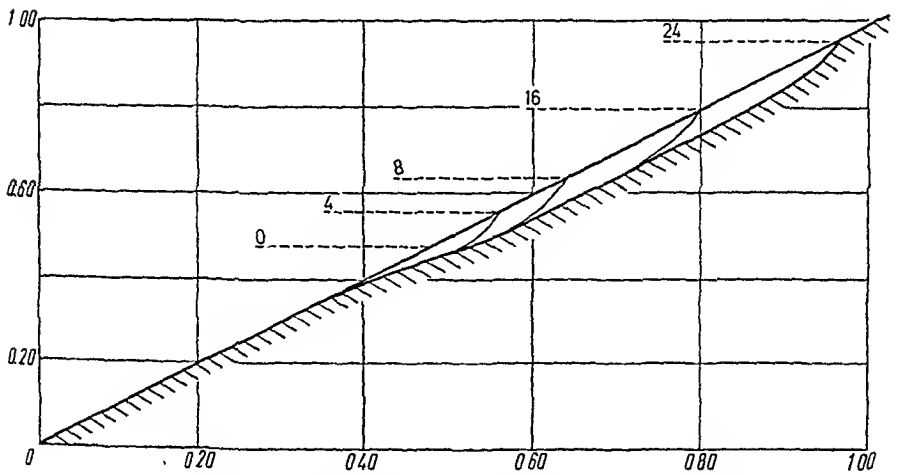

Fig 171. Effect of a rising sea level ($a=1\,0$, $\alpha=64\,0$, $t_{const}=2.0$, $Y_0=0\,48$. (After SCHEIDEGGER[1])

elaborate calculations by ESIN[2] who investigated slightly different expressions for the function Φ in Eq. (6.45-8).

6.46. Large-Scale Features on Coasts. Finally, one may look at coasts from a more macroscopic standpoint. One finds generally that a coast consists typically of a sequence of headlands and bays, the former

1. SCHEIDEGGER, A. E., *Geofis Pura Appl* **52**, 69 (1962)
2. ESIN, N.V.: In. Иссл. гидродин. и морфодинам. проц. береговой зоны моря. Izdatelstvo "Nauka", Moscow, p. 170 (1966).

representing a steep coast, the latter a shallow one with a concomitant beach. The question arises, therefore, why in one case a beach develops, whereas in another it does not. From the discussions given above, it is clear that this question is tied up with the nearshore circulation system: If the sediment supply is higher than what littoral drift can remove, a beach develops, otherwise it does not. The sequence of headland-bays is therefore somehow tied up with a similarly sequential (cellular) structure of the nearshore circulation system.

It was pointed out earlier that a coastline is a geomorphic line (Sec. 1.3). As such, it would, in principle, to treat it from a "systems" approach, using power spectra and such like, just like river meanders. This ought to give explanations of the observed large-scale characteristics. Unfortunately, however, this type of theory has not yet been sufficiently developed so that actual applications thereof could be presented at this time.

6.5. Dynamics of River Mouths

6.51. General Remarks. Rivers entering the sea or a large body of water cause a variety of peculiar features on the coast-line concerned. In Sec. 1.63, we have described the morphology of river mouths, and it will now be our endeavor to investigate the mechanical causes of the physiographic features mentioned there.

The physical background for a dynamical theory of river mouths will be supplied by a discussion of the general hydrodynamic conditions in a river mouth (Sec. 6.52). We shall then proceed to a description of the origin of the two most common types of river mouths: estuaries (Sec. 6.53) and deltas (Sec. 6.54). Finally, we shall conclude our survey with a brief description of the origin of sand bars off estuaries.

It will be found that the general dynamics of the evolution of a river mouth is not very well developed as of yet. There is a series of criteria indicating when a particular river mouth may be expected to be stable, but the problem of greatest interest to the geoscientist, viz. that of elucidating what happens when a river mouth is known to be unstable, has not yet been solved.

The theories to be presented here are contained in a variety of papers, mostly originating in engineering laboratories. Notable recent monographs dealing specifically with river mouths have been written by SAMOILOV[1] and by LAUFF[2]. Although they are mostly descriptive, some references to theoretical work are given.

1. SAMOILOV, I. V.: Устья рек. Moscow: Geografgiz (1954). German translation (title: Die Flußmündungen) by F. TUTENBERG. Gotha: Hermann Haack Verlag 1956.

2. LAUFF, G. H. (ed.): Estuaries. Washington: Amer. Assoc. Advanc. Sci. 1967.

6.52. General Hydrodynamic Conditions in a River Mouth. Where a river enters the sea, two agents act both at the same time: first, there is the influence of the river and second, there is the influence of the sea. The combination of these two influences has the result that the hydrodynamic conditions in a river mouth become very complicated.

The dynamics of a *river* has already been discussed in Chap. 4. It may be reckoned that the arguments presented there are still valid in the vicinity of a river's mouth. Since the dynamics of rivers has already been discussed, it is primarily the influence of the *sea* which deserves our attention in the present context. This influence is mostly due to the effect of the *tides* upon a river mouth. What one has to consider is the

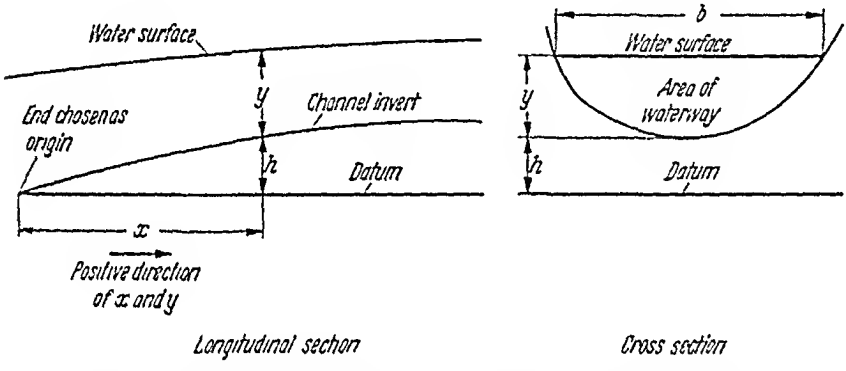

Fig. 172. Geometry of a river channel. After SCHOLER and GERMANIS[1]

unsteady-state problem of the motion of water in a channel under given time-dependent boundary conditions at its mouth. Combining the nonlinear shallow water wave theory (cf. Eq. 6.22-23) with MANNING'S friction formula (4.22-3), one obtains as equation of motion (see e.g. SCHOLER and GERMANIS[1])

$$\frac{\partial}{\partial x}(y+h)+\frac{1}{g}\frac{\partial v}{\partial t}+\frac{v}{g}\frac{\partial v}{\partial x}\pm\text{const}\frac{v^2}{y^{\frac{1}{3}}}=0 \qquad (6.52\text{-}1)$$

where the meaning of most of the symbols is evident from an inspection of Fig. 172. In addition, v denotes the mean flow velocity in the channel. Further to the equation of motion, one requires a continuity condition. The latter can be written as follows:

$$\frac{\partial Q}{\partial x}+\frac{\partial B}{\partial t}=0 \qquad (6.52\text{-}2)$$

1. SCHOLER, H. A., and E. GERMANIS: Inst. Eng. Australia, Civ. Eng. Trans. CEI, No. 1, 27 (1959).

where Q is the total discharge and B the area of the waterway. The area B has to be expressed as a function of height y and distance x which defines the geometry of the channel. The task, then, is to integrate the Eqs. (6.52-1) and (6.52-2). Needless to say, this problem is very difficult to solve as one has to integrate a system of nonlinear partial differential equations. The available methods have been collected in a book by DRONKERS[1]. Accordingly, there are in essence three types of methods available: The harmonic method, in which solutions for the individual harmonic components of the wave spectrum are sought, the method of characteristics, and digital numerical methods.

Because of the difficulty of solving the system of Eqs. (6.52-1/2) exactly, a variety of approximation methods for obtaining a solution has been suggested. These range from the application of the *linearized* shallow water theory (cf. Eq. 6.22-25) to various less severe simplifications of the exact differential equations. A review of some of the possibilities has been given by SCHOLER[2], by BRUUN and GERRITSEN[3] and in the book of DRONKERS[4] mentioned above. STOKER[5] also discussed a variety of solutions that have been applied to the design of breakwaters in harbors.

Accordingly, the simplifying assumptions that may be introduced are the following:

(i) the average elevation of the water surface is constant along a horizontal channel

(ii) tide is sinusoidal

(iii) friction term is linearized

(iv) differential equation itself is linearized.

According to how many simplifications are introduced, one obtains a more or less satisfactory description of the phenomena.

The basic nonlinear character of the fundamental differential equations (6.52-1/2) has some well-known consequences: a "shock" front may develop which represents a tidal "bore". This feature, of course, gets lost if the equations are linearized. The more exact calculations (particularly the digital ones) yield very acceptable results that seem to check with actually observed phenomena. DRONKERS' method was used for the calculation of the tides entering through gaps in the dykes of the Zuiderzee and the predictions were found to be very accurate.

---

1. DRONKERS, J. J.: Tidal Computations in Rivers and Coastal Waters, 518 pp. Amsterdam: North-Holland Pub. Co. 1964.

2 SCHOLER, H. A.: J. Inst. Eng. Austral. April-May, 1958, pp. 125 – 136.

3. BRUUN, P, and F. GERRITSEN: J. Waterways & Harbors Div., Proc. Amer. Soc Civ. Eng. 84, No. 3, 1644 – 1 (1958)

4. DRONKERS, J. J.: Tidal Computations in Rivers and Coastal Waters, 518 pp. Amsterdam: North Holland Pub. Co. 1964.

5. STOKER, J. J.: Water Waves. New York: Interscience 1957.

Because of the many variables involved, it is difficult to make general statements regarding the tidal currents that may be expected in any particular estuary. The calculations, preferably by means of electronic computers, have to be carried out separately for each case under consideration.

The tides are the principal influences induced by the sea in a river mouth. However, there are also other ones. Of some importance may be the *direct wind drag*[1] upon the water. The action of a strong upstream wind can be very similar to that of the tide entering the river mouth (cf. Fig. 173). In other cases, strong secondary currents may be set up

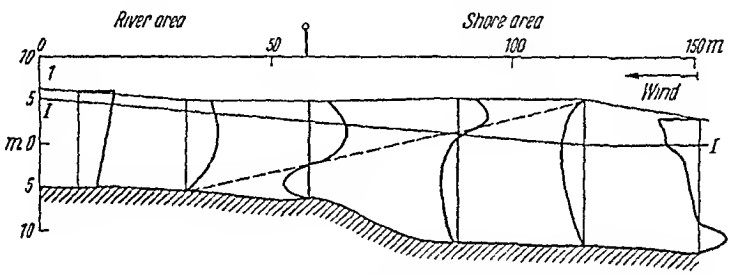

Fig. 173. Velocity distribution (heavy lines) and wave caused by wind I: Level without wind. After SAMOILOV[1]

which may form rather well defined solenoidal *convection cells* whose axes are parallel to the wind direction. The Coriolis force also may be of some significance[2,3].

The hydrodynamic conditions in a river mouth are also affected by the *swell*. However, the latter can be of geomorphological importance only if the river mouth is very wide indeed.

For a theoretical explanation of the development of the various types of river mouths, the hydraulics of the river and the effect of the tides are the most important factors. It is probably safe to neglect the other influences, at least in a first approximation.

6.53. River Estuaries. The background supplied in Sec. 6.52 makes it clear what would be required to set up an exact theory of the mechanics of the development of a given river estuary: First, the hydrodynamic régime (taking into account the river flow and the tides) at a specified time t has to be calculated. Then, the effect of the resulting currents upon the bottom and the sides of the estuary (using the methods of

1. Cf. SAMOILOV, I. V.: Устья рек. Moscow: Geografgiz 1954
2. SEKERZH-ZEN'KOVICH, T. YA.: Izv. Akad. Nauk, SSSR, Ser. Geofiz. No. 10, 1460 (1959)
3. LABEISH, V. G.: Izv. Akad. Nauk SSSR, Ser. Geofiz. No. 11, 1714 (1959).

Chap. 4) has to be established. This yields the *changes* that are taking place at time t by which it is possible to calculate the configuration of the estuary at time $t+dt$. The procedure can then be repeated over and over again to yield the development of the estuary with time. The above outline of the requirements for an exact theory of the evolution of a tidal estuary indicates that the procedure is rather involved. Although it ought not to be beyond the capacity of modern high-speed computers, it never seems to have been tried.

Because of the difficulties with an exact solution of the problem, the description of the evolution, or at least the establishment of equilibrium conditions, of a river estuary has also been tried by other means. First, there is a *shoal theory* by BRUUN and GERRITSEN[1] which is based upon an extremely simplified theoretical model of the hydrodynamic conditions in the estuary, and second, there are two theories aiming at criteria regarding whether a certain estuary is stable or not. The first of these, a *gorge theory* is also due to BRUUN and GERRITSEN; it only considers the material balance across the entrance ("gorge") to the estuary. The second is a *régime theory* of BLENCH[2] who tries to establish equilibrium criteria in a similar fashion as he had done this for rivers (cf. Sec. 4.64).

Turning first to the *shoal theory*, we assume (with BRUUN and GERRITSEN) that the whole of the estuary is subject to tidal currents. The change in cross-sectional area of the channel (ΔA) caused by deposits must be proportional to the net amount of material deposited (per unit length) ΔM:

$$\Delta A = c_1 \, \Delta M \tag{6.53-1}$$

or, integrated (the c_i's constants)

$$M = \frac{A - c_2}{c_1}. \tag{6.53-2}$$

Using one of the bed-load formulas (cf. Sec. 4.53), we can write for the material q_s transported per unit channel width

$$q_s = c_3 \, \sigma^{\frac{5}{2}} \tag{6.53-3}$$

where σ is the shear stress at the bottom. The last formula is a modification of (4.53-7) with $\sigma_{cr}=0$ and $m=\frac{5}{2}$. However, we can use the expression (4.22-11) for σ, viz.

$$\sigma = g \, \rho \, R S \tag{6.53-4}$$

1. BRUUN, P., and F. GERRITSEN: J. Waterways & Harbors Div., Proc. Amer. Soc Civ. Eng. **84**, No. 3, 1641 – 1 (1958).

2 BLENCH, T.: Proc. Minnesota Internat. Hydraulics Convent. 77 (1953).

where ρ is the density of the water, g the gravity acceleration, R the hydraulic radius and S the slope. We also have (from 4.22-3)

$$S = c_4 v^2 \tag{6.53-5}$$

and thus

$$q_s = c_5 v^5. \tag{6.53-6}$$

Let us assume that the velocity in the estuary due to the tides is (valid for one half-cycle)

$$v = v_{max} (\sin \omega t)^{\frac{1}{2}} \tag{6.53-7}$$

with $\omega = 2\pi/T$ (T being the tidal period). Then, the total amount of material dislodged during a tidal half-cycle is

$$\begin{aligned} M &= c_5 v_{max}^5 \int_0^{T/2} (\sin \omega t)^{\frac{5}{2}} dt \\ &= c_5 \frac{1.432}{2\pi} v_{max}^5 T. \end{aligned} \tag{6.53-8}$$

It is convenient now to introduce the *tidal prism* Ω which represents the total amount of water that flows into (and out of, if there is no river discharge) the estuary during one flood or ebb period. One obviously has a relationship of the form

$$v_{max} = c_6 \frac{\Omega}{AT}. \tag{6.53-9}$$

Thus,

$$M = c_7 \frac{1}{T^4} \left(\frac{\Omega}{A}\right)^5 \tag{6.53-10}$$

and, with (6.53-2)

$$A = c_1^{\frac{1}{6}} \left[c_7 \frac{1}{T^4} \Omega^5 + \frac{c_2}{c_1} A^5 \right]^{\frac{1}{6}} \approx \text{const } \Omega^{\frac{5}{6}}. \tag{6.53-11}$$

This is the equilibrium condition over one-half of a tidal cycle according to the shoal theory. As is noted, no modification can be made for the effect of the river. The shoal theory is thus restricted in its applicability to river mouths but does apply to tidal estuaries.

The *gorge theory* mentioned above (which is also due to BRUUN and GERRITSEN), however, lends itself to a modification to take the river discharge into account. As mentioned above, the gorge theory considers only the flow through the entrance of the estuary. Following BRUUN and GERRITSEN, we investigate a section dx of a gorge (see Fig. 174) and we denote by $Q_s dt$ the total amount of sand passing through that section during the time element dt. The mass erosion on the distance dx is then

obviously given by $(\partial Q/\partial x)\,dt\,dx$. If the estuary is to be stable, then the net erosion over a complete tidal cycle (time T) must be zero everywhere:

$$\int_0^T \frac{\partial Q_s}{\partial x}\,dt=0. \tag{6.53-12}$$

We assume that the total transport of material can be represented in the following form

$$Q_s=c_8\,v^n \tag{6.53-13}$$

where n is some empirical exponent. The velocity in the estuary is also expressed in terms of a semi-empirical relationship of the type

$$v=v_{\max}\cos^p\omega\,t \tag{6.53-14}$$

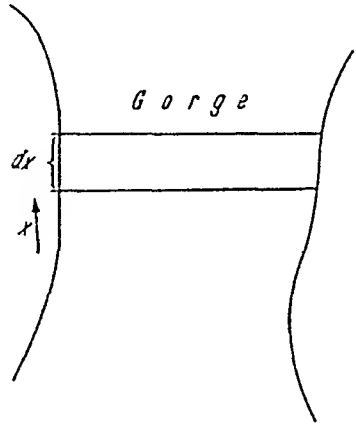

Fig. 174. Geometry of a gorge

which can be written, using (6.53-9), as follows

$$v=c_6\frac{\Omega}{AT}\cos^p\omega\,t. \tag{6.53-15}$$

The exponent p is purely empirical. Thus, the expression for Q_s becomes

$$Q_s=c_9\left(\frac{\Omega}{AT}\right)^n\cos^{pn}\omega\,t. \tag{6.53-16}$$

Stability is achieved if Eqs. (6.53-12) and (6.53-16) can be satisfied. Since only Ω and A are functions of x, this is obviously the case, if

$$\Omega=\text{const}\,A. \tag{6.53-17}$$

This is the stability condition.

The above theory can be modified to take the river flow into account. Instead of (6.53-14) we must set

$$v=v_{\text{river}}+v_{\max}\cos^p\omega\,t=\frac{Q_{\text{river}}}{A}+c_6\frac{\Omega}{AT}\cos^p\omega\,t \tag{6.53-18}$$

where Q_{river} is the total river discharge. Hence, (6.53-16) becomes

$$Q_s = c_9 \left(\frac{Q_{river}}{A} + c_6 \frac{\Omega}{AT} \cos^p \omega t \right)^n . \tag{6.53-19}$$

Thus, it is obvious that stability is achieved if

$$\frac{T Q_{river} + \Omega \cdot \xi}{AT} = \text{const}, \tag{6.53-20}$$

or if

$$\xi \frac{\Omega}{A} = \text{const}\, T - \frac{Q_{river} T}{A} \tag{6.53-21}$$

where ξ is a certain coefficient which originates from the integration with regard to time in the stability Eq. (6.53-12). Relationship (6.53-21) is exact for $n=1$ and approximate otherwise.

The shoal theory as well as the gorge theory yield semi-theoretical criteria indicating the conditions under which a river estuary ought to remain stable. The same is true for the entirely empirical *régime theory* of BLENCH who, from an analysis of data, comes up with an equation similar to (6.53-11).

The various stability criteria discussed above have been tested[1, 2] with regard to actual observations. It turns out that the linear relationship of the gorge theory (6.53-17) with

$$\text{const} = 1.56 \cdot 10^4 \text{ meters} = 1.17 \text{ acres/foot} \tag{6.53-22}$$

fits the observed data best. Results from a series of estuaries (after BRUUN and GERRITSEN[1] are shown in Fig. 175.

A consideration of the above remarks shows that there are sufficiently accurate relationships available which enable one to decide whether a certain estuary-configuration is stable or not. This, in fact, is sufficient for engineering purposes (harbor improvements etc.) for which these relationships have been developed. Unfortunately, they represent only the first step of an analysis that would be to the satisfaction of a theoretical geomorphologist. Although it is, of course, of some importance to know whether a certain estuary is stable or not, it would be of much more interest to know how an *unstable* estuary will *change* its shape. This problem has obviously not yet been solved.

Finally, it should be mentioned that a systems-type of approach to the problem of explaining the geometry of an estuary, has also been tried[3]. This approach is based on the principle of minimum variance (cf. Sec. 5.1). The discussion of this principle given in Sec. 5.1 applies also to its application to estuarine geometry.

1. BRUUN, P., and F. GERRITSEN: J. Waterways and Harbors Div., Proc. Amer. Soc. Civ. Eng. 84, No. 3, 1641–1 (1958).
2. JOHNS, B.: Geophys. J. Roy. Astr. Soc. 13, 377 (1967).
3. LANGBEIN, W. B.: Bull. Internat. Assoc. Sci. Hydrol. 8, No. 3, 84 (1963).

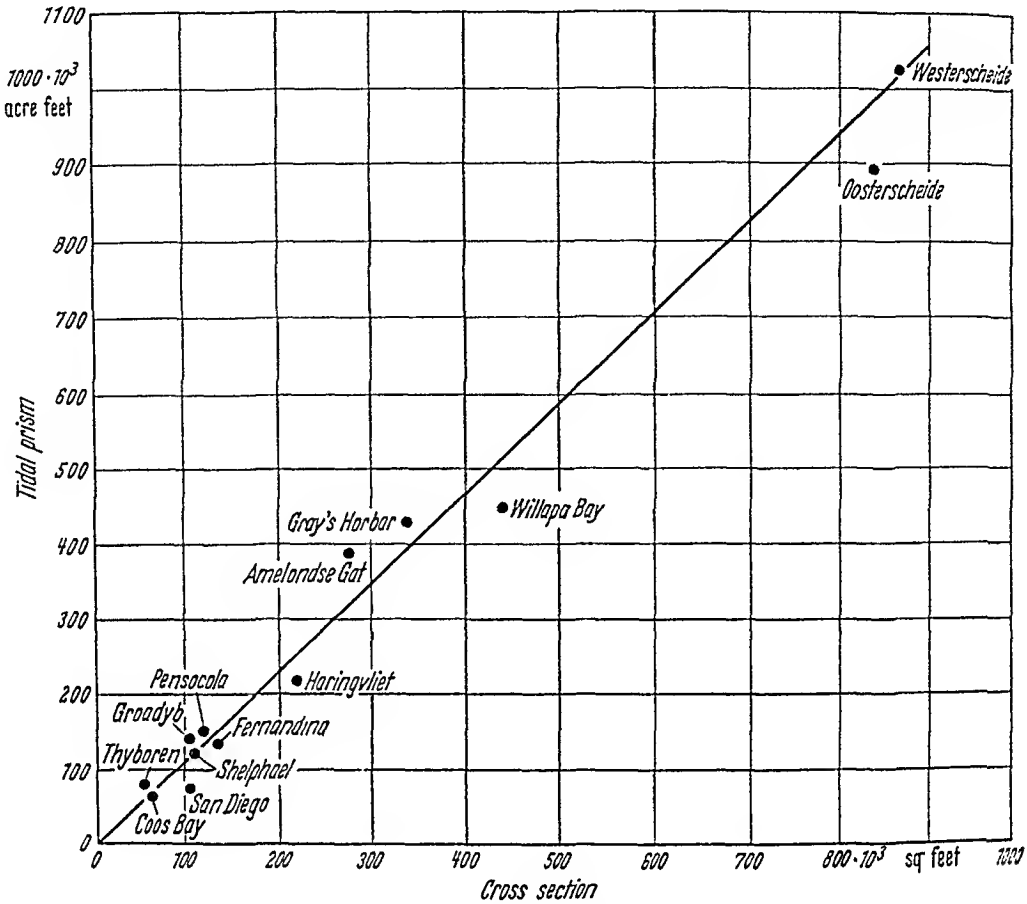

Fig 175. Statistical relationship between tidal prism and cross section for a variety of inlets. After BRUUN and GERRITSEN[1]

6.54. Formation of Deltas. When a river enters a large body of water, the velocity of the flow is retarded and it stands to reason that the sediment-carrying capacity of the water is thereby reduced. Thus, a large amount of material ought to be deposited at a river mouth, the latter is thereby lengthened and a delta should be the result. The theory of erosion and accumulation by water (see Sec. 3.45) should be adequate to explain the observed phenomena qualitatively[2].

It is possible, however, to refine the above statements somewhat. In Sec. 1.63, we have noted that there are two types of deltas: birds foot deltas and arcuate deltas. One might expect that there should be a rational explanation for the occurrence of these two types.

Such an explanation has been proposed by BATES[3]. Accordingly, the flow of water from the river mouth into the stagnant body of water can

1. BRUUN, P., and F. GERRITSEN: J. Wwys. Harbors Div., Proc. Amer. Soc. Civ. Eng. 84, No. 3, 1644 – 1 (1958).

2. See BAIDIN, S. S.: Trudy Gos. Okeanogr. In-ta 45, 5 (1959).

3. BATES, C. C.: Bull. Amer. Assoc. Petrol. Geol. 37, 2119 (1953).

be regarded as a turbulent jet of fluid entering still fluid from a nozzle. There are two types of flow that can occur: either one has an *axial* jet or one has a *planar* jet. These two types of jets simply refer to the three-dimensional and to the two-dimensional case, respectively. In their appearance, it turns out that the axial jet gets slowed down by mixing much more rapidly than the planar jet. Thus a certain fraction of the original velocity (say one-tenth) is reached 10 times sooner in the axial jet than in the planar jet. Furthermore, the planar jet always stays much narrower than the axial jet. There is a significant drop of velocity from the center line of the planar jet towards the sides, whereas in the axial jet this effect is small if it be compared with the slowing down of the jet as a function of a distance from the mouth.

If the density of the river water (including the suspension) is about the same as that of the still water which it is entering, then there is every reason to expect the jet to be an axial one. However, if the river water is considerably less dense than the still water (for instance if the latter is highly saline), then the jet will stay at the surface of the still water and one will have the characteristics of a planar jet. Similarly, if the river water is much denser than the still water, it will follow the bottom and one obtains a turbidity current (see Sec. 6.23).

BATES[1] now assumes that the two types of jets give rise to the two types of deltas, respectively: In an axial jet, the decrease of velocity is so rapid that sediments are deposited in an arc around the mouth of the river. Thus, the river constantly blocks its way, forces new channels and builds up a delta by adding new arcs. This, according to BATES, leads to an *arcuate* delta.

Contrariwise, in a planar jet, the decrease of velocity with distance from the river mouth is fairly small, but there is a significant velocity decrease sideways from the jet. Thus, sediments are deposited in lines paralleling the flow of the jet and the result is a *birds foot* delta.

The above theory of BATES has been criticized by CRICKMAY[2] who maintained that jet diffusion will have a plane (two-dimensional) pattern, no matter whether the density of the inflow is the same as that of the surrounding water or not. This view seems to be, in effect, correct[3]. The *type* of delta, then, which results would have something to do with the type and quantity of sediment transported by the river.

Assuming the delta formation to be connected with the diffusion of a planar jet, theoretical calculations of the attendant flow patterns and settling of sediments have been made by BONHAM-CARTER and SUTHER-

1. BATES, C. C : Bull. Amer. Assoc. Petrol. Geol. 37, 2119 (1953).
2. CRICKMAY, C. H.: Bull. Amer. Assoc. Petrol. Geol. 39, 1 (1955)
3. AXELSSON, V.: Geografiska Annaler 49A, 1 (1967).

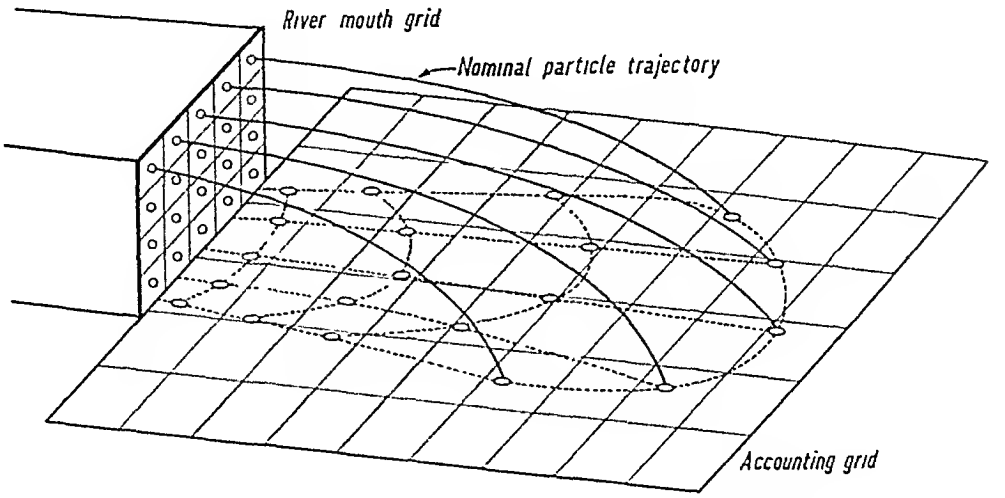

Fig. 176. Grid model of BONHAM-CARTER and SOTHERLAND[1]

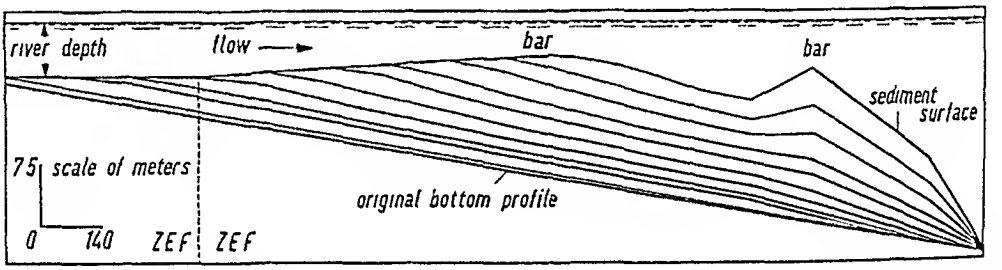

Fig. 177. Stratigraphic cross section along the jet centerline, showing "foreset" bedding. (After BONHAM-CARTER and SOTHERLAND[1])

LAND[1], using an electronic computer. The deposition of sediment is found by calculating the trajectories of nominal sediment particles which are subject to the forward transport by the jet and settling due to gravity. The schematic structure of these authors' model is shown in Fig. 176. During the calculation, the cells at the end of the trajectories on the accounting grid (see Fig. 176) are progressively built up until they are filled; the water depth is thereby progressively decreased. The settling trajectories have to be readjusted after each nominal time step. Thus, the sediment load of the river is progressively moved forward from the river mouth and deposited in the "delta". During a single nominal time step, a certain thickness of sediment will have been built up, forming a "bed". A sample of the results obtained by BONHAM-CARTER and SOTHERLAND[1] is shown in Fig. 177. The bar is the result of permitting the water depth to decrease as a function of current velocity. It is seen that a good simulation of a cross-section of a delta is obtained.

1. BONHAM-CARTER, G. F., and A J SOTHERLAND: Trans. Gulf Coast Assoc Geolog Soc. 17, 326 (1967).

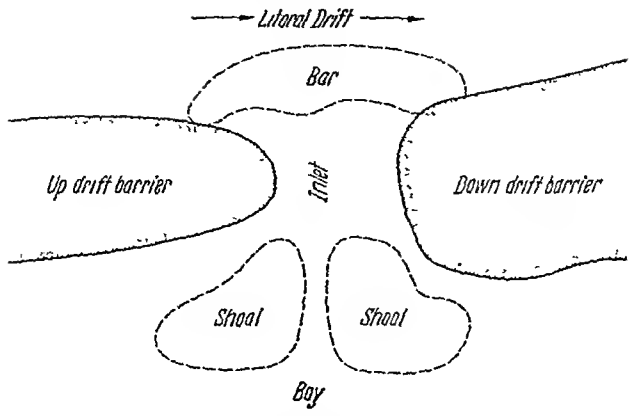

Fig 178. Bypassing of a river mouth by sand moving across a bar. After BRUUN and GERRITSEN[3]

The formation of deltas has also been studied in flume experiments by JOPLING[1, 2] who was able to produce "deltaic" type structures.

6.55. Barred River Mouths. If there is a strong longshore drift along a coast line, it is possible that sand accumulations develop off a river mouth causing the latter to be *barred*. The process by which this occurs is not quite clear although its general phenomenology appears explainable. A study has been reported by BRUUN and GERRITSEN[3] bearing upon the bar problem, in which an investigation was made regarding how the sand bypasses the river mouth over the bar. The contention is that the offshore bars are not solid features but exist only owing to a delicate balance between the sand which is deposited and the sand which is removed. This causes sand to "bypass" the river mouth from the updrift to the downdrift side. The general mechanics of the process is illustrated in Fig. 178.

From an analysis of observational data, BRUUN and GERRITSEN derived an empirical relationship expressing the conditions when bar-bypassing of the litoral drift can take place by an inlet. Involved is the ratio between the amount of tidal flow through the gorge of the inlet and the magnitude of the litoral drift. If this ratio is below a certain critical value, no bar can develop as the tides will sweep the channel clean.

Unfortunately, no further analyses of the mechanics of bar formation in terms of basic physics seem to be available.

1. JOPLING, A. V.: An Experimental Study on the Mechanics of Bedding Ph. D. Diss. Harvard Univ, Cambridge, Mass. 1960.

2. JOPLING, A. V.: Sedimentology 2, 115 (1963)

3. BRUUN, P., and F. GERRITSEN: J Waterways & Harbors. Div., Proc. Amer. Soc. Civ. Eng 85, No. WW 4, 75 (1959).

6.6. Theoretical Submarine Geomorphology

6.61. General Remarks. The last section in the present chapter on subaquatic effects has to deal with submarine geomorphology. The features to be analysed have been listed in Sec. 1.64. Unfortunately, no coherent attempts at an explanation of these features in theoretical-mechanical terms seem ever to have been reported in the literature. Thus although many qualitative arguments can be found scattered over a variety of sources, the substantiation of these arguments by numbers and equations is still mostly lacking. The treatises on the physiography of the sea bottom mentioned in Sec. 1.64 contain some information on theoretical submarine geomorphology; other items have been collected from various sources which will be mentioned in their proper context.

Our investigation will start with a review of the various agents that may affect submarine features (Sec. 6.62). We shall then proceed to a discussion of graded beds (6.63), of submarine canyons (6.64) and of the effect of bottom currents (6.65). Finally, we shall outline some speculations regarding the origin of the smoothened surface of abyssal plains (6.66) and of the sinking of coral atolls and guyots (6.67).

6.62. Agents Effective in Submarine Geomorphology. The striking similarity between many submarine and subaerial features has prompted some investigators to postulate an identical subaerial origin for the two. However, it is now beyond doubt that at least the deep water features are caused by *truly submarine processes*. One is therefore faced with the problem of finding agents that can produce submarine erosion, transportation and redeposition of material.

General reviews of the agents that may be effective in submarine geomorphology have been published by KUENEN[1, 2] and by HEEZEN[3, 4].

Accordingly, *erosion* in the general sense (i.e. the removal of material from its resting place) may be caused by submarine landslides[5] triggered by earthquakes or storms, by the erosive action of turbidity currents and by the drag of rip and bottom currents. In the very deep sea, bottom currents are probably the only erosive agents since turbidity currents have to be triggered by some external mechanism.

Submarine *transportation* of material occurs primarily by turbidity currents although the effect of ocean bottom currents is not entirely negligible. Material which is eventually deposited on the sea floor may

1. KUENEN, P. H.: J. Alberta Soc. Petrol. Geol. 5, 59 (1957).
2. KUENEN, P. H.: Geologie en Mijnbouw 21, 191 (1959).
3. HEEZEN, B. C.: Geophys. J. Roy. Astron. Soc. 2, 142 (1959).
4. HEEZEN, B. C.: J. Geol. 67, 713 (1959).
5. MORELOCK, J.: J. Geophys. Res. 74, 465 (1969).

also arrive there through the air: dust from the Sahara was found far out in the Atlantic. It obviously got there by the action of winds carrying it over large distances.

Finally, the *deposition* of material on the sea floor occurs by the transporting agent, whichever it may be, losing its carrying capacity: Turbidity currents coming to a halt, the wind letting the dust settle out, or ocean bottom currents slowing down.

In general, it may be stated that, although subaerial and submarine features are similar in many regards, *erosion* is the decisive factor on land, but *deposition* below the water level.

6.63. Graded Beds. Some of the features of submarine geomorphology that are amenable to a theoretical explanation are *graded beds.* The morphology of such beds was discussed at large in Sec. 1.65; they are generally thought to be laid down by turbidity currents. The mechanics of such currents was explained in Sec. 6.23; what remains to be done here is to discuss the mechanics of the actual deposition of the sediments.

This problem is a difficult one. Two types of approaches have been used to tackle it: Theoretical models and scaled experiments.

Turning first to the theoretical approach, we note that SCHEIDEGGER and POTTER[1, 2] have set up a model based on the following assumptions: (i) A turbidity current represents a slug of turbulent water moving downslope. It contains a size-distribution of sediment which is given by the sediment-source. (ii) When the current comes to rest, it decays according to standard laws. (iii) The sediment carrying capacity of the turbulent water is like that of a river.

The reason why a graded bed is deposited is that a sorting takes place during the decay-period of the turbulence: The coarse grains fall out first, then smaller and smaller ones and lastly the finest ones. The actual calculations for this process are rather tedious and the reader is referred to the original papers for the details. However, the final result can be stated by the following simple formula:

$$H = R(d_{\max}^{2p+5} - d_m^{2p+5}) \tag{6.63-1}$$

where R is a constant, $d_{\max}$ is the maximum grain size (a diameter) in the bed, d_m is the mean grain size found at the height H above the bottom of the graded bed in question, and p is a parameter connected with the grain size distribution of the source material. Eq. (6.63-1) is a relation between grain size and the level H in the bed, i.e. it is a grading relation. One sees that for $-1 > p > -2$ this relation is convex upward, for $p = -2$

1. SCHEIDEGGER, A. E., and P. E. POTTER: Sedimentology 5, 289 (1965).
2. POTTER, P. E., and A. E. SCHEIDEGGER: Sedimentology 7, 233 (1966).

it is a straight line, and for $-2.5<p<-2$ it is concave upward. Thus, the three characteristic grading curves observed in nature (cf. Sec. 1.65) are shown to be the result of the particle size distribution of the source material.

If d_m is set equal to zero in Eq. (6.63-1), the latter yields a relationship between the total thickness H_{TOT} of the bed and the maximum grain diameter found therein:

$$H_{TOT} = R\, d_{max}^{2p+5}. \tag{6.63-2}$$

The last relation can be used to explain the correlations between thickness and maximum grain size of naturally observed turbidite *sequences*: The physical model is based on the idea that the source-material has always the same p (particle size distribution), but that, depending on the force of the particular turbidity flow in question, only particles below a certain maximum size can be carried along. The "stronger" currents, as is natural, will deposit thicker beds; this is expressed by Eq. (6.63-2). The theory of SCHEIDEGGER and POTTER, thus, gives an excellent representation of the facts observed in nature.

Turning now to the experimental efforts for studying the depositional effects of turbidity currents, we note that the classic investigations have been made by KUENEN[1-5]. Turbidite type structures were shown to be the result of turbidity flows. MIDDLETON[6] has made similar tank-type experiments and claims that the deposition of sediment takes place immediately behind the "head" of the flow before the latter has begun to slow down. Finally, RIDDELL[7] also studied the suspension-effet of turbidity currents. It is seen, thus, that more than qualitative results have not yet been obtained from experimental investigation of the depositional characteristics of turbidity currents.

6.64. Submarine Canyons. Immediately after the discovery of submarine canyons, geoscientists have tried to explain their existence. The similarity of submarine canyons with subaerial valleys at first prompted investigators to ascribe a similar, subaerial origin to the two types of features. It soon became apparent, however, that tremendous changes in sea level would have been required to maintain such an explanation, particularly if one includes the Midocean Canyon in the Atlantic (see Sec. 1.64) with the submarine canyons.

1. KUENEN, P. H.: Repts. 18th Int. Geol. Congr., 8, 44 (1950).
2. KUENEN, P. H.: Spec. Pub. Soc. Econ Min. Paleont. 2, 14 (1951).
3. KUENEN, P. H.: Bull. Amer. Assoc. Petrol. Geol. 37, 1044 (1953).
4. KUENEN, P. H.: Proc. 17th Symp. Colston Research Soc. 47 (1965).
5. KUENEN, P. H.: Sedimentology 7, 267 (1966).
6. MIDDLETON, G. V.: Canad. J. Earth Sci. 4, 475 (1967).
7. RIDDELL, J. F.: Canad. J. Earth Sci. 6, 231 (1969).

Thus, an explanation different from subaerial erosion had to be sought after. Some of the proposals that have been advanced border on the fantastic (see reviews by KUENEN[1] and by SHEPARD[2]); at present it is generally agreed that it is turbidity currents which are responsible for the scouring agreed that it is turbidity currents which are responsible for the scouring out of least of the deeper submarine canyons. The first to propose this explanation was probably DALY[3]; the idea was later taken up by KUENEN[1] who made experiments to substantiate it.

There is little doubt that turbidity currents do exist (cf. Sec. 6.23) and also that they have some erosive power. The problem, therefore, is to investigate whether a reasonable number of turbidity flows can account for the size and shapes of the submarine canyons as the latter have been observed. KUENEN, in the paper mentioned above[1], makes some estimates in this regard; but they do not seem to be too well founded either upon theoretical or experimental considerations. In a later paper. KUENEN[4] notes that in any experiments he performed, the "velocity was never sufficient for the initial erosion to exceed the subsequent deposition". This would mean that all the material moving down a canyon would have to come from the collapse of a canyon wall or such like, with no net erosion taking place at all. However, KUENEN also notes that, if the scale of the experiment were enlarged, the reverse might be true. Thus, it must be held that to this date no satisfactory check of the supposed erosive power of turbidity currents with the actual size of submarine canyons has been obtained. Although the hypothesis of turbidity currents scouring out the submarine canyons appears as reasonable, it cannot really be accepted as proven until a quantitative check is produced.

6.65. Effects of Bottom Currents. The circulation in the sea at large has the effect that, in addition to the well-known surface currents, there also are bottom currents (cf. Sec. 6.25) in the deep ocean.

In very general terms, HANSEN[5] discussed the influence of the bottom relief of the ocean upon the currents and the reactions of the latter upon the former. However, aside from stating that ripple marks might be due to currents and noting that the velocities of the currents (up to 20 cm/sec) are sufficient to cause mass transport, he made no quantitative statements. CARTWRIGHT[6] studied the wave formation in a bottom current behind an obstacle; he obtained a result similar to that of LYRA for air waves behind an obstacle (see Fig. 39; Sec. 2.42). If the ocean floor con-

1. KUENEN, P. H.. Leidse Geol. Med. **8**, 327 (1937)
2. SHEPARD, F P · Proc 8th Pac Sci. Congr. **2A**, 820 (1956)
3. DALY, R A : Amer J. Sci. **31**, 401 (1936)
4. KUENEN, P. H.: Spec. Pub. Soc. Econ. Paleont. Min. **2**, 14 (1951).
5. HANSEN, W.. Geol. Rdsch **47**, 177 (1958)
6 CARTWRIGHT, D. E.: Proc. Roy. Soc. A **253**, 218 (1959)

sists of loose sand, the result of the wavy streamlines will be the creation of sand waves. Finally, HEEZEN and HOLLISTER[1] have made a comprehensive review of the geomorphic effects of bottom currents as observed in nature. Thus, no actual theoretical attempts at a quantitative analysis of the effect of bottom currents seem to be available. Thus, our knowledge of the dynamics of the evolution of the relief of the true ocean bottom is still inadequate.

6.66. Abyssal Plains. We have noted (cf. Sec. 1.64) that abyssal plains are covered by sediments. The general slowness of marine sedimentation, therefore, raises the question as to the origin and the mode of deposition of the sediments that smoothen out the original hilly relief of up to 300 m on the plains.

The answer seems to lie again in advocating turbidity currents[2] as the cause of the depositions, particularly where the latter encircle islands as "archipelagic aprons". However, no numerical estimates relating the size of the depositions to the turbidity currents seem to be available.

6.67. Atolls and Guyots. Finally, we shall discuss the phenomena of atolls and guyots. It appears that both these features have the same origin. They are volcanic cones thrown up onto the sea bottom which are thereafter sinking owing to their weight. If coral growth (cf. Sec. 6.34) is able to keep up with the sinking, an atoll is the result, otherwise one is faced with a guyot.

As noted, the most natural explanation of atolls and guyots is obtained by assuming them to be volcanic eruptions which, subsequently, sink until a state of isostatic equilibrium is attained[3]. However, such an explanation can be accepted only if the viscosity required to yield the observed rates of subsidence is of a reasonable order of magnitude. Assuming that a typical guyot is submerged to 500 fathoms and that it attains isostatic equilibrium, then, at an average rate of subsidence of 0.5 cm/century, it would take 18 million years (or approximately $1/k = 5 \times 10^{14}$ sec) to reach isostatic equilibrium. The radius of a guyot is of the order of $1/b = 5\,\text{km} = 5 \times 10^5$ cm. The viscosity η required to produce equilibrium at the given rate is, according to the Haskell theory[4]

$$\eta = \frac{\rho g}{2\sqrt{\pi k b}} \tag{6.67-1}$$

1. HEEZEN, B. C., and C. HOLLISTER: Marine Geology **1**, 141 (1964).
2. HEEZEN, B. C.: Geophys. J. Roy. Astron. Soc. **2**, 142 (1959).
3. SCHEIDEGGER, A. E.: J. Alberta Soc. Petrol. Geol. **6**, 266 (1958).
4. See e.g. SCHEIDEGGER, A. E: Principles of Geodynamics, 2nd Ed. p. 346 Berlin-Göttingen-Heidelberg: Springer 1963.

where $\rho(=3)$ is the density of the substratum and g is the acceleration due to gravity. Hence for a guyot:

$$\eta \cong 2.1 \cdot 10^{23} \text{ c.g.s.} \qquad (6.67\text{-}2)$$

Some guyots have a radius close to 20 km. Similarly, the assumed rate of subsidence may be of too low an order of magnitude. Together, these factors could raise the required value for the viscosity up to 10^{25} c.g.s. The first-quoted, low-viscosity value of approximately 10^{23} c.g.s is of the right order of magnitude, although it is somewhat high compared with the value for the viscosity which is obtained in a similar fashion by studying the uplift of Fennoscandia; i.e. the sinking rate of the guyots is "too slow". The same thing can also be expressed[1] by stating that the calculated time in which a large guyot would attain isostatic equilibrium is too fast in comparison with the observed time. SAITO[1] suggested that the presence of a yield strength in the Earth might counteract this. Nevertheless, it would appear that the proposed explanation for the formation and subsidence of guyots is entirely reasonable. If the high viscosity value is used, it may not be reasonable to advocate isosatic forces as the cause of the subsidence. One of the reasons for the high value of η might be that the rate of subsidence for guyots has been underestimated. This rate has been obtained by an investigation of the subsidence rate of atolls. The latter rate however, may be smaller than the rate for guyots since it is possible that atolls are close to isostatic equilibrium. Their rate of subsidence would therefore be small and this could be the reason that coral growth can keep up with the sinking.

1 SAITO, Y : J. Oceanogr. Soc. Japan 20th Ariv. Vol., 25 (1962)

VII. Niveal Effects

7.1. General Remarks

7.11. Principles of Ice Action. Many surface features of the Earth have been greatly affected by the action of ice and snow. It has been noted that, at various periods, the abundance of ice and snow upon the Earth's surface was much greater than it is at present. Such periods of increased abundance have been termed *ice ages*. Because of their geomorphological significance, we shall give in this book a brief review of the theories of such ice ages (Sec. 7.12).

Subsequently, we shall discuss the mechanical action of ice. In the main, the latter is due to the effects of *glaciers*. Glaciers are huge rivers of ice steadily flowing downhill. The explanation of the flow of glaciers still poses some problems; it appears that there are two modes of motion: internal motion and sliding. The glacier motion is most easily discussed in two dimensions (Sec. 7.2); i.e. along its bed if the thickness of the ice varies. The analysis of three-dimensional ice motion (Sec. 7.3) is much more complicated than the investigation of longitudinal glacier flow. However, its application to the explanation of the motion of ice caps and of cirque glaciers is of great geomorphological significance.

In the final section (7.4) we shall investigate some other effects that might properly be examined in the present context: these effects include the genesis of pingos, niveal solifluction and other periglacial effects.

7.12. Theories of Ice Ages. As noted earlier, the Earth has gone through periods of increased glaciation (ice ages) at various times of its history. It is of interest to discuss here some of the theories which have been proposed as an explanation of these ice ages. However, since the present treatise is concerned with geomorphology, i.e. with the effect of the ice upon the land, the reasons for the occurrence of increased glaciations are marginal to our subject and therefore the review of the various theories will be held brief[1].

Some physiographic evidence for the occurrence of ice ages has been listed in Sec. 1.71. Accordingly, their most notable features are: (a) the relative scarcity of ice ages throughout the history of the Earth (see Table 3) and (b) the periodic advances and retreats of the glaciers (glacial

1. A review has been given e.g. by SCHWARZBACH, M.: Eiszeitalter und Gegenwart 19, 250 (1968).

and interglacial stages) during any one ice age. For the Pleistocene ice age, the period in question was found to be about 40,000 years. It is possible that the Present Time represents an interglacial stage.

The theories that have been advanced for an explanation of these phenomena have sought the causes either in astronomical or else in endogenetic effects. A combination of these two types of effects has also been advocated. We shall discuss the various proposals in their turn.

Astronomical Causes. (a) Irradiation Fluctuations. The best known atronomical hypothesis of the origin of ice ages is that based upon irradiation fluctuations which had been postulated by MILANKOVITCH[1]. This theory is based on the fact that, because of the varying gravitational effects of the Moon, Sun and Planets upon the Earth (due to the different relative position of these heavenly bodies), the position of the equinoxes with respect to the perihelion, the obliquity of the plane of the Earth's ecliptic and the eccentricity of the Earth's orbit around the Sun vary in an oscillatory fashion with periods of roughly 21,000, 41,000 and 97,000 years, respectively. In the middle and high latitudes, this leads to a variation of insolation with a period of 41,000 years, in the low latitudes to a variation of insolation with a period of 21,000 years. The total insolation over one year stays approximately constant, as summer and winter effects vary in an opposite manner. However, it may be argued that a low summer insolation will generally favor the origination of an ice age, since the snow that has fallen in winter tends to remain permanently. In comparison with this, the extremities of cold reached in winter seem to be of little importance (this had been pointed out earlier by KÖPPEN and WEGENER[2]). Of greatest importance are the insolation fluctuations at middle and high latitudes; at these latitudes, they have a periodicity, as noted above, of 41,000 years. These could trigger climatic changes, assuming that the Earth's ocean-atmosphere system has two stable states (i.e. induce a "flip-flop" mechanism)[3]. The period of 41,000 years for climatic changes is of the right order of magnitude in comparison with the periodicity of glacial and interglacial stages during the Pleistocene. Thus, MILANKOVITCH fits the known record of glacial and interglacial stages with the insolation cycle.

The "Milankovitch theory" has been heavily criticized, but no fundamental argument against it has ever been produced. It is clear, how-

1. See particularly: MILANKOVITCH, M.: Kanon der Erdbestrahlung und seine Anwendung auf das Eiszeitenproblem. Ed. Spéc. Acad. Roy. Serbe Tome 133, Belgrade (1941). This summarizes MILANKOVITCH's life work Much of this theory of ice ages had been published earlier (starting 1920) in separate publications.

2. KÖPPEN, W, and A WEGENER· Die Klimate der geologischen Vorzeit. Berlin: Gebr. Borntrager 1924.

3 BROECKER, W. S.. Science 151, 299 (1966).

ever, that the insolation effect cannot be the only one that is present, simply because there were no ice ages during long periods of geological history.

(b) Solar Emission Theory. Another astronomical hypothesis of the origin of ice ages is the solar emission theory which assumes periodic fluctuations in solar radiation. It has been advocated, for instance, by FRITZ[1], SCHULMAN[2], ÖPIK[3,4], WILLET[5] and SIMPSON[6]. It is quite clear that the hypothesis of solar emission fluctuations cannot be tested easily. It is known that small emission fluctuations with short periods (cf. the sunspot cycle of 11 years) do indeed occur, but nothing is known with regard to the postulated long period of 40,000 years.

The solar emission theory also suffers from the difficulty that it should be applicable during all of the Earth's history, but that no ice ages have occurred during most of the time in question. The reasons for the occurrence of ice ages have therefore been sought in endogenetic causes rather than in astronomical ones.

Endogenetic Causes. *(a) Volcanism.* The first endogenetic cause we shall discuss is volcanism. A review of the hypothesis of the volcanic origin of ice ages has e.g. been give by FLINT[7,8]. Accordingly, volcanic activity may pollute the atmosphere with a large mass of volcanic dust which is an obstacle to the incoming short-wave radiation from the Sun, but does not interfere much with the outgoing long-wave radiation. Hence, its presence has a cooling effect upon the Earth which could cause an ice age. The rhythm of ice ages would then reflect the rhythm of volcanism. However, it is difficult to see why the volcanic activity of the Earth should be a rhythmic process.

(b) Submarine Tectonism. Some Russian investigators, notably SAKS and coworkers[9], advocated that submarine tectonics would be able to change the oceanic water circulation in such a fashion that an effective heat exchange between the seas of the world would be prevented; this

1. FRITZ, S.: In: MALONE, T. F. (ed.): Compendium of Meteorology. Amer. Meteorol. Soc., pp. 243–51 (1951).

2. SCHULMAN, E.: In: MALONE, T. F. (ed.): Compendium of Meteorology. Amer. Meteorol. Soc., pp. 1024–29 (1951).

3. ÖPIK, E. J.: A Climatological and Astronomical Interpretation of the Ice Ages and of the Past Variations of Terrestrial Climate. Armagh Obs. Contr. No. 9 (1953).

4. ÖPIK, E. J.: Irish Astron. J. **8**, 153 (1968).

5. WILLET, H. C.: In: SHAPLEY, H. (ed.): Climate Change, p. 51–71. Cambridge: Harvard Univ. Press 1953.

6. SIMPSON, G. C.: Proc. Linnean Soc. London **152**, 190 (1940).

7 FLINT, R. F.: Glacial Geology and the Pleistocene Epoch. New York: J. Wiley & Sons 1947.

8. FLINT, R. F.: Glacial and Pleistocene Geology. New York: J. Wiley & Sons 1957.

9. SAKS, V. N., N. A. BELOV, and N. N. LAPINA: Priroda 7, 13 (1955).

could produce an ice age. However, the rhythm of ice ages is again difficult to explain in this manner.

(c) Polar Wandering Theory. It is well known[1] that it has been postulated that the axis of rotation of the Earth may have had different positions with regard to the continents at various times during geologic history. This phenomenon has been called "polar wandering". Then, EWING and DONN[2–4] argue that every time the axis of rotation is such that one of the poles falls into a (nearly) enclosed sea (such as presently into the Arctic Ocean), a series of ice ages will be the result. The reason for this is that an enclosed sea at either pole, according to EWING and DONN, represents an unstable system. If the polar sea is frozen over, the supply of moisture in the polar areas is limited and existing glaciers recede. This, in turn, leads to a rise of sea level so that circulation in the oceans becomes such that a ready exchange of water and heat takes place between the polar and warmer seas. At this instant, the polar sea will thaw out. However, with an open polar sea, a ready supply of moisture is present which will accumulate in high latitudes as snow and give rise to glaciations. The process continues until so much snow is locked up in land areas that the sea level is sufficiently lowered to prevent an effective interchange of water between the polar and warm seas. At that stage, the polar sea suddenly freezes over and a new interglacial cycle starts.

The "pluvial" polar wandering theory described above has been criticized on the grounds that the temporal correspondence between the decrease of glaciation and the icing up of the Arctic Ocean has by no means been established[5,6]. Furthermore, COX[7] pointed out that, according to paleomagnetic evidence, the polar axis has been in its present position for an interval at least 10 times longer than the interval of recurrent glaciations.

A modification of the "pluvial" polar wandering theory has been proposed by WILSON[8] who assumed that the trigger in the flip-flop mechanism is not provided by the freezing and unfreezing of the Arctic Ocean, but by the build-up and decrease of the Antarctic ice sheet.

(d) Greenhouse Theory. Another theory of ice ages which is based upon phenomena taking place upon the Earth itself, has recently been pro-

1 Cf. e.g. SCHEIDEGGER, A. E.: Principles of Geodynamics. Second Ed. Berlin-Göttingen-Heidelberg: Springer 1963.

2. EWING, M., and W. L. DONN: Science 123, 1061 (1956). Second Ed.

3. EWING, M., and W. L. DONN: Science 127, 1159 (1958).

4. EWING, M.: J. Alberta Soc. Petrol. Geol. 8, 191 (1960).

5. SCHWARZBACH, M.: Z. Deutsche Geol. Gesellsch. 112, 309 (1960).

6. COLINVAUX, A. P.: Science 145, 707 (1964).

7. COX, A.: Meteorolog. Monogr. 8, No. 30, 112 (1968).

8. WILSON, A. T.: Nature 201, 147 (1964).

posed by GOSSELINK[1] who assumes that the climatic variations leading to ice ages result from changes in the water vapor and carbon dioxide content of the Earth's atmosphere. The water vapor and the carbon dioxide act as an effective shield for infrared radiation leaving the Earth and thereby cause a "greenhouse effect". According to GOSSELINK, an unstable state may be created: when for some reason the climate begins to become warmer, more water vapor will be in the air thereby increasing the greenhouse effect and the warming-up process. This will progress to an ultimate stage when a reversal of the process may take place. This would cause the oscillations represented in the cycle of glacial and interglacial stages.

Combined Theories. *(a) The Volcanic Combined Theory.* As noted above, the volcanic theory is by itself unable to account for the periodicity of the stages in an ice age. It has therefore been suggested that increased volcanism may have been able to produce a lowering of the over-all temperature of the world so that one of the astronomical causes considered above may have been able to imprint oscillations thereupon of the required periodicity. During long periods of the Earth's history, the volcanism may have been too weak to lower the temperature sufficiently to cause an ice age; this would account for the absence of glaciations during much of the Earth's evolution.

(b) Solar Topographic Theory. A more general formulation of a relationship between ice ages and topography may be obtained by not restricting oneself to volcanism as a temperature-depressing agent. It stands to reason that the atmospheric turbulence is greater during periods of high topographic relief than during periods of low relief. One might reason that the increased turbulence leads to increased cloud formation and thus to an increased albedo of the Earth. Increased albedo, in turn, will have the effect of reflecting more of the Sun's radiation away from the Earth and therefore lead to lowered temperatures. A connection between climate and orogenesis had, in fact, been postulated long ago by geologists[2]. A modern review of the above ideas has been given by EMILIANI and GEISS[3]. Accordingly, the two most recent sequences of ice ages coincide with the two most recent periods of increased orogenetic activity: the Pleistocene period and the Paleozoic period. The topographic changes produce a general lowering of the Earth's surface temperature, and some astronomical cause connected with solar irradiation or solar emission, impresses the required periodicity.

---

1. GOSSELINK, J. G.: Proc. Indiana Acad. Sci. 68, 294 (1958).
2. See e.g. RAMSAY, W.: Forh. Ofversight af Finska Vet. Soc. 52 (1910).
3. EMILIANI, C., and J. GEISS: Geol. Rdsch. 46, 576 (1959).

(c) An Eclectic Theory. A theory in which many of the possible causes of ice ages discussed above have been combined, has been proposed by FAIRBRIDGE[1]. Accordingly, polar wandering would put the Earth's poles into the Arctic Ocean and into the Antarctic Continent, Tertiary tectonism would close the Tethys Sea and cause high mountains (with attendant effects on the atmospheric circulation), the ice-build-up in Antarctica would increase the Earth's albedo, Milankovitch-type irradiation fluctuations would introduce cyclic changes in the heat available, solar radiation fluctuations would also be active, and the combination of all these factors would produce the characteristics of the present ice age.

One cannot decide to-date which is the correct theory of the origin of ice ages. However, it is seen that there are several, presently equally possible, hypotheses. We shall concern ourselves here mainly with the effects of ice action upon geomorphology and refer the reader interested in the details of ice ages theories, to the papers listed in the foot-notes.

7.2. Longitudinal Movement of Glaciers

7.21. General Remarks. The study of the movement of glaciers is an involved discipline into which much effort has been expended by various research workers. In connection with theoretical geomorphology, we are interested in glacier flow insofar as it has a bearing upon the land forms that have been affected by it. Unfortunately, when it comes to a study of the interaction of a glacier with its bed and the valley walls, studies available are very rare and incomplete indeed.

Of the various theories of glacier flow available at the present time, one of the variants of NYE's theories, based upon plasticity theory, is the most suitable for our purpose. It will be presented in Sec. 7.22. NYE'S theory explains the internal flow of a glacier only, it does not account for the sliding of a glacier over its bed. Questions concerned with the latter problem will be discussed in Sec. 7.23. Subsequently, we shall turn our attention to some special problems, viz. to the formation of glacier snouts and crevasses. Finally, some of the geomorphological implications of the above phenomena will be discussed.

All the discussions in these chapters are concerned with the longitudinal movement of glaciers only. If the three-dimensional movement of ice is under consideration, the mathematics involved becomes much more complicated. This will be investigated in Chap. 7.3.

1. FAIRBRIDGE, R. W.: Ann. New York Acad. Sci. 95, 542 (1961).

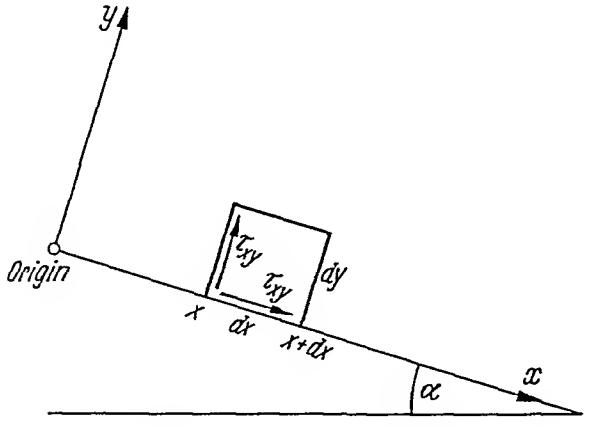

Fig. 179 Geometry of glacier flow

7.22. Theory of Longitudinal Flow of Glaciers. The flow of glaciers has been studied by many investigators. In the earliest attempts[1], a heuristic assumption was used for the connection between glacier thickness and flow velocity. Subsequently, the theory of glacier flow was based on a viscous-type flow law, later a plastic flow law was considered more appropriate and, finally, a power flow law was considered as most adequate. The plastic flow law can also be considered as a limiting case of the power flow law; the two laws lead, in many cases, to very similar results. Today, the best-known treatment of the glacier flow problem is probably that of NYE who first regarded it from the standpoint of plastic flow[2] and then from the standpoint of a power flow law[3]. It turned out that[4] the solutions for glacier flow obtained for the general flow law are very similar to those found for the plastic flow law. We shall therefore mainly discuss NYE'S earlier theory where a plastic flow law has been assumed as basic for glacier flow.

The theory thus obtained is, in fact, identical to the theory of the Rankine state of the slow downhill flowage of loose material (cf. Sec. 3.43). Accordingly, the flow may occur in an *active* or in a *passive* Rankine state. On a uniform slope of slope angle α (see Fig. 179) and in a plane strain state, the equations that have to be satisfied are (cf. 3.43-18/19)

$$\frac{\partial \sigma_x}{\partial x}+\frac{\partial \tau_{xy}}{\partial y}-\rho g \sin\alpha=0, \tag{7.22-1}$$

$$\frac{\partial \tau_{xy}}{\partial x}+\frac{\partial \sigma_y}{\partial y}-\rho g \cos\alpha=0 \tag{7.22-2}$$

1. FINSTERWALDER, S.: Z. Gletscherkunde 2, 81 (1907–8).
2. NYE, J. F.: Proc. Roy. Soc. A 207, 554 (1951).
3. NYE, J. F.: J. Glaciol. 2, 82 (1952); 2, 512 (1955).
4. NYE, J. F : Proc. Roy Soc. A 239, 113 (1957).

where σ and τ are normal and shear stresses, respectively, ρ is the density of the ice, g the gravitational acceleration and $+x$ is taken parallel to the slope, pointing downhill. To the above equation one must add the yield criterion (k being a constant):

$$(\sigma_x-\sigma_y)^2+4\tau_{xy}^2=4k^2.$$

If the velocity of flow is sought, one also has to heed the condition of incompressibility and the condition that the principal axes of stress and strain coincide. This will be dealt with below (cf. 7.22-8 and 7.22-9).

Assuming that the boundary conditions imply (k a positive number)

$$\tau_{xy}=-k$$

at the bed, that the velocity at the bed is zero, and that the shear stress vanishes at the surface of the glacier ($y=h$), the two possible stress solutions to the problem are:

$$\begin{aligned}
\sigma_x&=x\left(-\frac{k}{h}+\rho g\sin\alpha\right)+y\rho g\cos\alpha\pm 2k\sqrt{\left\{1-\left(1-\frac{y}{h}\right)^2\right\}}+a\\
\sigma_y&=x\left(-\frac{k}{h}+\rho g\sin\alpha\right)+y\rho g\cos\alpha+a \qquad (7.22\text{-}3)\\
\tau_{xy}&=-k\left(1-\frac{y}{h}\right).
\end{aligned}$$

Here, a is a constant which must be set equal to

$$a=-h\rho g\cos\alpha \qquad (7.22\text{-}4)$$

in order to have a free surface for $y=h$. Furthermore, for the same reason, the following condition must be imposed upon h

$$h=\frac{k}{\rho g\sin\alpha}=\frac{h_0}{\sin\alpha} \qquad (7.22\text{-}5)$$

with

$$h_0=k/(\rho g) \qquad (7.22\text{-}6)$$

for then σ_y and σ_x will also vanish on $y=h$.

Provided the condition (7.22-5) is satisfied, the possible stress solutions for glacier flow are therefore

$$\begin{aligned}
\frac{\sigma_x}{k}&=\frac{y-h}{h_0}\cos\alpha\pm 2\sqrt{\left\{1-\left(1-\frac{y}{h}\right)^2\right\}}\\
\frac{\sigma_y}{k}&=\frac{y-h}{h_0}\cos\alpha \qquad (7.22\text{-}7)\\
\frac{\tau_{xy}}{k}&=-1+\frac{y}{h}.
\end{aligned}$$

The corresponding velocity solutions (u parallel to x, v parallel to y) are obtained from the condition of incompressibility

$$\frac{\partial u}{\partial x}+\frac{\partial v}{\partial y}=0 \tag{7.22-8}$$

and from the condition that the principal axes of stress and stain rate coincide

$$\frac{\partial v/\partial x+\partial u/\partial y}{\partial u/\partial x-\partial v/\partial y}=\frac{2\tau_{xy}}{\sigma_x-\sigma_y}. \tag{7.22-9}$$

Hence:

$$u=C\pm\frac{Vx}{h}+2V\sqrt{\left\{1-\left(1-\frac{y}{h}\right)^2\right\}} \tag{7.22-10}$$

$$v=\mp Vy/h \tag{7.22-11}$$

where C and V are constants. The two solutions are illustrated in Fig. 180. It should be noted that in both solutions, a vertical velocity component is present. Thus, in order to keep condition (7.22-5) satisfied, material (snow) has to be either added or subtracted from the surface.

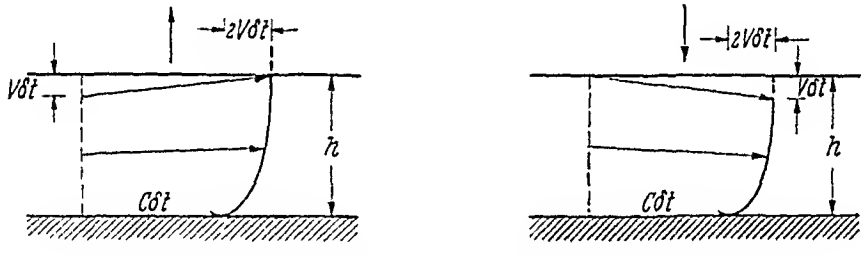

Fig. 180. The two velocity solutions for a glacier. After NYE[1]

The slip lines (trajectories of maximum shear stress) can be calculated for the above cases; in fact, this problem had been solved long ago by FRONTARD[2] and PRANDTL[3]. The result is shown in Fig. 181.

The above calculations are also roughly valid for a slope of varying slope angle. The interpretation of the approximate solutions for this case is that the ice always adopts the type of flow that maintains the critical thickness (Eq. 7.22-5). Accordingly, a concave bottom and loss of material would tend to favor the passive, a convex bottom and addition of material would tend to favor the active Rankine state.

Of particular importance is a discussion of glacial erosion. It appears that the slip lines discussed above have a connection with this. If the slip line is of the type PP' (Fig. 181), the differential movement at P might

1. NYE, J. F.: Proc. Roy. Soc. A **207**, 554 (1951).
2. FRONTARD, M.: C. R. Acad. Sci. (Paris) **174**, 526 (1922).
3. PRANDTL, L.: Z. angew. Math. Mech. **3**, 401 (1923).

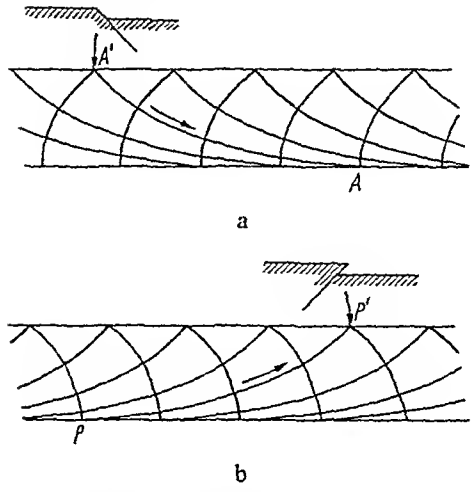

Fig. 181 a and b. The slip line fields and fault planes (a) in active flow and (b) in passive flow. After NYE[1]

tend to suck débris into the ice from the bottom, whereas in the case of a slip line of the type $A'A$, it would merely roll débris along. Thus, it might be expected that it is passive flow which causes erosion.

Thus, the picture of a glacier moving over a slope of varying slope angle might be envisaged as shown in Fig. 182 (after NYE). The places where erosion occurs are denoted by E.

The above theory is for a cross-section of an infinitely wide glacier. NYE[2] has also produced solutions of the basic equations for glacier flow in channels of rectangular, elliptic and parabolic cross-sections. MACKAY[3] has made analog-models for the solution of glacier flow problems.

As was noted earlier, the above theory has been extended to the use of flow laws different from that adopted in plasticity theory. However, the results obtained are very similar to those presented above and since our interest is essentially in the geomorphological effects of glacier flow, an improved theory is of little significance for us. Similarly, very interesting investigations into the propagation of surges[4,5] into wave formation on glaciers[6] and into travelling waves on glaciers[7] are presumably of little importance in connection with questions regarding the origin of the Earth's surface features.

1. NYE, J. F.: Proc. Roy. Soc. A 207, 554 (1951).
2. NYE, J. F.: J Glaciol. 5, 661 (1965).
3. MACKAY, J. R.: Geogr. Bull. 7, No. 1, 1 (1965).
4. NYE, J. F.: Nature (Lond.) 181, 1450 (1958).
5. NYE, J. F.: Proc. Roy. Soc. A 275, 81 (1963).
6. NYE, J. F.: Pub. Ass. Int. Hydrol. Sci. 47, 139 (1958).
7. WEERTMAN, J.: Pub. Ass. Int. Hydrol. Sci. 47, 162 (1958).

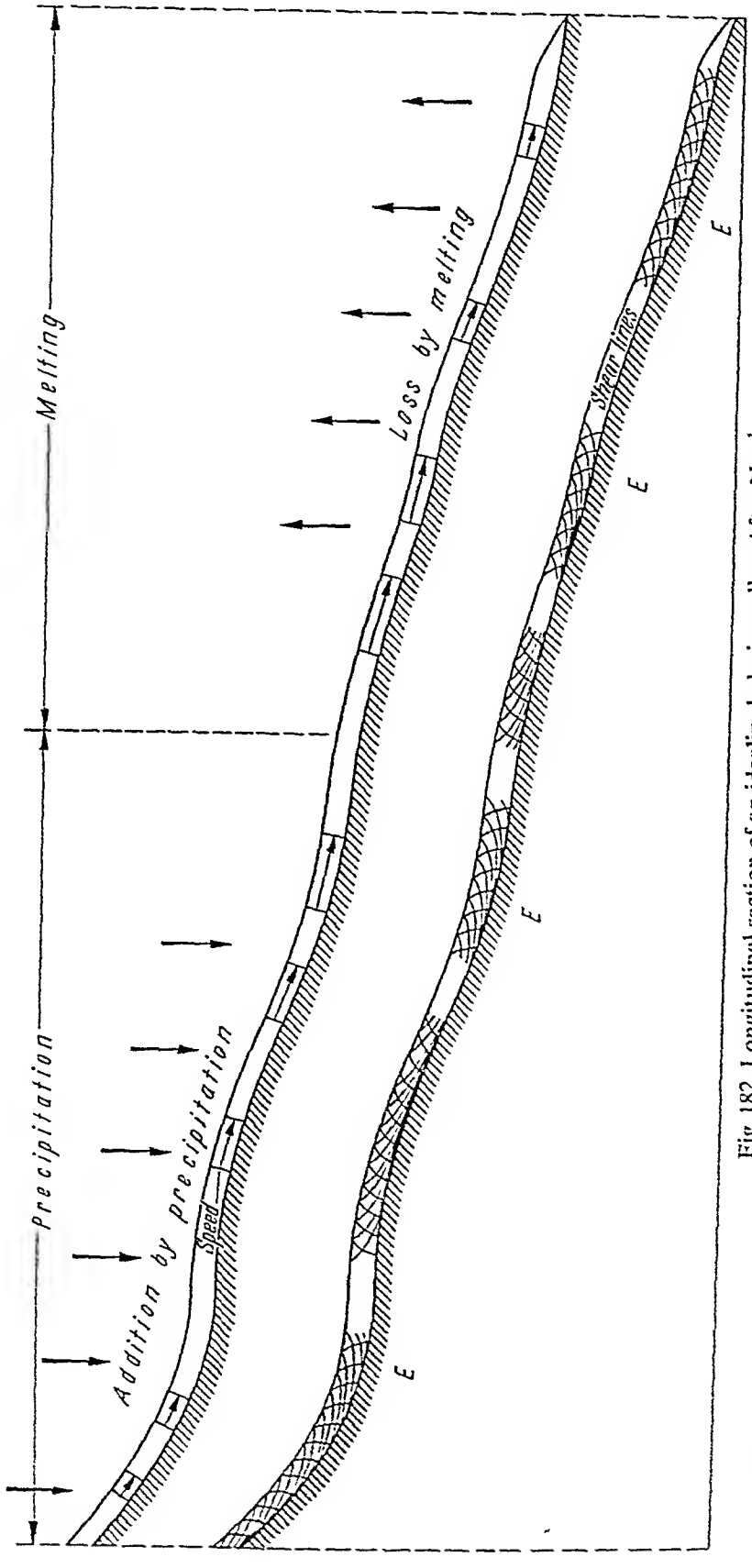

Fig. 182. Longitudinal section of an idealized glacier valley. After Nye[1]

1. Nye, J. F.: Proc. Roy. Soc. A 207, 554 (1951).

7.23. Theory of Longitudinal Sliding of Glaciers. The theory of glacier movement described above assumes as boundary condition that the velocity of the glacier vanishes at the bed. This is almost certainly an oversimplification, as it may be expected that a certain amount of sliding will always take place. The bed of a glacier is very uneven so that there are only two effects that can contribute much to sliding: the first is pressure melting, the second stress concentrations. A theory of glacier sliding based upon these two effects has been proposed by WEERTMAN[1,2].

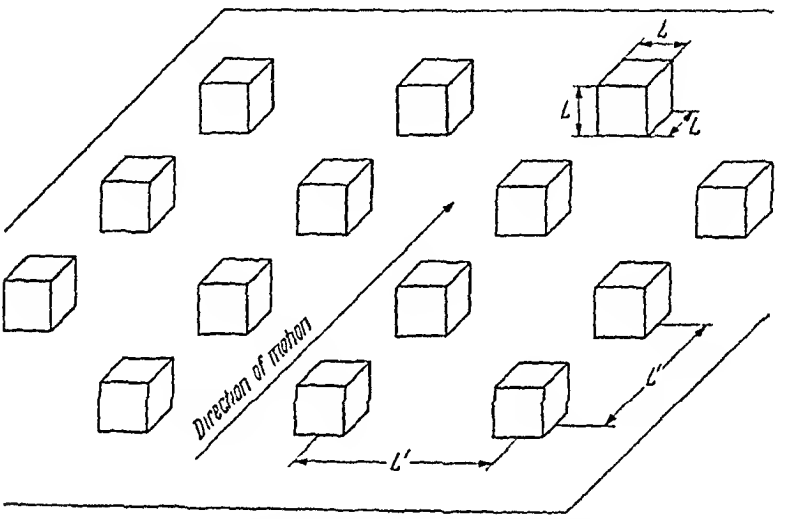

Fig. 183. Idealized glacier bed. After WEERTMAN[1]

In order to set up his theory, WEERTMAN had to assume an idealized glacier bed (see Fig. 183). Such a bed consists of cubical protuberances of edge length L which are centered on a square grid with grid length L'.

From the above model, it is first of all possible to calculate the difference ΔT in melting point temperature in front and behind an obstacle. If τ be the macroscopic shear stress at the glacier bottom, the average normal stress on one side of an obstacle is *equal* to $\tau L'^2/L^2$ if no hydrostatic pressure is present. If a hydrostatic pressure is present, then the stress increase caused by the obstacle must be *proportional* to the above value. Since the change of melting point ΔT is proportional to the stress change[3], we have the result that the latter will also be proportional to

$$\tau L'^2/L^2.$$

1. WEERTMAN, J.: J. Glaciol. 3, 33 (1957).
2. WEERTMAN, J.: J. Glaciol. 5, 287 (1964).
3. FERMI, E.: Thermodynamics. New York: Prentice-Hall 1937.

where $\rho g h$ is the mean pressure and $\Delta\sigma/2$ the maximum variation therefrom. Here, h is as usual the thickness of the glacier, ρ the density of the ice and g the gravity acceleration. The quantity σ_z is a principal stress; the other two principal stresses are

$$\sigma_y = \sigma_z = \rho g h. \tag{7.23-9}$$

The mean frictional traction τ is (setting the sine equal to the tangent)

$$\tau = \frac{1}{\lambda}\int_0^{\lambda} \sigma \frac{dz}{dx}\,dx = \frac{1}{\lambda}\int_0^{\lambda} \frac{\Delta\sigma}{2}\frac{a\pi}{\lambda}\cos^2\left(\frac{2\pi x}{\lambda} - \varphi\right) dx = \frac{\pi}{4} r\,\Delta\sigma \tag{7.23-10}$$

with r again being the rugosity as given by (7.23-7).

With the above concepts, it is possible to re-evaluate WEERTMAN's theory. Thus, considering first again "Process A", LLIBOUTRY noted that the difference in melting point temperature is again given by an equation of the type (7.23-1) which, however, reads now

$$\Delta T = \tfrac{1}{3} C\,\Delta\sigma \tag{7.23-11}$$

with the same value for C as adopted earlier. The heat flux across a protuberance of cross section a (referred to unit width) and average length $\lambda/2$ is

$$Q = C\frac{\Delta\sigma}{3}\frac{2a}{\lambda} D \tag{7.23-12}$$

where D is again the coefficient of heat conductivity of the rock. Following the same reasoning as above, this leads to a sliding velocity S_A of

$$S_A = \frac{Q}{aH\rho} = \frac{CD}{aH\rho}\frac{2}{3} r\,\Delta\sigma = \frac{CD}{aH\rho}\frac{2}{3}\frac{4}{\pi}\tau \tag{7.23-13}$$

where H is again the heat of fusion.

Considering now the "Process B", LLIBOUTRY assumes that the smooth flow of the ice is perturbed in a layer of thickness λ. Then the maximum compression (strain) will be of the order $a/\lambda = r$. It arises in the time interval $\frac{1}{2}\lambda/S_B$ and hence the strain rate $\dot{\varepsilon}$ is

$$\dot{\varepsilon} = r\frac{2S_B}{\lambda} = \frac{2S_B}{a} r^2. \tag{7.23-14}$$

The yield stress is according to general plasticity theory

$$k = \sqrt{\tfrac{1}{6}\Sigma(\sigma_i - \sigma_k)^2} \tag{7.23-15}$$

whose value is

$$k=\sqrt{\frac{2}{6}\left(\frac{\Delta\sigma}{2}\right)^2}=\frac{\Delta\sigma}{2\sqrt{3}}=\frac{2\tau}{\pi r\sqrt{3}}. \tag{7.23-16}$$

The power flow law for the ice yields then (cf. Eq. 2.33-1):

$$\frac{2S_B}{a}r^2=B\left[\frac{2}{\pi\sqrt{3}}\frac{\tau}{r}\right]^n \tag{7.23-17}$$

or

$$S_B=\frac{Ba}{2r^2}\left[\frac{2}{\pi\sqrt{3}}\frac{\tau}{r}\right]^n. \tag{7.23-18}$$

Taking now again a whole spectrum of protuberances, and requiring (with WEERTMAN) that the glacier speed due to process A equals that due to process B, LLIBOUTRY obtained a sliding velocity $S_A=S_B$ of 4 m/year (setting $n=3$, $B=0.18$, $\tau=1.83$, $r=0.1$, $CD/(H\rho)=0.0016$ in the system meter-bar-year). This is still too little. Of interest may be the observation that the protuberances required to produce the shear stress have a height of 0.7 mm. This indicates that the type of glacier sliding embodied in processes A and B applies only to very small obstacles. It represents a process which might produce glacial polish.

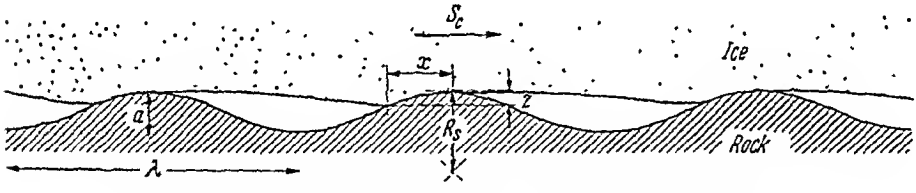

Fig. 185. Detachment of a glacier from its bed. After LLIBOUTRY[1]

Since the combination of processes A and B, either in WEERTMAN'S or in LLIBOUTRY'S form, cannot possibly produce the high sliding velocities of 30–3000 metres per year (cf. Sec. 1.72) observed in glaciers, LLIBOUTRY searched for a modification which might produce higher velocities. He found such a modification in the possibility that the glacier might detach itself from its bed. The picture would then be that represented in Fig. 185. This means, in effect, that the glacier bed is rough in only one direction.

According to Formula (7.23-8), the minimum normal pressure of the glacier bed is

$$\sigma_{z\,\min}=\rho g h-\frac{\Delta\sigma}{2}=\rho g h-\frac{2\tau}{\pi r}. \tag{7.23-19}$$

1. LLIBOUTRY, L.: Ann. Géophys. (Paris) **15**, 250 (1959).

If a detachment from the bed is to occur, this pressure must become zero which yields

$$\tau=\frac{\pi}{2} r \rho g h. \tag{7.23-20}$$

However, if detachment occurs, it appears likely that the resulting cavity fills itself with water which will be subject to an equilibrium pressure p at a temperature below 0° C. Hence, Eq. (7.23-20) should in fact be written as follows

$$\tau=\frac{\pi}{2} r(g \rho h-p). \tag{7.23-21}$$

The quantity $g \rho h-p$ is an "effective" stress, representing the excess of the prevaling stress over the prevailing hydrostatic pressure.

The above considerations lead to a process of sliding which has entirely different characteristics from the Processes A and B considered earlier. LLIBOUTRY called the new process "Process C". He envisaged[1] it as occurring in such a fashion that the ice rests over the length x (see Fig. 185) on the protuberances ($x \ll \lambda$), producing a rise Z in the underside of the glacier, equal to

$$Z=\frac{x^2}{2R_s} \tag{7.23-22}$$

where R_s is the radius of curvature at the top of the protuberance, which according to (7.23-6) is equal to

$$R_s=\frac{\lambda^2}{2\pi^2 a}. \tag{7.23-23}$$

Hence

$$Z=\pi^2 a \frac{x^2}{\lambda^2} \tag{7.23-24}$$

which is the value that now has to be used for the calculation of the strain rate $\dot{\varepsilon}$ (cf. 7.23-14)

$$\dot{\varepsilon}=2\pi^2 a S_c \frac{x^2}{\lambda^4} \tag{7.23-25}$$

where S_c now denotes the sliding velocity due to the Process C. The force-balance equation over a wavelength λ of the protuberance yields (approximately)

$$p(\lambda-x)+\sigma_z x=\rho g h \lambda; \tag{7.23-26}$$

hence

$$\sigma_z=(\rho g h-p)\frac{\lambda}{x}+p. \tag{7.23-27}$$

1. The following exposition is after LLIBOUTRY (loc. cit.). Note, however, that LLIBOUTRY'S paper contains many arithmetic errors which the present writer attempted to correct. The formulas given here, therefore, differ slightly from those in LLIBOUTRY'S paper.

The contact force between the ice and the solid bed forms an angle $x/(2R_s)$ with the vertical whose tangent is the coefficient of friction. The average effective normal pressure is $\rho g h - p$, hence the frictional force is (since $x/2R_s$ is small):

$$\tau_c = \frac{(\rho g h - p)\, x}{2R_s} = (\rho g h - p)\frac{\pi^2 a x}{\lambda^2}. \tag{7.23-28}$$

Inserting this into the equation for the shear rate, yields

$$\dot{\varepsilon} = \frac{2S_c \tau_c^2}{\pi^2 a (\rho g h - p)^2}. \tag{7.23-29}$$

On the protuberance, the effective stresses are

$$\sigma_z = (\rho g h - p)\,\lambda/x, \tag{7.23-30}$$

$$\sigma_x = \sigma_y = \rho g h - p. \tag{7.23-31}$$

If $x \ll \lambda$ as assumed earlier, σ_z is the dominating stress and one obtains for the yield stress k (cf. 7.23-15).

$$k = \frac{\rho g h - p}{\sqrt{3}}\,\frac{\lambda}{x} = \frac{(\rho g h - p)^2 \pi^2 a}{\tau_c \lambda \sqrt{3}}. \tag{7.23-32}$$

With the power law of flow, this yields

$$\frac{2S_c \tau_c^2}{\pi^2 a (\rho g h - p)^2} = B\left[\frac{(\rho g h - p)^2 \pi^2 a}{\tau_c \lambda \sqrt{3}}\right]^n. \tag{7.23-33}$$

It is obvious that S_c *increases* if the friction τ_c *decreases.* This is entirely different from what we had for the earlier processes. We now have a process in which the sliding becomes easier, the faster it occurs.

As representative values, LLIBOUTRY claims that, if one assumes

$$\rho g h - p = 6.5 \text{ bars},$$

then the set

$$\begin{aligned} r &= 0.1 \\ \tau_c &= 1.0 \text{ bar} \\ n &= 3 \\ a &= 0.21 \text{ m} \\ S_c &= 100 \text{ m/year} \end{aligned} \tag{7.23-34}$$

forms a consistent set of numbers, provided a suitable value is chosen for B. Thus, "Process C" at last represents a process in which high sliding velocities are possible.

As may by expected, there is a certain amount of controversy whether WEERTMAN'S or LLIBOUTRY'S theory should be used to describe glacier sliding[1,2]. The essential difference is that LLIBOUTRY assumes that the bed is rough only in one direction, because the glacier is in fact detached from its bed downstream of the obstacles. The question whether such "detachment" has to be invoked or not depends on whether the melting-regelation process is or is not possible, particularly in a "cold" glacier[3,4].

It may be assumed that in actual glacier flow, all three processes are possible. Processes *A* and *B* are responsible for the glacial polish on rocks, Process *C* for the high sliding velocities that may be observed in glaciers.

7.24. Dynamics of Glacier Snouts. One of the immediate effects of any climatic changes is upon the advance and the retreat of glaciers. In effect, even minor changes in mean temperature cause substantial glacier variations: Thus all the glaciers in the Alps have been in retreat since 1870[5]. Such advance and retreat takes place at the glacier snout. The problem of glacier snouts has been studied by FINSTERWALDER[6] at a very early date who, as noted in Sec. 7.22, based his analysis on an heuristic equation of the development of the ice surface similar to that of MATSCHINSKI in Sec. 7.31. It is

$$[(n+1)\,\kappa\,\Theta^n - a]\,\frac{\partial\Theta}{\partial x} + \frac{\partial\Theta}{\partial t} = -a. \tag{7.24-1}$$

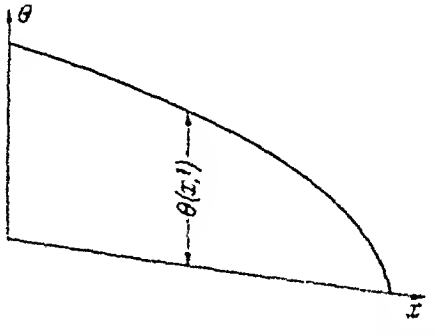

Fig. 186. Cross section through the end of a glacier

Here Θ is the height of the above the base x (cf. Fig. 186) and a is the melting constant giving the amount of ice loss per unit time. The above

1. LLIBOUTRY, L.: C. R. Acad. Sci. Paris 258, 1577 (1964).
2. WEERTMAN, J.: J. Glaciol. 6, 489 (1967).
3. WEERTMAN, J.: J. Geophys. Res. 72, 521 (1967).
4. LLIBOUTRY, L.: J. Geophys. Res. 72, 525 (1967).
5. FOREL, F.: Arch. Sci. Phys. Nat. 34, 209 (1895).
6. FINSTERWALDER, S.: Z. Gletscherkunde 2, 81 (1907).

picture is based on the heuristic assumption that the ice velocity is given by

$$v=\kappa\,\Theta^n \tag{7.24-2}$$

where κ depends on the bed slope of the glacier and n is a constant having a value between $\frac{1}{4}$ and $\frac{1}{2}$.

A numerical integration of the differential Eq. (7.24-1) has been given by COLLATZ[1], choosing $n=\frac{1}{3}$, $\kappa=0.075$, $a=\frac{1}{2}$. The result obtained is shown in Fig. 187.

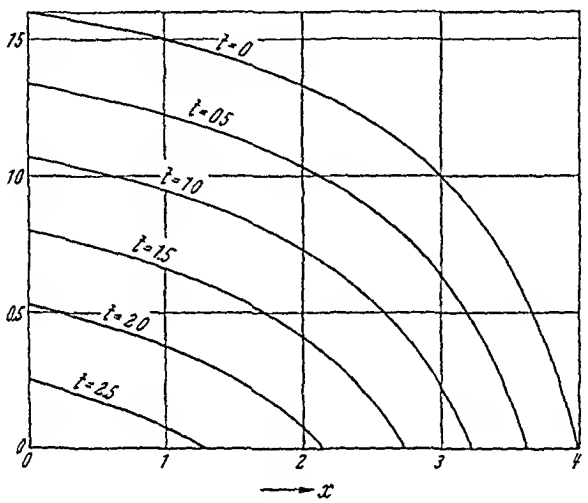

Fig. 187. Profile of glacier snout as a function of time. After COLLATZ[1]

The approach of FINSTERWALDER was put upon a somewhat more solid basis by NYE[2,3] (apparently entirely independently). Accordingly, the advance and retreat of a glacier snout is but a special case of a general theory of the response of a glacier to climatic variations. The theory of such variations has to be primarily based on a mass balance equation. In addition, the central assumption is made that the rate of discharge in the glacier at a point is a definite function of the thickness of the glacier and of the slope of its surface at that point [this is a generalization of Eq. (7.24-2)]. The actual response of the glacier to changes in the rate of nourishment and wastage can then be studied by means of a linearized perturbation theory; it turns out that the behavior of the perturbation is given by a diffusivity equation with a source term and a mass transport term. This can then be applied to a hypothetical reason-

1. COLLATZ, L Numerische Bchandlung von Differentialgleichungen. 2nd Ed. Berlin-Göttingen-Heidelberg: Springer 1955. See p 288
2. NYE, J F.: Proc. Roy. Soc A 275, 87 (1963)
3. NYE, J. F.: Geophys. J. Roy. Astron. Soc. 7, 431 (1963).

able snout-profile whose advance and retreat as a function of change in precipitation can be calculated.

Other studies of the mechanics of glacier snouts have been undertaken by LLIBOUTRY[1]. These were based upon the assumption that the glacier behaves as a rheological material. It will be noted that the results obtained upon this basis, as presented in Sec. 7.22, do not allow for a stationary front to be possible. LLIBOUTRY carried the solution to a further approximation, but the additional terms turned out to be quite negligible. It thus appears that, if the mechanics of ice is to be introduced [and not simply a semi-empirical equation like (7.24-1) is to be used], it is not sufficient to consider only the profile of the glacier snout, but that the effects of the valley sides have to be accounted for. This leads to a three-dimensional problem.

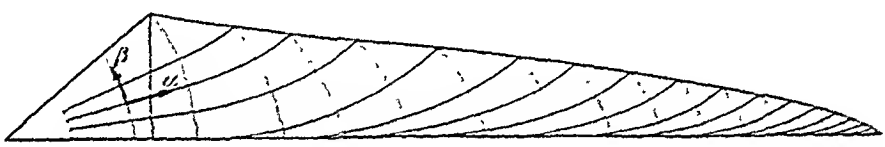

Fig. 188. NYE's plasticity solution for a glacier snout. After NYE[2]

The problem can be solved more easily if, instead of a general flow law, the plasticity theory of ice flow is used. Upon this basis, NYE[2] produced an equilibrium profile and slip line field of a glacier snout as shown in Fig. 188.

7.25. Transverse Crevasses. We now come to the attempts that have been made at explaining the presence of *crevasses* in glaciers. In the longitudinal case such crevasses are transverse reaching across the breadth of the glacier.

If we again revert to NYE's theory of plastic flow in glaciers, one may note that the stress solution given for active flow indicates (cf. Eq. 7.22-7) that the upper layer of the glacier is under tensile stress which stays tensile to a depth d of (according to NYE[3])

$$d=\frac{2h_0}{\sqrt{1+3\sin^2\alpha}}. \tag{7.25-1}$$

This might give rise to transverse fissures to this depth d, if the critical strain rate is exceeded[4].

The slip lines mentioned in Sec. 7.22 may also be associated with crevasses. If an actual displacement occurs along these lines, then it is

1. LLIBOUTRY, L.: Ann. Géophys. (Paris) 12, No. 4, 245 (1956).
2. NYE, J. F.: J. Glaciol. 6, 695 (1967).
3. NYE, J. F.: Proc. Roy. Soc. A 207, 554 (1951).
4. HOLDSWORTH, G.: J. Glaciol. 8, 107 (1969).

obvious that this will result in crevasses in the case of active flow. These crevasses will again be transverse as we are dealing here with linear geometry.

7.26. Geomorphological Effects of Longitudinal Glacier Motion. It remains to discuss the effects of longitudinal glacier movement on the terrain, with a view of possibly explaining the various features whose origin geomorphologists ascribe to the action of glaciers (cf. Secs. 1.73 and 1.74).

It stands to reason that the *longitudinal* profile of Alpine valleys can be explained by the *longitudinal* motion of glaciers. This concerns the step-shaped longitudinal profile of such valleys. With regard to the latter, we note that NYE's theory (Sec. 7.22) predicts that erosion should occur at places in the bed where the latter is concave. It thus appears that a glacier tends to deepen any existing hollows in its bed and thus to accentuate the existing relief. This view has been supported by RÖTHLISBERGER[1]. It is obvious that the end result of such a process will be a succession of pronounced hollows and steep steps. After the melting of the glacier, the hollows will be filled in by débris and the characteristic longitudinal profile of an Alpine valley results. NYE's theory may therefore be said to explain this profile.

Another effect of "longitudinal glacier erosion" is the scooping out of fjords[2,3]. As far as such fjords are drowned valleys, it simply is the glacial erosion as described above that might contribute to their deepening. However, the "glacier" may often, in effect, be a floating ice-sheet, and then the abrasion will occur at the sides of the inlet. A theory for this process was supplied by CRARY[3].

Another feature that might possibly be explained by reference to the longitudinal motion of a glacier is the existence of drumlins (see Sec. 1.74). It has been noted that the form of drumlins is very close to that of a streamlined body[4,5]. CHORLEY[6] has elaborated upon this supposition; he made comparisons of shapes of drumlins with that of aerofoils and found a good correspondence. He noted that the base contours of drumlins can be fitted rather well with lemniscate loops. An example of this fit is shown in Figs. 189 and 190. The lemniscate loops have the following equation

1. RÖTHLISBERGER, H.: Proc General Ass. Bern, Int. Ass Sci. Hydrol, Vol. "Snow and Ice", p. 87 (1967)
2. HOLTEDAHL, H.: Geografiska Annaler 49 A, 188 (1967).
3. CRARY, A. P.: Bull. Geolog. Soc. Amer. 77, 911 (1966).
4. FLINT, R. F.· Glacial and Pleistocene Geology. New York: J. Wiley & Sons 1957.
5. CHARLESWORTH, J. K.: The Quaternary Era with Special Reference to its Glaciation. London: E. Arnold & Co. 1957.
6. CHORLEY, R. J.: J. Glaciol. 3, No. 25, 339 (1959).

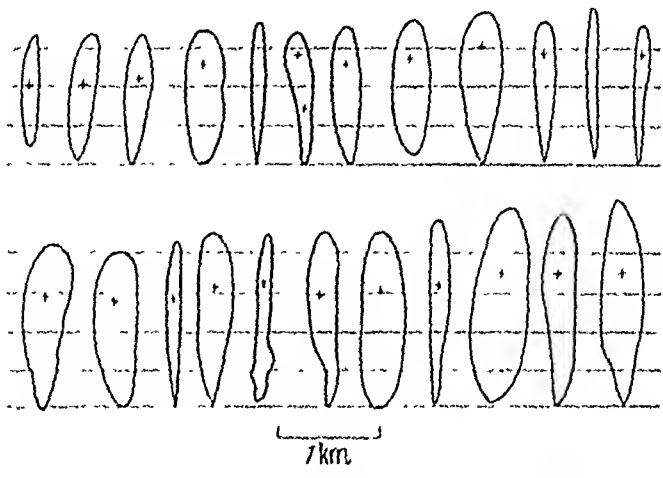

Fig. 189. Outlines of drumlin bases (as adapted from ALDEN[2] by CHORLEY[1]), the crosses indicating summits; Green Bay Glacier, Wisconsin

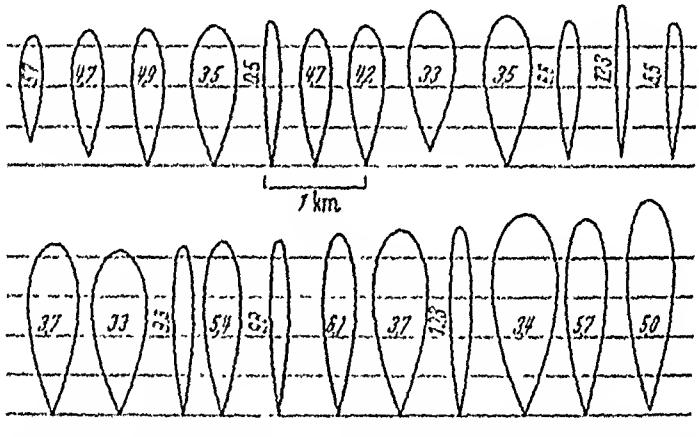

Fig. 190. Lemniscate loops fitted to the drumlins shown in preceding Figure. After CHORLEY[1]

in polar co-ordinates (ρ, Θ):

$$\rho = L\cos(k\,\Theta). \tag{7.26-1}$$

The constant L gives the length of the long axis, k is a measure of the elongation (k is 1 for a circle; for the lemniscate loops shown in Fig. 190, it has the values shown there; the latter were calculated by CHORLEY).

The outcome of the above discussion is that it is probably correct to regard each drumlin as a streamlined body sculptured by moving ice. A reason why the glacier dumps the material in the arrangement represented by a series of drumlins has been given by SMALLEY and UNWIN[3]

1. CHORLEY, R. J.: J. Glaciol. 3, No. 25, 339 (1959).
2. ALDEN, W. C.: U.S. Geol. Surv. Bull. 273, 18 (1905).
3. SMALLEY, I. J., and D. J. UNWIN: J. Glaciol. 7, 377 (1968).

who showed that the drumlin distribution is simply the result of random emplacement.

Finally, it may be assumed that the general bottom drag of glaciers is sufficient to produce the glacier ice-thrust features mentioned in Sec. 1.73.

7.3. Three-Dimensional Movement of Ice

7.31. Theories of Three-Dimensional Ice Movement. Thus far, we have only dealt with the longitudinal movement of glaciers. However, the three-dimensional motion of ice is also of particular geomorphological significance. Thus, one would like to know what happens at the valley wall of a glacier valley, how a glacial cirque is excavated and how ice caps spread at their edges. All these problems are three-dimensional.

In order to describe three-dimensional ice movement, one's first thoughts would be to try to generalize NYE'S theory of plasticity to this case. However, it becomes obvious that one soon ends up in great mathematical difficulties. Unless the geometry is very simple (such as in circular ice caps where the problem, essentially, reduces itself again to a two-dimensional one), no solutions can be obtained on the basis of plasticity theory or a related theory.

Therefore, a different approach has been sought after by MATSCHINSKI[1] who attempted to arrive at a differential equation of ice flow from purely logistic considerations. Thus, MATSCHINSKI postulated that any useful equation must be linear. Secondly, all functions of the co-ordinates must be invariants of co-ordinate transformations. Thirdly, the irreversibility of the ice flow process suggests that only odd-order time-derivatives are permitted. Finally, no space derivatives of a higher order than the second should occur.

The above four conditions suffice to set up an equation of ice flow. Let us denote the vertical co-ordinate of the ice surface by Θ, the position co-ordinates by x and y. Then it is possible to show that the only possible combination of derivatives satisfying the four assumptions is:

$$\frac{\partial \Theta}{\partial t}+\varepsilon \frac{\partial \operatorname{lap} \Theta}{\partial t}=h \operatorname{lap} \Theta+F \tag{7.31-1}$$

where h and ε are constants, and F is a function of t, x and y indicating external conditions.

It will be noted that the above equation is somewhat different from that of FINSTERWALDER (cf. Sec. 7.24) which was used for the discussion of a glacier snout. FINSTERWALDER'S equation is non-linear. However, it

1. MATSCHINSKI, M.: Pub. . 47, 213 (1958).

Stability questions (i.e. the equilibrium size) of ice caps were investigated with[1, 2] and without[3] the presence of a basal water layer; the latter decreases the maximum equilibrium size of such ice caps because of the decrease of the friction at the bed.

7.33. Various Problems. We have already discussed the flow of long glaciers as a two-dimensional problem. In such a discussion, we have of necessity not been able to take the effect of valley walls into account.

NYE[4] has attempted to make an estimate of the effects of the valley walls on the flow of a long glacier. However, he found that there is no satisfactory method to-date to describe a connection between the ice discharge of a real glacier and its bed configuration, let alone the action of a glacier on its sides.

The next topic of interest is the dynamics of more complicated types of ice sheets, such as of piedmont glaciers and cirque glaciers. The physiography of such glaciers has been described in Chap. 1 (cf. Sec. 1.72). In order to study such cases, one might first want to try to apply NYE's theorem (cf. Sec. 7.32). However, it is at once obvious that its two statements are not sufficient to determine the dynamics of piedmont and cirque glaciers.

The only possibility that remains, therefore, is to use MATSCHINSKI's logistic equation, although it is not very satisfactory. Nevertheless, MATSCHINSKI[5] has integrated his equation for the cases in question and obtained rather complicated expressions containing indetermined constants which must presumably be determined from boundary conditions.

It thus does not seem possible to make oneself a picture of what is essentially supposed to happen physically in piedmont and cirque glaciers.

7.34. Crevasses in Ice Sheets. Finally, it is of some interest to investigate the pattern of crevasses in multi-dimensional problems. We have already discussed crevasses in two-dimensional problems where the former of necessity cannot be anything but *transverse* features. Here we shall try to see how the problems discussed earlier will be modified by the presence of an additional dimension.

The problem has been investigated long ago from a general standpoint by HOPKINS[6], but we shall follow here a treatment suggested by NYE[4] which is based upon his plasticity theory of glacial movement.

NYE's theory applies only to a long glacier, but it does take the effects of the valley wall into account. According to NYE's theory of

1. WEERTMAN, J.: J. Geophys. Res. **66**, 3783 (1961).
2. LLIBOUTRY, L. A.: Sci. Jour. **5**, No. 4, 50 (1969).
3. WEERTMAN, J.: J. Glaciol. **6**, 191 (1966).
4. NYE, J. F.: J. Glaciol. **2**, No. 12, 82 (1952).
5. MATSCHINSKI, M.: Pub. Assoc. Hydrol. Sci. **47**, 213 (1958).
6. HOPKINS, W.: Phil. Trans. Roy. Soc. **152**, Pt. II, 677 (1862).

glacier flow (cf. Sec. 7.22), the stress σ_x at the surface of the glacier may be compressive (passive flow) or tensile (active flow). In either case, the theory of plasticity predicts that any *normal* stress σ_s caused by the valley wall will be subject to the following inequality[1]:

$$0 \leq |\sigma_s| < \tfrac{1}{2}|\sigma_x|. \tag{7.34-1}$$

The only shear component at the surface of the glacier is τ_{sx} which is zero in the center and increases (in absolute value) towards the sides. If all these stresses are taken together, one obtains for the surface-lines across which the greatest tensile stress occurs, the lines shown in Fig. 192.

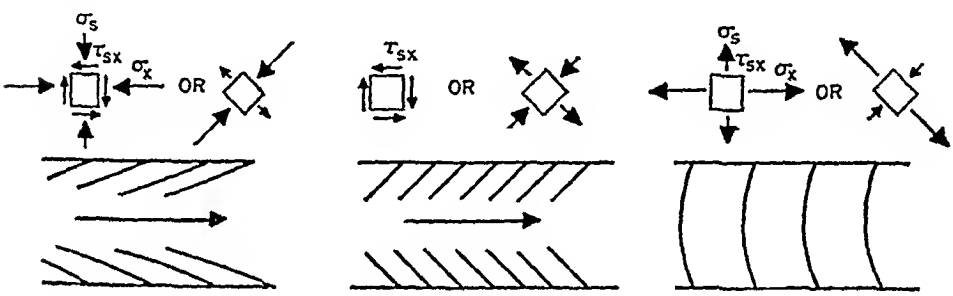

Fig 192. Theoretical positions of crevasses in a glacier for three possible cases. After NYE[2]

The possible stress states at the margin of the glacier are shown in the small diagrams on top of each main drawing. Which stress state is realized, of course, depends on the interaction between the valley wall and the glacier.

7.35. Geomorphological Effects. After having discussed the theory of three-dimensional glacier flow, it remains for us to examine the possibilities by which such flow can explain the glacial effects noted by geomorphologists (see Secs. 1.73 and 1.74). Part of these phenomena (viz. the longitudinal profile of Alpine valleys and the shape of drumlins) has already been explained by the theory of longitudinal glacier flow; here we shall investigate what can be said about the remaining features. These are (i) the transverse profile of glaciated valleys, (ii) glacial cirques, (iii) eskers and (iv) moraines. We shall discuss these features one by one.

(i) *The Transverse Profile of Glaciated Valleys.* Referring the reader to Sec. 1.73, we note that the task is to explain two phenomena: first the existence of a shoulder, and second the U-shape of the central trough. Unfortunately, it must be said that no satisfactory theory of either of

1 See HILL, R. Mathematical Theory of Plasticity, p. 129; Oxford: Clarendon Press 1950.

2. NYE, J. F., J Glaciol. 2, No. 12, 82 (1952).

these phenomena appears to be available. The stresses at the bottom of a flowing ice mass across a transverse profile seem to be quite unknown, and equally so the equilibrium profile of such a flowing ice mass if the *interaction* with the bed is taken into account. From the standpoint of mechanical theory, the transverse profile of an Alpine valley, therefore, remains a complete mystery. We have mentioned in Sec. 1.73 a few geomorphological interpretations of the observed facts, but the latter remain little more than hypotheses until a satisfactory mechanical model can be constructed.

(ii) *Glacial Cirques.* The situation with regard to the theoretical explanation of glacial cirques is somewhat less serious. Whereas the mechanical theory of cirque-shaped glaciers has not yet been satisfactorily established, their erosional action may at least be described qualitatively in terms of NYE's longitudinal glacier motion (see Sec. 7.22). The drainage basin which is being transformed by the glacier represents a highly concave feature. Such concave stretches in glacier flow are the places where, according to NYE, the erosion is a maximum. Hence it should be expected that an existing basin should be subject to maximum erosion and the transformation into a cirque is at least qualitatively understandable. However, it should be remembered that some of this so-called glacial cirques may, in effect, be stress-induced (Sec. 3.34).

(iii) *Eskers.* Little can be said with regard to a satisfactory theory of esker formation. It is possible that eskers are not directly caused by glacier action, but by depositional activity of melt water. Their layered cross-sections would appear to be an indication in this regard.

(iv) *Moraines.* We finally come to a discussion of moraines. The geomorphological interpretation postulating that the latter are débris left after the retreat of a glacier, appears to be substantially correct. The side moraines seem to represent possible stream lines of glacier flow;— as they should.

In conclusion, we may summarize the above discussion by saying that on the whole, the scouring effects of glaciers have been at least qualitatively explained by glacier flow theories. This is not true for the other incidental effects.

It may be noted that many of the difficulties of a theoretical explanation of glacial features arise from difficulties of mathematical analysis. In other disciplines, it is customary under such circumstances to resort to scaled experiments. In the case of glacier flow, this appears to have been tried only with regard to the origin of moraines[1] where a glacier has been represented by clay-mud. It stands to reason that this method could also be applied in connection with other problems of glacier flow.

1. MCCUTCHEN, W. T., and W. F. TANNER: Bull. Geol. Soc. Amer. 70, 1487 (1959).

7.4. Other Niveal Effects

7.41. General Remarks. Finally, we shall discuss the mechanics of some peculiar features which are due to frost action and which may therefore be considered in conjunction with niveal effects: This includes the genesis of pingos (Sec. 7.42), the occurrence of niveal solifluction (Sec. 7.43), ice-included stress features (Sec. 7.44) and the deposition of varves (Sec. 7.45).

There is a variety of theories which have been proposed for an explanation of the occurrence of the phenomena under discussion. Unfortunately, as will be demonstrated below, these theories are only very qualitative and no numerical tests for their predictions seem ever to have been undertaken. The investigation of niveal effects has thus obviously not yet been brought to a close.

7.42. Pingos. Although the physiography of any one pingo appears superficially as very much the same (cf. Sec. 1.75) as that of any other, there are indications that one must, in fact, discern between two genetically different types. This point has been particularly stressed by MÜLLER[1] who published a very extensive study of pingos.

According to MÜLLER, the first pingo type which occurs mainly in Greenland (and hence has been called "Greenland type") is an open ice-water system. Besides an ice lens, the interior of the pingo may contain unfrozen water. Isotopic analyses have yielded the result that the water is neither juvenile nor ancient, but identical to surface water. Therefore, MÜLLER reasoned that pingos of the Greenland type are primarily caused by an artesian effect. The forces active in the genesis of a Greenland type pingo (as envisaged by MÜLLER) are shown in Fig. 193.

The presence of springs in pingos certainly lends some credulity to MÜLLER's artesian hypothesis. However, it is not certain whether the suggested mechanism is thermodynamically sound. Since pingos occur only above permanently frozen ground, and since the melting temperature of ice is lower in a porous system (the soil) than in a large container, an artesian tube containing water cannot exist side by side with frozen ground. Drillings do not seem to have disclosed any water chambers below the ice lens in a pingo, since the water appears to have been found somewhere near the top. The mechanism suggested by MÜLLER, therefore, appears as physically questionable.

The same may be said for other attempts at an explanation of the genesis of Greenland type pingos. SVETOSAROV[2] thought that pingos are caused by the emergence of juvenile water and GUSSOW[3] proposed that

1. MÜLLER, F.: Medd. Grønland 153, No. 3 (1959).
2. SVETOSAROV, I. M.: Probl. Sovet. Geol. 4, No. 10, 119 (1934).
3. GUSSOW, W. C : Bull. Amer. Assoc. Petrol. Geol. 38, 2225 (1954)

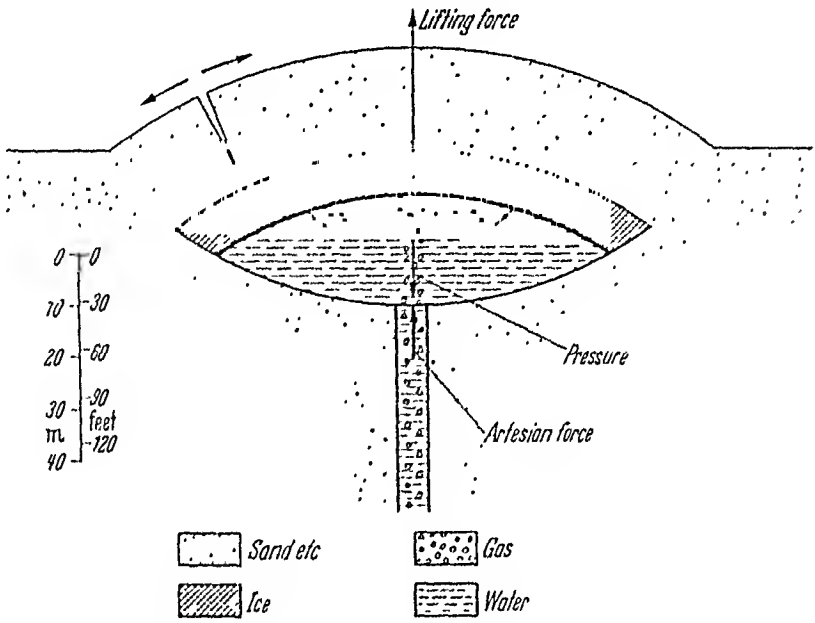

Fig. 193. Mechanism of a Greenland type pingo. After MÜLLER[1]

they are remnants of Pleistocene ice masses. Both these hypotheses do not agree with the observed isotopic composition of water and ice collected from these pingos.

In view of the above remarks, the writer suggests that Greenland type pingos are thermodynamically open systems alright. However, the water oozing out does not necessarily have to come from below the ice lens. The phenomenon can be regarded as analogous to a giant frost boil caused by the mechanism of water freezing in a porous medium (cf. Sec. 3.26). The freezing temperature in a porous system (soil) is lower than in bulk masses of water. Hence, once an ice lens has been started, it will grow by the addition of water which is in thermal equilibrium with the ice in the frozen ground, but which is supercooled as soon as it leaves the porous medium. Since there is a general temperature gradient near the surface by which the temperature (in summer) increases upward, ice will melt at the top of the ice lens. Thus, water in the form of ice, will move upward through the ice lens. If the process is equilibriated over the seasons, then the pingo will retain its size. Otherwise it will grow or shrink so as to achieve an energy balance. The melted water may escape immediately at the top of the pingo or collect in chambers inside the ice (but not below the ice lens) where it may be confined so as to be subject to relatively high pressures which, upon release, may give rise to a superficially artesian phenomenon.

1. MÜLLER, F.: Medd. Grønland **153**, No. 3 (1959).

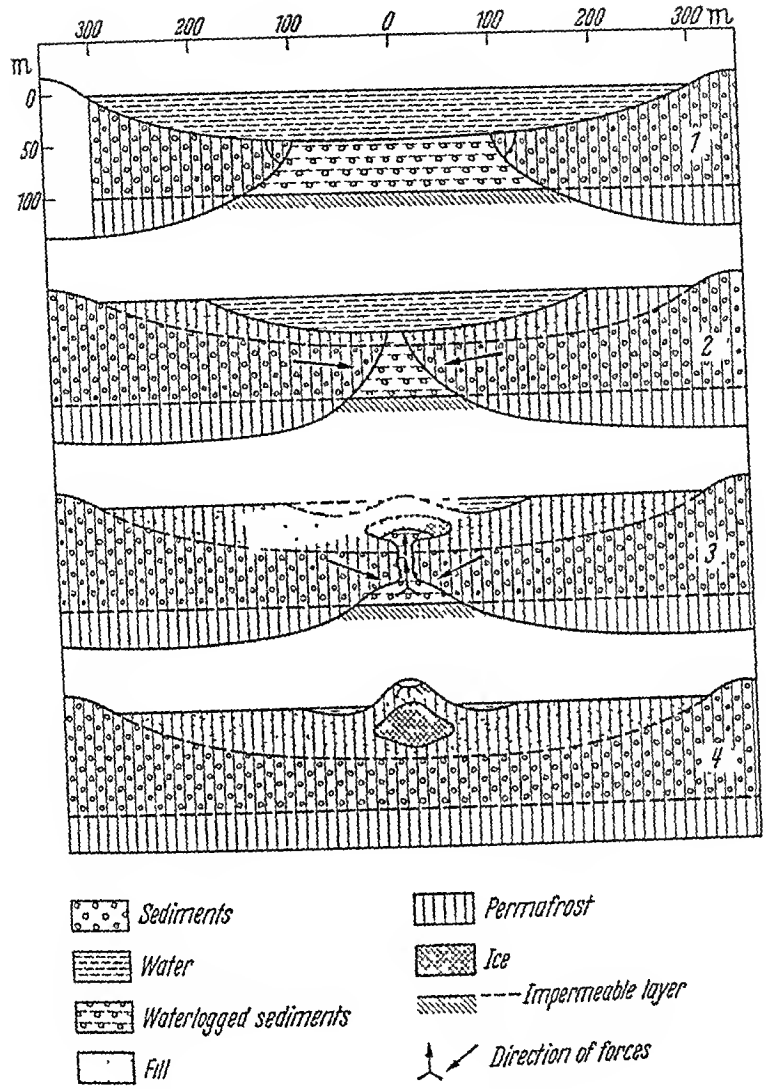

Fig. 194 Development of a Mackenzie type pingo. After MULLER[1]

The second type of pingos observed by MÜLLER[1] has been termed *Mackenzie type* by him. The structure of these pingos (with a central ice lens) is almost identical to that of the Greenland type pingos, but there is evidence that the ice lens was formed at a definite time, up to 28,000 years ago. There is also evidence that the ice was at one time water which contained vegetation. This prompted MÜLLER, who followed ideas suggested earlier by PORSILD[2], to postulate that these pingos developed at places where there was a lake at one time. In general, permafrost cannot

1. MÜLLER, F.: Medd. Grønland **153**, No. 3, 1 (1959).
2 PORSILD, A. E.: Geogr. Rev. 28, No. 1, 46 (1938)

exist below a lake of some 300 m or more in diameter. As silt and vegetation fill in the lake, its diameter decreases to a point where permafrost can exist below, and the lake freezes over. The volume expansion of the freezing water causes a pingo. The general scheme of this type of development is shown in Fig. 194 (after MÜLLER).

The diapirical appearance of pingos is accounted for by the theories outlined above as these theories do represent a kind of diapirism. It is, thus, not necessary to attribute a similar origin to pingos as to better known diapirical structures, such as salt domes.

7.43. Niveal Solifluction. The phenomenological aspects of niveal solifluction were discussed in Sec. 1.75. It is now our task to present what is known about the mechanics of the process.

As was noted earlier, the occurrence of freezing and thawing is essential in niveal solifluction. This will induce *frost heave* in the moving soil (cf. Sec. 3.26) which contributes to the downslope motion. The heaved condition persists into the thawed state of the soil[1]; the ice lenses which have become water, make the slope mobile. The strength reduction which

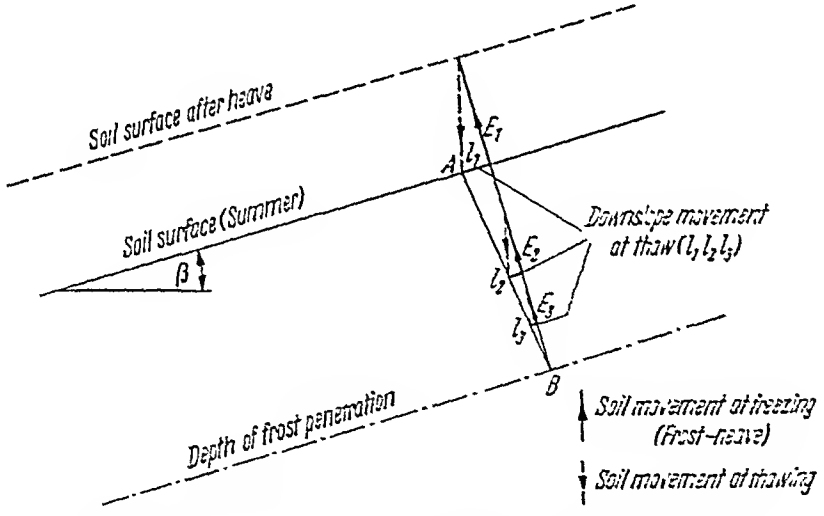

Fig. 195. Frost heave action and solifluction. After WILLIAMS[2]

gives rise to solifluction, is thus mostly caused by the lowering of the cohesion due to frost-heave action. WILLIAMS[2] has envisaged the mechanism of niveal solifluction in a manner as shown in Fig. 195. It may be noted that this mechanism is analogous to that of dry rock creep discussed in Sec. 3.43. Qualitatively it was invoked for the first time, it appears, for the explanation of frost-induced soil creep by DAVISON[3].

1. WILLIAMS, P. J.: Amer. J. Sci. 257, 481 (1959).
2. WILLIAMS, P. J.: Geogr. J. 123, 42 (1957).
3. DAVISON, C. A.: Geolog. Mag (3) 26, 255 (1889).

The line $A-B$ need not necessarily be straight. The increments Δl of downslope movement (cf. Fig. 196) are proportional to the increment of frost heave ΔE and to the tangent of the slope; hence

$$\Delta l = \tan \beta \, \Delta E. \tag{7.43-1}$$

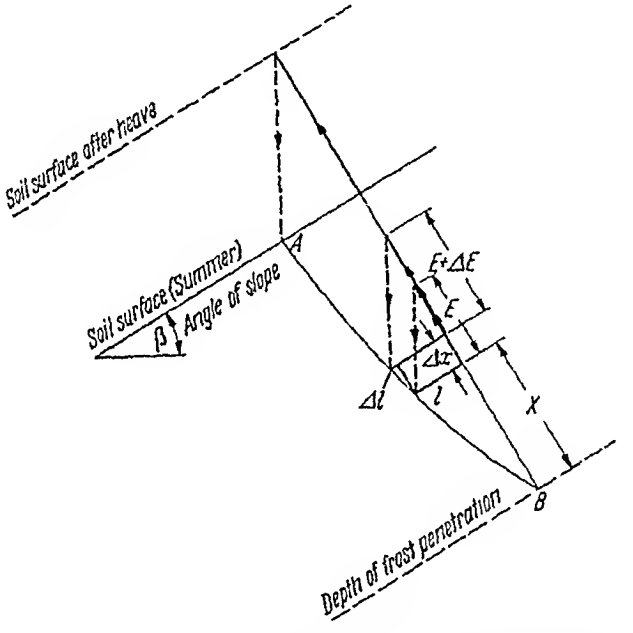

Fig. 196. Details of frost action in solifluction. After WILLIAMS[1]

However, the increment of frost heave ΔE is proportional to the time taken for Δx to freeze times the water flowing in during that time, Thus:

$$\Delta E = f(x) \, \Delta x, \tag{7.43-2}$$

where $f(x)$ is the quotient of water inflow rate over rate of freezing. Hence, by integration

$$l(x) = \tan \beta \int_0^x f(x) \, dx. \tag{7.43-3}$$

This yields the equation of the curve AB. Because of the conservation of mass, $f(x)$ must equal the amount of excess water present in the soil at the level x. It can thus be measured. Hence, the shape of the curve AB can be calculated in any practical case.

A somewhat more elaborate theory of essentially the same model of solifluction has been given by KIRKBY[2].

1. WILLIAMS, P. J.: Geogr. J. 123, 42 (1957).
2. KIRKBY, M. J.: J. Geol. 75, 359 (1967).

The above discussion elucidates somewhat the process of niveal solifluction. However, no comparisons between soil creep rates and frost heave rates seem to have been made.

7.44. Stress-induced Features in Periglacial Areas. In our discussion of physical geomorphology we have mentioned niveal pressure features (see Sec. 1.75). The generally accepted theory of the genesis of these features assumes that a thick permafrost layer existed ahead of the advance of the ice[1]. Upon breaking, parts of this layer were pushed forward by the advancing ice over the permafrost blow. This process produced the ridges.

RUTTEN[1] noted that, for the establishment of the required permafrost layer, the drainage pattern has to be *toward* the advancing ice. Since the drainage in the plains of the United States (as opposed to the drainage in Canada) was southward, away from the ice, this explains the absence of ridges in that country.

Finally, we mentioned in Sec. 1.75 that polygon patterns occur in the ground in periglacial areas. These features have been ascribed to contraction-stress patterns by LEFFINGWELL[2]. This hypothesis was examined from a mechanical standpoint by LACHENBRUCH[3]. Accordingly, small vertical fractures form in the frozen Arctic tundra in the winter owing to thermal contraction of the tundra surface. Then, in the spring, water from the melting snow forms ice wedges in these cracks in the permafrost, giving rise to a cycle that repeats itself year after year. The general physical picture envisaged is shown in Fig. 197.

The mechanical theory of LACHENBRUCH analyzes the mechanics of fracture, the stress before and after the crack formation, and also the multiple fracture patterns in a two-dimensional medium. LACHENBRUCH shows that polygons in patterned ground in permafrost can indeed be explained as contraction-crack polygons formed in many media due to a decrease in volume. In permafrost regions, this contraction is due to cooling in the Arctic winter.

7.45. Varves. We have pointed out (Sec. 1.76) the existence of varves in periglacial seas. It is held that the thickness of a varve is simply representative of the sediment deposited in one year. Varves are thought to be deposited in glacial basins off the edge of the glacier. Since the glaciers have been receding since the conclusion of the last ice age, the distance from the sediment source (i.e. the edge of the glacier) is progressively increasing with time, creating thereby the thickness decrease of varves observed in varve sequences.

1. See RUTTEN, M. G.: Amer. Sci. 258, 293 (1960).
2. LEFFINGWELL, E. DE K.: J. Geol. 23, 635 (1915).
3. LACHENBRUCH, A. H.: Spec. Pap. Geolog. Soc. Amer. No. 70 (1962).

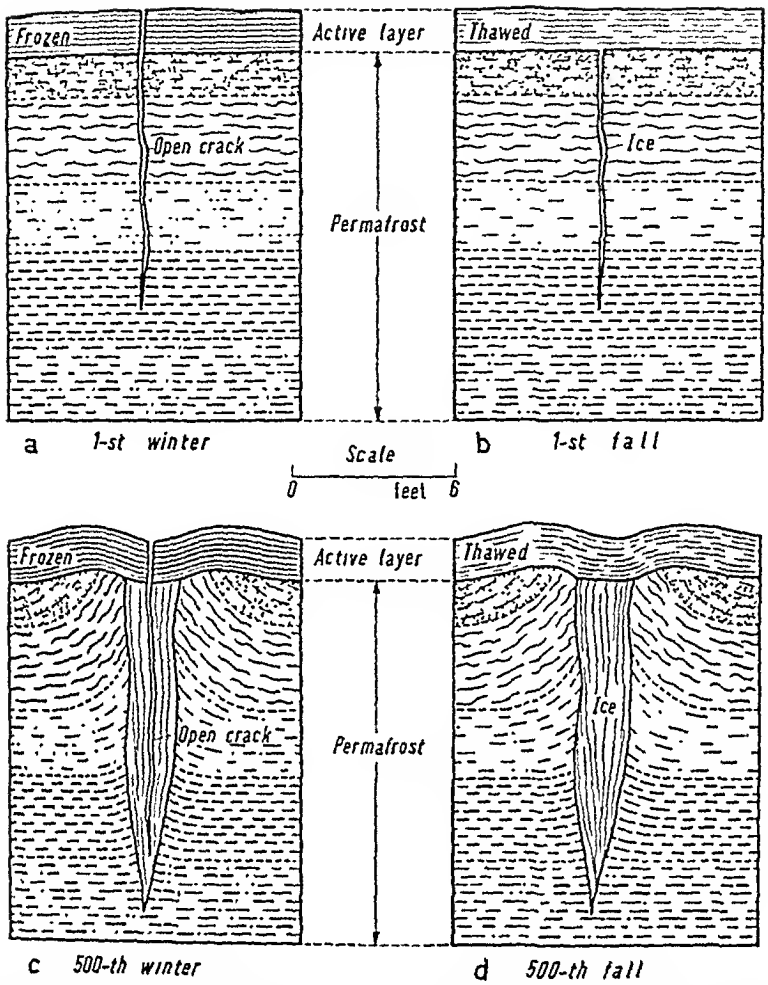

Fig. 197. Schematic representation of the evolution of an ice wedge according to the contraction-crack theory (width of crack exaggerated for illustrative purposes) After LACHENBRUCH[1]

The above qualitative physical model has been put upon a quantitative basis by SCHEIDEGGER[2]. Accordingly, one assumes a basin of constant depth to be filled with water in a turbulent state. The basin, assumed as subject to a plane geometry, may extend to one side into infinity. On the opposite side is a sediment source of constant strength which slowly retreats into the opposite direction with a constant velocity. Within the basin itself there is a current with a constant offshore velocity component carrying water (and therewith sediment) away from the sediment source. This sediment-carrying water is turbulent. It is assumed

1. LACHENBRUCH, A. H.: Spec. Pap. Geolog. Soc. Amer. No. 70 (1962).
2. SCHEIDEGGER, A. E.: Bull. Internat. Assoc. Scient. Hydrol. *10*, No 1, 68 (1965).

that the turbulence is created at the sediment source and that it slowly decays as it is carried along with the current.

The decay laws of turbulence are well known (see Eq. 2.24-2). Then, the sediment-carrying capacity (n particles per unit volume) of turbulent water with mean velocity fluctuation $\overline{u'^2}$ is given by (cf. Eq. 4.52-6 with $\varphi \sim \overline{u'^2}$)

$$n = C_1 e^{-C_2/\overline{u'^2}} \tag{7.45-1}$$

which yields, using (2.24-2) to eliminate u'

$$n = C_1 e^{-C_3 t^m} \tag{7.45-2}$$

where $C_1, C_2, \ldots$ etc. are constants. The rate of sedimentation is the negative derivative of this with regard to t

$$\begin{aligned} s &= C_1 C_3 e^{-C_3 t} && \text{for } m=1 \text{ (initial range)} \\ s &= \tfrac{5}{2} C_1 C_3 t^{\frac{3}{2}} e^{-C_3 t^{\frac{5}{2}}} && \text{for } m=\tfrac{5}{2} \text{ (terminal range).} \end{aligned} \tag{7.45-3}$$

If we remember the assumption that the glacier retreats at a constant speed and that the speed of the offshore current is also constant, the above equations yield directly a quantity proportional to the varve thickness, as a function of time. The corresponding curves, plotted on semilog paper, yield almost straight lines which can be compared with the varve-thickness decrease curves given in Fig. 31 (Sec. 1.76). There is, therefore, a good agreement between theory and observation.

VIII. Theory of Aeolian Features

8.1. The Significance of Wind Action

The present Chapter (VIII) will deal with the theory of the geomorphological action of *wind*. This action is caused by the fact that wind is able to pick up and transport loose particles over very large distances.

There are in essence two modes of transportation of particles by the wind: Some particles may be held in suspension for long periods by the *turbulence of the wind alone*, others have to *return to the ground* at short intervals. Particles which remain suspended in the air for long periods of time are commonly referred to as *dust* particles, the others as *sand* particles.

The two modes of transportation by wind are fundamentally different and it will thus be necessary to treat them separately.

Wind action is particularly important in deserts where a variety of features is caused by it. After studying the physics of particle movement by wind, it will be our endeavor to present the theories of the origin of the various features in question, as they exist to-date.

8.2. The Physics of Sand Movement

8.21. General Remarks. We shall first turn our attention to the motion of *sand* (as contrasted with *dust*). The classical investigations on this subject have been undertaken by BAGNOLD[1] who described them in a monograph. Consequently, the present exposition can be held brief, the reader being referred to BAGNOLD'S excellent book for most details. However, we shall describe (in Sec. 8.24) some effects which were not considered by BAGNOLD and which may have a geomorphological significance: This concerns the creation of static electricity when sand is being acted upon by wind. Otherwise we shall generally follow BAGNOLD'S thoughts (but not his exposition), adding references to newer work wherever feasible.

8.22. Wind Velocity Near the Ground. In order to study the motion of blown sand, it will first of all be necessary to obtain an idea about the

1. BAGNOLD, R. A.: The Physics of Blown Sand and Desert Dunes London: Methuen & Co. 1941 (reprinted 1954).

wind velocity in those regions into which the moving sand is likely to penetrate.

It turns out (from field observations) that any wind velocity which is large enough to start sand grains moving, is such that the wind will be in turbulent motion. Since air and water are simply two *examples* of *fluids*, one would expect that the same velocity distributions laws hold for streaming air as for streaming water. We have deduced earlier (cf. Sec. 4.23) the velocity distribution for water in turbulent motion near a wall: we have shown that in that case, KARMAN'S logarithmic law of velocity distribution holds (cf. Eq. 4.23-6). It stands to reason that the same law applies when air is streaming by a wall in turbulent motion[1]. This supposition has been checked by BAGNOLD in wind-tunnel experiments who found a full confirmation thereof. He writes the law in the following fashion

$$u = 5.75\, u_* \log_{10} \frac{z}{k} \tag{8.22-1}$$

where z is the vertical co-ordinate, k a constant indicative of the surface roughness, and u_* the drag velocity

$$u_* = \sqrt{\frac{\sigma_m}{\rho}}. \tag{8.22-2}$$

Here, σ_m is the bottom drag force and ρ the density of the air. From experimental investigations, one was able to deduce that the constant k is approximately $\frac{1}{30}$ of the diameter of the particles causing the surface roughness.

The theory of flow of turbulent air over the ground is therefore entirely analogous to the theory of flow of turbulent water in a channel.

If the blowing wind is sand-laden, it may be expected that formula (8.22-1) has to be modified since it stands to reason that the sand content will affect the flow behavior of the wind. BAGNOLD shows that, under these conditions, the altered velocity distribution u' can be described as follows

$$u' = 5.75\, u'_* \log_{10} \frac{z}{k'} + u_t \tag{8.22-3}$$

where k' is approximately equal to 0.3 cm for a fine uniform sand and equal to 1 cm for dune sand. Furthermore, u_t is the "impact threshold velocity" whose significance will be described more fully in the next Section (8.23).

1. Cf. SUTTON, O. G.: Micrometeorology. New York: McGraw-Hill Book Co. 1943, also FRENKIEL, F. N., and P. A. SHEPPARD: Atmospheric Diffusion and Air Pollution. New York: Academic Press 1959. A newer review is by ZILITINKEVICH, S. S. et al.: Izv. Akad. Nauk SSSR, Atmos. and Ocean. Phys. 3, No. 3, 297 (1967).

8.23. Grain Movement. Just like the bottom particles in a river, the sand grains acted upon by wind are subject to essentially two forces: first to the gravity force and second to the drag force caused by the wind. In order to start the sand grains moving, the drag exerted by the wind must achieve a critical value. Corresponding to Eq. (4.43-2) for water, the fundamental equation of the drag theory for the sand grains may be written as follows

$$v_{cr}=A\sqrt{\frac{\delta-\rho}{\rho}g\,d} \tag{8.23-1}$$

where δ is the density of the sand (2.65 g cm^{-3} for quartz), ρ the density of air, g the gravity acceleration, and d the diameter of the grains. The quantity A is a constant approximately equal to 0.1. Furthermore, v_{cr} is the critical drag velocity which will just start the grains moving. According to BAGNOLD, the above Eq. (8.23-1) holds for sand grains in air exceeding 0.2 mm diameter. The deduction of Eq. (8.23-1) can be performed in the same fashion as the deduction of the corresponding equation for the movement of bottom particles in rivers (cf. Eq. 4.43-2). The above equation can be made valid for sand grains with a diameter smaller than 0.2 mm provided the "constant" A is adjusted accordingly: the smaller the grains, the larger the constant.

Once grain movement is started by the wind, it can be maintained by a wind velocity below the critical value which would be necessary to dislodge resting particles. This is due to the fact that sand grains move by *saltation* caused by impact. When grains strike the ground, their momentum may be sufficient to start other particles moving. Thus, in addition to a critical drag velocity of the wind, there is also an impact threshold velocity u_t which is sufficient to keep the above-mentioned "impact" mechanism operative indefinitely. Upon being struck, a grain may rise from the ground at any angle, usually almost vertically if it is to rise to any height at all. Its terminal forward velocity will be close to that of the wind v_w, its terminal downward velocity will be close to its settling velocity (cf. Sec. 4.42) v_s. Hence, the angle β by which it will strike the ground is

$$\tan\beta=\frac{v_s}{v_w}. \tag{8.23-2}$$

Typical grain paths (after BAGNOLD) are shown in Fig. 198.

For the impact threshold velocity u_t, BAGNOLD gives the following equation

$$u_t=5.75\,A\sqrt{\frac{\delta-\rho}{\rho}g\,d}\log_{10}\frac{k'}{k} \tag{8.23-3}$$

where $A=0.08$. This equation has been obtained from the drag equation (8.23-1); inserting the latter (v_{cr} denoting a shear velocity) into (8.22-1)

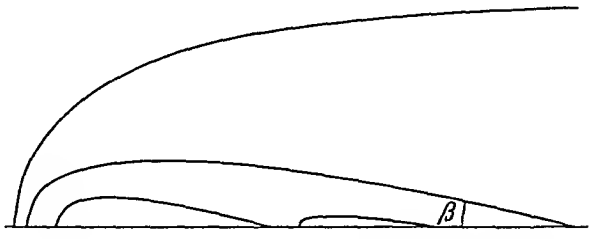

Fig. 198. Typical grain paths. After BAGNOLD[1]

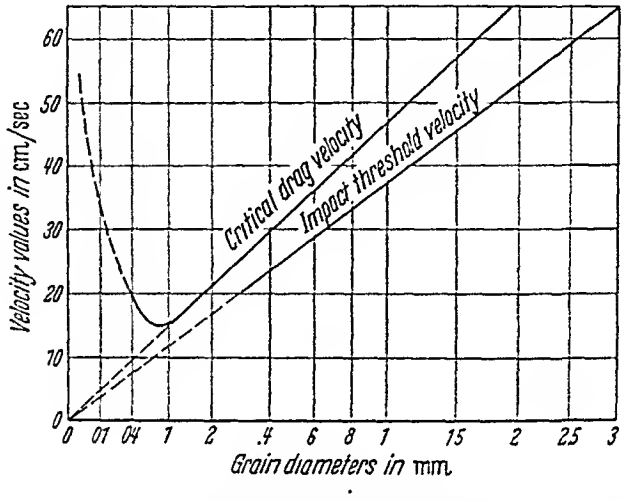

Fig. 199. Relation between critical drag velocity and impact threshold velocity. After BAGNOLD[1]

and calculating the velocity for $z=k'$ yields an equation for the impact threshold velocity. In other words, k' is that height from which on downward the velocity no longer changes if the impact mechanism is fully developed. It should be noted however, that k' is, in fact, a parameter which has been adjusted *a posteriori* so that the above equations become self-consistent. The relation between v_{cr} and u_t are shown in Fig. 199 (after BAGNOLD) which also takes account of the change of the coefficient A for small grain sizes mentioned earlier.

In addition to saltation, another mechanism of sand movement may also occur. This has been called "*reptation*" or "*surface creep*". This mechanism refers to grains being pushed along the surface by the impact of the saltating grains; the grains in reptation never actually leave the surface. BAGNOLD notes that about one-quarter of the grains move in reptation, the rest in saltation.

It remains to relate the rate of sand movement to the wind velocity. BAGNOLD does this by assuming that each grain moving in saltation extracts all of its maximum forward momentum from the air. Thus, the

1. BAGNOLD, R. A.: The Physics of Blown Sand and Desert Dunes. London: Methuen & Co. 1941.

loss of momentum from the air to move a sand mass q_s per unit time and width is $q_s v$, where v is the velocity attained by the grains. The loss of momentum is distributed over the length l where l is the length of a saltation jump so that the loss of momentum per unit time and area equals $q_s v/l$. However, this quantity must be equal to the boundary stress σ_m; hence

$$\sigma_m = q_s \frac{v}{l}. \tag{8.23-4}$$

Using (8.22-2), this yields

$$\rho u_*^2 = q_s \frac{v}{l}. \tag{8.23-5}$$

BAGNOLD now makes the arbitrary assumption that

$$l/v = B u_*/g$$

where B is a constant which depends on the surface. It then follows

$$q_s = \frac{B}{g} \rho u_*^3. \tag{8.23-6}$$

The formula can be modified by writing u'_* (corresponding to 8.22-3 embodying the reaction of the sand-load onto the wind velocity) instead of u_*. The constant B can be adjusted in such a manner as to express that only $\frac{3}{4}$ of the sand are transported in saltation, the rest in reptation. Since reptation and saltation are proportional to each other, a formula of the type of (8.23-6) can be written down to express the *total* sand movement.

A slight modification of BAGNOLD'S formula was given by KAWAMURA[1] who wrote

$$q_s = \frac{C}{g} \rho (u_* - u_{*t})(u_* + u_{*t})^2 \tag{8.23-7}$$

where u_{*t} is the threshold shear velocity. The two formulas, evidently, do not differ much from each other.

8.24. Electrical Effects. In addition to the physical phenomena connected with the motion of blown sand, which have already been discussed above, there is evidence[2, 3] that electrical effects may also occur. A significant set of experiments has been reported by GILL[4] who claims that, when sand grains are rubbing against one another, the smallest particles become positively charged and the larger ones negatively charged. GILL claims that the actual sand grains in a sand storm are always negatively charged; the positive charges are carried in the dust ahead of and above the sand.

1. KAWAMURA, R.: Rept. Inst. Sci. Technol., Univ. Tokyo 5, Nos 3/4 (1951).
2. BONING, P.: Z. tech. Phys. 8, 385 (1927).
3. BEAVERS, A. N.: Science 126, 1285 (1957).
4. GILL, E. W. B.: Nature (Lond.) 162, 568 (1948).

GILL's experiments show that a sand cloud may become charged which explains the thunder and lightening that is often observed in dust and sand storms. GILL also mentioned the peculiar behavior of radio antennas during such storms.

Another set of experiments has been carried out by WALTER[1-3] who also showed that electrical effects may occur during sand storms. However, WALTER's conclusions have opposite signs for the charges involved as compared with those of GILL, inasmuch as WALTER's experiments seem to indicate that the *small* particles, carried ahead of a sand storm, are *negatively* charged and that the *sand* itself is *positively* charged. From statements in the literature alone, it is not possible to resolve this discrepancy.

WALTER also indicated that the electrical effects may affect the mechanical behavior of sand grains. Accordingly, at the beginning of a sand storm, the surface of a dune becomes negatively charged. When the positively charged sand grains arrive, certain grains will be entrapped by the negative charges which would not be entrapped otherwise, – until the negative surface charge is neutralized. This may lead to a layering of dunes. Similar geometrical effects in dunes have been ascribed to electrical effects also by GABRIEL[4].

8.3. Geomorphological Effects of Blown Sand

8.31. Outline of Sand Action. Our task is now to apply the basic physics of sand movement to an explanation of the various desert features described in Sec. 1.82.

In order to do this, we shall have to analyse first the distribution of sand concentration with height above the ground in a sand storm. This will yield a means to explain the grading of grain size distribution in some desert features. After these preliminaries have been dealt with, it will be possible to give an explanation for some of the small-scale (ripples) and large scale (dunes) desert features.

Finally, we shall give a brief description of the theory of corrasive action of blown desert sand as far as this is possible with our present-day knowledge.

8.32. Distribution of Sand Concentration in a Storm. In a sand storm, grains driven by the wind rarely ascend higher than 1 m above the ground.

1. WALTER, W.: Dünenstudien im Schwanheimer Wald bei Frankfurt. Heft 28 der Rhein-Mainischen Forschungen, Frankfurt, 1950.

2 WALTER, W.: Rev. Géomorphol. Dynamique **2**, No. 6, 242 (1951).

3 WALTER, W.: Neue morphologisch-physikalische Erkenntnisse über Flugsand und Dunen. Heft 31 der Rhein-Mainischen Forschungen, Frankfurt, 1951.

4. GABRIEL, A.: Mitt. Österr. Geogr. Ges **107**, No 3, 125 (1965).

The average height is generally much less, of the order of 10 or 20 cm. The top of the sand cloud appears to have a rather sharp edge.

One would like to explain the distribution of sand concentration with height above the ground in terms of the physics of grain movement discussed in Sec. 8.23. Unfortunately, no complete theory of the concentration distributions seems to be available, and it is only possible to explain *some* of the features that are being observed.

Above all, there is the occurrence of the sharp edge of the sand cloud which can be explained by the fact that sand grains travelling in a wind of velocity v, will reach a terminal velocity equal to c

$$c=\sqrt{v^2+w^2} \tag{8.32-1}$$

where w is the terminal settling velocity in question. Thus, the velocity by which a sand grain strikes the ground on its path is c. If it bounces off the ground, the maximum height it can reach is obviously attained if it leaves the ground in a vertical direction. The maximum initial velocity will be equal to c if the impact is completely elastic. Thus, sand grains (of a given size) can only reach a finite maximum height in a sand storm; this explains the existence of a sharp upper surface of a sand cloud. The exact height of this upper surface depends on the terminal falling velocity of the grains, on the wind velocity and also on the air resistance offered to the grains bouncing upwards. Numerical checks seem to give values for the height reached by the sand grains which are in reasonable agreement with that observed in sand storms. These numerical checks are empirical because the air resistance of sand grains cannot be determined mathematically. The procedure is thus one of taking sand grains of a certain size and actually measuring the height attained (or else measuring the resistance encountered at various speeds and integrating) if they are shot upward into the air with an initial velocity c.

The above discussion can be expanded somewhat if a more detailed analysis is made of the saltating motion of the single grains.

The path of a grain leaving the ground with velocity c at a certain angle can be calculated approximately by the use of semi-empirical relationships. BAGNOLD[1] writes that the air resistance p to a grain travelling with the velocity u relative to the air is given by

$$p=C\,\tfrac{1}{2}\rho\,a\,u^2 \tag{8.32-2}$$

where ρ is the density of the air and a the cross-sectional area of the grain. Unfortunately, C depends on the Reynolds number Re and thus on the velocity u. Tables of $C(Re)$ are available.

1. BAGNOLD, R. A.: The Physics of Blown Sand and Desert Dunes. London: Methuen & Co. 1941.

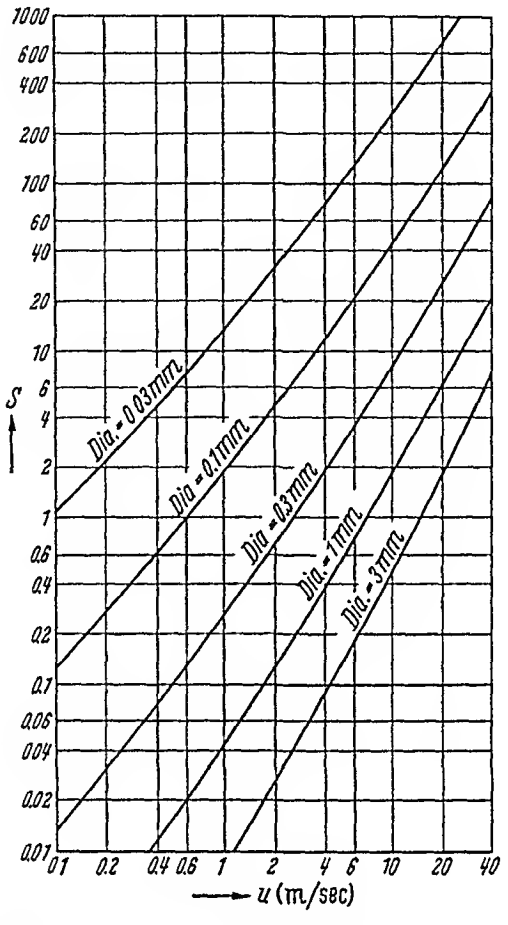

Fig 200. Susceptibility curves for the entrainment of sand. After BAGNOLD[1]

It is convenient to introduce the *susceptibility* S which is defined as the ratio of the air resistance p to the gravity force

$$S=\frac{p}{m\,g}. \tag{8.32-3}$$

Eq. (8.32-3) and empirical values of $C(Re)$ have been used by BAGNOLD to construct susceptibility diagrams. An example is shown in Fig. 200 (after BAGNOLD[1]).

Using the susceptibility values, it is possible to calculate the path of a grain. At each instant of its trajectory, the acceleration is known: that due to gravity is g in a downward direction, that due to the air drag is gS parallel to the tangent of the trajectory in a co-ordinate system moving with the wind. The path, thus, can be computed by numerical integration.

1. BAGNOLD, R. A.: The Physics of Blown Sand and Desert Dunes. London: Methuen & Co. 1941.

From a series of such paths it is, in principle, possible to calculate the distribution of concentration of sand as a function of height above ground. If it be assumed that many grains are leaving the ground at a certain angle, say α, then the total time percentage spent in any height interval (say $y, y+dy$) is proportional to the concentration of these grains. If the calculation be repeated for all possible angles α (varying from 0 to 180 degrees), assuming that these angles are evenly and randomly attained by the grains, and averaging the results, one ought to obtain a theoretical grain density distribution. Although the calculation could be made in principle, this does not seem to have been carried out owing to the large amount of computation involved.

8.33. Grading of Grain Size Distribution. It stands to reason that the prevailing wind strength will have an effect upon the grain size distribution on the surface of a sandy area. Unfortunately, it has not been possible to-date to devise an exact analytical theory for determining the grain size distribution that is to be expected in a given area under the prevailing climatic conditions. It has only been possible to make more or less qualitative statements regarding the general processes that are at work.

Thus, according to BAGNOLD[1], during the evolution of a sand storm, there is a definite sequence (or "cycle") of the events which are taking place. As the wind increases at the beginning of a storm, the fine particles are picked up. This leaves a certain surface roughness of the ground. TRIKALINOS[2] referred to a surface in such a state as being in a "state of flocculation". In a wind of steady strength, the intensity of sand flow increases downward until equilibrium is reached. This means that grains can be picked up only from a limited area. At a given wind strength, grains only up to a certain size can be picked up as was shown in the discussion of Sec. 8.23. Thus, the area from which sand is removed moves continually downwind.

At the end of the cycle the sand picked up by the wind will have to be deposited somewhere. If this occurs due to the wind losing its strength, one speaks of *true sedimentation:* the falling grains have no longer the strength to keep up their saltating motion. There are, however, other possibilities by which deposition can take place. One of them is *accretion* which is due to the surface becoming so irregular that the local wind strength in the lee of the irregularities is too small to carry the grains forward. This causes obstacles to grow larger by the accretion of sand

1. BAGNOLD, R. A.: The Physics of Blown Sand and Desert Dunes. London: Methuen & Co. 1941.

2. TRIKALINOS, J.: Peterm. Geogr. Mitt. 74, No. 9–10, 226 (1928).

thereto. During accretion, the grains may creep along the surface after impact until they find a quiet hollow in which to come to rest.

The final mode of deposition is by *encroachment* which is a large-scale version of accretion. It is connected with large-scale discontinuities in the surface, such as steps. A step encroaches downwind because grains are sheltered in its lee from aerial entrainment.

The validity of the above general and qualitative statements (as noted above, a more accurate theory does not exist) has been checked experimentally by BAGNOLD[1] who made observations of the grading changes (i.e. changes of grain size distribution) of various sands under a variety of conditions. It appears that the observed grading changes conform well with those expected. For the details of the experiments, the reader is referred to BAGNOLD'S[1] book.

8.34. Surface Ripples. As with the grain size distribution curves of desert sand, no analytical theory exists which could claim to explain the existence of *sand ripples* adequately. As was noted earlier (cf. Sec. 1.82), sand ripples are distinguished from larger features not only by their size, but also by the fact that in ripples the grading of the sand is such that the coarsest material is found at the crests, the finer material in the throughs. In larger desert features the reverse is true.

A good early review of the various attempts that have been made at achieving an explanation of the existence of desert sand ripples has been given by TRIKALINOS[2]. BAGNOLD[1] in his book has, in fact, little to add to TRIKALINOS' article.

The earliest attempts at an explanation of ripples, due to DARWIN[3] and CORNISH[4], assumed that the mechanism is analogous to that responsible for the formation of ripples in a river bed. Accordingly, some mechanism involving resonant turbulence or a "traffic jam" (cf. Sec. 4.62) may be invoked. However, although experiments involving fluvial ripples and wind ripples yield the result that the two phenomena are superficially similar, it turns out that there is a fundamental difference between them: In wind ripples the grains are sorted with regard to size, in fluvial ripples this is not the case. Therefore, there seems to be a fundamental difference between the two kinds of ripples.

Other research workers (BASCHIN[5], SOLGER[6]) attempting an explanation of sand ripples (due to wind) have assumed that there is a fundamen-

1. BAGNOLD, R. A.: The Physics of Blown Sand and Desert Dunes. London: Methuen & Co. 1941.
2. TRIKALINOS, J.: Peterm. Geogr. Mitt. **74**, No. 9/10, 266 (1928).
3. DARWIN, G. H.: Proc. Roy. Soc. A **34**, 18 (1884).
4. CORNISH, V.: Geogr. J. (Lond.) **9**, 278 (1897); **13**, 624 (1899).
5. BASCHIN, O.: Z. Ges. Erdk. (Berl.) **34**, 408 (1899).
6. SOLGER, F.: Forsch. Z dtsch. Landes- u. Volksk. **19**, No. 1, 1 (1910).

tal resemblance between the rippling of a water surface and the rippling of a sand surface by wind. However, it can again be shown that this resemblance is merely superficial and cannot be used as basis for an explanation of the phenomenon of sand ripples. If a very uniform sand is taken, no sand ripples will form although, if the phenomenon were analogous to the creation of water waves, this should be the case. An attempt by EXNER[1] to treat the origin of ripples as an instability phenomenon in a layered fluid in which the density increases downward, suffers from the same deficiency as the attempts by BASCHIN and SOLGER.

It remains to try to explain the formation of desert ripples by assuming that they are a phenomenon which is truly due to the differential movability of grains of various sizes. This is an assumption which has been advanced by TRIKALINOS. It was later also maintained, independently of TRIKALINOS (as it appears) by BAGNOLD. Thus, ripples can form only if there is a spread in grain sizes in the sand. Ripples are ephemeral phenomena which change their shape, size and orientation with the prevailing wind direction. Unfortunately, as noted at the beginning of this Section, no quantitative theory based upon the above hypothesis is available as of yet. Its qualitative aspects, however, have been confirmed by observations in wind tunnels and deserts.

8.35. Large Scale Effects. We now turn our attention to the large-scale geomorphological effects caused by the motion of desert sand. In this connection, it is particularly the phenomenon of wandering *dunes* which captures one's imagination. However, in order to explain this phenomenon, it will first of all be necessary to have a close look at the mechanism of deposition of sand under conditions in which the direction and the strength of the wind vary. This will yield a possibility of explaining the two types of dunes (barchan dunes and seif dunes; cf. Sec. 1.82) which have been observed in nature. Finally, the slip face on a barchan dune will be discussed. Most of the pertinent investigations into the mechanism of formation of dunes have been undertaken by BAGNOLD[2] who gives an extensive description thereof in his book.

Starting with the mechanism of sand deposition we note that the intensity q of sand flow was given earlier (cf. 8.23-6) as equal to

$$q = B \frac{\rho}{g} u_*^3 \tag{8.35-1}$$

where B is a constant which depends on the surface, ρ is the density of the air, g is the gravity acceleration and u_* is the drag velocity. If for

1 EXNER, F. M.. Geografiska Annaler 9, 80 (1927).

2 BAGNOLD, R. A.. The Physics of Blown Sand and Desert Dunes. London: Methuen & Co. 1941.

some reason on a coarse, pebbly (with sand between the pebbles) surface a sand patch has been formed, the constant B will have a value B_1 on the coarse surface and B_2 on the sand patch with

$$B_1 > B_2. \tag{8.35-2}$$

This yields the result that deposition must take place over the sand patch at a rate q_d equal to

$$q_d = q_1 - q_2 = (B_1 - B_2)\frac{\rho}{g} u_*^3. \tag{8.35-3}$$

This indicates that a sand patch, once it has been started, should grow by increasing its height, i.e. it will tend to form a dune.

In the formation of sand accumulations, one must distinguish between winds of various strengths. A "gentle" wind will be able to entrain particles from the fine-sand surface, but not from the coarse (pebbly) surface. A "strong" wind will be above the threshold velocity for both types of surfaces. It is the "strong" winds which tend to build up dunes, the "gentle" winds have the opposite effect.

Generally, winds are constant neither in strength nor in direction. Designating the azimuth of the wind (with regard to North) by Θ, the total mass flow dm per unit area at an observation point during the time dt is (setting $B\rho/g = b$)

$$dm_N = -b\, u_*^3 \cos\Theta\, dt, \tag{8.35-4}$$

$$dm_E = -b\, u_*^3 \sin\Theta\, dt \tag{8.35-5}$$

where the suffixes N and E stand for the North and East component, respectively. Integrated over time for a long period T this yields

$$M_N = \int_0^T dm_N = -b \int_0^T u_*^3 \cos\Theta\, dt, \tag{8.35-6}$$

$$M_E = \int_0^T dm_E = -b \int_0^T u_*^3 \sin\Theta\, dt. \tag{8.35-7}$$

The mean rate Q of sand flow over a long period is then

$$Q_N = M_N/T, \tag{8.35-8}$$

$$Q_E = M_E/T, \tag{8.35-9}$$

$$Q = \sqrt{M_N^2 + M_E^2}/T. \tag{8.35-10}$$

The mean direction $\bar{\Theta}$ of sand flow is given by

$$\bar{\Theta} = \arctan\frac{M_E}{M_N}. \tag{8.35-11}$$

It is convenient to separate the total sand flow into flow caused by gentle winds $Q^{(g)}$ and flow caused by strong winds $Q^{(s)}$ since the effects of the two wind types are somewhat different. It then appears as logical to hypothesize (BAGNOLD[1]) that longitudinal (or seif) dunes occur if the directions of $Q^{(s)}$ and $Q^{(g)}$ differ, and that barchan dunes occur if the directions of $Q^{(s)}$ and $Q^{(g)}$ nearly coincide. In this connection, however, the terms "gentle" and "strong" refer to a surface studded with dunes: a gentle wind is one whose strength is such that the corresponding intensity of sand movement is less than that required to give the surface an equivalent roughness equal to the actual roughness of the surrounding

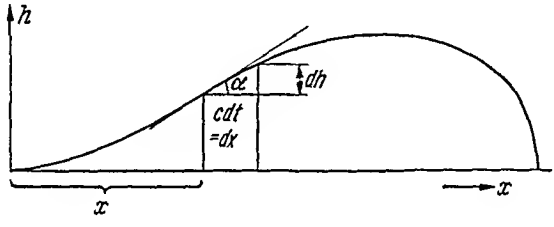

Fig. 201. Cross section of a dune

area. In a "strong" wind the reverse is true. The hypothesis regarding dune shapes and wind direction enounced above cannot be proven mathematically. One can convince himself only qualitatively that it is reasonable as will be seen from the arguments that follow below.

Turing first to the longitudinal profile of a dune, we note that its leeward side is generally steeper than its windward side. If a dune is progressing downwind with a velocity c without changing its shape, the horizontal component of the sand removal at any point must exactly correspond to the velocity c, which yields

$$\frac{dQ}{\rho_{BS}} = dV = c\,dt\,dh \tag{8.35-12}$$

where dQ is the mass (and dV the volume) per unit width of sand removed during the time dt, ρ_{BS} is the bulk density of the sand and dh is the height increase of the original dune corresponding to a shift by the distance $dx = c\,dt$ at the bottom (cf. Fig. 201). Hence the rate of sand removal per unit time (and width) must be

$$dq = \frac{dQ}{dt} = c\,\rho_{BS}\,dh \tag{8.35-13}$$

1. BAGNOLD, R. A.: The Physics of Blown Sand and Desert Dunes. London: Methuen & Co. 1941.

or

$$\frac{dq}{dx}=c\,\rho_{BS}\frac{dh}{dx}=c\,\rho_{BS}\tan\alpha. \tag{8.35-14}$$

If the leeward side of a dune becomes too steep, it will collapse and form a *slip face* corresponding to the angle of repose (cf. Sec. 3.31) for sand. All the sand passing over the rim of the slip face will contribute to its advance. If the rate of sand movement (per unit width) over the rim of the slip face be given by Q, and the slip face have the height h, we have from (8.35-13) (note $dh=h$)

$$c=\frac{Q}{\rho_{BS}\,h}. \tag{8.35-15}$$

If the above consideration be applied to a circular mound of sand which has a slip surface at the leeward side, it becomes obvious that, in a cross-wind section, the height of the slip face must decrease from a maximum at the middle to near zero at the extremities. If the sand flow Q is nearly the same across the dune, it follows immediately (from Eq. 8.35-15) that the extremities must advance more rapidly than the center. Presumably, an equilibrium is reached if the extremities advance so far into a region sheltered by the rest of the dune so that the sand flow Q is reduced to such an extent that the whole dune proceeds at equal speed. This at once explains the crescentic shape of a barchan dune. The explanation holds if the wind blows predominantly always from the same direction.

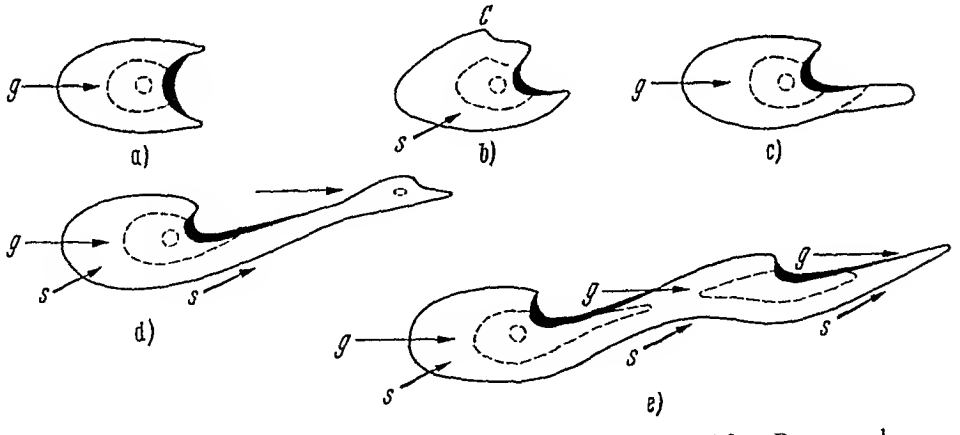

Fig 202 Transition of a barchan dune into a seif dune. After BAGNOLD[1]

If the wind is not unidirectional, it stands to reason that the barchan dune will develop into a seif dune. The procedure is illustrated in Fig. 202 (after BAGNOLD) where g denotes the direction of gentle winds and s the direction of strong winds. The argument is entirely qualitative; no

1. BAGNOLD, R. A.: The Physics of Blown Sand Desert Dunes. London: Methuen & Co. 1941.

exact mathematical theory can be given of the development. It has, in fact, been questioned by VERSTAPPEN[1] who assumed seif dunes to be due to different earlier climatic conditions.

8.36. Corrasive Action of Sand. We have noted on Sec. 1.82 that blown sand may have a pronounced corrasive action upon rocks which happen to rise above the general level in a desert. In this instance the sand attacks the rocks directly in a manner which is similar to the action of a sandblasting apparatus. It is known that weird, pillar- or mushroom-like structures may be the result of the corrasion caused by the blown sand.

Because of the distribution of the sand concentration in a sand storm (discussed in Sec. 8.32), which indicates that more sand is transported near the bottom than higher up, the corrasion of desert features is more pronounced at the base than at the top. This explains the mushroom-shaped rocks that have been observed in deserts.

Unfortunately, no calculations seem to exist which would endeavor to determine, by analytical means, the corrasive effect of blown sand upon desert features and the evolution of the shape of the latter.

Aeolian corrasion is also effective with regard to the grains themselves which constitute the sand. Experimental investigations of this effect have been made by KUENEN[2] who was able to show that aeolian abrasion of sand is far more effective than the aqueous abrasion of pebbles (for the latter, see Sec. 4.75). As in aqueous abrasion, there is also a lower limit for aeolian abrasion below which aeolian corrasion ceases to be effective. This limit, however, is much smaller than in aqueous abrasion; for aeolian abrasion it has been shown to occur at grain diameters of about 0.05 mm. It stands to reason that grains below that size move in suspension as "dust".

8.4. Physics of Dust Movement

8.41. Basic Principles. Dust particles, by definition, are so fine that their transport in the air occurs by *suspension.*

Natural dust is very similar to many man-made pollutants and therefore the movement of such particles has been studied fairly extensively by sanitary engineers[3–5].

---

1 VERSTAPPEN, H · Z. Geomorph 12, 200 (1968)

2 KUENEN, P. H.: J. Geol. 68, 427 (1960).

3 MAGILL, P. L., et al.: Air Pollution Handbook, New York: McGraw-Hill Book Co. 1956

4. FRENKIEL, F N., and P A. SHEPPARD (ed.): Atmospheric Diffusion and Air Pollution (Adv in Geophysics, Vol. 6). New York: Academic Press 1959.

5. MCCABE, L (ed): Air Pollution. New York· McGraw-Hill Book Co. 1952.

The chief phenomenon influencing the movement of dust is that of atmospheric diffusion. We shall therefore first discuss the theory of atmospheric diffusion and then apply the latter to the problem of dust movement.

8.42. Theory of Atmospheric Diffusion. We shall first turn our attention to the general theory of atmospheric diffusion. A good review of this subject has, for instance, been given by MONIN[1]. Accordingly, diffusion is a phenomenon which, in the lower layers of the Earth at least, can be attributed to *turbulence*. Simply using the empirical fact of the existence of atmospheric diffusion, one can then, for purely heuristic reasons, write down the following diffusivity equation for the movement of a "dust" cloud:

$$\frac{\partial c}{\partial t}+u\frac{\partial c}{\partial x}=\frac{\partial}{\partial x}K_x\frac{\partial c}{\partial x}+\frac{\partial}{\partial y}K_y\frac{\partial c}{\partial y}+\frac{\partial}{\partial z}K_z\frac{\partial c}{\partial z}. \qquad (8.42\text{-}1)$$

Here, x, y, z, are Cartesian co-ordinates (z is vertical), u is the wind-velocity, assumed as parallel to the x-direction, K_x, K_y and K_z are empirical diffusion coefficients and c is the dust concentration. The diffusivity equation (8.42-1) can be justified theoretically by the existence of eddy diffusion in turbulent flow (cf. Sec. 2.22). It is assumed that the dust particles are so small that their motion is identical to that of the surrounding microscopic elemental volumes of air. The diffusivity equation as written above does not allow for the gravitional settling of the dust particles. If the latter is also to be taken into account, a term $-w(\partial c/\partial z)$ should be added to the left hand side, where w is the settling velocity.

The diffusion coefficients K_x, K_y, K_z are not constant. The term containing K_x is usually neglected in comparison with $u\,\partial c/\partial x$. The values of the other coefficients depend on the turbulence of the air. For further investigations, we shall use the Karman law for the turbulence in the air near the ground (cf. 8.22-1 or 4.23-6) in the following form:

$$\frac{u(z)}{u_*}=\frac{1}{k}\,\text{lognat}\,\frac{z}{z_0} \qquad (8.42\text{-}2)$$

where u_* is the usual shear velocity given by (8.22-2) and z_0 is a constant. We now introduce the assumption that, near the Earth's surface, the shear stress is independent of height; we have then:

$$\sigma(z)=\sigma_m. \qquad (8.42\text{-}3)$$

1. MONIN, A. S.: Advanc. Geophys. 6, 29 (1959).

where $u(z)$ is given by (8.42-2) and $K_z(z)$ by (8.42-10). The boundary conditions for a line source are

$$\left.\begin{aligned} c&=0 && \text{for } x=\infty,\ z=0\\ K_z\frac{\partial c}{\partial z}&=0 && \text{for } z=0,\ x>0\\ c&=\infty && \text{for } x=z=0\\ \int_0^\infty u\,c(x,z)\,dz&=Q && \text{for } x>0. \end{aligned}\right\} \tag{8.43-2}$$

The integration of Eq. (8.43-1) has to be achieved numerically as the result is not expressible in terms of simple functions. However, it is possible to give analytical solutions of the equation if $u(z)$ and K_z are approximated by powers of z instead of being taken as given by Eqs. (8.42-2) and (8.42-10) respectively. Thus, let us set

$$u(z)=u_1\left(\frac{z}{z_1}\right)^m, \tag{8.43-3}$$

$$K_z(z)=K_1\left(\frac{z}{z_1}\right)^n, \tag{8.43-4}$$

then, the solution of (8.43-1) can be shown to be[1] (z_1 = unity)

$$c(x,z)=\frac{Q}{u_1\,\Gamma(s)}\left[\frac{u_1}{(m-n+2)^2\,K_1\,x}\right]^s\exp\left\{-\frac{u_1\,z^{m-n+2}}{(m-n+2)^2\,K_1\,x}\right\} \tag{8.43-5}$$

with

$$s\equiv\frac{m+1}{m-n+2}. \tag{8.43-6}$$

It has been found empirically that for a smooth or short-grass surface,

$$\begin{aligned} m&=\tfrac{1}{7}\\ n&=\tfrac{6}{7} \end{aligned} \tag{8.43-7}$$

and then we have

$$c(x,z)=\frac{Q}{(1\tfrac{2}{7})^{\frac{6}{9}}\,\Gamma(\tfrac{8}{9})\,K_1^{\frac{1}{9}}\,u_1^{\frac{1}{7}}\,x^{\frac{8}{9}}}\exp\left\{-\frac{u_1\,z^{\frac{9}{7}}}{(1\tfrac{2}{7})^2\,K_1\,u}\right\}. \tag{8.43-8}$$

This gives the shape of a dust cloud caused by a line source of fine dust.

An alternative approach to that given above has been suggested by SUTTON[2], who considered the motion of the dust particles directly as a statistical process. If the standard deviation σ of a particle after time t be assumed as expressible by an expression of the form (u being the

1. See SUTTON, O. G.: Micrometeorology. New York: McGraw-Hill Book Co. 1953.
2. SUTTON, O. G.: Proc. Roy. Soc. A 146, 701 (1934).

Turning first to ash flows, we note that nuées ardentes have much in common with *turbidity currents* in the sea (cf. Sec. 6.23). However, a mixture of air, gravel and sand does not flow downhill on a moderate slope as does a turbidity current in water or a nuée ardente. An additional effect must therefore be operative to account for the mobility of a nuée ardente. The various theories that have been advanced have been reviewed, for instance, by McTAGGART[1].

Accordingly, the gas emission hypothesis, first stated by ANDERSON and FLETT[2], is the most widely accepted theory of the mobility of a nuée ardente. According to this theory, gas is emitted from the lava and rocks thrown out by the volcanic eruption while they are cooling, which is so plentiful that it keeps the individual particles in suspension. The gas emission hypothesis was accepted by very many authors; REYNOLDS[3] added the specific statement that this gas emission produces *fluidization* in the cloud.

McTAGGART made a quantitative check of the gas emission hypothesis by comparing the suspension time of a particle in a nuée with the suspension time of a single particle in an air stream. However, he used an orifice formula to make his estimates whose applicability to the case in question is somewhat doubtful. Let us therefore compare the nuée with a fluidized bed for which measurements are available.

In order to keep a fluidized bed in suspension, the pressure drop Δp across it has to be at least as great as the (buoyant) weight of the bed[4]:

$$\Delta p = L(1-P)(\rho_{sed} - \rho_{fluid})\, g \tag{8.45-1}$$

where L is the depth of the bed, P its porosity, ρ_{sed} the density of the particles, ρ_{fluid} the density of the fluid and g the gravity acceleration.

In order to correlate the pressure drop Δp with the flow velocity, we take one of the available correlations[5], in particular, we take the correlation proposed by KLING[6] for turbulent flow at low Reynolds numbers:

$$\lambda = 94/(Re)^{0.16} \tag{8.45-2}$$

where λ is the "friction factor"

$$\lambda = \frac{2\delta\, \Delta p/L}{P^2 v^2 \rho_{fluid}} \tag{8.45-3}$$

---

1. McTAGGART, K. C.: Amer. J. Sci. 258, 369 (1960).
2. ANDERSON, T., and J. S. FLETT: Phil. Trans. Roy. Soc. London A 200, 353 (1903).
3. REYNOLDS, D. L.: Amer. J. Sci. 252, 577 (1954).
4. Cf. e.g. LEVA, M., et al.: Fluid Flow Through Packed and Fluidized Systems. Washington: Bureau of Mines Bulletin No. 504 (1951).
5. Cf. SCHEIDEGGER, A. E.: The Physics of Flow Through Porous Media. 2nd ed. Toronto: Univ. of Toronto Press 1960.
6. KLING, G.: Z. Ver. dtsch. Ing. 84, 85 (1940).

This shows that velocities of the right order of magnitude to cause fluidization can indeed be obtained. Therefore, McTaggart's supposition appears to be reasonable.

A modification of the above process has been proposed by Shreve[1] who advanced the hypothesis that the pyroclastic flow, in fact, develops a cushion of gas at the bottom upon which it slides. This process allows for a much greater mobility than mere flow in a fluidized state. The cushion of gas consists partly of air and partly of gas emitted from the debris.

Turning now to the phenomenon of *ash falls*, we note that the characteristic downwind size decline of the deposits can be explained as a case of aeolian particle gradation. This hypothesis was advanced by Scheidegger and Potter[2] and its mechanical implications were carefully studied. The physical model is that of a turbulent "slug" of air (containing suspended particles) being transported downwind. During the downwind motion, the turbulence decays according to standard laws. Thereby, the carrying capacity for sediment diminishes, and a sorting of the particles results: First the heavy particles, then the lighter and lighter ones fall out. The process is much like that considered in the theory of varve deposition (Sec. 7.45); except that, in addition to the *amount* of sediment deposited down-current, the particle *size* has to be considered. The theory yields an excellent correlation with observation.

8.5. Geomorphological Effects of Dust Movement

In the Chapter on physical geomorphology (cf. Sec. 1.83) we have already stated in qualitative terms what the geomorphological effects of dust movement are: first the erosion of soil and desert dust in large quantities, and second the deposition of dust over large areas to form loess, the area of deposition being hundreds or thousands of miles removed from that of the origin of the dust.

It would be nice if it were possible to account for the *amount* of dust removed from or deposited in an area under given climatic conditions. Unfortunately, as far as the writer was able to ascertain, studies to determine this amount either theoretically or experimentally do not seem to have been undertaken as of yet.

This leaves one solely with the task of explaining theoretically the large distances over which dust movement has actually been observed to occur. In this regard, the atmospheric diffusion theory, applied to "light" particles (cf. Sec. 8.43) immediately furnishes the required explanation: a sufficient cross-wind with reasonably turbulent air can keep dust in suspension indefinitely.

1. Shreve, R. L.: Bull. Geolog. Soc. Amer. **79**, 653 (1968).
2. Scheidegger, A. E., and P. E. Potter: Sedimentology **11**, 163 (1968).

forces, but is a consequence of the prevailing flow potentials. It has been closely studied by REINER[1] and by KELLER[2].

If we neglect gravity forces for one moment, then it can be shown that there are various possible flows when a jet of fluid leaves a nozzle with parallel walls. KELLER[2] made a study of this and came up with a variety of flows. He calculated the flow potentials for the planar case where a jet is confined between two parallel plates. The plates end, say, at $x=0$ and the jet moves on. There are four possibilities. One is that the jet moves straight on, another that it turns around the upper as well as around the lower plate, filling the whole space. The remaining two possibilities are where the jet turns either around the upper or around the lower plate. This is almost the teapot effect. In the course of his investigations, KELLER found an additional flow which has a direct bearing upon the problem of the hoodoos. We shall discuss it below.

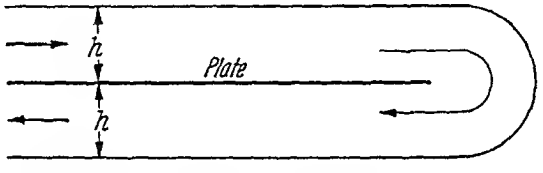

Fig. 203. Flow around a plate. After KELLER[2]

Assume that there is a plate extending along the x-axis (in cross section) towards minus infinity ending at $x=0$. Then it can be shown that a free surface flow is possible whose surface has (at minus infinity) the distance $\pm h$ from the plate. The geometry of this flow is then as shown in Fig. 203.

The complex potential for this flow is calculated by making a series of conformal mappings until the boundaries are of such a form that the potential can be written down easily. In order to do this, one must assume that the stream function (the imaginary part of the complex potential) is zero on both sides of the plate (since this represents one streamline) and that on the free surface, it is equal to a constant Q representing the total flux. The equation between the complex potential w and the complex variable z turns out to be

$$z=-\frac{4h}{\pi}\,\text{lognat}\cosh\frac{\pi w}{4Q}. \tag{9.22-1}$$

One can indeed convince himself that $w=w(z)$ satisfies, with its real and imaginary parts, the Laplace equation and that the boundary conditions as stated are also satisfied. One therefore has the required solution.

1. REINER, M.: Physics Today, No. 9, 16 (1956).
2. KELLER, J. B.: J. Appl. Phys. 28, 859 (1957).

In hydrodynamic stability calculations it is, then, usually assumed that the flow will actually become unstable (i.e. detach itself) after it has travelled a distance of $10\,L$.

9.23. Bearing of Teapot Effect on Hoodoos. Let us now investigate the significance that the above-mentioned discussion might have with regard to the formation of hoodoos.

In the case of hoodoos, the eroding agent is water. In the case of water, one has $T=80$ dynes/cm, $\rho=1$ g/cm^3, $g=980$ cm/sec^2; thus

$$\text{(a)} \qquad \text{if} \quad 12h^2 \ll 1, \quad \text{then} \quad L=\frac{u}{h^{\frac{1}{2}}}\times 0.0183, \tag{9.23-1}$$

$$\text{(b)} \qquad \text{if} \quad 12h^2 \gg 1, \quad \text{then} \quad L=u\times 0.0275 \tag{9.23-2}$$

where all units are in the c.g.s.-system.

The distance L, as has been explained above, is that distance in which the most significant disturbance grows by the factor e as stated above. In hydrodynamic stability theory, it is usually assumed that the instability will become predominant (i.e. the flow will detached itself) in a distance equal to ten times L. It turns out that the case (b) applies if h is greater than about $\frac{1}{3}$ cm. Then

$$10\,L \cong u\times 0.28 \text{ cm} \tag{9.23-3}$$

irrespective of the thickness h of the flow. It is difficult to estimate the velocity u in the flow. In a good cloudburst it will probably reach about $1-2$ m/sec at the edge of the overhang. This means that the flow can continue on the underside for about $28-56$ cm before detaching itself. According to earlier remarks about the mechanism of erosion, this distance of $28-56$ cm is the distance by which the "hat" of the hoodoos can overhang, for, in order to erode the soft material below, the water must obviously first reach it.

It thus appears that the values postulated above from a discussion of the teapot effect are in good agreement with those actually found in the hoodoos measured. This would serve to substantiate the theory proposed here.

9.3. Geysers

As noted in Sec. 1.93, geysers are intermittent hot springs. Since they occur in young volcanic areas, it is not difficult to see why they are hot. What needs an explanation, however, is the intermittency of their flow.

There is a whole series of theories of geyser action in existence which have been reviewed, for instance, by BLOSS and BARTH[1, 2] and by

1. BLOSS, F. D., and T. F. W. BARTH: Bull. Geol. Soc. Amer. 60, 861 (1949).
2. BARTH, T. F. W.: Publ. Carnegie Inst. Wash. 587, 1 (1950).

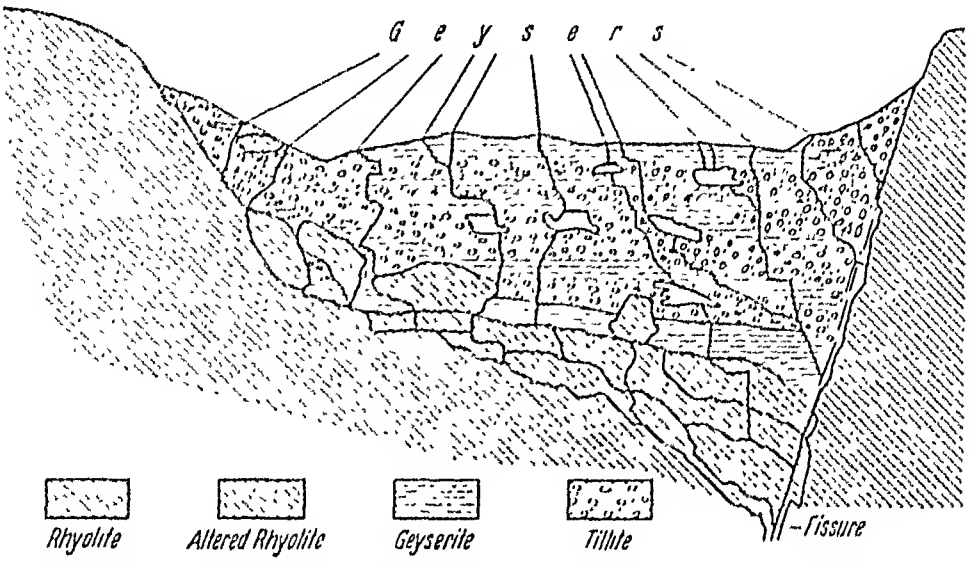

Fig. 204. Imaginary cross section through a Geyser basin. Modified after BAUER[1]

A further theory of geyser action has been suggested by THORKELSSON[2] who based his argument on the presence of dissolved gases in the geyser water. From the top to a certain depth in a geyser tube (in the quiescent state), the temperature increases to a depth l_1 at which bubbles of the dissolved gases can form. Below that point, no gas bubbles exist because the hydrostatic pressure is too high. The temperature above this point decreases with height because the bubbles, as they form, are continuously withdrawing heat from the column. The gases may collect in caverns etc. As the process continues, an increasing amount of water will be displaced from the geyser column (above l_1) by gases which results in a reduction of the hydrostatic pressure. Thus, the formation of bubbles now can occur at a level lower than l_1 – in fact, it begins to move downward at a certain rate of speed, as water spills on top, further reducing the hydrostatic pressure, until a new level, l_2, is reached which again corresponds to an equilibrium state. This represents the eruption.

BLOSS and BARTH[3] made a study of some Yellowstone geysers to test the above theory. It was found that in some geysers, the temperature in the column does not increase regularly between eruptions, but fluctuates widely, which excludes this theory at least for these geysers.

In other geysers, the volume of spring gases contained in the eruption water is very small which is at variance with the basic premises of

1 BAUER, C. M.: Yellowstone, its Underworld. Albuquerque: Univ. New Mexico Press 1953.

2. THORKELSSON, T.: On Thermal Activity in Iceland and Geyser Action. Reykjavik: Isafoldarprentsmidja 1940.

3. BLOSS, F. D., and T. F. W. BARTH: Bull. Geol. Soc. Amer. 60, 861 (1949).

where C is the concentration of solute, v the local flow velocity and D, as indicated above, the diffusivity factor. As noted above, the dissolution of limestone at the wall is very rapid so that the boundary condition can be formulated by stating that the solution must be saturated at the wall.

WEYL has solved the above Eq. (9.42-2) (steady state case) for a fissure of width d which contains a fluid flowing laminarly with an average velocity $\bar{v}$ parallel to its walls; he found for the distance L at which the bulk of the fluid is 90% saturated

$$\begin{aligned} &\text{if} \quad \bar{v}\, d/D \gg 1 \qquad L = 0.304\, d^2/D \\ &\text{if} \quad \bar{v}\, d/D \ll 1 \qquad L = d. \end{aligned} \tag{9.42-3}$$

For $\bar{v} = 1$ cm/sec, $d = 1$ mm, this works out to

$$L = 1.52 \text{ meters}. \tag{9.42-4}$$

WEYL's theory is valid only for very fine fissures in which one may assume laminar flow. In limestone caverns the flow of water is presumably turbulent so that the rate of mass transfer out of the vicinity of a wall is increased many times. At any rate, WEYL concludes from his investigations that water inside rock is essentially in chemical equilibrium with its surroundings. The solution-reaction occurs in times which are short compared with the times during which the water remains in the rock.

Thus, the leaching out of a cavern is entirely determined by the amount of water that percolates through it and by the solubility of the limestone in the water. There is no danger that water will percolate through a cavern without becoming completely saturated while doing so.

The solubility of calcium carbonate (calcite) in water containing carbon dioxide has also been investigated by WEYL[1]. Accordingly, the oder of magnitude of equilibrium molal calcium ion concentration in cold (10° C) water is approximately equal to the initial molal CO_2 concentration. The question regarding the dissolving potency of water, thus, depends on determining the initial CO_2 content. For the solubility of CO_2 in water, the Handbook of Chemistry and Physics (38th ed.) gives, at 10° C, 2.32 g per liter at a partial CO_2 pressure of 760 mm Hg. Thus, for saturated water one obtains a solubility of calcite equal to $2.32 \times 100.9/44$ g/liter which equals about 5 g/liter. However, it can hardly be assumed that the water can be fully saturated with carbon dioxide at a partial pressure of 1 atmosphere. One may assume that an enrichment of CO_2 in water can indeed occur to perhaps $\frac{1}{10}$ of that partial pressure. Thus, it may be reasonable to assume that 1 liter water can dissolve 0.5 g of limestone. For the Carlsbad Cavern (cf. Sec. 1.94) we have a volume of $1.2 \times 10^5 \times 18{,}000 \times 9{,}000\ \text{cm}^3 = 1.9 \times 10^{13}\ \text{cm}^3$ or

1. WEYL, P. K.: Geochim. et Cosmochim. Acta 17, 214 (1959).

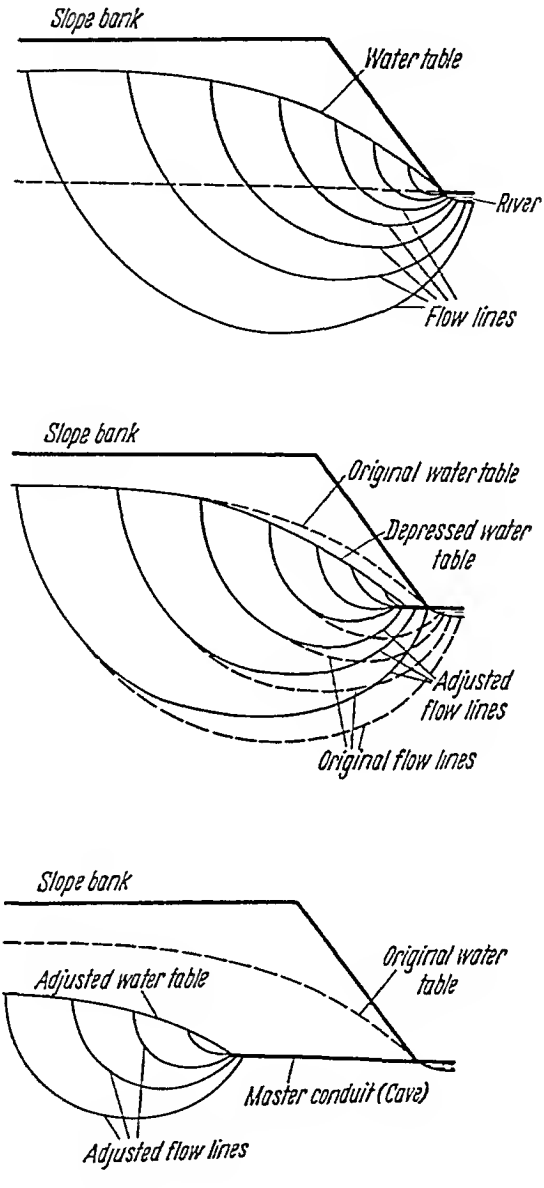

Fig. 205. Three stages of the development of a cave. Modified from RHOADES and SINACORI[1]

9.44. Stability of Caves. In order to investigate the stability of caves, we shall analyse the stresses around a cavity in a geological stress state. Beginning with the simplest case, we take the stresses far away from the cavity as being represented by a pure compression (pressure p) and the cavity as spherical (radius a). Furthermore, the rock will be treated as elastic and fracture will be assumed to occur when the maximum stress difference reaches a critical value (i. e. exceeds the "strength" of the rock).

The problem of calculating the stresses around a spherical cavity in a homogeneous elastic medium under pressure has been solved long ago

1. RHOADES, R., and M. N. SINACORI: J. Geol. 49, 785 (1941).

one has proven the result that, in an uniaxial stress, the stresses on the surface of a spherical cavity are independent of the size of the cavity. However, a general triaxial geological stress state is nothing but the superposition of three uniaxial stress states, and hence we see that the stability of a spherical cave is independent of its size, at least as long as the stress field far away from the cavity is homogeneous (i.e. gravity is neglected) and as long as the rock can be assumed as being elastic.

It may be of some interest to note that a similar result also applies to cylindrical cavities in a uniform stress field. The stress distribution around cylindrical cavities has been studied by mining engineers (e.g. by VAN ITERSON[1] or BOSHKOV[2]) because such cavities may be taken to

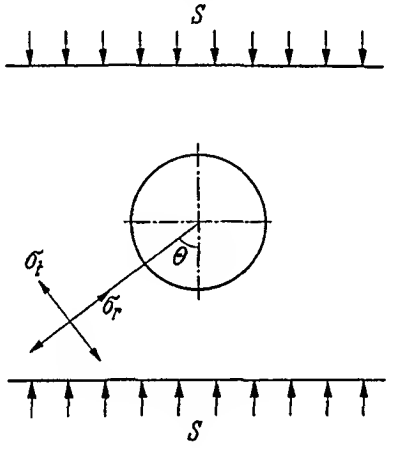

Fig. 207. Stresses around a cylindrical hole

represent mine shafts. The stresses around a cylindrical cavity of radius a have been given by e.g. MILES and TOPPING[3] as follows

$$\sigma_r = \frac{S}{2}\left\{1-\frac{a^2}{r^2}+\left(1-4\frac{a^2}{r^2}+3\frac{a^4}{r^4}\right)\cos 2\Theta\right\}, \qquad (9.44\text{-}24)$$

$$\sigma_t = \frac{S}{2}\left\{1+\frac{a^2}{r^2}-\left(1+3\frac{a^4}{r^4}\right)\cos 2\Theta\right\}, \qquad (9.44\text{-}25)$$

$$\tau = -\frac{S}{2}\left(1+2\frac{a^2}{r^2}-3\frac{a^4}{r^4}\right)\sin 2\Theta, \qquad (9.44\text{-}26)$$

where the meaning of the symbols is explained in Fig. 207. It is again at once obvious that the stresses at the surface of the cavity ($r=a$) are independent of the radius a of the cavity. Thus, if a cylindrical cavity is

1. VAN ITERSON, F. K. T.: Geologie en Mijnbouw **10**, 198 (1948).
2. BOSHKOV, S.: Trans. Canad. Inst. Min. Met. **59**, 264 (1956).
3. MILES, A. J., and A. D. TOPPING: Trans. AIME **179**, 186 (1949).

Author Index

Subject Index

Fotosatz, Druck und Bindearbeit Universitätsdruckerei H. Stürtz AG Würzburg

$L'/L=4$, $H=80$ cal $\cdot g^{-1}$, $D=0.005$ cal deg^{-1} sec^{-1} cm^{-1}, $\tau=1$ bar, $B=0.017$ bar$^{-4.2}$ year^{-1}, $n=4.2$) for the constants in (7.23-5), obtained a value of about 1 m/year. This is far less than what is observed in natural glaciers. The situation can be improved by slightly changing the roughness-value (L'/L), because of the high value of n attached to the latter.

Modifications of the above theory have been attempted by LLIBOUTRY[1,2] who noted that the idealized glacier bed considered by WEERTMAN (Fig. 183) represents too gross an oversimplification. Thus, LLIBOUTRY suggested that, instead of a bed with square obstacles, one should consider a bed made up of parallel sine waves, as shown in

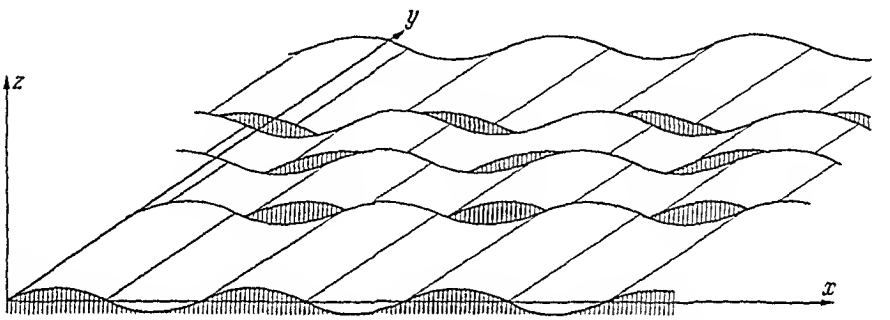

Fig 184. LLIBOUTRY's model of an idealized glacier bed. After LLIBOUTRY[1]

Fig. 184. The equation of the glacier bed (in the co-ordinate system indicated in Fig. 184) is then

$$z=\frac{a}{2}\sin\left(\frac{2\pi x}{\lambda}-\varphi\right). \tag{7.23-6}$$

In order to approach reality, one can allow different phase angles φ for different intervals on the y-axis. The quantity r

$$r=\frac{a}{\lambda} \tag{7.23-7}$$

may be called the *rugosity* of the bed.

The ice exerts a pressure upon the bed which will be greater in front of the waves than behind; thus LLIBOUTRY assumes a harmonic variation for this pressure:

$$\sigma_z=\rho g h+\frac{\Delta\sigma}{2}\cos\left(\frac{2\pi x}{\lambda}-\varphi\right) \tag{7.23-8}$$

1 LLIBOUTRY, L : Ann Géophys. (Paris) **15**, No 2, 250 (1959)
2. LLIBOUTRY, L.: Pub Assoc. Int. Hydrol. Sci. 79, 33 (1967).